A GLOBAL ANALYSIS OF APPARENT TRENDS IN ABUNDANCE AND RECRUITMENT OF LARGE TUNAS AND BILLFISHES INFERRED FROM JAPANESE LONGLINE CATCH AND EFFORT DATA

by

ROBERT NORMAN MATTHEW AHRENS

A THESIS SUBMITTED IN PARTIAL FULFILLMENT OF THE
REQUIREMENTS FOR THE DEGREE OF

DOCTOR OF PHILOSOPHY

in

THE FACULTY OF GRADUATE STUDIES
(Zoology)

THE UNIVERSITY OF BRITISH COLUMBIA
(Vancouver)

March 2010

Abstract

There has been substantial debate in recent years about the extent to which industrialized fishing has affected tunas and other large pelagic predator populations and altered the pelagic community. Variations in the type of data incorporated into assessments, statistical treatment of catch rate information, and different assessment methodologies have lead to diverging interpretations of stock levels and the sustainability of current large-scale industrialized fisheries. Simple nominal catch rates derived from Japanese longline catch and effort data paint a biased picture of the impact of industrialized fishing on the large pelagic tuna and billfish community, suggesting that abundance as of 2002 was only 10% of pre-1950 levels. Methods that correct for the spatial expansion, shift in distribution, and change in species targeting of the Japanese fleet, by averaging catch rates over spatial areas while imputing missing catch rate values, indicate a less severe decline with tuna and billfish stock reduced to an average of 50% of pre 1950 levels. For the majority of stocks, simple assessment methods indicate these relative abundance trends may still be biased and additional information sources are necessary to constrain assessments and evaluate the status of the stocks. With the incorporation of prior information on current fishing mortality rates and in some instances stock productivity, assessments indicate that a number of stocks are over-fished and experiencing over-fishing. Optimization models based on the same catch and effort data, aimed a redistributing fishing effort to maximize profits subject to fishing mortality constraints, suggest economic efficiencies can be gained in the long term if effort reductions are coupled with closed areas. Areas open to fishing should be placed where potential value and recruitments into the fishery are high. Fisheries are complex adaptive systems and it is not necessarily apparent how data resulting from fishing activities relate to the states of the assemblage of species captured. Careful consideration must be given to the nature of the sampling processes that give rise to these data. Without such consideration or alternative sources of information, inferences about impacts of fisheries on natural systems can be severely distorted.

Contents

List of tables

List of figures

Acknowledgements

This work would not have been possible without the assistance and support of many individuals.

I owe a great debt to my mentor Dr. Carl Walters for guiding me through this endeavor and for providing endless opportunities and challenges. He has been a great inspiration throughout my education. Dr. Villy Christensen has been exceptionally generous with his input and time on both this thesis and other endeavors. I thank Dr. Ussif Rashid Sumaila for his contributions. Dr. Steven Martell was a guiding light through much of the modeling in *AD Model Builder* and I am truly appreciative of the time he gave and the rigor of his intellectual contribution. I am grateful to Dr. John Sibert who provided me with funding and many opportunities early in this venture that allowed me to meet many of the individuals involved in tuna assessment and acquire the necessary data. The funding he provided was through Cooperative Agreement NA17RJ1230 between the Joint Institute for Marine and Atmospheric Research (JIMAR) and the National Oceanic and Atmospheric Administration (NOAA). Funding through the Apex Predator Workgroup from the University of Wisconsin, Madison was provided by Dr. Jim Kitchell and afforded me many opportunities to meet with colleagues in Hawaii. I am truly thankful for his support.

Japanese longline data from the Pacific Ocean used in this thesis were provided by the Fisheries Agency of Japan. I am grateful to Dr. Ziro Suzuki and Naozumi Miyabe from the National Research Institute of Far Seas Fisheries, Shimizu, Japan, for their assistance in acquiring data. I am also indebted to Dr. Hiroyuki Kurota for many discussions and facilitating my communication with individuals at the Far Seas Laboratory.

I have had the great pleasure of meeting many of the individuals involved in the assessment of tuna and billfish and thank them for their kindness and intellectual contributions: John Hampton, Shelton Harley, David Kirby, Adam Langley, Peter Williams, Simon Hoyle, Valérie Allain, Michael Hinton, Robin Allen, Mark Maunder, Pierre Kleiber, Keith Bigelow, and Chris Boggs. Public domain data was made available through the dedication of many other individuals at the SPC-OFP, IATTC, IOTC, ICCAT, and CCSBT.

Robyn Forrest and Nathan Taylor inspired me through this process and provided much advice. I also thank Bob Lessard for discussions and support in the early days. Many other friends and colleagues at the Fisheries Centre and Zoology department have made the process enjoyable and I am grateful. This thesis has been a long time coming and I thank my friends for enduring and my parent for their endless support and having faith that the end would come.

Finally, I thank my beloved, Andrea Rambeau for her unwavering love and support.

"Our knowledge, our attitudes, and our actions are based to a very large extent on samples."

William G. Cochran

"How should scientists operate when they must try to explain the results of history, those inordinately complex events that can occur but once in detailed glory?"

Stephen Jay Gould

Chapter 1 General introduction

Context

Reported landings of principle market tunas and billfishes captured by industrialized fisheries steadily increased from 0.4 million tonnes in 1950, reaching ~4 million tonnes by 2002 (Figure 1.1). Approximately 40% of the cumulative ~100 million tonnes of landings is skipjack tuna, followed by yellowfin tuna (~30%), albacore and bigeye tuna (~10% each), bluefin tuna sp. (~4%), and billfish sp. (~6%). Removals from the Pacific Ocean account for ~65% of the reported catch, followed by the Indian (~20%) and Atlantic (~15%) oceans. The majority of catches were taken by purse seine, longline, pole-and-line, and troll vessels. During the 1940s and 1950s, Japan was the first to develop large-scale industrial fisheries within the western Pacific Ocean. Japanese fleets, particularly the Japanese distant-water longline fleet, advanced into and throughout the world's oceans by the 1970s. Spain, France, the Republic of Korea, Taiwan Province of China, and the United States followed during the mid 1960s and developed large-scale operations. Driven by technological advances, market forces, and political constraints, tuna fisheries have undergone substantial changes over time. Excluding skipjack tuna fisheries, early-industrialized fishing was dominated by longlines, targeting older and larger individuals. During the 1980s, a rapidly increasing purse seine fishery, targeting smaller individuals, emerged as the dominant gear. Though most fleets target tuna, some specialized fleets targeting billfish, particularly swordfish, emerged.

Attempts to assess potential yields of tuna stocks began early in the history of industrialized tuna fishing (Schaefer 1957, Shimada and Schaefer 1956). Assessments of the major tuna and billfish stocks are currently conducted in all major oceans by Regional Fisheries Management Organizations (RFMOs). Japanese longline catch and effort data, having broad temporal, spatial, and species coverage, has been used often as the primary information source to derive relative abundance indices for assessments. Recently, spatial catch and effort data have become available in the public domain, and variations in the type of data incorporated into assessments, statistical treatment of spatial catch rate information, and assessment methodology utilized have lead to widely divergent interpretations of stock levels and the sustainability of current large-scale

industrialized fisheries. At one extreme, Japanese pelagic longline catch (in numbers) and effort (in hooks) data were used as the sole indicator of large pelagic predator community status (Myers and Worm 2003). In that analysis, simple exponential model fits to trends in longline 'nominal' catch-per-unit-effort (*cpue*, calculated as total catch summed over species and areas divided by total effort), suggested large pelagic predators communities were rapidly depleted (by 80%) within 15 years of industrial fishing commencing and are currently at 10% of abundances before 1950. Such an analysis was contrary to current single species stock assessments, which generally utilize a broader suite of data. For the more abundant tuna stocks, recent assessments indicated fishing mortality rates are at or near levels that produce the maximum sustainable yield (F_{msy}), and stock biomasses are at or near levels that produce the maximum sustainable yield (B_{msy}) (IATTC 2008, ICCAT 2009, IOTC 2008, ISC 2007, WCPFC 2008). There are some exceptions; assessments suggest bluefin stocks are likely below B_{msy} ('over-fished') and fishing mortality rates are above F_{msy} ('over-fishing') (CCSBT 2006b, ICCAT 2009, ISC 2008c). Furthermore, when assessments are available, similar results are found for some marlin stocks (ICCAT 2006c, Uozumi 2003).

Much literature warns of biases that may be introduced into stock assessment due to errors in understanding the mechanisms that give rise to relative abundance observations or the misspecification of processes that govern dynamic behaviour (Haddon 2001, Hilborn and Mangel 1997, Hilborn and Walters 1992, Quinn II and Deriso 1999, Walters and Martell 2004). The analysis presented by Myers and Worm (2003) has been criticized for presenting a misleading picture of the status of large pelagic communities and the severity of management actions implied (Hampton et al. 2005b, Polacheck 2006, Sibert et al. 2006). There is no disagreement concerning the trends presented. Nominal *cpue* aggregated over the major species captured in Japanese longline operations did decline rapidly after 1950 in the Pacific Ocean, after 1952 in the Indian Ocean, and after 1956 in the Atlantic Ocean. Rapid change in apparent abundance appears incongruous in relation to relatively small catch removals in the early 1950s. As a result, various unsubstantiated explanations for the rapid change in nominal *cpue* have been proposed (Polacheck 2006). Although the mechanisms that gave rise to changes in nominal catch rates are not well understood, a number of critical assumptions must be met if changes in nominal *cpue* are to be interpreted as indicative of changes in large pelagic predator abundance.

A number of papers suggest that nominal *cpue* is unlikely to reflect changes in tuna and billfish, given historical changes in the Japanese longline fishery (Hampton et al. 2005b, Maunder et al. 2006b). Developing abundance trends using methods that explicitly account for changes in the spatial distribution of the fishery has been recommended (e.g., Walters 2003). Kleiber and Maunder (2008) demonstrated the possibility of hyperdepletion of *cpue* aggregated over species, due to differences in catchability and productivity among species in the overall catch. Hampton et al. (2005b) point out that the spatial scale used by Myers and Worm (2003) is inappropriate. The definitions of eco-regions used by Myers and Worm (e.g., tropical, sub-tropical) do not necessarily span the core range of some species. Finally, stock assessments generally rely on data as catch removals or composition in addition to *cpue* to make inference about population scale and productivity relationships. Using *cpue* alone, particularly to infer impacts at a community level is generally not accepted; even the simplest of assessments should account for fishery impacts (Hampton et al. 2005b).

The primary motivation for this thesis was to investigate the differing intepretations of Japanese catch and effort data that gave rise to such divergent views of population status and rates of decline of large pelagic predators. Concerns highlighted above regarding methodology and interpretation makes a reexamination of the Japanese longline catch and effort data a worthwhile exercise. Heeding the litany of advice regarding development of abundance indices and stock assessment, apparent impacts of industrialized fishing on tuna and billfish stocks globally were reassessed using Japanese longline data. More specifically, status of the component of those stocks that are of a size vulnerable to longline gear was reassessed.

This thesis does not attempt to reproduce assessments performed by the various RFMOs. Instead, similar methods and assessments were applied to all stocks in all oceans to: 1) highlight how and why different methodologies produced widely different relative abundance trends; 2) demonstrate when such trends in conjunction with known removals are sufficient to assess stock status or when additional information is required; 3) highlight which stock-specific relative abundance trends derived from Japanese catch and effort data may not be proportional to abundance even when more appropriate methods are applied; and 4) assess apparent status of tuna and billfish stocks globally. Finally, given concerns regarding over-exploitation of a number

of stocks, a global spatially explicit multi-species model was developed to explore potential equilibrium effort distributions that maximize profit subject to the constraint of not over-fishing any stock within the multi-species fishery.

Thesis structure

This thesis contains five main sections, presented in the same basic order as a fisheries assessment. Chapter 2 presents background information required for most assessments. The first section in Chapter 2 presents a brief history of the Japanese longline fishery, highlighting major developments over time that may have altered species-specific catchability or fishing power. The second section of Chapter 2 introduces biological, distributional and fisheries information for each species considered in this thesis: albacore tuna (*Thunnus alalunga*), bigeye tuna (*Thunnus obesus*), yellowfin tuna (*Thunnus albacares*), Southern bluefin tuna (*Thunnus maccoyii*), Pacific bluefin tuna (*Thunnus orientalis*), Atlantic bluefin tuna (*Thunnus thynnus*), blue marlin (*Makaira nigricans*), striped marlin (*Tetrapturus audax*), Atlantic white marlin (*Tetrapturus albidus*), black marlin (*Makaira indica*), swordfish (*Xiphias gladius*). Within each ocean, species were broken down in to stocks. Table 1.1 presents the stock designation used along with a short code to identify each stock. Stock definitions do not necessarily conform to those used by RFMOs. Sailfish and spearfish are captured by Japanese longline but have been excluded for analyses due to major changes in data reporting requirements during the first few decades of the fishery. The final section in Chapter 2 details the development of various data sets spanning 1950-2002 for the species listed above: global 5°x5° Japanese longline catch and effort, global 5°x5° longline catch of all other nations combined, global 5°x5° catch of longline vulnerable-sized individuals in other gear and nominal catches by species.

In Chapter 3, various methods for constructing relative abundance trends for each stock are presented and compared. The emphasis in this chapter is to develop so-called 'folly and fantasy' spatial estimators (Walters 2003) for trends in relative abundance, so as to correct for gross violation of statistical assumptions about representative sampling of spatial density patterns by the fishing fleets. The basic approach in the development of such estimators is to recognize that the estimation procedure must assign a catch per effort index value to every spatial cell

frequented by each stock, for every historical time period used in assessment, whether or not the spatial cell was actually fished in every period. The 'folly and fantasy' methods involve trying to make better assumptions about unsampled cells than the hidden, common assumption in catch rate data analysis that such unsampled cells had the same average catch rate as the cells that were fished.

In Chapter 4, relative abundance trends developed in Chapter 3 in conjunction with nominal catches are used to explore stock productivity and abundance using assessment models. These models range from simple stock-recruitment reconstructions based on recruitment trends estimated from relative abundance and catch data, to age-structured models fit to the relative abundance data using a stochastic approach to stock reduction analysis.

In Chapter 5, a global, spatially explicit multi-species model with movement is developed and parameterized. For this model, spatial movement rates among 5x5 degree cells are estimated from trends in spatial relative abundance and catch, where the essential idea is to estimate the movement between cells that must have occurred to explain observed catches.

Finally, in Chapter 6 the global spatial model is used in a gaming and optimization framework to identify optimized spatial distributions of fishing effort given constraints on allowable fishing mortality rates on all species considered in the analysis. A key aim in this chapter is to identify a spatial mosaic of large-scale closed areas (marine protected areas) that would meet target fishing mortality constraints at minimum cost in terms of lost profits from fishing.

Throughout this thesis, a number of terms and acronyms that can have multiple interpretations are used. To avoid confusion these terms are defined here and a list of acronyms is presented in Table 1.2. The term 'stock' is used to define a management unit. This may be part of a population or multiple populations. Within this thesis, with the exception of albacore tuna, a stock is defined as the individuals of the same species within an ocean basin. Maximum sustained yield (MSY) is the largest yield that can be taken on a continuing basis from a stock. Associated with MSY is the stock abundance in biomass (B_{msy}) or numbers (N_{msy}) that produces, on average, the largest surplus. The fishing mortality rate that captures this surplus is termed the

fishing mortality rate that produces MSY (F_{msy}). In this thesis, 'overfishing' indicates the fishing mortality rate (F) exerted on a stock is greater than the fishing mortality rate that would reduce the stock abundance to a level that produces the greatest yield and capture the surplus production ($F>F_{msy}$). When a stock is referred to as 'overfished', stock abundance is below the level that would produce MSY ($B<B_{msy}$ or $N<N_{msy}$).

Table 1.1 Stock breakdown and short identifier coded associated with each species.

Species	Stock (short code identifier)
Albacore tuna	Indian (IALB) North Pacific (PNAB) South Pacific (PSAB) North Atlantic (ANAB) South Atlantic (ASAB)
Bigeye tuna	Indian (IBET) Pacific (PBET) Atlantic (ABET)
Yellowfin tuna	Indian (IYFT) Pacific (PYFT) Atlantic (AYFT)
Southern bluefin tuna	Global (GSBT)
Pacific bluefin tuna	Pacific (PBFT)
Atlantic bluefin tuna	Atlantic (ABFT)
Blue marlin	Indian (IBUM) Pacific (PBUM) Atlantic (ABUM)
Striped marlin	Indian (ISTM) Pacific (PSTM)
Atlantic white marlin	Atlantic (AWHM)
Black marlin	Global (GBLM)
Swordfish	Indian (ISWO) Pacific (PSWO) Atlantic (ASWO)

Table 1.2 A description of acronyms used in this document.

Acronym	Description
cpue	Catch-per-unit-effort
RFMO	Regional Fisheries Management Organization
IOTC	Indian Ocean Tuna Commission
CCSBT	Commission for the Conservation of Southern Bluefin Tuna
WCPFC	Western and Central Pacific Fisheries Commission
SPC-OFP	Secretariat of the Pacific Community
IATTC	Inter-American Tropical Tuna Commission
ICCAT	International Commission for the Conservation of Atlantic Tunas
ISC	Interim Scientific Committee for Tuna and Tuna-like Species in the North Pacific Ocean
MSY	Maximum Sustainable Yield
Fmsy	Fishing mortality rate that on average produces MSY over the long term
Fcur	Current fishing mortality rate
Nmsy	Population size in numbers that on average produces MSY
Bmsy	Population biomass that on average produces MSY
ALB	Albacore tuna
BET	Bigeye tuna
YFT	Yellowfin tuna
PBFT	Pacific bluefin tuna
ABFT	Atlantic bluefin tuna
GSBT	Southern bluefin tuna
BUM	Blue Marlin
BLM	Black Marlin
STM	Striped Marlin
WHM	White Marlin
SWO	Swordfish
EEZ	Exclusive Economic Zone
HPB	Hooks-per-basket – the number of hooks between floats in a longline set
MLE	Maximum Likelihood Estimate
GLM	Generalized Linear Model
GAM	Generalized Additive Model
GIS	Geographic Information System
MPA	Marine Protected Area

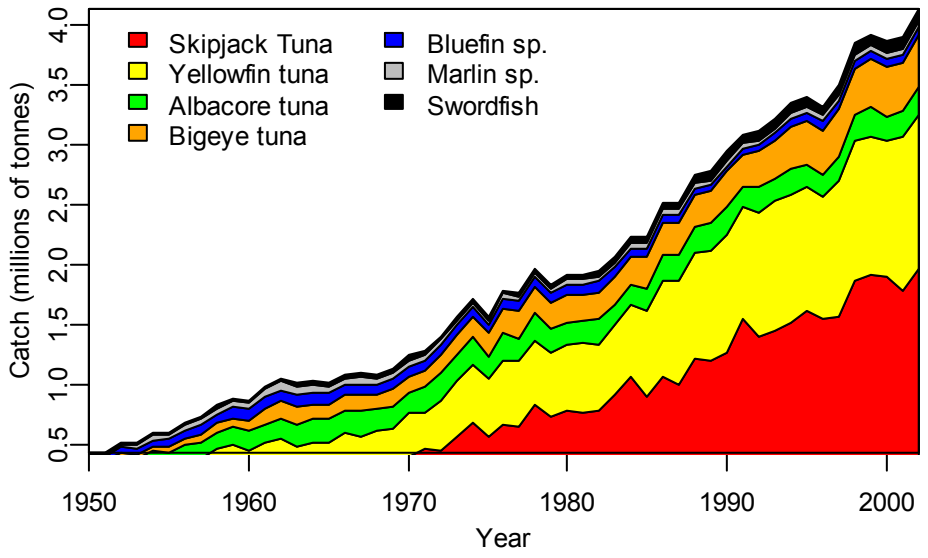

Figure 1.1 Global catch of principal market tuna and billfish from 1950-2002. Bluefin sp. includes Atlantic, Pacific, and southern bluefin and marlin sp. includes blue, black, white, and striped marlin.

Chapter 2 Background information

Basic information pertaining to species biology and fisheries as well as methods used to generate the data sets required for the construction of relative abundance trends and assessments of stocks are presented within this chapter. In the first section, a brief history of the Japanese longline fishery is presented highlighting major fishery developments related to fleet distribution, fleet composition, targeting practices, and technological advances. Changes in the fishery altered fishing power, species-specific catchability, and the spatial relationship between fishing effort and species distributions. These factors must be considered when developing relative abundance indices. The second section emphasizes aspects of species biology and fisheries. Various life history trait parameters required for the assessment models used in later chapters are presented. Attention is also given to aspects of species distribution, movement, and habitat use that should be considered when interpreting fisheries data. A brief description of the fisheries is also presented to emphasize changes in fishing intensity over time and the diversity of gears used. The final section of this chapter details the development of various global catch and effort data sets spanning 1950-2002.

Development of the Japanese longline fishery

It is critical to recognize potential sources of change in species-specific catchability and fishing power when interpreting fisheries dependent catch and effort information. Failing to account for shifts in these components, which relate catch rate to stock abundance, may lead to erroneous interpretations of fishery impacts, population change, or population distribution. Catch and effort data from Japanese distant-water longliners are no exception. During the expansion of industrialized fishing by Japan after World War II, the distant-water fleet underwent changes in available technology, targeted species, and was subject to economic and political constraints. A number of authors have documented operational and procedural changes in the Japanese longline fleet (Beverly et al. 2003, Matsuda and Ouchi 1984, Miyake 2004, Miyake et al. 2004, Okamoto 2004, Ward and Hindmarsh 2007). Some of the major developments are reviewed in this chapter, as they influence the interpretation of catch and effort data. In particular, it is important to

recognize how such developments may have affected species-specific catchability, fishing power, and the spatial relationship between fishing effort and species captured over time.

Governmental development and promotion of Japanese costal and distant-water tuna fisheries is traced to Meiji Era (1868-1912) policies responding to foreign fishery activity in waters around Japan. Catches for tuna fisheries around Japan were recorded as early as 1894 (Matsuda and Ouchi 1984). By 1906, the advent of power-driven vessels aided in the formation of distant-water fisheries and by 1914 offshore tuna fisheries emerged. The Japanese territory expanded in 1915 facilitating the expansion of tuna fisheries into the western central Pacific through development of overseas fishing bases. Shoulder season fishing by bait-boat operators targeting skipjack tuna (*Katsuwonus pelamis*) soon proved the viability of yellowfin and bigeye fisheries. In the 1930's, longline fisheries that were initially restricted to more temperate species (albacore, northern Pacific bluefin, swordfish, and striped marlin) expanded into the western central Pacific. These ventures were mothership operations that primarily targeted yellowfin for canning. Distant-water fisheries continued to increase production until the commencement of World War II (Figure 2.1). In 1942, Japanese vessels came under military control and suffered significant losses during wartime activities. Post-war fleets were reduced by 60%, and all overseas fishing bases were lost (Matsuda and Ouchi 1984). Following the war, Japanese fishing activities were restricted to the use of wooden vessels within 12 nautical miles of the coast (Matsuda and Ouchi 1984). By September 22, 1945, all vessels were allowed access to waters within 12 nautical miles. Successive relaxations (Figure 2.2) of restrictions on Japanese fishing activities were demarked by 'MacArthur Lines' (Morita 1998). By September 22, 1945, vessels <100 gmt were allowed to fish outside the 12 nautical mile zone. On October 13, 1945, vessels >100 gmt were also given permission to expand beyond 12 nautical miles. These two expansions were combined on November 3, 1945, to form the first MacArthur Line. Fishing activities were further expanded on June 22, 1946, and September 19, 1949. The establishment of the third MacArthur Line in 1949 allowed Japanese vessels to access fully their historical grounds. On May 11, 1950, 'mothership' operations were allowed access to fishing ground to the south and on April 25, 1952, the MacArthur Lines were abolished. Concurrent with the removal of the MacArthur lines was the development of a vessel licensing program (1949) and refinement of catch reporting to the species level (1951, Okamoto 2004). Thus, available catch and effort

records from 1950 and 1951 are from mothership operations only and after 1952 from an increasing number of large (>100 gmt) longliners. Species-specific catchability and fishing power between and within vessel classes is likely to have changed during these first few years though it is unknown to what extent. Changes in license restrictions, government promotion, and programs aimed at reducing economic inefficiencies altered the distribution and composition of the Japanese fleet following 1952. Up to the mid 1960s, a shifting mosaic of vessel classes, many equipped with -25°C air blast freezers, expanding into the Indian and Atlantic oceans increasing landings (Figure 2.1) and the geographic range of the fishery (Figure 2.3).

Pacific expansion was eastward as well as north and south from western equatorial waters. In the Indian Ocean, the fleet extended westward and to the south. In the Atlantic, the pattern was generally north and south from equatorial waters. As a result, in all oceans a greater portion of each stock's range was sampled (Figure 2.4). During the first few years of fishing within each ocean, effort was concentrated within a few months (Figure 2.5). As fisheries expanded, so did the seasonal distribution of fishing effort. This effect is very prominent in the Pacific where the seasonal pattern of mothership effort in 1950 and 1951 was different from the seasonal effort distribution after 1952. Seasonal expansion of fishing effort also occurred in each new 5°x5° area; initially fished for only a few months (Figure 2.6), new areas were later fished for a greater period. These patterns hint at a methodical exploration: new areas were initially probed for fishing opportunity for a few months. If fishing was successful, effort expanded into the areas and the fishing season was extended. Spatial heterogeneity in stock distribution and seasonal migratory patterns relative to the effort distribution complicates the interpretation of catch rates from aggregated catch and effort data, particularly from the early expansion period.

In the late 1960s and early 1970s, the expanding Japanese fleet underwent significant changes. Further modifications were made to the 1949 New Fisheries Law, to include area specific vessel size restrictions aimed at promoting fishery development (Matsuda and Ouchi 1984). Advances in freezing technology allowed longer trips but the majority of products were still destined for canning. Line-casting devices and other labor saving measures were introduced to improve efficiency and increase profit (Miyake 2004). By the late 1960s, increasing operational costs and increasing numbers of larger longliners with freezing technology resulted in a substantial

reduction in mothership operations. A single mothership operation was operating in the western Pacific after 1965 and the last mothership operation occurred in 1975 (Miyake 2004). Improvements in blast freezing technology (<-40°C), prevented product from browning during thawing and allowed frozen product to be sold as higher valued sashimi. By 1969, -55°C freezers were common on longliners and a large proportion of the fleet changed fishing strategy (Miyake 2004). When fisheries were targeting tuna for canning during the 1950s and 1960s, areas of high catch rate were a primary objective, and albacore and yellowfin tuna were target species. On the sashimi market, bigeye and bluefin tuna are preferred species and fetch higher prices. This economic incentive resulted in a targeting switch to these colder water species. During this relatively rapid transition period (late 1960s to late 1970s), significant changes occurred in the fleet. Many vessels began setting deeper longlines to target bigeye tuna, which altered the relationship between the depth of gear and captured species. Although new areas were still being explored during this period and later, particularly in the North Atlantic, the Japanese fleet had reached its greatest level of occupancy in each ocean (Figure 2.7). Seasonal effort distribution over the range of most species also changed during this time (Figure 2.5) though less apparent in the Pacific where southern albacore were targeted year round. General patterns in the Indian Ocean suggest a shift from a northern winter dominated distribution to dominance by summer fishing. Patterns in the Atlantic appear more haphazard, and effort tended to be spread throughout the year. The impact of seasonal effort shifts must be considered when interpreting aggregated data.

The energy crisis in the mid 1970s resulted in several cost saving measures. Trip routes were optimized to reduce fuel consumption. Ship hulls were redesigned to improve efficiency through reduced drag. Freezing technology was improved to reduce energy loss and propeller design was changed to decrease fuel consumption. In addition, the Japanese government provided support in the form of fuel subsidies, product price support, and low interest loans (Matsuda and Ouchi 1984). The Fisheries Special Reconstruction and Adjustment Act (1976) provided loans and subsidies for the withdrawal of vessels from the longline fleets, and in the Pacific, ~20% of the longline fleet was removed. These cost-saving measures also helped to stimulate expansion of the more economical purse seine fleet. In the late 1970s and early 1980s, a significant number of countries declared 200 nautical mile exclusive economic zones (EEZ). With the exception of the

Banda Sea agreement with Indonesia, Japan possessed no bilateral agreements with other countries requiring Japan to develop agreements usually requiring new joint ventures or access fee agreements (Matsuda and Ouchi 1984). In the Indian and Atlantic oceans this transitional period resulted in a decline in area occupied (Figure 2.4), followed by increase again after 1980. Declines in area occupied in the Pacific were more gradual but continued after 1980. The general result of these changes was a gradual contraction of Japanese effort from northern and southern extremes, except in the North Atlantic. Seasonal effort distribution during this period remained stable until the late 1990s.

Communication, navigation, and information systems improved dramatically over time (Ward and Hindmarsh 2007). Radio communication and echo sounders, prevalent by the late 1950s were replaced. Satellite navigation and communication, and weather facsimiles dramatically changed navigation, positioning, and communication by the 1980s. The introduction of global positioning systems, Doppler current profilers, multi-directional sonar, remote sensing images, and information integration further enhanced the information available to longliners into the 1990s, allowing for more accurate targeting of specific oceanographic features. Amidst advances aimed at improving targeting, navigation, and communication was the modernization of gear materials such as monofilament for mainline and leaders, and stainless steel for hooks. Refinements also occurred in setting techniques aimed at reducing setting time, increasing hook fishing time and hook exposure during crepuscular periods (Hayasi 1974, Ward and Hindmarsh 2007). Distributional changes in fishing effort both spatially and temporally, coupled with technological advances and shifts in target species, resulted in an appreciably different Japanese fleet by the mid 1980s and 1990s than that of the 1950s. The overall effect of changes in the Japanese fleet for interpreting catch rates and their relationship to species abundance is significant, and comparisons between methods that do or do not attempt to account for some of these changes are presented in Chapter 3.

Species biology and fisheries

The biology and fisheries for tuna and billfish are diverse. Variability in terms of life-history strategy, habitat use, and the nature of the fishing gears utilized must be considered when interpreting fisheries data and developing assessment models given the multi-species nature of the longline fisheries and the historical changes in fishing practices that have occurred. Growth, mortality, maturity, and allometric relationships are essential information for any stock assessment, and though it is possible to estimate some of these quantities using composition information, in many instances values must be obtained from basic scientific studies or meta-analyses. Species horizontal and vertical distributions as well as seasonal and daily shifts in distribution must also be considered as changes in the spatial distribution of Japanese longline fisheries and change in species targeting altered the spatial relationship between species and gear. Consideration must also be given to the diversity of gears capturing tuna and billfish and the size of individuals captured. Longline gear tends to capture large individuals. However, there are overlaps in the size distributions between gears. Although large individuals may comprise only a small fraction of the catch in some gears, the biomass harvested by some alternate gears was substantial and the resulting number of large individuals removed must be considered. The removal of individuals by other gears of size vulnerable to longline gear is an important consideration for the analyses in later chapters.

In the open ocean, tuna and billfish are commonly categorized by habitat use according to photic zone and surface water temperature. Yellowfin and marlin are categorized as epipelagic (shallow) and tropical, bigeye is mesopelagic and tropical, swordfish are mesopelagic and temperate, and albacore and bluefin tunas are epipelagic and temperate. Furthermore, marlins are generally considered a by-catch species while tuna and swordfish are targeted. Marlin and swordfish are mainly solitary, observed sometimes in spawning or feeding aggregations, while tuna aggregate in schools according to size. Much of this categorization stems from fishery-based observations of larger individuals, mainly captured by daytime longline sets. As knowledge of tuna and marlin biology has increased, particularly through acoustic, archival, and satellite tag development as well as a greater understanding of physiological constraints, a richer picture of life history strategies and spatial ontogeny has emerged. Billfish and tuna, at least

those examined here, use tropical waters to spawn and remain in epipelagic waters during the night and for brief periods during the day. Juvenile tuna are found in mixed-species schools in tropical waters, so niche differentiation appears to emerge as individuals grow. The daytime foraging behaviour of yellowfin and bigeye appear distinctively different, as does the behaviour of marlins and swordfish. Adult Atlantic bluefin are observed to forage where the Gulf Stream meets cooler sub-arctic waters, then return to the Mediterranean Sea and Gulf of Mexico to spawn. These differences in habitat use, migration, and life history are worthwhile mentioning as they complicate the interpretation of fisheries data particularly, as is the case with the Japanese longline fleet, when data are collected from a fleet that altered its distribution and target species over time. Furthermore, a wide variety of fleets and gears had developed to exploit theses species throughout their ontogeny.

The subsections that follow provide some details of the biology and fisheries for individual species in each ocean. Data for tuna are more readily available than that for billfishes and information for species in the Indian Ocean is sparse. Life history parameters such a mortality, growth rates, length-to-weight conversions, and estimates of age at 50% maturity used in the creation of data sets as well as stock assessments and gaming simulations are presented at the end of each biology subsection, and are also summarized for all species in Table 2.1. In a number of instances, information was not available, and reasonable guesses had to be made as noted in the table. Brief descriptions of fisheries for each species are provided to highlight the variety of gears used and the magnitude of removals by each gear. A more detailed breakdown of catch by county and gear can be found in Miyake (2004) or on the FAO website.

Albacore tuna (*Thunnus alalunga*)

Biology

Distributed in temperate to tropical waters of the Pacific, Atlantic, and Indian oceans as well as the Mediterranean Sea, albacore tuna are generally found in epi- to mesopelagic waters where surface temperature ranges between >10-25° C. Though commonly taken with surface gears particularly in more temperate waters, individuals are observed to depths of ~600 m (Collette and Nauen 1983) with an apparent preference for cooler temperatures (~15° C). Lower lethal

oxygen levels estimated for albacore vary depending on body size and model assumption (1.67 mg l^{-1} at 50 cm, 1.39 mg l^{-1} at 75 cm (Sharp 1978), 5 mg l^{-1} (Graham et al. 1989)). As with most Scombroids, albacore show a preference for surface waters during the night. Unlike yellowfin, which make repeated forays to depth during the day, albacore appear to spend a substantial proportion of the day at intermediate depths (Bard 2001, Chen et al. 2005, Dagorn et al. 2000, Saito 1973). In the Pacific and Atlantic oceans, warm equatorial waters are assumed to be a barrier to migration which has resulted in distinct northern and southern populations (Nakamura 1969). In the Indian Ocean, no such north-south differentiation exists. Generalized migratory patterns have been proposed for most populations. Mature adults migrate from temperate to subtropical waters to spawn. Young of the year rear for a time in tropical waters then migrate toward temperate waters. Sub-adults and adults outside the spawning season tend to migrate east west, concentrating along convergence zones (Jones 1991, Nakamura 1969, Wang 1988).

In the Indian Ocean, albacore are distributed between 25° N-45° S with a main spawning area off eastern Madagascar (Koto 1969). Life history stages appear segregated by major current systems (Chen et al. 2005). Mature individuals are mainly found north of 10° S, where the monsoon-driven current prevails, in temperatures >15° C. Spawning occurs in the austral summer between 10-30°S within the subtropical gyre zone at depth, where surface temperatures are >24° C and the mixed layer is deep (Ueyanagi 1969). Immature albacore are predominantly found >30° S within circumpolar currents in the austral autumn, migrating northward to 25° S in the austral winter, then to between 15-25° S in the austral spring and returning south of 30° S in the austral summer.

Northern Pacific albacore appear to range between 0-50° N with immature individuals making large trans-Pacific migrations (Nakamura 1969). Kimura (1997) expanded upon previous migration models proposing an anti-clockwise migration for both immature and mature albacore. Immature albacore concentrate between 25-35° N between October to March, dispersing widely and up to 45° N in the North Pacific during the summer. Winter movement depends upon the Kuroshio Current meander. In years with little extension of the Kuroshio into eastern Pacific waters, immature individuals appear to migrate in an anti-clockwise direction during the winter from 120-180° E. This pattern extends eastward when the Kuroshio's influence extends into the

eastern Pacific. Mature individuals appear to follow an anti-clockwise migration centered on 20° N and 170° E. During the summer, mature individuals are found spawning south of 20° N between 150° E-160° W moving north and east in the fall and westward between 25-35° N in the winter.

Distribution and migration patterns of southern Pacific albacore are not as well understood (Nakamura 1969). Distributed between ~0-<50° S, southern Pacific albacore appear to spawn within the western Pacific during the southern summer with juveniles migrating south to the Subtropical Convergence Zone (Roberts 1980) before returning to spawn in more tropical waters when mature. Catch rates of mature individuals are high in the southern summer between 15-25° S and between 30-40° S in the southern winter (Wang 1988). Both immature and mature southern albacore are thought to migrate west to east within the subtropical convergence (Jones 1991).

In the Atlantic Ocean, albacore are distributed between 45° S-50° N (Collette and Nauen 1983). North Atlantic albacore are assumed to be distributed between 5-<50° N (Bard 1981) with spawning grounds located in waters offshore of Venezuela, the Sargassum Sea, and the Gulf of Mexico. Spawning occurs from April-November, peaking in the summer (Nishikawa et al. 1985). Mature individuals are thought to migrate eastward in the winter months (Grant 1969). Juvenile individuals appear to migrate toward the eastern Atlantic. Immature albacore undergo a seasonal migration associated with warming surface waters (Bard 2001). In the spring, young albacore migrate northward and eastward from the Azores to the Bay of Biscay and Celtic Sea, potentially moving westward to concentrate on the front of the Gulf Stream. During the summer, individuals are found in two feeding areas, on the continental slope of Bay of Biscay and the Celtic Shelf as well as Gulf Stream fronts and south of the Grand Banks.

Distribution and movement of albacore in the Mediterranean is poorly understood. Mature individuals are distributed discontinuously with concentrations in the Tyrrhenian, Ionian, Adriatic, and Aegean seas (Megalofonou 2000). Tagging studies suggest exchange between areas within the Mediterranean and limited exchange with the north Atlantic (Arrizabalaga et al. 2002)

South Atlantic albacore are assumed to be distributed between 50° S-5° N. Spawning is observed to occur off the eastern Brazilian coast during the austral summer (Koto 1969). Mature individuals appear to migrate eastward in the winter concentrating off Angola and Southwest Africa (Grant 1969). Coimbra (1995) proposed that all life stages of southern albacore follow the south Atlantic subtropical gyre. The Brazil current transports larvae southward to the inter-tropical convergence zone. Immature individuals move eastward and spread northward up the west coast of Africa toward the Gulf of Guinea in the Benguela current. Mature individuals migrate westward in the south equatorial current and Brazil current to the northeast Brazilian coast.

Maximum life span is assumed 13 years, though Mediterranean albacore are estimated to reach a maximum age of 9 years (Megalofonou 2000). Age at 50% maturity is estimated to be around 80-90 cm (~ 5 years) in the Pacific, Atlantic and Indian oceans, and >62 cm in the Mediterranean Sea. Length-at-age varies with location and sex, with recent estimates for the von Bertalanffy curvature coefficients between 0.14-0.54 $year^{-1}$ and mean asymptotic lengths from 78-142 cm. Natural mortality rate is commonly assumed to be between 0.2-0.4 $year^{-1}$ for older ages, though estimates range as high as 0.56 $year^{-1}$ (Chen and Watanabe 1988, Labelle and Hampton 2003). Sex ratio appears to diverge from 1:1 after the age of maturity, with males having apparent lower mortality, slower growth, and larger body size (Collette and Nauen 1983).

Fisheries

Albacore are captured using both surface (troll, pole-and-line/baitboat, purse seine, and drift gillnet) and subsurface (longline) gears with relative contribution of each gear to total catch depending on ocean and stock. Surface gears tend to target immature albacore, 40-80 cm, and longlines target fish >65 cm.

Albacore fisheries in the Indian Ocean are dominated by longline. Japanese vessels began large-scale longline operations in the Indian Ocean in 1952, primarily targeting yellowfin and albacore. Albacore catch increased until the early 1960s from less than 5000 tonnes to ~15,000 tonnes (Miyake et al. 2004). Through the late 1960s, catches declined rapidly as vessels outfitted

with super-cold freezers began targeting southern bluefin and bigeye. Coinciding with the decline in Japanese catch was a rapid increase in Taiwan's catch. A number of other nations contributed to total longline removal, though Taiwan's catch contribution accounts for the majority of the ~40,000 tonnes caught in the late 1990s (Miyake et al. 2004). The only other fishery removals of note are a small amount of purse-seine by-catch reported by the European Community and a sizeable Taiwanese drift gillnet fishery that operated during the mid 1980s until 1992 with catches peaking around 20,000 tonnes.

Unlike Indian Ocean fishery development, north Pacific albacore has had a long history of targeted exploitation. Japanese total catch of tuna increased steadily after the beginning of the 20th century to around 85,000 tonnes by 1940 (Matsuda and Ouchi 1984), and it is likely that a sizable proportion of this catch was comprised of albacore. By 1950, the Japanese albacore catch was ~75,000 tonnes (Miyake et al. 2004). The development of the U.S. commercial albacore fishery off the coast of California began decades prior to 1950, and was comprised of 3,000 vessels by 1950 (Laurs and Dotson 1992) catching ~20,000 tonnes. Miyake et al. (2004) note that prior to the late 1980s the largest component of north Pacific albacore catch was taken by the Japanese baitboat fleet. Peak catches of >100,000 tonnes occurred in the 1970s. In the mid 1970s to 1991 Japanese, Taiwanese and Chinese drift gillnet fishery catch increased, surpassing all other gears by the late 1980s. Longline fishery catch surpassed baitboat catch in the early 1990s though total catch had declined substantially. By 1999, catches had increased again to levels seen in the 1970s.

Fisheries for albacore in the South Pacific Ocean are predominantly longline operations. Japanese longline catch increased from low levels in 1952 to ~30,000 tonnes by the early 1960s. As in the Indian Ocean, the Japanese catch declined as vessels shifted to targeting bigeye, and were replaced by Taiwanese and Korean longliners. Drift gillnet fisheries began in the late 1980s but ended in the high seas by 1992. Troll fisheries developed in the late 1970s between New Zealand and 140° W along the southern convergence zone. Total removals from the south Pacific stock has not exceeded ~50,000 tonnes (Miyake et al. 2004).

North Atlantic albacore were caught prior to 1950 mainly by French and Spanish troll fleets in the Bay of Biscay, producing a stable catch of 30-40,000 tonnes (Miyake et al. 2004). Troll fishery catch declined in the late 1950s as the Spanish fleet converted to baitboats and in the 1980s as French trollers converted to trawls and drift gillnets. After 1956, Japanese longliners began targeting albacore and yellowfin but, as in the Indian and Pacific oceans, switched to bigeye and bluefin in the late 1960s with fleets from Korea and Taiwan taking their place. Total longline catch from the 1960s through the 1980s varied between 10-20,000 tonnes declining in the 1990s with Taiwan remaining the dominant longline fleet. Total catch of northern albacore from the mid 1960s to the late 1980s varied between 50-60,000 tonnes. Miyake et al. (2004) remark that the southern Atlantic albacore fishery is predominantly a longline fishery with Japanese catches increasing in the late 1950s followed by Korea and Taiwan. By the early 1970s, longline catch peaked around 30,000 tonnes, varying between 10,000-30,000 tonnes since. Taiwanese catch accounts for a high proportion of the biomass captured in recent years. In the early 1980s, baitboat fisheries developed off Namibia and South Africa with catches quickly reaching 10,000 tonnes. Albacore fisheries in the Mediterranean Sea are also predominantly longline fisheries with a reported catch of ~5,000 tonnes.

Bigeye tuna (*Thunnus obesus*)

Biology

Bigeye tuna occur in tropical and subtropical oceanic waters of the Pacific, Atlantic, and Indian oceans. Bigeye, an epi- and mesopelagic species, are found where surface waters range between >10-29° C (Collette and Nauen 1983) with an apparent adult temperature preference of 11-15° C (Brill 1994). Spawning is thought to occur year round in surface waters >24° C, with a seasonal peak during the summer months at depths >50 m (Miyabe 1994). Bigeye are found to have the lowest dissolved oxygen tolerance limit of the major tuna species though estimates vary depending on size and method (0.52 mg l^{-1} at 50 cm, 0.65 mg l^{-1} at 75 cm (Sharp 1978), 1.3 mg l^{-1} (Hanamoto 1987)). Low temperature and oxygen tolerance afford bigeye tuna a distinct depth distribution and vertical movement pattern. Remaining in surface waters during the night, individuals mirror the vertical movement of the deep scattering layer (Brill et al. 2005) reaching depth >500 m during the day but making short forays into warm shallow water possibly to

recover thermal or oxygen debts (Holland et al. 1990b, Matsumoto et al. 2005, Schaefer and Fuller 2002). Bigeye tunas appear to spend daytime hours below the thermocline. Arrizabalaga (2005) noted an exception to this behaviour in Azorean waters where bigeye made repeated dives to depth but remain in surface waters. A crude migratory pattern is apparent from purse seine and longline catch rate for bigeye tuna (Fonteneau et al. 2005). As spawning season approaches, adults move toward warm equatorial waters where the sea surface temperatures is >24° C. Juveniles rear within warm equatorial surface waters in mixed schools with yellowfin and skipjack until sufficient thermoregulatory ability is achieved allowing them to move to deeper colder waters. Adults tend to migrate from spawning areas to feeding zones in more temperate waters.

In the Indian Ocean bigeye are distributed north of 40° S. Lee et al. (2005) note that movement patterns of bigeye within the Indian Ocean appear tied to the 6 month cycle of north-east and south-west prevailing monsoons as the inter-tropical convergence zone shifts north to south across the equator. The migration pattern is poorly defined though adults appear to concentrate between 15° S-10° N during the northeast monsoon season (austral summer) for spawning. Juveniles appear in the purse seine fishery in the western ocean in mixed species schools. Adults appear to move into temperate waters outside the spawning season.

Information that is more detailed is available on the distribution of bigeye in the Pacific Ocean (Miyabe 1994). Pacific bigeye tunas are distributed between 40° S-40° N in the west and 30° S-40° N in the east, except near coastal waters off Central America. Gonadosomatic index measurements suggest year round spawning with peak spawning in June and July west of 140° E within the equatorial counter current. Size of individuals and proportion spawning tends to increase from west to east. However, bigeye tuna associate with the thermocline and such a pattern is explainable if catchability of larger individuals increases as the thermocline shallows west to east. Peak spawning is observed between 140-180° E from April-July shifting to between February-July at 140-100° W. Mature bigeye are often caught from April-September between 10° S-10° N in the west (Kikawa 1962) and from January-September at 0-10° N and January-June at 0-10° S in the east (Kume and Joseph 1966). Miyabe (1994) notes that along 30° N and off Chile,

immature individuals are caught in winter fisheries. Japanese baitboat fisheries in the northwestern Pacific targeting immature individuals move northeast from spring to summer and return south to southwest in the fall. This north-south movement is also apparent in the eastern Pacific as well as the Southern Ocean. Such observations support the notion of spawning (tropical) to feeding (temperate) ground migration with immature individuals tending to reside temperate areas moving north and south in response to seasonal changes in sea surface temperature.

The main spawning area for Atlantic bigeye is between 10° S-10° N within the Gulf of Guinea (Alvarado Bremer et al. 1999). Fonteneau (2005) suggests mature bigeye return to this area to spawn during northern winter and summer months depending on feeding ground location (north or south). Juveniles appear to rear within the Gulf of Guinea as indicated by capture in the purse seine fisheries. Based on tagging studies and fisheries information, Hallier (2005) suggest immature individuals north of the Equator move northward of along the African coast during spring and summer returning south during winter months. Tagging studies suggest some individuals move northwest to the Azores and westward. Individuals tagged further south (Cape Lopez) have displayed southward movement along the coast toward Angola and westward movement in the south equatorial current. Proposed feeding grounds for mature and larger immature bigeye in the northern hemisphere are located between 10-20° N in the western Atlantic as well as spanning the Atlantic between 20-40° N in the east and 35-45° N in the west (Fonteneau et al. 2005). Southern feeding areas are hypothesized between 30-40° S in the west and 10-35° S in the east.

Longevity estimates based on natural mortality rates suggest a maximum age of >12 years (Hampton and Williams 2005) to 16 years (Farley et al. 2006). Maturity is observed to occur at sizes >100 cm or >2 years though estimates depend on geographic location (Calkins 1980, Nikaido et al. 1991, Schaefer et al. 2005) with age at 50% maturity assumed to be around 3.5 years. Estimates of growth parameters are also highly variable depending on method and location. Estimates for the von Bertalanffy curvature coefficient range from 0.14-0.45 $year^{-1}$ and estimates of asymptotic mean length from 166-250 cm. Natural mortality is estimated to decrease with size until maturity (~130 cm). As with albacore and yellowfin tuna, increasing male sex

ratios after maturity suggest an increase in female mortality or differential growth associated with spawning. As a result, estimates of mortality rate in some assessment models increase around the age of maturity and decline as the proportion of females decreases (Fonteneau et al. 2005, Hampton et al. 2005a, Maunder and Hoyle 2006a). Estimates of natural mortality for mature bigeye vary between 0.25-0.7 $year^{-1}$ depending on size, though a reasonable estimate is around 0.4 $year^{-1}$ (Fonteneau et al. 2005, Hampton et al. 1998).

Fisheries

Bigeye tunas are targeted in all three oceans using longline, baitboat, and purse seines though longline is the dominant gear type. Longlines target individuals >100 cm while baitboat and purse seine fisheries capture immature individuals <100 cm. In the Indian, Pacific and Atlantic oceans, fisheries for bigeye have undergone three major changes. In the late 1970s, longliners equipped with super-cold freezers (<-40° C) began targeting bigeye and bluefin for the sashimi market. This shift in target species resulted in gear configurations aimed at targeting bigeye at greater depth (Suzuki et al. 1977). Purse seine development in the 1980s resulted in increased catches of immature bigeye associated with natural floating object. The use of man-made fish aggregating devices (FADs) increased in mid to late 1990s resulted in a substantial increase in the catch of small juvenile bigeye in mixed schools with yellowfin and skipjack (Miyake et al. 2004).

In the Indian Ocean, bigeye tuna were first captured by Japanese longline fleets targeting yellowfin and albacore for canning in 1952. Catch increased as fleets from Korea and Taiwan joined the fishery in the 1960s. Catches peaked at 40,000 tonnes in the late 1960s. When vessels switched to targeting bigeye for the sashimi market in the late 1970s, catches stabilized between 40,000-60,000 tonnes. With other nations entering the fishery and the use of 'flags of convenience', catches increased to over 100,000 tonnes by the late 1990s (Miyake et al. 2004). French, Spanish, and to a lesser extent Japanese purse seine fisheries for yellowfin and skipjack developed in the early 1980s resulting in an increase in juvenile bigeye catch because of mixed schooling. By the early 1990s, catch of juvenile bigeye increased to 20,000 tonnes. The development of FAD fishing in the early 1990s resulted in further increases, again of primarily

small bigeye, to approximately 40,000 tonnes by the late 1990s (Miyake et al. 2004). Baitboat and gillnet catches are small in comparison, accounting for <2,000 tonnes.

As in the Indian Ocean, catches of bigeye in the Pacific are predominantly from longline operations though catch by purse seine and baitboat operations does occur. Bigeye in the western Pacific likely caught prior to 1950 in baitboat and longline operations off Japan (Matsuda and Ouchi 1984). With the expansion of the Japanese longline fishery, catch of bigeye increased rapidly to 60,000 tonnes by the mid 1960s. Targeting of bigeye in the late 1970s resulted in a further increase in the Japanese catch, peaking around 100,000 tonnes in the mid 1980s to mid 1990s then declining to 60,000 tonnes in the late 1990s. Taiwan, Korea and China also developed fleets in the mid 1960s and total longline catch peaked at ~160,000 tonnes during the mid 1980s to late 1990s declining to <100,000 tonnes by the late 1990s. Miyake et al. (2004) note that expansion of purse seining fleets started in the 1970s. Japanese, U. S., Korean, and Taiwanese fleets catch increased in the western Pacific to ~20,000 by the 1990s primarily targeting free schools or schools associated with natural floating objects. Eastern Pacific catches peaked in the mid 1970s at ~16,000 tonnes primarily using dolphin associated sets. In 1993, within the eastern Pacific, and 1998 in the western Pacific bigeye catch increased substantially with the development of FAD fishing. In the western Pacific, catch of bigeye also occurs in the Japanese baitboat fishery as well as artisanal fisheries in Indonesia and the Philippines. Prior to the expansion of the Japanese longline operations in the late 1950s, Atlantic bigeye, primarily large fish, were captured using baitboats within the Azores, Madeira and Canary islands (Miyake et al. 2004). Japanese catch increased as in other oceans as longliners switched to targeting bigeye in the late 1970s. Korean and Taiwanese vessels commenced longline operations in the 1960s. Total catch of bigeye varied between 40,000-60,000 tonnes through the 1970s and 1980s (Miyake et al. 2004). Attempts to account for IUU fishing in the 1990s resulted in a further increase in reported catch from longlines to ~70,000 tonnes. Purse seine fisheries developed in the Gulf of Guinea in the late 1960s with catches varying between 10,000-15,000 tonnes in the mid 1970s. Catches declined through the 1980s but increased during the 1990s with the introduction of FAD fisheries, to ~20,000 tonnes. In 1962, Japanese baitboats established a small fishery off Ghana (Miyake et al. 2004). Korea, Panama, and Ghana joined the fishery but currently only Ghana produces notable catches.

Yellowfin tuna (*Thunnus albacares*)

Biology

Yellowfin tuna occur in tropical and subtropical oceanic waters within the epipelagic zone. Distribution is generally restricted to where surface water range between 18-31° C (Collette and Nauen 1983) though yellowfin are most commonly caught in temperatures >20° C (Fonteneau 2005). Spawning is observed to occur year round in surface waters >24° C (Kikawa 1966) though seasonal peaks vary with location. Field observations and laboratory investigation show that yellowfin require higher dissolved oxygen concentration than bigeye, though potentially lower than albacore (1.49 mg l^{-1} at 50 cm, 2.32 mg l^{-1} at 75 cm (Sharp 1978), <2.5 mg l^{-1} (Dizon 1977), 2.1 mg l^{-1} (Bushnell and Brill 1992)). Archival tagging studies indicate that yellowfin are predominantly within surface waters during the night, and spend 90% of their daytime activity above 100 m making forays to depths near the thermocline provided temperature is no less than 8° C colder than surface temperature (Block et al. 1997, Brill et al. 1999, Holland et al. 1990b). However, Dagorn (2006) and Schaefer (2007) observed deep diving behaviour in yellowfin tuna, observing forays up to >1000 m in depth. During these dives water temperatures encountered were more that 8° C cooler that surface temperature though dives were terminated as body temperature approached 15° C. Korsmeyer (1996) and Brill (1998) point out that at 15° C cardiac function in yellowfin is impaired likely limiting vertical distribution.

Indian Ocean yellowfin are mainly distributed north of 30° S. Spawning occurs year round concentrated between 10° S-10° N (Mimura 1963). Areas of high larval density can be found within this geographic band in the western ocean south to Madagascar and in the eastern ocean within the Malay Archipelago during the Austral summer (Conand and Richards 1982, Mimura 1963). North-South migration of adult individuals is likely tied to seasonal changes in water temperature and currents, with higher densities in the north during the austral winter. Juveniles also appear to migrate north to south in response to seasonal changes, though their distribution is closer to coastlines. Mimura (1963) notes an apparent geographic distribution in adult sex ratio with a higher proportion of males north of 10° S, equal ratio between 10-15° S and a higher female ratio south of 15° S.

In the Pacific Ocean yellowfin are distributed in tropical and sub-tropical waters between 35° S-40° N in the western ocean and 33° S-35° N in the east (Cole 1980). Spawning occurs in the tropical Pacific year round and at higher latitudes when sea surface temperature is greater than 24° C (Suzuki 1994). Peak spawning in the western and central tropical Pacific is observed December-January between 120°-180° E, and April-May between 180° E-140° W, May-June in the Kuroshiro Current, and November-December in the East Australia Current (Cole 1980, Kikawa 1966). Suzuki (1994) notes that within Philippine waters, peak spawning occurs March-May and to a lesser extent November-December. Wild (1994), in a summary of eastern yellowfin spawning, indicates year round spawning off the coasts of Mexico, Central America as well as between 0-10° N and 130-190° W. Between 0-10° S and 130-190° W, spawning peaks from January-June and is suppressed in the second half of the year due to the intrusion of water colder than 26° C. As in the Indian and Atlantic oceans, north-south movements of both adults and juveniles are observed. Seasonal changes in thermal and current structure limit latitudinal extent of distributions with the highest latitudes reached in the summer (Suzuki 1994). Nakamura (1969) notes an apparent west to east cline in yellowfin tuna size distribution within the western and central Pacific. It is uncertain if such a cline is the result of size related ontogeny or differential exploitation rates. Several authors suggest western, central, and eastern individuals comprise separate stocks (Schaefer 1955, Suzuki et al. 1978) with potential further differentiation between eastern individuals north and south (Diaz-Jaimes and Uribe-Alcocer 2006). Yellowfin appear to show limited dispersal (Bayliff 1979, Fink and Bayliff 1970, Schaefer et al. 2007, Sibert and Hampton 2003) while recent tagging information indicates limited movement across the Pacific though large scale migratory behaviour is not apparent (Hampton et al. 2006b).

Distribution in the Atlantic extends from 50° S-50° N, though predominantly in tropical and sub-tropical waters. Spawning occurs along the West African coast in the Gulf of Guinea (January-March). Juveniles move north and south along the African coast within coastal currents and in response to seasonal temperature changes, ranging north to the Canary Islands and south off Angola. In the western Atlantic, spawning areas are found in the southeast Caribbean Sea (July-

September) and in the Gulf of Mexico (May-August) (Arocha et al. 2001, ICCAT 1991). In the western Atlantic, juveniles found off Brazil are likely spawned in the southeast Caribbean Sea. As in the eastern Atlantic, north-south movement is also observed. Adult yellowfin make transatlantic migrations within equatorial currents (ICCAT 1991) as well as north-south migrations along both the western and eastern Atlantic coasts.

Yellowfin tuna likely live 7-10 years. Size and age at 50% maturity is estimated to occur at sizes of 85-100 cm or 2-3 years age, though estimates depend on geographic location (Fonteneau 2005, Maunder and Hoyle 2006b). Growth parameters are also highly variable depending on method and location. Estimates for the von Bertalanffy curvature coefficient range from 0.26-0.66 $year^{-1}$ and estimates for asymptotic mean length from 166-230 cm. Departures from the standard von Bertalanffy growth model have been noted by a number of authors with growth apparently slowing around 40-70 cm (Lehodey and Leroy 1999, Wild 1986). Natural mortality is generally thought to decrease with size until maturity (~100 cm). As with bigeye and albacore, there is an almost linear increase in male sex ratio after maturity and potential differences in sex specific growth result in estimates of age specific natural mortality increasing with the onset of maturity. Thus, estimates of adult mortality vary considerably 0.55-1.2 $year^{-1}$. Hampton (2006b) estimate a minimum mortality of 0.6-0.8 $year^{-1}$ for sub-adults (<1.25 years). Similar estimates are made by Hoyle (2007) with sub-adult (<1.5 years) instantaneous mortality estimated at 0.8 $year^{-1}$ increasing to 1.2 $year^{-1}$ by age 3 and slowly declining back toward 0.8 $year^{-1}$.

Fisheries

Yellowfin tuna are fished in the Indian, Pacific, and Atlantic oceans using primarily longline, baitboat, and purse seine gears though catch in the Pacific and Indian oceans is also taken using gillnet and artisanal gears. In general, longlines targets individuals >90 cm, while baitboat and purse seine fisheries capture immature individuals <90 cm. Free and dolphin-associated purse seine sets in the eastern Pacific Ocean capture larger individuals. Since the 1980s, purse seining has been the dominant method of capture, with the exception of the eastern Pacific where purse seining dominated since the 1960s (Miyake et al. 2004). Japanese longline fleets began targeting yellowfin and bigeye in the Indian Ocean in 1952. Taiwan and Korea followed by the 1960s. Catch rose to 20,000-60,000 tonnes from the late 1950s to the mid 1980s though Japanese catch

had declined to 10,000 in the mid 1970s due to vessels targeting bigeye and southern bluefin. Increased catch by Taiwan and Indonesia resulted in peaks of 160,000 tonnes in the early 1990s, fluctuating between 80,000-100,000 tonnes by the late 1990s. French and Spanish purse seine fisheries began in the early 1980s with catches rising quickly and fluctuating from 80,000-100,000 tonnes through the 1990s with total purse seine catch fluctuating from 100,000-160,000 tonnes in the late 1990s. Purse seine catch in the Indian Ocean is primarily on FADs (Miyake et al. 2004). Baitboats have been operating out of the Maldives sine the early 1950s with catches around 10,000 tonnes in the 1990s. Sri Lankan and Iranian gillnet fisheries developed in the 1980s with catches >60,000 tonnes in the late 1990s.

Differences in fishery development in the western and eastern Pacific are striking. Commercial ventures for yellowfin were in place well before 1950 in both the western and eastern Pacific (Laurs and Dotson 1992, Matsuda and Ouchi 1984). Japanese baitboat and longline vessels operated in the western Pacific and U.S. baitboats operated in the eastern Pacific. With the expansion of the Japanese longline fleet in 1952, yellowfin catch in the western and central Pacific increased quickly. Taiwan and Korea commenced longline operations in the late 1950s and early 1960s. By the early 1980s longline catch had peaked at >100,000 tonnes but with fleets switching to target bigeye and the expansion of purse seining, catch declined and fluctuated between 50,000-100,000 tonnes (Miyake et al. 2004). Japanese purse seine fleets targeting free schools were in operation in the western Pacific before 1950. Until the development of fleets by the U.S., Korea, and Taiwan, in the 1980s, catches were small. Expansion of purse seine fishing, mainly on free schools, resulted in catch increasing to >200,000 tonnes in the 1990s. FAD fishing which commenced in 1998 has been used extensively since (Miyake et al. 2004). Eastern Pacific longline fisheries contribute little to total catches. The development of the U.S. purse seining fleet in the late 1950s resulted in catch increasing to >200,000 tonnes by the mid 1970s primarily using dolphin associated sets. Catch restrictions and El Niño conditions resulted in catch declines as the U.S. fleet shifted to the western Pacific. Catches increased in the mid 1980s with the development of Latin American fleets and FAD fishing in the early 1990s. Catch rose to between 250,000-300,000 tonnes (Miyake et al. 2004). Artisanal fisheries of Indonesia and the Philippines in the western Pacific are poorly documented but catches in recent years are estimated to have reached 140,000 tonnes (Miyake et al. 2004).

Japanese longlines began targeting yellowfin in the Atlantic Ocean after 1956. Catch increased rapidly to 50,000 tonnes by the early 1960s and declined through the 1970s. Taiwanese and Korean vessels entered the fishery in the 1960s and catches have been stable ranging from 20,000-30,000 tonnes since the 1980s (Miyake et al. 2004). Baitboat fisheries by France and Spain developed in the late 1950s in the eastern tropical Atlantic with catches increasing to 20,000 tonnes. In the 1960s, Japan developed a baitboat fishery based in Ghana followed by Korea, Panama, and Ghana. With French and Spanish fleets switching to purse seining, catch by baitboat has been stable at around 20,000 tonnes (Miyake et al. 2004). In the mid 1960s, French and Spanish purse seining fleets developed in the Gulf of Guinea with catches peaking at 130,000 tonnes in the early 1970s. Catches declined through the 1970s and vessels moved to the Indian Ocean. Catches increased through the 1980s and peaked with the introduction of FADs at around 130,000 tonnes in the early 1990s (Miyake et al. 2004). Since 1995, catches have declined.

Southern bluefin tuna (*Thunnus maccoyii*)

Biology

Southern bluefin tuna are a single stock with a near circumpolar distribution in the southern ocean (Proctor et al. 1995). Distribution is delimited by a broad temperature spectrum in epipelagic and mesopelagic waters (5-30° C) though outside of the spawning season, 5-20° C appears to be the preferred temperature range (Olson 1980). Cardiac performance of bluefin tunas allows them to exploit waters below 2° C (Blank et al. 2004). Southern bluefin remain in surface waters at night and, like bigeye, appear to follow the scattering layer during the day while returning to surface waters to warm (Gunn and Block 2001). Observation from tracking studies on southern bluefin (Davis and Stanley 2002, Gunn and Block 2001) and other bluefin (Block et al. 2001, Block et al. 2005, Brill et al. 2005, Lutcavage et al. 2000, Teo et al. 2007) suggest temperature tolerance is related to body size, allowing larger individuals to exploit deeper depths.

Southern bluefin are distributed between 10-50° S though individuals north of 30° S are either juveniles or spawning adults. The main distribution is thought to occur between 30-50° S (Nakamura 1969). Southern bluefin spawn in water temperatures between 25-30° C in a restricted area in the eastern Indian Ocean south of Java, with the major spawning area between 10-20° S and 110-125° E and a minor areas 20-30° S and 110-125° E (Nakamura 1969). Spawning occurs between September-March (Mimura and Warashina 1962, Serventy 1956) with peaks in abundance during October and February (Farley and Davis 1998). Distribution and migration of southern bluefin is reasonably well established (Farley et al. 2006, Olson 1980). Young of the year appear to take one year to migrate southward along the western Australian coast, within the Leeuwin Current, to the southwestern Australian coast. Juveniles move eastward into the Great Australian Bight (GAB) off southern Australia. Juveniles age 2-4 years appear to winter in the GAB making eastward migrations south of Tasmania and up the southeastern Australian coast, or westward migrations within the southern Indian Ocean gyre to the African coast. After the age of four, juveniles move into the West Wind Drift and migrate east and west centered on 35° S. Upon reaching maturity, adults undertake seasonal migrations back to the spawning ground in the eastern Indian Ocean. Distribution of southern bluefin is not continuous within the West Wind Drift. Areas of high abundance are found off Southern Africa, the southeast Indian Ocean, Tasmania, and New Zealand.

Southern bluefin tuna are estimated to live >20 years (Caton 1994), with the oldest age observed being estimated at 41 years (Farley et al. 2007). Age at 50% maturity is estimated to occur at sizes 150-160 cm or 11-12 years (Davis et al. 2001). Growth parameters estimates for southern bluefin are reasonably well defined though asymptotic length is variable depending on the size range of individuals sampled. Estimates for the von Bertalanffy curvature coefficient range from 0.1-0.146 $year^{-1}$ and estimates for mean maximum asymptotic length between 180-260 cm. Polacheck et al. (2004) suggest, given an apparent reduction in growth rate during the transition between juvenile to sub-adult, that a two stage growth model is more appropriate for southern bluefin tuna. Increases in growth rate and decreased asymptotic size since 1960 have also been observed (Polacheck et al. 2004). Farley (2006) notes an increase in male sex ratio with size after maturity suggesting potential differences in male and female growth with males reaching a larger

asymptotic size. Natural mortality is estimated to decrease with size (Polacheck et al. 2006) with adult natural mortality between >0.05-0.2 $year^{-1}$ (CCSBT 2006a, Polacheck et al. 2006).

Fisheries

Southern bluefin are targeted using longline and purse seine gear. Reported catches from Japanese vessels commenced in 1952 with the expansion of the fleet into the Indian Ocean. Catches, primarily for canning, peaked at 20,000 tonnes in the late 1950s. With the development of freezing technology, southern bluefin was targeted for the sashimi market and catch peaked at 79,000 tonnes in 1961. By the early 1980s, catches had declined to 30,000 tonnes and decreased continuously to 6,000 tonnes by the 1990s. Taiwan began longline fishing in the late 1970s with catches reaching 1,000 to 1,500 tonnes in the 1990s. Reported catches from New Zealand longline vessels began in 1980 and fluctuated from 150-500 tonnes. Taiwan and Indonesia began longline operations in 1991 and 1986, with a combined catch of ~3,500 tonnes in the late 1990s. Australian catch (baitboat, troll, and purse seine) increased to 20,000 tonnes from 1950 through the early 1980s but declined rapidly to around 6,000 tonnes in the 1990s (Miyake et al. 2004). Australian catch prior to the 1980s was primarily for canning. However, because of the high price for southern bluefin on the Japanese sashimi market, farming operations have developed since the 1980s, where juveniles are purse seined and fattened in sea pens for a few months (Miyake et al. 2004). Total catch of southern bluefin in the 1990s was <20,000 tonnes. Perhaps the most alarming aspect of the southern bluefin fishery is the recent documentation that market assessments indicate the total reported catches may be only 50% of the actual catch removals (CCSBT 2006b).

Pacific bluefin tuna (*Thunnus orientalis*)

Biology

Pacific bluefin are a highly migratory species found in tropical and subtropical epipelagic waters of the Pacific Ocean in surface water temperatures ranging between 14-30° C, with larger individuals preferring 14-23° C outside the spawning season (Bell 1963, Uda 1957). In the western Pacific, bluefin are distributed 40° S-50° N from Sakhalin Island to southwestern

Australia and New Zealand (Bayliff 1994). In the eastern Pacific, the distribution is narrower and predominantly off the coasts of California and Mexico (roughly 20-35° N). Juveniles have been recorded along the Chilean, Oregon, and British Columbian coasts suggesting a potential range of 37° S-47° N, (Bayliff 1994). Archival tagging studies on immature pacific bluefin indicate a strong preference for surface waters with dives extending down to or below the thermocline (Itoh et al. 2003a, b, Kitagawa et al. 2006, 2007, Kitagawa et al. 2000, Kitagawa et al. 2002, Marcinek et al. 2001). However, Blank et al. (2004) demonstrated that Pacific bluefin are capable of tolerating very low temperatures so that larger individuals may exploit much deeper depths as they grow (Kitagawa et al. 2006). Such behaviour is also observed in Atlantic bluefin tuna (Block et al. 2001).

Migration of Pacific bluefin is described in Bayliff (1994). Spawning is restricted to the western central Pacific between the Philippines and Japan (April-June), southern Honshu (July) and the Sea of Japan (August) (Nishikawa et al. 1985, Yamanaka 1963). Larvae, post larvae and juveniles are transported northward within Kuroshio Current waters, then migrate southward in winter months. After the first year of life, juveniles either remain in the western Pacific while seasonally migrating north-south, or make transpacific migrations to eastern Pacific waters within the Kuroshio meander and the north Pacific current where they remain for 1-6 years. Immature individuals that remain in the western Pacific show a north-south movement. After reaching maturity, Pacific bluefin appear to remain within the western Pacific while migrating north to south.

Longevity is estimated to be >13 years (Hsu and Chen 2006). Age at 50% maturity is assumed around 150 cm or 5 years (Harada 1980). Growth parameters for the von Bertalanffy growth model are reasonably well defined though growth studies are limited. Asymptotic mean length is estimated between 320-325 cm and the curvature coefficient between 0.11-0.135 $year^{-1}$. Natural mortality is estimated to be 0.276 $year^{-1}$ for older individuals (Bayliff et al. 1991) and 1.6 $year^{-1}$ for age 0 individuals (Takeuchi and Takahashi 2006).

Fisheries

Pacific bluefin are mainly captured by Japanese fleets, using a variety of gears: purse seine, longline, baitboat, trolls, gillnet, and trap net. Purse seine is the dominant gear in both the western and eastern Pacific (Miyake et al. 2004). Pacific bluefin were likely caught in moderate quantities prior to 1950 particularly in the waters surrounding Japan (Matsuda and Ouchi 1984, Miyake 2004). Longline fisheries specifically targeting pacific bluefin only occur near the spawning grounds within the western Pacific, though non-targeted catch occurs throughout the Pacific in regions that are more temperate. Taiwanese and Korean catch of Pacific bluefin is relatively minor compared to Japan with a combined catch in the late 1990s of <5,000 tonnes. Japanese longline catch through the 1960s was significant with catches >5,000 tonnes. When compared to purse seine catches, longline catches in recent years are small. In general, purse seine vessels capture intermediate sized individuals, though substantial variation in length is observed depending on location, cohort strength, and time of year (Itoh 2006, Nakamura 1969). Juveniles are captured in the winter and adults in the summer. Japanese vessels account for a significant proportion of the total purse seine catch varying between 5,000-20,000 tonnes. Korean purse seines have operated since 1980. Within the Eastern Pacific, U.S. and Mexican purse seines catch <5,000 tonnes. Japanese baitboat, troll, trap, and gillnet fisheries account for around 10,000 tonnes though catches have been low through the 1990s (Miyake et al. 2004).

Atlantic bluefin tuna (*Thunnus thynnus*)

Biology

Atlantic bluefin are a highly migratory species found in tropical to sub-arctic epipelagic waters of the Atlantic Ocean. Eastern and western Atlantic stocks are assumed to exist with separate spawning grounds in the Mediterranean Sea and the Gulf of Mexico (Fromentin and Powers 2005, Mather et al. 1995) though mixing occurs in the North Atlantic (Block et al. 2005). Atlantic bluefin have a wide distribution though predominantly in the northern hemisphere. Information of migration and distribution are summarized in Fromentin (2005) and Mather (1995). In the eastern Atlantic, bluefin are distributed as far north as 70° N down to the equator and from 25° S-50°N in the west with a west-east distribution from the Gulf of Mexico to the

Black Sea. Spawning occurs in the Gulf of Mexico and Mediterranean Sea where surface waters are >24° C (Baglin 1982, Richards 1976). Spawning individuals appear to show site fidelity (Block et al. 2005). As with other bluefin species, Atlantic bluefin spend nighttime hours as well as a large proportion of daylight hours in surface waters (Block et al. 2001, Brill et al. 2002, Lutcavage et al. 2000, Wilson et al. 2005). However, dives into deep (500-1000 m) cold (<4° C) water for prolonged periods have been observed; depth and temperature limits appear to depend on body size (Block et al. 2001, Brill et al. 2002, Lutcavage et al. 2000). Diving behaviour is thought to be associated with foraging in the deep scattering layer. Western Atlantic bluefin are assumed to originate from spawning in the Gulf of Mexico where spawning occurs between April-June within the Gulf or the Straight of Florida (Baglin 1982). In the Gulf of Mexico, larval densities are highest below 200m between 23°-30° N and 84°-94° W. Spawning in the Straight of Florida appears to occur west of Bimini Island (Mather et al. 1995). Young of the year individuals appear to spread widely through the Strait of Florida into waters surrounding the Bahamas and Greater Antilles, moving northward along the eastern coast of the U.S. to nursery grounds between Cape Hatteras and Cape Cod. After the first year of life, individuals seasonally migrate during the spring-summer feeding period along the coast and within frontal structures of the Gulf Stream. The extent of this southwest to northeast migration depends on size. During winter months individuals move into offshore waters. Transatlantic migrations have been observed for individuals older than age 1, with tag recaptures occurring predominantly in the Bay of Biscay. After leaving, the Gulf of Mexico, post-spawning adults move either northward along the coast to feeding areas in the North Atlantic reaching as far as the coast of Norway, or move southward to areas off Brazil. Tagging data suggest substantial mixing of the eastern and western stocks in the north Atlantic (Block et al. 2001, Block et al. 2005). Eastern Atlantic bluefin spawn within the Mediterranean Sea from June to August (Richards 1976). Spawning is thought to occur in both the west (Balearic Islands, Malta Island and the Tyrrhenian Sea) (Corriero et al. 2003, Medina et al. 2002, Susca et al. 2001) and east (Ibero-Moroccan embayment and Black Sea) (Karakulak et al. 2004). Young of the year move towards the Atlantic coast of Morocco by age 1. As individuals emerge from the Mediterranean, migration is to the north within the Bay of Biscay, toward the north coast of Spain, or south along the Atlantic coast of Africa. During winter months, individuals appear to move offshore. Older individuals move northward as far as the northern coast of Norway or southward crossing the Atlantic to the

coast of Brazil. Substantial movement into the middle of the north Atlantic is also seen (Block et al. 2005). Such migratory patterns are generalizations as individuals of all sizes are found within the Mediterranean throughout the year.

Longevity is estimated to be > 25 years (Mather et al. 1995). Length at 50 % maturity for eastern Atlantic females is estimated at 103 cm or 3-5 years age (Cort 1991). Western Atlantic individuals appear to mature at older ages, 190-240 cm, or 8-12 years (ICCAT 1997). Growth parameters for the von Bertalanffy growth model are reasonably well defined though estimation of age for larger-sized individuals is problematic due to small sample size (Mather et al. 1995). Currently accepted values for asymptotic mean length are 318-325 cm with the curvature coefficient between 0.093-0.11 $year^{-1}$. Differences in sex specific growth have been noted (Caddy et al. 1976) as well as strong seasonal growth pattern (Mather et al. 1995). Natural mortality is estimated at 0.165 $year^{-1}$ for mature individuals in the eastern Atlantic and 0.14 $year^{-1}$ for the western stock (ICCAT 1997).

Fisheries

Atlantic bluefin, particularly eastern Atlantic bluefin, were caught at significant levels prior to 1950 (Mather et al. 1995, Miyake et al. 2004). Records of trap catches of bluefin within the Mediterranean Sea date back for centuries (Ravier and Fromentin 2001) with estimates of total catch varying from 7,000-30,000 tonnes with 15,000 tonnes caught on average (Ravier and Fromentin 2002). Longline, purse seine, trap nets, baitboat, gillnet, harpoon, hand line and recreational gear are used to catch Atlantic bluefin. Since the 1970s, removals using purse seines have dominated the catch. Japanese longliners began targeting bluefin off the coast of Brazil in the late 1950s with catches increasing rapidly to 12,000 tonnes by the mid 1960s. Catches declined in the late 1960s as the fleet expanded to the Gulf of Mexico, New England Coast, and the Bay of Biscay. Stringent quotas on western Atlantic catch pushed the fleet to the Mediterranean in the early to mid 1980s. Much of the fleet left the Mediterranean in the 1990s for new fishing grounds in the North Atlantic (Miyake et al. 2004). Since the mid 1970s, Japanese catch has fluctuated between 2,000-6,000 tonnes. Other longline operations in the Mediterranean are operated by France, Spain, or classified as IUU. Purse seining in the western Atlantic by U.S. vessels increased during the mid 1960s peaking over 5,000 tonnes. Catch

restrictions since the 1980s resulted in a lower biomass taken. The only other significant fisheries for bluefin in the western Atlantic are recreational and trap fisheries, and catches under the current quota system are small. Purse seining in the eastern Atlantic from 1930 to the mid 1960s was by Norwegian vessels with catches in the 1950s between 5,000-15,000 tonnes. Declining catches in the 1960s resulted in the fishery shifting to other resources in the early 1970s. France started purse seining in the Mediterranean in the late 1960s followed by Spain and Italy. Greece, Croatia, Algeria, and Turkey also joined the fishery. Catches in the Mediterranean peaked in the mid 1990s around 25,000 tonnes but declined into the late 1990s. An increasing proportion of the purse seine catch since the 1990s has been used for farming operations (Miyake et al. 2004). French and Spanish baitboats have operated in the Bay of Biscay since the 1930s with catches varying, but usually <5,000 tonnes. Trap fisheries in the Mediterranean had peak catches of 20,000 tonnes in the late 1950s declining to <5,000 tonnes by the early 1970s.

Blue marlin (*Makaira nigricans*)

Biology

Blue marlins occur in epipelagic tropical and sub-tropical oceanic waters of the Indian, Pacific, and Atlantic Oceans between 45° S-45° N. The 24° C isotherm is thought to delineate northern and southern range extents (Nakamura 1985). Blue marlins are solitary individuals with preference for open ocean waters. Tagging data from the Atlantic suggest blue marlin follow cyclical migration paths with spawning site fidelity (Ortiz et al. 2003). Migration patterns and spawning sites are not well determined for stocks in the Pacific or Indian oceans. Trans-oceanic migration and inter-oceanic migrations have been observed. Pepperell (2000b) notes that females appear to migrate further into subtropical waters than males in the Indian Ocean. The ability of females to tolerate colder temperatures is likely related to their larger size and potential thermal inertia. Tagging studies exploring habitat use indicate blue marlin spend a substantial proportion of time in surface waters >25 m making excursion to the top of the mixed layer with dive depth limited to 200-300 m depending on location (Block et al. 1992, Holland et al. 1990a, Saito and Yokawa 2006) though Goodyear (2006) noted dives up to 800 m. As with other billfish, blue marlin have evolved a ‘brain heater’ (Block 1986) which maintains brain and eye temperature above ambient temperature.

In the Indian Ocean, blue marlins are distributed north of 45° S in the west and north of 35° S in the east. Seasonal concentrations are found off Sri Lanka, the Maldives, and Laccadive Islands (December to August), around Mauritius (December to February), between 0-13° S off the east coast of Africa (April to October) and year round between Java and northwestern Australia with peak abundance from November to April (Nakamura 1985, Pepperell 2000b). Larval blue marlins have been observed around the Maldives, Mascalene Islands, Java, and Sumatra (Nakamura 1985).

In the Pacific Ocean, blue marlin distribution extends from 35° S-45° N in the west and 25° S-35° N in the east though abundance declines along a west to east cline (Nakamura 1985). Within the western and central Pacific, concentrations have been observed between 8-26° S from December to March, between 2°-24° N from May to October and 10° S-10° N from April to November (Nakamura 1985). Larvae have been collected in both tropical and subtropical waters of the western and central Pacific suggesting year-round spawning in equatorial waters and seasonal spawning in more subtropical waters (Nakamura 1985). Tagging data from the Pacific indicate trans-oceanic migrations though no apparent cyclical migration patterns (Ortiz et al. 2003).

Atlantic blue marlins are distributed from 40° S-45° N in the western ocean and 30° S- 45° N in the east. Nakamura (1985) notes two seasonal concentrations of blue marlin in the western Atlantic, from January to April between 5-30° S and from June to October between 10-35° N. Spawning has been observed from January to February at 17-23° S and 37-42° W (Amorim et al. 1998). Martins (2007) observed spawning between 20° S-7° N west of 15° W from June to August. Spawning around the Bahamas occurs in Exuma Sound around July (Serafy et al. 2003). In the eastern Atlantic where blue marlin abundance is lower, areas of higher abundance are off the African coast between 25° S-25° N (Nakamura 1985). In the western North Atlantic, significant movement occurs between the US mid-Atlantic coast and the Gulf of Mexico to Venezuelan waters, hinting at a cyclical migration between these two areas for feeding and spawning (Ortiz et al. 2003). Trans-Atlantic movements have been observed in a small fraction of recaptures as well as movement from the Atlantic Ocean into the Indian Ocean (Ortiz et al. 2003).

Life history information on mortality, growth, and maturity of blue marlin is sparse. Longevity for Pacific blue marlin in waters around Hawaii has been estimated at 27 years for females and 18 years for males (Hill et al. 1989). Blue marlin growth over the first year of life can be considerable, with individuals reaching >100 cm (Prince et al. 1991). Blue marlins are sexually dimorphic with females reaching larger body size than males. Pepperell (2000b) notes that males rarely exceed 180kg (~300cm) while females have been caught >800 kg (>400 cm). Skillman (1976) estimated asymptotic mean length in males between 368-370 cm and 626-660 cm for females with a curvature coefficients between 0.285-0.315 $year^{-1}$ and 0.116-0.123 $year^{-1}$ respectively. Age at 50 % maturity is poorly determined. Nakamura (1985) suggested males first mature at 130-140 cm (lower jaw fork length LJFL) and females >200 cm. Pepperell (2000b) indicates weight at first maturity for males around Hawaii was 31 kg (~170 cm) for males and 80 kg (~230 cm) for females, whereas Arocha (2006) observed female Atlantic blue marlin size at 50% mature around ~250 cm. These observations suggest males mature at age 2-3 years while females mature at age 4-5 years. Estimates of instantaneous natural mortality based on growth rates are higher for males. Boggs (1989) estimated male natural mortality at 0.53 $year^{-1}$, female natural mortality at 0.21 $year^{-1}$. Hinton (2001) estimated male mortality between 0.38-0.41 $year^{-1}$ and female between 0.18-0.19 $year^{-1}$ using meta-analysis in Pauly (1980) and growth equations derived by Skillman (1976).

Fisheries

Blue marlins are primarily caught on longlines as by-catch in tuna fisheries though catch is taken in gillnet, harpoon, purse seine, and recreational rod-and-reel fisheries. Longliners targeting blue marlins generally use modified tuna gear to fish shallow (Nakamura 1985). Prior to 1970, Japanese longline removals dominated blue marlin catch in the Indian Ocean with peak catches in the mid 1950s around ~5,000 tonnes declining after the early 1970s and varying around 200-1,000 tonnes. As Japanese catch declined in the 1970s, Taiwanese catch increased and has varied between 1,000-4,000 tonnes. Catches in the Indian gillnet fishery increased in the early 1970s and accounts for a significant proportion of the gillnet catch from the Indian Ocean. By the late 1990s, reported catches varied between 1,000-2,500 tonnes. Total reported catch for the late 1990s fluctuated between 6,000-10,000 tonnes. Japanese catch of Pacific blue marlin peaked in

the early 1960s at >25,000 tonnes but declined through the 1970s and has remained stable around 10,000-15,000 tonnes. Since the mid 1950s, Taiwanese catches increased to 5,000-10,000 tonnes. In the 1990s, Indonesia, the Philippines, Korea, and the U.S. also report blue marlin catch though total reported catch is a small fraction of the Japanese and Taiwanese catch. Harpoon fisheries do not necessarily target blue marlin but incidental catch does occur in fisheries off southern Japan and Taiwan. Total reported catch of Pacific blue marlin was >20,000 tonnes through the 1990s. In the Atlantic Ocean, Japanese catch of blue marlin peaked in the early 1960s at <9,000 tonnes, declining rapidly to 2,000 tonnes by the late 1960s, and <100 tonnes by the early 1980s. Japanese catches through the 1990s fluctuated around 1,000 tonnes. Since the late 1960s, Chinese Taipei, U.S., Korean, Venezuela, Cuba, Brazil, and, since 1990, Ghana have contributed to total catches. Recreational rod-and-reel catch is significant, accounting for a large proportion of catch designated as 'other' in fisheries statistics. Total catch in the 1990s varied between 2,500-4,000 tonnes.

Striped marlin (*Tetrapturus audax*)

Biology

Striped marlins occur in tropical to temperate epipelagic waters of the Indian and Pacific Oceans. Distribution is generally restricted to tropical and subtropical waters though striped marlins appear to tolerate cooler water than other marlins, particularly in the Pacific, resulting in an observed distribution between 45° S-45° N (Nakamura 1985). Striped marlins also possess a heat-producing tissue beneath the brain and adjacent to the eyes allowing blood temperature within these areas to remain above ambient. As with other marlins, striped marlin vertical distribution is generally restricted to depth above the thermocline, with a substantial proportion of time in depths <90 m (Brill et al. 1993, Domeier et al. 2003). Dives below the thermocline, to depth <200 m have been observed though dive duration is short. Ortiz's (2003) summary of conventional tagging data indicates that striped marlin are capable of long distance migrations and potential trans-oceanic movement. Tagging in Australian waters indicates some site fidelity or cyclical migration paths.

In the Indian Ocean, striped marlin are found north of 45° S in western waters and north of 35° S in the east. Concentrations are found off the coast of Africa (0-10° S), south and west in the Arabian Sea, the Bay of Bengal, and waters northwest of Australia (Merrett 1971, Nakamura 1985, Pillai and Ueyanagi 1978). Spawning likely occurs in waters west of Madagascar between 6° S-6° N from December to January (Pillai and Ueyanagi 1978) and to the southeast from 20-25° S and 55-60° E (Nishikawa et al. 1978). Spawning potentially occurs in the Bay of Bengal from March to May given the presence of mature females (Nakamura 1985). In the eastern Indian Ocean, spawning occurs from January to February in the Timor and Banda seas (Ueyanagi and Wares 1975) and from July to December in waters (10-18° S and 110-125° E) to the northwest of Australia (Pillai and Ueyanagi 1978). In the western and eastern ocean, seasonal north and south range expansion is observed (Ueyanagi and Wares 1975). Individuals appear to move northward to warmer waters during the Austral summer into waters off southeastern Africa. Northward movement in spring may occur in the western Arabian Sea (Ueyanagi and Wares 1975). In the western ocean, individuals appear to move from waters northwest of Australia in late summer, to the Bay of Bengal.

Pacific striped marlins are distributed 45° S-45° N in the western ocean and 30° S-45° N in the east (Nakamura 1985). Distribution is not uniform as catch rates in western equatorial waters are low and indicate a U-shape distribution with the bottom of the U along the Central American coast (Nakamura 1985). Genetic analyses indicate potential stock structure within the Pacific with significant heterogeneity between northwestern, north-central, eastern, and southwestern individuals (Graves and Mcdowell 1994, 2003). The highest densities of striped marlin occur in the central eastern Pacific in waters off Baja California (Nakamura 1985, Squire 1974). Spawning occurs in the summer and autumn near the mouth of the Gulf of California (Armas et al. 1999) and in waters to the southwest (Eldridge and Wares 1974). Movement north and south is observed from tagging data suggesting seasonal shifts in density with long distance movement to the southeast (Domeier 2006, Ortiz et al. 2003). Westward unidirectional migration into Hawaiian waters from Baja California has also been observed (Ortiz et al. 2003). Hyde (2006) confirmed spawning within Hawaiian waters during May which is contrary to the previously held notion that striped marlin use Hawaiian waters only as a feeding ground (Squire and Suzuki 1990). Spawning in the north western Pacific is observed to occur from May to June west of 180°

W between 10-30° N (Nakamura 1985). Squire (1990) suggests a northerly movement of striped marlin in the northwest Pacific during the summer month, with fish returning south in the winter to areas in the East China Sea and South China Sea. In the southwestern Pacific, tagging data suggest cyclical migration (Ortiz et al. 2003). Spawning is thought to occur in the Coral Sea 15-25° S during the Austral summer (November and December) (Hanamoto 1978). After the spawning season individuals move south and southeastward down the coast of Australia to the Tasman Sea. Tagging data indicate northeastward movement to waters off Fiji and the Marquesas Islands (Ortiz et al. 2003). Aggregations are observed in September to October around underwater ranges of Lord Howe Rise and Norfolk Ridge (Squire and Suzuki 1990).

Life history information on mortality, growth, and maturity is sparse for this species. Striped marlins are thought to live for at least 10–12 years (Kopf et al. 2005, Melo-Barrera et al. 2003). As with other billfish, growth in the first year can be considerable with individuals reaching 45% of asymptotic length by age 1 (~100 cm) (Melo-Barrera et al. 2003). In the few studies examining size-at-age, growth parameters vary considerably depending on the method and size range sampled. Unlike swordfish, blue marlin, and black marlin, large sexual dimorphic differences are not seen in striped marlin though females tend to be heavier (Kopf et al. 2005, Melo-Barrera et al. 2003). Skillman (1976) estimated asymptotic length (measured as total length) for males at 277 cm and 251 cm for females with corresponding curvature parameters of 0.417 $year^{-1}$ and 0.696 $year^{-1}$ for striped marlin in Hawaiian waters. Skillman's asymptotic mean length estimates are similar to those of Melo-Barrera (2003), but Kopf (2005) estimated maximum mean length at 301 cm. Both the Melo-Barrera and Kopf estimates for the von Bertalanffy curvature parameter are considerably lower (0.23 $year^{-1}$ and 0.22 $year^{-1}$). Discrepancy in growth rate is likely due to Skillman using modal progression in length frequencies. Age at 50% maturity is poorly determined for striped marlin. Nakamura (1985) notes that size at first maturity occurs around 140-160 cm in the western Pacific. Skillman and Kopf suggest maturity occurs around 2-4 years. Boggs (1989) and Hinton (2002) estimated natural mortality rates for males (0.569 $year^{-1}$-0.79 $year^{-1}$) and females (0.818 $year^{-1}$-1.33 $year^{-1}$) using growth curves from Skillman. Natural mortality rates were also estimated at 0.369 $year^{-1}$-0.49 $year^{-1}$ from other growth data (Boggs 1989, Hinton and Bayliff 2002).

Fisheries

Striped marlins are harvested commercially in both the Indian and Pacific oceans. Catch is taken primarily as by-catch by longlines in tuna fisheries, and by some directed longline fisheries. Additional catch is taken in harpoon fisheries off Taiwan and Japanese gillnet fisheries, or as incidental catch in purse seines. Recreational catch of striped marlin is small compared to the commercial but is economically important in local areas (Bromhead et al. 2004, Holdsworth et al. 2003, Ortega-Garcia et al. 2003, Whitelaw 2003).

The reported catch in the Indian Ocean prior to 1970 was mainly taken by Japanese longline vessels. Japanese catch increased steadily from 1952, reaching ~4000 tonnes by 1967, but declined to ~500 tonnes by 1973. In the late 1970s and 1980s, catches ranged from 500-1,500 tonnes, remaining below 1,000 tonnes since. The Taiwanese reported catch began in 1954, but did not increase significantly until the late 1970s reaching >4,000 tonnes. Since the 1980s, catch has varied from < 1,000 tonnes to > 4,000 tonnes. Korea, Sri Lanka, and Indonesia also participated in the fishery early in the 1970s. Total catches of striped marlin peaked in the early 1990s and have declined since.

Total estimated catch from the Pacific Ocean peaked in the mid 1960s at >28,000 tonnes, primarily from Japanese vessels. By the mid 1970s, catches declined to ~10,000 tonnes and have since fluctuated between 6,000-13,000 tonnes. Catches from the Western Pacific account for around 67 % of the total reported catch. A significant proportion of catch in the eastern Pacific are from waters southwest of Baja California and the mouth of the Gulf of California (ISC 2006). Catch rates within this area have been 20 times higher than in other Pacific areas. Significant changes in fishery regulations by the Mexican government to control removals from this area have occurred over time. Squire and Muhlia-Melo (1993) note that prior to 1967 longlines were not permitted within 9 nautical miles of the Mexican coast, though Japanese operations were permitted in the 9-12 nautical miles zone. This zone was extended in 1983 to 50 nautical miles and in 1987 to encompassing waters southwest of Baja California, the Gulf of California mouth, and Tehuantepec Bight. Although Japanese catches are a large proportion of total reported catch, Taiwanese, Korean, Mexican and Costa Rican operations contribute to overall catches.

Atlantic white marlin (*Tetrapturus albidus*)

Biology

White marlins occur in tropical to temperate epipelagic waters of the Atlantic Ocean. Distribution is roughly delimited by the 22° C isotherm resulting in an observed geographic range of 45° S-45° N in the western ocean and 35° S-45° N is the east (Nakamura 1985). Genetic analysis does not suggest heterogeneity between locations, indicating white marlins comprise a single stock (Graves and McDowell 2003). Spawning is mainly in tropical waters of the western Atlantic during spring and summer in the respective hemispheres. In the northern Atlantic, spawning is observed in the Gulf of Mexico, Straits of Florida, and northeast of Hispaniola and Puerto Rico (Arocha and Marcano 2006, Baglin 1979). Between 5° S-5° N, spawning is observed between May and June (Oliveira et al. 2007) and from November to March at 18-26° S and 40-46° W (Amorim et al. 1998). Conventional tag recoveries of predominantly north Atlantic individuals suggest site fidelity and seasonal cyclic migrations with maximum displacement half way through the year around 3,000 nautical miles (Ortiz et al. 2003). Maximum displacement distances agree with average daily displacement (7.8-14.2 nautical miles) measured from archival tags (Horodysky et al. 2005). Trans-oceanic movements for a few individuals have also been observed. Archival tagging indicates a strong preference for surface waters with individuals spending a large proportion of time at depths <25 m (Horodysky et al. 2004, Prince et al. 2005). Daytime dives, presumably for foraging, have been observed to depth >300 m, though most are observed around 100-200 m. Prince (2006) suggest the minimal oxygen concentration for white marlin is ~4.6 mg l^{-1}.

Longevity is estimated to be >15 years (Ortiz et al. 2003). No growth model has been developed for white marlin. Maximum total length is estimated at 280 cm with males reaching smaller asymptotic size than females (Nakamura 1985). Recent studies (Arocha and Marcano 2006, Oliveira et al. 2007) suggest length at 50% maturity of around 140 cm for males and 150-190 cm for females. If white marlin growth were similar to that of other marlin, such sizes would suggest age at 50% maturity of around 2-4 years. Longevity would suggest natural mortality is low for

older ages. Mather (1972) estimated instantaneous natural mortality at 0.32 $year^{-1}$ based on tagging studies.

Fisheries

Although white marlins are captured as targeted or incidental catch in longlines, there are also important gillnet and recreational fisheries. Japanese catch after 1956 increased rapidly peaking at > 4,500 tonnes by 1965, and declining to around 1,000 tonnes by the late 1960s and early 1970s. Catches declined as a greater number of Japanese vessels switched to targeting bigeye and bluefin, reaching less than 100 tonnes by the late 1990s. Taiwanese and Korean catches increased in the early 1960s with Korean catches peaking at <600 tonnes in the early 1970s and declining after. Taiwanese catch has varied over time between 200-1,350 tonnes. Cuba, Venezuela, and Brazil also operate longline fleets that take white marlin as by-catch. Total longline catches since the early 1970s have varied between 1,000-2,000 tonnes.

Black marlin (*Makaira indica*)

Biology

Black marlins are primarily distributed (45° S-40° N) in epipelagic tropical and sub-tropical waters of the Pacific and Indian oceans though some fish have been observed in Atlantic waters off the west coast of Africa (Nakamura 1985). Black marlins demonstrate a greater propensity to school and associate with landmasses and continental shelf areas than do blue or striped marlin (Pepperell 2000a). Black marlins are found in water temperatures of 15-30° C though their distribution is scattered in areas that are more temperate. Spawning is associated with temperatures ~27-28° C. From limited tagging data, vertical distribution and movement appears restricted to the mixed layer (<100 m) with infrequent excursions to deeper depths (~200 m) (Gunn et al. 2003). Ortiz's (2003) summary of conventional tagging data suggests site fidelity and cyclical migrations patters for individuals tagged off eastern Australia, with displacements midway through the year of between 400-3,000 nautical miles. Trans-oceanic movements from eastern Australia to eastern Pacific waters and Hawaii as well as movements into the Indian Ocean have been observed.

Stock structure in the Indian Ocean is not known, but concentrations of black marlin are observed in waters to the northwest of Australia and the Timor Sea (November to March), south of Java (May to September) with both areas assumed to support spawning (Pepperell 2000a). Black marlin abundance peaks in Mauritian waters around November with concentrations also occurring off eastern South Africa, the southwestern Arabian Sea, and the Bay of Bengal (Campbell and Tuck 1998). Black marlin are found throughout the Indian Ocean north of 45° S but catches are highest north of 15° S. It is likely, as with blue marlin, that spawning occurs in waters off Mauritius and the Maldives.

In the Pacific, the black marlin range has been estimated to be 45° S-40° N in the west and 35° S-35° N in the east (Nakamura 1985). Areas of concentration within the northwest, southwest, and eastern ocean are apparent though it is not clear if these represent separate stocks (Pepperell 2000a). Spawning is known to occur in the northwest Coral Sea (October to December) with individuals moving southward along the eastern Australian coast (December to April) and offshore after April before returning to spawn the following summer (Ortiz et al. 2003). Spawning occurs January to April in the Banda Sea, May to June near Hainan Island in the South China Sea, and August to October off Taiwan (Nakamura 1985). Black marlin are thought to move north during the spring and summer in the Sea of Japan and East China Sea returning south during the autumn and winter.

Life history information on mortality, growth, and maturity is very sparse for black marlin. Longevity has been estimated to be up to 30 years for females, and is likely lower for males (Pepperell 2000a). As with other billfish, growth in the first year can be considerable with individuals reaching > 80cm by age 1 (Speare 2003). Growth curve parameters have not been estimated for black marlin due to difficulties in ageing older individuals. Growth appears similar to that of blue marlin given length-at-age estimates for individuals up to age 6 (Speare 2003). Maximum size is observed to be >400 cm (Nakamura 1985) though the majority of individuals >170 kg (~250 cm) are female (Pepperell 2000a). As with other marlins, there is sexual dimorphism, and males may reach maturity earlier than females and have higher mortality rates (Pepperell 2000a). Size at 50% maturity has not been established though Pepperell (2000a) notes first maturity is potentially 2-3 years in males and 3-4 years for females. Nakamura (1985)

indicates the majority of longline caught individuals are between 170-210 cm. Assuming the majority of catches were taken in spawning areas estimate of length-at-age would suggest maturity at ~4 years (Speare 2003). No mortality estimate is available for black marlin; however, given the similarity to blue marlin and apparent longevity, mortality is likely to be low for older individuals.

Fisheries

Black marlins are principally captured as targeted or incidental catch in longline fisheries, and are targeted in important harpoon, troll, gillnet, and recreational fisheries. In the Indian Ocean, Japanese longline catches increased to 1,000-1,500 tonnes in the late 1950s and 1960s. As vessels switched to targeting more temperate species through the 1970s (Miyake 2004) catches declined to 200-800 tonnes through the 1980s and was only 80-200 tonnes in the 1990s. Taiwanese catch has been relatively stable over time at 400-1,100 tonnes. Korean vessels reported some catch in the mid 1970s to 1980s but catches since have been small. Sri Lankan and Indian catches using a variety of gears have become a large fraction of total black marlin catch removals. In the late 1990s, catches varied from 500-900 tonnes and 200-900 tonnes respectively. Reported catch of black marlin peaked in the late 1960s at slightly greater than 2,000 tonnes, and varied around 2,000 tonnes through the 1990s.

It is difficult to partition black marlin catches in the Pacific by nation, given reporting problems and lack of stock assessment. It is reasonable to assume that early in the 1950s the majority of black marlin catch resulted of Japanese fleet expansion, although Korean and Taiwanese longliners were quick to follow. Peak catches of over 4,000 tonnes were reported in the early 1970s. However, catches declined in 1980s and 1990s fluctuating around 2000 tonnes. Incidental catch in purse seine fisheries was estimated to be 200-400 tonnes (SPC-OFP 2006b). Both Taiwan and Japan operate harpoon and gillnet fisheries in the western Pacific and account for 200-500 tonnes.

Swordfish (*Xiphias gladius*)

Biology

Of the billfish, swordfish tolerate the broadest range of temperatures, resulting in a wide distribution in all oceans between 50° S-60° N. Range extent is approximately delimited by surface waters >13° C though individuals are observed where surface waters are as low as 5° C. Apparent preferred temperatures are 18-22° C (Nakamura 1985). Spawning occurs year-round in surface waters >24° C (Nakamura 1985). In general, swordfish feed in temperate waters during the summer and migrate towards warmer waters during the autumn for spawning and over wintering (Nakamura 1985, Takahashi et al. 2003). Although swordfish are capable of long-range migrations, they appear to show fidelity to particular locations (Takahashi et al. 2003). Unlike tuna, swordfish are unable to maintain elevated body temperature. They do however possess a 'brain heater' (Carey 1982) that allows blood flowing to the eyes and brain to be maintained at temperatures above ambient. As a result, swordfish are able to exploit depths of 1000 m where temperature is below 5° C (Carey and Robison 1981, Takahashi et al. 2003). Swordfish appear to follow the deep scattering layer, residing in surface waters during the night and swimming at depth (>200 m) during the day (Carey and Robison 1981, Dagorn et al. 2000, Takahashi et al. 2003). Swordfish are also seen 'basking' in surface waters during the day, likely to recover thermal losses.

Swordfish in the Indian Ocean are distributed north of 45° S. Spawning appears to occur in two main areas. In the eastern ocean, spawning occurs in equatorial waters east of 80° E, southwest of Java and around northwestern Australia (Nishikawa and Ueyanagi 1974). In the western ocean, spawning occurs from October to April in waters around Madagascar (Poisson et al. 2001). Migration patterns of swordfish in the Indian Ocean are not known.

In the Pacific Ocean, swordfish appear distributed between 45° S-50° N in the west and 35° S-50° N in the east. There is some indication that swordfish are not a homogeneous population given apparent spawning site fidelity. Based on mtDNA analysis, Reeb (2000) suggests that there are northwestern, southwestern and eastern stocks in a horseshoe shape much like striped marlin.

Spawning in the northwest occurs within the Kuroshio Current area from March to July and within the East Australian Current area from September to December (Nakamura 1985). Hinton et al. (1997), estimated spawning to occur in the eastern Pacific from May to August in the north, year-round in equatorial waters and from October to March in southern waters. There is some debate as to a north-south split in the eastern Pacific (Sakagawa and Bell 1980).

Atlantic swordfish are distributed between 45° S-50° N in the west and 50° S-60° N in the east. Three separate stocks are believed to exist: northern, southern and Mediterranean (Bremer et al. 2005, Greig et al. 1999). Northern individuals are observed to spawn within the northern Caribbean Sea, Strait of Florida, and the southern Sargasso Sea from December to March, moving northward to feed off Georges Banks during the summer (Greig et al. 1999). Southern swordfish spawn off Brazil and Uruguay west of 10° W between 5°S-5° N and from 20-40° W between 15-35° S, likely moving to the Gulf of Guinea to feed (Arocha and Lee 1995). In the Mediterranean, spawning occurs mainly in spring to summer, peaking in June and July around the Balearic Islands, southern and central Tyrrhenian Sea, Ionian Sea, and the Strait of Messina (ICCAT 2004b).

Longevity is estimated to be 25 years though males reach asymptotic mean length by around age 9 and females by around age 15 (Wilson and Dean 1983). Swordfish are sexually dimorphic with females reaching larger sizes. Age at 50% maturity is estimated to occur at 117-130 cm or ~2 years age for males and 160-175 cm or ~5-6 years age for females. Maturity is observed to occur at younger ages in the Mediterranean Sea (~3.5 years for females). Growth rate slows considerably after age 1 but during this time swordfish can reach 90 cm (Ehrhardt 1992). Growth parameter estimates are highly variable depending on method and location. Estimates of the von Bertalanffy curvature coefficient for females/males range from 0.026-0.21 $year^{-1}$/0.1-0.24 $year^{-1}$. Asymptotic mean length is estimated between 240-365 cm/190-250 cm for females and males respectively. Males are observed to grow faster and reach smaller asymptotic sizes than females in all regional studies, with the highest growth rates estimated for Mediterranean individuals. Natural mortality is poorly determined, but assumed low for larger sized individuals, varying between 0.2-0.4 $year^{-1}$.

Fisheries

Swordfish are targeted in all oceans using primarily longline gear, followed by gillnets and harpoon. Reported longline catch of swordfish is either as by-catch in tuna directed fisheries or as the result of targeted fisheries. Longliners targeting swordfish increased after 1970 when the U.S. (Miyake 2004) lifted mercury-content restrictions. Unlike tuna longline operations, gear is set shallow at night and light sticks are utilized to attract swordfish (Miyake 2004). Some fleets target swordfish using conventional tuna longline gear, but set lines at night and add floats so that hooks fish shallower. Summaries of swordfish catches presented below for the Indian, Atlantic, and Mediterranean Sea are taken from Miyake et al. (2004). A synthesis of catch data was not available for swordfish in the Pacific Ocean. Summary information for the Pacific was compiled from nominal catch statistics of the Inter-American Tropical Tuna Commission (ICCAT Database 2006) and the Secretariat of the Pacific Community Oceanic Fisheries Programme (SPC-OFP Database 2006).

In the Indian Ocean, Japanese catch of swordfish was minor, varying around 1-2,000 tonnes. Taiwanese vessels began harvesting in the 1960s but catch remained low until the 1980s. Taiwanese catch increased rising dramatically in the 1990s to >15,000 tonnes. A number of other nations, particularly in the 1990s, operated small longline operation with catches around 1,000-2,000 tonnes. Total longline catch in the late 1990s exceeded 30,000 tonnes. The only other significant swordfish fishery within the Indian Ocean is the Sri Lankan gillnet fishery that began reporting catches in 1985. Total catch from this fishery fluctuated between 2,000-4,000 tonnes annually in the 1990s.

In the Pacific Ocean, Japanese catch increased to ~20,000 tonnes in the early 1960s primarily from operations in the North Pacific, but declined and has remained around 8,000 tonnes. Taiwan, U.S., Spain, Chile, Australia, and New Zealand are responsible for the majority of the other longline catches reported. Through the 1970s and 1980s, catches varied between 10,000-15,000 tonnes. By the mid 1980s, catches increased, with a noticeable increase again in the 1990s. Increased catches in the 1990s were likely due to an influx of vessels (Spanish and U.S.)

from the Atlantic Ocean (Miyake et al. 2004) as well as the expansion of Central and South American fleets.

Swordfish catch in the Atlantic Ocean is predominantly due to longline operations though gillnet catches in the Mediterranean Sea are likely on par with longline catches. Prior to 1960 harpoon harvest by Canadian fishers dominated the catch, but the fishery never recovered after a ban on swordfish due to mercury contamination was lifted in the late 1970s (Miyake et al. 2004). Spanish and U.S. longline fleets account for a high proportion of the swordfish caught in the northern Atlantic. Catches are also taken by Canada, Japan, and Portugal. Total catch in the north Atlantic increased to ~20,000 tonnes by the late 1980s, but declined to ~10,000 tonnes due to catch restrictions. Catch in the southern Atlantic is taken predominantly by Spain, Japan, Brazil, and Taiwan. Total reported catch in the 1990s had increased to 15,000-20,000 tonnes. Catches from the Mediterranean were ~15,000 tonnes in the late 1990s, taken mainly using longline, gillnet, and harpoon gears. Italy, Spain, Greece, and Morocco account for the majority of the catches although catch statistics are considered poor (Miyake et al. 2004).

Catch and effort data

Development of a global spatial catch and effort database for major tuna and billfish stocks of sizes vulnerable to longline gear required synthesizing public domain catch and effort data from various Regional Fisheries Management Organizations (RFMOs) and the Japanese Fisheries Agency. Four data sets spanning 1950-2002 were developed: Japanese longline monthly 5°x5° catch and effort, monthly 5°x5° catch for longline operations of all other countries combined, monthly 5°x5° catch for all other gears and all other nations (including Japan) combined, and yearly nominal catch for all gears and all countries combined. For all data sets, the number of individuals caught of size vulnerable to longlines was estimated, and effort was measured in hook lifts. This section presents a description of the methods and assumptions required to create each data.

Stocks were defined as all individuals within an ocean basin with no distinction made between the Atlantic Ocean and Mediterranean Sea. Exceptions were made for Pacific and Atlantic

albacore tuna, which were split in to northern and southern stocks. Black marlin and southern bluefin tuna were considered as single stocks though their distributions span multiple basins. In all cases, data available from RFMOs and the Japanese Fishery Agency were assumed to reflect the true catches from each country. In a number of instances, this is known not to be accurate (Tsuji 2007).

Japanese 5°x5° monthly longline catch and effort data

Japanese longline monthly 5°x5° catch (in numbers) and effort (in hooks) data from 1950-2002 for the major tuna and billfish species vulnerable to longline gear in the Pacific Ocean was obtained from the Secretariat of the Pacific Community Oceanic Fisheries Program (SPC-OFP) under permission from the Japanese Fisheries Agency. Similar data for the Indian and Atlantic oceans (including the Mediterranean Sea) was acquired using task II (spatial catch, effort, and size) public domain datasets available from the Indian Ocean Tuna Commission (IOTC, IOTC Database 2006) and the International Commission for the Conservation of Atlantic Tuna (ICCAT, ICCAT Database 2006). Combining all datasets produced a global Japanese longline spatial dataset. Spatial overlap in the ICCAT and IOTC datasets occurred from 20-30°E, and for this area, values from the IOTC database were used. Although each dataset contained catch and effort information for southern bluefin tuna, records were compared to the public domain data available from the Commission for the Conservation of Southern Bluefin Tuna (CCSBT, CCSBT Database 2004). The CCSBT database was assumed correct when discrepancy in either the catch or effort was found. Average catch by decade at a scale of 5°x5° for the Japanese longline by species is presented in Figure 8.2 to Figure 8.21 in the Appendix to Chapter 2.

5°x5° monthly longline catch for all other countries

Total longline catches by other countries from the Pacific Ocean for all species except southern and northern Pacific bluefin were estimated from monthly 5°x5° catch (in numbers) public domain data from the SPC-OFP (SPC-OFP Database 2006). The difference between SPC-OFP spatial records by species and the Japanese Pacific Ocean catches was assumed to represent total longline catches by all other countries combined.

Southern bluefin tuna catch (in numbers) by other countries was included from the CCSBT public domain spatial data, which has been expanded to reported nominal catch (the total reported biomass of a species harvested in a year) by the commission. Estimating catch (in numbers) of North Pacific bluefin required some assumptions. Although SPC-OFP data has separate catch records for each species, some reporting countries did not distinguish Pacific bluefin from southern bluefin. To obtain an estimate of Pacific bluefin catch by other countries it was necessary to combine SPC-OFP records for the two species. Removing Japanese catch of both species and CCSBT spatial catch of southern bluefin by countries other than Japan resulted in catches assumed to reflect total northern bluefin catches of all other countries combined. Although no validation of this method could be performed, the ratio of southern bluefin to Pacific bluefin in other nations' data was similar to that observed in the Japanese longline data. SPC-OFP data cover longline operations throughout the Pacific Ocean for all countries except those in South American (primarily Mexico). Monthly 5°x5° catch (in numbers) public domain data obtained from the Inter American Tropical Tuna Commission (IATTC, IATTC Database 2006) were used to fill in catch records for these countries. No information was available to include estimates of longline catches classified as Not Elsewhere Included (NEI) or Illegal, Unregulated, and Unreported (IUU), or discards. The SPC-OFP also caution that estimates of numbers caught for some fleets may be problematic due to conversion using mean weight from other fleets.

Spatial catch records for longline operations by all other countries within the Atlantic Ocean available from ICCAT are not comprehensive, and spatial catch records represent a variable proportion of total nominal catch reported by each member country (Figure 2.8 as well as Table 8.1 in the Appendix to Chapter 2). Longline catches classified as NEI, IUU, and discards were not included. A procedure to allocate reported nominal catch by species, for each country to 5°x5° areas and to convert biomass catch to numbers was developed. All spatial records were assigned to a 5°x5° cell, requiring records reported at 1°x1° to be aggregated to 5°x5°. Records reported at larger scales were distributed to 5°x5° cells in proportion to the spatially reported catch of all countries combined within the areas for the year and month of the record. The resulting 5°x5° country-specific records for each species were used to estimate proportions of the catch by area and month, which were then used to allocate nominal catch of each country. In

years where nominal catch was reported prior to spatial records being available, area-month proportions estimated from the first available spatial records were used. The previous year's area-month proportions were used to allocate catch for years missing spatial records after the first year of reporting. Nominal harvests for countries without spatial records were allocated in proportion to the catch reported by all countries for the given year by area and month.

Country-specific records of length or weight frequency (from ICCAT Task II size data) by species were used to estimate mean weight of catch, and convert biomass to numbers for catch records from corresponding time-area strata. Size data reported for areas larger than 5°x5° were assumed representative for all 5°x5° cells within the area. Lengths were converted to weight using coefficients presented in Table 2.1. If country-specific size data were not available for a time area combination, numbers were estimated using a weighted average of mean weight estimated for each country that did report size information. If mean weights were not available for a time-area strata, mean weight (see Figure 8.1) for a given year was used, calculated as a spatially weighted average with each 5°x5° record weighted by cell area.

A similar procedure was followed to estimate spatial catch records for longline operations by all other countries within the Indian Ocean. As in the Atlantic, spatial catch records were not comprehensive (see Figure 2.8 and Table 8.2) and a portion of nominal catch for most reporting countries had to be distributed spatially. Longline catches classified as NEI, IUU, and discards were not included. Biomass was converted to numbers using a similar procedure to that outlined for the Atlantic. However, spatial size composition data available from the IOTC was sparse. In many instances, weight averaged over all strata (see Figure 8.1) was used to convert biomass to numbers.

The catch allocation procedure above relies on a number of key assumptions that likely introduce bias in the overall catch distribution. These biases may affect the spatial analysis presented in later chapters. Assuming spatially reported catches are representative of a country's catch distribution could be problematic if large catches from specific areas have been misallocated. Misallocations may be large for countries reporting a small proportion of nominal catch spatially. For those countries without spatial records, the allocation procedure is obviously erroneous,

particularly if catches came from local waters. In many instances, reported harvests by these countries was small in comparison to the larger fleets (Miyake et al. 2004) and contribute little to removals in a 5°x5° cell when assumed to have been broadly dispersed. If catches were removed from local waters, impacts may be underestimated. Substantial differences in the size of individuals captured by longlines, not represented in the size data used to convert biomass to numbers, will have resulted in biased estimates of the number of individuals.

The 5°x5° average catch by decade for non-Japanese longline fleets by species is presented in Figure 8.2 to Figure 8.21 in the Appendix to Chapter 2.

5°x5° monthly catch by other gears all countries combined

Developing the 5°x5° dataset of combined catch for all countries by all other gears required multiple approaches depending on available data. The other gear classification included purse seine, baitboat, troll, gillnet, harpoon, rod and reel, and other artisanal gear. In all cases, each species-gear combination required an estimate of mean weight in the catch, to convert biomass to numbers, and the proportion of the catch vulnerable to longline gear. Estimating the number of individuals captured of a size vulnerable to longline gear required use of a threshold size criterion. For each species-ocean combination, this threshold was set as the 10^{th} percentile of a cumulative length frequency distribution of longline catches averaged across all countries reporting size data. The proportion of catch greater than this threshold for each gear type was considered part of the longline vulnerable population. This calculation varied for each ocean as detailed below.

Catch data and size data for other gears in the Pacific Ocean are not as complete as longline records, and are not available in the public domain for some species-gear combinations. Although catch statistics were available as nominal catch for all species by gear, spatial distribution of catch was not available for the following species-gear combinations, resulting in a significant underestimate of spatial catch: no spatial records for other gear types were available in the public domain for Pacific bluefin, northern albacore tuna, and Pacific swordfish (see

Figure 2.10). As a result, these stocks were excluded from some of the spatial analyses presented in later chapters. A much smaller proportion of catch by other gears could not be allocated spatially for striped marlin, blue marlin, and black marlin. Spatial data were also unavailable for southern albacore troll fleets. Longline size thresholds were estimated from longline catch average length frequency distribution from the following sources: southern albacore (Langley 2006), western Pacific yellowfin tuna (Hampton et al. 2006b), eastern Pacific yellowfin tuna (Maunder and Hoyle 2006b), western Pacific bigeye tuna (Hampton et al. 2006a), eastern Pacific bigeye tuna (Maunder and Hoyle 2007), blue marlin (Kleiber et al. 2002), and swordfish (ISC 2008b). Striped marlin and black marlin lengths were assumed similar to estimates made for the Indian Ocean from length frequency data available from the IOTC (IOTC Database 2006). Monthly 5°x5° or 1°x1° spatial catch data raised to nominal catch for the remaining stock by gear type combinations were accessed through the SPC-OFC database and the IATTC database. Data at a resolution of 1°x1° were aggregated to 5°x5°. Spatial catch for purse seines was estimated separately for associated and unassociated sets in the western Pacific and for associated, unassociated, and dolphin set in the eastern Pacific. Mean weight estimated from averaged length frequency information was used to convert biomass to numbers. Mean weights used are presented with references in Table 2.2 and conversion of length to weight was done using parameter values in Table 2.1. Aggregate length frequencies were also used to determine the proportion of gear specific catch greater than the size threshold estimated above (see values in Table 2.2).

The 5°x5° quarterly harvests expanded to nominal catch and aggregated across country available from ICCAT (CATDIS) were utilized to determine the numbers of longline vulnerable individuals caught in other gear in the Atlantic. Although ICCAT task II data are available for multiple gear types, the CATDIS database accessed aggregated gear into baitboat, purse seine, and 'other' categories. Harpoon, gillnet, rod and reel, trap, troll, trawl and 'other' gear are aggregated into the 'other' category. Task II size data were used to determine mean weight of individuals harvested by gear, size threshold used to define longline vulnerable individuals, and the proportion of individuals greater than the threshold size (see values in Table 2.2). Size data were converted to weight when necessary using length-to-weight values in Table 2.1, and averaged over, years, fleets, and spatial areas to determine gear-specific mean weight of the

catch. Mean weight of the 'other' category was also averaged over all gears in that category. The resulting averaged length frequency distributions were also used to determine the proportion of the catch greater than the longline threshold that had been determined from Task II longline length frequency records. Such a method is likely biased due to variation in size data reporting by country, but paucity of length frequency records and the nature of the CATDIS dataset necessitated its use.

A more complex method was required to generate a dataset for the Indian Ocean since spatial data for other gear types had not been expanded to total landings. As detailed for Indian and Atlantic longline fleets, task II spatial data by gear type and country were used to allocate nominal catch to spatial areas by month assuming spatial catch records represented the spatial distribution of catch for gear/fleet combinations for which spatial data were not reported. Years missing spatial records were filled following the same procedure described for longline fleets. Catch from countries without spatial records for a gear type were allocated spatially in proportion to the countries' spatial records aggregated for all gear types. If such data were not available, catch was distributed in proportion to a country-aggregated catch for the gear type in question. IOTC Task II size frequency data were used to determine mean weight of gear specific catch by species and to determine the proportion of individuals of longline vulnerable size (see values in Table 2.2). Size data were converted to weight when necessary using length-to-weight values in Table 2.1 and averaged over years, fleets, and spatial areas.

The 5°x5° average catch by decade for other gear types and countries combined by species are presented in Figure 8.2 to Figure 8.21 in the Appendix to Chapter 2.

Annual nominal catch all gear all countries combined

A nominal catch dataset of longline vulnerable individuals by all gear and all countries combined for the Indian and Atlantic oceans (Figure 2.9 to Figure 2.11 and Table 8.3) was generated by aggregating catch over spatial area, gear, and month using spatial datasets developed above. Additional information not available spatially for other gear was added to the Pacific data for northern albacore and bluefin tuna, swordfish, striped marlin, and blue marlin. Additional nominal catch records for northern albacore were acquired from the ISC (ISC 2008a) and

estimates of longline vulnerable numbers caught were made using values in Table 2.2. Pacific bluefin tuna data were acquired from an ISC report (ISC 2008c). Targeting of strong year classes by purse seine gear required the numbers of longline vulnerable individuals caught to be approximated from estimated purse seine catch of medium and large bluefin tuna (Takeuchi 2007a) and changes in purse seine size composition over time (Takeuchi 2007b). Additional catch statistics for striped marlin and swordfish in the North Pacific were available in ISC documentation (ISC 2008b). Catch estimates of blue, striped, and black marlin from other gears were obtained as nominal catch estimates derived by the SPC-OFP (SPC-OFP 2006a), and estimates of mean weight by gear type and proportion vulnerable to longlines were calculated using values in Table 2.2. Catches not reported spatially were a significant proportion of the total catches estimated for northern bluefin, northern albacore, and swordfish in the Pacific Ocean.

Table 2.1 von Bertalanffy growth equation parameters, instantaneous annual natural mortality rates, age, or size at 50% maturity, and length-to-weight conversions parameters for tuna and billfish stocks by ocean. von Bertalanffy growth equation parameter K is an annual rate and t_0 is in years. Where multiple values are presented, bold values indicate parameters used for conversions in this thesis. Unless otherwise stated, length for tunas is fork length (cm) and weight is round weight (kg). For billfish, length is lower jaw fork length (cm) and weight is round weight (kg). EFL indicates eye fork length. Male and female relationships are designated with m and f. Mortality rates designated with † are approximated from mortality at age schedules for longline vulnerable individuals. Repeated references are indicated with (").

	Albacore tuna (*Thunnus alalunga*)	
Indian Ocean		
Growth	**L_∞=128.13 K=0.16 t_0=-0.897**	(Huang et al. 1990)
	L_∞=136 K=0.159 t_0=-1.6849	(Hsu 1991)
Mortality	0.206	(Lee et al. 1990)
	0.22	(Lee and Liu 1992)
Maturity	Assumed as Pacific	
Length-to-weight	(m) a=3.383 x10^{-5} b=2.8676	(Lee and Kuo 1988)
	(f) a=4.1830 x10^{-5} b=2.8222	"
North Pacific		
Growth	(m) L_∞=131.3 K=0.184 t_0=-1.771	(ISC 2005)
	(f) L_∞=110.1 K=0.282 t_0=-1.27	"
Mortality	0.3	"
Maturity	~85 cm ~5 years	"
Length-to-weight	**a=4.66 x10^{-5} b=2.829**	"
	a=2.5955 x10^{-5} b=2.9495	(Nakamura and Uchiyama 1966)
South Pacific		
Growth	L_∞=121 K=0.134 t_0==-1.9322	(Labelle et al. 1993)
Mortality	0.2-0.4	(Langley 2006)
	0.3	(Labelle et al. 1993)
Maturity	~82 cm ~5 years	(Ramón and Bailey 1996)
Length-to-weight	**a=6.9587 10-^{6} b=3.2351**	(Langley and Hampton 2005)
	a=8.8405 x10^{-5} b=2.6822	(Nakamura and Uchiyama 1966)
North Atlantic		
Growth	L_∞=124.74 K=0.0.23 t_0=-0.9892	(Bard 1981)
Mortality	0.3	(ICCAT 2007a)
Maturity	~90 cm ~5 years	(Bard 1981)
Length-to-weight	a=1.339 x10^{-5} b=3.1066	(Santiago 1993)
South Atlantic		
Growth	L_∞=142.28 K=0.1454 t_0=-0.674	(Lee and Yeh 1993)
Mortality	0.3	(ICCAT 2007a)
Maturity	~90 cm ~5 years	(Bard 1981)
Length-to-weight	a=1.3718 x10^{-5} b=3.0793	(Penney 1994)

Continued on next page

Table 2.1 cont.

Mediterranean		
Growth	L_∞=94.7 K=0.258 t_0=-1.354	(Megalofonou 2000)
Mortality	0.3	(ICCAT 2007a)
Maturity	~62 cm ~3 years	(Arena et al. 1980)
Length-to-weight	a=3.1190 x10^{-5} b=2.88	(Megalofonou 1990)
	Bigeye tuna (*Thunnus obesus*)	
Indian Ocean		
Growth	L_∞=211.5 K=0.45 t_0=-0.1205	(Praulai 1998)
	L_∞=178.41 K=0.176 t_0=-2.5	(Farley et al. 2006)
	L_∞=169 K=0.32 t_0=-0.336	(IOTC 2008)
Mortality	?	
Maturity	~100cm ~3 years	"
Length-to-weight	a=1.63 x10^{-5} b=3.0388	(Praulai 1998)
	a=2.396 x10^{-5} b=2.98	(IOTC 2005)
	a=3.661 x10^{-5} b=2.90182	(IOTC 2008)
Pacific Ocean		
Growth	**L_∞=228.59 K=0.226 t_0=-0.425**	(Lehodey et al. 1999)
	L_∞=166.3 K=0.3494 t_0=-0.389	(Hampton et al. 1998)
	L_∞=208.7 K=0.201 t_0=-0.9991	(Sun et al. 2001)
Mortality	0.361	(Hampton et al. 1998)
	0.44-0.68	(Murphy and Sakagawa 1977)
	0.45†	(Maunder and Hoyle 2006a)
	0.46†	(Hampton et al. 2005a)
	0.477	(Kume and Joseph 1966)
Maturity	100-130 cm ~2.5-3 years	(Calkins 1980)
	~135 cm ~3.5 years	(Schaefer et al. 2005)
	>100 cm >2.5 years	(Nikaido et al. 1991)
Length-to-weight	**a=3.0 x10^{-5} b=2.9278**	(Sun et al. 2001)
	a=3.661 x10^{-5} b=2.90182	(Nakamura and Uchiyama 1966)
Atlantic Ocean		
Growth	**L_∞=217.3 K=0.18 t_0=-0.709**	(Hallier et al. 2005)
	L_∞=247.29 K=0.14 t_0=-0.54	(Alves et al. 2002)
Mortality	0.4	(Fonteneau et al. 2005)
Maturity	~115cm ~3 years	(ICCAT 2005)
Length-to-weight	a=2.396 x10^{-5} b=2.9774	(Parks et al. 1982)

Continued on next page

Table 2.1 cont.

	Yellowfin tuna (*Thunnus albacares*)	
Indian Ocean		
Growth	L_∞=194 K=0.66 t_0=-0.27	(Praulai 1998)
Mortality	0.6	(Fonteneau 2005)
Maturity	~95cm ~2-3 years	"
Length-to-weight	a=1.80 x10^{-5} b=2.9841	(Praulai 1998)
	a=4.1 x10^{-5} b=2.8	(IOTC 2005)
	a=1.886 x10^{-5} b=3.0195	(IOTC 2008)
Pacific Ocean		
Growth	**L_∞=199.6 K=0.39 t_0=-0.177**	(Lehodey and Leroy 1999)
	(m) L_∞=202.1 K=0.276 t_0=0	(Yabuta et al. 1960)
	(f) L_∞=176.9 K=0.372 t_0=0	
	(m) L_∞=175 K=0.3 t_0=0	(Yesaki 1983)
	(f) L_∞=173 K=0.32 t_0=0	
Mortality	0.6	(Francis 1977)
	0.55-1.05	(Schaefer 1967)
	0.67-0.91	(Murphy and Sakagawa 1977)
	~0.91†	(Maunder and Hoyle 2006b)
	~0.88†	(Hampton et al. 2006b)
Maturity	~85 cm ~2 years	(Maunder and Hoyle 2006b)
	~100cm ~2 years	(Hampton et al. 2006b)
Length-to-weight	**a=2.5120 x10^{-5} b=2.9396**	"
	a=1.387 x10^{-5} b=3.086	(Wild 1986)
Atlantic Ocean		
Growth	**L_∞=230.7 K=0.267 t_0=-0.081**	(Lessa and Duarte-Neto 2004)
	L_∞=196.5 K=0.474 t_0=-0.847	(Bard 1983)
	L_∞=166.4 K=0.864 t_0=-1.292	"
	L_∞=192.4 K=0.37 t_0=-0.003	(Draganik and Pelczarski 1984)
Mortality	0.6	(ICCAT 1984)
Maturity	~100 cm ~2.5 years	(ICCAT 2004a)
Length-to-weight	a=2.153 x10^{-5} b=2.976	(Caveriviere 1975)
	Northern Pacific bluefin tuna (*Thunnus orientalis*)	
Growth	L_∞=320.5 K=0.135 t_0=-0.07828	(Yukinawa and Yabuta 1967)
	L_∞=325 K=0.1098 t_0=-0.3993	(Hsu and Chen 2006)
Mortality	0.276	(Bayliff et al. 1991)
Maturity	~150cm ~5 years	(Harada 1980)
Length-to-weight	**a=2.977 x10^{-5} b=2.9103**	(Shingu et al. 1974)
	a=5.4535 x10^{-5} b=2.7946	(Bayliff 2000)
	a=6.2033 x10^{-5} b=3.3335	"

Continued on next page

Table 2.1 cont.

	Atlantic bluefin tuna (*Thunnus thynnus*)	
Eastern Atlantic		
Growth	L_∞=318.85 K=0.093 t_0=-0.97	(Cort 1991)
Mortality	0.165	(ICCAT 1997)
Maturity	135-165 cm 5-7 years	"
	(f) 103 cm 3 years	(Corriero et al. 2005)
Length-to-weight	a=2.95 x10^{-5} b=2.899	(ICCAT 1997)
Western Atlantic		
Growth	**L_∞=382 K=0.079 t_0=-0.707**	(Turner and Restrepo 1994)
	(m) L_∞=286.64 K=0.134 t_0=-0.3278	(Caddy et al. 1976)
	(f) L_∞=277.315 K=0.116 t_0=-0.78	"
Mortality	0.14	(ICCAT 1997)
Maturity	190-240 cm 8-12 years	"
Length-to-weight	a=2.861 x10^{-5} b=3.0092	(Parrack and Phares 1979)
	Southern bluefin tuna (*Thunnus maccoyii*)	
Growth	**L_∞=261.3 K=0.108 t_0=-0.157**	(Thorogood 1987)
	L_∞=219.7 K=0.135 t_0=0.04	(Yukinawa 1970)
	L_∞=180.8 K=0.146 t_0=-0.011	(Murphy and Sakagawa 1977)
Mortality	0.2	(CCSBT 2005)
	0.45 age 1 >0.05 age 5	(Polacheck et al. 2004)
Maturity	150-160cm 11-12 years	(Davis et al. 2001)
Length-to-weight	a=1.7913 x10^{-5} b=3.02	(CCSBT 2005)
	Blue marlin (*Makaira nigricans*)	
Indian Ocean		
Growth	Assumed as Pacific	
Mortality	Assumed as Pacific	
Maturity	Assumed as Pacific	
Length-to-weight	a=1.73 x10^{-6} b=3	(IOTC 2005)
Pacific Ocean		
Growth	(m) L_∞=371.1 K=0.285 t_0=0.106	(Skillman and Yong 1976)
	(f) L_∞=659.1 K=0.116 t_0=-0.161	"
Mortality	(m) 0.53 (f) 0.21	(Boggs 1989)
	(m) 0.38-0.41 (f) 0.18-0.19	(Hinton 2001)
Maturity	(m) ~150cm ~2-3 years (?) (f) ~220cm ~4 years	(Pepperell 2000b)
Length-to-weight	**a=2.79 x10^{-6} b=3.24**	(Wang et al. 2006)
	(m) a=7.08 x10^{-5} b=2.6	(Prince et al. 1991)
	(f) a= 1 x10^{-7} b=3.81	"

Continued on next page

Table 2.1 cont.

Atlantic Ocean		
Growth	Assumed as Pacific	
	24 cm in ~40 days, 190 cm in ~1.37 years	(Prince et al. 1991)
Mortality	>0.05	(Goodyear and Prager 2001)
Maturity	(f) ~256cm ~4(?) years	(Arocha and Marcano 2006)
Length-to-weight	**(m) $a=2.468 \times 10^{-6}$ b=3.2243**	(Prager et al. 1995)
	(f) $a=1.903 \times 10^{-6}$ b=3.2842	"
	Striped marlin (*Tetrapturus audax*)	
Indian Ocean		
Growth	Assumed as Pacific	
Mortality	Assumed as Pacific	
Maturity	Assumed as Pacific	
Length-to-weight	Assumed as Pacific	
Pacific Ocean		
Growth	(m) L_∞=277.4 K=0.417 t_0=-0.521	(Skillman and Yong 1976)
	(f) L_∞=251 K=0.696 t_0=0.136	
	L_∞=221 K=0.23 t_0=-1.6	(Melo-Barrera et al. 2003)
	L_∞=301 K=0.22 t_0=-0.04	(Kopf et al. 2005)
Mortality	0.49-1.33	(Boggs 1989)
	0.389-0.818	(Hinton and Bayliff 2002)
Maturity	<170cm	(Squire and Suzuki 1990)
	first maturity 165-190 cm	(Nakamura 1985)
	~2-4 years	(Skillman and Yong 1976)
Length-to-weight	**$a=2 \times 10^{-8}$ b=2.88**	(Kopf et al. 2005)
	$a=1.91 \times 10^{-6}$ b=3.25	(Wang et al. 2006)
	$a=8 \times 10^{-5}$ b=2.523	(Melo-Barrera et al. 2003)
	Atlantic white marlin (*Tetrapturus albidus*)	
Growth	Assumed as Pacific Striped Marlin	
Mortality	0.32	(Mather et al. 1972)
Maturity	(m) ~139cm ~2-4 (?) years (f) 147cm ~ 2-4 (?) years	(Oliveira et al. 2007)
	(f) 189.9cm	(Arocha and Marcano 2006)
Length-to-weight	(m) $a=1.9556 \times 10^{-5}$ b=2.7487	(Prager et al. 1995)
	(f) $a=3.9045 \times 10^{-6}$ b=3.0694	"

Continued on next page

Table 2.1 cont

	Black marlin (*Makaira indica*)	
Growth	0+ ~120 cm 1+ ~130-140 cm 2+ ~150-165 cm	(Speare 2003)
	3+ 160-170 cm 4+ 180-200 cm	"
	5+ 210-220 cm 6+ 240-260 cm	"
Mortality	Assumed as Pacific blue marlin	
Maturity	first maturity (m) 2-3 years (f) 3-4 years	(Pepperell 2000a)
Length-to-weight	a=1.518 x10^{-6} b=3.361	(Speare 2003)
	a=6.62 x10^{-6} b=3.07	(Wang et al. 2006)
	a= 8.1 x10^{-6} b=3.033	(IOTC 2005)
	Swordfish (*Xiphias gladius*)	
Indian Ocean		
Growth	(m) L_∞=210.058 K=0.157 t_0=-3.162	(Vanpouille et al. 2001)
	(f) L_∞=240.704 K=0.134 t_0=-2.361	"
Mortality	Assumed as Pacific	
Maturity	(m) 119.8cm ~2 years (f) 170.4cm ~6 years	(Poisson et al. 2001)
Length-to-weight	a=6.33 x10^{-6} b=3.1605	(IOTC 2005)
Pacific Ocean		
Growth	(m) L_∞=224.17 K=0.14 t_0=-3.089	(Sun et al. 2002)
	(f) L_∞=281.809 K=0.101 t_0=-3.204	"
	(m) L_∞=250 K=0.3216 t_0=-0.7545	(Barbieri et al. 1998)
	(f) L_∞=282 K=0.2925 t_0=0.1085	"
Mortality	0.22	(Boggs 1989)
	0.21-0.39	(Hinton et al. 2004)
Maturity	(m) 117cm ~2 years (f) 162cm ~5.5 years	(DeMartini et al. 2000)
	(f) 168.2cm ~6 years	(Wang et al. 2003)
Length-to-weight	a= 1.3528 x10^{-6} b=3.4297	(Sun et al. 2002)
	a= 6.48 x10^{-6} b=3.12	(Wang et al. 2006)
	EFL to RW a=1.299x10^{-5} b=3.074	(DeMartini et al. 2000)
Atlantic Ocean		
Growth	(m) L_∞=189.58 K=0.105 t_0=-0.41	(Ehrhardt et al. 1996)
	(f) L_∞=364.69 K=0.0262 t_0=-0.556	"
	(m) L_∞=223.12 K=0.1522 t_0=-3.4875	(Arocha et al. 2003)
	(f) L_∞=312.27 K=0.0926 t_0=-3.762	"
Mediterranean	(m) L_∞=203.08 K=0.241 t_0=-1.205	(Tserpes and Tsimenides 1995)
	(f) L_∞=226.53 K=0.210 t_0=-1.165	"
Mortality	0.2	(ICCAT 1987)
Maturity	(m) 129cm ~2 years (f) 176cm ~5years	(Arocha 1997)
Mediterranean	(f) 142cm 3.5 years	(ICCAT 2004b)
Length-to-weight	a= 3.4333 x10^{-6} b=3.2623	(Mejuto et al. 1988)

Table 2.2 Values used to convert gear specific catches to number of longline vulnerable individuals in the catch. W is the mean weight in kilograms (kg) estimated by gear type. $L_{90\%}$ is the average ocean specific length for which 90% of longline caught individual are larger. Proportion (p) > $L_{90\%}$ is the estimated proportion of the gear specific catch greater than the minimum longline size, and treated as part of the longline-vulnerable catch . Weight for all species is round weight (kg). Length for tuna is fork length (cm) and length for billfish is lower jaw fork length (cm). For yellowfin and bigeye tuna, purse seine A, U and D indicate associated, unassociated and dolphin sets respectively. Pacific northern bluefin tuna conversions for purse seine are presented as decadal averages. Repeated references are indicated with (").

Stock	Gear	W(kg)	$L_{90\%}$	p > $L_{90\%}$	Reference
Albacore Tuna					
Indian	Purse Seine	26	80	0.95	(IOTC Database 2006)
	Baitboat	Assumed as Purse Seine			
	Gillnet	Assumed as Purse Seine			
	Other	Assumed as Purse Seine			
North Pacific	Purse Seine	Assumed as Baitboat			
	Troll (Canada)	7.15	75	0.23	(Stocker 2005)
	Troll (U.S.)	7.86	75	0.34	"
	Gillnet	Assumed as South Pacific Gillnet			
	Baitboat	6.65	75	0.19	(Langley 2006)
South Pacific	Gillnet	7.16	75	0.13	"
	Troll	6.16	75	0.05	"
North Atlantic	Purse Seine	24.78	82	0.75	(ICCAT Database 2006)
	Baitboat	16.51	82	0.54	"
	Other	9.13	82	0.15	"
South Atlantic	Purse Seine	24.80	82	0.94	"
	Baitboat	10.85	82	0.29	"
	Other	12.85	82	0.41	"
Bigeye Tuna					
Indian	Purse Seine	8.94	100	0.098	(IOTC Database 2006)
	Baitboat	Assumed as Purse Seine			
	Gillnet	Assumed as Purse Seine			
	Other	Assumed as Purse Seine			
Western Pacific	Purse Seine (A)	5.17	90	0.0325	(Hampton et al. 2006a)
	Purse Seine (U)	12.88	90	0.27	"
Eastern Pacific	Purse Seine (A)	24.3	90	0.44	(Maunder and Hoyle 2006a)
	Purse Seine (U)	32.94	90	0.64	"
	Baitboat	32.94	90	0.64	"
Atlantic	PS	8.70	100	0.08	(ICCAT Database 2006)
	Baitboat	16.49	100	0.20	"
	Other	33.67	100	0.47	"

Continued on next page

Table 2.2 cont.

Stock	Gear	W(kg)	$L_{90\%}$	$p > L_{90\%}$	Reference
Yellowfin Tuna					
Indian	Purse Seine	17.15	88	0.39	(IOTC Database 2006)
	Baitboat	3.39	88	0.031	"
	Gillnet	10.6	88	0.22	"
	Other	10.72	88	0.22	"
Western Pacific	Purse Seine (A)	14.22	90	0.25	(Hampton et al. 2006b)
	Purse Seine (U)	21.81	90	0.57	"
	Baitboat	23.21	90	0.28	"
Eastern Pacific	Purse Seine (A)	14.66	90	0.18	(Maunder and Hoyle 2006b)
	Purse Seine (U)	15.19	90	0.24	"
	Purse Seine (D)	19.82	90	0.34	"
	Baitboat	16.49	90	0.18	"
Atlantic	Purse Seine	24.04	106	0.37	(ICCAT Database 2006)
	Baitboat	7.47	106	0.05	"
	Other	23.08	106	0.30	"
Southern Bluefin Tuna					
	Surface Gears	6.69	100	0.05	(CCSBT Database 2004)
Pacific Bluefin Tuna					
Western Pacific	Purse Seine 1950	101.3	160	0.42	(Bayliff 2000)
	Purse Seine 1960	104.3	160	0.43	(Takeuchi 2007b)
	Purse Seine 1970	76.57	160	0.37	"
	Purse Seine 1980	45.96	160	0.14	"
	Purse Seine 1990	49.88	160	0.21	"
	Purse Seine 2000	50.93	160	0.22	"
	Other	Assumed no catch > min length			
Eastern Pacific	All	Assumed no catch > min length			
Atlantic Bluefin Tuna					
Atlantic	Purse Seine	94.30	142	0.44	(ICCAT Database 2006)
	Baitboat	65.89	142	0.20	"
	Other	195.99	142	0.72	"
Blue Marlin					
Indian	Purse Seine	Assumed as Gillnet			
	Baitboat	Assumed as Gillnet			
	Gillnet	69.5	155	0.93	(IOTC Database 2006)
	Other	Assumed as Gillnet			
Pacific	Purse Seine	Assumed as Atlantic Other			
	Other	Assumed as Atlantic Other			

Continued on next page

Table 2.2 cont.

Stock	Gear	W(kg)	$L_{90\%}$	$p > L_{90\%}$	Reference
Atlantic	Purse Seine	Assumed as Other			
	Baitboat	Assumed as Other			
	Other	104.39	139	0.89	(ICCAT Database 2006)
Striped Marlin					
Indian	Purse Seine	40	150	1	(IOTC Database 2006)
	Baitboat	Assumed as Purse Seine			
	Gillnet	Assumed as Purse Seine			
	Other	Assumed as Purse Seine			
Pacific	Purse Seine	Assumed as Indian Purse Seine			
	Other	Assumed as Indian Purse Seine			
White Marlin					
Atlantic	Purse Seine	Assumed as Other			
	Baitboat	Assumed as Other			
	Other	25.50	124	0.88	(ICCAT Database 2006)
Black Marlin					
Pacific	Purse Seine	Assumed as Indian Gillnet			
	Other	Assumed as Indian Gillnet			
Indian	Purse Seine	Assumed as Gillnet			
	Baitboat	Assumed as Gillnet			
	Gillnet	89	150	0.95	(IOTC Database 2006)
	Other	Assumed as Gillnet			
Swordfish					
Indian	Purse Seine	Assumed as Other			
	Baitboat	Assumed as Other			
	Gillnet	Assumed as Other			
	Other	24.33	110	0.6	(IOTC Database 2006)
Pacific	All Gears	40	100	1	(ISC 2008b)
Atlantic	Purse Seine	28.37	104	0.97	(ICCAT Database 2006)
	Baitboat	28	104	0.97	"
	Other	52	104	0.75	"

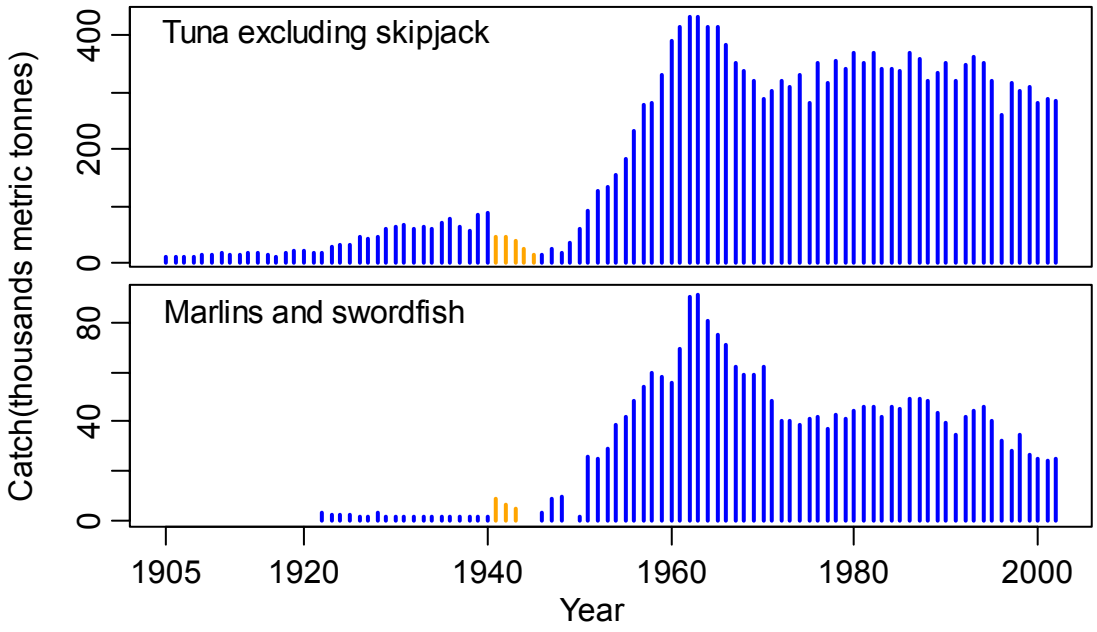

Figure 2.1 Japanese catch (thousands of metric tonnes) of tuna and billfish from 1905-2002. Tuna catches excluded skipjack. Orange bars indicate the years of World War II.

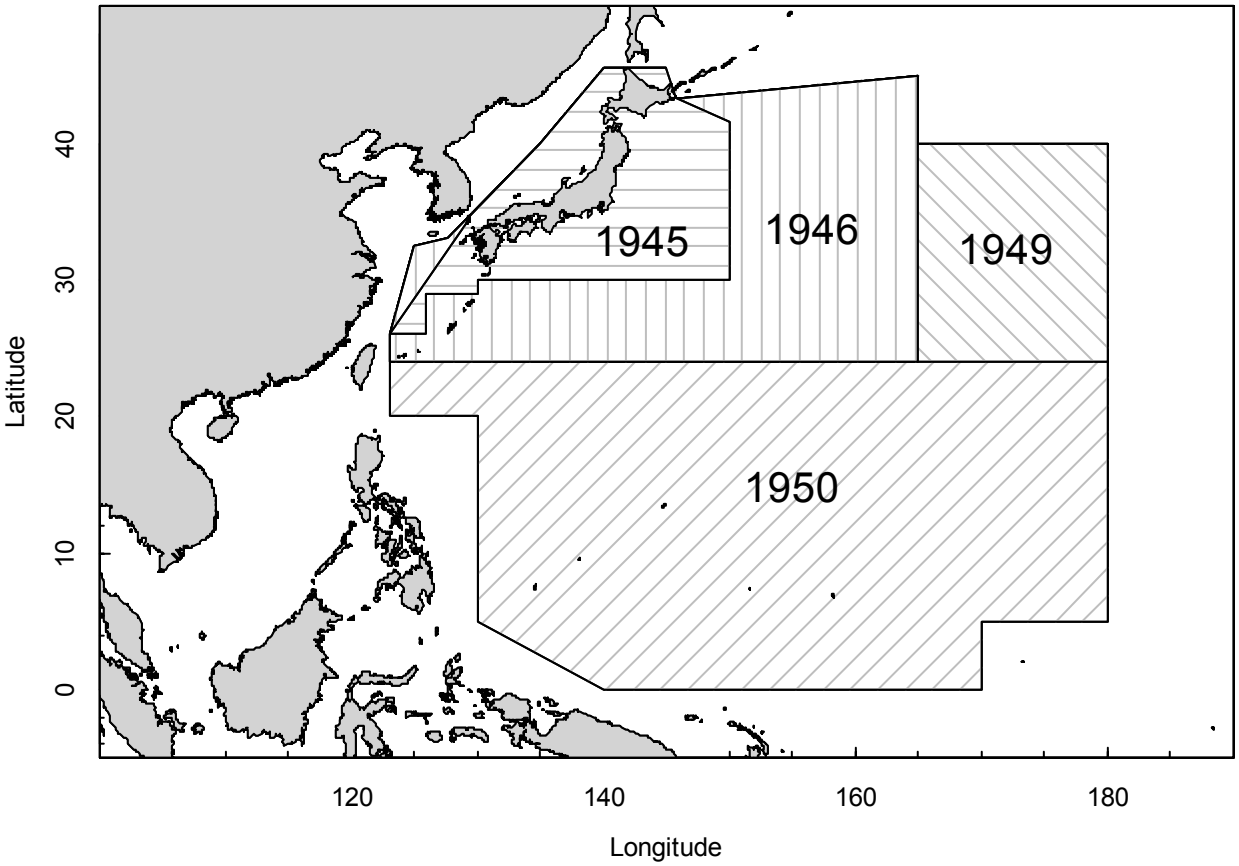

Figure 2.2 Map of the Northwest Pacific and MacArthur Lines. Immediately after World War II, Japanese fishing activity was restricted within 12 nautical miles of the coast. This restriction was relaxed with the formation of the first MacArthur Line in 1945. 1946 and 1949 refer to expansions of the original 1945 line and 1950 allowed for the expansion of tuna mothership operations only. In 1952, the MacArthur Lines were abolished.

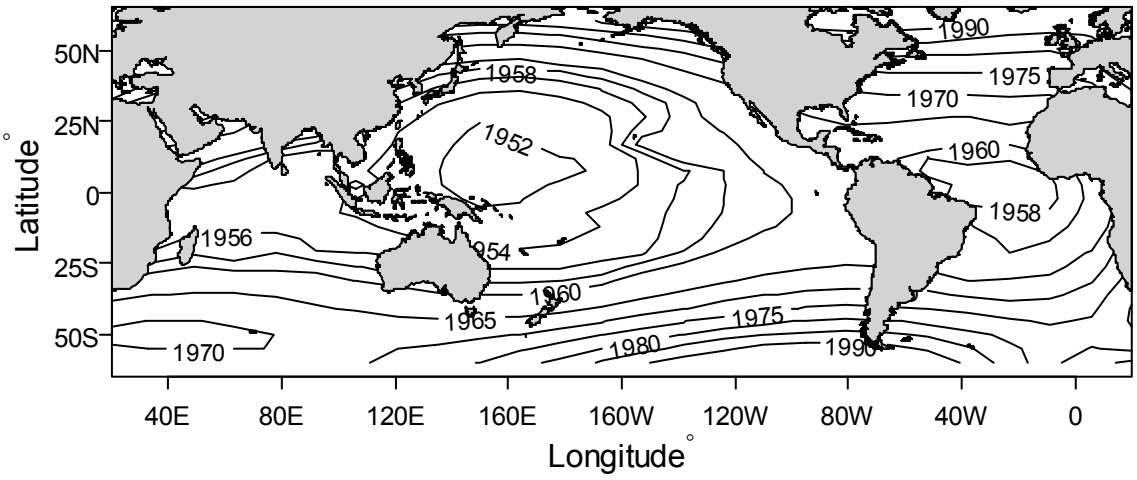

Figure 2.3 Contour plot of the approximate year when areas were first fished by the Japanese longline fleet.

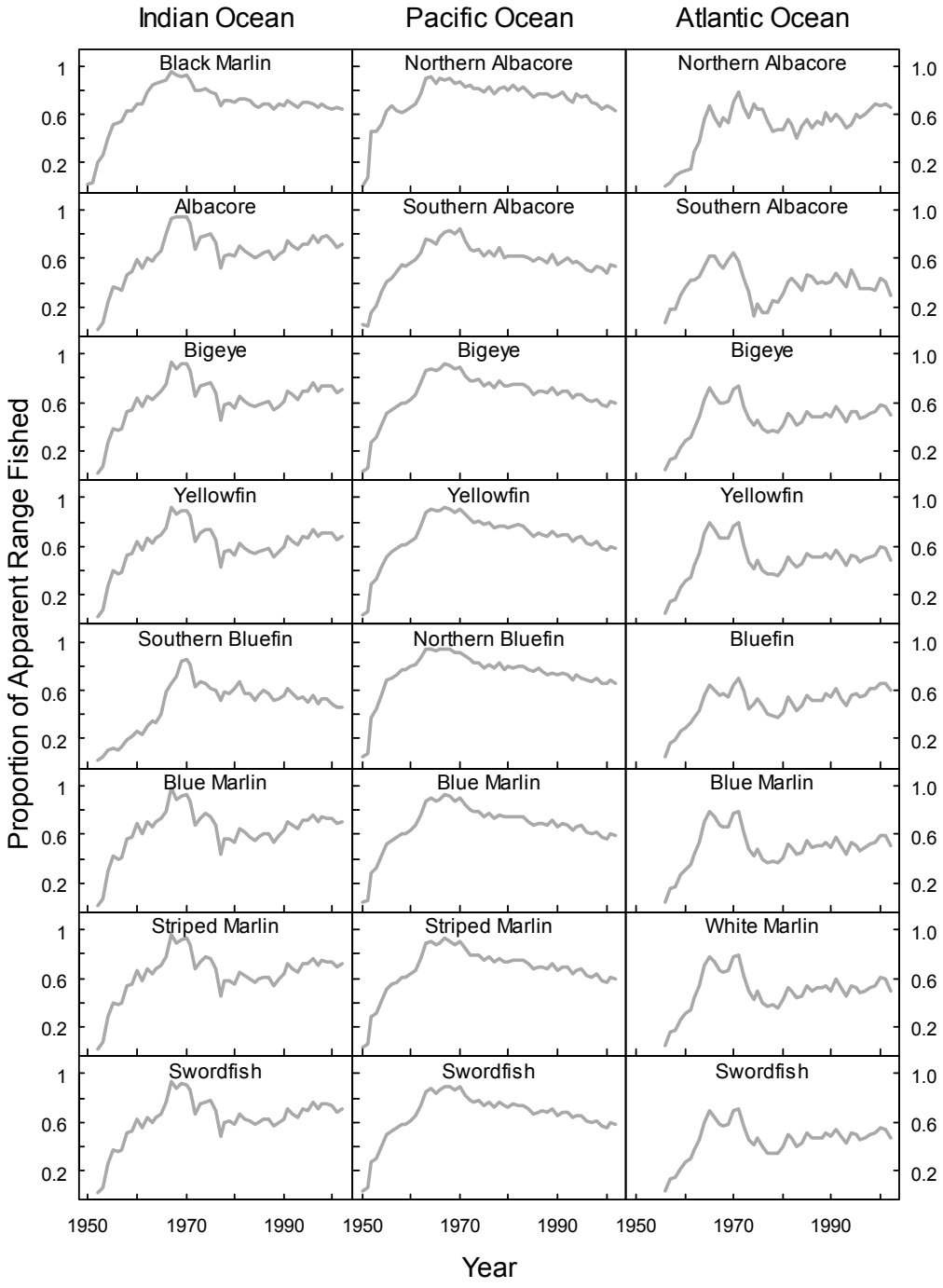

Figure 2.4 Proportion of each stock's distribution area fished by Japanese longline gear from 1950-2002 measured as the proportion of 5°x5° areas fished. Areas that produced catch for any gear or country combination from 1950-2002 were included in a stock's range. Stocks in each ocean are presented in columns with the exception of black marlin and southern bluefin tuna, which span multiple oceans, and are presented under the Indian Ocean.

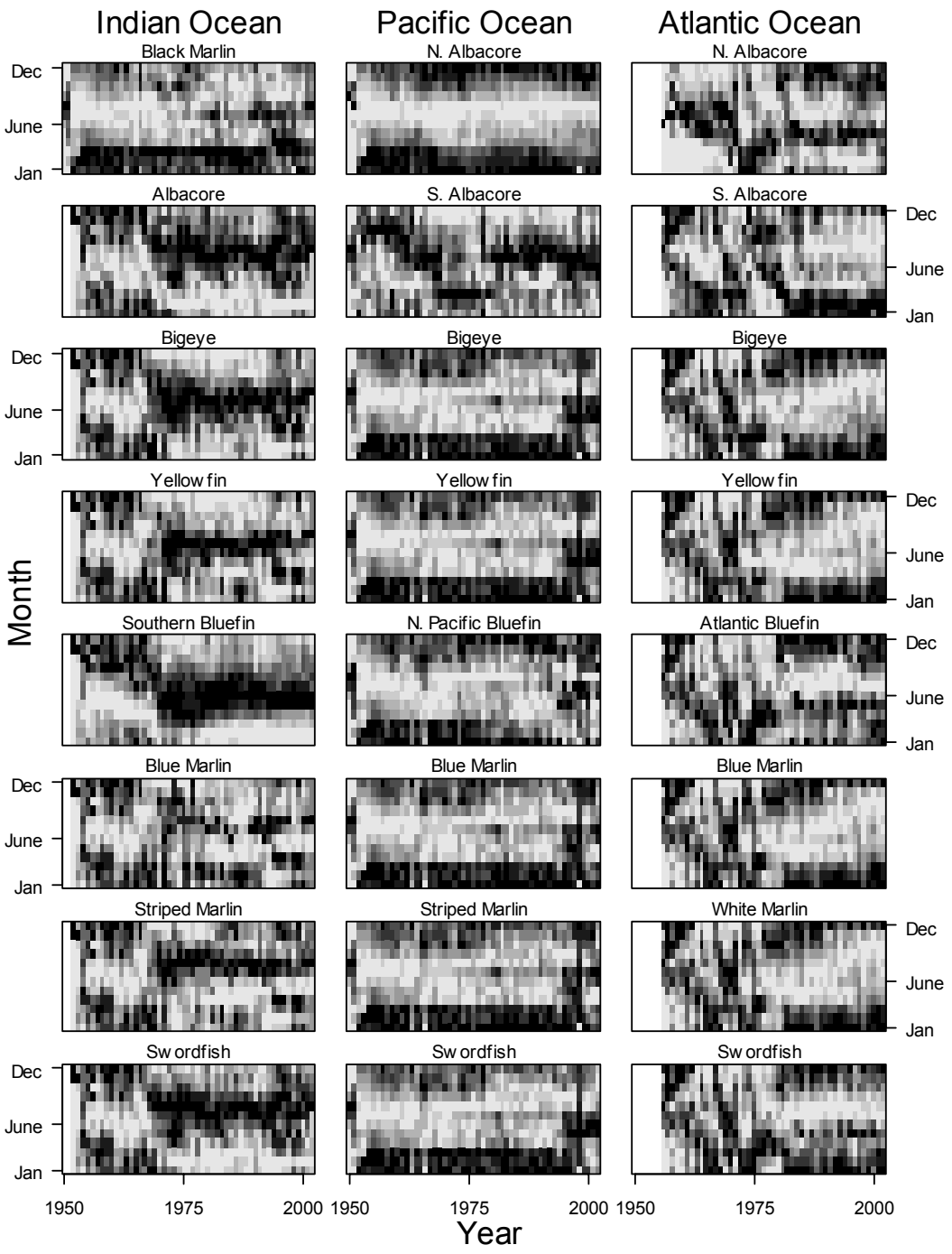

Figure 2.5 Temporal changes in the seasonal distribution of fishing effort for each species. Only those areas considered to be within a stocks distribution were included. Black indicates a higher proportion of the effort grading to white which indicate little to no effort. Stocks in each ocean are presented in columns with the exception of black marlin and southern bluefin tuna, which span multiple oceans, but are presented under the Indian Ocean.

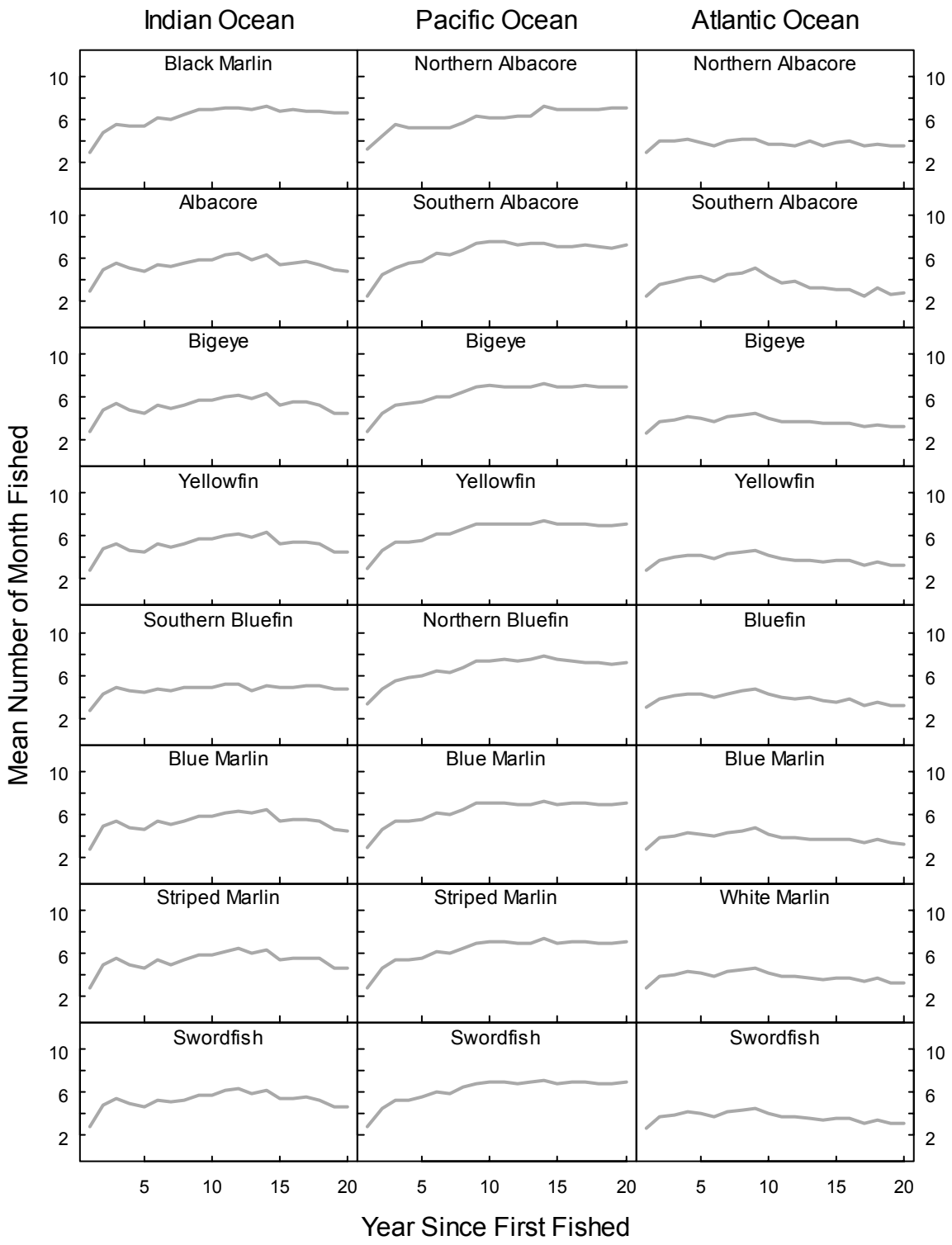

Figure 2.6 Average number of months that areas were fished by Japanese longline after first receiving effort. Stocks in each ocean are presented in columns with the exception of black marlin and southern bluefin tuna, which span multiple oceans, and are presented under the Indian Ocean.

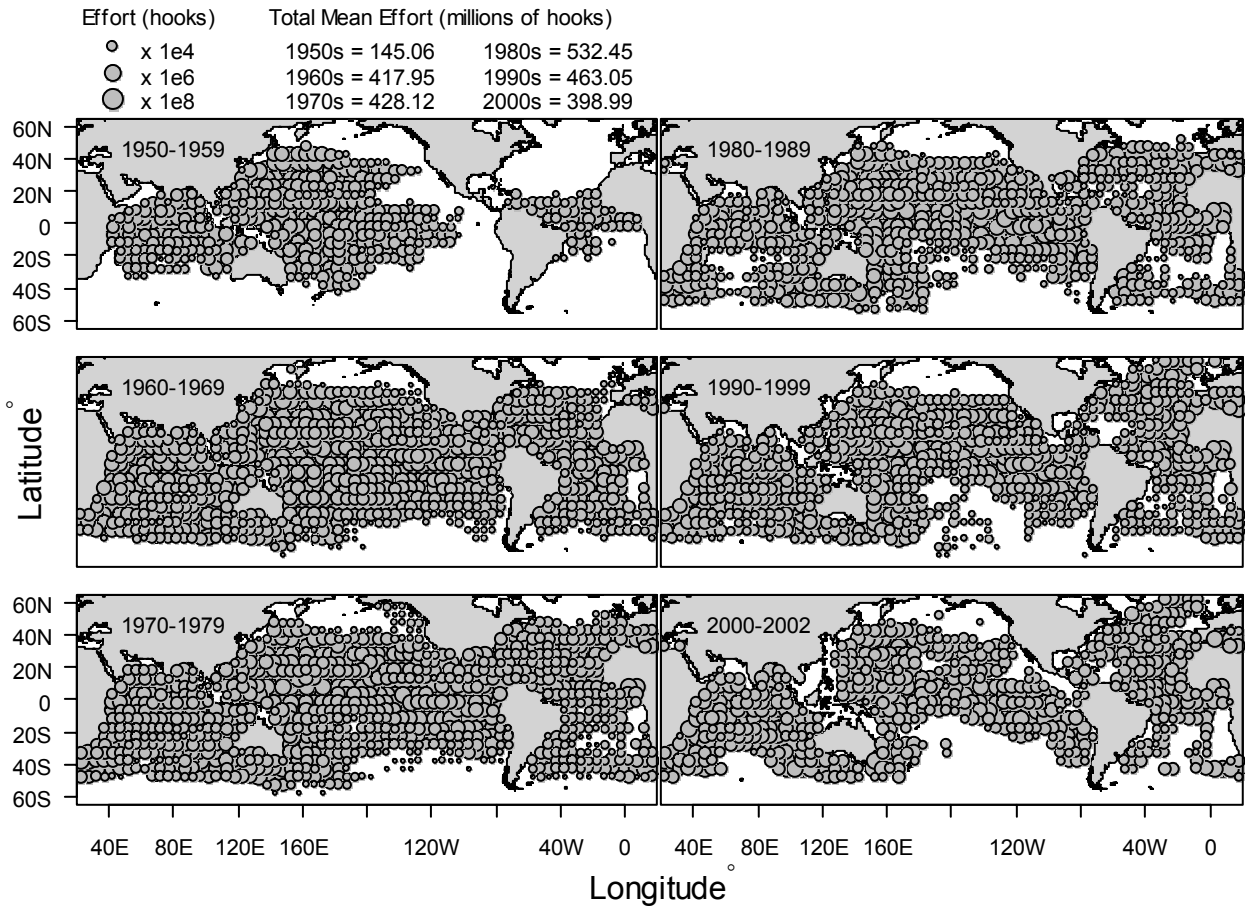

Figure 2.7 Decadal average 5°x5° effort distribution of the Japanese longline fleet from 1950-2002. Area of each grey circle is proportional to the average number of hooks set per year.

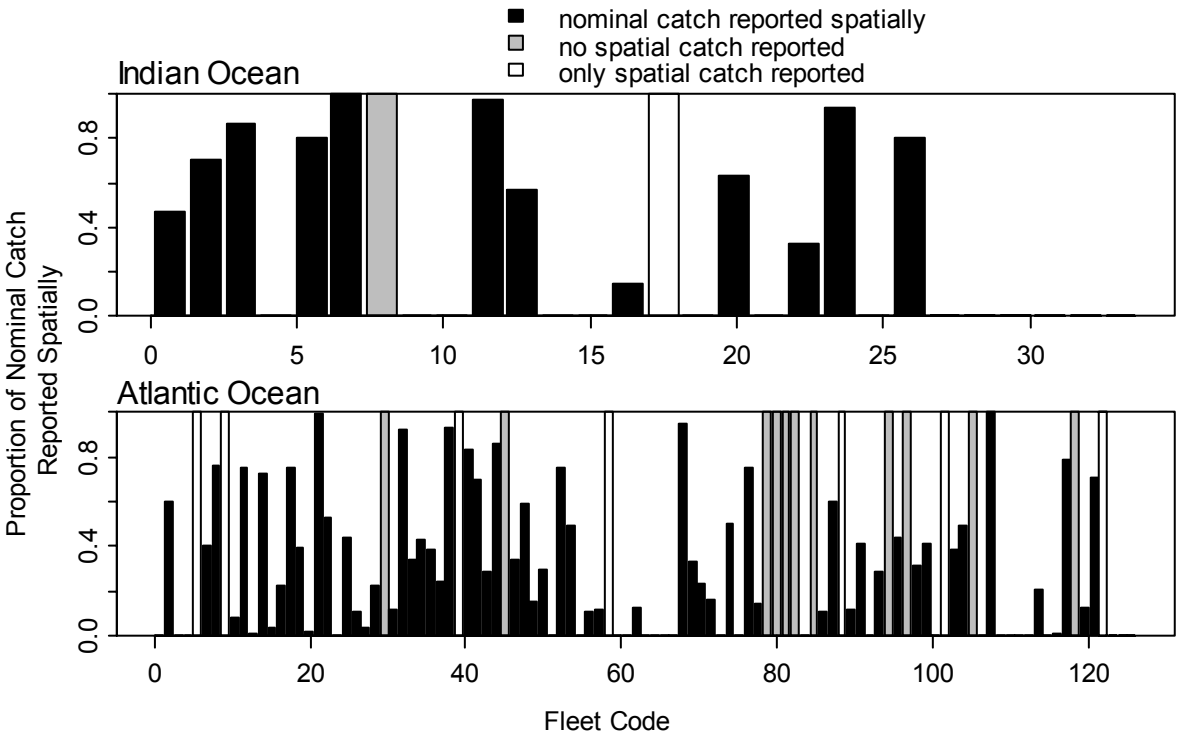

Figure 2.8 Proportion of nominal longline catch accounted for in spatial records (black bars) for countries reporting catch from the Indian and Atlantic oceans. White bars indicate countries that reported spatial catch but no nominal catch and grey bars indicate countries that reported nominal catch but no spatial catch. The countries associated with each numeric code can be found in Table 8.1 and Table 8.2.

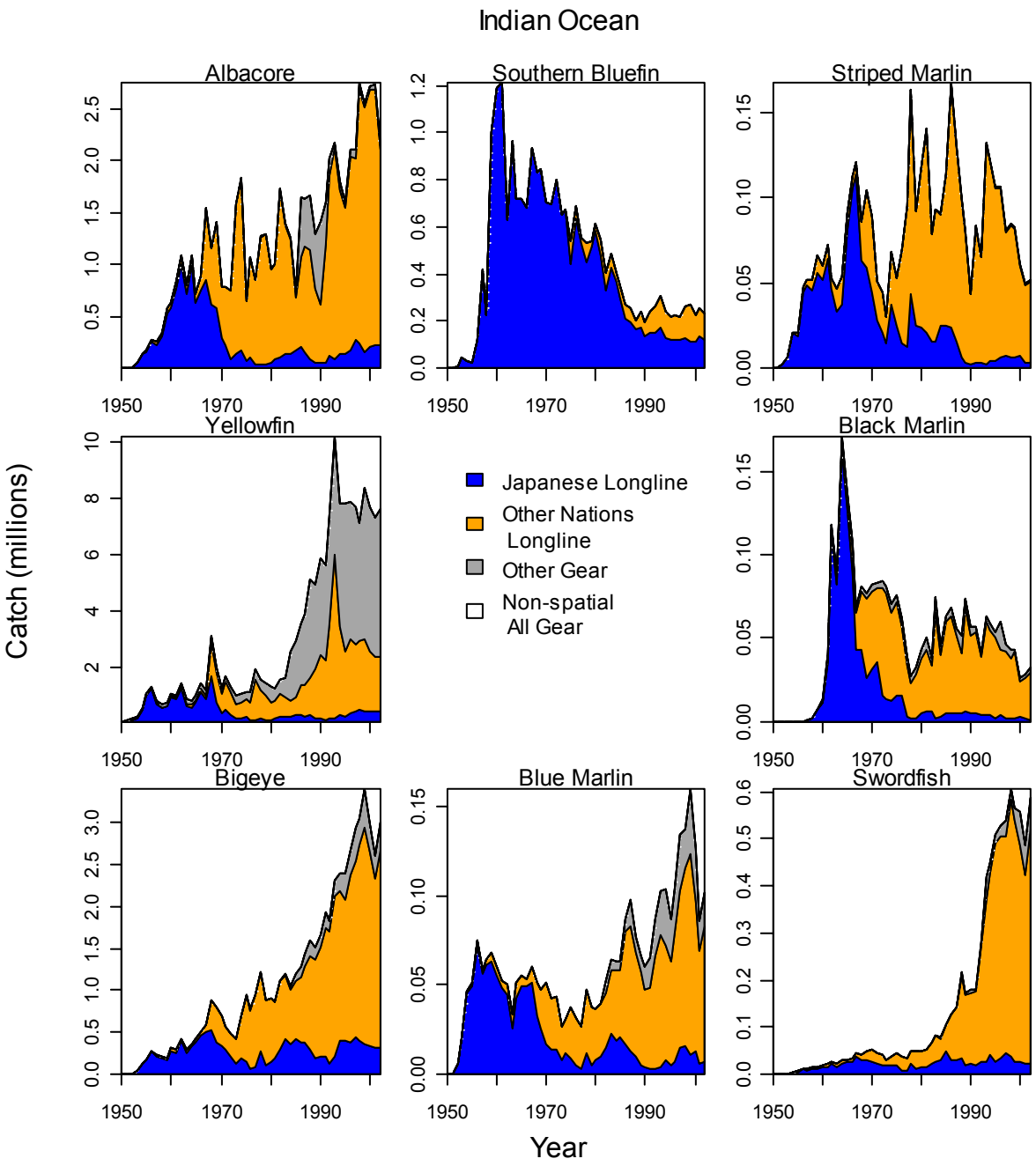

Figure 2.9 Total estimated catch, in millions, of individuals of size vulnerable to longlines captured by Japanese longline (blue), the longlines of all other nations combined (orange), other gear types (light grey), and all other gear types not reported spatially (white) for the Indian Ocean (1950-2002).

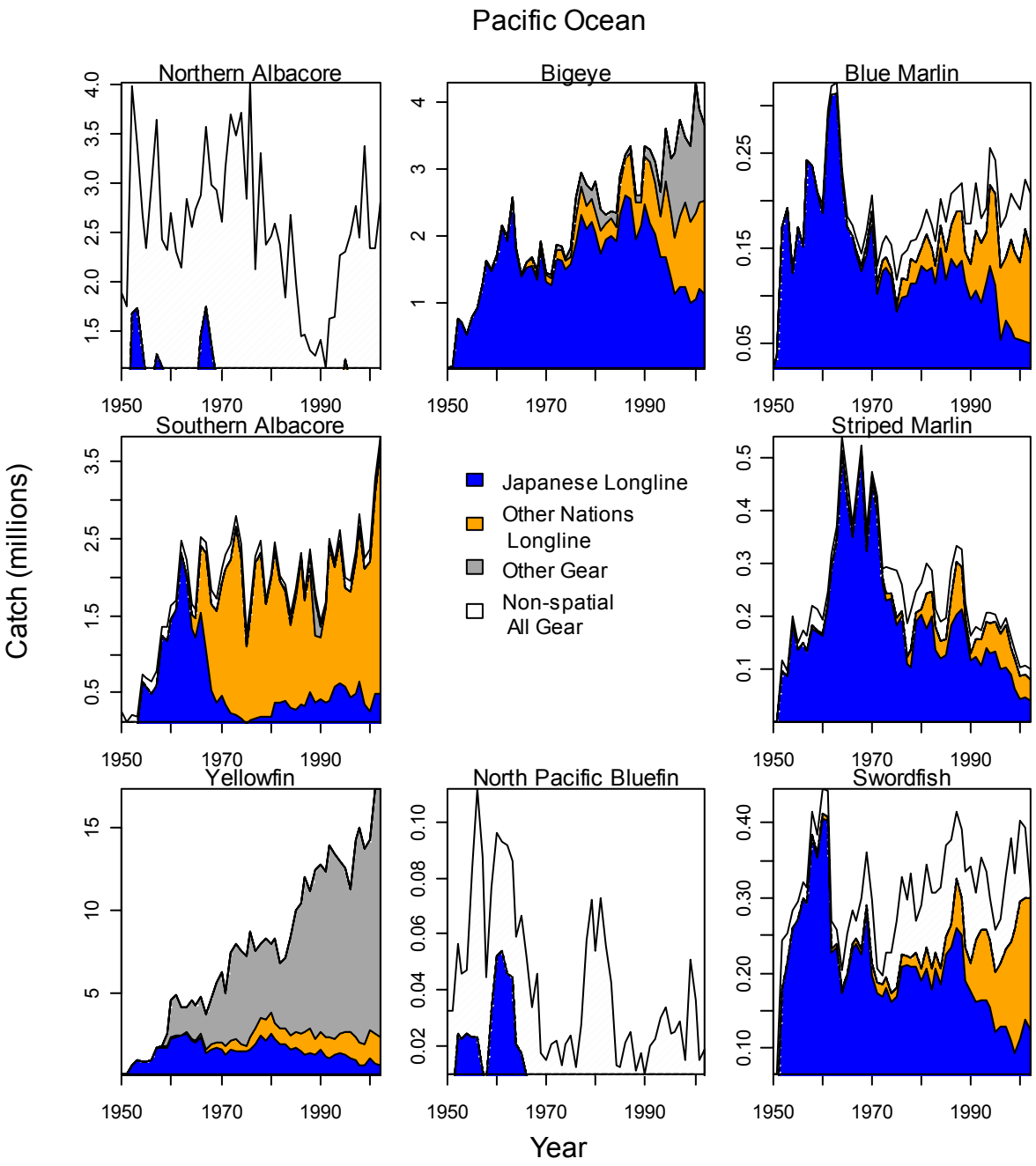

Figure 2.10 Total estimated catch, in millions, of individuals of size vulnerable to longlines captured by Japanese longline (blue), the longlines of all other nations combined (orange), other gear types (light grey), and all other gear types not reported spatially (white) for the Pacific Ocean (1950-2002).

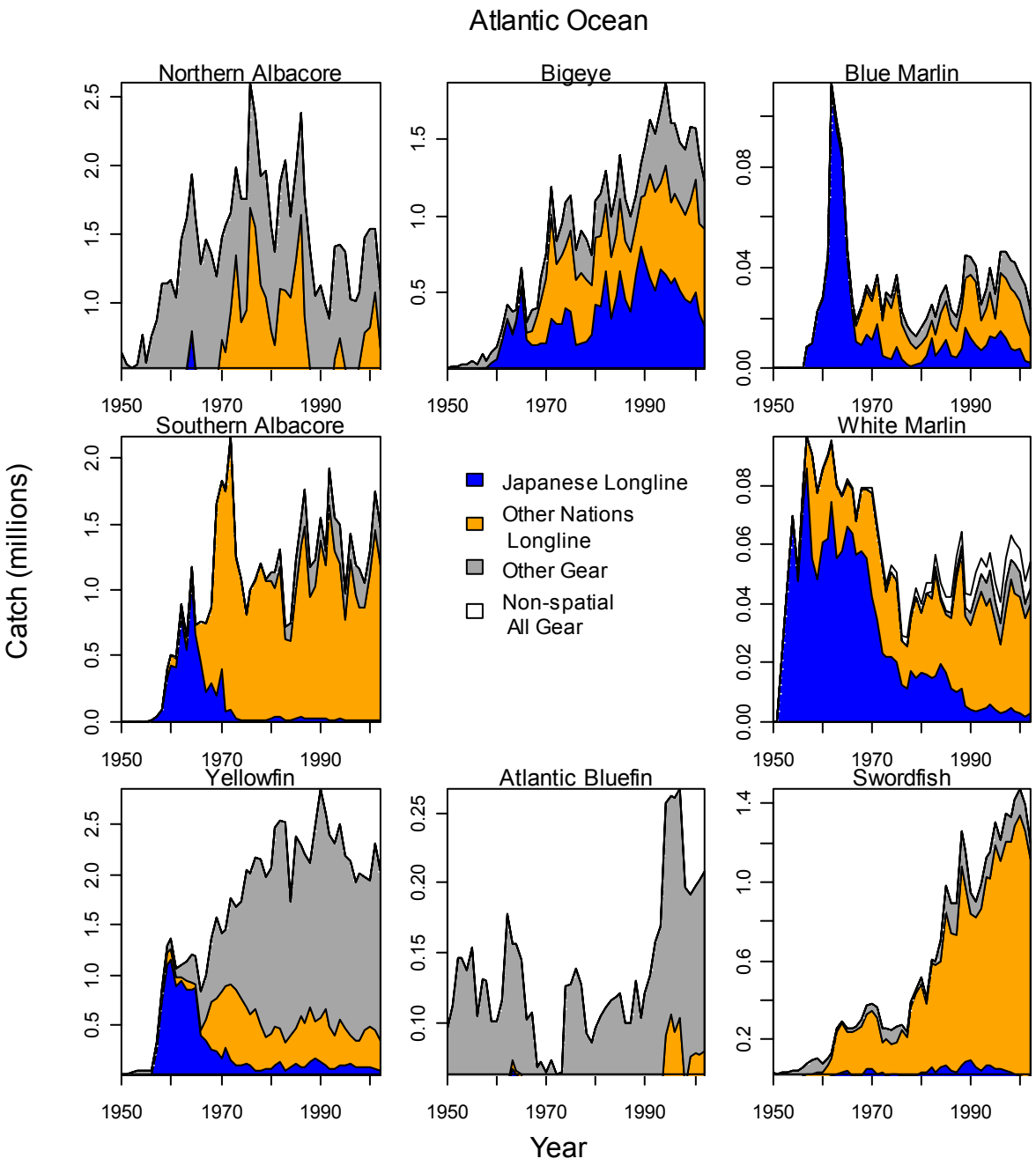

Figure 2.11 Total estimated catch, in millions, of individuals of size vulnerable to longlines captured by Japanese longline (blue), the longlines of all other nations combined (orange), other gear types (light grey), and all other gear types not reported spatially (white) for the Atlantic Ocean (1950-2002).

Chapter 3 Deriving relative abundance trends from spatial catch and effort data

Introduction

Commercial or recreational catch rates (catch per unit effort, *cpue*) are often the only information available to develop relative abundance trends, an essential component for most long-term stock assessments. It is common to assume that *cpue*, calculated as the ratio of total catch (C) to total effort (E) is proportional to abundance,

3.1) $C/E = qN$

Here N is stock abundance, and q, the catchability coefficient, is the proportion of a stock removed by one unit of effort. Unfortunately, such *cpue* indices derived from fishery data are often not proportional to abundance. Inappropriate metrics for effort, species biology, changes in fishing practices as well as fisher behaviour can bias simple ratio estimators such as nominal or 'raw' *cpue* (total catch over total effort) (Gulland 1974, Harley et al. 2001, Hilborn and Walters 1992, Maunder et al. 2006b, Paloheimo and Dickie 1964, Swain and Sinclair 1994, Swain and Wade 2003). Effort is generally 'standardized' in an effort to remove such biases so that indices do not decline faster than population abundance (hyperdepletion) or slower than abundance (hyperstability) (Hilborn and Walters 1992). Early standardization methods controlled for differences in vessel efficiency relative to a 'standard' vessel (relative fishing power) to harmonize effort units (Beverton and Holt 1957, Gulland 1956, Honma 1974). In such an approach, effort from vessels fishing in the same fishery at the same time is scaled to a specified 'standard' configuration by comparing differences in catch rates. Such an approach becomes difficult to implement over longer times as paired comparisons with the 'standard' vessel become impossible, and will still produce wildly biased trend indices if fishing effort is not distributed randomly over a stock's range. More recent standardization techniques use generalized linear models (GLMs Nelder and Wedderburn 1972), which can facilitate consideration of a greater variety of effects (i.e. area or seasonal effects) for which paired comparisons are not necessarily available (Allen and Punsly 1984). Maunder and Punt (2004)

reviewed a wide variety of statistical modeling approaches that have proliferated since, with GLMs the most common method applied.

When using GLMs to develop relative abundance time series, a variety of explanatory variables that account for differences in catch rates (year, area, quarter, longitude, latitude, gear configuration, etc.) are selected. After accounting for effects of these factors, year effects are extracted and used as a relative abundance trend. Provided all factors are sampled in a representative manner, relative abundance trends should be proportional to stock size. However, often (as is the case with Japanese longline catch and effort data) assuming representative sampling of all factors over the full history of a fishery is not possible. Fleet expansion coupled with systematic changes in fleet distribution or gear configuration result in particular spatial factors not being sampled. In terms of a GLM, interaction terms including the year must be considered but biases will occur because interactions were not sampled representatively. In these instances, standardization is only possible for those periods when all factors were representatively sampled. Campbell (2004) notes that missing information causes biases in GLM based abundance indices.

In terms of proceeding with stock assessments, two options exist. If reliable composition information is available to facilitate the determination of fishing mortality rates, then the depletion information from the early years of a fishery are not necessarily required. However, if composition information is not available or if recruitment, mortality, and selectivity influences giving rise to patterns in composition information are complex so that fishing mortality rate effects are confounded with other effects, (e.g., dome-shaped size selection), then abundance trends spanning the history of a fishery are desirable.

The Japanese longline fleet expanded over the world's oceans from tropical to temperate waters. If a relative abundance series from 1950 onwards is required, the non-representative sampling problem must be addressed. When spatial catch and effort data are available, estimators that are more appropriate than simple nominal *cpue* can be calculated as weighted averages of the ratios for individuals areas, where area specific statistical stratum weight depends on area size (Walters 2003). However, to construct such a stratified sampling estimator of relative abundance, catch

rate observations are required for every stratum; i.e., every area and time combination is considered. Ignoring time-area strata with no effort in calculating average *cpue* is equivalent to assuming that these areas behaved as the mean of the strata that were sampled (fished). Such an assumption can result in severely biased abundance trends as fisheries expand, shift or contract over large areas. Missing catch rate data must be imputed, and surely, there are better estimates for unsampled areas than simply the mean of areas that were sampled. Methods used to assign values to missing strata (data imputation) become the central question when developing indices of abundance. Walters (2003) suggests a number of options to address this spatial and temporal gap-filling problem. His simplest approach is to perform a form of trend analysis within a given stratuma, interpolating or extrapolating over non-sampled periods using observed values near the beginning and/or end of such periods. Methods that are more complex could incorporate information from surrounding areas such as kriging (Clark 1979) or fitting time-space data to an assessment model that explicitly account for spatial dispersal and/or migration processes. In addition to imputing missing values, fishing effort should be standardized to account for known factors that alter catchability over time and space (i.e., gear configuration or technological improvements). Furthermore, the spatial scale of each stratum or spatial cell must be sufficiently small to make it reasonable to assume that sampling within each stratum was effectively random (i.e., that catch rates were proportional to abundance within the stratum).

Often, the fundamental assumption that catch rate (at the spatial resolution considered in the standardization) is proportional to local abundance is inappropriate. Handling time effects (Deriso and Parma 1987), fisher interference (Gillis and Peterman 1998), non-random species distributions within strata combined with small-scale response of effort to that distribution (Clark and Mangel 1979, Rose and Kulka 1999, Rose and Leggett 1991), gear saturation (Beverton and Holt 1957, Rodgveller et al. 2008, Sigler 2000), and local depletion effects (Hilborn and Walters 1992) can all make catch rate not proportional to abundance at even the smallest scale. Even at small spatial scales, hyperstability or hyperdepletion in *cpue* is a reality. The extent to which these local scale biases influence the Japanese longline data is unknown.

Analysis of a 1°x1° subset of the Japanese longline data indicated a high degree of variability in the proportion of each 5°x5° larger cell fished. Three common patterns in the proportion of area

fished were observed. Either the proportion of area fished increased over the first years of fishing and then declined, remained high, or remained a small proportion of the area. When only a small proportion of a 5°x5° area was fished, it is not possible to determine if stocks were concentrated into a few areas or if insufficient effort occurred in an area to warrant effort expansion. If the former mechanism were true then the area specific weighting used in averaging over larger (5x5 cell) strata would be over estimated. One would expect areas of high catch rate within a 5°x5° to be targeted as suggested by catch rates maps presented in Matsuda (1984) and Okamoto (2004) however, it is unknown if such areas were persistent or ephemeral. This potential bias due to non-representative sampling of fishing effort even at small spatial scales is an unfortunate reality when relying on fishery dependent data.

In this chapter, relative abundance trends are derived using variations of the simple method proposed by Walters (2003) for species captured in Japanese longline operations from 1950-2002. Resulting trends (referred to as 'spatial filling' trends) are compared to nominal *cpue*, the average *cpue* from fished areas (referred to as 'average *cpue*'), abundance trends generated assuming a temporally stable relative population distribution (referred to as 'Poisson model' trends), and trends utilized in current stock assessments by using various standardization methods.

Methods

Generating species and ocean specific abundance trends from Japanese longline monthly catch and effort data at a spatial resolution of 5°x5° required a number of assumptions. Species distributions in Chapter 2 are loosely defined by oceanographic characteristics. For catch rate analysis, stock distribution was defined more precisely using presence or absence in all spatial catch and effort data sets. Strata (5°x5° cells) were assumed to be within a stocks distribution if the observed total catch within the cell, summed over all periods, was greater than 0.01% of the maximum total catch for any cell. As a result, it is likely that stock distribution may not encompass the full species distribution for a given ocean. However, if significant accessible abundances existed outside the geographic extent of the fishery, it would be reasonable to expect

such areas to attract fishing effort. Fishing effort is assumed sufficiently random within a 5°x5° cell to generate a proportional relationship between catch rate and stock abundance within the cell. As mentioned earlier, it is difficult to determine if such an assumption is reasonable at a 5°x5° scale. However, finer scale data for all oceans over the period examined were not available in the public domain leaving 5°x5° data as the finest resolution available for longline data analysis.

Calculating ratio estimators

The simplest estimator (y_t) from spatial catch and effort data is 'nominal' *cpue*,

$$3.2) \qquad y_t = \sum_i C_{t,i} \left(\sum_i E_{t,i} \right)^{-1}$$

where catches ($C_{t,i}$) and efforts ($E_{t,i}$) are summed over all cells (i) to produce a single ratio of total catch to total effort. Such an estimator places more weight on those cells with more effort. Walters (2003) suggest a better estimator for ratios is to treat catch and effort data as a stratified random sample. The spatially weighted average catch rate from fished cells is calculated as,

$$3.3) \qquad y_t = \left(\sum_i w_i \right)^{-1} \sum_i w_i C_{t,i} E_{t,i}^{-1} \qquad if \quad E_{t,i} > 0$$

Here w_i is the size of cell (i) whose relative area can be approximated using the cosine of the latitude of each 5°x5° area. Equation 3.3 will still produce biased abundance trends if fishing effort is not randomly distributed over a species' distribution, since areas not sampled are assumed to behave as the mean of sampled areas.

Japanese longline effort is known to have spread from a few areas within the western central Pacific throughout the world's ocean. To avoid biases caused by assuming the cells fished to be representative of all cells it is necessary to make assumptions about catch rates in cells prior to first fishing (and post fishing for cells that were not fished in later years). Furthermore, strong seasonal changes in species distribution and the fishery must be considered when the space-time grid of fine-scale catch rate estimates is filled. Aggregating catch and effort over longer periods, one year, is likely to cause bias in the filling as species with seasonal movement patterns are

'smeared' across areas. Using a monthly period commonly results in insufficient catch records within cells to interpolate or extrapolate catch rates. A temporal aggregation of 3 months was used to calculate a spatially weighted average catch rate for each quarter (q).

3.4) $$y_{t,q} = \left(\sum_i w_i \right)^{-1} \sum_i w_i C_{t,q,i} E'^{-1}_{t,q,s,i}$$

In equation 3.4, effort E′ is standardized for changes in catchability due to set depth for each area. The estimator for a year was then calculated as the average of the quarterly estimators,

3.5) $$y_t = 0.25 \sum_i y_{q,t}$$

Four filling methods were explored for imputing $C_{t,q,i}$ for unfished cells. For the first three, catch rate in an area before fishing for each quarter was estimated as the average quarterly catch rate in the first three consecutive years that the cell was actually fished. If three consecutive years were not available, remaining years were used. If effort was no longer present in an area after some year, catch rate was assumed equal to the last observed catch rate (labeled SF31) or 0 (labeled SF30). Thus, local abundances were assumed not to have increased once effort departed or had been driven to 0. For both the methods, effort was standardized for each species to account for changes in catchability due to set depth. For comparison, a third method was explored similar to SF31 but where effort was not standardized (labeled SF31NE). The final method was a variation of SF31 where averaging over quarterly trends was not performed (see equation 3.5). In this instance catch rates for a given strata were calculated as the ratio of total catch summed over the year divided by total effort over the year. Imputed values prior to fishing were still taken to be the average of the first three observed annual catch rates and were assumed equal to the last observed catch rate once fishing effort had vacated an area (SF31NQ). In general, methods where missing values were imputed are referred to as 'spatial filling' methods.

Correcting for changes in catchability due to hook depth

In addition to accounting for the spatial distribution of fishing effort, significant changes in fishing technology and species targeting occurred over the history of the fishery. An attempt was made to standardized effort to account for changes in gear depth that may have influenced species catchability. Ward and Hindmarsh (2007) provide a review of historical changes in

pelagic longline gear and provide some estimation of potential changes in gear efficiency over time. Unfortunately, detailed information is not available in the public domain and the relative impact of each component on efficiency over time cannot be fully analyzed. However, some attempt was made to account for changes in species targeting by approximating depth of gear from coarse information on gear configuration such as hooks-per-basket (HPB; sets with higher HPB have a larger proportion of hooks fishing deeper). Average monthly HPB for 5°x5° areas in the Pacific Ocean for 1966 and 1975-2002 were calculated from 1°x1° effort and HPB data. HPB for areas prior to 1966 and before 1975 were assumed equal to HPB values for 1966. No spatially detailed HPB information could be obtained for Japanese longline operation in the Indian and Atlantic oceans, so average HPB by year for the Atlantic and Indian oceans were calculated from information on the proportion of sets using various HPBs configurations each year in each ocean. 1975-2000 HPB values for the Atlantic were obtained from Ward and Myers (2005a) and values for the Indian Ocean were taken from Dowling and Campbell (2002). For each ocean, average HPB prior to 1975 was assumed equal to estimated for 1975 and values post 2000 were assumed the same as 2000 values. Although such an approximation of changes in hook depth does not account for spatial heterogeneity in targeting specific depths, the general trend toward increasing depth of sets (higher HPB) is captured. Species-specific catchability varies with hook depth (Bigelow et al. 2002, Suzuki et al. 1977, Ward and Myers 2005a), decreasing for epipelagic species such as marlins as mean hook depth increases, and increasing for more mesopelagic species such as bigeye tuna. The strength of this effect is tied to oceanographic conditions such as thermocline depth and oxygen concentrations (Maunder et al. 2006a, Prince and Goodyear 2006). Unfortunately, the geographic extent of data on such effects is limited and only Ward and Myers (2005a) provide coefficients for a number of species to calculate changes in species-specific catchability as a function of mean hook depth. The Ward and Myers (2005a) study is restricted to 4 regions in the Pacific Ocean covering mainly tropical and sub-tropical waters within the central ocean, and it is unlikely that catchability corrections from their study apply precisely to areas with disparate oceanographic characteristics. However, the general trend in catchability for most species should be similar to that predicted from HPB changes for the Pacific studies.

The relationship between HPB and hook depth can be approximated from caternary geometry following the equation developed by Yoshihara (Suzuki et al. 1977). The depth of each hook (D_j) given its sequence (j), up to the middle hook(s), along the length of the mainline (L) within a basket, is a function of branch line length (h_a), float line length (h_b), number of HPB+1 (N), and the angle (φ) between the horizontal and tangential line of the mainline where the float line was attached (degrees from horizontal)

$$3.6) \qquad D_j = h_a + h_b + 0.5L\left\{\left(1+\cot^2\varphi\right)^{0.5} - \left[\left(1-2\frac{j}{N}\right)^2 + \cot^2\varphi\right]^{0.5}\right\}$$

Using values in Bigelow et al. (2006), h_a and h_b were set at 15m, mainline length was calculated assuming a branched line spacing of 50m as 50*(HPB+1), and φ was assumed a linear function of HPB increasing from ~52° at 5 HPB to ~65° at 20 HPB. Bigelow et al. (2006) indicate that hook depth estimated from this method is biased upward as longlines shoal in current, so that observed hook depth can be 10-50% shallower than predicted. Depths calculated using equation 3.6 were reduced by 20% in attempts to account for shoaling. Average hook depth given HPB was then calculated given estimated depth of each hook. Coefficients (Table 3.1) provided in Ward and Myers (2005a) were used to estimate how species-specific catchability changes with mean hook depth or HPB. Ward and Myers(2005a) predict relative catchability (q_D) using a third order polynomial,

$$3.7) \qquad q_D = \exp\left(\alpha + k_1 D + k_2 D^2 + k_3 D^3\right)$$

where k_1-k_3 are regression coefficients from Ward and Myers(2005a), D is depth (in this case average set depth), and α was selected so that relative catchability of a 5 HPB set was 1.

Coefficients for the q_D vs. hook depth relationship were not available for bluefin tuna species or Atlantic white marlin. Striped marlin values were used for white marlin, and yellowfin tuna values were used for bluefin tuna species. The catchability pattern for yellowfin was selected because it showed little change with depth. Although this pattern is not necessarily representative of the pattern for yellowfin in areas with shallower thermoclines and cooler surface waters, a degree of neutrality in relation to hook depth is reasonable to assume. Such an assumption was important for bluefin species as detailed spatial HPB information could not be obtained for the Indian and Atlantic oceans and only general trends in increasing set depth were used. Bluefin are

generally targeted using shallower sets and given bluefin tuna's high market value after the advent of deep-freezing, it is likely they were targeted if present. Assuming catchability change is relatively neutral with depth attempts to account for this depth targeting.

Relative changes in catchability given hook depth (Figure 3.1) for each cell for each species ($q_{D,s,i,t}$) were then used to rescale effort for each species, as

3.8) $$E'_{t,q,s,i} = q_{D,s,i,t} E_{t,q,i,t}$$

Since q_D was scaled to vary around 1.0 (for HPB=5), this rescaling results in effective efforts that increase over the long term (with long term increases in HPB) for some species, but decreases for others.

Estimators derived assuming a stationary population distribution

An alternative method for extracting relative abundance trends from catch rate data is to assume species have a stable spatial distribution, on average. Under this assumption, expected relative abundance ($\bar{y}_{t,m,i}$) for a given month, year, and area can be modeled as,

3.9) $$\bar{y}_{t,m,i} = p_{m,i} qN_t$$

where $p_{m,i}$ is the proportion of a stock in area i in month m and qN_t is the relative abundance for the total stock over its distribution in year t. If the probability of observing a given catch rate $y_{t,m,i}$ in any area in a given year and month ($p(y_{t,m,i})$) can be described using a Poisson distribution,

3.10) $$p(y_{t,m,i}) = \frac{e^{-\bar{y}_{it,m,i}} \bar{y}_{t,m,i}^{\,y_{t,m,i}}}{y_{t,m,i}!}$$

Then the total log likelihood (L) of observing all catch rate data can be written as,

3.11) $$L \propto -\sum_{t,m,i} p_{m,i} qN_t + \sum_{t,m,i} y_{t,m,i} \ln(p_{m.i} qN_t) \quad \text{if} \quad E_{t,m,i} > 0$$

Maximum likelihood values of $p_{m,i}$ and qN_t can be solved for using equations 3.12 and 3.13.

3.12) $$\frac{\partial L}{\partial p_{i,m}} = -\sum_{i,t} qN_t + \sum_{i,t} \frac{y_{i,m,t}}{p_{i,m}} \therefore \quad p_{i,m} = \frac{\sum_t y_{i,m,t}}{\sum_t qN_t}$$

3.13) $$\frac{\partial L}{\partial qN_t} = -\sum_{i,m} p_{i,m} + \sum_{i,m} \frac{y_{i,m,t}}{qN_t} \therefore \quad qN_t = \frac{\sum_{i,m} y_{i,m,t}}{\sum_{i,m} p_{i,m}}$$

Given an arbitrary initial $p_{m,i}$, such as $1/(n \times m)$, where n is the number of spatial areas and m is months, qN_t can be solved for. The resulting qN_t can then be used to determine updated values for $p_{m,i}$. This iterative process is continued until values converge to the maximum likelihood estimates implied by equations 3.12-3.13 (estimates for which $\partial L/\partial p=0$). An important condition for convergence of this estimation process is that only those areas that received effort be included. Bias in the estimation of qN_t or $p_{m,i}$ are likely to arise if effort is not sufficiently distributed in space and time to infer random sampling.

Results

Comparison between methods

Differences in relative abundance trends generated using the various methods described above for each ocean are quite substantial (Figure 3.2 to Figure 3.4). Of particular note are the large differences between averaging over all spatial cells (with imputation of missing space-time observations), compared to nominal *cpue* or to only averaging over fished areas, or, in many instances, to the Poisson method. In general, across most stocks analyzed, spatial filling trends imply fishery removals had less impact on population abundance than would be inferred from the other methods. Apparent variability in stock abundance is also considerably reduced. Nominal *cpue* trends tend to indicate the most severe declines, and have high inter annual-variation. Patterns for trends produced from averaging over fished only areas are less variable and suggest less population change, in most cases. Variability and apparent stock changes are further dampened in indices calculated with the Poisson model. Though these general patterns apply across most stocks examined, there are a number of exceptions and groupings of stock patterns that merit mention.

When missing catch rates values were not imputed, there was a tendency for mean catch rate to increase over the first few years, as for Indian Ocean bigeye or Atlantic yellowfin, or increase over the first 5-10 years, as with southern bluefin tuna or Atlantic Ocean southern albacore. After peaking, catch rates tended to decline at a similar rate as estimated during the increase. In some instances, rapid catch rate increases were followed by gradual declines, as calculated for bigeye tuna in the Pacific and Indian oceans. In contrast, catch rates for swordfish in the Atlantic and Indian oceans, as well as Atlantic bigeye, increase over time. The most dramatic declines in catch rate were estimated for yellowfin tuna, bluefin tuna, and blue marlin in the Pacific Ocean. A rapid decline in *cpue* in the late 1960s followed by a rapid increase was estimated for Atlantic bluefin tuna (Figure 3.3).

When missing catch rate values were imputed, catch rates were estimated to have declined more gradually over time as did trends generated using the Poisson model. Poisson model trends did tend to deviate from imputed trends during early years. This discrepancy is particularly noticeable for Pacific yellowfin and blue marlin. Discrepancies between these two approaches are even greater for trends in Atlantic Ocean stocks (Figure 3.2).

Table 3.2 presents apparent decline/increase in stock abundances inferred from the four different relative abundance indices calculated as the percentage difference between the average relative abundance over the first decade of fishing and an average of the last decade. First year of fishing activity in the Indian Ocean is assumed to be 1952, 1950 for the Pacific, and 1956 for the Atlantic. Differences in stock change indicated by each method are obvious and tend to agree with the trend patterns described above; spatial filling methods suggest less reduction in most instances. Relative abundance changes inferred from nominal *cpue* are markedly different from those inferred with spatial filling. Differences in trends for Pacific bluefin tuna (nominal *cpue* 8% compared to spatial filling 24%), Atlantic yellowfin (8% compared to 27%), and Atlantic white marlin (3% compared to 46%) are striking examples. In the Indian Ocean, nominal *cpue* trends suggest an increase in bigeye tuna relative to the early decade (108%). This is in stark contrast to the decline (59%) indicated using spatial filling. In a few instances, the various methods agree (i.e. southern bluefin tuna, northern Atlantic albacore tuna, and Indian Ocean yellowfin tuna).

Comparison between methods with imputation

Four variations of the spatial filling method for each stock are presented in Figure 3.5 to Figure 3.7 (SF31, SF30, SF31NE, and SF31NQ). For all stocks, trends generated using the SF30 method suggest more rapid population declines with greater amplitude fluctuations. This pattern is very noticeable for all albacore stocks, except north Pacific albacore, as well as white marlin in the Atlantic, striped marlin in the Pacific and to a lesser degree yellowfin and blue marlin in all oceans. SF30 indices suggest more rapid declines during the mid 1960s to mid 1970s. In a number of instances, not averaging across quarterly trends (SF31NQ) produces a similar though less dramatic result. Albacore and yellowfin stocks are clear examples of this effect as well as blue marlin in the Atlantic and Pacific oceans. There are some differences between SF31 trends and those produced using nominal effort (SF31NE). For species such as bigeye and albacore, where catchability was assumed to increase substantially with average hook depth, trends using nominal effort suggest less decline. In the case of northern Pacific albacore, the suggestion is greater increase. The difference for marlin stocks, where catchability was assumed to decline with hook depth, is less dramatic with trends using nominal effort suggesting a slightly greater decline than when effort is standardized.

Comparison with indices used in stock assessment

Ultimately, relative abundance trends are incorporated into stock assessments, and it is worthwhile to compare the results from the spatial filling method for the Japanese longline data with the trend estimates utilized in stock assessments produced from the tuna RFMOs. Figure 3.8 to Figure 3.10 present a comparison between trends used by RFMOs and SF31 trends. Trends have been broken down for the smaller sub areas utilized in stock assessment (particularly in the Pacific Ocean). For some stocks, comparison was not possible because assessments were not available, official abundance trends had not been developed, or catch and effort data from a different fleet had been used. For those stocks where comparisons were possible, the geographic stratification used by the RFMOs and stock assessment documents from which the relative abundance indices were taken are presented in Table 3.3.

In the Pacific Ocean, there is general agreement between abundance trend indices. Here, agreement implies similarity in trend and relative overall change. Discrepancies do arise early in the time series, with stock assessment trends suggesting initial declines that were greater and more rapid than indicated by SF31. Comparisons for eastern Pacific yellowfin and northern albacore tuna agree over the period of overlap, though no comparison can be made for earlier years.

Indian Ocean trends agree less. Eastern swordfish, southern bluefin, and bigeye tuna track each other over the period of overlap. The albacore index used for assessment suggests less of a decline over the period. The trend used for yellowfin tuna assessment suggests a more rapid decline in abundance.

In the Atlantic, the index used for southern albacore suggest a substantially greater decline in abundance than does SF31, as does the trend used for white marlin. Eastern bluefin trends near the end of the time series are contrary, with the assessment trend indicating a stock decline.

Discussion

Each the four methods presented required a number of underlying assumptions for estimates to be proportional to population abundance. It is not possible, given the data available for this analysis, to explore all violations of those assumptions, particularly for processes that may cause hyperstabilty or hyperdepletion in catch rate at the 5°x5° scale. However, major differences in relative abundance trends produced can be explained by the failure of some methods to account for historical changes in the Japanese longline fleet. In particular, it is easily seen how spatial and seasonal expansion and redistribution of the Japanese fleet, in response to changes in primary target species and development policies, impacted the way species distributions were sampled. It is worth exploring the differences on a case-by-case basis to highlight how such strong biases arose in nominal *cpue* trends, and to highlight the importance of imputing missing space-time observations.

One important case to consider is that of yellowfin tuna given its prevalence in the longline catch and the dominant influence it has when catch is aggregated over species to calculate community level catch rates such as those used by Myers and Worm (2003). Nominal *cpue* of Pacific Ocean yellowfin tuna declined dramatically in the first three years (Figure 3.3). This rapid decline is mitigated to some degree when catch rates are averaged over areas fished in attempts to eliminate biases due to disproportionate effort sampling, but early patterns in *cpue* are dominated by spatial and temporal expansion as well as changes in fleet composition. As mentioned in Chapter 2, catch and effort data for 1950 and 1951 are from a few mothership operations working in 16 or 17 5°x5° areas within the western central Pacific for 6 months of the year with effort concentrated in a few months (Figure 2.5). The spread of effort seasonally from 1950 to 1951 is apparent. These motherships were operating in the core of yellowfin tuna habitat. The first decline in nominal *cpue* was due to an extension of the fishing season, not overall stock reduction: *cpue* declined because effort spread into months when catch rate was lower. By 1952, restrictions on Japanese fleet movements were lifted and effort increased substantially. Licensing restrictions and an active promotion of fishery expansion resulted in fishing effort being distributed outside the core yellowfin areas. Thus, new effort entering the fishery expanded into areas with lower *cpue*. This effect can be clearly seen when the average *cpue* is calculated over cells grouped by the first year the cells were fished, and plotted over time (Figure 3.12). It is obvious from such plots that fishing effort expanded into areas of lower catch rates (areas that had lower *cpue* when first fished), and these areas were more numerous and effort was substantially larger. As a result, nominal *cpue* averaged over fished areas declined quickly. It is important to note that catch rates in those areas initially fished in early years remained high throughout the record, and in fact even initially increased. This increase in catch rate for mothership operations is also confirmed in records presented by Matsuda (1984). There is a similar effect in the Indian and Atlantic oceans (Figure 3.2 and Figure 3.4), except *cpue* in areas initially fished were low and it was in subsequent years that core areas for yellowfin tuna were found (Figure 3.11 - Figure 3.13). One troubling trend can be seen in the Atlantic Ocean, where *cpue* in the core area did not remain above other areas but instead declined quickly and became similar to that of other clusters of cells first fished later. This difference warrants further discussion.

A similar pattern apparently occurred for the tropical blue and black marlin. Fishing effort was initially concentrated in tropical areas, and as the fishery expanded into areas that were more temperate and across seasons it progressed out of core tropical habitats so that nominal *cpue* declined. Nominal and averaged *cpue* trends fail to account for non-representative sampling of time area strata and as a result, abundance indices show hyperdepletion.

A similar analysis of average *cpue* aggregated over cells by years when the cells were first fished helps to explain the patterns of nominal *cpue* trends in albacore and bigeye tuna (Figures 3.11-3.13). Low initial catch rates for north Pacific albacore are easily explained because data for the first 2 years came from mothership operations in the tropical western Pacific that were targeting yellowfin. By 1952, a much larger fleet was included in the statistics, and catches from core albacore areas were included in the statistics. As a result, nominal catch rates increased. It is clear in Figure 3.12 that the core areas produced relatively high *cpue* compared to other areas, over most of the history of the fishery. South Pacific albacore *cpue* increased as the fishery expanded into core habitat, as was the case with Indian and Atlantic oceans albacore tuna. However, much like patterns for yellowfin tuna in the Atlantic and unlike the pattern for north Pacific albacore, catch rate in all areas became homogeneous and low by about the mid 1970s. Interpreting this pattern is difficult. The simplest interpretation is that all areas were depleted. Unfortunately, this interpretation does not explain the high catches and catch rates achieved by other nations in subsequent years.

By the mid 1970s, much of the Japanese fleet had switched from targeting yellowfin and albacore tuna to bigeye and bluefin tuna. As a result, areas of high albacore catch rate within a given 5°x5° area were potentially abandoned causing average catch rate of each area to decline. During the mid 1970s, there was a noticeable shift in the seasonal timing of effort (Figure 2.5) and the decline in albacore *cpue* in each area could be due at least partly to shifts in the seasonal effort weighing. However, when data by year first fished cell clusters are averaged over quarters, the low catch rate effect remains. No attempts were made in this study to correct average *cpue* for potential changes in species-specific catchability arising from alterations in gear configuration other than hook depth, and it is entirely possible that such changes had an impact on albacore catch rates.

The trend in all oceans for bigeye tuna is straightforward to explain. The Japanese fleet moved into areas of high bigeye catches rates, causing nominal *cpue* to increase. As the fishery began targeting bigeye, catch rates further increased in some areas. This effect is dramatic in the Atlantic Ocean where catch rates on average increase over most of the period examined. Figure 3.2 to Figure 3.4 clearly show how the spatial filling method corrects the biases introduced by shifting effort distributions relative to the bigeye tuna distribution.

Nominal *cpue* patterns for southern and Pacific bluefin tuna can also be explained by shifts in the spatial distribution of effort relative to species distributions, although strong year classes likely dominate the pattern for Pacific bluefin. However, attempts to explain the pattern in the nominal *cpue* for Atlantic bluefin stocks or striped marlin and white marlin expose some of the weaknesses in the spatial filling approach, as well as weaknesses in attempts to standardize for changes in catchability. Nominal *cpue* patterns for Atlantic bluefin tuna are strongly influenced by the shifting mosaic of Japanese longline effort (Figure 2.7); rapid increase in *cpue* up to 1965 and then decline to 1970 likely resulted from the discovery and subsequent depletion in an aggregation of bluefin tuna off the east coast of South America. Catch rates then increased again as the fleet expanded northward, and new aggregation were encountered sequentially in the Gulf of Mexico, off the eastern coast of North America, in the Mediterranean Sea and finally near the end of the 1990s in the northern Atlantic Ocean. The spatial filling methods attempt to account for shifts in effort distribution by back filling over time. However, it is difficult to determine what catch rates would be appropriate for backfilling given the long duration of the backfilling period and the migratory nature of Atlantic bluefin tuna. In particular, it is quite possible that many spatial cells had abundance declines well before they were first fished, due to fishing impacts on the overall abundance of fish available to migrate into those cells.

Patterns seen in the *cpue* averaged by first year fished for Atlantic white marlin (Figure 3.13) also call into question the appropriateness of only standardizing effort for changes in catchability due to changes in hook depth. As catch removals increased in the early 1960s, *cpue* in most areas increased. When *cpue* is spatially averaged and missing time area data are imputed, an increase in mean *cpue* is still apparent (Figure 3.4). While some learning by the fleet is expected in new

areas, hence the necessity of averaging over the first few years of *cpue* when back filling, the strong increasing pattern hints at changes in catchability over time due to some factor beyond learning. Similar patterns can also be seen in catch rates for Pacific striped marlin (Figure 3.12) and striped marlin in the Indian Ocean (Figure 2.5), with *cpue* increasing in the mid 1960s, followed by an abrupt decline through the 1970s and an increase again in the 1980s. There is evidence that a component of the Japanese fleet was actively targeting striped marlin during the high *cpue* periods (ISC 2006), and white marlin may have been targeted as well. Although this targeting partly involved low HPB (to keep hooks near the surface), altered float line or branch line length would have further reduced gear depth and depth corrections applied in this study would not fully capture the targeting methods.

Spatial effects had an overriding impact on trends in nominal *cpue* or *cpue* averaged over only those areas fished each year, particularly when a fishery expands or significantly shifts its distribution. However, changes in species targeting by tactics other than choice of fishing region are also an important consideration. Standardizing effort for changes in species-specific catchability has a noticeable effect on estimated abundance trends when such changes are predicted to be large. In Figure 3.5 to Figure 3.7 (compare SF31 with SF31NE), correcting for changes in bigeye catchability as hook depth increased had a substantial effect on relative abundance trends. In all cases, abundance declines are estimated to have been larger over the period in question. Ward and Hindmarsh (2007) demonstrated the potential impact that changes in gear configuration or technology can have on species-specific catchability over time. One of the limitations in the analysis presented in this chapter is sole reliance on spatial or aggregated HPB information to capture such effects. In the method presented here, correcting for changes in catchability with hook depth relied on observations from a restricted area of the Pacific Ocean and do not necessarily reflect changes that occurred in areas with differing oceanography. Suzuki (1977) demonstrated a different impact of depth on the catchability of yellowfin and albacore tuna, in western versus eastern Pacific areas. Prince and Goodyear (2006) noted how cold hypoxic water in the eastern tropical Pacific and Atlantic oceans restricted the vertical distribution of tuna and billfish. Habitat compression could result in a noticeably different relationship between hook depth and catchability than that measured in the central Pacific where the thermocline is deeper. Bigelow and Maunder (2007) suggested that considering only hook

depth can lead to serious misinterpretations when developing relative abundance trends, due changes in species-specific vertical distributions in response to temperature and oxygen. The analysis presented here does not account for all factors that could have influence catchability over time and the method applied to account for changes in hook depth is problematic. Applying observation from a restricted area within the Pacific to all areas in the world oceans and assuming effects are similar is obviously erroneous. Unfortunately, until operational-level information is made available or more studies are performed to separate the relative impact of various factors on catchability, further correction is not possible.

Walters (2003) stresses that missing data cannot be ignored and deliberate consideration must be given to assumptions that are made when filling missing time-area strata. Some concerns regarding the spatial filling methods used have already been raised, but a more thorough examination of the methods applied is required. The values used to fill missing strata have a noticeable impact on the resulting abundance indices (compare methods SF30 with SF31 in Figure 3.5 to Figure 3.7). Given the number of nations involved in tuna fisheries, it would seem logical that once Japanese effort abandoned areas, catch rates from other longline fleets still fishing could be utilized to extend the trend patterns. Unfortunately, it is not possible to develop an informative correlation between Japanese *cpue* and that of any other fleet, because there is very little overlap in space and time. It is also unlikely that Japanese vessels abandoned areas because the catch rate had declined to 0, considering that other nations fished the same areas later and apparently found them still profitable.

Filling forward in time with the last observed *cpue* is also problematic, particularly for long periods. For example, forward filling in Figure 3.14 panel C, may seem a reasonable approach since the period filled is relatively short and data are available after each filling period. However, this ignores the possibility that abundance in the areas was in fact patchy, possible due to inter-annual variability in species distribution, and indeed declined to 0 resulting in effort leaving. However, the analysis also included examples like Figure 3.14 panel E, where the same *cpue* was used to fill forward for 30 years. It is unrealistic to assume abundance within the area did not change over such a long time. The pattern presented in panel E is quite typical for areas near the

edge of species distributions, and it is possible that such areas were fished out completely; however; it is more likely that low catch rates in these areas made them unattractive.

There are also a number of concerns about filling backward in time prior to the start of Japanese longline fishing. If one were developing trends for a sessile organism, it might be reasonable to backfill with the first observed *cpue* and to assume that within each area the organisms were at equilibrium abundance until first fished. However, tuna and billfish are highly mobile and in some cases follow migratory routes, so there is considerable potential for harvesting impacts in one area to cascade into other areas. There are also clear indications (see Figure 3.11 to Figure 3.13) that catch rates increased over the first few years of fishing as experience was gained in new areas. When filling backward in time, the relative impact of learning effects should be considered and some diagnostics aid in determining which effects dominate the observed patterns. Figure 3.15 presents result from a simple spatial simulation where the impact of varying levels of fishing intensity on population abundance in surrounding cells was explored under various simple movement scenarios. For the simulation presented, movement was assumed purely diffusive and recruitment into each area was assumed constant. When fishing mortality rates were low, the simulated impact on surrounding areas was minor except when mean dispersal distance was low. In these instances, a small effect was evident. As fishing rates were increased, the impact of local depletion increased in surrounding areas. As mean dispersal distance increased, local impacts spread further but were diluted resulting in similar abundances in all areas.

Plots of mean *cpue* of areas grouped by first year fished should contain distinct patterns depending on the combination of fishing mortality and movement rates that occurred during the initial expansion of the Japanese fishery. If fishing mortality and movement rates were low, *cpue* patterns in such plots should represent expansion into areas of high or low abundance because the impact of local fishing mortality on area clusters fished later should be negligible. For higher mortality rates but low movement rates, local depletion effects should be seen. Cpue of each area grouping should have declined but impacts should not have filtered into areas fished later, so that declines seen in those areas fished later should appear independent of the declines in areas first fished earlier. If fishing mortality was moderate and movement high, then areas should have

responded to both local and widespread depletion, i.e., should have behaved less independently such that all areas should have declined along the same trajectory. Inspection of Figure 3.11 to Figure 3.13 suggests initial fishing mortality rates were low and as fishing mortality increased, clusters appear to deplete independently suggesting lower mixing rates. There are, however, exceptions: blue marlin in the Pacific and Atlantic as well as yellowfin tuna in the Atlantic. It is difficult to know if the patterns for these stocks are the result of higher movement rates or if there was confounding with the shift to targeting bigeye and bluefin. Such an analysis also raises concern with the forward filling method used. It is likely that as mortality rates increased, the impact on surrounding areas also increased to at least some degree, implying that filling forward with the last observed *cpue* may be inappropriate, as fishing in surrounding areas would deplete local abundance. In the end, a three-year average was chosen for backfilling to balance depletion effects due to movement and increasing *cpue*, potentially due to gaining experience with an area. For short periods, filling with an average value seemed reasonable (Figure 3.14 panel D) however, for the reason mentioned above (Figure 3.14 panels E and A), confidence in using a simple mean value is weakened.

Seasonal changes in species distribution and targeting of a fleet must be considered when backfilling. For fisheries that operate within a single season such effects are likely negligible, but for fisheries that operate throughout the year, ignoring seasonal effects can introduce bias particularly when backfilling is required. Abundance trends should be developed for each quarter to avoid 'smearing' fish across areas due to seasonal movement patterns and to prevent biases introduced by giving more weight to seasons with more effort. For each quarterly trend, spatial backfilling and forward filling are required. The biases introduced by not averaging over quarterly trends can be seen in Figure 3.16, or compare the SF31 trend to SF31NQ in Figure 3.5 to Figure 3.7 where the range and average of quarterly trends is compared with no averaging for stocks in the Pacific Ocean. The effect for yellowfin tuna and blue marlin is noticeable. Not averaging over quarters caused abundance trends to decline faster than quarterly trends. Such a result is somewhat counter intuitive. The expectation, in the absence of quarterly averaging, would be a more variable trend bounded by quarterly trends. However, it is the bias introduced by backfilling over time with *cpue* values biased by seasonal effort concentrations that causes at least some hyperdepletion. As shown in Figure 2.6, effort in most areas was only focused in a

few months. These were months when catch rates were high and not representative of the average catch rate throughout the year.

One final concern when imputing missing catch rates is the potential impact of targeting changes. While spatial impacts appear to have a substantial effect on trends produced, in some instances species specific targeting may have also had a noticeable effect. Panel A in Figure 3.14 for Atlantic bluefin tuna is particularly worrisome. Effort in the late 1960s and early 1980s did not produce high catch rates of Atlantic bluefin tuna. However, when effort returned in the 1990s, catch rates steadily increased. This is a common pattern for bluefin tuna in the north Atlantic. It is possible to interpret this pattern in a number of ways. In earlier periods, effort was not targeting bluefin tuna; in the 1990s, targeting of bluefin occurred and as experience was gained, catch rates increased. Such an interpretation would indicate that all values prior to fishing in the 1990 should have been filled with a higher *cpue* even though catch rate was observed to be 0. Alternatively, abundance in the area could have increased in the 1990s due to distributional shifts or increasing stock abundance. If this were the case, the filling method used would be inappropriate. Information about such subtleties at the operational level, such as which species were targeted, are necessary to make more informed decisions regarding which *cpues* are appropriate when filing space/time strata.

It is common practice to derive relative abundance trends using established statistical procedures such as GLMs. Provided all factors being standardized for have been sampled representatively, simulation studies have shown that the extracted year effects track population abundance well (Campbell 2004, Maunder and Punt 2004). However, there are clearly strong time interactions due to the expansion and shift in targeting that occurred in the Japanese fleet, so that seasonal and spatial sampling was not representative. To circumvent this complication, many abundance trends have been standardized only for periods when Japanese effort had sufficient spread to cover most areas; further, assessments using such trends have also relied on additional information such as stock composition to determine fishing mortality rates. The comparison between the abundance trends used in stock assessments and those derived with spatial filling (Figure 3.8 to Figure 3.10) suggests in many instances that the trends match well for the period of comparison. Within the Pacific, discrepancies that arise early in the *cpue* time series for

western yellowfin and bigeye likely resulted from biased sampling over space and time. A similar bias can be seen in trends produced using the Poisson model (Figure 3.6) which also declines faster in the first few years. Comparison between the three methods suggests average seasonal distributions within areas and average population distribution can be resolved from the *cpue* data. However, the year effect was not sampled representatively in the early years of the fishery. This pattern can also be seen for blue and striped marlin. In the Atlantic Ocean, where discrepancies from assessment trends for southern albacore tuna and white marlin compared to spatial filling are likely due to strong time-area interaction that were not accounted for in the standardization models. Both of the marlin assessment trends closely match the Poisson model (Figure 3.7), indicating that time-area and time-season interaction were not sampled in a representative way. The discrepancy in trends for Atlantic bluefin tuna is not so easily explained and may hint at biases introduced when backfilling over long periods. In the Indian Ocean, disagreement between methods for yellowfin in the early years can be explained by non-representative sampling of time interactions with season and space. Here again, the assessment standardized trend is more similar to the trends produced from the Poisson model.

When spatial catch and effort data are available, Walters (2003) stresses the importance of imputing missing catch rate data when averaging over spatial areas to create relative abundance trends. Careful consideration should be given to the appropriateness of the method used to impute missing values. Ignoring missing space-time strata can cause severe bias in relative abundance time series particularly during expansion, shifts, or contraction of a fishery's distribution. Using nominal *cpue* or *cpue* averaged over only those areas fished is akin to imputing missing *cpue* values as equal to the effort weighted mean *cpue* or the average *cpue* of fished areas. In instances where spatial data are not available, great care must be taken when using nominal *cpue* as an abundance trend. Expansion of the Japanese fleet to areas outside the core distribution of yellowfin tuna stocks in all oceans resulted in severely biased nominal *cpue* trends and in trends produced from GLM standardization when records back to 1950 were used. When nominal *cpue* trends were aggregated across species this bias in the yellowfin trend dominated the resulting trend, leading to an erroneous interpretation of the overall impact of industrialized fishing on the larger pelagic tunas and billfishes. Had a method of imputing missing time-area strata been used to develop abundance trends, a different conclusion as to the

effects of industrialized fishing would have been drawn. Comparing the first decade of fishing to the last decade examined here, the overall pelagic stock appears to have been depleted by 51% (Table 3.2) though the variability is high (CV= 0.76). Even if apparent depletion levels were presented for each stock, such information only allows the use of general rule of thumb to evaluate stock status in relation to targets. Without a better understanding of underlying production relationships, it is difficult to draw conclusion about stock status.

Table 3.1 Coefficients for determining changes in catchability due to hook depth for species considered in the analyses presented in this thesis; coefficient estimates from Ward and Myers(2005a)

Species	k_1	k_2	k_3
Albacore tuna	9.44	-20.34	13.81
Bigeye tuna	7.83	-12.25	7.2
Yellowfin tuna & Bluefin tuna sp.	1.73	-6.05	5.32
Blue marlin	-3.77	1.83	1.86
Striped & white marlin	-3.82	-2.3	6.29
Black marlin	-9.48	22.77	-16.81
Swordfish	2.74	-11.45	11.84

Table 3.2 Apparent change in stock abundance using four different relative abundance indices calculated as the percentage difference between the averaged over the first decade of fishing and the last decade. First year used for the Indian Ocean is 1952, for the Pacific is 1950, and for the Atlantic is 1956. Columns represent the different methods shown in Figure 3.2 to Figure 3.4. **Nominal** is nominal *cpue*, **mean fished** is the average *cpue* from fished areas, **Poisson** is derived assuming a Poisson model and **spatial** is derived averaging over all areas with missing space/time strata imputed (see description of SF31 in methods).

Stock	Nominal	Mean Fished	Poisson	Spatial
IALB	36	11	11	14
IBET	108	47	47	59
IYFT	27	17	18	23
GSBT	19	19	7	20
IBUM	9	8	9	15
ISTM	8	11	10	27
GBLM	3	4	5	20
ISWO	208	134	132	126
PNAB	21	71	114	170
PSAB	34	16	39	42
PBET	53	25	32	34
PYFT	34	20	39	46
PBFT	2	7	12	24
PBUM	17	12	23	27
PSTM	26	44	50	60
PSWO	20	54	67	92
ANAB	18	13	11	18
ASAB	2	4	4	24
ABET	243	105	88	75
AYFT	8	9	9	27
ABFT	104	105	47	63
ABUM	17	15	22	35
AWHM	3	6	9	46
ASWO	236	145	133	93

Table 3.3 Areas subdivisions and references for relative abundance trends used in stock assessments by RFMOs. Repeat references are marked with (").

Ocean & Stock	Area	Reference
Indian Ocean		
Albacore	All	(IOTC 2004b)
Bigeye	All	"
Yellowfin	All	"
Southern Bluefin	All	(CCSBT 2006a)
Blue Marlin	All	No Assessment
Striped Marlin	All	No Assessment
Black Marlin	All	No Assessment
W. Swordfish	<80E	(IOTC 2004b)
E. Swordfish	>80E	"
Pacific Ocean		
N. Albacore	>0N	(ISC 2008a)
S. Albacore	<0N	(Langley 2006)
WCPO Bigeye NW	<170E, >20N	(Hampton et al. 2006a)
WCPO Bigeye NE	>170E->150W, >20N	"
WCPO Bigeye W	<170E, <20N->10S	"
WCPO Bigeye E	>170E->150W, <20N->10S	"
WCPO Bigeye SW	<170E, <10S	"
WCPO Bigeye SE	>170E->150W, <10S	"
EPO Bigeye R8	<150W, >15N	(Maunder and Hoyle 2007)
EPO Bigeye R9	<150W, <15N	"
WCPO Yellowfin NW	<170E, >20N	(Hampton et al. 2006b)
WCPO Yellowfin NE	>170E->150W, >20N	"
WCPO Yellowfin W	<170E, <20N->10S	"
WCPO Yellowfin E	>170E->150W, <20N->10S	"
WCPO Yellowfin SW	<170E, <10S	"
WCPO Yellowfin SE	>170E->150W, <10S	"
EPO Yellowfin N	<150W, >15N	(Hoyle and Maunder 2007)
EPO Yellowfin S	<150W, <15N	"
Northern bluefin	All	No Assessment
Blue marlin	All	(Kleiber et al. 2002)
Striped marlin	All	(ISC 2006)
NE swordfish	<150W, >5S	(Hinton et al. 2004)
SE swordfish	<150W, <5S	"
Atlantic Ocean		
N. albacore	>5N	(ICCAT 2007a)
S. albacore	<5N	"
Bigeye	All	(ICCAT 2005)
Yellowfin	All	(ICCAT 2004a)
Western bluefin	>10N, <45W and <10N, <25W	(ICCAT 2003a)
Eastern bluefin	Remaining Area	"
Blue marlin	All	(ICCAT 2006c)
White marlin	All	(ICCAT 2003c)
N. swordfish	>5N	(ICCAT 2003b)
S. swordfish	<5N	"

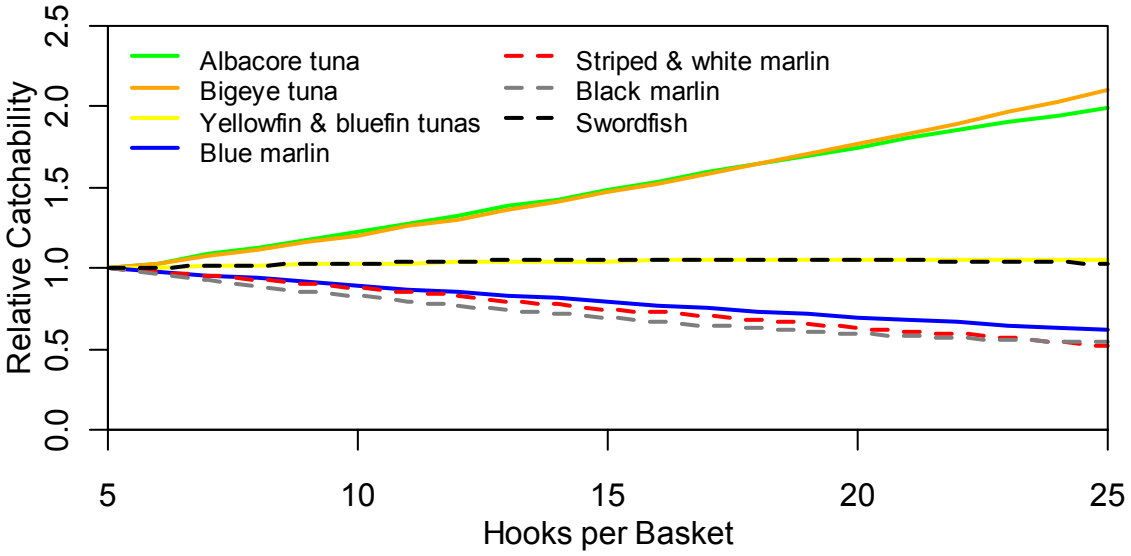

Figure 3.1 Relative changes in species catchability estimated as a function of hooks between floats.

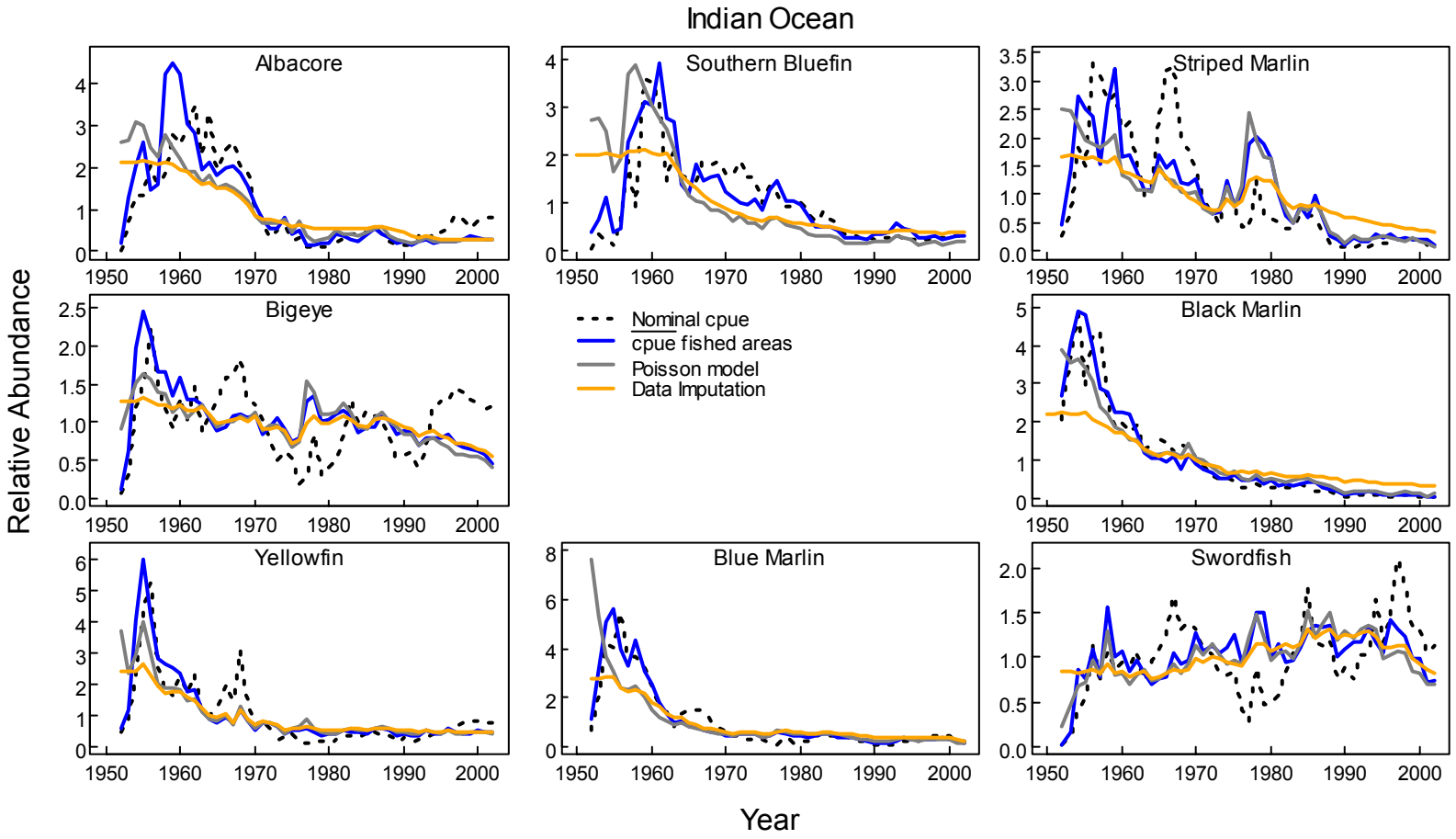

Figure 3.2 Relative abundance indices developed using four different methods, standardized to their mean, for stocks in the Indian Ocean from 1952-2002. Indices demarked by dashed black lines are nominal *cpue*. The blue lines were produced by averaging *cpue* over only those areas fished. The grey lines indicate indices created using the Poisson model. The orange lines are the spatially weighted average of all areas, where missing values were imputed using the SF31 variation. Note that black marlin and southern bluefin tuna are found in multiple oceans.

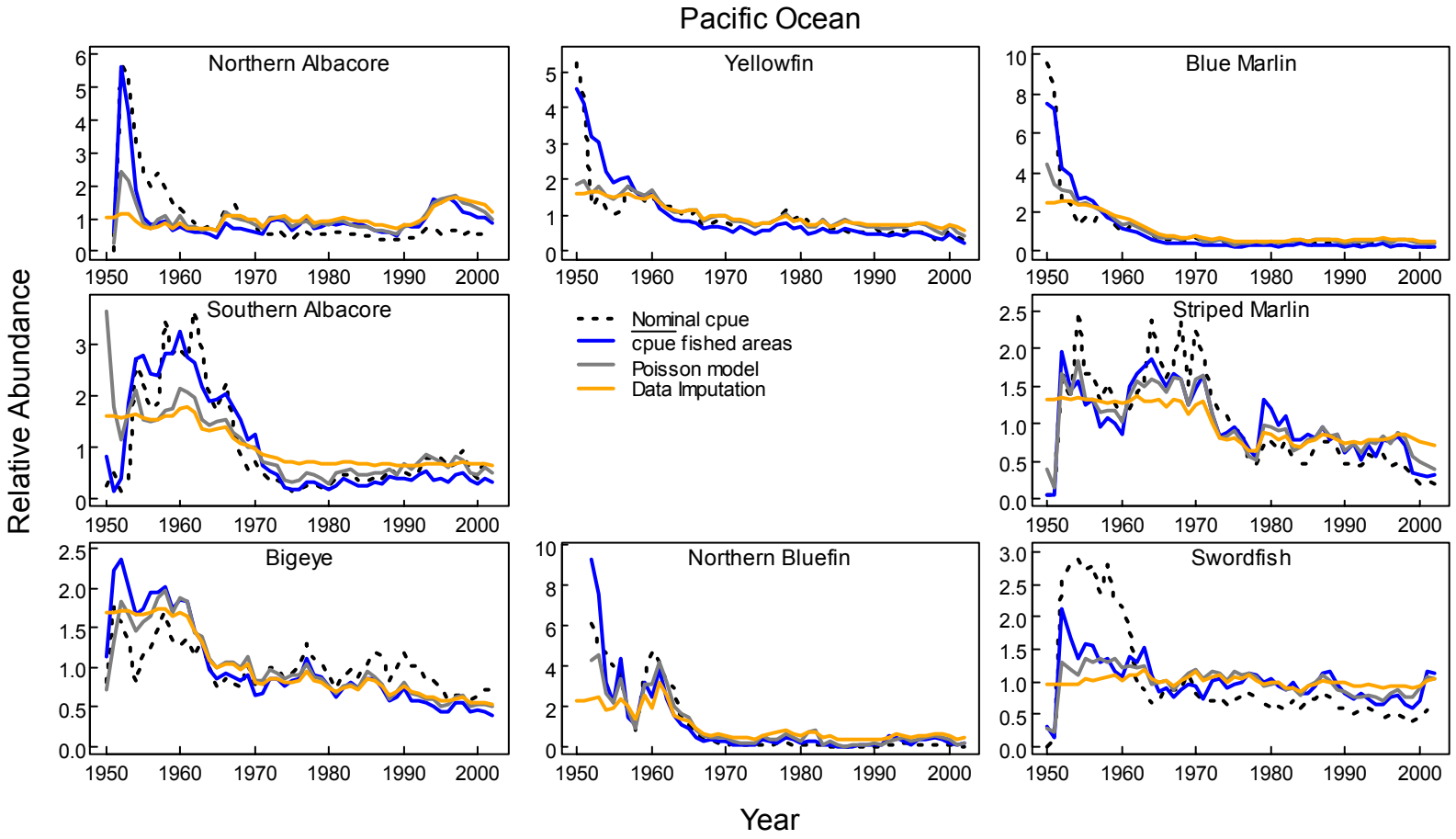

Figure 3.3 Relative abundance indices developed using four different methods, standardized to their mean, for stocks in the Pacific Ocean from 1950-2002. Indices demarked by dashed black lines are nominal *cpue*. The blue lines were produced by averaging *cpue* over only those areas fished. The grey lines indicate indices created using the Poisson model. The orange lines are the spatially weighted average of all areas, where missing values were imputed using the SF31 variation. Note that black marlin and southern bluefin tuna are found in multiple oceans.

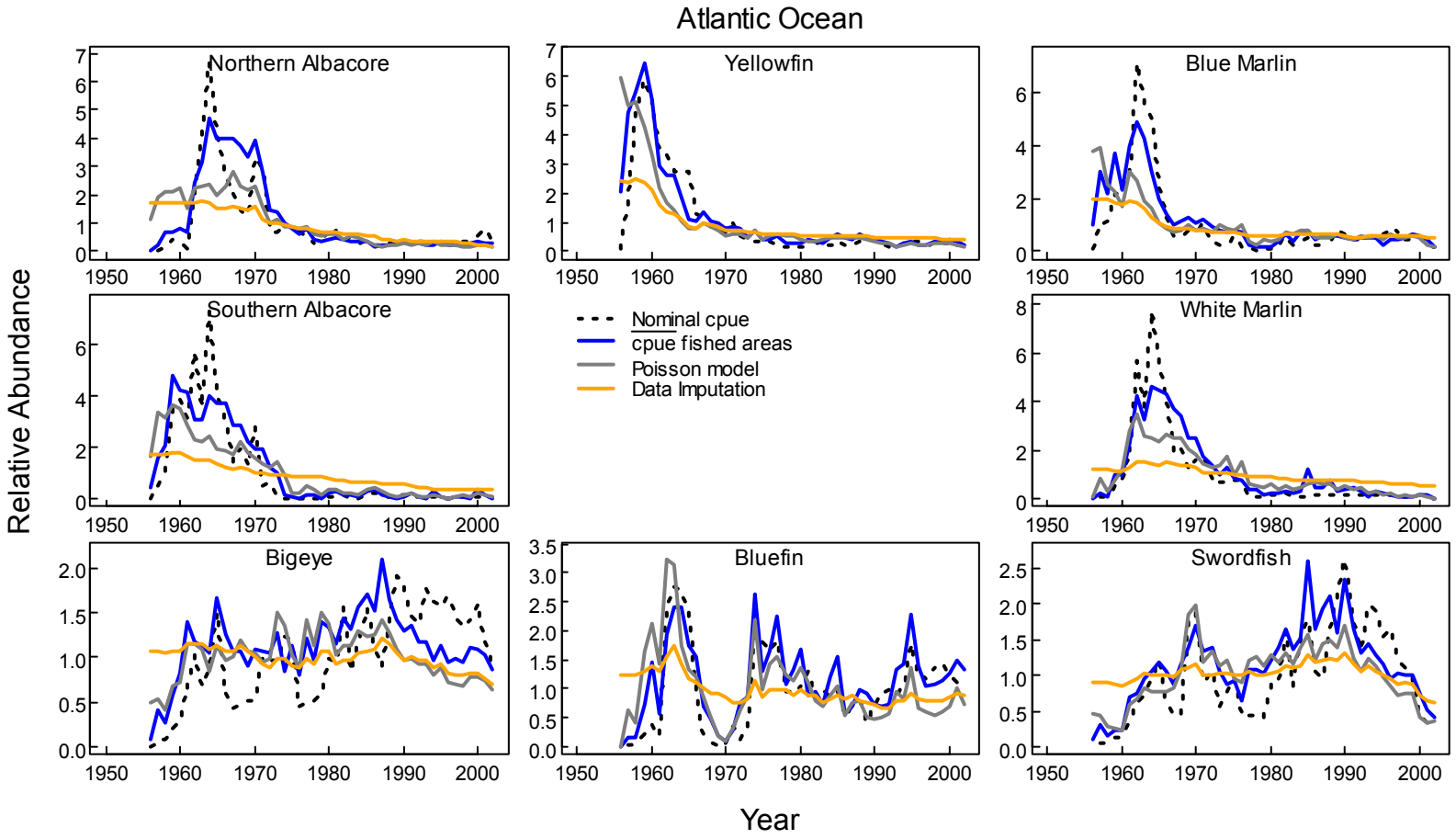

Figure 3.4 Relative abundance indices developed using four different methods, standardized to their mean, for stocks in the Atlantic Ocean from 1956-2002. Indices demarked by dashed black lines are nominal *cpue*. The blue lines were produced by averaging *cpue* over only those areas fished. The grey lines indicate indices created using the Poisson model. The orange lines are the spatially weighted average of all areas, where missing values were imputed using the SF31 variation. Note that black marlin and southern bluefin tuna are found in multiple oceans.

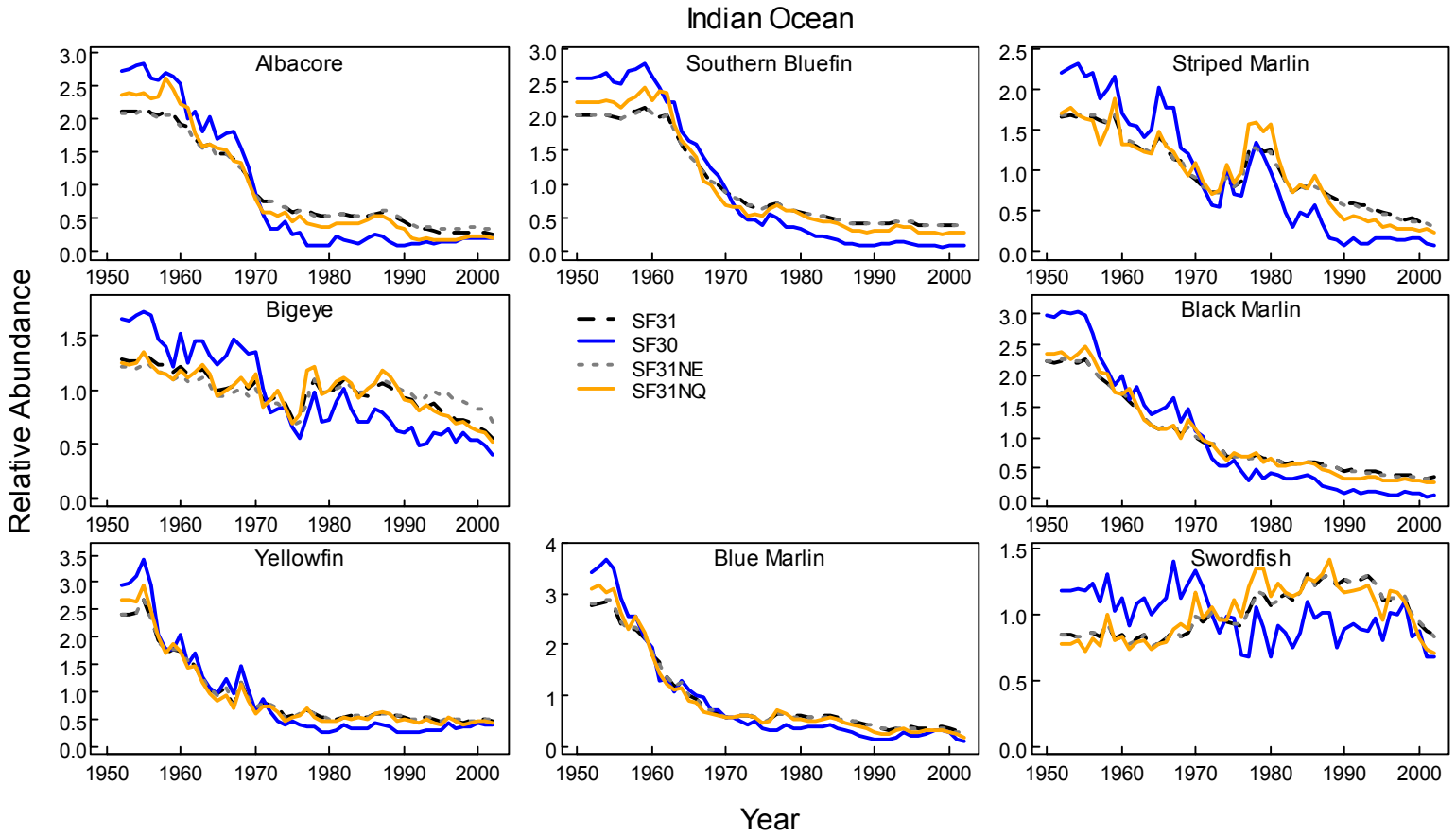

Figure 3.5 Relative abundance indices developed using four variations of the spatial filling method, standardized to their mean, for stocks in the Indian Ocean from 1952-2002. Indices demarked by a dashed black line were developed using the SF31 variation where missing values were imputed as the average of the first 3 years fished prior to fishing and the last observed *cpue* once abandoned. The blue line, SF30, is similar to SF31 but *cpue* was assumed 0 once and areas was abandoned. The dotted light grey line is similar to SF31 but effort has not been standardized for changes in hook depth. The orange line is similar to SF31 but averaging is not done across trends derived for each quarter. Note that black marlin and southern bluefin tuna are found in multiple oceans.

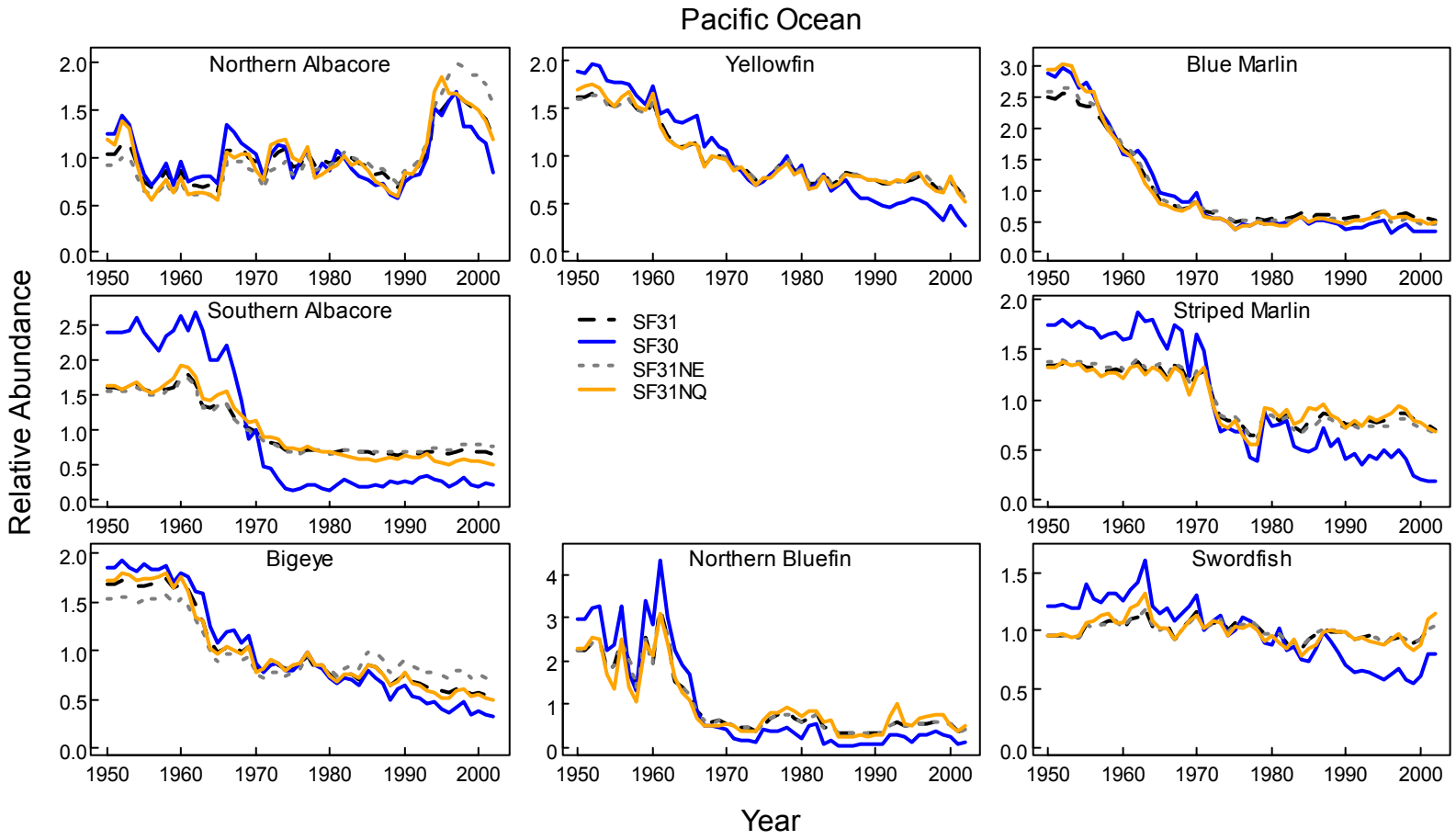

Figure 3.6 Relative abundance indices developed using four variations of the spatial filling method, standardized to their mean, for stocks in the Pacific Ocean from 1950-2002. Indices demarked by a dashed black line were developed using the SF31 variation where missing values were imputed as the average of the first 3 years fished prior to fishing and the last observed *cpue* once abandoned. The blue line, SF30, is similar to SF31 but *cpue* was assumed 0 once and areas was abandoned. The dotted light grey line is similar to SF31 but effort has not been standardized for changes in hook depth. The orange line is similar to SF31 but averaging is not done across trends derived for each quarter.

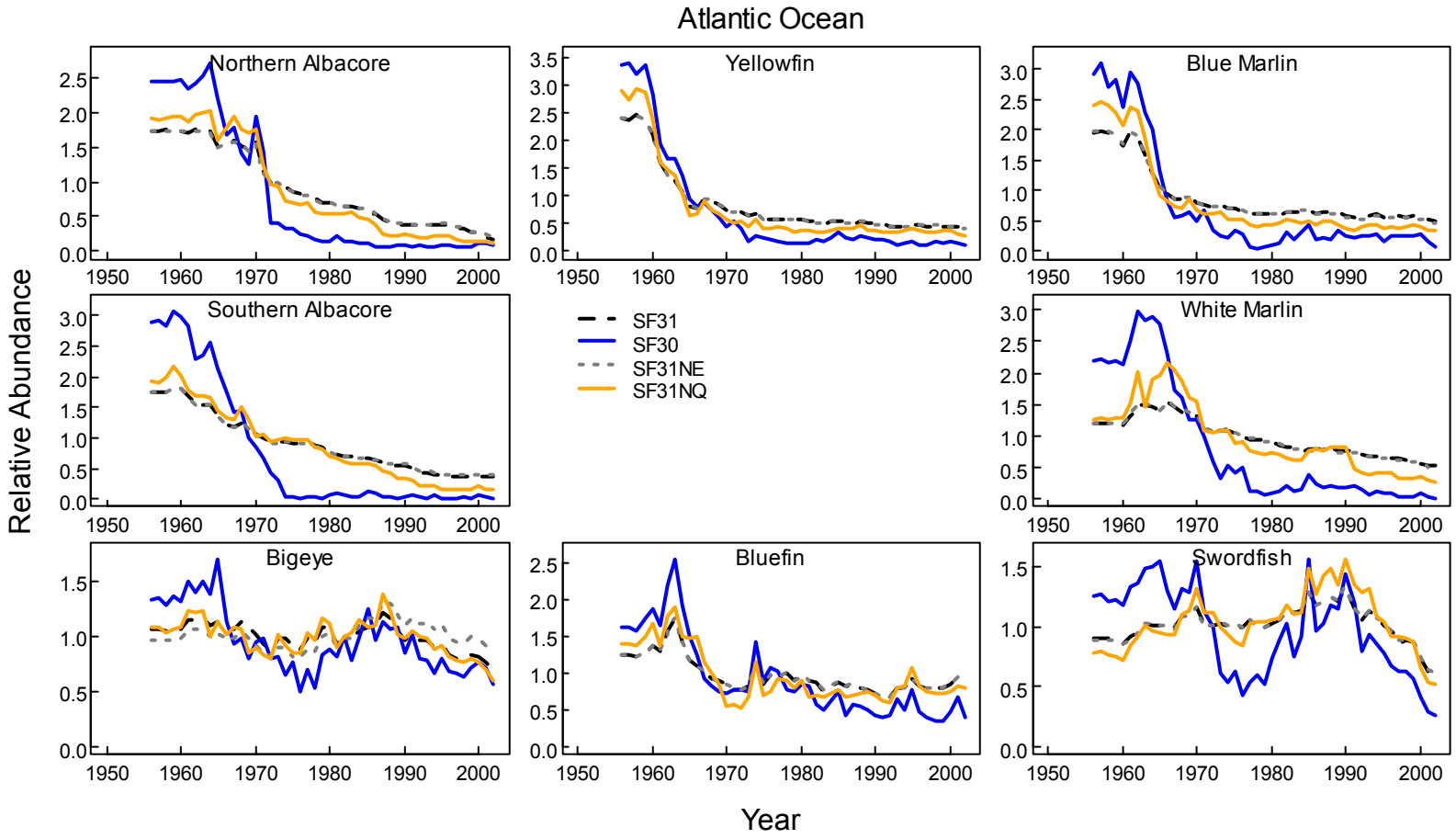

Figure 3.7 Relative abundance indices developed using four variations of the spatial filling method, standardized to their mean, for stocks in the Atlantic Ocean from 1956-2002. Indices demarked by a dashed black line were developed using the SF31 variation where missing values were imputed as the average of the first 3 years fished prior to fishing and the last observed *cpue* once abandoned. The blue line, SF30, is similar to SF31 but *cpue* was assumed 0 once and areas was abandoned. The dotted light grey line is similar to SF31 but effort has not been standardized for changes in hook depth. The orange line is similar to SF31 but averaging is not done across trends derived for each quarter.

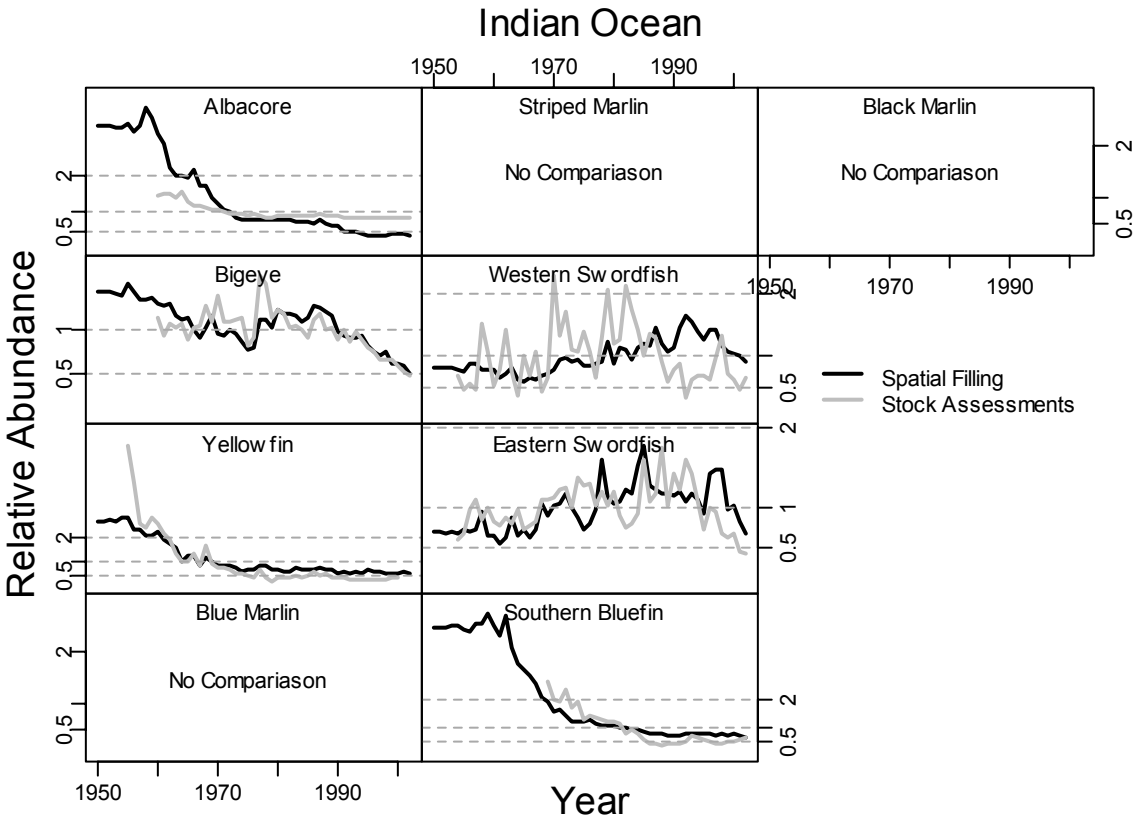

Figure 3.8 Comparison between relative abundance indices derived for stock assessment in the Indian Ocean using Japanese longline data and relative abundance trends developed using the SF31 variation of the spatial filling method.

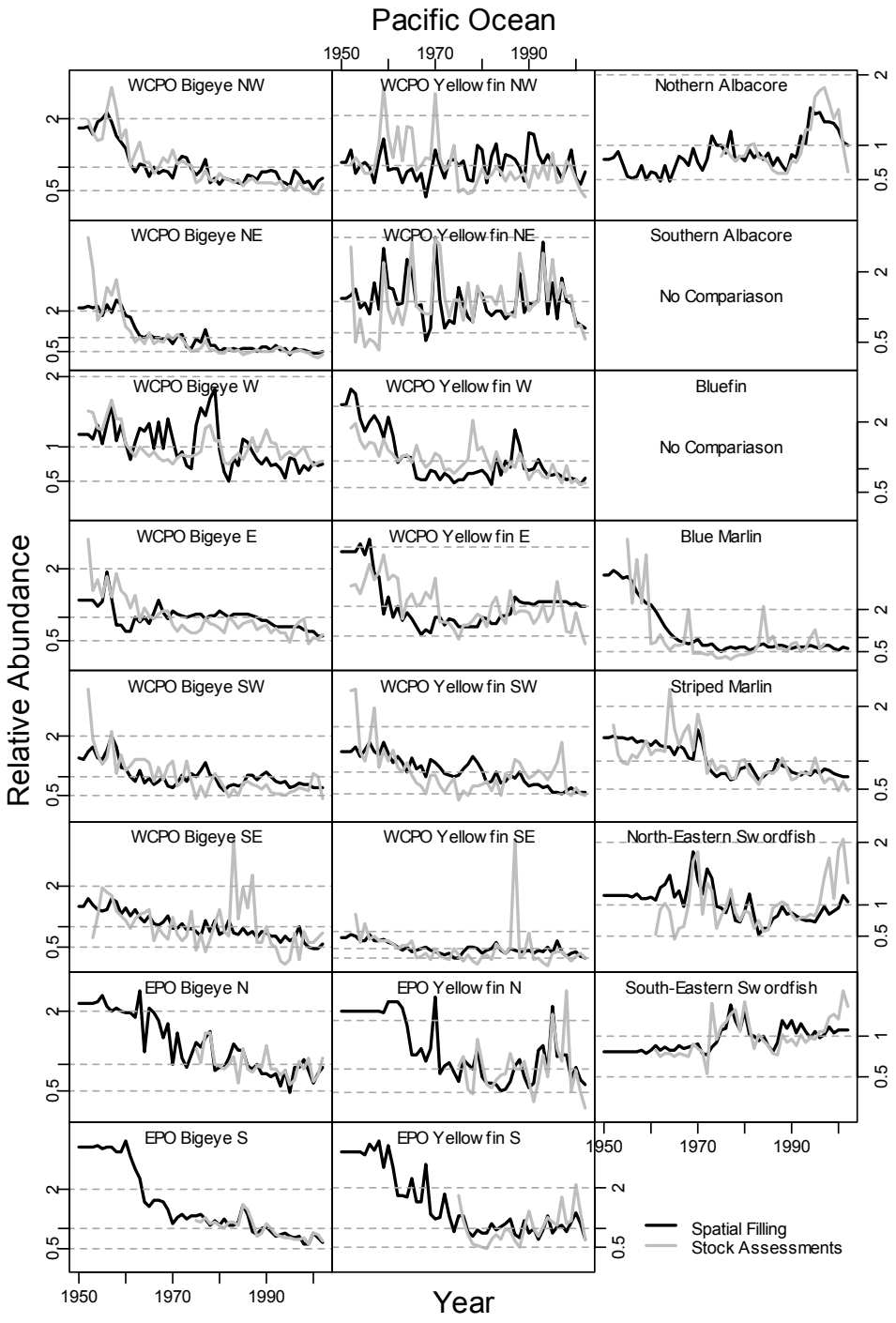

Figure 3.9 Comparison between relative abundance indices derived for stock assessment in the Pacific Ocean using Japanese longline data and relative abundance trends developed using the SF31 variation of the spatial filling method.

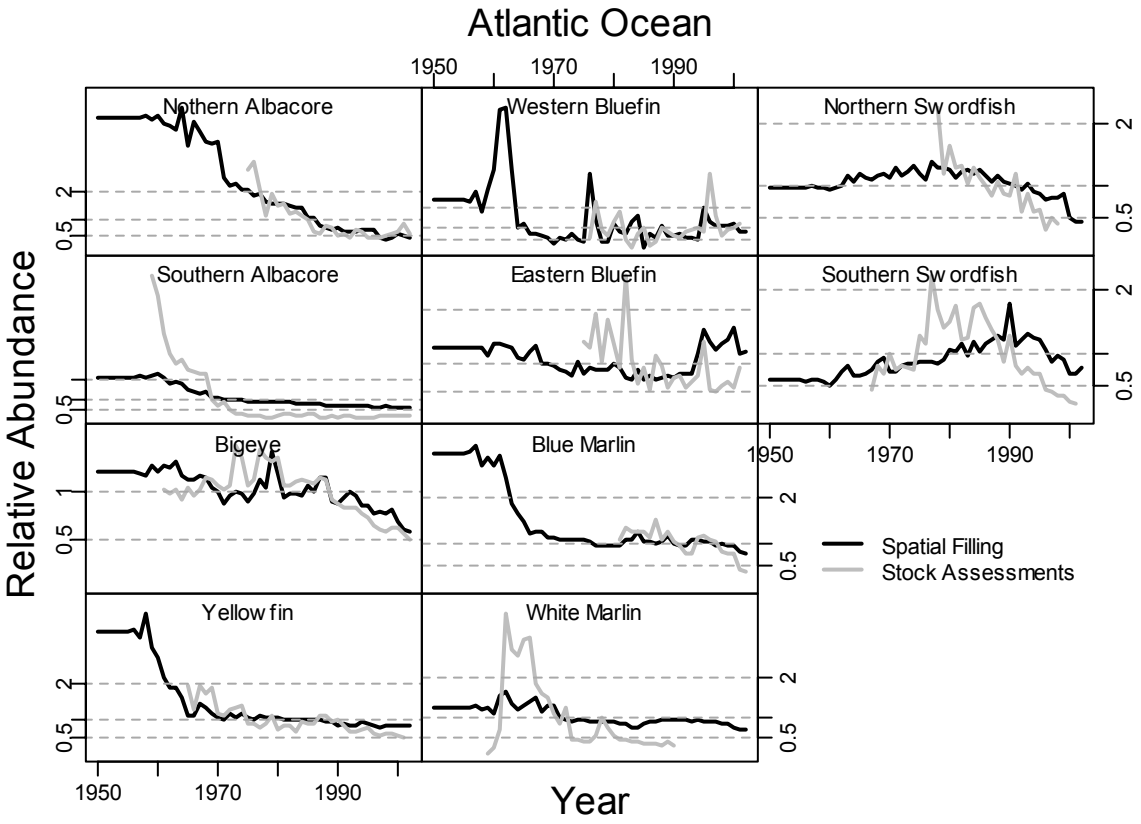

Figure 3.10 Comparison between relative abundance indices derived for stock assessment in the Atlantic Ocean using Japanese longline data and relative abundance trends developed using the SF31 variation of the spatial filling method.

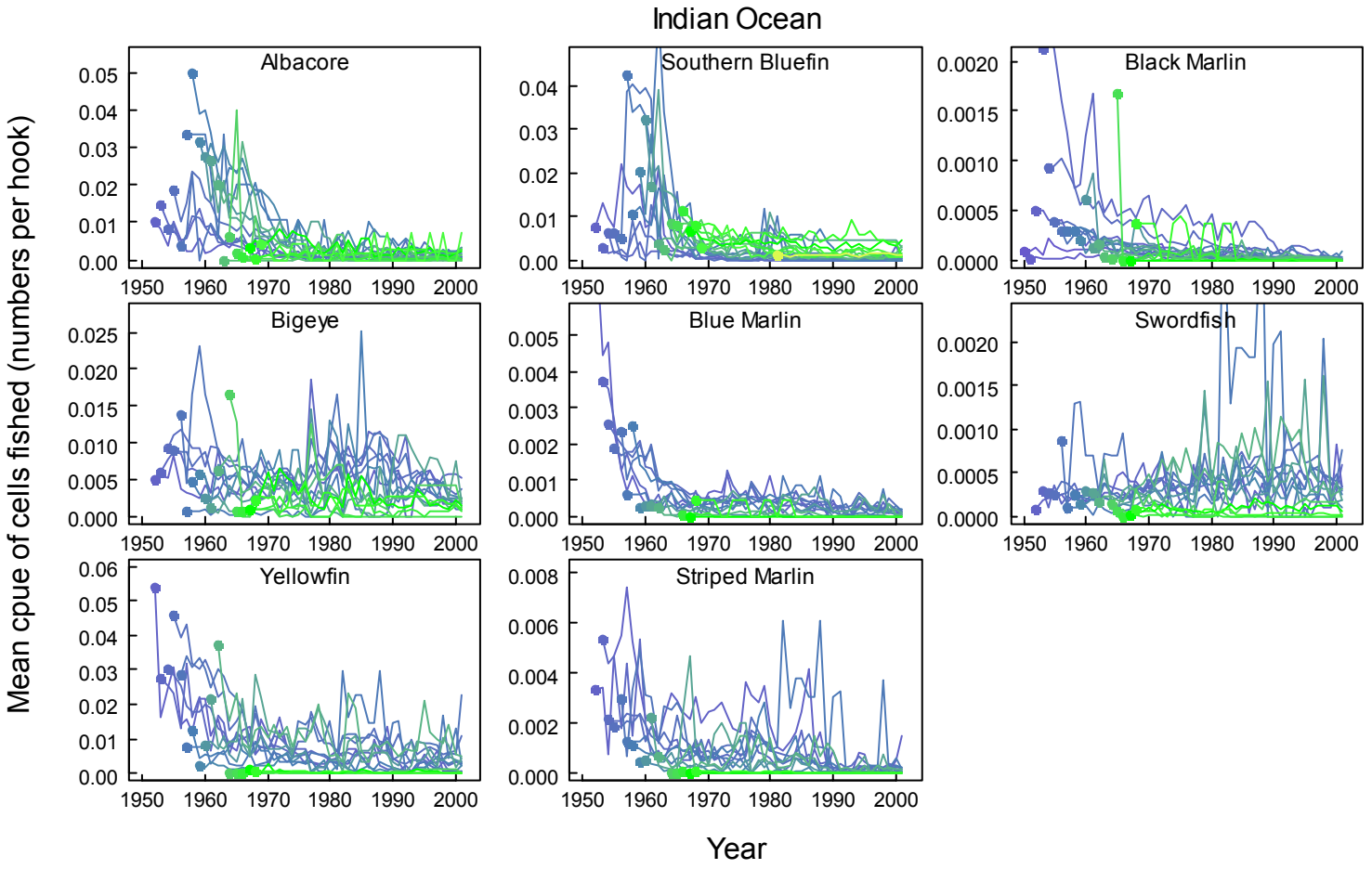

Figure 3.11 Mean *cpue* trend for species in the Indian Ocean grouped by the years areas were first fished. Trends for groupings in the early years are shaded in blue progressing throught green, yellow, orange, and red for later years.

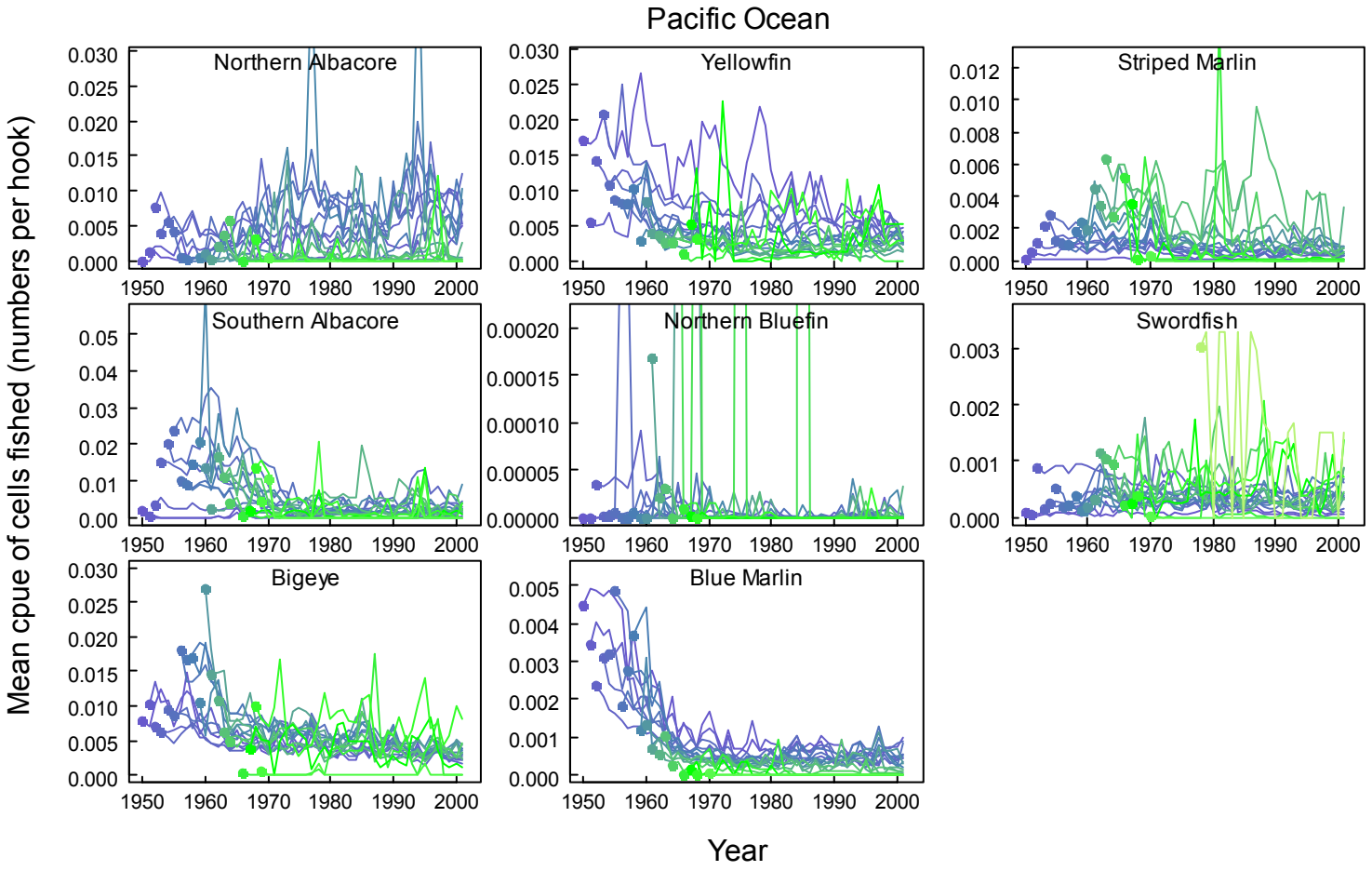

Figure 3.12 Mean *cpue* trend for species in the Pacific Ocean grouped by the years areas were first fished. Trends for groupings in the early years are shaded in blue progressing throught green, yellow, orange, and red for later years.

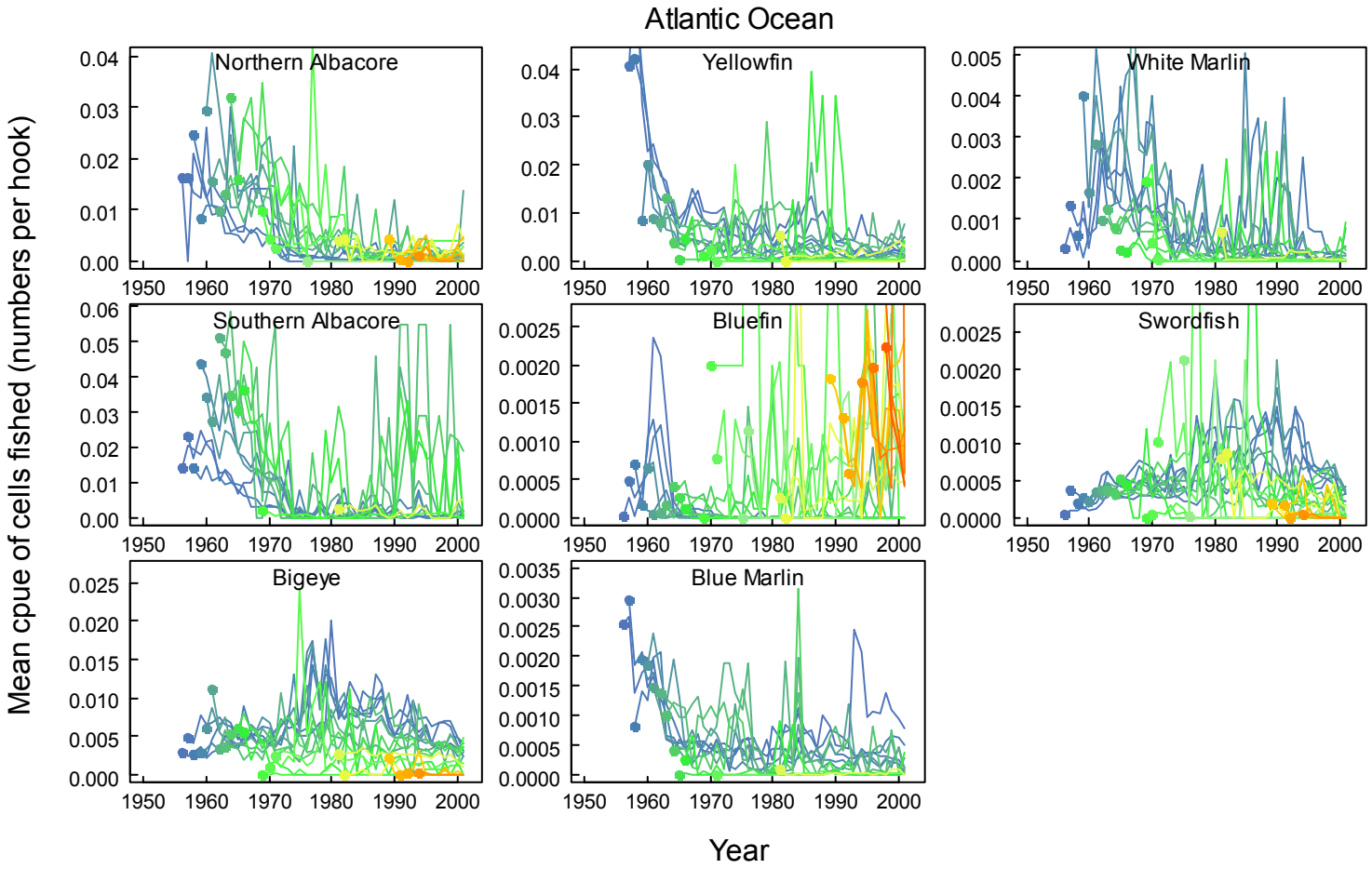

Figure 3.13 Mean *cpue* trend for species in the Atlantic Ocean grouped by the years areas were first fished. Trends for groupings in the early years are shaded in blue progressing throught green, yellow, orange, and red for later years..

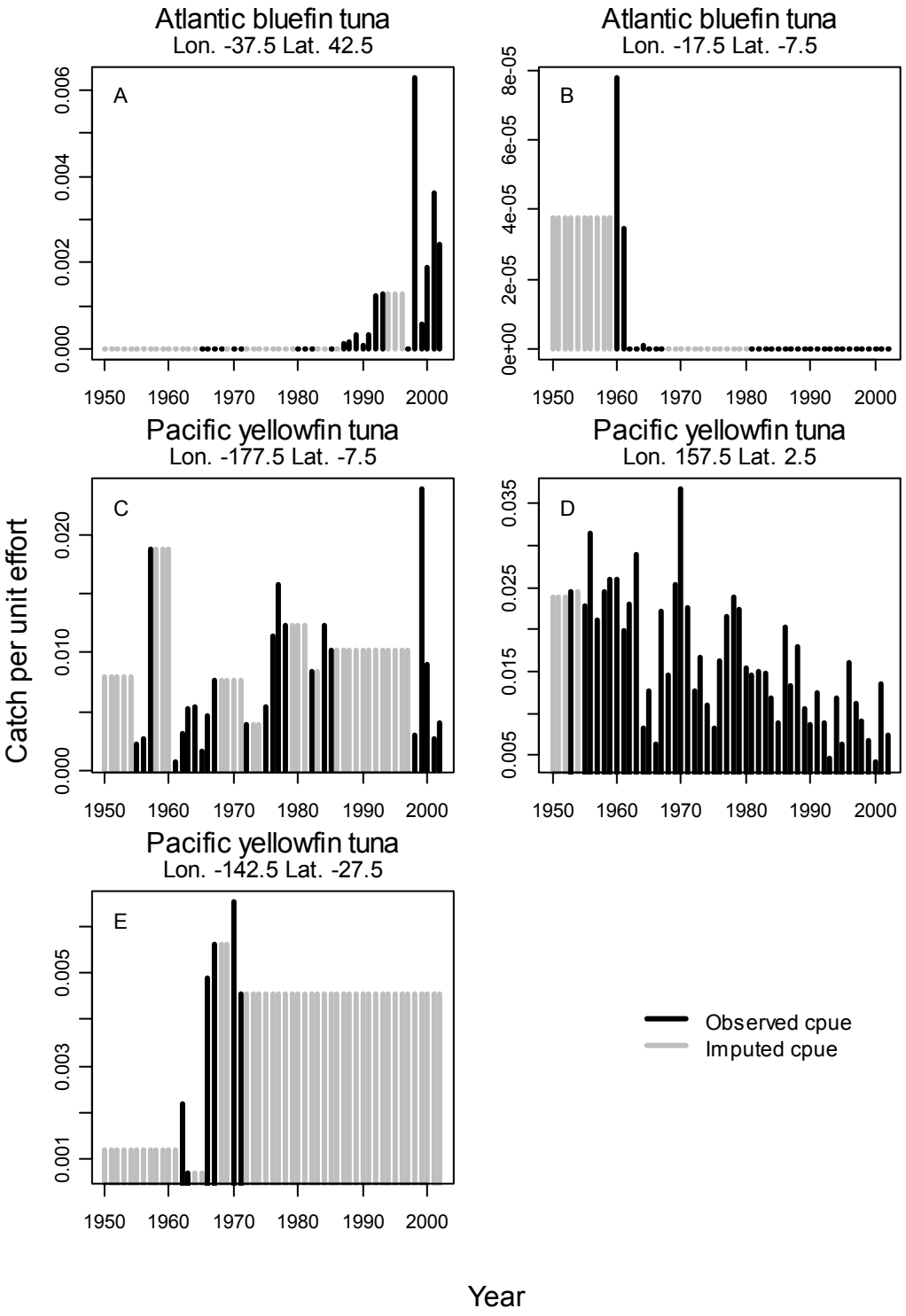

Figure 3.14 Examples of various forward and backward filling conditions. Black vertical lines are observed *cpue* averaged across quarters and grey vertical lines are imputed values. Each graph represents the *cpue* time pattern for one 5^{o}x5^{o} spatial cell.

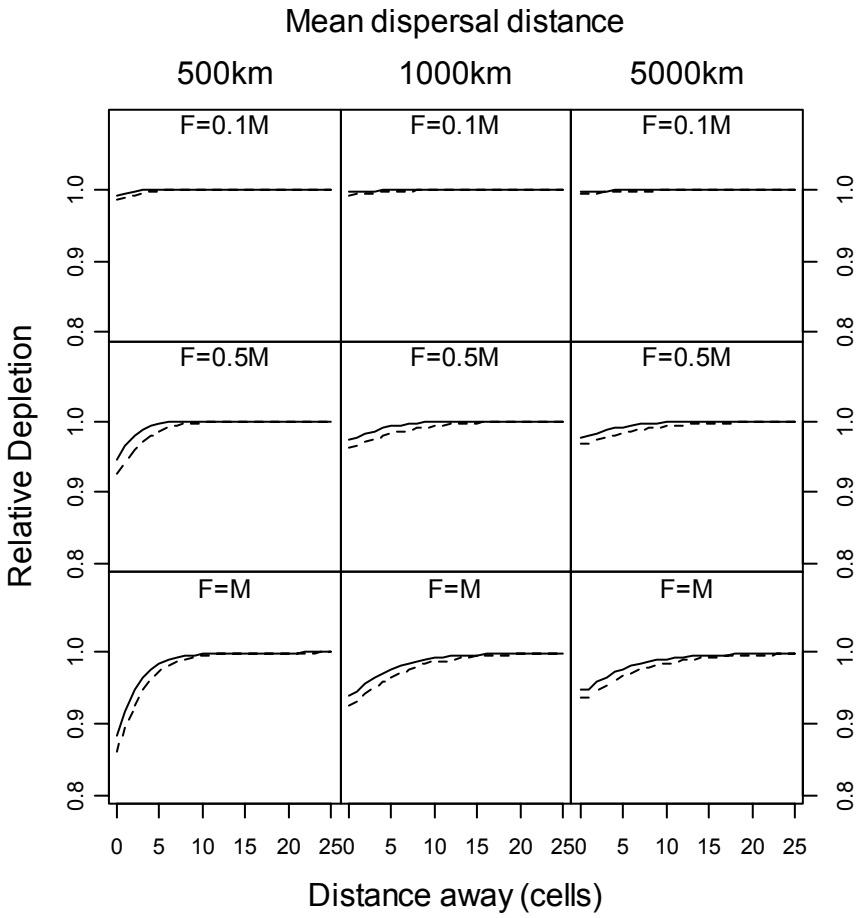

Figure 3.15 Relative level of depletion as a function of fishing mortality rate relative to natural mortality (M=0.4) for three diffusive movement scenarios. In each scenario, recruitment is assumed constant. Fishing mortality is applied to cell 0 only. Solid back line indicates the level of depletion after 1 year. The dashed line delineates depletion levels after 10 years assuming the same fishing mortality rate is applied in cell 0. Cell width used was 500km.

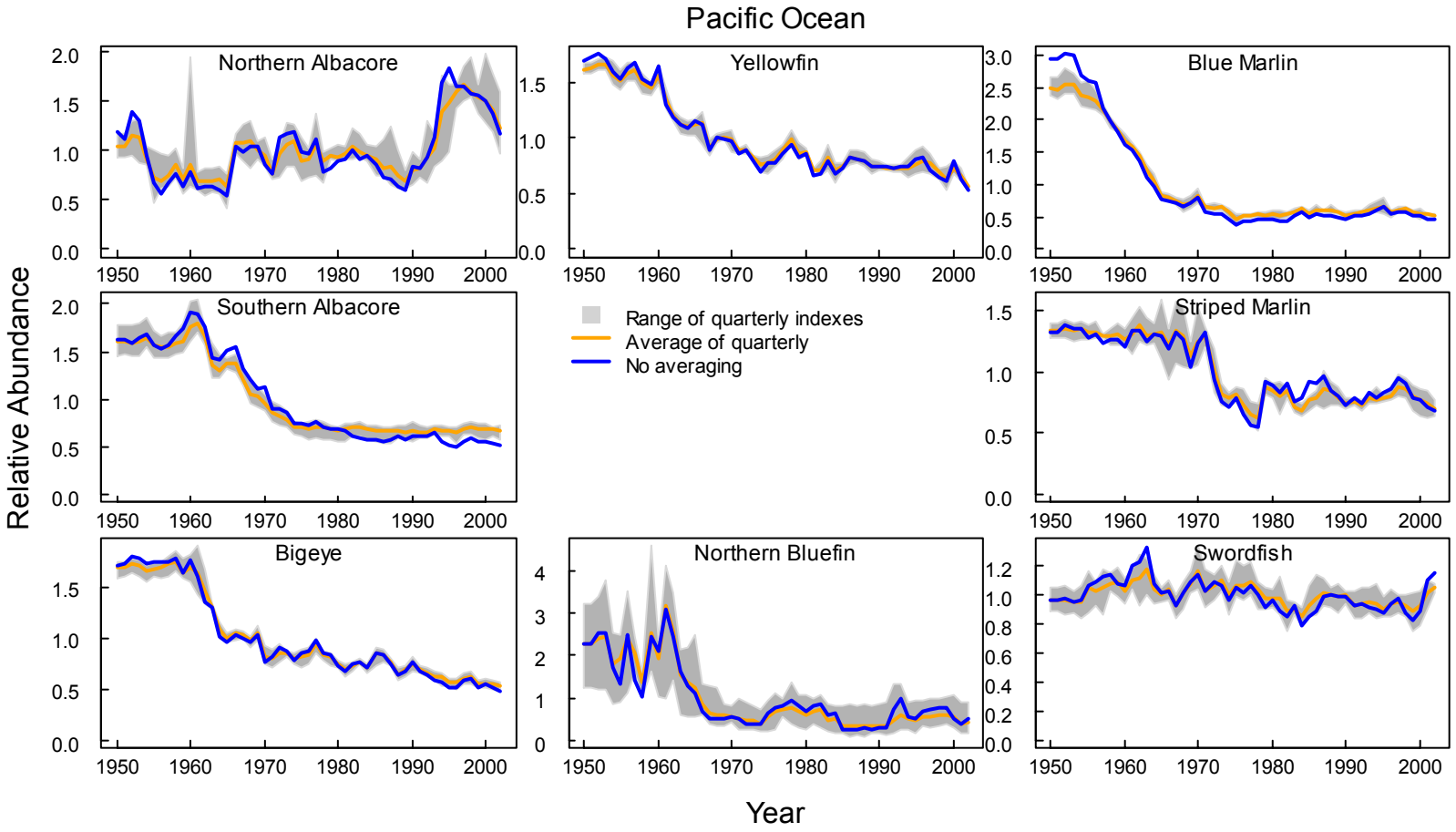

Figure 3.16 Relative abundance trends developed for various stocks in the Pacific Ocean. The grey polygon demarks the range of indices developed for each quarter from the SF31 method prior to averaging. The solid orange line is the average of the quarterly trends and the blue line indicates abundance trends resulting from the SF31NQ method.

Chapter 4 Assessment of recruitment and productivity using catch and relative abundance information

Introduction

The objective of most stock assessments is to develop an understanding of biological processes ('state dynamics') that describe stock dynamic behaviour so management may make informed decision regarding stock status relative to reference points, the potential impact of catch recommendations, and the possible ramifications of longer-term policies. To this end, an assortment of assessment techniques has been developed to parameterize some underlying state dynamics models given a history of observed disturbance (Hilborn and Walters 1992, Quinn II and Deriso 1999). Much of the complexity in assessment methods is intended to extract information about underlying state dynamics from a wide assortment of data sources. In models where the underlying production relationship is assumed stationary, a limited number of parameters are of key interest and determine stock productivity and stock scale; remaining parameters generally characterize assumed relationships between various data sources and state dynamics ('observation models') or describe fishery characteristics such as size specific removals. In all assessments, simplifying or structural assumptions are necessary and influence conclusions about key parameters (Walters and Martell 2004). Furthermore, if data sources pertaining to key biological parameters such as natural mortality rates are not available it is necessary to assume these parameters are known (Punt and Hilborn 1997). Such assumptions are often necessary even when detailed composition (age, size) data are available, since a wide range of parameters defining state and observation models can typically fit such composition data equally well (Gavaris and Ianelli 2002). The ability to estimate parameters and the degree of certainty in estimated values, under an assumed biological structure, depends on how informative available data are and the nature of the assumptions made (Magnusson and Hilborn 2007).

For simple, non-age structured, biomass dynamic, or stock reduction models, which have a limited number of parameters, data must contain sufficient contrast for confounded parameters to be resolved. It is typical, given an observed history of removals, to fit such models to relative abundance trends. The resulting state dynamic model is used to predict an expected pattern of

observations over time and in general, parameter values that minimize residual deviation under an assumed error structure are deemed credible with the degree of credibility depending on apparent variability around the expected pattern. Unfortunately, even if a population is assumed unfished at the start of the time series, a simple linear or exponential decline in relative abundance with increasing catch (a common pattern in developing fisheries) can be equally well explained by a wide range of parameter combinations. Parameter combinations representing a large unproductive stock typically fit such 'one-way trip' data as well as parameter combinations representing a small but highly productive stock (Hilborn 1979, Hilborn and Walters 1992). Assumptions made about sources of variability in observed data can also influence where along this trade off (large-unproductive vs. small-productive) the 'best' parameter estimates fall (Schnute 1987). If variability is assumed to have arisen due to inaccuracies in observation, there is a tendency for parameter estimates to shift toward the large population, low productivity end of the trade off. If more of the variation is assumed to have arisen from variability in state dynamics ('process error'), parameter estimates shift toward high productivity, low stock size (Polacheck et al. 1993).

Often a Bayesian framework is used in assessments to quantify uncertainty and to incorporate prior information to limit the range of parameter combinations when data are uninformative (Hilborn et al. 1993, Mcallister et al. 1994, Walters and Ludwig 1994). Fits to some abundance trends may result in parameter estimates beyond the range that is considered biologically reasonable. At the extremes, parameters may suggest a population that is infinitely large or infinitely productive. In such instances, informative priors are required to constrain the estimation procedure to a realm that is believed to be biologically possible. In such instances and perhaps always, it is worthwhile to turn the question around and ask, given what we understand to be a reasonable model for state dynamics, have inappropriate assumptions been made about the observation model? (Walters and Martell 2004). In doing so, failures in basic assumption (such as whether relative abundance trends are proportional to changes in the stock) are challenged and insight is potentially gained into factors that may be biasing assumed relationships.

In this chapter, productivity, abundance, and status of the longline vulnerable component of tuna and billfish stocks are assessed using relative abundance trends developed in Chapter 3 in conjunction with nominal catch data compiled in Chapter 2. Three simple assessment methods are employed. The first is a reconstruction of recruitment under various hypotheses about current fishing mortality rate, assuming the natural mortality rate is known. Productivity estimates, abundance, and status are evaluated from the recruitment estimates, assuming recruitment patterns can be described by a Beverton-Holt or Ricker relationship. Second, stochastic stock reduction analysis (stochastic SRA, Walters et al. 2006) is then employed under two extreme assumptions regarding errors-in-variables, where residuals are assumed mainly due to observation error versus where residuals result from process error. The SRA assumes a Beverton-Holt recruitment pattern, but includes effects of stochastic variation in recruitment in prediction of relative abundance over time when observed catches are subtracted from predicted abundances (a 'conditioned-on-catch' approach). The third assessment procedure involves fitting observed catch to a simple balance model as assumed in the second approach (with assumed Beverton-Holt recruitment relationship), but using a time series of relative fishing mortalities rather than subtracting observed catches from predicted abundances. Such a procedure requires the estimation of an additional parameter to rescale the relative fishing mortality series. The aim of these assessments is to evaluate current stock status, patterns in recruitment relationships, the influence particular recruitment patterns have on parameter estimation, and to determine if there is any indication of further bias in the relative abundance trends developed in Chapter 3.

Methods

Recruitment reconstruction

A simple method to reconstruct apparent historic recruitment patterns, which can be used to explore stock status relative to management reference points, was proposed by Walters and Hilborn (2005). They suggest recruitment trends may be recovered from simple relative abundance trends by using methods similar to those proposed by Schaefer (1954, 1957) for estimating surplus production. Provided a relative abundance series is proportional to stock abundance, recruitment can be calculated each year given an estimate of the catchability coefficient and natural mortality rate. Walters and Hilborn (2005) point out that recruitments

estimated using such a method have high variance due to having two measurement errors along with process error in each recruitment estimate. Abundance indices can be smoothed to reduce, at least in part, variance due to measurement error (see discussion in Walters and Hilborn 2005). In the method presented here, relative abundance trends are smoothed using a three point moving average (MA-3) as suggested by the authors.

Assume the state dynamics are adequately described by the differential equation

4.1) $dN/dt = R_t - C_t - MN_t$

where M is the instantaneous natural mortality rate, N_t, C_t, and R_t are the population abundance, the catch of longline vulnerable individuals across all gears, and recruitment in numbers of individuals of size vulnerable to longline. Assuming that recruitment and catch are piecewise constant over time steps of one year, dynamic change in N over each year is given by the integral of equation 4.1:

4.2) $N_{t+1} = (R_t - C_t)/M + [N_t - (R_t - C_t)/M]e^{-M}$

Assume that N_t can be estimated from the smoothed relative abundance series as

4.3) $\hat{N}_t = y_t^{MA-3}/q$

where y_t^{MA-3} the smoothed relative abundance estimate for year *t* and *q* is is an estimate of the catchability coefficient. Estimates of recruitment each year can then be obtained from the rearrangement of equation 4.2 as

4.4) $R_t = (\hat{N}_{t+1} - \hat{N}_t e^{-M})M(1 - e^{-M})^{-1} + C_t$

One of the challenges of this approach is to obtain an estimate of the catchability coefficient. Reasonable estimates of *q* can be obtained if an estimate of current fishing mortality rate can be provided. In some instances, tagging data or swept area methods may be used to evaluate current fishing mortality rates. An alternative is to reconstruct recruitment patterns for a range of

assumed values of current fishing mortality rates. Given a current fishing mortality (F_{cur}), the catchability coefficient can be estimated as

4.5) $$q = \frac{F_{cur}}{\overline{E}^*}$$

Here, $\overline{E}^*$ is the ratio $\overline{F}/q$ or a measure of average relative fishing mortality rate estimated over the most recent years (t) of the fishery, calculated from catch and relative abundance information as

4.6) $$\overline{E}^* = \frac{\overline{F}}{q} = \frac{\sum_t C_t}{\sum_t \overline{y}_t} \quad given \quad \overline{F} = \frac{\overline{C}}{\overline{N}} = q\frac{\sum_t C_t}{\sum_t \overline{y}_t} \quad and\ provided \quad \overline{y}_t = qN$$

At this point, if recruitment estimates are assumed to have come from some underlying average functional relationship, an assessment of average population productivity and capacity can be made. This information may then be used to assess current population status in relation to management reference points such as the fishing mortality rate (F_{msy}) that produces maximum sustainable yield (MSY). Beverton and Holt (1957) as well as Ricker (1975) recruitment curves were fit to the stock-recruitment (N_t, R_t) series reconstructed using the above method under various hypotheses regarding current fishing mortality rates. A management-oriented parameterization (see Forrest et al. 2008, Martell et al. 2008, Schnute and Kronlund 1996, Schnute and Richards 1998) of the underlying recruitment relationships was used. The productivity (a) and scale (b) are parameters of the Beverton-Holt model (Equation 4.7), where a defines the maximum number of recruits per spawning individual (N_t) and a/b determines the maximum number of recruits, are replaced with equations 4.8 and 4.9. Here, assuming 'knife edge' selectivity and maturity, the compensation ratio (Ω), as defined by Goodyear (1980), is parameterized using F_{msy} and instantaneous natural mortality rate (M) as leading parameters. The scale parameter (b), is defined using F_{msy}, maximum sustainable yield (MSY) as a second leading parameter, along with a and total instantaneous mortality rate (Z_{msy}). The parameter k is the approximate age that individuals become vulnerable to longline gear.

4.7) $R_t = aN_{t-k}\left(1 + bN_{t-k}\right)^{-1}$

4.8) $a = \Omega M \quad where \quad \Omega = \left(F_{msy} / M + 1\right)^2$

4.9) $b = F_{msy} / MSY\left(a / Z_{msy} - 1\right) \quad where \quad Z_{msy} = F_{msy} + M$

For the Ricker model (Equation 4.10), the maximum recruits per mature individual (a) is parameterized in terms of F_{msy} using equation 4.11, while b which determines how quickly recruits per mature individual declines as N_t increases, is parameterized in terms of MSY and a using equation 4.12.

4.10) $R_t = aN_{t-k}e^{-bN_{t-k}}$

4.11) $a = \Omega M \quad where \quad \Omega = e^{F_{msy}/Z_{msy}} Z_{msy} / M \qquad and \qquad Z_{msy} = F_{msy} + M$

4.12) $b = F_{msy} / MSY \ln\left(a / Z_{msy}\right)$

For the results presented here, recruitments were reconstructed for three hypotheses about current fishing mortality (F_{cur}). For each stock, F_{cur} was scaled relative to instantaneous natural mortality, to F_{cur} values of 0.25M, M, and 3M. Natural mortality was assumed to be known precisely and set to the mean values presented in Table 4.1. Maximum likelihood estimates of the leading parameters F_{msy} and MSY where determined using *AD Model Builder* (Fournier 2001) assuming deviations from the log recruits per spawner relationships were normally distributed. Equation 4.13 gives the concentrated log likelihood (L) used in the estimation, where μ_i and x_i and are the observed and predicted log recruits per mature individual respectively.

4.13) $L = -0.5n \ln\left(\sum_{i=1}^{n}\left(x_i - \mu_i\right)^2\right)$

Marginal and joint posterior distributions for leading parameters and joint posterior distribution for management reference points were estimated using a Markov Chain Monte Carlo (MCMC)

procedure. The MCMC procedure was implemented using *AD Model Builder*, which employs a version of the Metropolis-Hasting algorithm (Gelman et al. 1995). Two common management reference points were calculated, the ratio of current stock size to that expected at equilibrium if the population is fished at F_{msy} (N_{cur}/N_{msy}) as well as the ratio of current fishing mortality rate to F_{msy} (F_{cur}/F_{msy}).

Stochastic stock reduction analysis

A somewhat more complex method for determining stock size and productivity is a variation of the stochastic stock reduction analysis (stochastic SRA) presented by Walters et al. (2006), a stochastic implementation of the SRA approached initially proposed by Kimura and Tagart (1982) and Kimura et al. (1984). Assuming stock dynamics can be adequately described using equation 4.1, integrating over a yearly time step, population in the next year is expressed as in equation 4.2 but with recruitments R_t predicted from a stock-recruitment equation.

4.14) $$N_{t+1} = (R_t - C_t)M^{-1} + \left[N_t - (R_t - C_t)M^{-1}\right]e^{-M}$$

where R_t are assumed to vary around a Beverton-Holt relationship:

4.15) $$R_t = aN_{t-k}\left(1 + bN_{t-k}\right)^{-1} e^{\left(v_{t-k} - \sigma_v^2/2\right)}$$

with variation around the mean relationship assumed lognormal. Again, a management-oriented parameterization of the recruitment relationship is used (see equations 4.8 and 4.9). Recruitment anomalies (v_t) are assumed to be drawn from a normal distribution with a mean of 0 and standard deviation of σ_v. No deviation was applied in the first year (t=1) as the initial population size N_0 was not necessarily assumed to be at the expected unharvested equilibrium value (equation 4.16). Population in the first year (N_0) and for k years prior was allowed to vary but constrained so that the ratio of N_0 to $\hat{N}_{eq0}$ was close to 1. This constraint was relaxed for stocks assumed to have experienced significant catches prior to 1950.

4.16) $$\hat{N}_{eq0} = \left(aM^{-1} - 1\right)b^{-1}$$

For stocks assumed near unfished equilibrium, deviation from the expected ratio of 1 were tightly constrained with the standard deviation in log space set at 0.05. For stocks (see Table 4.1) that experienced significant historical catch removals, such that it would be unrealistic to assume they were near an unfished state in 1950, this constraint was relaxed and the standard deviation was assumed 0.8.

Given a known history of removal C_t over T years (1950-2002), predicted population trajectories were fitted to relative abundance time series derived using method SF31 (Chapter 3). Assuming relative abundance (y_t) is proportional to stock size and observation errors (w_t) have a lognormal distribution Walters and Ludwig (1994) suggest integrating over the catchability coefficient (q) such that the observation anomaly in any year t can be expressed as

$$4.17)\ w_t = \left(\ln\left(\frac{y_t}{N_t}\right) - T^{-1}\sum_{t=1}^{T} \ln\left(\frac{y_t}{N_t}\right) \right)$$

Here, w_ts are assumed normally distributed with a mean of 0 and a standard deviation of σ_w. The total log likelihood (L) of the observed relative abundance time series is then proportional to

$$4.18)\ L \propto -n_{vt}\ln(\sigma_v) + \sum_{t=1}^{n}\left(v_t + 0.5\sigma_v^2\right)^2 \Big/ \left(2\sigma_v^2\right) - n_{wt}\ln(\sigma_w) + \sum_{t=1}^{m}\left(w_t\right)^2 \Big/ \left(2\sigma_w^2\right)$$

where n_{vt} is the number of recruitment anomalies and n_{wt} the number of relative abundance observations. One challenge of this quasi state-space approach (Schnute and Kronlund 2002), admitting both process (σ_v) and observation error (σ_w) (Schnute 1987), is variance partitioning, since only a total variance (τ) can be estimated. With no prior knowledge of the variance components or even their relative differences, the proportion of the total variance contributed by each component can only be hypothesized. σ_v can be expresses as $\sigma_v = \left(p\tau\right)^{0.5}$ and σ_w can be expressed as $\sigma_w = \left((1-p)\tau\right)^{0.5}$. For the result presented, p was assumed either 0.1 to represent variation mainly due to observation error, or 0.9, variation due mainly to recruitment deviations.

Posterior distributions for the leading parameters F_{msy}, MSY, M, N_0, τ, and 'nuisance' recruitment anomalies as well as the management reference points described in the recruitment reconstruction section and an estimate of current fishing mortality rate were approximated using *AD Model Builder* as described previously. An informative prior was used for natural mortality and assumed log-normally distributed around a mean $ln(\overline{M})$ with standard deviation σ_M (see Table 4.1 for values). As already mentioned, N_0 was also constrained with an informative prior. For a number of stocks, informative priors were also applied to either F_{cur} or F_{cur} and F_{msy}. In all cases F_{msy} or F_{cur} were assumed to have lognormal prior distributions with means $ln(\overline{F}_{msy})$ and $ln(\overline{F}_{cur})$ and standard deviations σ_{fmsy} and σ_{fcur} (see Table 4.1 for values). Prior distribution for F_{msy} were developed from compensation ratios (Ω) estimated by Myers et al. (1999). The mean compensation ratio estimated for the genus *Thunnus* in the Myers analysis was 5.672. Assuming a Beverton-Holt recruitment relationship, equation 4.8 can be restructured such that a prior estimate of F_{msy} can be expressed as F_{msy} = 1.38M if the mean compensation value above is used. Prior estimates of F_{cur} were taken from recent stock assessment documents and references are provided in Table 4.1. It was assumed that composition information utilized in these more complex assessments (either VPA or stock synthesis methods) were interpreted correctly so that the average fishing mortality rates calculated for longline vulnerable individuals from 2000-2002 were accurate.

Relative fishing mortality forced numbers dynamic model

Another simple assessment model is to drive the basic dynamic model (equation 4.1) with estimates of the relative fishing mortality rates (E^* forced models), and fit the observed catch. In this method, assuming recruitment is piecewise constant, state dynamics are described as

4.19) $dN/dt = R_t - Z_t N_t \qquad where \quad Z_t = F_t + M$

when integrated over a one year time step, results in the equation for population in the following year as

4.20) $N_{t+1} = R_t/Z_t + \left[N_t - R_t/Z_t\right]e^{-Z_t}$

Expected catch in any year is estimated as

4.21) $\hat{C}_t = F_t / Z_t \left[R_t + N_t \left(1 - e^{-Z_t} \right) \right]$

where F_t is the estimated fishing mortality rate. Similar to the description in equation 4.6, a time series of E*s (an estimate of "effective effort" for each year) can be derived as

4.22) $E_t^* = \frac{F_t}{q} = \frac{C_t}{\bar{y}_t} \quad if \quad \bar{y}_t = qN_t$

Using the same relative abundance trend data as for the SRA, the observed catch C_t and an estimate of average current fishing mortality rate ($\overline{F}$), the catchability coefficient (q) can be estimated using equation 4.5, and time series of fishing mortality rates (F_t in equation 4.23) can then be estimated from 'effective effort' calculated in equation 4.22.

4.23) $F_t = qE_t^*$

In equation 4.23, q was calculated assuming $\overline{F}$ was applied over the last few years (2000-2002). In this approach, recruitment and initial population size were parameterized and modeled as descried for the SRA with the exception that process error was not explicitly modeled. The concentrated total log likelihood (L) of the observed catch was taken to be

4.24) $L = -0.5n \ln\left(\sum_{i=1}^{n} \left(\ln\left(\hat{C}_t\right) - \ln\left(C_t\right) \right)^2 \right)$

where n is the number of years of data. Marginal and joint posterior distributions of the leading parameters F_{msy}, MSY, F_{cur}, M, and N_0 were estimated using *AD Model Builder* as described previously using the prior distributions described in the stochastic SRA section.

Results

Recruitment reconstruction

In general, both the Ricker and Beverton-holt recruitment relationships produced similar fits to reconstructed stock recruitment data for the range of current fishing mortality estimates explored (Figure 4.4 to Figure 4.6). In all instances, use of the Ricker model resulted in lower estimates of

the compensation ratio (Ω). Increasing estimates of current fishing mortality usually resulted in increasing estimates of recruitment compensation, and lower estimates of unfished stock size. Reconstruction results can be grouped into four general categories.

The first category is a recruitment pattern that forms a scatter of points for most estimates of current fishing mortality rate. This pattern occurred for swordfish in all oceans, Atlantic bigeye and bluefin tuna, and north Pacific albacore tuna. The resulting effect on stock-recruitment parameter estimation of this pattern is presented in Figure 4.7 for Atlantic bigeye tuna. The marginal posterior distribution for F_{msy} was poorly defined, as was the distribution for MSY. As a result, the compensation ratio was estimated to be very large, i.e. no apparent relationship between stock size and recruitment, for the Beverton-Holt model. The Ricker model had a tendency to fit a domed relationship in these instances. The exception in this categorization was swordfish from the Indian Ocean. In this instance, as estimated current fishing mortality was increased, the scatter of points shifted toward a linear pattern with a positive slope and then to a pattern of rapid decline in recruitment at large population sizes (referred to as a 'hooking' pattern). In these instances, recruitment compensation was estimated to be very low.

Southern and Pacific bluefin tuna fall into a second category where at low current fishing mortality rates, recruitment compensation was estimated to be high but, as assumed current fishing mortality was increased, estimated compensation ratio declined followed by a progressive increase as expected (Figure 4.8). MSY was also poorly defined for these two stocks when current fishing mortality was estimated to be low.

Recruitment reconstructions for six stocks: Atlantic blue marlin and southern albacore as well as Pacific striped and blue marlin, Indian Ocean striped marlin, and black marlin represent a third category, where estimates behaved as expected when observations can be explained by assuming either a large unproductive stock or a small productive one. Estimated productivity increased as current fishing mortality estimates increased. In these cases, marginal posterior distributions for F_{msy} were well defined over a broad range of current fishing mortality estimates (Figure 4.9). Marginal posteriors for MSY were also well defined. There is however some tendency for distributions to be truncated when current fishing mortality was assumed low.

The remaining stocks fall into a final category as illustrated in Figure 4.10 for Indian Ocean yellowfin tuna. Though similar to the previous category, there was a tendency for posterior distributions of F_{msy} to be truncated at either lower or upper bounds indicating recruitment relationships where recruitment is assumed proportional to stock abundance (very low productivity) or independent of abundance (very high productivity) are credible fits to estimated stock recruitment points.

A few other general patterns are worth noting. There was a tendency for marginal and joint posterior distributions for management parameters estimated using the Ricker model to have lower standard deviations when compared to the Beverton-Holt model. Most reconstructed recruitment relationships, particularly those in the last two categories, possessed some degree of 'hooking' pattern. In a number of instances (Figure 4.4 to Figure 4.6), when current fishing mortality was assumed to be low, negative correlation between biological reference point estimates was reduced or was shifted to positive. Plots of parameter joint posterior distributions, marginal posterior distributions, and joint posteriors for biological reference points for all stock are presented in Figure 10.1 to Figure 10.24 in the Appendix to Chapter 4. The most credible estimates and 95% credible intervals for F_{msy} and MSY for various recruitment reconstructions are presented in Table 10.1 along with the associated natural mortality rates and current fishing mortality rate estimates. The same statistics for management reference points are presented in Table 10.2.

MCMC sample results for all recruitment reconstructions were summarized by locating each stock in a joint biological reference point space (Figure 4.15). In this 'stock status' plot, reference points were generated by combining results over all current fishing mortality rate hypotheses and both recruitment models explored assuming equal weight. Only Pacific striped marlin falls within the category of being over-fished ($N_{cur}<N_{msy}$) but over-fishing ($F_{cur}>F_{msy}$) is not occurring. Stocks classified as not over-fished and over-fishing not occurring were bigeye - tuna from the Indian and Atlantic oceans, Atlantic bluefin tuna as well as Pacific northern albacore and swordfish. Remaining stocks are all estimated to be over-fished and experiencing over-fishing with the exception of Indian Ocean blue marlin, Pacific Ocean southern albacore

tuna, and yellowfin tuna from the Pacific Ocean. These three stocks were categorized as experiencing over-fishing but not being over-fished. Only the 10% and 50% quantile contours are indicated on the plot for each stock. Displaying the 95% quantile contours cover a much larger area resulting in stock classification spanning multiple categories.

SRA and relative effort forced models

Stochastic stock reduction analyses (sSRA) where the variance in recruitment deviations was assumed high, captured most of the variability in relative abundance trends (Figure 4.11 to Figure 4.13). There was a tendency in such assessments for compensation ratios to be estimated higher and stock size lower than when variance in recruitment was assumed low. When recruitment variability was assumed low, declines in stock abundance were underestimated relative to abundance trends for most albacore and yellowfin tunas, as well as blue marlin stocks, though north Pacific and south Atlantic albacore were exceptions. The SRA model fits with low assumed recruitment variation also overestimated the *cpue* decline in Atlantic white marlin and produced poor fits to Indian and Atlantic swordfish trend data.

When stocks were assessed using E^* forced model, fits to relative abundance trends could be classified as in between sSRA fits. In general, this method resulted in estimated compensation ratios higher for most stocks than estimates from sSRA regardless of the assumed variability in recruitment. Predicted and observed catches using the E^* forced method typically matched well (not surprising since catch was used in the E^* time series estimation) though there were some notable exceptions. Catches of Pacific blue marlin were under predicted during the early period and over predicted during intermediate years. A similar pattern occurred in the Indian Ocean, except that blue marlin harvests in recent years were under predicted. Early high harvests of Pacific bluefin tuna were under predicted and recent high catches of Indian Ocean swordfish were under predicted.

Compensation ratio was estimated below 5, using all three assessment methods, for those stocks not requiring prior information for current fishing mortality rate or F_{msy}. Compensation ratio for Pacific bigeye tuna and Atlantic southern albacore tuna resulting from E^* forced assessment were exceptions (Table 4.2). In a number of assessments, the value was below three. In instances

where prior information was needed for current fishing mortality rate only, estimates of compensation ratio were also low and generally below three. Even when prior information was utilized, posterior modes tended to shift to lower values as apparent in Figure 4.14 for north Atlantic albacore. Such a noticeable shift in posterior distribution also occurred for Atlantic and Indian yellowfin tuna, as well as Atlantic white marlin and swordfish. However, in general, little difference was seen between prior and posterior distributions. When differences did occur, discrepancies were minor.

Plots of parameter joint posterior distributions, marginal posterior distributions, and joint posteriors for biological reference points for all stock are presented in Figure 10.25 to Figure 10.48 in the Appendix to Chapter 4. Values are presented in Table 10.3 and Table 10.4.

All stocks assessed can again be classified within a stock status space by combining reference point values across SRA assessments with high and low observation error variances as well as results for E^* forced models (Figure 4.16). When compared to the status plot generated using the recruitment reconstruction approach (Fig. 4.15), there is a noticeable reclassification for a number of stocks. No stock was categorized solely within the 'recovering' domain where a stock was estimated to be over-fished but over-fishing is not occurring. All swordfish stocks, Atlantic bluefin and bigeye tuna, Indian ocean bigeye and yellowfin tuna and blue marlin, as well as Pacific northern albacore tuna and striped marlin fell within the 'healthy' domain where stock are above the abundance that would produce MSY and over-fishing is not occurring. In the Pacific, southern albacore and yellowfin tuna were above the abundance that produces MSY but over-fishing was estimated to have occurred. The remaining stocks were classified as over-fished and experiencing over-fishing as of 2002. As mentioned before, only the 10% and 50% quantile contours are indicated on the plot for each stock and the 95% quantile contours cover a much larger area resulting in stock classifications spanning multiple categories.

Discussion

There are at least two possible causes of bias in the stock-recruitment analyses presented in this chapter that are due to using relatively simple models and are independent of issues related to use of catch per effort as an index of abundance. First, the total longline-vulnerable stock N_t may be

a poor predictor of annual reproduction (potential recruitment), as opposed to say spawning stock biomass or annual total egg production estimated from stock size or age composition and fecundity schedules. For most of the stocks, N_t should be close to total adult abundance, and the available size composition data do not indicate large changes in average body size, but it is still possible that mean fecundity (per N) declined over the period of analysis as some stocks were depleted; if so, early egg production was disproportionately high compared to N_t, implying that recruitment compensation was somewhat higher than estimated (recruitment points should be shifted to the right on the stock-recruit plots, to higher effective spawning stock sizes). Second, recruitment rates to the longline-vulnerable stock R_t may have declined over time in some stocks, particularly yellowfin and bigeye tuna, due to pre-recruit fishing mortality caused by fisheries such as purse seine fishing. Such decreases, when correlated with decreasing N_t, probably tended to cause underestimation of recruitment compensation.

Assessing stock-recruitment relationships and stock status with simple assessment models that relied only on changes in relative abundance and catch removal had limitations. It was necessary to assume, as is generally the case for simple assessment modelling that natural mortality rates were known. Therefore, any biases that existed in the referenced studies (more complex assessments, meta-analyses, or tagging studies) were carried forward in to the assessments presented here. For other leading parameters (F_{msy}, MSY, and F_{cur}), obtaining estimates with a certain degree of precision is only possible if sufficient contrast exists in fishery removals and relative abundance information ('informative' data) such that three points within the productivity, population size and catchability space are defined (Hilborn and Walters 1992). Information must be available for periods when population abundance is high and exploitation is low, when population is low and exploitation is low, as well as a period when stock is low and exploitation is high. Of the 24 stocks examined, only seven stocks have catch histories and relative abundance trends with sufficient contrast to meet these criteria: southern and pacific bluefin tuna, Indian and Pacific Ocean striped marlin, Indo-pacific black marlin, and Atlantic southern albacore tuna and blue marlin. Abundance trends for the remaining stocks either declined continuously with increasing removals ('one-way trip') or appeared relatively flat over the majority of the period examined.

When data were informative, assessment results tended to follow a predictable pattern. In recruitment reconstructions, increasing estimates of catchability (F_{cur}) reduced the influence of changes in relative abundance relative to observed catch removals on the resulting stock recruitment plots. As a result, estimates of stock productivity increased with increasing F_{cur}. Posterior distributions at each F_{cur} level for F_{msy} and MSY were well within the bounds set. As expected, Ricker model estimates of productivity were lower than the Beverton-Holt model estimates. The pattern of increasing productivity with increasing estimates of F_{cur} was common in some reconstructions using uninformative data series as well. With informative data series, F_{cur} could be estimated using SRA and E* forced models, leading parameter distribution were well defined within specified bounds and shifted predictably along shifts along the productivity-population size trade-off. Observation error weighted models produced results indicating low productivity and large stock size, while process error models indicated the converse as found by (Polacheck et al. 1993). Given the nature of the relative fishing mortality calculation in E^* forced models, results were expected to fall somewhere within the observation-process error range. Results were likely to shift towards higher productivity, in E^* forced models, when relative fishing mortality changes were estimated to be large likely due to a misspecification of the source of variability. In these instances increases in catch were attributed to increases in fishing mortality when it reality such changes may have resulted due to recruitment variability. As a result, a higher estimate of stock productivity was necessary to explain observed catches. Although shifts along the productivity-population scale trade-off did occur, assessments of stock status and recommended MSY were consistent.

When data were uninformative, two general classifications of assessment problems occurred. In the first category, relative abundance data could be classified as a 'one-way trip' and there was insufficient contrast to estimate all leading parameters. When prior information on F_{cur} (q) was assumed available, the remaining leading parameters could be estimated within specified bounds. The general patterns described in relation to shifts along the productivity-population size trade-off were also observed and estimates of stock status and MSY were similar between assessment methods. In the second category, even when prior information was assumed available for F_{cur}, productivity estimates fell outside the bounds of what was determined to be biologically reasonable. Recruitment was assessed as either proportional to abundance or independent of

abundance and in some assessments, depending on estimates of catchability, flipped between the two extremes. These 'flips' between radically different recruitment relationships implied divergent policies. To provide more reasonable estimate of stock status and MSY, productivity was constrained using informative priors based on values that had previously been estimated for tuna and billfish stocks. As a result, the assessments of stock status presented in these situations are conditioned on prior assumptions on all leading parameters except MSY. It is possible to obtain reasonable fits to observed relative abundance trends using alternative state dynamic models. Figure 4.18 presents an alternate hypothesis regarding current fishing mortality rate and natural mortality rate of Pacific Ocean yellowfin tuna (compare with Figure 4.12), which produced plausible fits to relative abundance data but suggests a much larger stock; in this scenario, current fishing mortality rate is also estimated to be higher than that which would produce the maximum sustainable yield.

The assessments presented in this chapter indicate that simple models are insufficient to estimate productivity and population scale for the majority of the tuna and billfish stocks analyzed using catches and relative abundance trends alone. If additional sources of information (i.e., mark-recapture data) were available, such information could be integrated into simple assessment models (perhaps as informative prior distributions or independent measures of current fishing mortality rate) to constrain parameter estimation. Often only fishery-dependent composition information (catch-at-age or catch-at-length) is available; more complex assessment model may be used to extract information about leading parameters such as catchability as well as natural mortality. Recruitment, mortality, and selectivity all influence the patterns in observed composition information and as a result, certain assumptions about the form of relationship, stationarity in the relationship, and variability for each source of change are required. If only length frequency information is available, an understanding of underlying growth patterns and changes in growth patterns is also required. More complex assessment models may provide the necessary framework to assess those stocks where only F_{cur} information was required. However, productivity estimates would ultimately be influenced by underlying assumption about patterns and variability in recruitment, mortality, and selectivity. Given the number of assumptions required to incorporate composition information and the influence such assumptions can have on assessment results particularly when shift in mortality or selectivity patterns are suspected, it

would be worth while to move toward more direct measures of catchability or mortality. Direct measures of fishing mortality rates and natural mortality rates would skirt many of the potential biases introduced in to assessment when composition data are required. More complex assessment models would also not improve the assessment of productivity for those stocks requiring informative prior distributions on productivity. Walters and Hilborn (2005) stress the utility of recruitment reconstruction for exploring long-term recruitment patterns. If relative abundance trends are proportional to stock abundance and a measure of the catchability coefficient can be obtained, (e.g., directly from tagging studies, Martell and Walters 2002), such an approach can circumvent the need for more complex assessments. Stock productivity, scale, and resulting reference point comparisons can be determined by fitting an underlying recruitment model to the reconstructed recruitment pattern. If catchability cannot be estimated, a range of hypotheses can be explored that provides insight into potential problems arising in more complex assessments as well as indications of potential biases in relative abundance trend.

The inability to estimate productivity within reasonable bounds even when informative priors were placed on catchability suggests relative abundance trends may not be proportional to stock abundance even though attempts to standardize effort were made. There are indications that abundance trends may not be proportional to abundance in the odd 'hooking' pattern seen in a number of the recruitment reconstructions. In the most extreme cases, (e.g., Atlantic Ocean yellowfin tuna), recruitment estimates at high stock sizes fell along a vertical line. As calculated population abundance declined, points fell concave to the horizontal (stock size) axis, and ended in a cluster. While it is possible for such a pattern to have arisen by chance alone, repetition of the pattern in all oceans, the steady growth in catch removals, and the prominence of the pattern in yellowfin tuna, albacore tuna, as well as blue marlin in suggests otherwise. Reoccurrence of this pattern suggests that something fundamental was not accounted for while developing trends in Chapter 3.

Both observation and process-weighted assessments indicate auto-correlation in residuals. Such patterning is possibly the result of auto-correlation in recruitment and using observation error weighted models or E^* forced models causes misspecification of the source of variability in abundance trends. A number of authors have noted correlation between changes in tuna

population and climate variables, and there is no reason to assume that models representing high variability in recruitment are inappropriate (Lehodey et al. 2006, Lehodey et al. 1997, Lehodey et al. 2003, Lehodey et al. 2008). However, pattern in observation anomalies (Figure 4.17), particularly patterns observed for yellowfin tuna, blue marlin, and albacore tuna, relative to the historic development in the Japanese longline fleet, warrant further consideration.

Transition from positive to negative residuals for these stocks tended to occur in the mid 1960s to the 1970s. This shift was estimated to be gradual for stocks such as Pacific Ocean blue marlin and abrupt for stocks such as Indian Ocean albacore. It is plausible that a particular subset of each stock was removed early in the development of the fishery. Such populations could have been composed of older, less productive individuals that were more vulnerable to longline gear and had accumulated over time, or an accumulation of individuals that were merely more aggressive. Early fisheries rapidly depleted these stock components and the remaining populations were more difficult to catch, hence lower catchabilities. Differences in individual behaviour have been observed and can have consequences for vulnerability to fishing gears (Biro and Post 2008, Mangel and Stamps 2001, Stamps 2007). Anomaly patterns like those estimated for Indian Ocean blue marlin or Pacific blue marlin could be interpreted with such a model. However, apparent increases in catchability for stocks such as Pacific striped marlin or Atlantic white marlin early in the fishery render such an argument is less convincing. Furthermore, abrupt declines in catchability of some stocks, (e.g., Atlantic and Pacific yellowfin tuna or Indian Ocean albacore tuna) were estimated to occur within the 1960s to the1970s suggesting abrupt changes in species targeting or catch reporting not the erosion of a stock component. Apparent changes in catchability during this period are often attributed to changes in species targeting because a large portion of the Japanese fleet switched to targeting bigeye and bluefin tuna. However, for a number of stocks the decline began prior to this major transition. A variety of other factors may have contributed to catchability declines. From the mid 1950s and into the 1980s the Japanese fleet was a shifting mosaic of vessel classes with new smaller vessels extending into areas earlier reserved for mothership operations. Furthermore, mothership operations began disappearing from the fishery during this period. It is entirely possible that the effectiveness of these new vessels was lower. Hisada (1973) notes a significant increase in yellowfin (4 times) and bigeye (26 times) catch rates in the Coral Sea at particular times of the year, when hand-lining longlines.

It is plausible that operational level differences between vessels resulted in substantially different catchabilities. Furthermore, Hayasi (1974) suggested reduced competition for space during the early years allowed sets to be placed with greater care along thermal and current fronts resulting in higher catch rates earlier in the fishery. Ward and Hindmarsh (2007), also highlight potential impacts of operational level details such as gear material or bait type on catchability. It is likely that a myriad of operational level details, which in conjunction with a change in species targeting, resulted in noticeable declines the catchability of particular species. Catchability for bigeye tuna, a targeted species, in the Indian and Pacific oceans may also have declined during this period, suggesting changes in catchability were not simply due to targeting. Furthermore, apparent synchronous changes in catchability of each bluefin tuna species suggest very structured targeting within the Japanese fleet throughout the fishery history. While much of the decline in nominal catch rates can be explained by failing to account for spatial interaction, the apparent hyperdepletion remaining when estimators that are more appropriate are used is puzzling. Gaining more insight into these potential changes would require operational level information that is currently not available in the public domain.

Stock status estimates, averaging over variance hypotheses in stochastic SRA assessments and E^* forced assessments tended to be more pessimistic for tuna stocks than RFMO published assessments (Figure 4.19 and Table 4.3) that were generally age structured, incorporate a wider array of data, and abundance trends. When comparisons were possible, assessments of billfish stocks generally agreed. Many of the assessment results are not directly comparable due to differences in the assumed spatial distributions of the stocks. However, differences in assessed stock status are more likely the result of differences in the relative abundance trends used and assumed prior distributions on productivity. Many of the RFMO assessment models assume a modal value for steepness of 0.7, which equates to a compensation ratio of approximately 10, almost double the value used for the assessments presented in this chapter. Differences in the assessment of yellowfin and bigeye tuna in the Pacific Ocean could be attributed to this difference as well as the incorporation of younger age classes. The large discrepancies in assessment result for Indian Ocean albacore and Atlantic Ocean bluefin tuna are mainly due to the relative abundance trends used. For Atlantic Ocean bluefin tuna, the relative abundance trend used for mature individuals declines over the more recent years of the time series whereas the

trend used in the assessments presented in this chapter increases. Abundance trends used by ICCAT come from a variety of other fleets. Relative abundance trends used to assess Indian Ocean albacore indicate less of a decline than abundance trends used in this chapter and as a result, the RFMO's assessment of stock status is less pessimistic. Discrepancies in the assessment of Atlantic Ocean southern albacore are due to the use of additional relative abundance trends from different fleets in the ICCAT assessment that suggest less of a decline in population abundance. The more optimistic assessment of Atlantic Ocean bigeye tuna presented in this chapter result from the use of a more optimistic relative abundance time series. The WCPFC assessment of southern albacore tuna presented used Taiwanese catch rates to derive relative abundance trends, which indicated less of a decline in albacore abundance compared to Japanese catch rates.

The assessments presented in this chapter do not indicate a rapid decline in all large tuna and billfish with the commencement of industrialized fishing. However, fishing mortality on a number of stocks was estimated to be higher than what was estimated to produce the maximum sustainable yield, and a number of stocks appear to be depleted below the abundance estimated to produce MSY. In many assessments, additional information was required to constrain parameter estimation because relative abundance trends were uninformative. Although it is possible to obtain more information about composition data, direct measures of fishing mortality rates would markedly improve assessments. Assessments not requiring prior information for stock productivity suggest there is relatively weak recruitment compensation in large tuna and billfish populations suggesting the lower value of compensation used when informative priors were needed was appropriate and the use of higher values in RFMO assessment may be overly optimistic. When assessment models were constrained using prior information, population trajectories declined slower than the relative abundance trends suggesting critical factors were not accounted for when standardizing effort.

Table 4.1 Fixed parameter values and leading or derived parameter prior probability distribution values. *k* is the assumed age at first vulnerability to longline gear. For the recruitment reconstruction (figure legend letters A-F) M is fixed and three hypothesis of F_{cur} are explored. For the stochastic SRA and Effort Forced analyses, prior distributions, where applicable, are assumed lognormal with means given below and standard deviations shown in parentheses. References are provided for F_{cur} mean values. Stock identified with a * indicate substantial catches prior to 1950.

Method	**All**	**Recruitment Reconstructions**				**Stochastic SRA & Effort Forced**			
Parameter	**k**	**M**	**F_{cur}=0.25M**	**F_{cur}=M**	**F_{cur}=3M**	**M**	**F_{cur}**	**F_{msy}**	**F_{cur} reference**
IALB	5	0.27	0.068	0.27	0.81	ln(0.27) (0.05)	ln(0.58) (0.23)	ln(0.37) (0.15)	(IOTC 2004a)
PNAB*	5	0.27	0.068	0.27	0.81	ln(0.27) (0.05)	ln(0.40) (0.16)	ln(0.37) (0.15)	(Stocker 2005)
PSAB	5	0.27	0.068	0.27	0.81	ln(0.27) (0.05)	ln(0.21) (0.08)	-	(Hoyle et al. 2008)
ANAB*	5	0.27	0.068	0.27	0.81	ln(0.27) (0.05)	ln(0.40) (0.16)	ln(0.37) (0.15)	(ICCAT 2007a)
ASAB	5	0.27	0.068	0.27	0.81	ln(0.27) (0.05)	-	-	
IBET	4	0.4	0.1	0.4	1.2	ln(0.40) (0.08)	ln(0.30) (0.12)	ln(0.55) (0.22)	(IOTC 2007)
PBET	4	0.4	0.1	0.4	1.2	ln(0.40) (0.08)	ln(0.45) (0.18)	-	(Langley et al. 2008)
ABET	4	0.4	0.1	0.4	1.2	ln(0.40) (0.08)	ln(0.18) (0.07)	ln(0.55) (0.22)	(ICCAT 2007b)
IYFT	3	0.7	0.18	0.7	2.1	ln(0.70) (0.14)	ln(0.60) (0.24)	ln(0.97) (0.39)	(Nishida and Shono 2007)
PYFT	3	0.7	0.18	0.7	2.1	ln(0.70) (0.14)	ln(0.35) (0.14)	-	(Hampton et al. 2006b)
AYFT	3	0.7	0.18	0.7	2.1	ln(0.70) (0.14)	ln(0.51) (0.20)	ln(0.97) (0.39)	(ICCAT 2004a)
GSBT	5	0.1	0.025	0.1	0.3	ln(0.10) (0.02)	-	-	
PBFT*	5	0.28	0.07	0.28	0.83	ln(0.28) (0.06)	-	-	
ABFT*	6	0.15	0.038	0.15	0.45	ln(0.15) (0.03)	ln(0.18) (0.07)	ln(0.21) (0.08)	(ICCAT 2006a)
IBUM	5	0.25	0.062	0.25	0.75	ln(0.25) (0.05)	ln(0.20) (0.08)	ln(0.21) (0.08)	Assumed
PBUM	5	0.25	0.062	0.25	0.75	ln(0.25) (0.05)	ln(0.10) (0.04)	ln(0.21) (0.08)	(Kleiber et al. 2002)
ABUM	5	0.25	0.062	0.25	0.75	ln(0.25) (0.05)	-	-	
ISTM	3	0.5	0.125	0.38	1.14	ln(0.50) (0.10)	-	-	
PSTM	3	0.5	0.125	0.38	1.14	ln(0.50) (0.10)	-	-	
AWHM	3	0.32	0.16	0.38	1.14	ln(0.32) (0.06)	ln(0.20) (0.08)	-	(ICCAT 2006c)
GBLM	5	0.15	0.038	0.15	0.45	ln(0.15) (0.03)	-	-	
ISWO	5	0.21	0.052	0.21	0.63	ln(0.21) (0.04)	ln(0.30) (0.12)	ln(0.29) (0.12)	(IOTC 2008)
PSWO*	5	0.21	0.052	0.21	0.63	ln(0.21) (0.04)	ln(0.15) (0.06)	ln(0.29) (0.12)	(Kolody et al. 2006)
ASWO	5	0.21	0.052	0.21	0.63	ln(0.21) (0.04)	ln(0.40) (0.16)	ln(0.29) (0.12)	(ICCAT 2006b)

Table 4.2 Compensation ratio estimates for various stocks from sSRAs where process error was assumed low versus high and from F/q forced assessments. Stocks without values were assessed with priors on F_{msy}.

Stock	SRA σ_v low	SRA σ_v high	F/q forced
IALB			
PNAB			
PSAB	2.51 (1.58-3)	2.65 (1.58-3)	3.15 (2.34-4.49)
ANAB			
ASAB	3.81 (2.55-5.3)	4.46 (2.07-5.14)	5.11 (3.46-8.11)
IBET			
PBET	2.59 (1.59-4.75)	3.17 (1.61-4.04)	9.76 (3.7-56.92)
ABET			
IYFT			
PYFT	1.72 (1.26-2.68)	1.27 (1.17-1.98)	3.03 (1.86-46.62)
AYFT			
GSBT	2.4 (2.07-2.71)	2.58 (1.91-3.09)	2.36 (2.03-2.68)
PBFT	1.41 (1.09-1.76)	4.42 (1.25-3.02)	2.01 (1.15-3.06)
ABFT			
IBUM			
PBUM	1.22 (1.01-1.57)	1.28 (1.06-1.59)	1.25 (1.01-1.61)
ABUM	2.26 (1.48-2.86)	2.76 (1.71-3.45)	3.24 (2.08-5.43)
ISTM	1.46 (1.02-1.88)	2.72 (1.16-2.52)	1.77 (1.01-2.63)
PSTM	1.29 (1.01-1.47)	1.45 (1.03-1.72)	1.31 (1.07-1.5)
AWHM	1.54 (1.43-2.16)	1.88 (1.65-4.6)	2.12 (1.75-3.02)
GBLM	2.52 (1.84-3.18)	3.01 (1.82-3.44)	2.98 (2.21-4.03)
ISWO			
PSWO			
ASWO			

Table 4.3 Point estimates of reference points from assessments produced by RFMOs. The year column indicates the assessment year. The B ratio column presents the ratio of current biomass to the biomass that produces MSY and the F ratio column is the ratio of current fishing mortality rate to the fishing mortality rate that would produce MSY.

Code	Sub-Area	Year	B ratio	F ratio
IALB		2007	1.67	0.7
IBET		2007	1.34	0.81
IYFT		2007	1.03	1.25
ISWO		2006	1.31	0.67
PSAB		2008	1.26	0.44
WC-PBET	Western Central	2006	1.27	1.32
E-PBET	Eastern	2007	1.15	1.22
WC-PYFT	Western Central	2007	1.1	0.95
E-PYFT	Eastern	2007	0.96	0.88
SW-PSWO	South Western	2004	1.47	0.71
ANAB		2006	0.81	1.5
ASAB		2003	0.91	0.63
ABET		2006	0.92	0.87
AYFT		2006	1.09	0.84
E-ABFT	Eastern	2007	0.35	3.42
W-ABFT	Western	2007	0.57	1.27
ABUM		2006	0.43	2.03
AWHM		2006	0.47	0.98
N-ASWO	Northern	2005	0.99	0.86

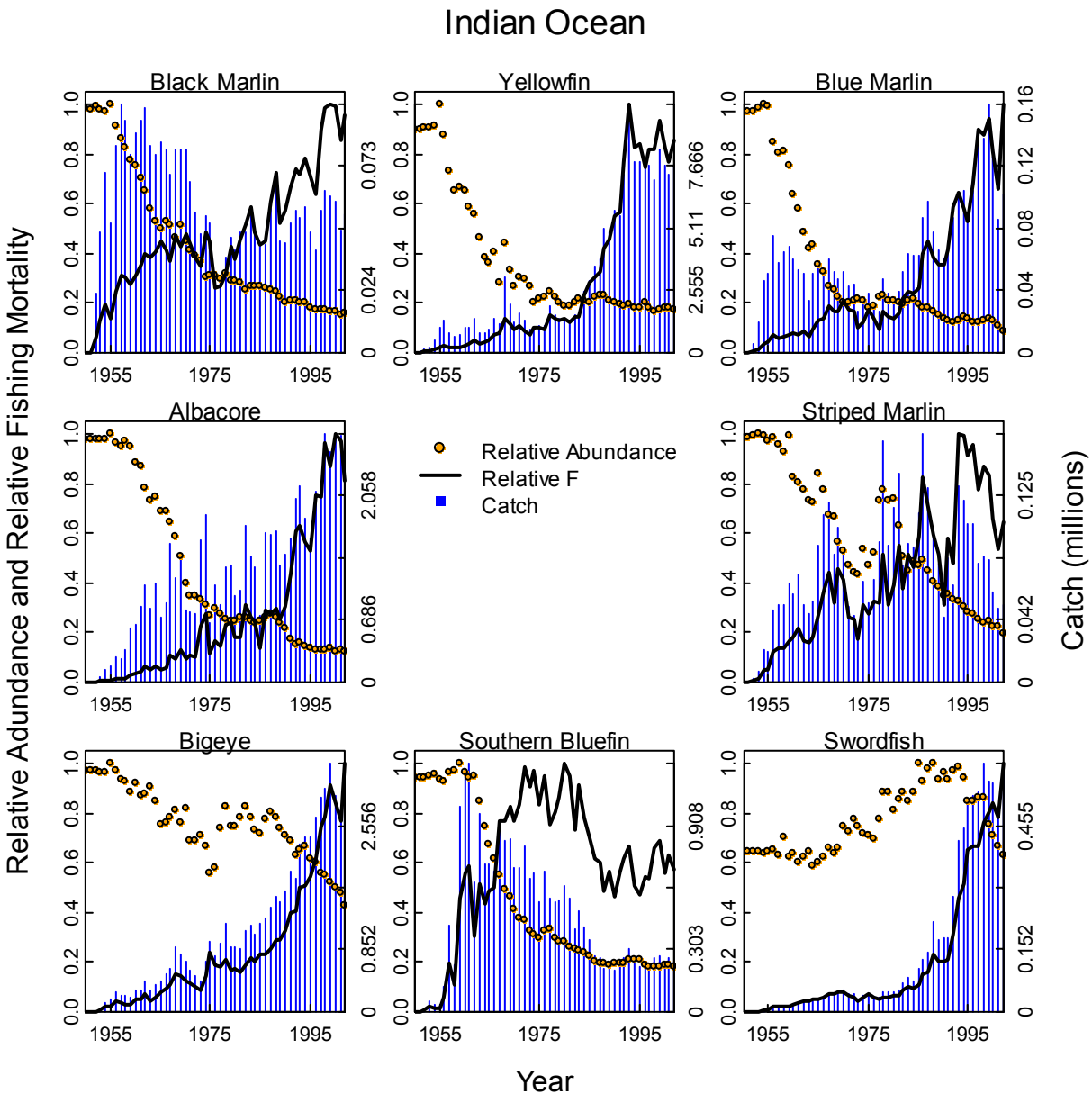

Figure 4.1 Input data for assessments and reconstructions for Indian Ocean stocks. Orange circles are relative abundance trends. Black line indicates relative fishing mortality trends and blue vertical bars indicate estimated catch removals

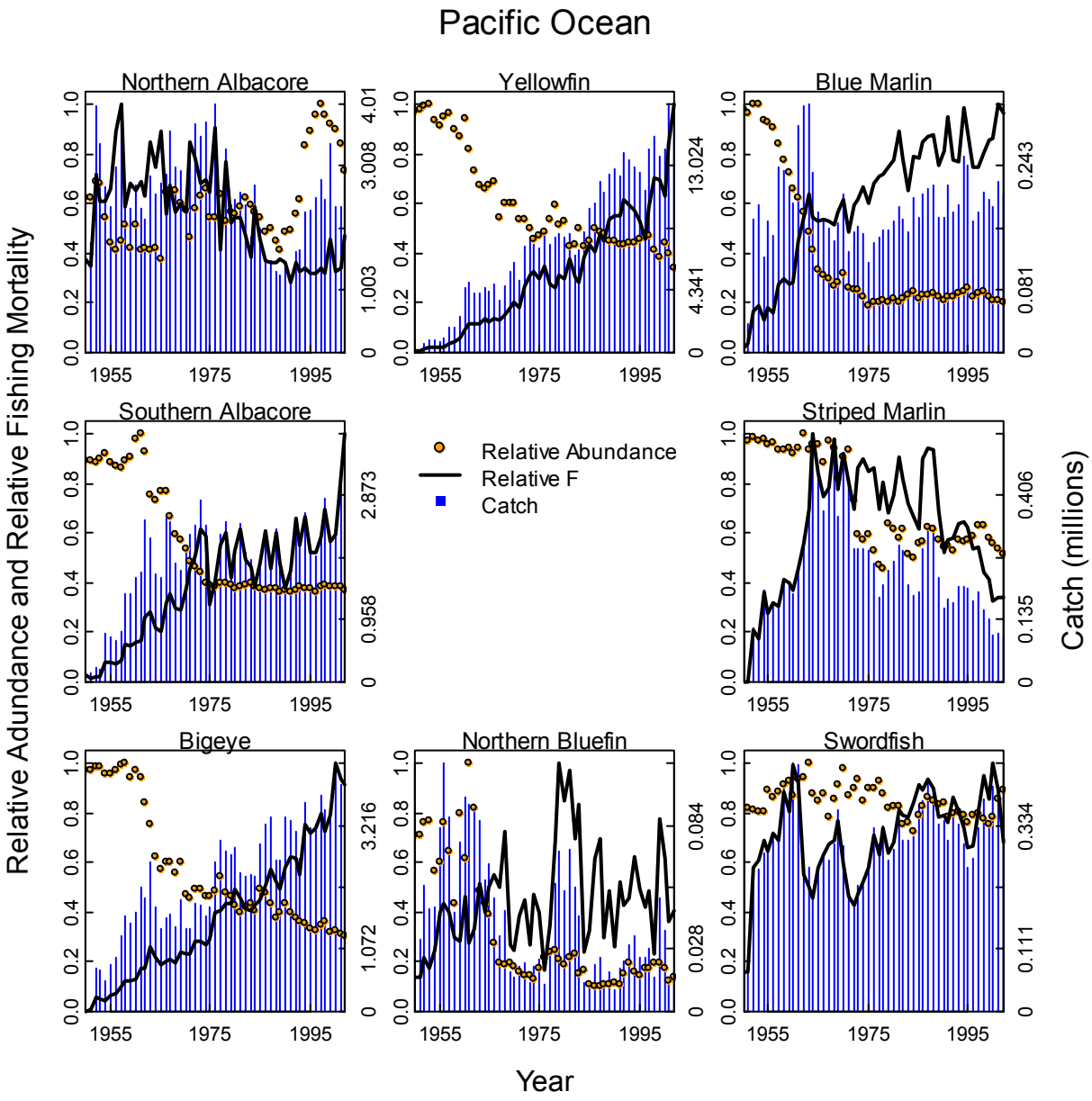

Figure 4.2 Input data for assessments and reconstructions for Pacific Ocean stocks. Orange circles are relative abundance trends. Black line indicates relative fishing mortality trends and blue vertical bars indicate estimated catch removals

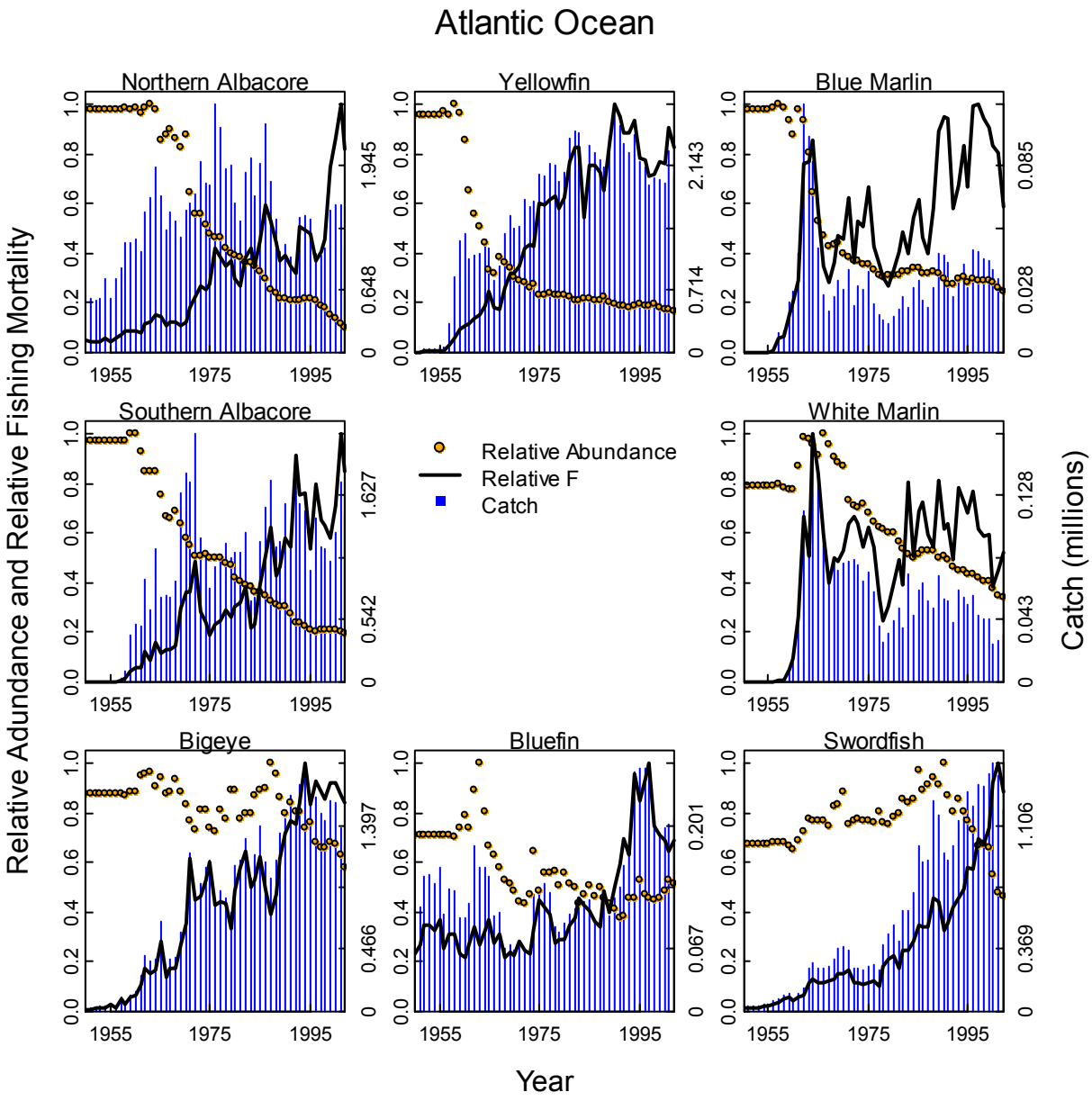

Figure 4.3 Input data for assessments and reconstructions for Atlantic Ocean stocks. Orange circles are relative abundance trends. Black line indicates relative fishing mortality trends and blue vertical bars indicate estimated catch removals

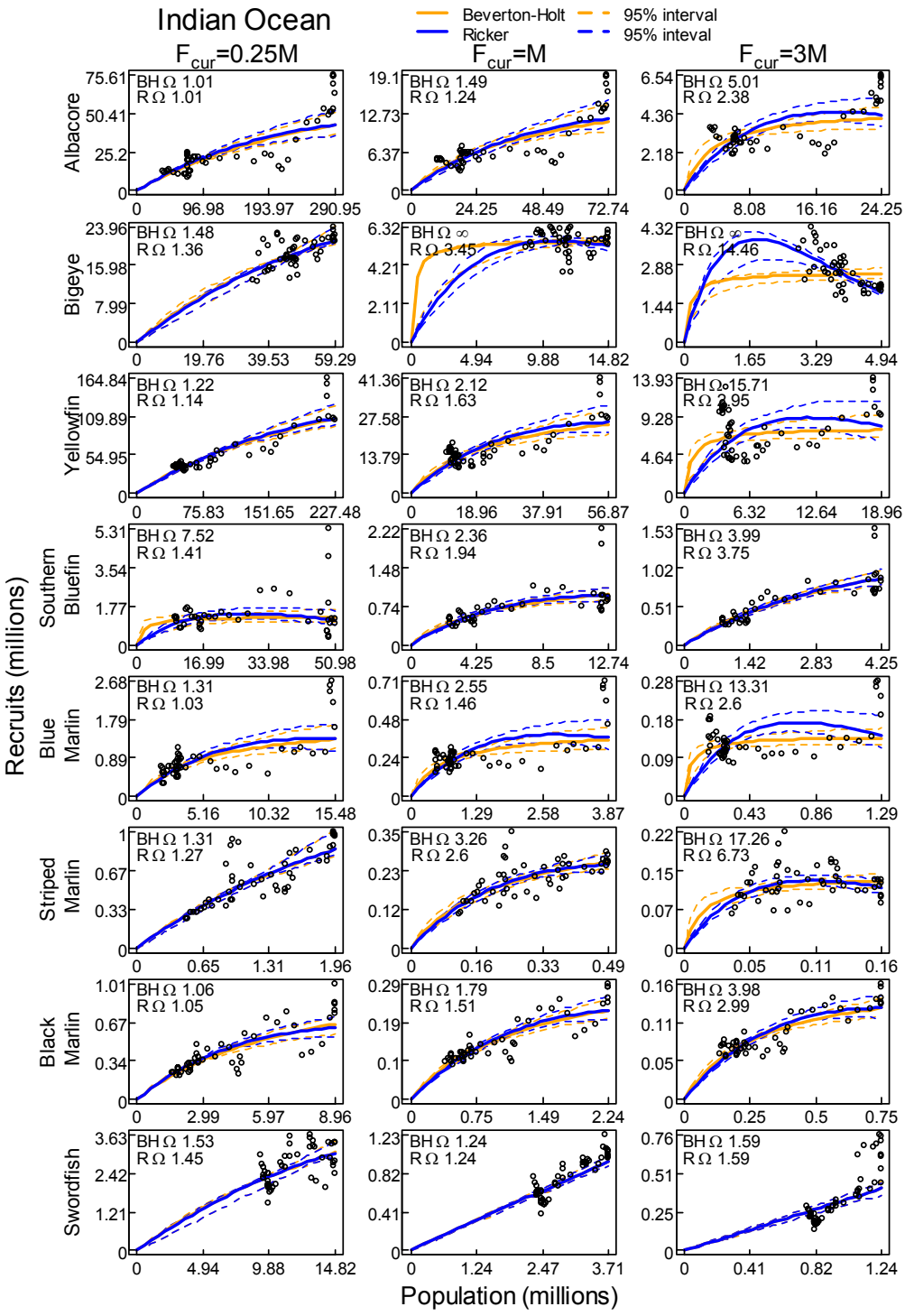

Figure 4.4 Stock recruitment reconstructions and best fits for stocks in the Indian Ocean. Fits are for the Beverton-Holt (BH, orange line) and Ricker (R, blue line) recruitment relationships under three estimates of current fishing mortality rate (F_{cur}) and a fixed natural mortality rate. Ω is the MLE estimate of the compensation ratio.

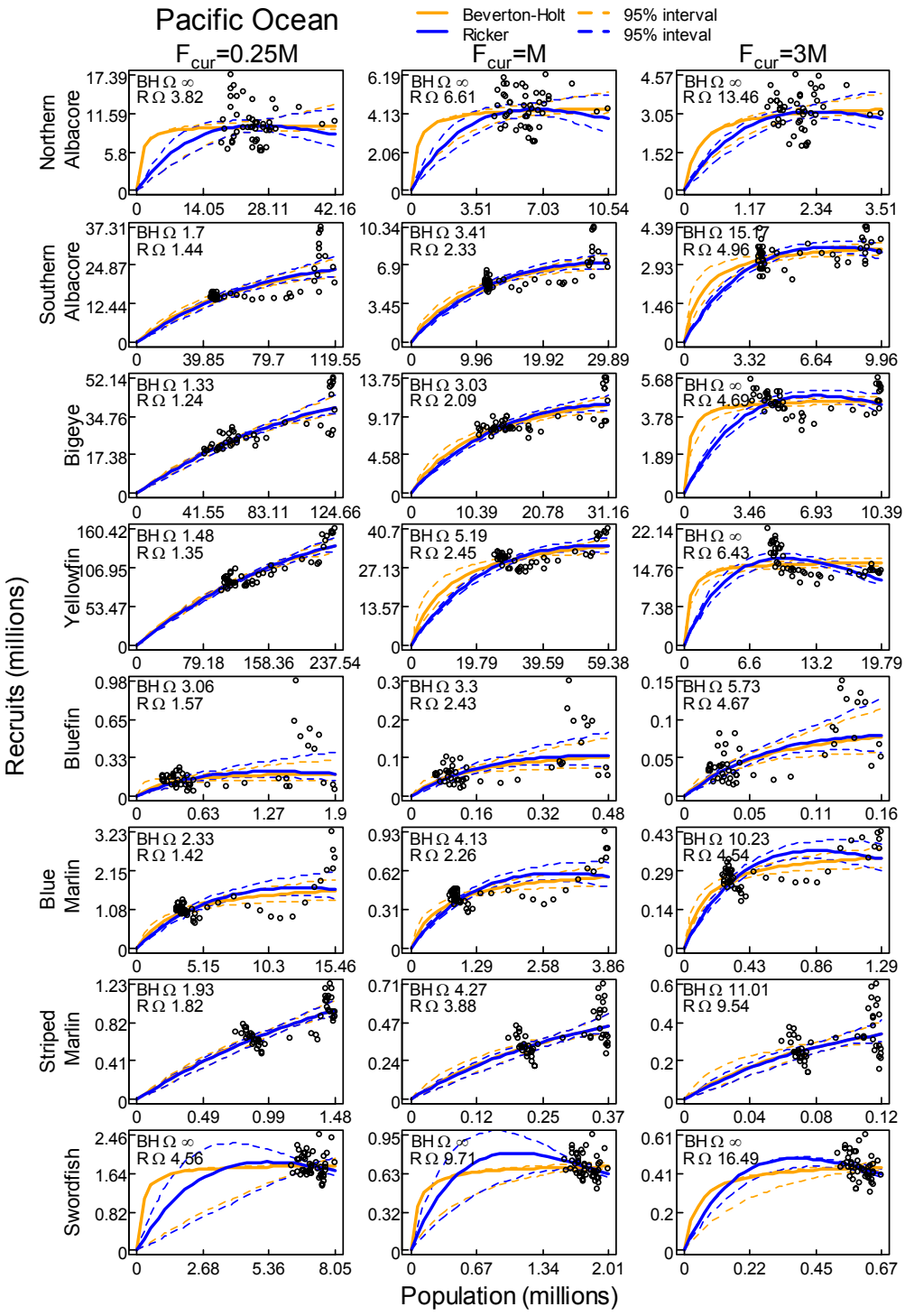

Figure 4.5 Stock recruitment reconstructions and best fits for stock in the Pacific Ocean. Fits are for the Beverton-Holt (BH, orange line) and Ricker (R, blue line) recruitment relationships under three estimates of current fishing mortality rate (F_{cur}) and a fixed natural mortality rate. Ω is the MLE estimate of the compensation ratio.

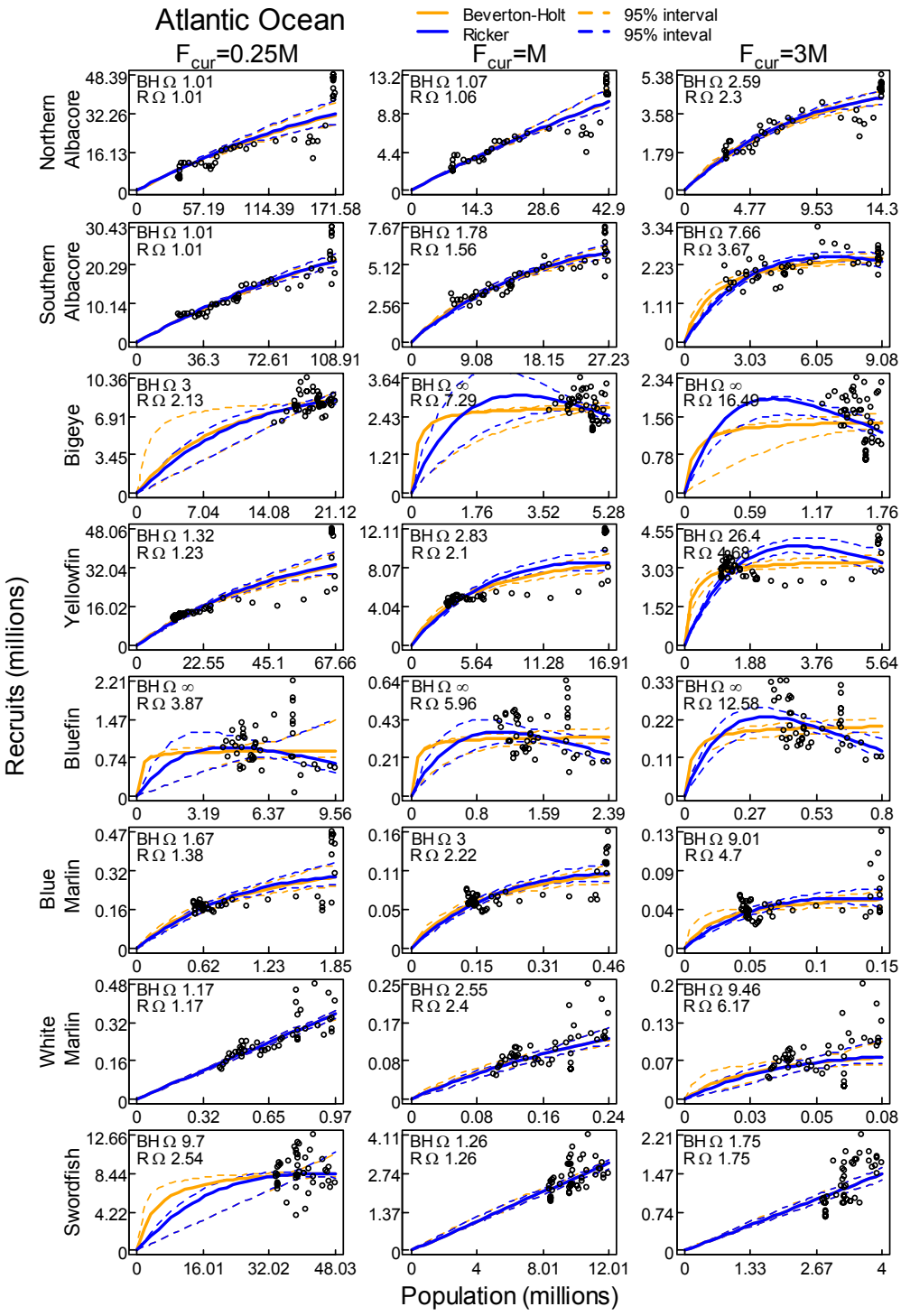

Figure 4.6 Stock recruitment reconstructions and best fits for stock in the Atlantic Ocean. Fits are for the Beverton-Holt (BH, orange line) and Ricker (R, blue line) recruitment relationships under three estimates of current fishing mortality rate (F_{cur}) and a fixed natural mortality rate. Ω is the MLE estimate of the compensation ratio.

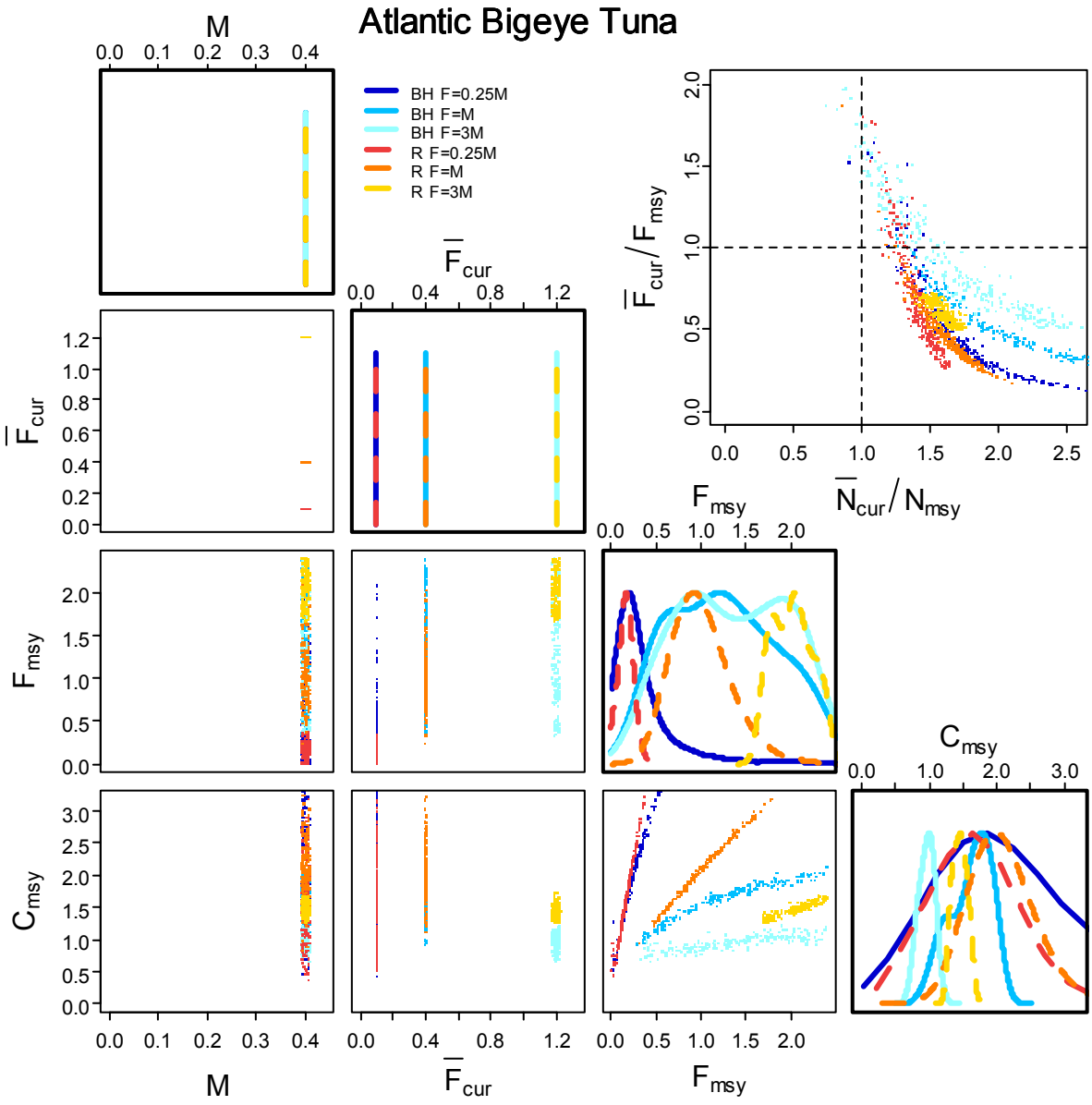

Figure 4.7 Atlantic Ocean bigeye tuna leading parameter joint distribution (lower triangular), marginal posterior distributions (diagonal) and biological reference points (upper triangular) for F_{msy} and MSY (C_{msy}) estimated from recruitment reconstructions assuming Beverton-Holt (BH) and Ricker (R) recruitment relationships for three current fishing mortality estimates (F_{cur} or F) and a known natural mortality rate M. Biological reference points are the ratio of current fishing mortality to the fishing mortality which produces MSY, and the ratio of current stock size to the stock size that produced MSY when fished at F_{msy}. Filled circles outside the upper triangular plot indicate ratios greater than 5. If both ratios are greater than 5 the filled circles lay in the top right corner.

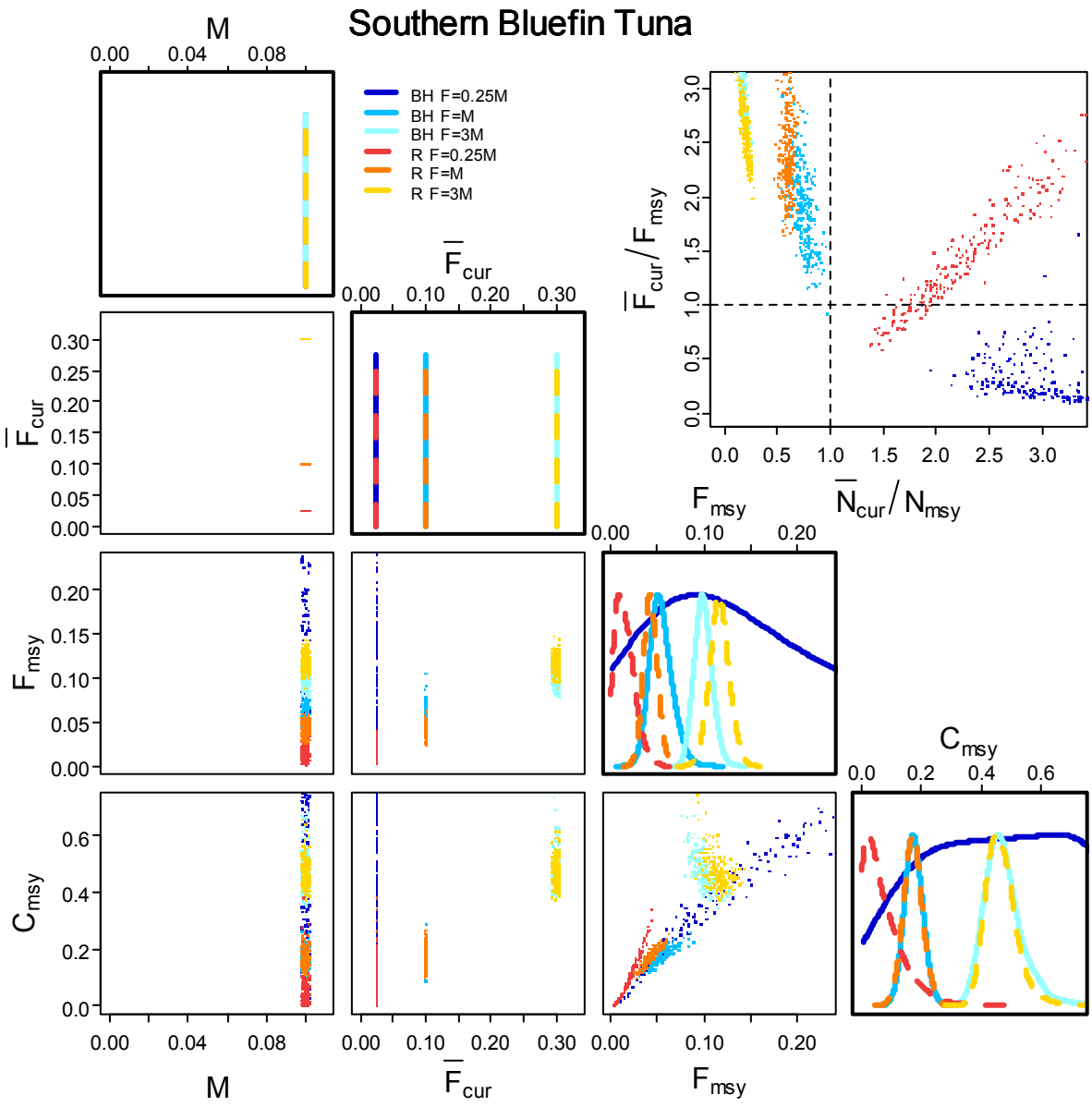

Figure 4.8 Southern bluefin tuna leading parameter joint distribution (lower triangular), marginal posterior distributions (diagonal) and biological reference points (upper triangular) for Fmsy and MSY (C_{msy}) estimated from recruitment reconstructions assuming Beverton-Holt (BH) and Ricker (R) recruitment relationships for three current fishing mortality estimates (F_{cur} or F) and a known natural mortality rate M. Biological reference points are the ratio of current fishing mortality to the fishing mortality which produces MSY, and the ratio of current stock size to the stock size that produced MSY when fished at F_{msy}. Filled circles outside the upper triangular plot indicate ratios greater than 5. If both ratios are greater than 5 the filled circles lay in the top right corner.

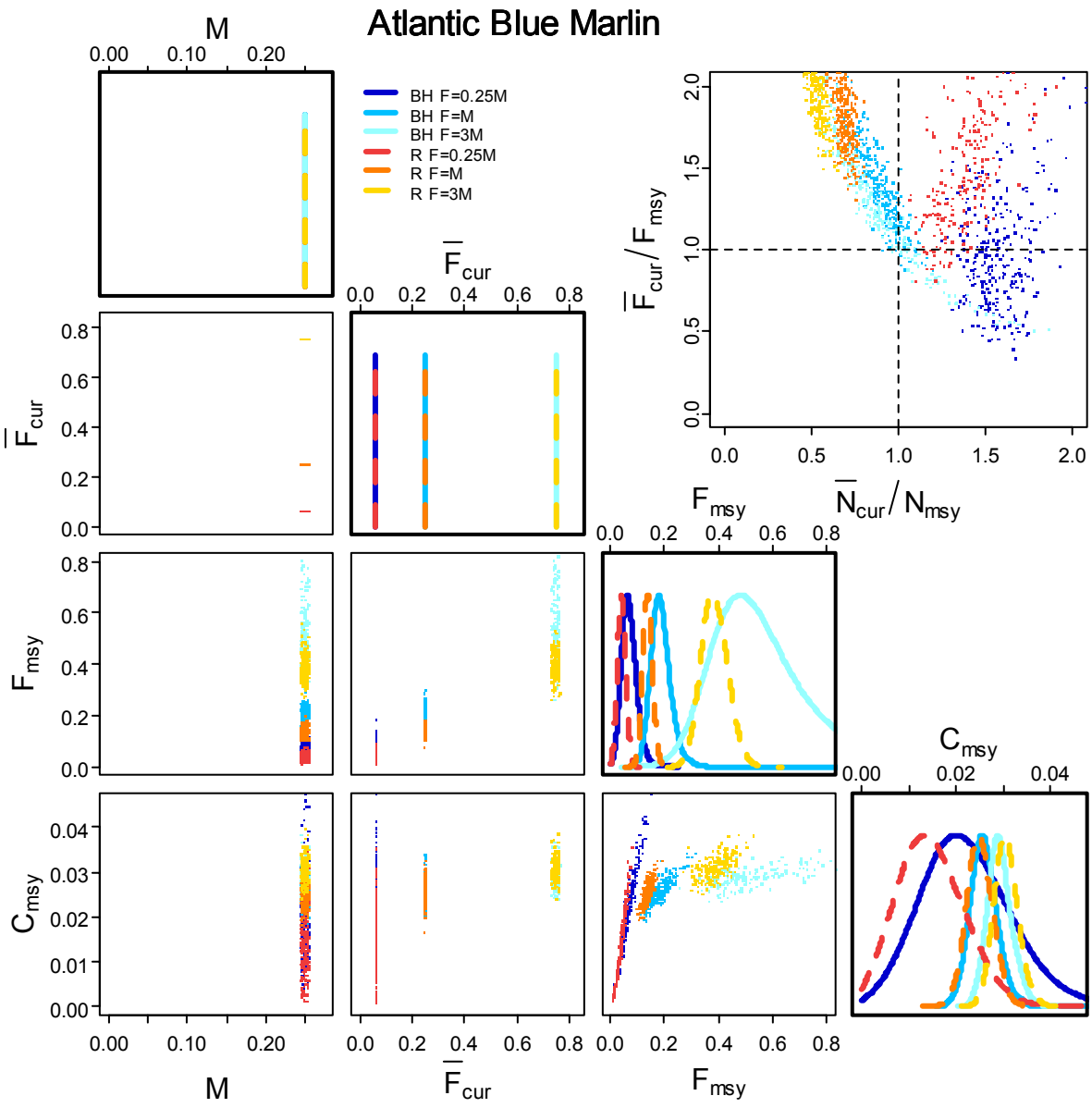

Figure 4.9 Atlantic Ocean blue marlin leading parameter joint distribution (lower triangular), marginal posterior distributions (diagonal) and biological reference points (upper triangular) for F_{msy} and MSY (C_{msy}) estimated from recruitment reconstructions assuming Beverton-Holt (BH) and Ricker (R) recruitment relationships for three current fishing mortality estimates (F_{cur} or F) and a known natural mortality rate M. Biological reference points are the ratio of current fishing mortality to the fishing mortality which produces MSY, and the ratio of current stock size to the stock size that produced MSY when fished at F_{msy}. Filled circles outside the upper triangular plot indicate ratios greater than 5. If both ratios are greater than 5 the filled circles lay in the top right corner.

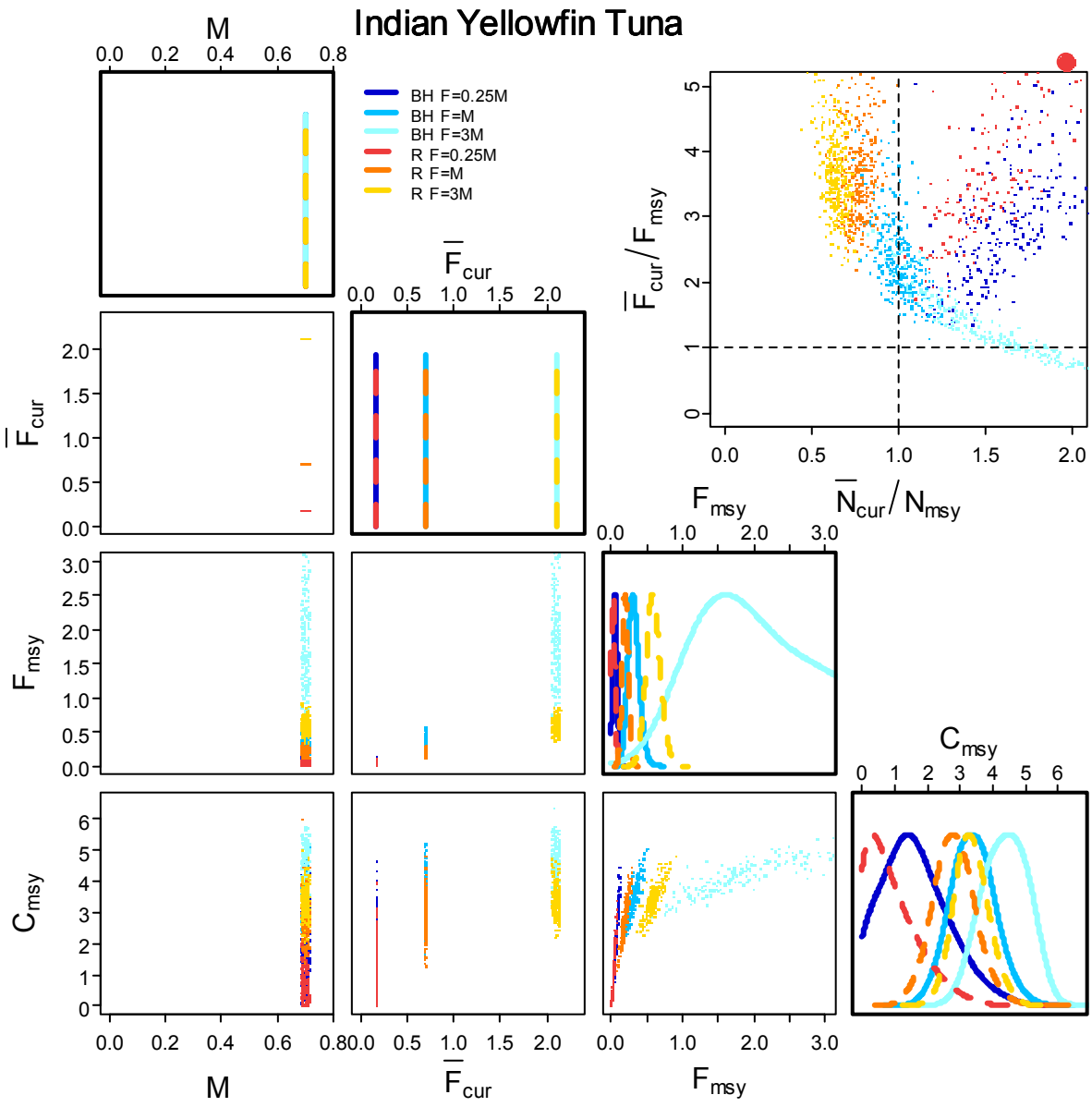

Figure 4.10 Indian Ocean yellowfin tuna leading parameter joint distribution (lower triangular), marginal posterior distributions (diagonal) and biological reference points (upper triangular) for F_{msy} and MSY (C_{msy}) estimated from recruitment reconstructions assuming Beverton-Holt (BH) and Ricker (R) recruitment relationships for three current fishing mortality estimates (F_{cur} or F) and a known natural mortality rate M. Biological reference points are the ratio of current fishing mortality to the fishing mortality which produces MSY, and the ratio of current stock size to the stock size that produced MSY when fished at F_{msy}. Filled circles outside the upper triangular plot indicate ratios greater than 5. If both ratios are greater than 5 the filled circles lay in the top right corner.

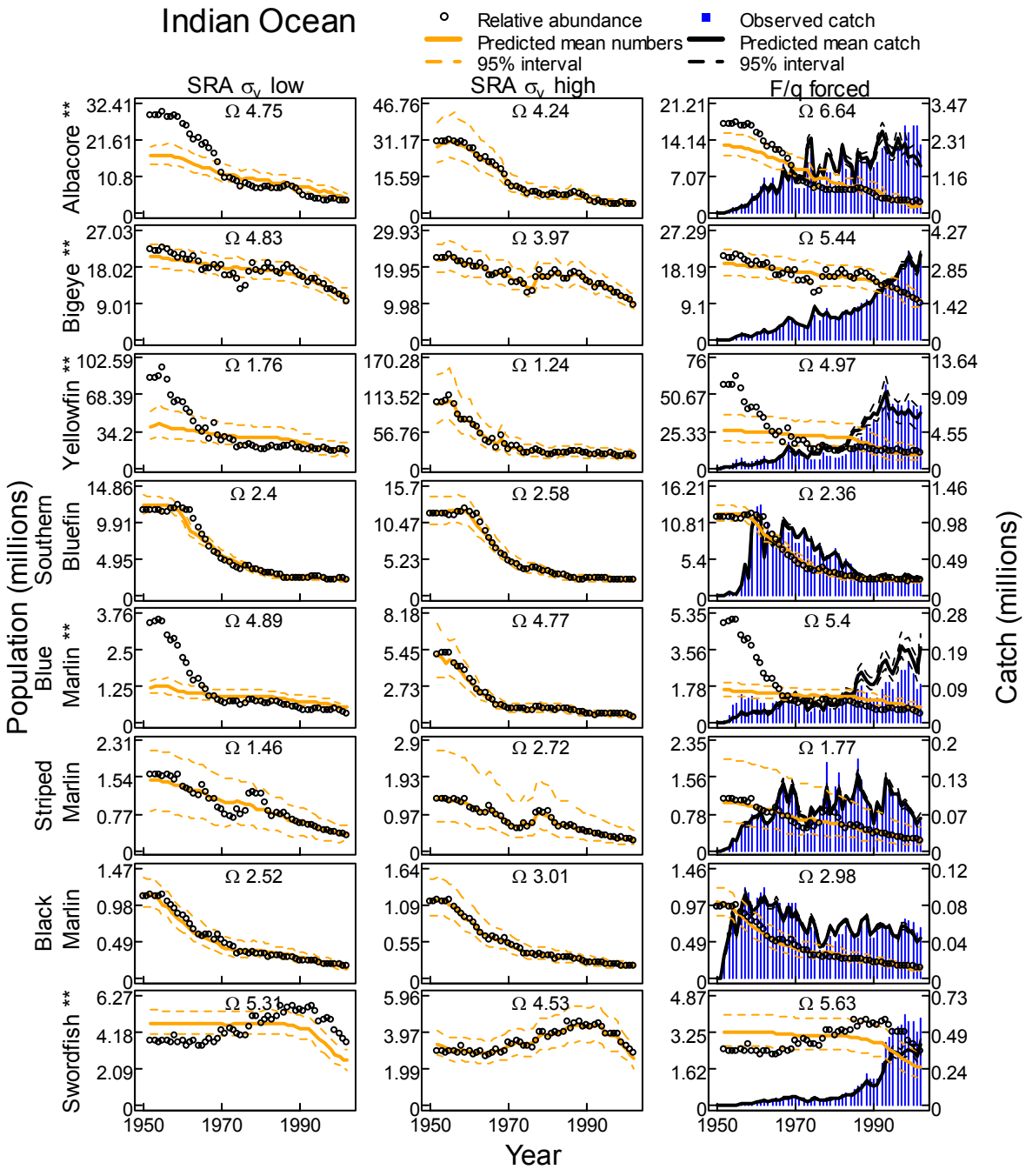

Figure 4.11 Fit and confidence bounds for SRA and F/q forced models for stock in the Indian Ocean. SRA σ_v low column are results from SRA where variance in recruitment anomalies was assumed low. SRA σ_v high are from SRA where variance in recruitment anomalies was assumed high. The F/q forced columns are results from the relative fishing mortality rate forced numbers dynamic model. Open circles represent relative abundance trends. Orange lines and orange dashed lines are mean population estimates and 95% intervals. Blue vertical bars are observed catch and black lines and dashed black lines are predicted catch and 95% interval. Ω is the MLE estimate of the compensation ratio. * indicates a prior on F_{cur} and ** indicates priors of F_{cur} and F_{msy}.

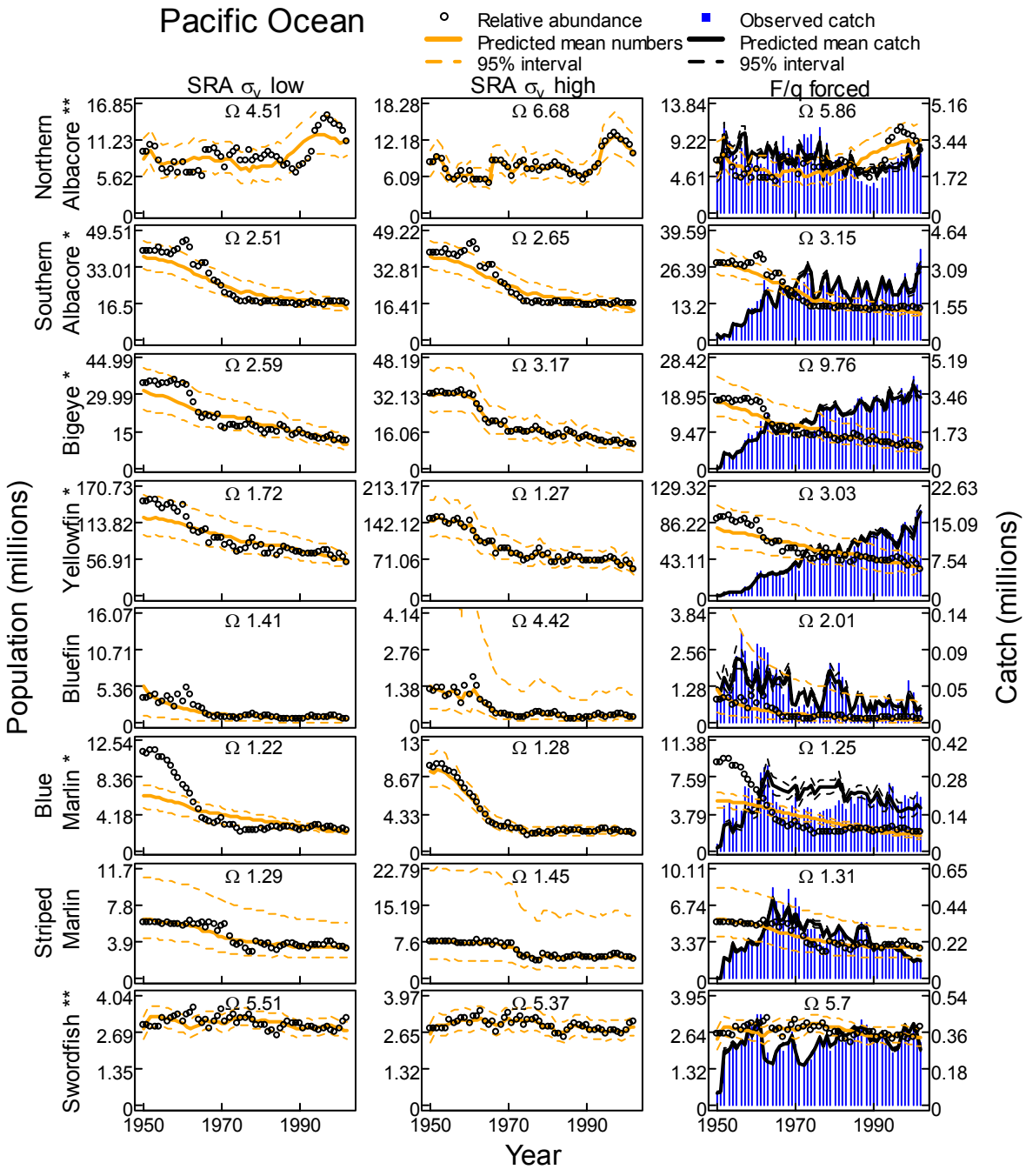

Figure 4.12 Fit and confidence bounds for SRA and F/q forced models for stocks in the Pacific Ocean. SRA σ_v low column are results from SRA where variance in recruitment anomalies was assumed low. SRA σ_v high are from SRA where variance in recruitment anomalies was assumed high. The F/q forced columns are results from the relative fishing mortality rate forced numbers dynamic model. Open circles represent relative abundance trends. Orange lines and orange dashed lines are mean population estimates and 95% intervals. Blue vertical bars are observed catch and black lines and dashed black lines are predicted catch and 95% interval. Ω is the MLE estimate of the compensation ratio.* indicates a prior on F_{cur} and ** indicates priors of F_{cur} and F_{msy}.

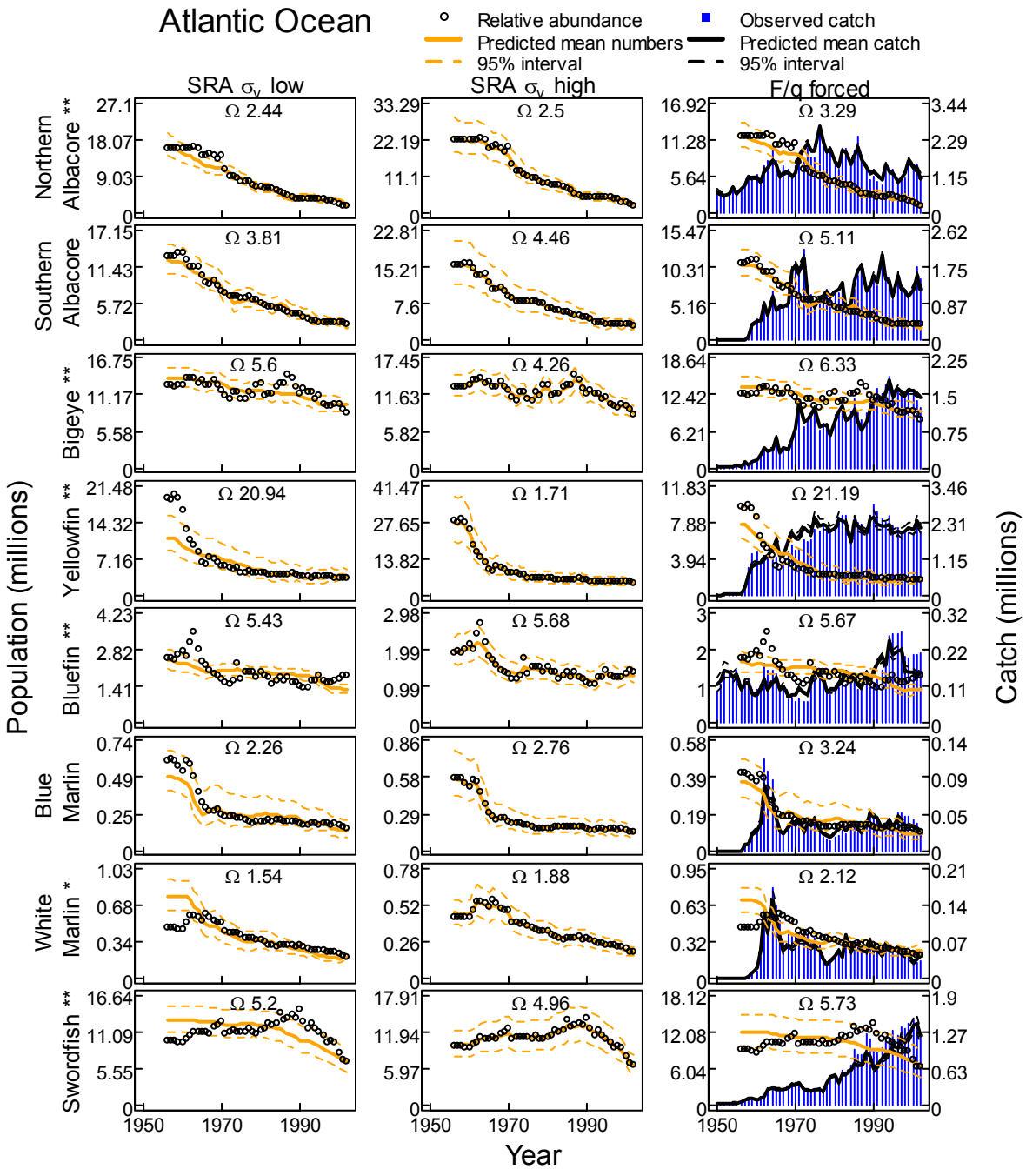

Figure 4.13 Fit and confidence bounds for SRA and F/q forced models for stocks in the Atlantic Ocean. SRA σ_v low column are results from SRA where variance in recruitment anomalies was assumed low. SRA σ_v high are from SRA where variance in recruitment anomalies was assumed high. The F/q forced columns are results from the relative fishing mortality rate forced numbers dynamic model. Open circles represent relative abundance trends. Orange lines and orange dashed lines are mean population estimates and 95% intervals. Blue vertical bars are observed catch and black lines and dashed black lines are predicted catch and 95% interval. Ω is the MLE estimate of the compensation ratio. * indicates a prior on F_{cur} and ** indicates priors of F_{cur} and F_{msy}.

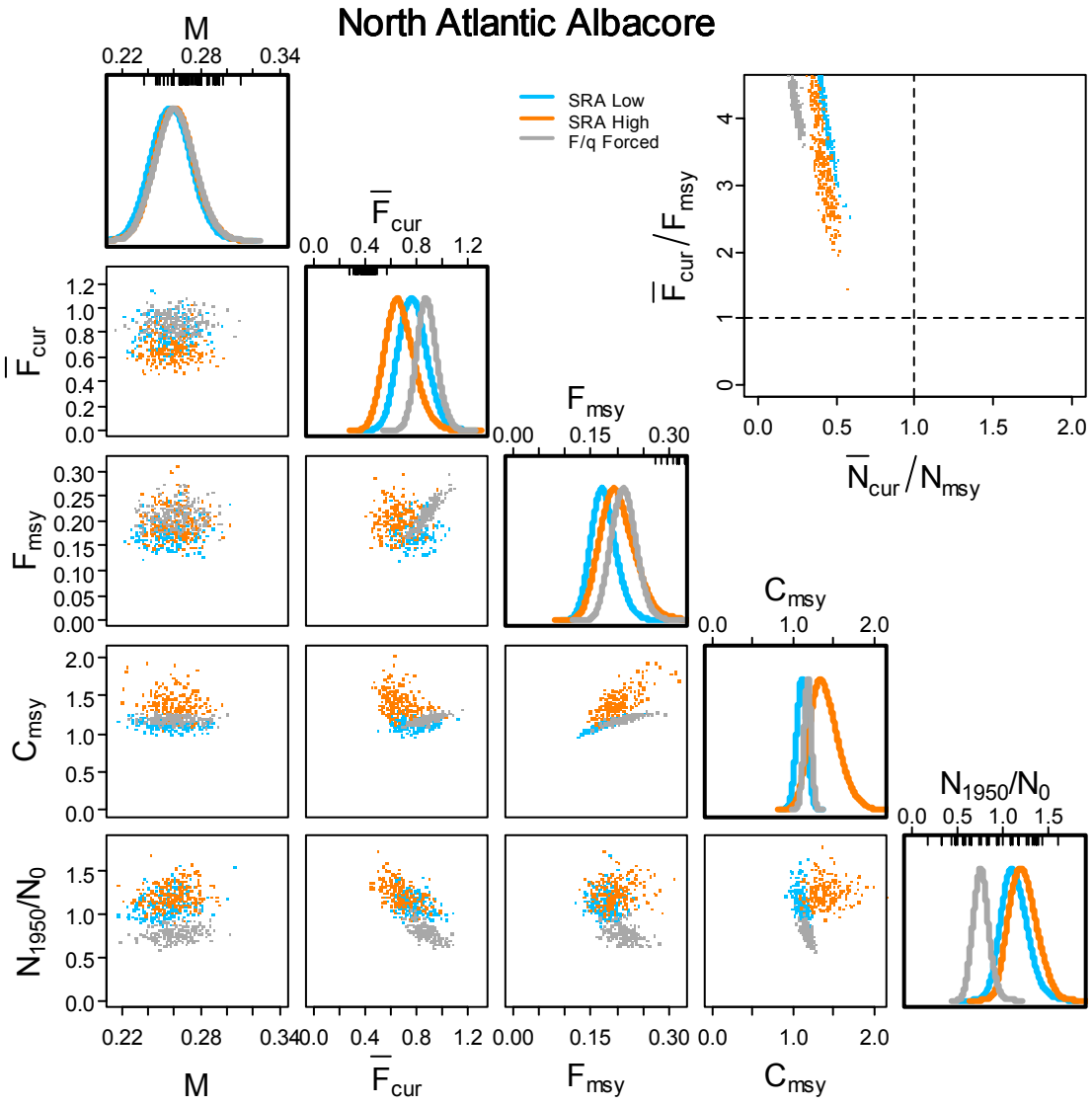

Figure 4.14 Atlantic Ocean northern albacore tuna leading parameter joint distribution (lower triangular), marginal posterior distributions (diagonal) and biological reference points (upper triangular) for natural mortality (M), current fishing mortality (F_{cur}), fishing mortality that produced MSY (F_{msy}), MSY (C_{msy}) and the ratio of population in 1950 to that expected in the absence of fishing. Black lines and points are SRA where variance in recruitment anomalies was assumed low. Medium grey lines and points are from SRA where variance in recruitment anomalies was assumed high. Light grey lines and points are from the relative fishing mortality rate forced numbers dynamic model. Rug plots on the top of distributions on the diagonal demark prior distributions.

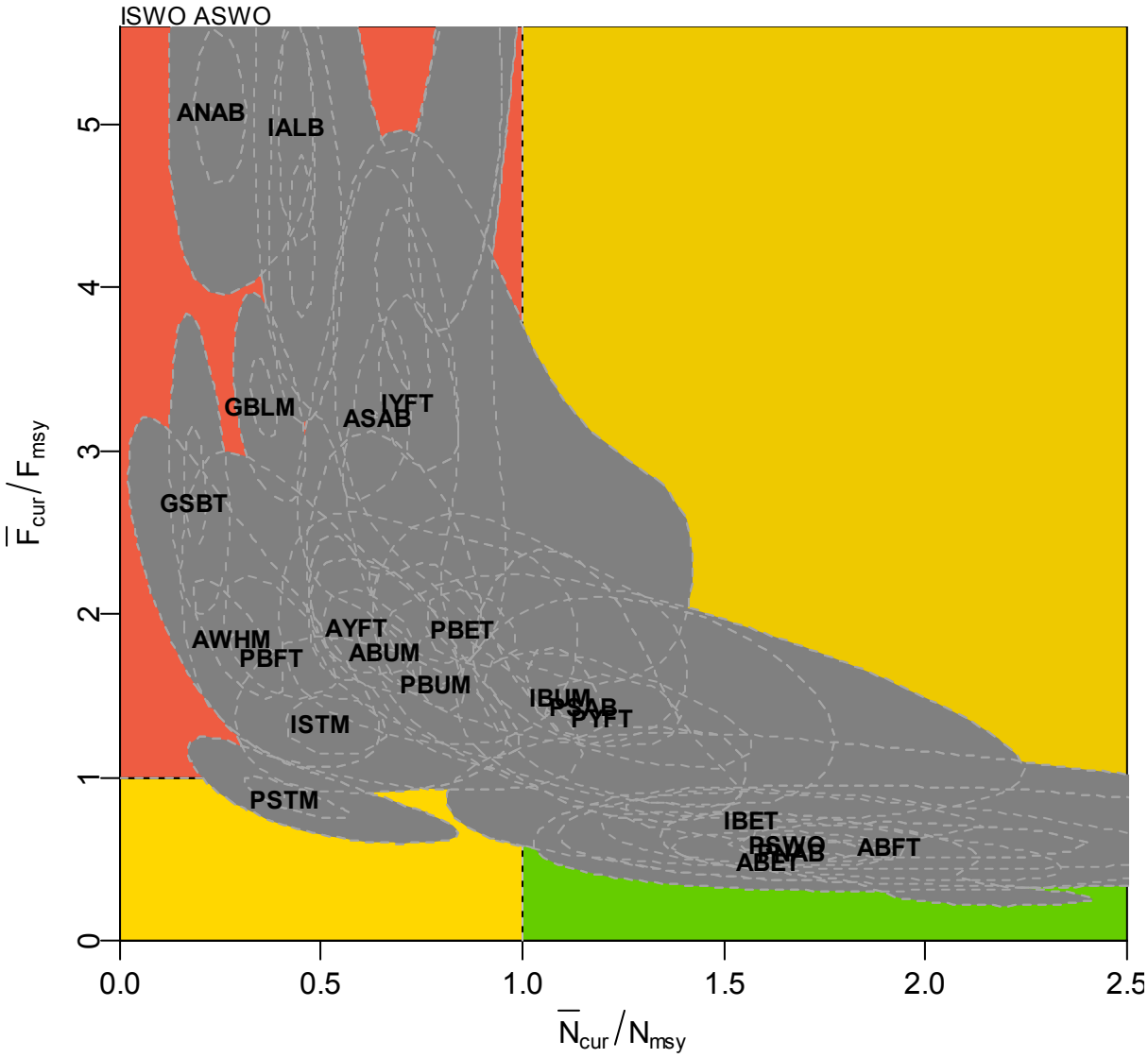

Figure 4.15 Joint distributions for biological reference points for recruitment reconstructions for all hypothesized current fishing mortality rates as well as Ricker and Beverton-Holt recruitment functions. Stock names demark the centre of the 1% quantile. Darker grey shading with lighter grey lines indicate the 10% and 50% probability contour. Ratios greater than 5 were not included for plotting clarity and stock identifiers are placed in the margin.

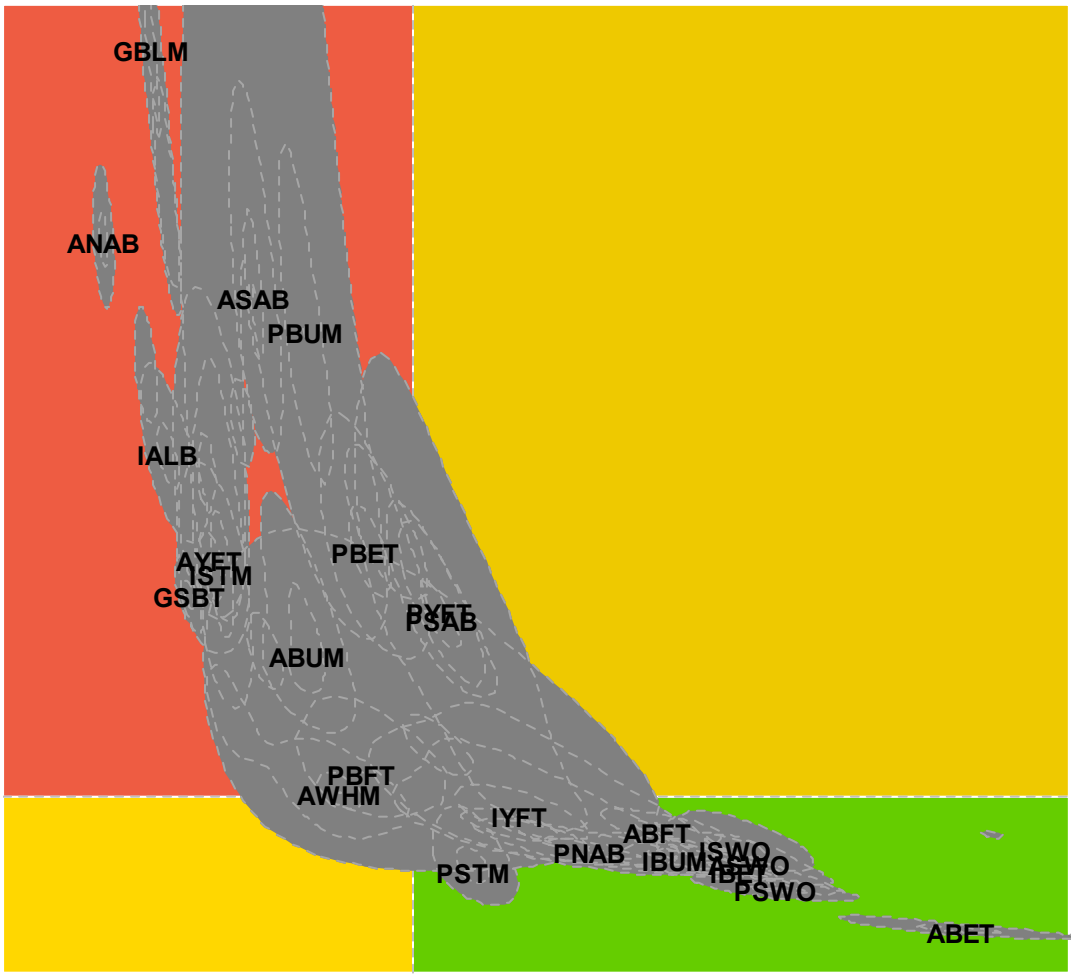

Figure 4.16 Joint distributions for biological reference points for SRA estimations and E^* forced simulations combined. Stock names demark the centre of the 1% quantile. Darker grey shading with lighter grey lines indicate the 10% and 50% probability contour. Ratios greater than 5 were not included for plotting clarity and stock identifiers are placed in the margin.

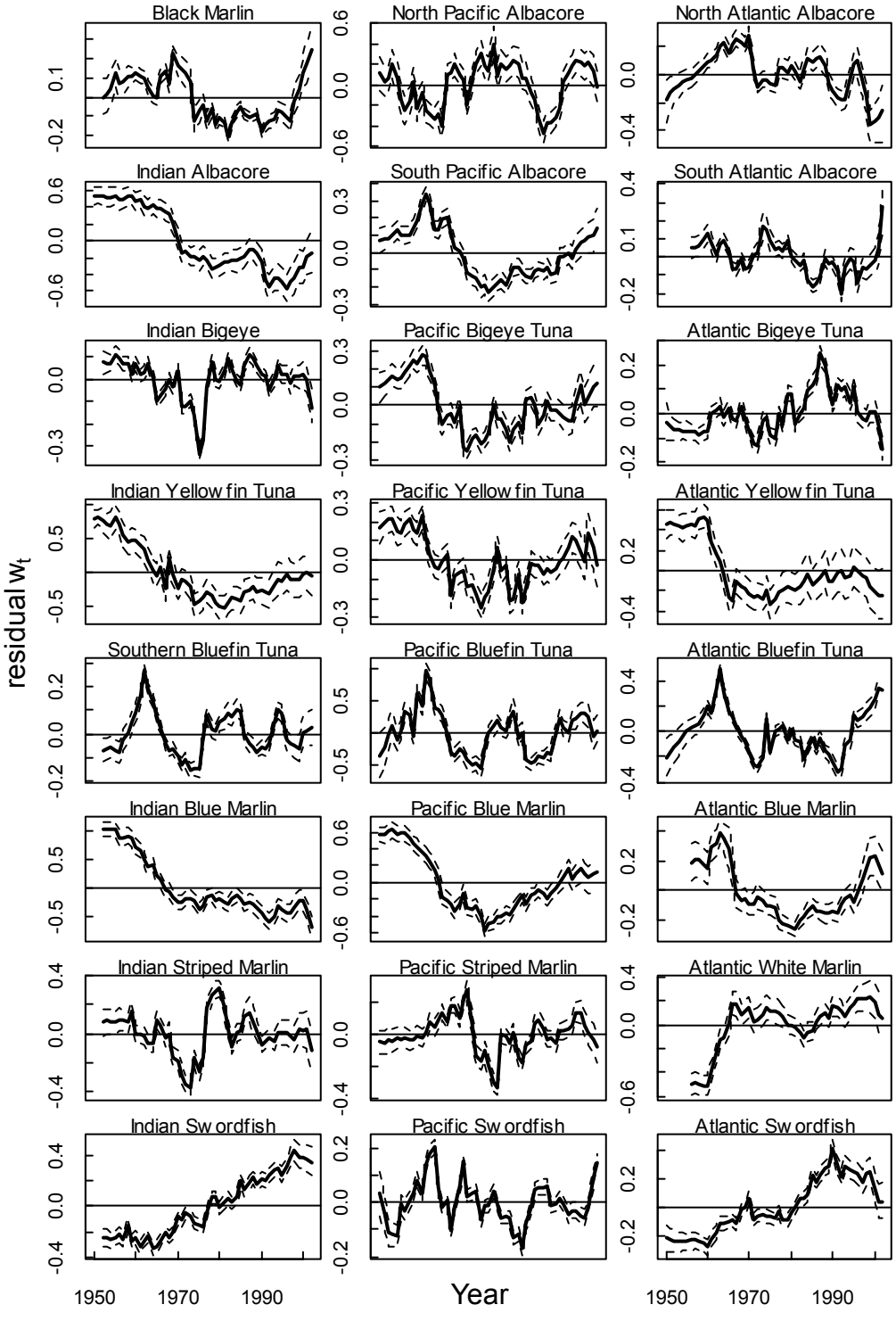

Figure 4.17 Observation residuals and 95% credible intervals from stochastic SRA assessment of each stock assuming a high proportion of total variability in relative abundance trends was due to observation error.

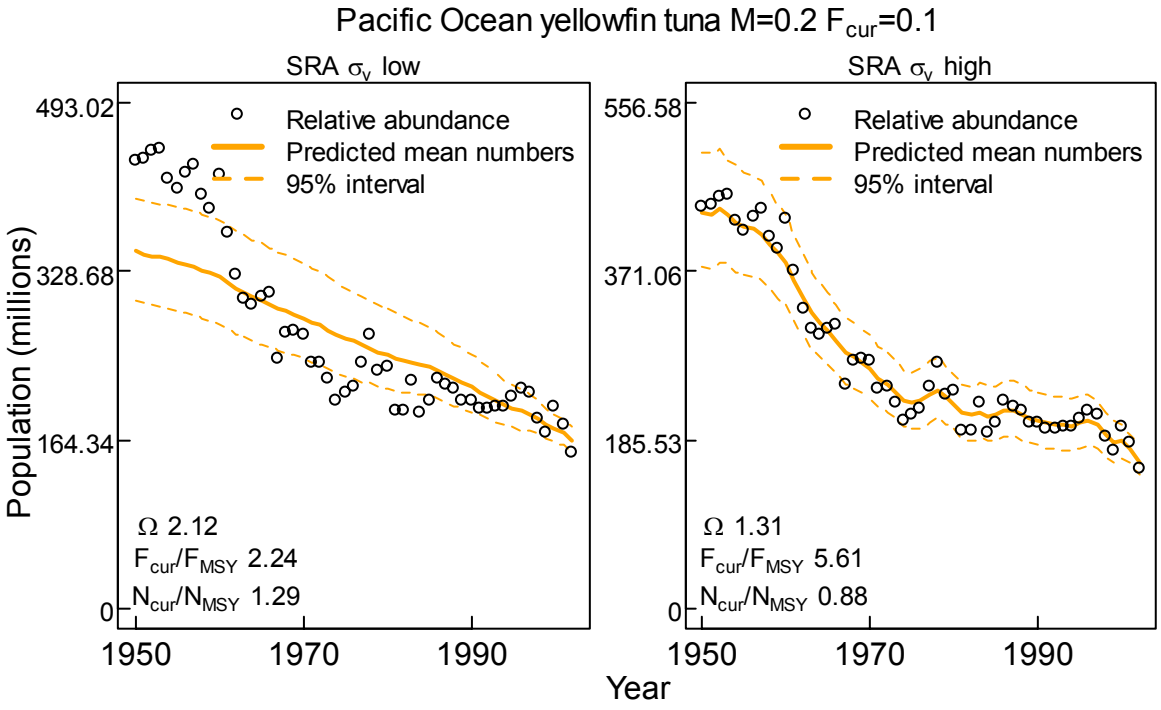

Figure 4.18 Estimated abundance trends, compensation ratio (Ω), and reference points for Pacific Ocean yellowfin tuna from stochastic SRA with alternate hypothesis of natural mortality (M) and current fishing mortality (F_{cur}). Open circles designate relative abundance trends. Orange lines are MLE estimates of population size and dotted grey line delineate 95% credible intervals.

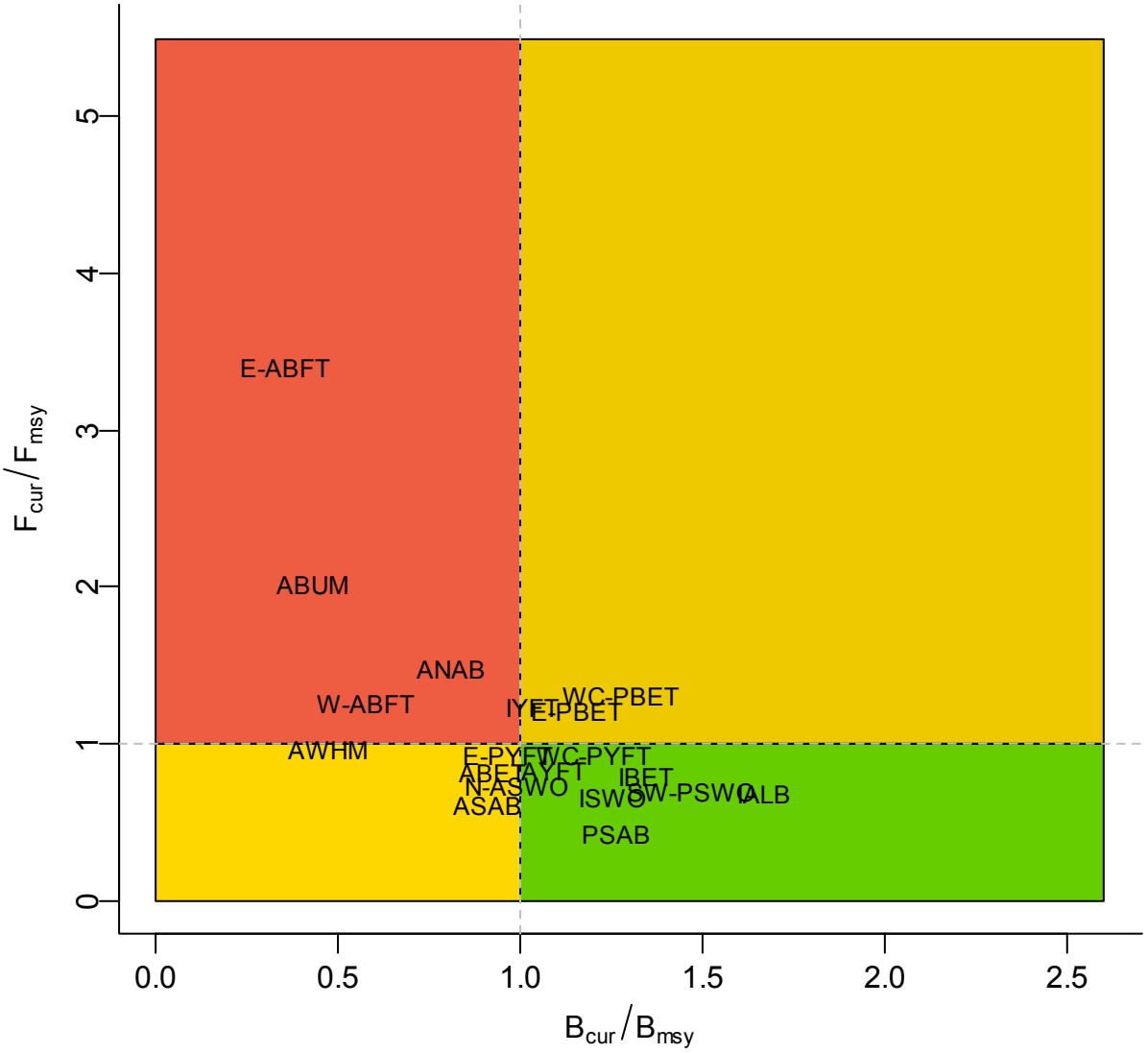

Figure 4.19 Point estimates of biological reference points from stock assessments produced by RFMOs.

Chapter 5 A spatially explicit population dynamics model to assess apparent recruitment, productivity, distribution, and movement patterns

Introduction

Spatial distributions of tuna and billfish stocks and the fisheries pursuing them are inherently heterogeneous. Disregarding this changing patchwork of species and fisheries interactions has obvious consequences for the management of these resources. Spatially aggregated 'dynamic pool' assessment models do not capture fishery impacts on local abundances, sub stocks, or potential spill over effects on neighboring abundances of local exploitation. Furthermore, spatial heterogeneity creates opportunity to enhance fisheries while conserving stocks of concern, by using spatial regulations to target effort at particular times or in specific areas (Goodyear 2003, Walters and Martell 2004). Obvious spatial heterogeneity coupled with complex fishery dynamics, biological potential for long distance movements, and availability of large tagging and recapture data sets has stimulated significant advancement in incorporating spatial movement into assessment models for tuna and billfish.

Two basic types of models have been developed to quantify fish movement in fishery assessment models, and have been applied to tuna over recent decades. The first type ('Eulerian') represents abundance changes over a fixed grid or set of irregular spatial areas, with movement represented as fluxes between the areas. Within the Eulerian class of movement models, Beverton and Holt (1957) introduced the concepts of bulk transfer models and diffusion models in fisheries. A number of studies have used tagging data to parameterize mixing (transfer) coefficients (Hampton 1991, Hampton and Gunn 1998, Hilborn 1990). Advection-diffusion models have been parameterized by estimating cross-boundary transfer rates from tagging data (Kleiber and Hampton 1994) or Markovian transition matrices (Deriso et al. 1991). Sibert and Fournier (1994) developed a general advection-diffusion-reaction model for fisheries assessment and applied it to skipjack tuna (Sibert et al. 1999). More elaborate advection-diffusion models have attempted to predict movement from basic biological principles, using habitat gradients and biological constraints determined from life-history characteristics (e.g., Bertignac et al. 1998, Lehodey et al.

2006, Lehodey et al. 1997, Lehodey et al. 2003, Lehodey et al. 2008). The second type of model ('Largrangian') represents populations as individuals (or packets of individuals) each with spatial coordinate attributes, and movement is represented by changes in the coordinates of each individual. Such models have also been utilized to assess movement and evaluate fishery impacts (e.g., Meester 2000, Porch 1995, Tyler and Rose 1994). However, although some assessments have incorporated movement mainly using Eulerian representations, (e.g., Hampton and Fournier 2001, Hampton et al. 2006a, Hampton et al. 2006b, ICCAT 2006a), many assessments of tunas and billfishes are either spatially disaggregated stock synthesis models with no movement between areas (e.g., Fournier et al. 1998, Kolody et al. 2006, Maunder and Hoyle 2007), or are spatially aggregated (e.g., ICCAT 2003b, c, ISC 2008b).

A multi-species, spatially explicit (5°x5° spatial cells) population dynamics model was developed and parameterized for the species examined in this thesis. Unlike many of the previously mentioned models and assessments, only spatial catch and effort data along with basic information from tagging studies were used to infer stock distribution and movement. This model provided a framework to map stock spatial distribution over time, highlight areas of apparent high recruitment, and map an ostensible static or average advection-diffusion field for each stock. One of the advantages of a spatially linked model is that it provides a framework to assess stock depletion on a smaller scale based on an underlying biological structure instead of inferring stock changes directly from local relative abundance trends. Incorporating movement fields allowed the impact of local fishing on surrounding areas to be assessed which in turn provided insight into the appropriateness of backfilling assumptions used in Chapter 3. Finally, a spatially explicit model is essential when exploring spatial effort distributions policies, which will be the topic of Chapter 6.

Methods

The spatially explicit assessment model presented in this section is an extension of the simple E^* forced dynamic model presented in Chapter 4. It is to be understood in the following that all parameters and variables are subscripted by species as well as spatial cell (i) and year (t); species subscripts are suppressed for clarity in presenting model equations. The dynamics of a species

for any given spatial cell (i), in this instance at a resolution of 5°x5°, is modeled using an 'Eulerian' approach assuming mixing rates across boundaries are constant over time and season:

5.1) $$dN_i/dt = R_{i,t} - F_{i,t}N_{i,t} - MN_{i,t} - \sum_{i\to j} v_{i\to j}N_{i,t} + \sum_{j\to i} v_{j\to i}N_{j,t}$$

In this model, the rate of change of the population of individuals vulnerable to longline gear in cell i depends on (1) local recruitment of individuals growing into vulnerable size ($R_{i,t}$); (2) natural mortality losses ($MN_{i,t}$), (3) removals due to fishing ($F_{i,t}N_{i,t}$), (4) movement of individuals out of cell i ($v_{i\to j}N_{i,t}$) to the surrounding 4 cells j , and (5) movement of individuals from surrounding cells j ($v_{j\to i}N_{j,t}$) into cell i. Solution of equation 5.1 over annual time steps was done using the second-order Adams-Bashforth method (Benyon 1968) with a numerical integration time step of 1 day.

Prediction of cell-specific recruitment, fishing mortality, and exchange rates each required specific assumptions. A Beverton-Holt function (equation 5.2) was used to predict total recruitment each year, and this total was distributed over spatial cells assuming that the proportion of individuals recruiting to each cell is stable over time. As in Chapter 4, a management-oriented parameterization for total recruitment was used (equation 4.8 and equation 4.9):

5.2) $$\sum_i R_{i,t} = a\sum_i N_{i,t-k}\left(1 + b\sum_i N_{i,t-k}\right)^{-1}$$

Cell specific recruitment was assumed to be unaffected by local depletion, and total recruitment was distributed as a fixed proportion of total recruitment to each cell. The proportion of total recruitment (pR_i) allocated to each cell i was estimated from an average recruitment for the cell, calculated over all years (T):

5.3) $$pR_i = \overline{R}_i \Big/ \sum_i \overline{R}_i \qquad where \quad \overline{R}_i = T^{-1}\sum_t \hat{R}_{i,t}$$

Cell-year specific recruitments ($\hat{R}_{i,t}$) were reconstructed following a method similar to that presented in Chapter 4, but while including effects of movement to and from adjacent cells. Given a cell- specific MA-3 smoothed relative abundance time series ($y_{i,t}^{MA-3}$) where missing observations had been imputed (in this case following the SF31 method in Chapter 3), recruitment in cell *i* for any year was estimated as

$$\hat{R}_{i,t} = \hat{N}_{i,t+1} - \hat{N}_{i,t} + M\left(\hat{N}_{i,t+1} + \hat{N}_{i,t}\right)/2 + C_{i,t} + \sum_{i\to j} v_{i\to j}\, 0.5\left(\hat{N}_{i,t+1} + \hat{N}_{i,t}\right) - \sum_{j\to i} v_{j\to i}\, 0.5\left(\hat{N}_{j,t+1} + \hat{N}_{j,t}\right) \quad where \quad \hat{N}_{i,t} = y_{i,t}^{MA-3}/q^{*} \tag{5.4}$$

Here *q* is the catchability coefficient (assumed constant over *i*), $0.5\left(\hat{N}_{i,t+1} + \hat{N}_{i,t}\right)$ are time averages over year t of the cell-specific populations, used as a predictors of natural mortality loss and mixing rate over the year, and mixing rates *v*'s are initially set equal for all areas and directions.

However, for some cells, total recruitment summed over the entire time was predicted by equation 5.4 to be negative, indicating either a problem with the estimation of local population abundance or a diffusion imbalance. Assuming negative recruitment arose from diffusion imbalances, negative recruitment predictions were redressed by reducing the total inflow component of 5.4 (the sum of flow from j surrounding cells calculated over the entire period) by the negative of total recruitment. This was achieved by assuming that cell inflows equaled outflows over the entire period (equation 5.5) for each surrounding area.

$$v_{i\to j}\sum_{T} 0.5\left(\hat{N}_{i,t+1} + \hat{N}_{i,t}\right) = vnew_{j\to i}\sum_{T} 0.5\left(\hat{N}_{j,t+1} + \hat{N}_{j,t}\right) \tag{5.5}$$

Provided total recruitment into the surrounding cell (j) was positive and the sum of time averaged population estimates larger than that for cell *i*, the new flow rate from *j* to *i* (*vnew*) was calculated as,

$$vnew_{j\to i} = v_{j\to i}\sum_{T} 0.5\left(\hat{N}_{i,t+1} + \hat{N}_{i,t}\right)\Big/\sum_{T} 0.5\left(\hat{N}_{j,t+1} + \hat{N}_{j,t}\right) \tag{5.6}$$

where $v_{j\rightarrow j}$ was the initial mixing rate. Total recruitment in cell j was reduced to account for the reduction in outflow over the entire period, potentially resulting in negative values. As a result, the procedure was iterated until total recruitment was non-negative in all areas. This method of adjusting the v's changed the model from being purely diffusive to one with v's that represented both advection and diffusion.

One obvious constraint that had to be applied in adjusting the movement v's was to restrict movement to only those cells (stock ranges) actually sampled by fisheries. It may be reasonable to assume that cells with relatively high abundance would have attracted fishing effort, thus areas not fished likely had inconsequential abundance. However, this assumption ignores two possible scenarios. The first is that there may be areas that were considered to dangerous to fish or too difficult to fish, despite containing large portions of a population. The second is that there may be cells where fishing access was restricted or where data had not been collected. Absent additional information, it was not possible to correct for these possibilities.

Catchability (q^* equation 5.4) was derived from an estimate of average fishing mortality (F_{cur}) in recent years (i.e. 2000-2002) following similar reasoning to that presented in Chapter 4:

$$5.7)\quad F_{cur} = \frac{\overline{C}}{\overline{N}} = \frac{\sum_{i,t} C_{i,t}}{\sum_{i,t} y_{i,t} / q^*} \qquad if \quad y_{i,t} = q^* N_{i,t} \qquad \therefore \qquad q^* = F_{cur} \frac{\sum_{i,t} y_{i,t}}{\sum_{i,t} C_{i,t}}$$

It is interesting to note, and a useful conversion when q cannot be assessed directly, that the ratio of q^* from equation 5.7 and the total stock-scale catchability coefficient (q) estimated in Chapter 4 is simply the ratio of the sum of cell-specific relative abundances (y_i) to the average relative abundance. Predictions of cell-specific fishing mortality rates ($F_{i,t}$) were calculated using the q^* derived above along with estimates of cell-specific effective effort ($E_{i,t}$*).

$$5.8)\quad E^*_{i,t} = C_{i,t} / y_{i,t}$$

Estimated area specific relative fishing mortality rates were expected to be highly erratic in some cells, due to variability in *cpue* in those cells. To prevent numerical instability due to large values

of $F_{i,t}$, $E_{i,t}$* was expressed relative to an effective effort calculated across all species (j) considered. Thus,

5.9) $E^*_{i,t} = r_{i,t}\overline{E}^*_{i,t}$ *where* $r_{i,t} = \dfrac{C_{i,t}/y_{i,t}}{\sum_j C_{j,i,t} \Big/ \sum_j y_{j.i.t}}$ *and* $\overline{E}^*_{i,t} = \sum_j C_{j,i,t} \Big/ \sum_j y_{j.i.t}$

Here $r_{i,t}$ was constrained for numerical stability to be no greater than 5, and j was the number of species considered.

Determining realistic base mixing rates was a difficult challenge, since information on average yearly displacement or estimates of diffusivity are not readily available in the literature. From equations 5.10 and 5.11, taken from Kleiber and Hampton (1994) mixing rates (v) were approximated from estimates of mean displacement distance (r^*) or diffusivity (D) given the width (Δx) of 5° area at the equator. Kleiber and Hampton show that D, r*, and v are related as:

5.10) $D = \left(0.5r^*\right)^2 \pi$

5.11) $v = \Delta x^{-2} D$

Data presented in Ortiz (2003) on minimum distance traveled from billfish tag recaptures indicates a high proportion of recaptures occur within 2,000 km of the release point, which translates into mixing rates v<10. Diffusivity (D) of skipjack tuna averages 200,000 nm^2 per year from results presented in Sibert et al. (1999), which corresponds to a mixing rate of v~0.65. Sibert and Hampton (2003) suggested the lifetime displacement for yellowfin tuna within the Western-Central Pacific to be ~320 nautical miles, corresponding to a mixing rate of v~1. Averaging diffusivity estimates for tagged bigeye tuna presented in Sibert et al. (2003) results in estimates of D in the range 50,000-700,000 nm^2 or mixing rates v in the range 0.5 to 8.0. The higher value results when individual diffusivity estimates of 0 are excluded from the averaging. Schaefer and Fuller (2005) reported annual displacement distances for bigeye tuna in the eastern Pacific ranging from 3-3000 nautical miles, implying a range of mixing rate from 0 to 80. Hampton and Williams (2005) presented a similar range of values for bigeye tagged in the western and central Pacific, though the majority of recapture were within 500 nautical miles.

These studies suggest that a reasonable range of mixing rates to explore in the model would be 0.7-10, which correspond to mean displacement distances of 500-2000 km.

The model was fit for each species to observed catch summed over all 5°x5° areas. The concentrated total log likelihood (L) of the observed catch can be written as

$$5.12)\ L = -0.5n\ln\left(\sum_{t=1}^{n}\left(\ln\left(\hat{C}_t\right)-\ln\left(C_t\right)\right)^2\right)$$

where n is the number of years of data, $\hat{C}_t$ is the predicted total catch and C_t is the observed total catch. Normal approximations to the marginal posterior and joint posterior distributions for leading parameters F_{msy}, F_{cur}, MSY, M, and N_0 as well as the management reference points described in Chapter 4 were taken from the Hessian, estimated using *AD Model Builder* over a range of hypothesized initial mixing rates (v=0.7, 2, 5, 10). Plots of marginal posterior and joint posterior distributions were generated from 10,000 random samples drawn from a multivariate normal distribution using the covariance matrix generated in *AD Model Builder*. As described in the stochastic SRA section in Chapter 4, informative prior distributions were used for some parameters (see Table 4.1). Due to missing spatial catch data for some gears, some species could not be included in the fitting, as missing spatial catch was a large proportion of total catch removed. In the Pacific Ocean, northern albacore and bluefin were excluded as well as swordfish.

An attempt was made initially to fit the model to cell-scale log catches $ln(C_{it})$ rather than aggregated total catch as in equation 5.9, in hopes that the local catch time series might provide information about mixing rates not included in the calculated mean recruitments and recruitment proportions pR. The attempt failed badly, giving very high estimates of recruitment compensation and unfished biomass so as to 'flat line' predicted biomasses for some species. This flat line effect was apparently due to trying to fit erratic catch time series for substantial numbers of cells near species range boundaries, for which no temporal pattern was evident or cells where catch and *cpue* increased over time. Catches from such marginal cells were given the

same statistical weight in the $ln(C_{it})$ criterion as cells that did show informative variation over time.

Results

Overall fits

Fits to observed catch data and relative abundance trends under various initial mixing rate assumptions (*v)* were similar, for a number of stocks, to those obtained from the spatially aggregated E* forced model presented in Chapter 4 (Figure 5.1 to Figure 5.3). There was a tendency for normal approximation to the marginal posterior distributions of leading parameters derived from the Hessian to have a larger variance than distribution mapped in Chapter 4. Approximated joint posterior distributions for derived biological reference points were more tightly correlated (Figure 11.1 to Figure 11.21 in the Appendix to Chapter 5). Noticeable differences in fits occurred for some stocks in all oceans.

Productivity for southern bluefin tuna was estimated to be lower and stock size smaller when using the spatially disaggregated model, leading to an underestimation of population decline relative to the decline indicated by relative abundance trends. Similarly, population decline for Indian Ocean albacore tuna was estimated to have been less with the spatially explicit model. In this case, posterior estimates of current fishing mortality rate shifted closer to prior values as flow rates were increased. There was a tendency in Indian Ocean striped marlin assessments for estimates of F_{cur}, F_{msy}, and MSY to be higher than for the spatially aggregated model, though there is little impact on overall fit to observed catch. A similar trend is seen for Indo-Pacific black marlin. Little difference was seen between assessment methods for Indian Ocean swordfish, blue marlin, yellowfin tuna, or bigeye tuna.

In the Pacific Ocean, yellowfin tuna and southern albacore tuna spatial assessments differed little from aggregated assessments. Declines in striped marlin were estimated to be greater than indicated by relative abundance trends, and current fishing mortality rates and productivity were estimated to be higher than those estimated using spatially aggregated models. Productivity and stock size were estimated to slightly higher for blue marlin, resulting in better fits to observed

catch data when mixing rates were assumed low. Assuming low mixing rates for bigeye tuna resulted in under estimation of population decline and productivity. Estimated current fishing mortality rates were similar to prior values.

Spatially explicit models produced poorer fits to observed catches and population trends for stocks in the Atlantic (Figure 5.3) when compared to aggregated models (Figure 4.13). Early catches and population declines of northern albacore were underestimated, except when mixing rates were assumed high. At a high mixing rate, population decline was overestimated. In contrast to posterior distributions produced from spatially aggregated models, when movement rates were assumed low current fishing mortality rates were estimated closer to prior values, as was productivity. Atlantic yellowfin tuna abundance was estimated to decline slower than indicated by relative abundance trends, and catch was over-predicted in later periods. Current fishing mortality rate and F_{msy} posterior modes were similar to prior modes, which were not observed for spatially aggregated models. Population decline in white marlin was estimated to be greater and more rapid than indicated by the spatially aggregated E* forced model, though fits to observed catch were similar. Predicted trends in population decline for bigeye tuna, blue marlin, and swordfish were similar to E* forced model fits though in later periods catches were over-predicted for bigeye, and highly variable for swordfish. Catch of southern albacore matched observed values reasonably well though population decline was underestimated. Fits to observed catch of Atlantic bluefin tuna were also reasonable though modeled abundance patterns are very difference from relative abundance trends. Population size in 1950 was also estimated to be a smaller portion of unexploited population than estimated from spatially aggregated models.

Estimated abundance distributions

Estimated initial population distributions, averaged over quarters, are similar to those described in Chapter 2 (Figure 5.4-Figure 5.7). This result is not surprising since early longline data were an important information source used to determine species distributions.

In the Indian Ocean, yellowfin tuna and bigeye tuna and blue marlin were estimated to have higher densities in equatorial waters. There was an increasing westward trend in density for

yellowfin tuna and an apparent concentration of blue marlin off northwestern Australia. Albacore appeared concentrated between latitudes -35°S to -20°S with a concentration off Madagascar. Concentrations of striped marlin were estimated off Somalia, western India, Sri Lanka, within the northern Bay of Bengal, and northwestern Australia. Highest densities of swordfish appear to be in the western Indian Ocean. The highest abundances of southern bluefin tuna were estimated northwest of Australia, east of New Zealand, and within the Tasmanian Sea. Concentrations were also predicted between 40-55° S to with patches of higher density off South Africa. Highest densities of black marlin appeared to be in the Coral Sea, the South China Sea, the East China Sea, the Bay of Bengal, and off Sri Lanka. In the Pacific Ocean, high densities of albacore were predicted within the northern and southern subtropical convergence zones with a westward increasing trend. Blue marlin appeared concentrated in equatorial waters within the central Pacific. High densities of yellowfin tuna were estimated in western and central equatorial waters with lower concentration in the eastern ocean. Striped marlins have a horseshoe distribution with its base in eastern Pacific waters. The highest apparent densities of striped marlins occurred off Baja California. Swordfish and bluefin tuna were estimated to have highest densities in northwestern waters near the northern Kushiro current. Bluefin tuna distribution was skewed to the west with minor concentration off New Zealand. Concentrations of swordfish also had a less obvious horseshoe shape with high densities in the eastern Pacific off Baja California. Bigeye tuna seemed concentrated in equatorial waters with an eastward skew in distribution. A lobe of the bigeye distribution pushed into northern waters in the central Pacific. In the Atlantic Ocean, yellowfin tuna were concentrated in equatorial waters spanning from the Gulf of Guinea to the Gulf of Mexico. Blue marlins also shared this distribution though apparently more diffuse. Southern albacore appear concentrated off Brazil while the highest concentrations of northern albacore appeared in the Bay of Biscay. Bigeye tuna appeared concentrated in the eastern ocean centered on the Gulf of Guinea. Swordfish had no obvious core distribution though areas of high density were estimated off the northeastern seaboard of North America. White marlins appeared concentrated off southern Brazil, northern Venezuela, and the Gulf of Mexico. Highest densities of Atlantic bluefin tuna are estimated to occur within the northeastern Atlantic off Norway, in the eastern Atlantic west of the Mediterranean Sea, and within the Mediterranean Sea.

Maps of total abundance change in large pelagic tunas and billfishes by 5°x5° area from 1950-2002 were generated under various movement scenarios (Figure 5.8). It is important to note that Pacific Ocean northern albacore, swordfish, and bluefin tuna are not included in the presentation. However, their impact on total population change is likely small as northern albacore and swordfish were estimated using spatially aggregated models to have changed little over the period, and bluefin tuna numbers are much lower than other species. For the other stocks, assuming average flow between cells was low (v=0.7 initially), the average ratio of predicted abundance in 2002 to predicted abundance in 1950 was 0.42 with a standard deviation of 0.18. Therefore, on average large pelagic tuna and billfish were estimated under this movement scenario to have been reduced by 58%. Areas of more severe depletion were estimated in the southern Indian Ocean, the western Indian Ocean, the eastern Pacific, the Gulf of Guinea, off Brazil, and the central Atlantic. If average mixing rates between cells were assumed higher (v=10 initially) total population decline was estimated to be 63% and to be more spatially homogeneous. A noticeable anomaly in both scenarios was that little population change was estimated in the northeastern Atlantic, for cells dominated by Atlantic bluefin tuna (Figure 5.8).

Estimated recruitment distributions

The impact of initial mixing rates on estimated distributions of recruitment (pR) is demonstrated in Figure 5.9 to Figure 5.11 for Indian Ocean yellowfin tuna. When initial mixing rates were assumed low (v=0.7), recruitment was estimated to be broadly distributed. As initial mixing rate was increased, estimated recruitment was concentrated into fewer and fewer cells (Figure 5.9). The net result was to concentrate recruitment into areas where catch rates were observed to be the highest and have net harvestable additions to N_{it} in most other cells estimated to have resulted from movement into those cells. The static advection-diffusion fields that resulted from redressing apparent flow imbalances changes as movement rates were progressively increased (Figure 5.10). There is no obvious pattern as to how flow rates changed as initial mixing rates increased. There was however, a consistency to the general flow pattern out of areas estimated to have higher recruitment. Although higher mixing rates concentrated recruitment in to fewer cells, initial population distributions were more diffuse that those that resulted from lower mixing rates (Figure 5.11).

Estimated management reference points

When parameter estimates from the spatial model were placed within a stock-status space, positioning changed relative to results obtained from spatially aggregated models (Figure 5.12). When averaged over mixing rate hypotheses, reference points shifted noticeably for some species. Categorization for stocks within the Indian Ocean changed little, though there were shift within each stock-status quadrant. For the Pacific Ocean, an estimate for striped marlin shifted into the 'recovering' quadrant where a stock is assessed as 'over-fished' but 'over-fishing' is not occurring. Estimates for bigeye and yellowfin tuna shifted into the 'healthy' quadrant where a stock is assessed as not over-fished and over-fishing is not occurring. Southern albacore shifted to being classified as over-fished and experiencing over-fishing (though much closer to 'optimal' exploitation levels). For the Atlantic Ocean stocks, northern albacore and swordfish were reclassified as over-fished but above N_{msy} levels, while yellowfin tuna shifted into the 'recovering' quadrant. Like the stock status classifications in Chapter 4, the classification presented here is general and posterior distributions span multiple quadrants.

Discussion

In the method presented, spatial catch and effort data were used to parameterize an advection–diffusion model with constant, annual mixing rates over time. Unfortunately, catch and effort data alone are insufficient to estimate overall mixing rate, and alternative possible values must be provided. The results indicate that in most cases, alternative estimates of overall mixing rate do not significantly alter the fit to observed catch data or substantially influence inferences about leading parameters, though there are differences in the estimated initial recruitment, movement, and population spatial distributions.

Estimated mixing patterns obviously do not fully represent closed seasonal migrations or changes in stock movement patterns in response to annual changes on oceanographic conditions. There are two important implications of using a single annual movement field. Tuna stocks are known to respond to changes in oceanographic conditions brought about by climate shifts such as El Niño (Lehodey et al. 2006, Lehodey et al. 1997, Lu et al. 1998). If significant shifts in stock distribution occurred and such shifts were uncommon, observed catch rates and harvests

would be inconsistent with those predicted from estimated relative fishing mortality rates and expected abundance, to cause predicted catches in those areas and years to be substantially underestimated. Furthermore, seasonal migration patterns are observed for a number of species (e.g., Atlantic bluefin tuna) and tagging data suggest predictable migratory patterns for others (Ortiz et al. 2003). The annual, constant movement (v) dynamics used in the model does not capture this migratory behaviour. Although some attempt has been made to mitigate this effect by averaging over seasonal abundance trends, the impact of area-specific seasonal movement and targeting by fisheries is likely underestimated.

The recruitment model used in this analysis assumes that local recruitment of individuals vulnerable to longline gear and local population abundance are decoupled, in the sense that recruitment to each cell is assumed to have arisen from overall spawning abundance across all cells used by each stock. As a result, the model predicts that local abundance can be depleted completely with no impact on recruitment, provided overall population abundance remains high. It is difficult determine if such an assumption is realistic. Given how long it takes tunas and billfishes to become vulnerable to longline gear, as well as their potential to move large distances, there is no reason to assume that areas into which individuals recruit bear any relationship to areas where those individuals were spawned. Areas of apparent higher recruitment are possibly better spawning or feeding grounds, but could also simply be areas where individuals are more susceptible to longline gear. There is however, evidence that tuna have strong site fidelity (Schaefer et al. 2007) and tuna are observed to spawn in locations where they were born (Block et al. 2005). It is likely that the best possible model lies somewhere between the alternative assumptions of fully local versus fully mixed recruitment processes. A component of each population is likely highly migratory, and the remainder highly localized, as evidenced in Atlantic cod (Beacham et al. 2002, Ruzzante et al. 2000). There is also the possibility of meta-population structures with somewhat distinct populations linked through dispersal as evidenced by recent work on striped marlin (McDowell and Graves 2008). If stocks were in reality aggregations of locally recruiting populations, local depletions, or recoveries were likely underestimated with the model structure used. However, the data suggest that abundances in cells at the extremes of distributions tended not to persist, i.e., to be depleted soon after first fishing and not to sustain later fishing activity. Catch rates appear not to have recovered in such

areas, suggesting that initial abundances were due to immigration from 'core' population areas rather than local reproduction.

To interpret differences in parameter estimates and fits to catch data between the spatial model and the spatially aggregated models of Chapter 4, it is important to recognize that the spatial model differs only in the prediction of overall fishing mortality rates F_t. Given the same stock size and population parameters (stock-recruitment and natural mortality), the spatial model predicts exactly the same total recruitment and natural mortality loss as the aggregated models.

Poor fits to observed catches (compared to spatially aggregated models) for some Atlantic Ocean stocks suggest that the spatial model gave poor estimates of overall historical fishing mortality rates. The spatial model was forced with historical relative fishing mortality rates, and these relative fishing mortality rates were calculated as catch observed within each time/area cell divided by the relative abundance index for that cell (equation 5.6). Relative abundance trends for each area were estimated from only Japanese longline catch and effort data, and missing values were imputed when time/area data were missing. Provided there was actually a Japanese catch rate observation when catches were removed from an area within a quarter, this assumption is reasonable. However, for a number of stocks, removals by other fleets prior to and post Japanese fishing activity resulted in a lack of time-area co-occurrence between fleets, particularly in the Atlantic. The result for any spatial cell where this occurred was to have catch rate remain constant (due to imputation) while catches were removed. In such cases, relative changes in fishing mortality rates were underestimated, and this likely contributed to bias in estimates of leading parameters. Such apparent insensitivity of catch rate to catch removals created discord with observations where catch rates were observed to change in response to fishery removals. The net result for Atlantic northern albacore tuna was to overestimate the impact of harvesting and underestimate stock productivity relative to spatially aggregated models. For Atlantic bluefin tuna, estimated population size for most years was increased, and estimated initial population size in 1950 was decreased. While this effect of imputation was mitigated to some degree in spatially aggregated models, its impact on parameter estimation was unavoidable in the spatially disaggregated model when catches were taken from core areas. Catch rate in every cell was assumed a representative sample of the catch rates that resulted from

removals. If effort redistributed or refocused target species within an area that contained a large portion of total stock biomass, catch rate declines may not reflect the impact of removals. Japanese effort off the Baja California, a core striped marlin area, is known to have redistributed in response to changes in Mexican access policy. However, Japanese vessels did not abandon the 5°x5° cells within this region, but were required to shift outside sub-areas of high catch rate. The relative contribution of these areas to total striped marlin abundances, and the apparent contradiction in the catch and effort data caused by the policy-driven *cpue* decrease, resulted in an over estimation of fishery impacts and productivity relative to the spatially aggregated model. There was also a striking contrast in the estimate of productivity for southern bluefin tuna. Spatially disaggregated models resulted in a substantially lower estimate of productivity, due to apparent rapid depletion of local abundances. Here an apparent sequential depletion of areas was masked by imputation in spatially aggregated models.

Three areas of concern have been raised with the model structural assumptions used in this chapter, in relation to movement parameterization, local recruitment dynamics, and the relationship between relative abundance and local abundance. From the examples given it would seem prudent to avoid using such a modeling structure when violations of such key assumptions are obvious. When tagging data are available to help parameterize changes in seasonal movement, a more complex model might be used. It is also possible to model recruitment as dependent on local abundance or a mixture of both local and global abundance effects and explore the impact various recruitment mechanism have on estimated parameters. The imputation method presented is simplistic and developing a method that can draw upon additional information, (e.g., correlative catch rates between fleets) would alleviate some of the confounding introduced by the lack of sensitivity in relative abundance trends to fishery removals.

In addition to providing a framework to explore spatial policy options, population trajectories evaluated at MLE estimates of stock dynamics parameters under various movement hypotheses may be used to evaluate the imputation methods applied in Chapter 3. Population trajectories estimated using the spatial model for stocks in the Indian Ocean, aggregated by the year cells were first fished, are presented in Figure 5.13 and Figure 5.14. When mixing rates between cells

were assumed low, estimated low harvest rates during early periods of the fishery had little impact on those areas fished later. After nearly two decades, when harvest rates dramatically increased, were deletion impacts noticeable, (e.g., southern bluefin tuna). In two instances, yellowfin, and albacore tuna, there was a slight decline in simulated abundance in cells before those cells were first harvested. Such impacts are minor and likely less significant than increases in catch rate due to gaining experience in a particular area. Thus using an average of the first 3 years of observed catch rates appears reasonable for imputation of catch rates for cells before they were first fished. Little change in abundance is apparent in the spatial simulation results even when flow rates between areas are assumed high. Southern bluefin tuna is an exception, as high exploitation rates were experienced early in the period; for this species, areas fished later are estimated to have undergone a noticeable decline, so that filling backward in time with an average of the first few observed catch rates are predicted to cause underestimation of overall population impacts in early years. In instances where harvest rates are high early in the fishery, a more elaborate imputation method is likely required to account for depletion impacts on neighboring areas. In such cases, developing a simple movement model like the one presented in Chapter 3 can help guide reasonable imputation methods provided estimates of harvest rates independent of fitting to abundance trends during the early period of fishing can be made. These values can then be used to infer changes in cells not yet fished over time and hence allow appropriate adjustment to imputed values for those cells.

Over a range of hypothesized mixing rates v, the spatially disaggregated model indicated over harvesting of a number of stocks, similar to findings with spatially aggregated models. Furthermore, a number of stocks are estimated to be below levels that would produce their maximum sustainable yield. Given these apparently robust results despite misgivings about various quantitative parameter estimates, it would seem prudent to utilize the spatial model developed in this chapter to determine whether spatial segregation of populations is sufficient to allow continued exploitation of those stocks deemed healthy while redistributing effort to reduce exploitation rates on others. In the next chapter, an exploration of such spatial policies is presented for a number of hypotheses about the current economic state of the fishery.

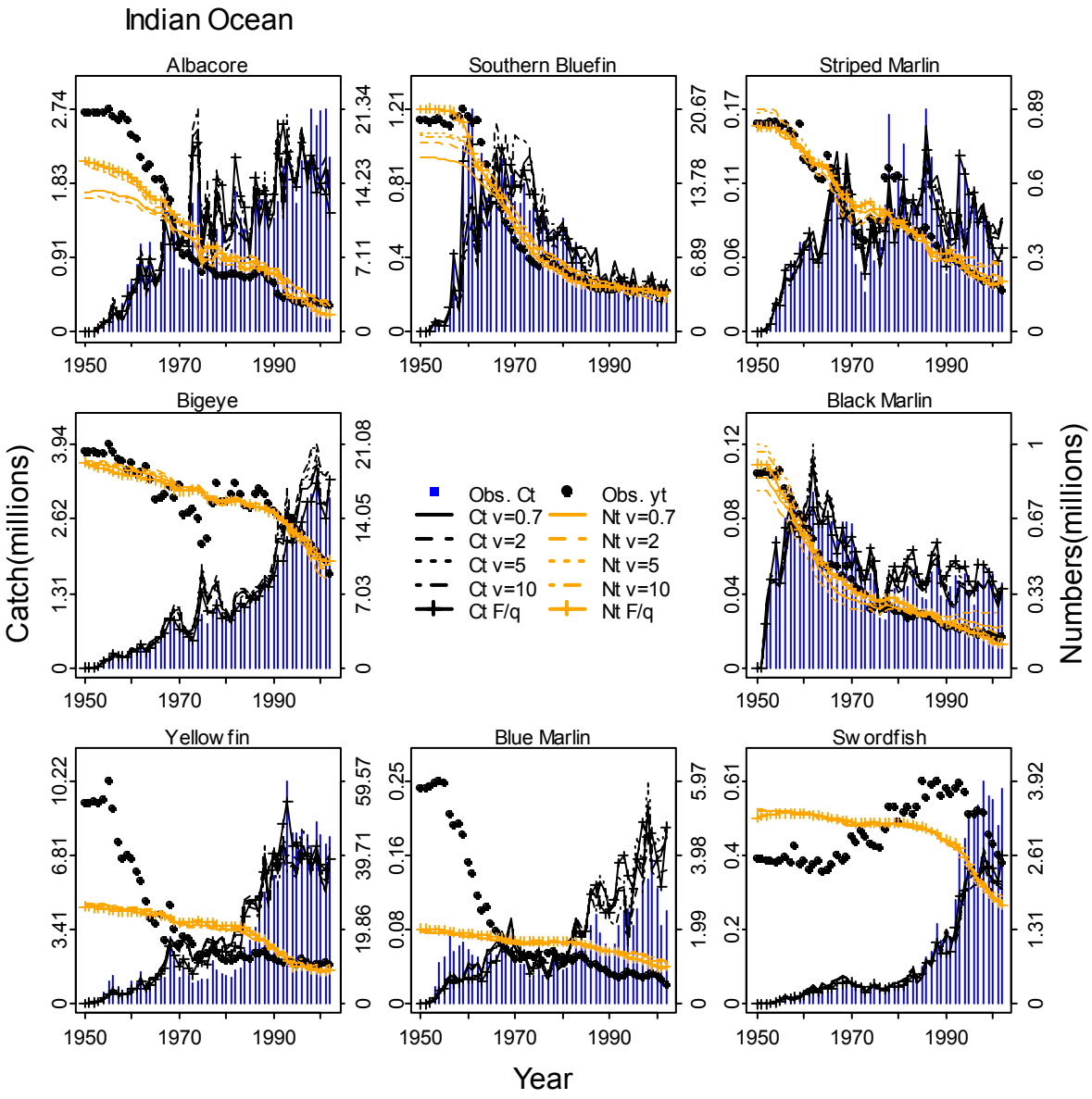

Figure 5.1 Fit to catch and relative abundance trends for stocks in the Indian Ocean. Blue vertical bars indicate observed catch (Obs. C_t). Solid circles are relative abundance trends (Obs. y_t). Black lines (solid, dashed, dotted, and dash-dotted) represent predicted catch (C_t) for various initial movement rates. Orange lines (solid, dashed, dotted, and dash-dotted) represent predicted numbers (N_t) for various initial movement rates. Hashed black and grey lines are predicted catch and numbers from the spatially aggregated numbers dynamic model with relative fishing mortality rate forcing (F/q).

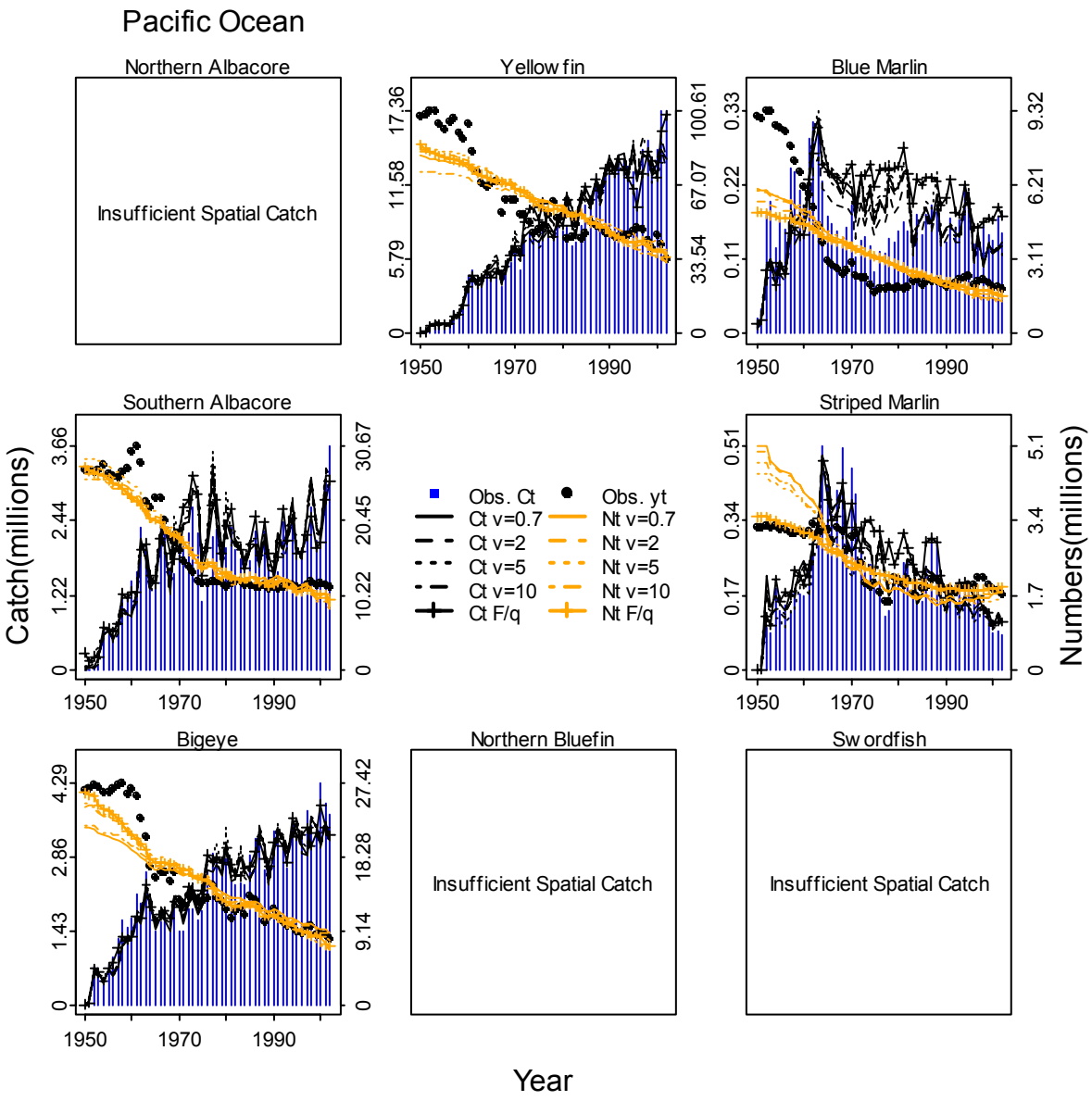

Figure 5.2 Fit to catch and relative abundance trends for stocks in the Pacific Ocean. Blue vertical bars indicate observed catch (Obs. C_t). Solid circles are relative abundance trends (Obs. y_t). Black lines (solid, dashed, dotted, and dash-dotted) represent predicted catch (C_t) for various initial movement rates. Orange lines (solid, dashed, dotted, and dash-dotted) represent predicted numbers (N_t) for various initial movement rates. Hashed black and grey lines are predicted catch and numbers from the spatially aggregated numbers dynamic model with relative fishing mortality rate forcing (F/q).

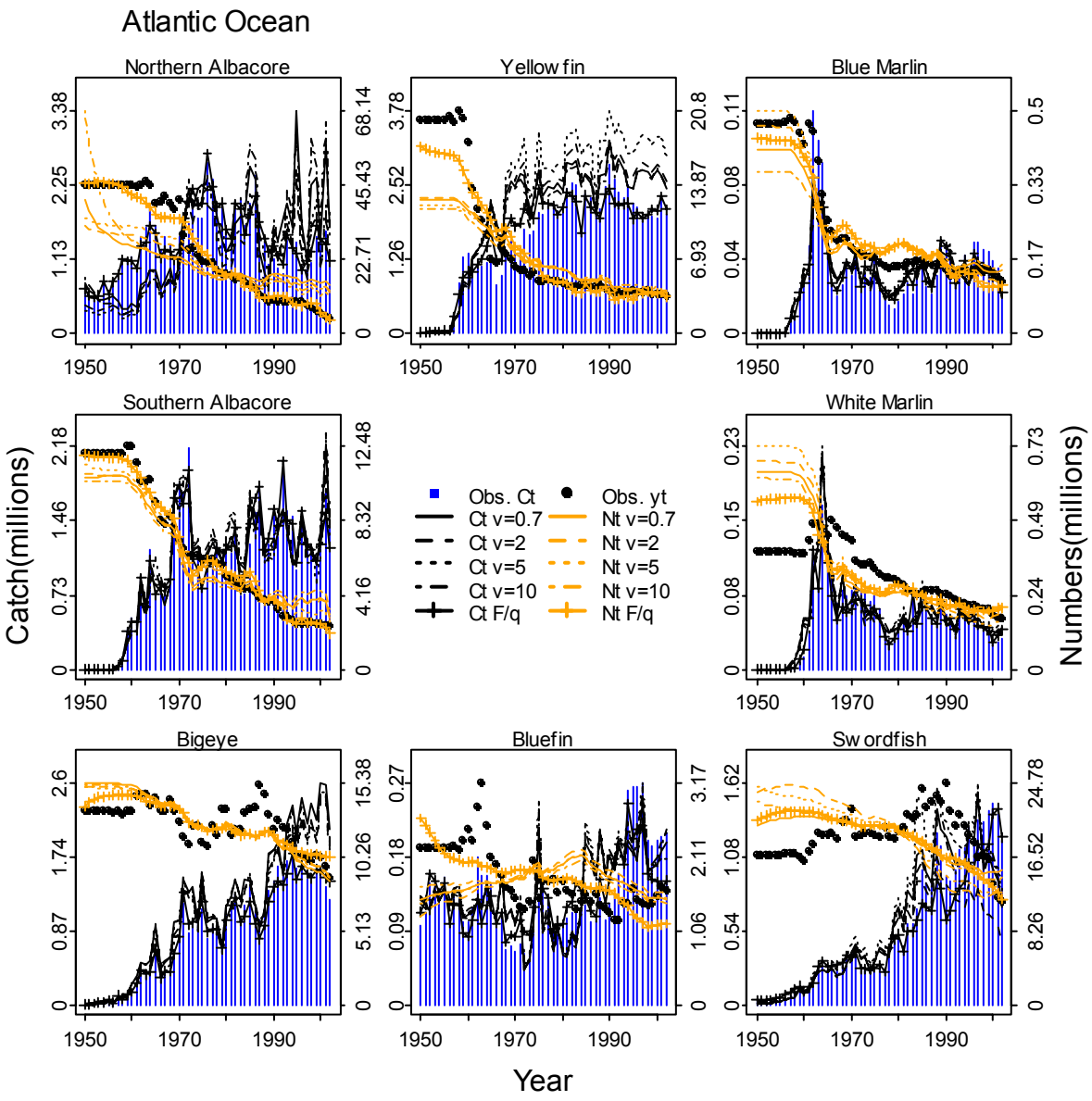

Figure 5.3 Fit to catch and relative abundance trends for stocks in the Atlantic Ocean. Blue vertical bars indicate observed catch (Obs. C_t). Solid circles are relative abundance trends (Obs. y_t). Black lines (solid, dashed, dotted, and dash-dotted) represent predicted catch (C_t) for various initial movement rates. Orange lines (solid, dashed, dotted, and dash-dotted) represent predicted numbers (N_t) for various initial movement rates. Hashed black and grey lines are predicted catch and numbers from the spatially aggregated numbers dynamic model with relative fishing mortality rate forcing (F/q).

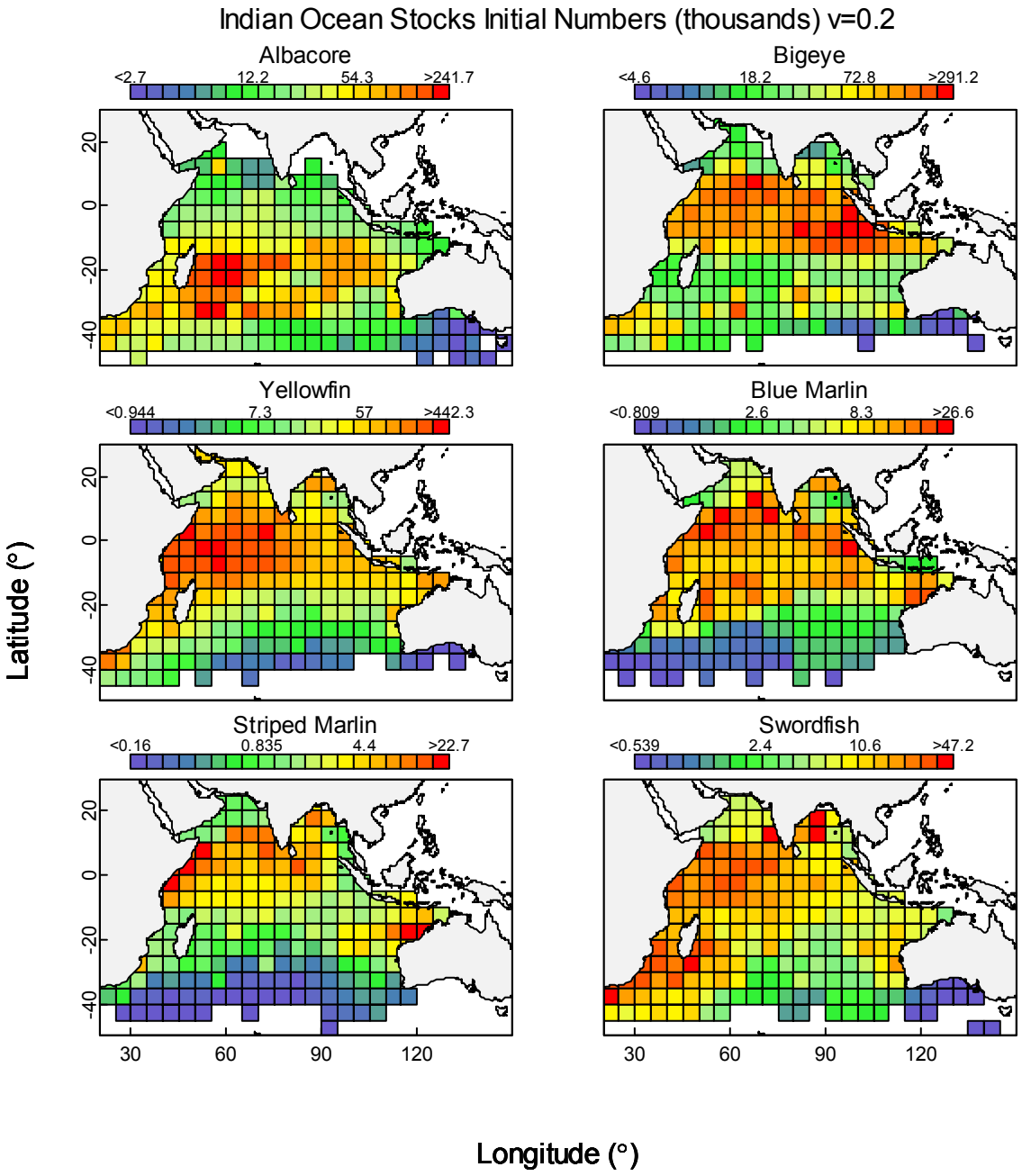

Figure 5.4 Estimated population numbers by 5°x5° area in 1950 for stocks in the Indian Ocean. Colour scale key for each stock is located above the individual plots.

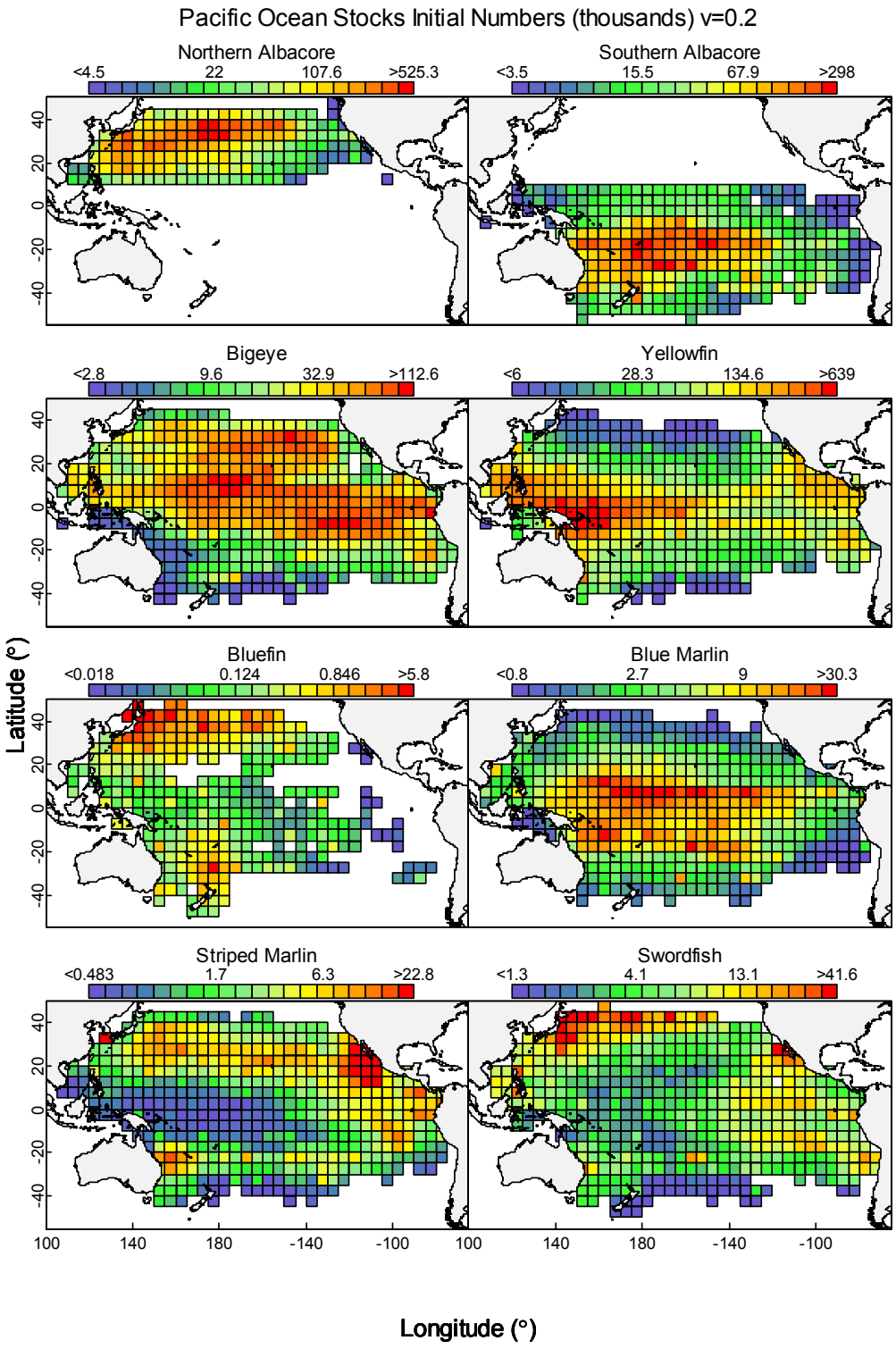

Figure 5.5 Estimated population numbers by 5°x5° area in 1950 for stocks in the Pacific Ocean. Colour scale key for each stock is located above the individual plots.

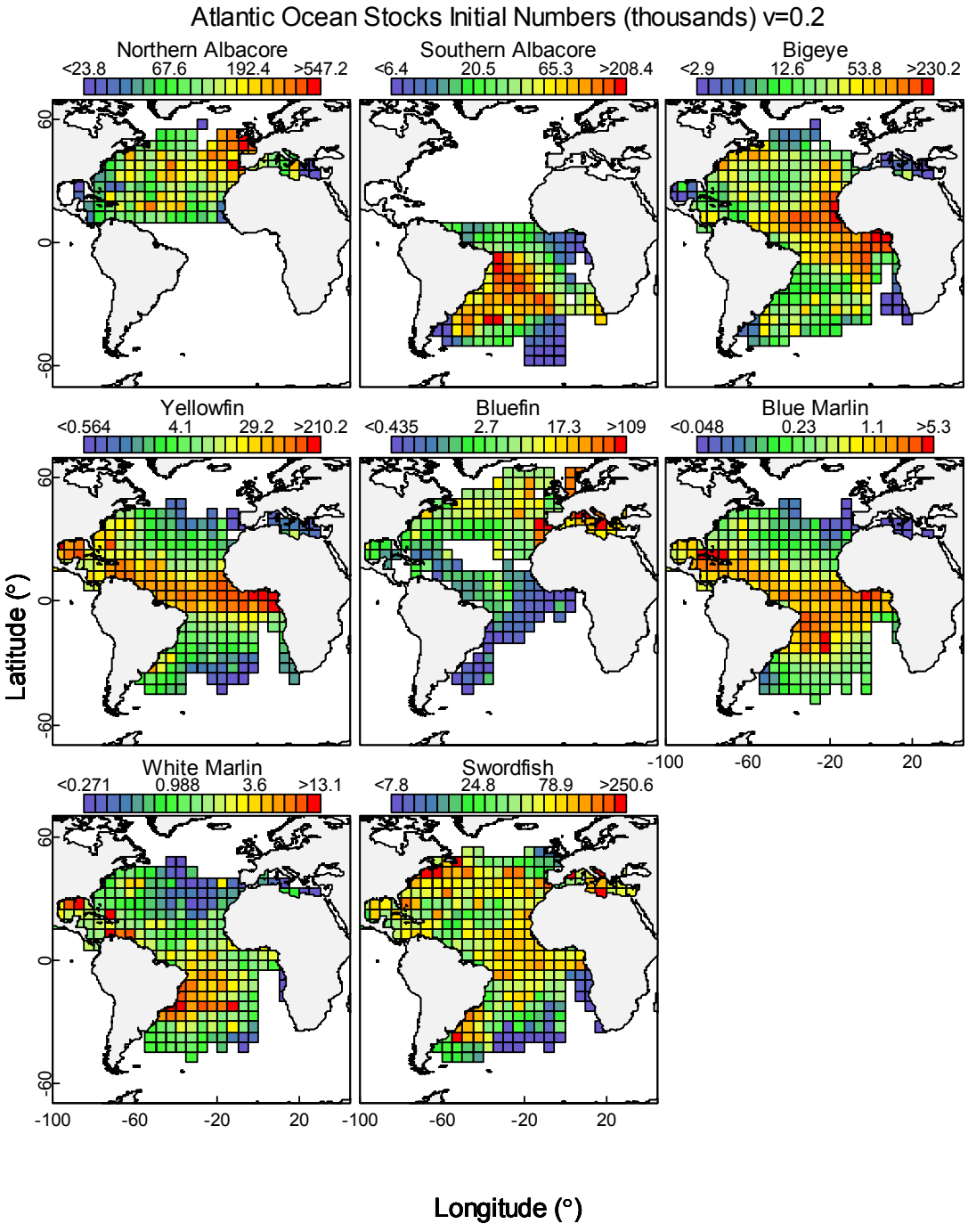

Figure 5.6 Estimated population numbers by 5°x5° area in 1950 for stocks in the Atlantic Ocean. Colour scale key for each stock is located above the individual plots.

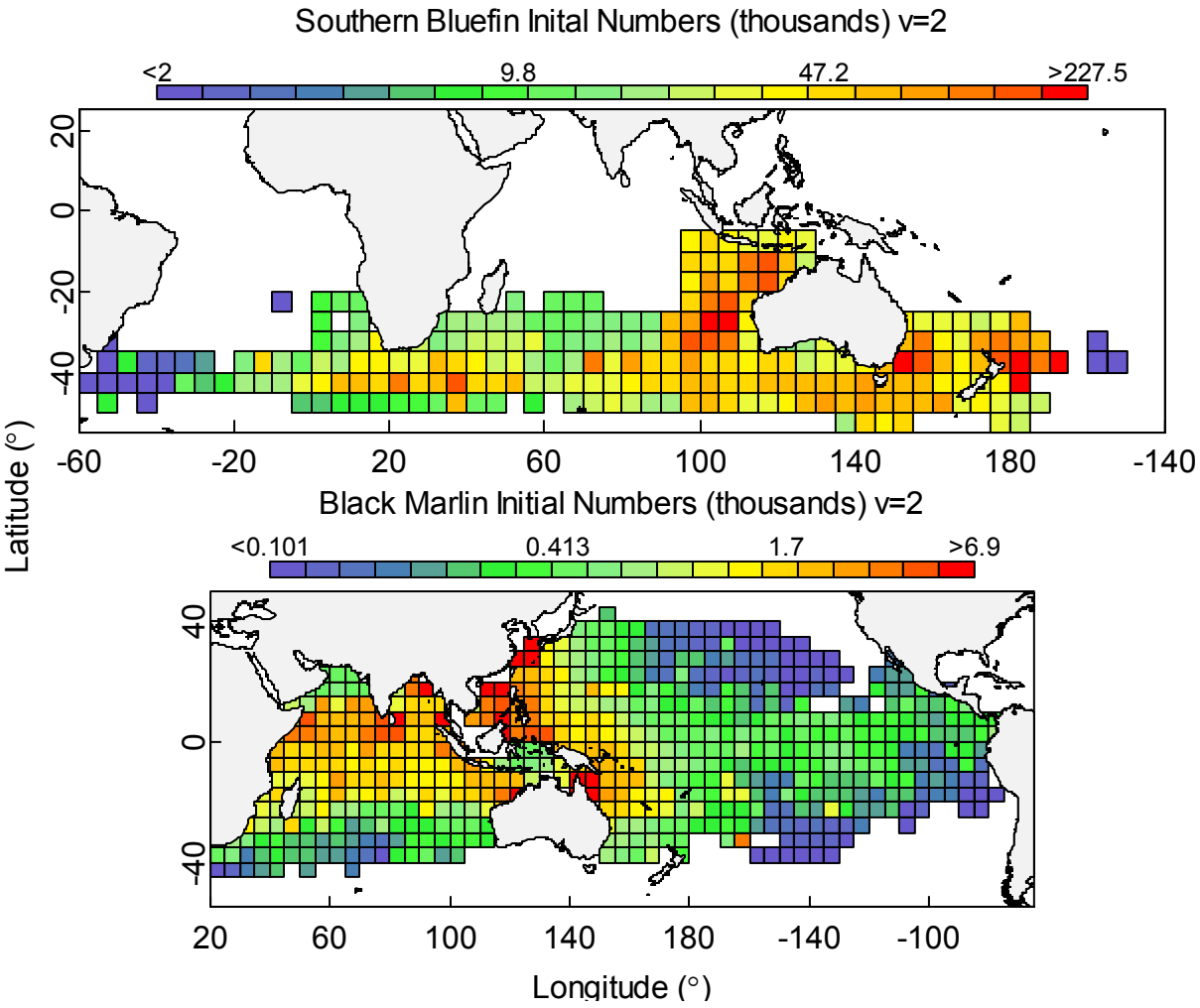

Figure 5.7 Estimated population numbers by 5°x5° area in 1950 for southern bluefin tuna and Indo-Pacific black marlin. Colour scale key for each stock is located above the individual plots.

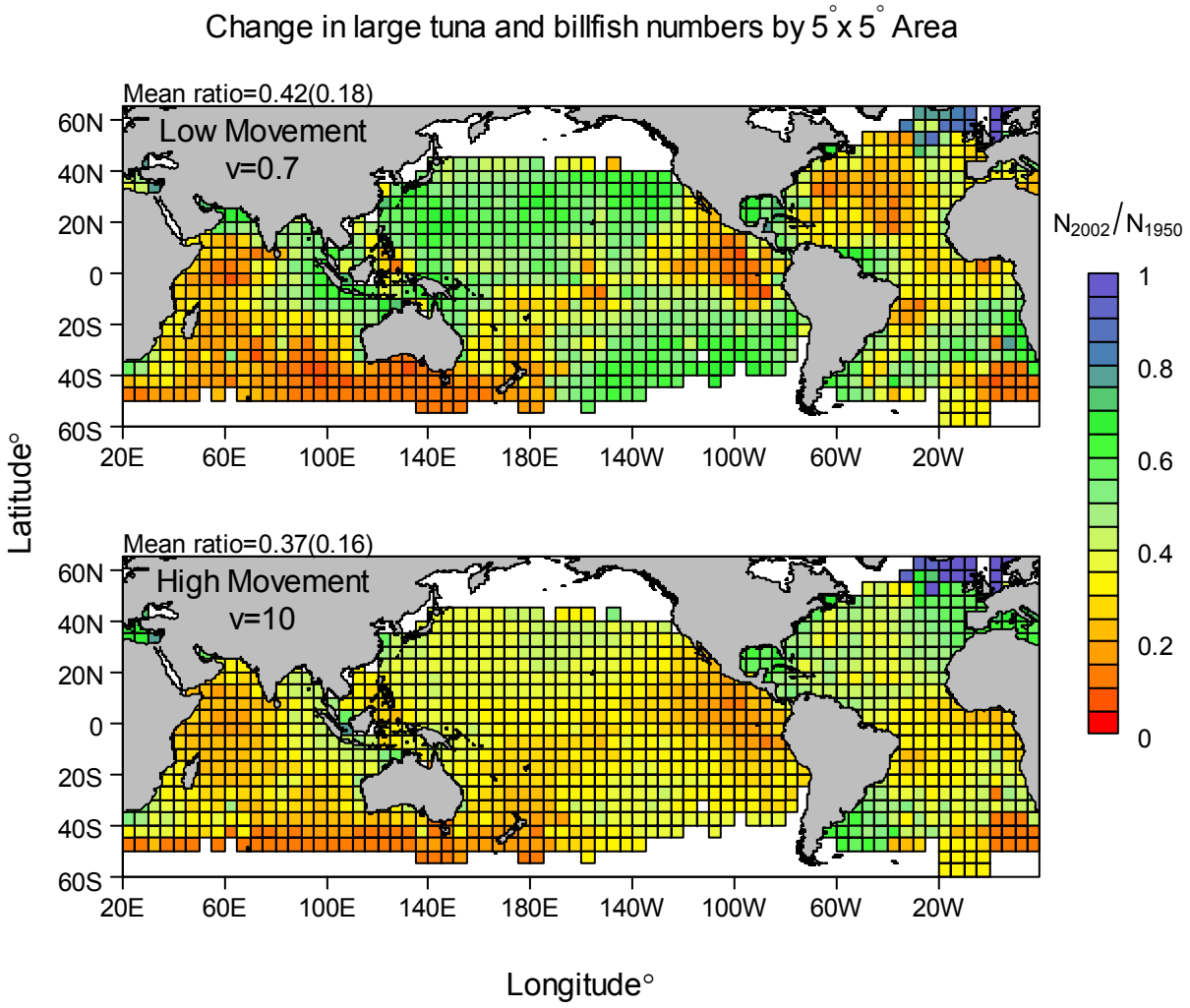

Figure 5.8 Ratio of estimated population in 2002 to that in 1950 by 5°x5° area, evaluated at MLE estimates for leading parameters for all stocks. Movement rates are assumed low in the top panel (v=0.7) and high in the lower panel (v=10). Warmer colours indicate more severe depletion

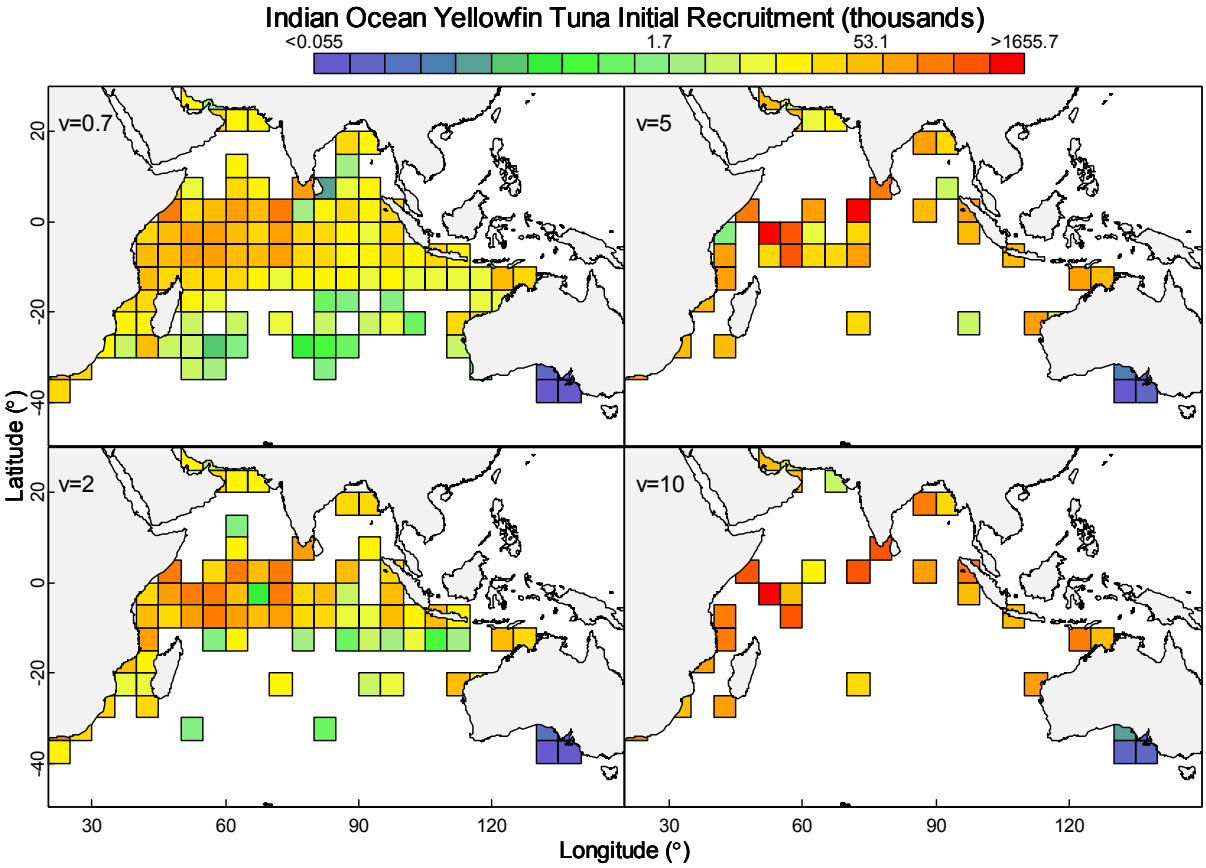

Figure 5.9 Estimated recruitment in numbers by 5°x5° cell in 1950 for Indian Ocean yellowfin tuna. Colour scale key for each panel is located above the plot. Note concentration of estimated recruitment into fewer cells as assumed mixing rate *v* is increased.

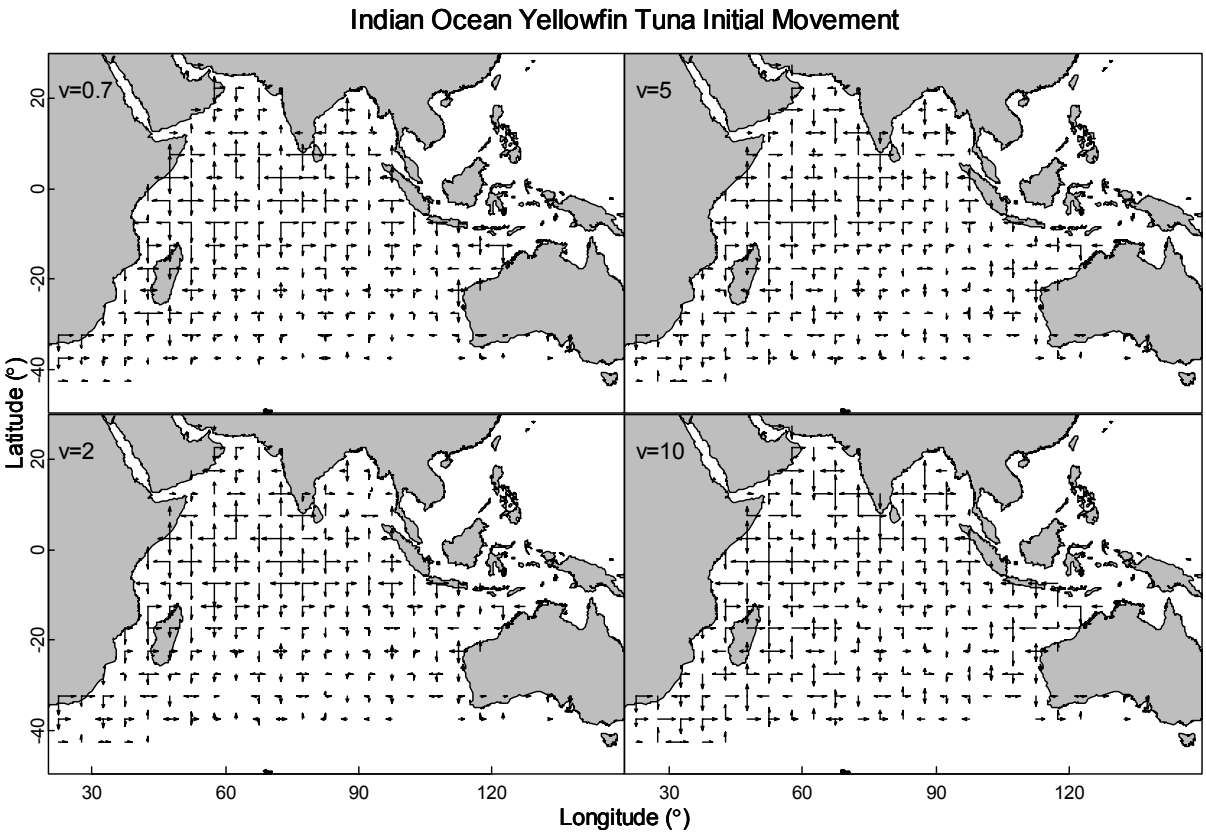

Figure 5.10 Estimated net flow (movement of individuals) into or out of each 5°x5° area given population size in 1950 for Indian Ocean yellowfin tuna.

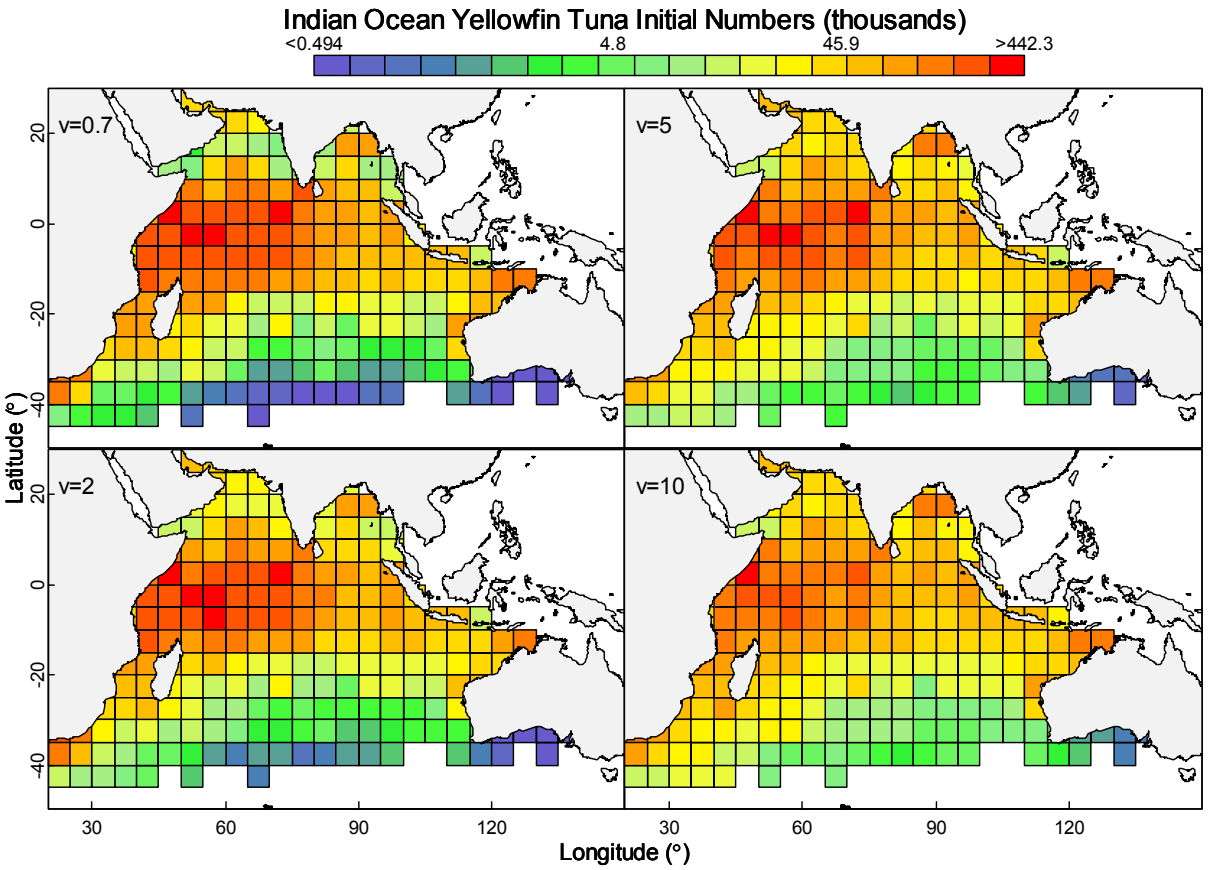

Figure 5.11 Estimated numbers by 5°x5° area in 1950 for Indian Ocean yellowfin tuna, estimated with different assumed mixing rates *v* as indicated.

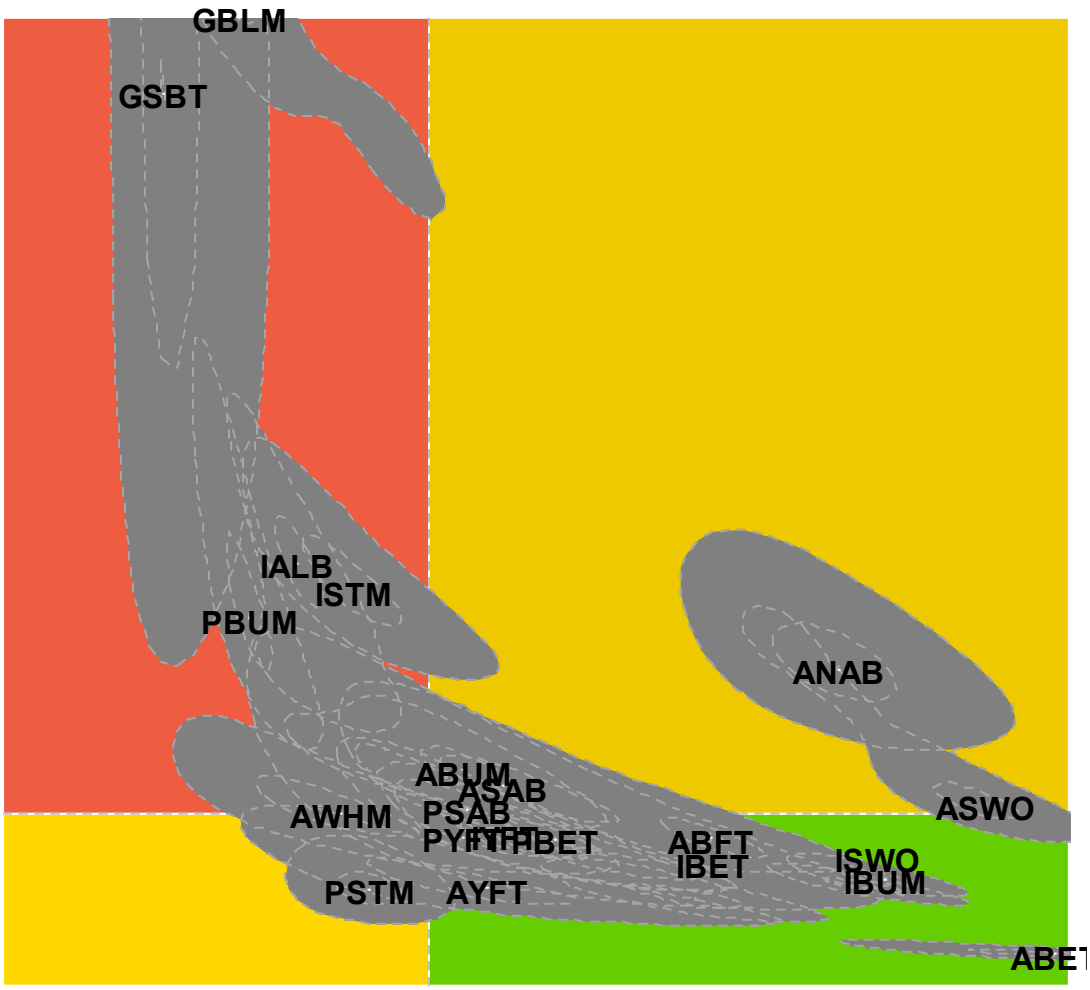

Figure 5.12 Joint distribution of biological reference points produced by combining the randomly generated points from all movement scenarios. Stock names demark the centre of the 1% quantile. Darker grey and lighter grey shading indicate the 10% and 50% probability contour. Ratios greater than 5 were not included for plotting clarity and stock identifiers for these cases are placed in the margin.

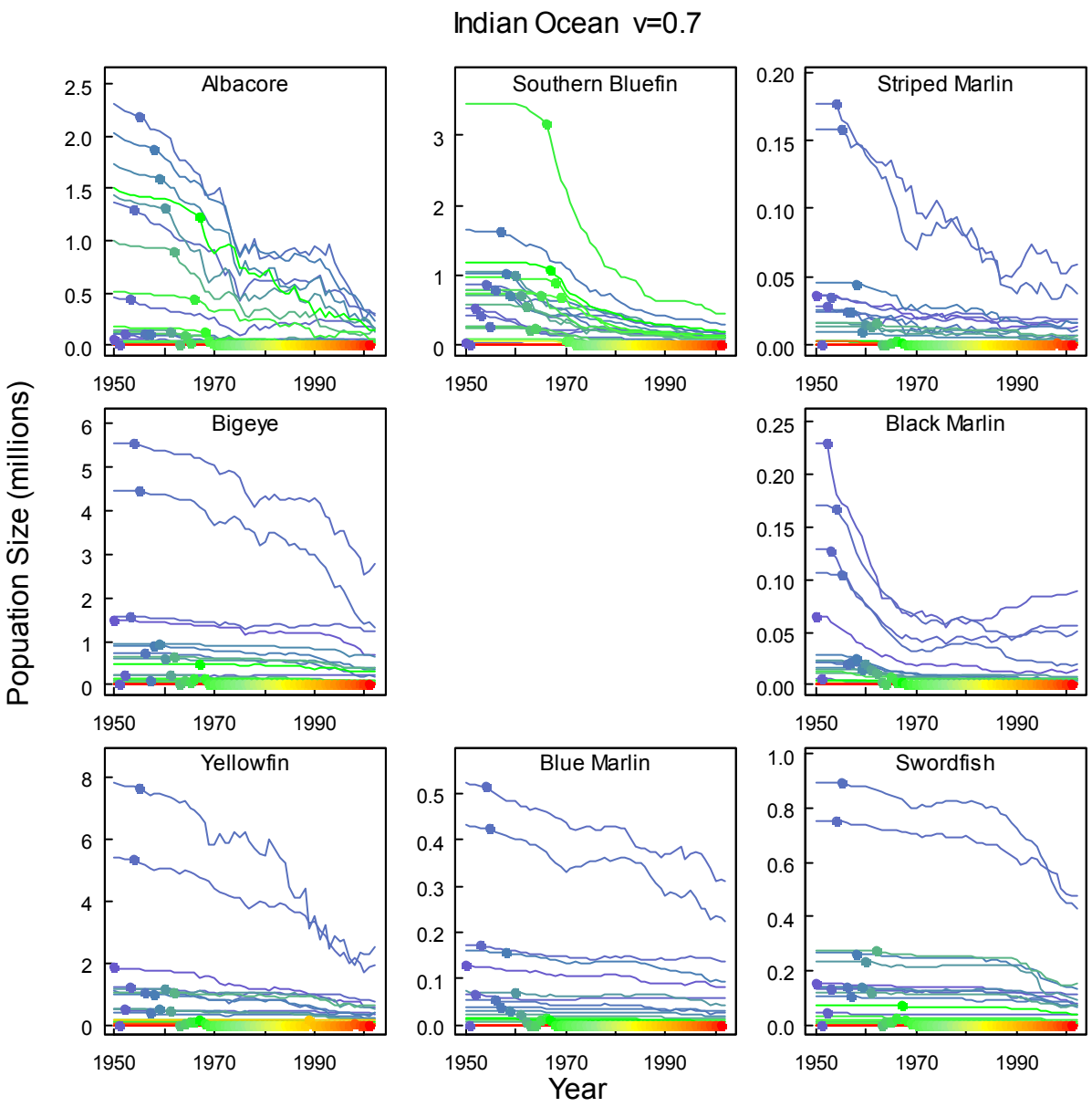

Figure 5.13 Simulated population trends of spatial cells aggregated by the year they were first fished for stocks in the Indian Ocean. Trends estimated using the spatial model with MLE parameter estimates and an assumed overall mixing rate v=0.7. Trends occurring prior to the dot (year of first fishing) on each trend line represent predicted stock declines due to reduced immigration caused by fishing in other cells.

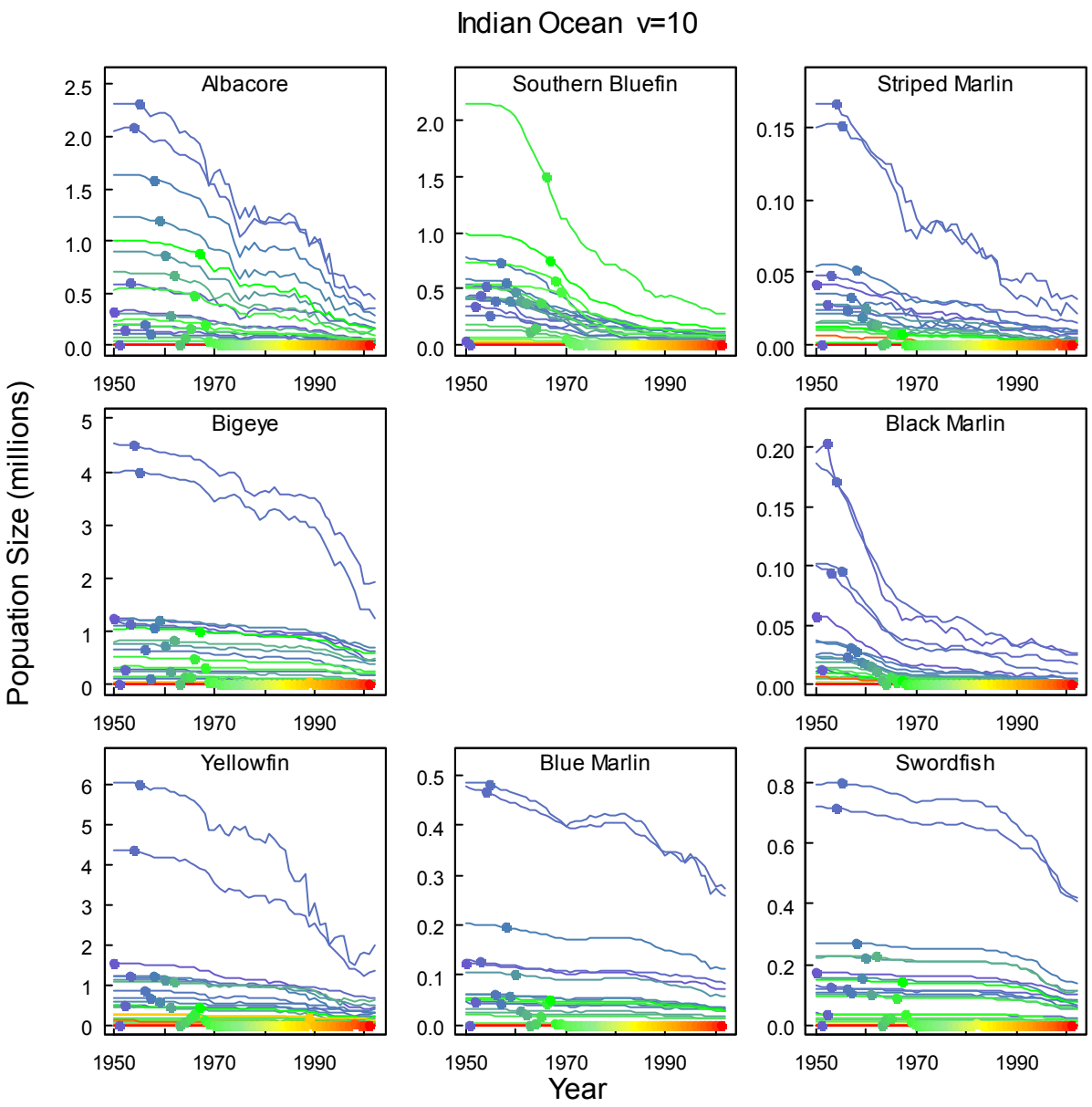

Figure 5.14 Simulated population trends of spatial cells aggregated by the year they were first fished for stocks in the Indian Ocean. Trends estimated using the spatial model with MLE parameter estimates and an assumed overall mixing rate v=10. Trends occurring prior to the dot (year of first fishing) on each trend line represent predicted stock declines due to reduced immigration caused by fishing in other cells.

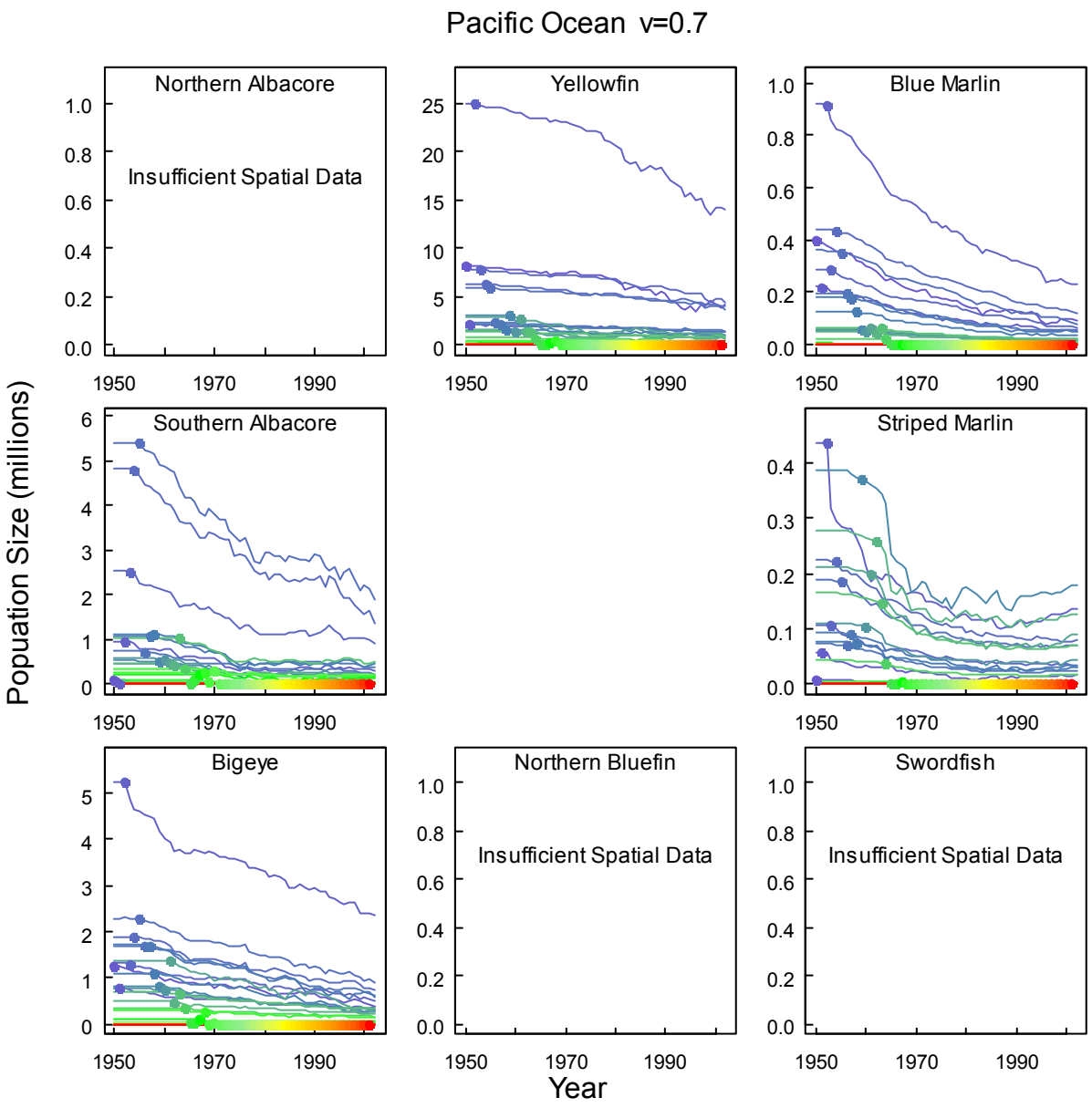

Figure 5.15 Simulated population trends of spatial cells aggregated by the year they were first fished for stocks in the Pacific Ocean. Trends estimated using the spatial model with MLE parameter estimates and an assumed overall mixing rate v=0.7. Trends occurring prior to the dot (year of first fishing) on each trend line represent predicted stock declines due to reduced immigration caused by fishing in other cells.

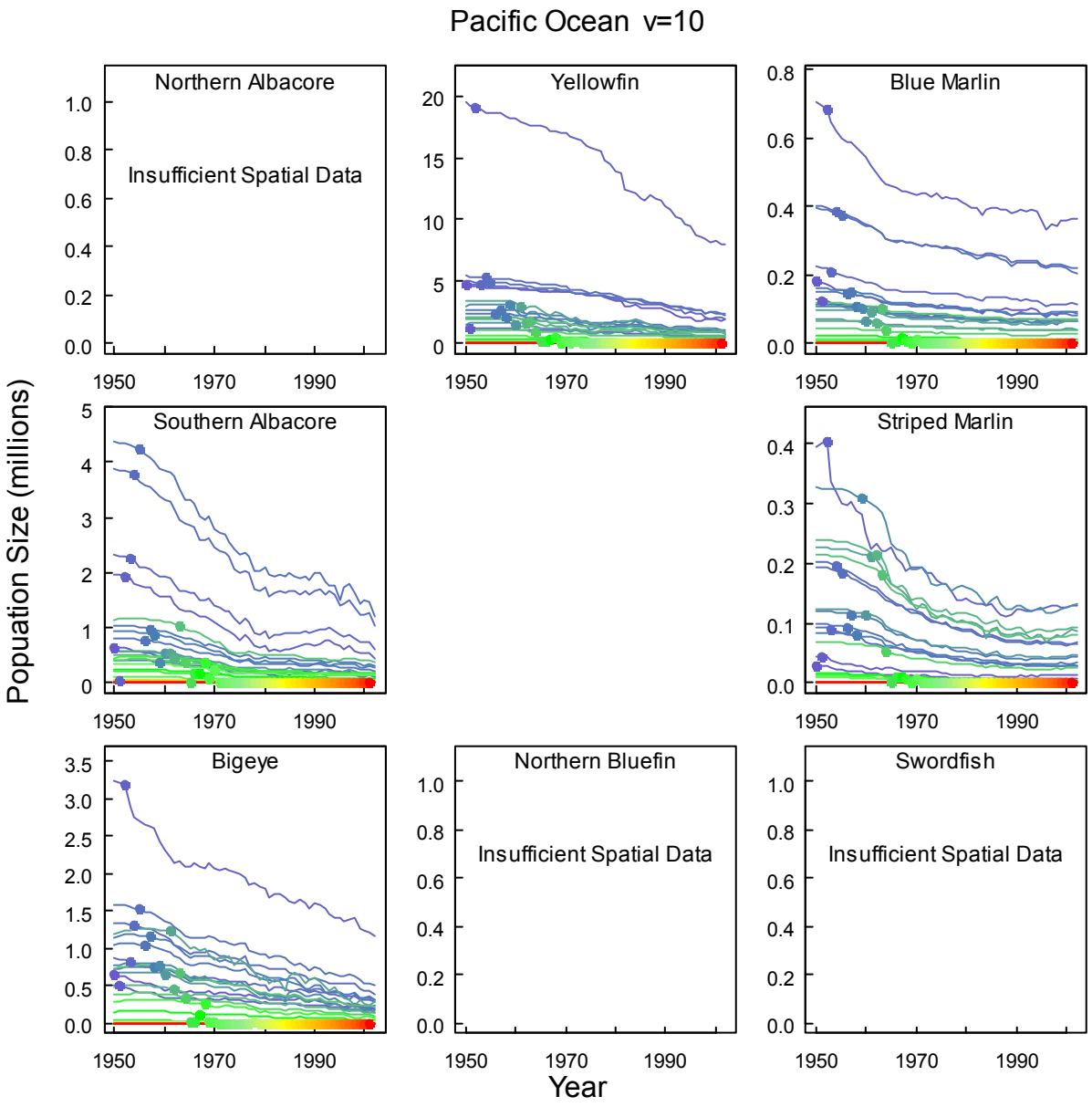

Figure 5.16 Simulated population trends of spatial cells aggregated by the year they were first fished for stocks in the Pacific Ocean. Trends estimated using the spatial model with MLE parameter estimates and an assumed overall mixing rate v=10. Trends occurring prior to the dot (year of first fishing) on each trend line represent predicted stock declines due to reduced immigration caused by fishing in other cells.

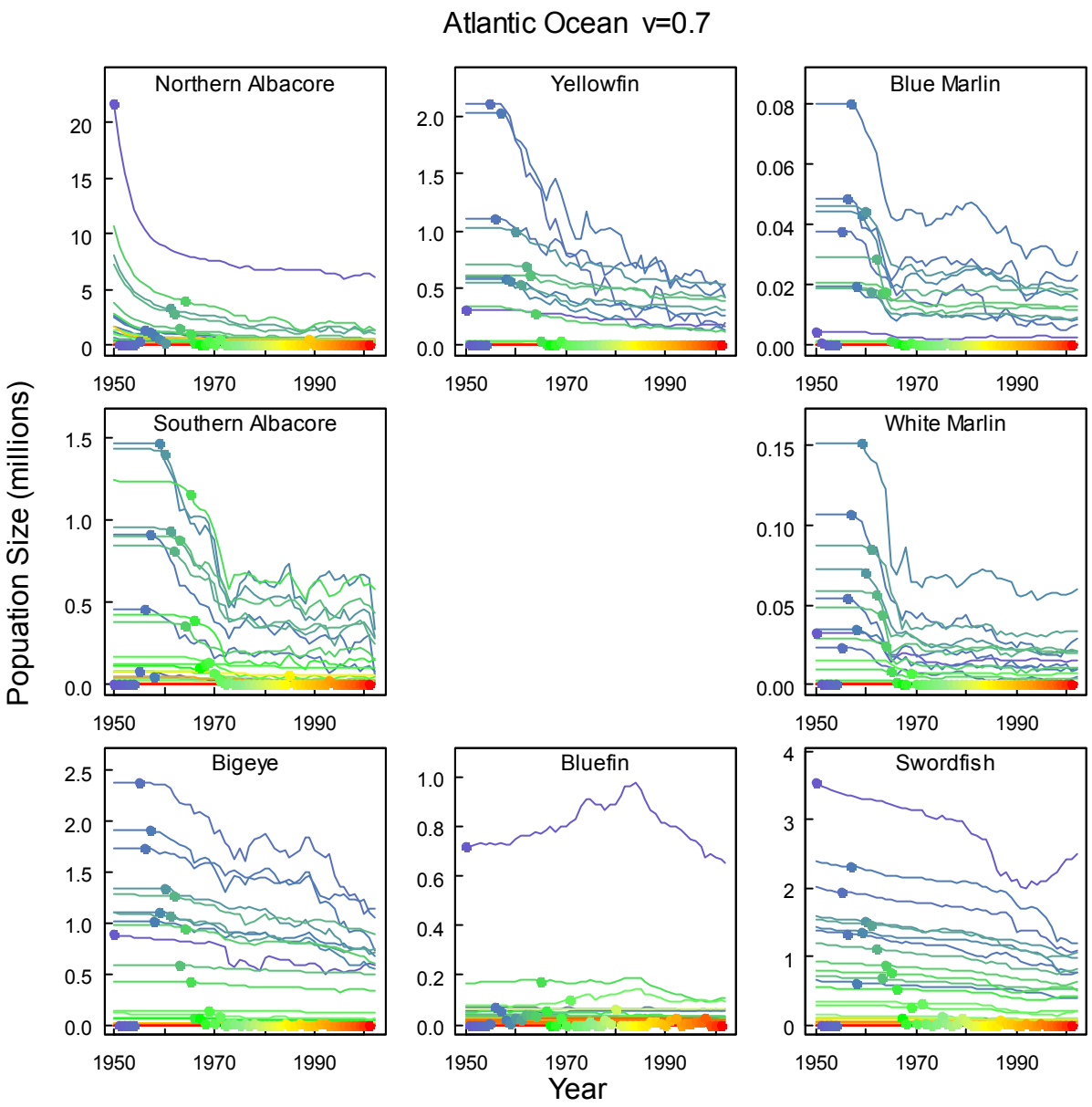

Figure 5.17 Simulated population trends of spatial cells aggregated by the year they were first fished for stocks in the Atlantic Ocean. Trends estimated using the spatial model with MLE parameter estimates and an assumed overall mixing rate v=0.7. Trends occurring prior to the dot (year of first fishing) on each trend line represent predicted stock declines due to reduced immigration caused by fishing in other cells.

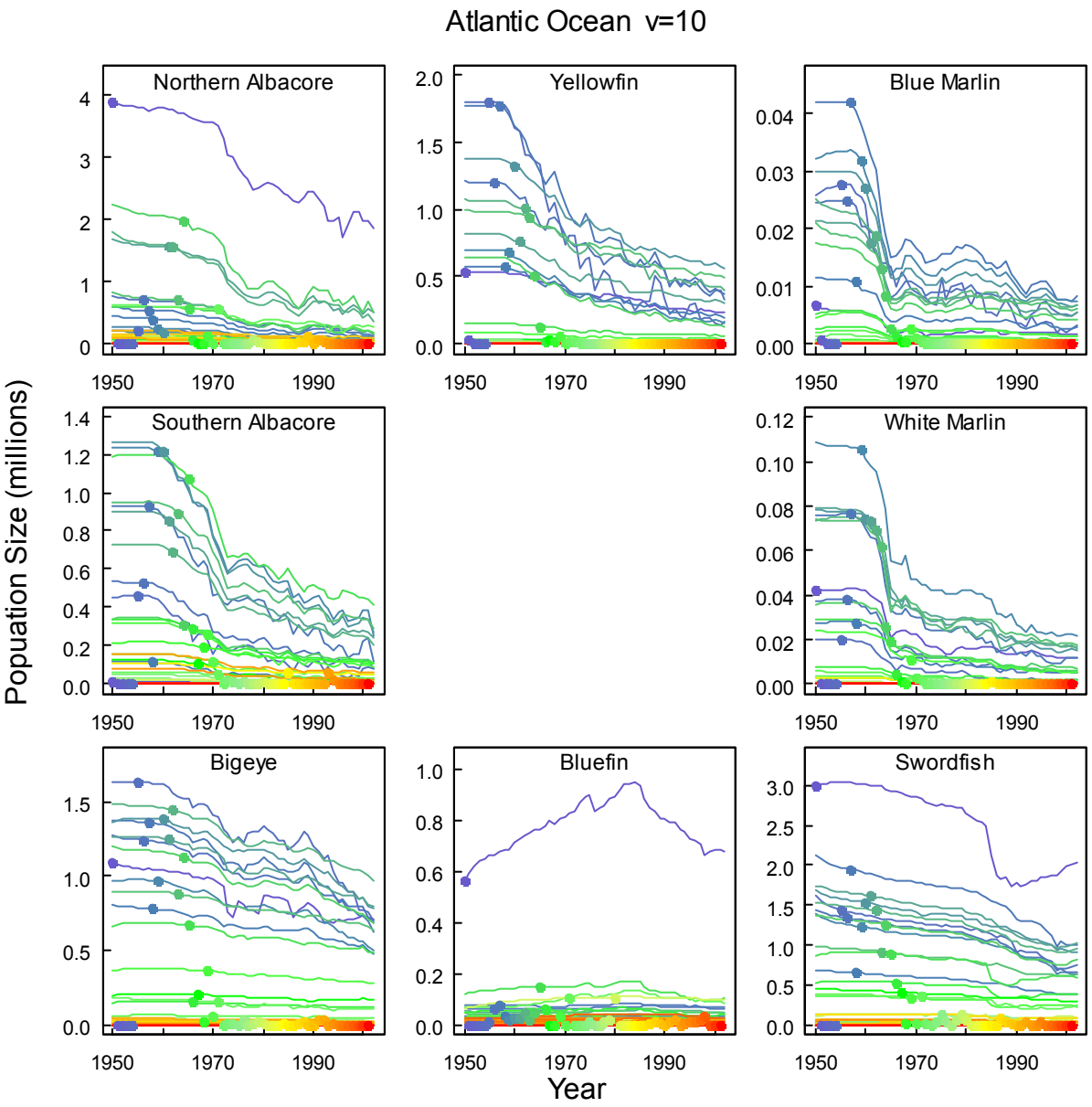

Figure 5.18 Simulated population trends of spatial cells aggregated by the year they were first fished for stocks in the Atlantic Ocean. Trends estimated using the spatial model with MLE parameter estimates and an assumed overall mixing rate v=10. Trends occurring prior to the dot (year of first fishing) on each trend line represent predicted stock declines due to reduced immigration caused by fishing in other cells.

Chapter 6 A simulation approach to assessing a mosaic of closures to meet multi-species fishing rate constraints while maximizing profits

Introduction

The severity and timing of impacts on large pelagic tuna and billfish stocks from industrialized fishing has sparked much recent debate (Myers and Worm 2003, Polacheck 2006, Sibert et al. 2006, Ward and Myers 2005b). The focus of this debate has been on the appropriateness of alternative methodologies for inferring such impacts (Kleiber and Maunder 2008, Maunder et al. 2006b, Walters 2003). Although views about how to interpret assessment data are divergent, there is little debate that current fisheries removals are having an unprecedented impact on many of these stocks (Mullon et al. 2005, Sibert et al. 2006, Worm et al. 2009). In particular, there is general recognition that many stocks are experiencing exploitation rates above what is deemed optimal using conventional reference points. Furthermore, a number of stocks are estimated to be depressed to below levels considered optimal (IATTC 2008, ICCAT 2009, IOTC 2004b, ISC 2007, Uozumi 2003, WCPFC 2008). Assessment results presented in Chapters 4 and 5 are in general agreement with these current assessments of stock status.

Given the current status of many stocks, stock assessment scientists have been advising for a number of years that exploitation levels on many stocks should be reduced if the management objective is to maintain all stocks at optimal levels. Further to this stock assessment advice, there have been calls to consider the use of marine protected areas (MPAs) at a large scale (Allison et al. 1998, Game et al. 2009, Lauck et al. 1998, Roberts et al. 2006, Worm et al. 2006, Worm et al. 2003) in order to protect overall biodiversity and stocks that are particularly sensitive to harvesting. However, closing areas to fishing does not necessarily ensure a reduction in exploitation rate (Walters et al. 1999, Walters and Bonfil 1999), and reducing fishing effort does not ensure a sufficient reduction in exploitation rate if remaining effort concentrates in areas where some species are particularly vulnerable. To complicate matters, although longline fisheries target specific species, they are inevitably multi-species fisheries with incidental capture of non-target species depending on geographic location. A final and equally important

consideration is the economic well being of the fishery. It makes little sense to place closures or reduce effort in such a way as to introduce gross economic inefficiencies into the fishery. Thus, some attempt at reaching a balance should be considered (Hilborn et al. 2004). Analysis of Japanese longline data suggests there are areas of high species overlap (Worm et al. 2003) as well as temporal-spatial locations where over-exploited stocks such as Atlantic blue marlin appear to be particularly vulnerable while catch rates of other, target species are lower (Goodyear 2003). This spatial mosaic of species overlaps should afford opportunities to reduce exploitation rates on those stocks that are over-exploited, through redistribution of fishing effort to areas where spatial overlap with particularly vulnerable species is lower. Such a redistribution of effort necessarily requires consideration of economic viability within the fishery.

Economic theory in relation to the dissipation of rent and profit optimization in fisheries is well established (Clark 1976, Gordon 1954). In open access fisheries, over capitalization and dissipation of rent is expected to occur over time, and stocks are generally expected to be depleted below the abundances that provide MSY. In instances where fisheries are viewed as having a sole owner, optimal resource use is expected to occur at efforts lower than and at abundances higher than that producing MSY. The difficulty with such prescriptions is that spatial heterogeneity is ignored, and though effort levels may appear optimal in relation to target species, the spatial distribution of effort can result in over exploitation of non-target or less valued species. Recently, spatial interactions have been considered in economic optimizations (Costello and Polasky 2008, Sanchirico and Wilen 1999). These analyses suggest that optimum equilibrium patterns of effort and population abundance are dependent upon bionomic conditions at the area-specific level, as well as the linkage between areas. For systems where production is linked to local abundance, effort targets areas of higher profit. These can be areas of lower relative cost or higher productivity or both. Effort is expected to be reduced in areas where expected profit is low due to high fishing costs or low fish abundance. Even in instances where economic incentives would indicate an attraction of effort, it is not necessarily optimal to utilize such areas fully; it may be better to protect them to allow them to act as ‘sources’ of production for other areas. The optimization analyses also indicate that area closures alone are insufficient to prevent rent dissipation in open access fisheries; overall effort limitations are required (Hannesson 1998, Sumaila and Charles 2002).

In this chapter, a method for optimizing the global equilibrium effort distribution is applied to tuna and billfish stocks based on the model developed in Chapter 5. The optimization aims to distribute effort to maximize total profit of the fishery. However, unlike the studies mentioned above, the multi-species nature of the fishery for larger size individuals was considered, and effort levels and distributions were progressively constrained so that target exploitation rates for every stock were not surpassed. Static advection-diffusion fields derived in Chapter 5 were used to represent mixing of fish between areas. Recruitment was assumed to depend on total population abundance rather local abundance in each spatial cell.

Methods

Walters and Martell (2004) suggested an approach to the assessment of space-time closures that would maximize profits from fishing over a long time horizon, subject to species-specific target fishing mortality rates treated as constraints (upper bounds on species Fs). Their approach involves finding the effort distribution that would maximize total profit over areas and/or times i where species j is caught. In this study, only area was considered, as seasonal changes in species distribution were not modeled. The overall value to be maximized (Π) is total profit, a function of income and cost of fishing, penalized for exceeding fishing mortality targets. Considering only income to the fishers, Π can be expressed as

$$6.1)\ \Pi = \sum_{i,j} q_j^* E_{i,j}^* N_{i,j}^{eq} w_j p_j - \sum_i c_i E_i - c_p \sum_j \left(F_j / F_j^* \right)^d$$

In equation 6.1 w_j is the average weight of a longline caught individual of species j and p_j is the price per unit weight of species *j*. c_i is an estimate of the area-specific unit cost of effort in cell *i*. $N^{eq}_{i,j}$ is the predicted equilibrium abundance of species *j* in cell *i*, predicted from the spatial dynamic model of Chapter 4 (equations 5.1-5.3). The last term in 6.1 is a penalty for exceeding target fishing mortality rates. q_j^* is the species j cell-scale catchability coefficient and $E_{i,j}^*$ is the relative effort applied in area *i* on species *j* calculated as,

$$6.2)\ E_{i,j}^* = \bar{r}_{i,j} E_i$$

Here $\bar{r}_{i,j}$ is the relative effort scale calculated in equation 5.9 average over 2000-2002 and E_i is the optimized effort for area *i*. This equation assumes that gear configurations within a given area do not change and relative differences in species targeting are preserved. The overall penalty for exceeding target fishing mortality rates is scaled by c_p and *d* determines how quickly the penalty changes as species-specific fishing mortality rates deviate from target values. The penalty term is only applied in instances when F_j exceeds F^*_j and F^*_j is a specified target fishing mortality rate. Equilibrium population abundance of each species in each area ($N^{eq}_{i,j}$) depends on the intensity of fishing (E_i). Overall fishing impact by species, F_j, depends on the effort distribution E_i and the predicted stock distribution; in particular, F_j can be written as

$$6.3) \quad \begin{aligned} F_j &= q^*_j \sum_i E^*_{i,j} N^{eq}_{i,j} \Big/ \sum_i N^{eq}_{i,j} \\ &= q^*_j \sum_i E^*_{i,j} s_{i,j} \qquad where \quad s_{i,j} = N^{eq}_{i,j} \Big/ \sum_i N^{eq}_{i,j} \end{aligned}$$

where $s_{i,j}$ is the equilibrium proportion of stock *j* fish vulnerable to fishing in area *i*. The basic idea behind seeking a maximum of profit (Π) that may involve a mosaic of closures is that the spatial distributions $s_{i,j}$ typically differ among species, implying the possibility of concentrating fishing in some areas that might minimize impact on 'sensitive' (low F^*_j) species.

Walters and Martell point out that maximizing equation 6.1 amounts to finding the 'ideal free distribution' (IFD) of efforts where profitability (measured as income-costs-contribution to penalty cost) is equalized across areas. The resulting solution satisfies $\partial\Pi/\partial E_i=0$ for all non-closed areas, and $\partial\Pi/\partial E_i<0$ at $E_i=0$ for all areas that should be closed. They suggest finding this IFD solution by a numerical procedure that involves successively finding the E_i that solve the $\partial\Pi/\partial E_i=0$ equations, essentially inching the E_i values toward the solution that maximizes equation 6.1. An alternative approach to identifying the effort distribution that maximizes Π is to utilize a nonlinear search routine, and that approach was used in this study by using *AD Model Builder* to do the optimization search. Optimal effort distributions were estimated and mapped for three estimated cost fields under different movement scenarios, using the most credible estimates of leading parameters (F_{msy}, MSY, M) from Chapter 5. Scenarios were mapped with increasing values of the penalty parameter *cp* with a modification to the penalty component of

equation 6.1 that only applied when fishing mortality exceeded target values (equation 6.4). Target fishing mortality (F^*_j) rates were assumed equal to F_{msy} for all species, with the F_{msy} estimates being the maximum likelihood values from Chapter 5 for each movement scenario from (see Table 11.1 in the Appendix to Chapter 5).

6.4) $$c_p \sum_j \left(F_j^* - F_j\right)^2$$

Either optimization approach required simulating population dynamics (N_{ij}) to determine equilibrium population distributions and fishing mortality rates, given any distribution of fishing effort. The spatially explicit model developed in Chapter 5 provided the necessary framework, with the simple addition of a routine to perform the calculation of Π at the predicted spatial equilibrium of the model N_{ij} for any given E_i pattern (that might be tested during the optimization search). To find the spatial equilibrium given E_is, a computationally inefficient method would be to integrate equations 5.1-5.3 over time until the N's stop changing. A much more efficient relaxation method was used instead, based on setting the left hand side of equation 5.1 to 0, then iteratively solving for each $N_{i,j}$ with R and other N_{ij} fixed at estimates from the previous iteration. This method converges to N^{eq} in about 500 iteration steps, while solving the equations over time typically required several thousand solution-steps to reach equilibrium.

One challenge in either optimization approach is to determine the per unit effort cost of fishing in each area (c_i). Absent detailed information on fishing cost in each area, cost fields can only be hypothesized using a reasonable set of assumptions. Three approaches were used in this study, each assuming that fishing cost is a portion (ψ) of revenue generated. The first assumed cost was related to distance (Figure 6.1) from port (d_i) such that $c_i=\xi d_i$. The scalar (ξ) was chosen so that equation 6.5 balanced assuming cost was and arbitrary 40% of total revenue ($\psi=0.4$).

6.5) $$\psi \sum_{i,j} \overline{C}_{i,j} w_j p_j = \sum_i c_i \overline{E}_i^*$$

6.6) $$\psi \sum_j \overline{C}_{i,j} w_j p_j = c_i \overline{E}_i^*$$

For this calculation, effort ($\overline{E}_i^*$) is similar to that from equation 5.9 but averaged over the last few years of data (1998-2002) for each area. Observed catch for each species in each cell ($\overline{C}_{i,j}$) was also averaged over the last few years of data. In this approach, total cost (summed over cells) was assumed 40% of the total revenue generated (summed over cells), which resulted in some cells generating a greater profit and some areas potential being fished at a loss. The second approach was to assume cost for each area equaled 40% ($\psi=0.4$) of the 1998-2002 historical mean revenue generated in a cell using equation 6.6. The difficulty with this approach was that costs for those areas that appear to generate much higher profits, costs were estimated to be very high; in reality, such areas might be exceptionally profitable. The third approach assumed a uniform cost field (c_i in equation 6.5 equal for all cells) with cost scaled so that total cost equaled 40% of total revenue.

The global maritime port database was used for the calculation of d_i. Port information was obtained from the National Aeronautics and Space Administration (NASA) Global Change Master Directory (http://gcmd.nasa.gov/records/GCMD_Maritime_Port_Boundary.html). d_is were calculated as the great circle distance from the closest port location to the center of a 5°x5° area using the *rdist.earth* function from the *fields* package (*v5.02*) in R (R Development Core Team 2008).

Relative average prices (Table 6.1) were calculated from monthly ex-vessel prices for 1998-2002. A landings-weighted average of monthly ex-vessel price at Japanese ports was calculated from data compiled by the US National Marine Fisheries Service, Sustainable Fisheries Division (http://swr.nmfs.noaa.gov/fmd/sfd.htm). Price for each species was taken as the average of monthly prices for fresh and frozen product again weighted by landings. Mean weights (Table 6.1) were calculated from length frequency information or paired numbers and biomass catch records (see Chapter 2).

Optimal effort distributions were described using simple linear models with total cell value, cost, total species recruitment, and tuna and marlin richness as explanatory variables. For these models, 'total cell value' as a predictor variable was calculated as the sum over species of initial population estimates multiplied by relative price and species weights. Species richness was

calculated using the method presented in Worm et al. (2005). The expected number of species $E(S_n)$ arising in a sample of n=100 individuals from a cell was calculated as,

$$6.7)\quad E(S_n) = \sum_{j=1}^{S}\left[1 - \binom{N - m_j}{n} \Big/ \binom{N}{n}\right]$$

In equation 6.7 S is the number of species, N is the total number of individuals in a sample, and m_j is the number of individuals of species j in the sample. Assuming a sample of N=1000 individuals $m_j=p_jN$. Where p_j was calculated as, a species initial population size divided by the total initial population size summed over all species in an area. Changes in the linear model predictors total value, recruitment and species richness as a function of movement rates are presented in Figure 12.1 to Figure 12.3 in the Appendix to Chapter 6.

Results

Estimated optimum fishing effort patterns and associated fishing mortality summaries for the various cost and movement scenarios are presented in Figure 6.2 to Figure 6.17. The most noticeable pattern in all scenarios, independent of assumed movement rate and impacted only slightly by assumed cost structure, was the mosaic of cells with no predicted effort, i.e., cells estimated to not be profitable (as an example, Figure 6.2). In general, these cells amounted to ~30% of all cells (Table 6.2), and occurred on the margins of tuna and billfish distributions. Comparison of Figure 6.2 and Figure 6.6 indicates some differences in the no-fishing pattern in the southern oceans when cost was assumed proportional to distance from port. As initial mixing rate was increased, and recruitment focused into fewer areas, the optimum effort became more concentrated near such recruitment areas, resulting in a higher proportion of areas with no effort even though such areas could generate profit (Figure 6.2 to Figure 6.4).

In general, optimized distributions resulted in a >150% increase in predicted total profit relative to the value used to determine cost fields. Effort was decreased to 20-60% of levels estimated for 1998-2002 with effort reduced more in scenarios where cost were assumed uniform (Table 6.2).Within a given scenario and concurrent with the increase in closed areas with increasing initial mixing rate, was an increase in total effort and value generated. Although optimized effort

levels were lower than levels estimated for 1998-2002 in all scenarios, optimized effort was highest when mixing rate was high v=10. There was a tendency for scenarios with a movement rate v=2.0 to have lower value and effort than scenarios with movement v=0.7 suggesting a parabolic relationship.

Common to all cost scenarios with low mixing rates and no penalty for exceeding target fishing rates (referred to here after as 'penalty'), was an obvious reduction in fishing effort and a restriction of effort distribution. This reduction and restriction resulted in a reduction of fishing mortality to below or near MSY levels for a number of stocks (Table 6.2 and Figure 6.5, Figure 6.9, Figure 6.13, and Figure 6.17). In most scenarios, despite effort reduction and spatial restriction, optimized efforts resulted in an increase in fishing mortality for those stocks estimated to be currently fished well below MSY levels, such as bigeye in the Atlantic Ocean or yellowfin in the Pacific Ocean (Figure 6.5). For a number of stocks that were estimated to be over-exploited in 2002, such as Indian Ocean albacore or North Atlantic albacore, reductions in fishing mortality rates (Figure 6.9) to below levels that would produce MSY were observed. A number of marlin species and southern bluefin tuna were subjected to fishing mortality rates above target values. These stock-specific exploitation levels were reasonably consistent across costs scenarios.

As initial mixing rate was increased in no penalty scenarios target fishing mortality rates were exceeded for a larger portion of the stocks (Table 6.2). For some stocks, fishing mortality increased even though fishing mortality had been reduced in the lower initial mixing rate scenarios (e.g. Figure 6.5). The underlying cost field had a noticeable impact on the degree to which exploitation rates changed for some species particularly when initial mixing rate was at higher values, (e.g., Indian Ocean striped marlin).

As the penalty for exceeding target fishing mortality rates increased, within a mixing rate scenario, areas open to fishing tended to decrease, effort increased, and value decreased. In some instances, the number of areas open to fishing was greater when the penalty was highest. Under these high penalty scenarios, the most noticeable increases in open areas occurred in the equatorial Atlantic Ocean, western Indian Ocean and south-central Pacific Ocean though the

extent of the increase was moderated by underlying costs. In other words, as exceeding target fishing mortality rates was severely penalized, effort distributions were not restricted further but diffused into a greater number of areas.

In all initial mixing rate and cost scenarios, linear models suggest a significant positive relationship between optimum effort and total initial value (Table 6.3). In scenarios where cost was variable, effort was always negatively related to cost though not significantly in all cases (using α=0.05). When effort was assumed a function of distance to port, the cost effect was estimated to be larger. In most scenarios, effort was negatively related to species richness; however, as with cost the relationship was not statistically significant except in a few initial mixing rate scenarios when cost was assumed uniform. A significant positive relationship was found between total recruitment and effort when movement rate was assumed lower. However, as initial mixing rates were increased (and modeled recruitment more concentrated), there was a tendency for this relationship to switch to negative. The proportion of variability described by linear models was low (<0.4) and decreased as initial mixing rates and the penalty were increased.

Increasing the penalty for exceeding target fishing mortality rates resulted in an expansion of the closed area mosaic. This pattern was particularly noticeable in low movement rate scenarios (compare Figure 6.6 through Figure 6.8 top panel). In the Pacific Ocean, a large closure occurred in the eastern Pacific Ocean with additional noticeable concentration of closures in the southern ocean and central northern ocean. As the fishing mortality penalty was increased, these areas fused due to closed area expansion. Thus when the penalty was high, a thick band of closed areas was observed between 0-20°N in western waters shifting south moving into eastern waters. Surrounding this band was a complex mosaic of smaller closures. There was also a cluster of closed areas off southeastern Australia. In the Indian Ocean, closures initially occurred in southern waters with a large portion of waters surrounding Australia closed. As fishing mortality penalty was increased, closures expanded northward and westward to meet fishing mortality targets for striped and black marlin as well as southern bluefin tuna. In the Atlantic Ocean, closures expanded from three main areas, the south and central ocean, as well as northern central waters to meet fishing mortality targets for white marlin.

The general patterns of closed area expansion became less obvious when initial mixing rates were increased and modeled recruitment concentrated because large contiguous areas of closed cells were estimated. Under higher initial mixing rates, spatial pattern are easier to describe as a complex mosaic of a few open areas. However, as noted above, under a high penalty for exceeding target fishing rates there was a tendency for effort to increase slightly compared to lower mixing rate scenarios with fewer areas closed (Table 6.2). This spatial 'dilution' of effort was very apparent in scenarios where fishing cost was assumed proportional to distance from port and fishing mortality penalty was high (Figure 6.6 to Figure 6.8). This noticeable change in the mosaic of open areas between moderate and severe penalty scenarios occurred as effort was shifted out of areas of high recruitment of over exploited species that overlapped with other less impacted species, to less valuable areas. In the Atlantic Ocean, these changes were very noticeable.

In scenarios where billfish catchability was halved (Figure 6.14 to Figure 6.16), assuming changes in gear configuration or fishing methods could be adopted to reduce billfish catchability, there was a slight increase in fishing effort under high penalty scenarios though total fishery value was somewhat lower. The number of open areas also increased as did the amount of effort in areas where marlin overlap was higher, (e.g., equatorial waters). This effect was more pronounced when movement rates were assumed higher.

Discussion

The underlying dynamic model used to explore profit optimization scenarios contains a number of complexities: spatial connectivity through advection-diffusion fields, multiple stocks with variability in stock productivity, spatial heterogeneity in recruitment, spatial cost variability, and stock-specific management constraints. Despite these complexities, when the assumed management objective for tuna and billfish fisheries was to maximize of total global profit, and management constraints were ignored, some general patterns emerged. Perhaps the most obvious was a substantial reduction in overall fishing effort. This result is not surprising as many stocks were estimated to be experiencing over-fishing under average 1998-2002 fishing intensities, and classic economic theory predicts profit to be maximized, when cost are assumed proportional to

effort, in single species fisheries when effort is below F_{msy} levels. Given the multi-species nature of the simulated fishery, profit optimization appeared to be dominated by a few species that make up a high proportion of total value (biomasses *x* prices). In each ocean, yellowfin, bigeye, and albacore tuna dominate total biomass, and effort levels were reduced by the optimization so that these species were harvested below or at F_{msy} levels. The optimal solution that emerges when a sole owner is assumed in single species fisheries appears to apply in multi-species fisheries provided a few stocks dominate total value. Not all of the dominant stocks are harvested below F_{msy} levels. When the cores of stock distributions overlap, the optimal effort distributions resulted in somewhat less valuable stock being harvested closer to or at F_{msy}. Potential profit generated from one stock was forgone in lieu of greater profits from the other stock(s), maximizing total profit. Exploitation rates on less valuable billfish stocks (less productive, smaller, and/or lower priced) above F_{msy} values depended on the degree of overlap with the core distribution of more valuable stocks and F_{cur} estimates. Significant overlap between weaker and dominant stocks generally resulted in the weaker stock being exploited at levels above F_{msy} particularly if F_{cur} was estimated to be above F_{msy}. However, reduction in (and redistribution of) effort also reduced fishing mortality rates on less abundant billfish species. When effort reductions were sufficient to prevent over-fishing it was not possible to discern if reductions in mortality resulted from optimizing profits for a particular stock or were simply a by-product of optimizing for species that contributed more to total value. In instances where spatial overlap was high, it was likely the latter.

Walters and Martell (2004) point out that in such spatial optimizations, the solution typically contains a mosaic of closed areas when fishing mortalities are constrained to target values. In the results presented here, this effect is evident even when fishing mortality constraints are ignored, because a number of major stocks were estimated to be exploited at levels above F_{msy} and to increase profits, fishing mortality on these stock had to be reduced. This 'first level' of closures arose because fishing mortality reductions were achieved by removing effort in areas estimated to have very low value due to differences in species composition, abundances, and cost. These areas also become less profitable through cascade effects resulting from spatial connectivity. Effort in high values areas, primarily areas of high yellowfin, albacore, and bigeye recruitment, reduced value in neighboring locations through reductions in numbers of fish dispersing to the

'sink' areas. At the margins of stock distributions, or in areas where initial profitability was low cascade effects resulted in some cells becoming unprofitable. It is likely that closing such areas increased overall profit by establishing a 'source-sink' dynamic as found by Costello and Polasky (2008).

The underlying structure of the recruitment model used (assuming recruitment into each cell was a function of total stock size, and not local abundance) was also likely to affect the shift of effort out of 'sink' areas. Basing recruitment on total population size allowed exploitation rates in cells that received a greater proportion of total recruitment a high level without necessarily affecting recruitment into the cells. However, although the optimized effort distributions correlated with areas of higher recruitment for more abundant species, there were a number of instances where effort was excluded from high recruitment areas. This effect was more apparent as movement rates were increased so that areas of estimated high recruitment were concentrated. It is likely that the mechanism determining the opening or closing of 'source' areas is similar to that found by Sanchirico and Wilen (1999). If areas of high recruitment have higher cost and provide a high net flow of individuals into neighboring areas with lower cost, profit is likely to increase by fishing surrounding areas. If cost is lower in the high recruitment areas then profit is maximized by placing effort into these areas.

Increasing the penalty for exceeding target exploitation rates further restricted fishing effort distribution. Effort was shifted out of areas where over-exploited species were most abundant. To meet fishing mortality constraints, a larger proportion of area was closed to fishing. Potential losses of profit from such closures were mitigated to some extent by moving effort to less profitable areas resulting in an increase in total effort. When recruitment was concentrated and resulted in strong species overlap in high value areas, larger reductions in fishing effort, number of open cells, and total value were necessary to meet target fishing mortality constraints. However, simulations in which billfish catchability was reduced showed that effort reduction and area closures could be substantially less severe if such reductions in catchability could be achieved. Here it was assumed that alteration in fishing practices or gear configuration could be made to either reduce the catch rate of billfish species or reduce release mortality (Beverly et al. 2009, Serafy et al. 2009). Another possible way to reduce catchability of billfish and other

sensitive species would be by implementing dynamic space-time closures focused on particular areas and seasons where by-catch impacts are highest (Game et al. 2009, Goodyear 2003, Grantham et al. 2008).

The results presented for optimization simulations generally agree with the findings of previous investigations. Effort was reduced so stocks that have the greatest impact on total value were fished below F_{msy}. Profit was further increased when effort was shifted out of areas of lower value and higher cost as well as allowing some areas of higher recruitment to act as 'source' areas. To prevent target exploitation rates of less values species from being exceeded, effort was excluded from areas where such species were particularly abundant. Effort exclusion could be mitigated through the adoption of methods aimed at reducing the catchability of vulnerable species. Recently protected areas within the open pelagic have been proposed. The spatial arrangement of closures estimated in this chapter that would optimize returns to the longline fishery for tunas and billfishes are generally more complex than closure patterns developed from expert judgment (Roberts et al. 2006) or indices of species diversity (Worm et al. 2006). Substantial overlaps between area closures predicted from optimizations and those based on other criteria do occur. When mixing rates were assumed high, a much larger area of the world's oceans is closed compared to previous proposals. In contrast, MPA classification using static GIS based models (Game et al. 2009) produce a far more complex network of optimal areas that do not necessarily account for mixing between areas.

The general management prescriptions arising from the optimization presented appears robust and have been reproduced in previous works. However, the main objective of management should not necessarily entail the maximization of profit or prevent all stock from being exploited above F_{msy} levels (Bromley 2009, Christensen *In press,* Christensen and Walters 2004, Hilborn et al. 2004, Walters et al. 2005). Optimization scenarios do not necessarily bear any relation to what would be optimal if a more realistic multi-nation/multi-fleet optimization model were explored. Furthermore, the details of the equilibrium effort distribution presented under each scenario were dependent on the underlying cost structure, state dynamics, species-specific catchability given current gear configurations, and movement fields assumed. In particular, species-specific average catchability was calculated from estimates of relative fishing mortality

and adjusted for each specific area. When effort was allocated to an area, area specific catchability was assumed not to change. In other words, the composition of gears that generated observed catches of larger sized individuals in a given area was assumed not to change. There is a potential for catchability to change as the composition of gears changes, particularly in areas when gears other than longlines (unassociated purse seine sets or baitboats) are effective at capturing larger tuna, (e.g., areas with shallow thermoclines).

Seasonal migration patterns and inter-annual variability in stock distribution in response to changing oceanographic conditions were not considered in optimization scenarios. If seasonality were considered, the optimum effort distribution would likely shift in response to seasonal shifts in value, potentially reducing fishing mortality on more vulnerable species if overlap with more valued species were reduced (Grantham et al. 2008). Larger-scale changes in ocean conditions such as progressive shifts in large oceanographic structures, (e.g., convergence zone) or major events such as El Niño significantly alter the distribution and catchability of a species. These major changes in oceanography would likely result in noticeably different effort distributions.

Although the exercise presented here is essentially 'gaming' due to the arbitrary nature of the cost fields used, some insights into potential management options for tuna and billfish stocks were gained. Stock assessments presented in this thesis, in agreement with those performed by RFMOs, indicate over-fishing in many stocks and assessment scientists have recommended effort reductions for a number of years. Profit optimization scenarios presented in this chapter suggest economic efficiencies can be gained in the long term if effort reductions are coupled with closed areas. If and how such reductions and restrictions are to be achieved is unknown, and attempts to implement such strategies will likely rest on the member nations of RFMOs. In addition to increasing the available economic rent, reducing effort on the major tuna species captured by longlines should also result in reduced harvest rates on by-catch species, particularly if area closures are placed in areas of overlap.

Fishery removals have had profound impacts of on marine ecosystems, and there has been growing demand to increase the number and sizes of marine reserves (Allison et al. 1998, Myers and Worm 2003, National Research Council 1995, 1999, Pauly et al. 1998, Worm et al. 2006,

Worm et al. 2009). If such areas are intended to reduce exploitation on large pelagic tuna and billfish, optimizations presented here suggest that closures many result in net economic benefits to the fishery provided total effort be reduced. Simply closing areas without reducing effort can potentially increase exploitation rates (Walters and Bonfil 1999) and degrade the economic performance of the fishery (Costello and Polasky 2008). Simulations suggest it is optimal to close a large proportion of the pelagic area (>30-60%) though the optimum proportion is highly dependent on assumed movement rates and recruitment patterns. Provided effort is reduced, there may be potential long-term economic benefits to the fishery even if a simpler closed area mosaic were implemented.

Table 6.1 Mean weights and relative ex-vessel prices for species considered in Chapter 6.

Species	Mean Weight (kg)	Relative Price
Albacore Tuna	15	1.67
Bigeye Tuna	40	4.94
Yellowfin Tuna	40	3.09
Southern bluefin tuna	100	11.68
Northern Pacific bluefin tuna	160	11.68
Atlantic bluefin tuna	133	11.68
Blue marlin	60	1
Striped marlin	20	2.76
White marlin	20	2.76
Black marlin	50	1.68
Swordfish	50	4.03

Table 6.2 Optimization model results expressed as percentages relative to average values for 1998-2002 for relative change in average fishing mortality, value, areas status, as well as the number of stocks for which target fishing mortality was exceeded. Results are presented for various cost and movement rate (v) assumptions. In the final uniform cost scenario, billfish catchability (q) is halved.

Scenario	F penalty	Initial v	F/q (x10^6)	Value	Areas Open	Areas Closed	No Profit	F > Ftarget
Mean Effort 1998-2002	Nil	0.7/2/5/10	7479	3515	1213			11/9/10/9
Area Cost 40% of Area Revenue	Nil	0.7	27	147	34	39	27	5
		2	27	143	23	50	27	7
		5	26	139	17	56	27	7
		10	29	147	10	63	27	8
	Moderate	0.7	27	147	33	40	27	5
		2	27	143	21	51	27	5
		5	26	139	16	57	27	7
		10	31	147	10	64	26	8
	High	0.7	28	145	36	37	27	0
		2	29	140	21	52	27	2
		5	27	138	16	57	27	0
		10	31	144	9	64	27	1
Cost proportional to Distance from port	Nil	0.7	38	158	31	40	29	7
		2	39	154	18	69	30	7
		5	37	147	13	57	30	9
		10	40	157	7	63	30	10
	Moderate	0.7	39	158	29	42	29	6
		2	40	153	18	52	30	5
		5	37	147	13	57	30	6
		10	40	157	7	63	30	9
	High	0.7	44	154	30	41	21	0
		2	43	151	19	51	30	1
		5	37	146	18	52	30	0
		10	41	153	16	55	30	1
Uniform Cost	Nil	0.7	20	152	36	36	28	6
		2	17	147	23	48	29	7
		5	15	141	17	54	28	8
		10	16	148	9	63	28	9
	Moderate	0.7	20	146	35	36	28	5
		2	18	146	21	50	29	6
		5	16	140	14	56	28	7
		10	17	148	9	62	28	7
	High	0.7	21	150	34	37	28	0
		2	21	143	22	49	29	1
		5	17	139	18	54	28	0
		10	17	144	10	62	28	1
Uniform Cost Billfish q half	Nil	0.7	20	152	36	36	28	6
		2	17	148	24	24	29	7
		5	15	141	18	18	28	7
		10	16	149	10	10	28	8
	Moderate	0.7	20	151	35	37	28	6
		2	17	147	23	48	29	5
		5	15	141	18	54	28	6
		10	16	148	10	62	28	7
	High	0.7	21	150	32	40	28	0
		2	19	145	24	47	29	1
		5	16	140	21	51	28	0
		10	17	144	11	61	28	1

Table 6.3 Linear model coefficients for predicting optimized cell effort, along with R-squared values and significance codes for optimization scenarios for various cost assumptions and initial movement rates. In the final uniform cost scenario, billfish catchability (q) is halved. Codes "***", "**", "*", "." indicate p-values of < 0.001, <0.01, <0.05, <0.1.

Scenario	F penalty	Initial v	Intercept	Value	Cost	Recruitment	Richness	R^2
Area Cost 40% of Area Revenue	Nil	0.7	0.8 **	0.23 ***	-1.34	9.16 *	-0.17 **	0.226
		2	1.16 **	0.23 ***	-1.57	16.58 ***	-0.22 **	0.132
		5	0.75	0.23 ***	-1.55	14.96 **	-0.09	0.075
		10	1.41 *	0.33 ***	-2 ***	17.08 **	-0.35 *	0.055
	Moderate	0.7	0.75 **	0.21 ***	-1.31	9.86 *	-0.15 *	0.207
		2	1.22 **	0.23 ***	-1.6 ***	17.19 ***	-0.24 **	0.121
		5	0.84 .	0.24 ***	-1.61	16.12 **	-0.12	0.074
		10	1.66 *	0.34 ***	-2.17	21 **	-0.41 *	0.055
	High	0.7	0.83 **	0.22 ***	-1.37	8.77 .	-0.14 *	0.175
		2	1.28 **	0.2 ***	-1.64	18.75 ***	-0.17 .	0.093
		5	0.93 .	0.25 ***	-1.7 ***	17.82 ***	-0.14	0.073
		10	1.58 *	0.34 ***	-2.17	17.33 *	-0.37 *	0.047
Cost α to distance from port	Nil	0.7	1.53 **	0.27 ***	-4.44	22.34 **	-0.12	0.172
		2	2.6 **	0.26 ***	-5.29	38.94 ***	-0.28 .	0.102
		5	2.53 *	0.23 **	-5.25	42.55 ***	-0.21	0.063
		10	2.99 *	0.36 **	-6.27	16.11	-0.31	0.035
	Moderate	0.7	1.52 *	0.31 ***	-4.39	14.11	-0.16	0.164
		2	2.61 **	0.32 ***	-5.15	27.84 **	-0.34 *	0.091
		5	2.56 *	0.29 ***	-5.24	34.1 ***	-0.27	0.057
		10	2.93 *	0.36 **	-6.23	16.08	-0.31	0.033
	High	0.7	1.97 **	0.36 ***	-4.82	5	-0.22	0.139
		2	2.81 **	0.34 ***	-5.44	19.99 .	-0.32 .	0.084
		5	2.59 *	0.3 ***	-5.03	40.94 ***	-0.34	0.059
		10	2.86 *	0.37 **	-6.24	19.75	-0.31	0.034
Uniform Cost	Nil	0.7	-0.29 *	0.2 ***		9.62 ***	-0.14	0.453
		2	-0.17	0.2 ***		14.84 ***	-0.18	0.317
		5	-0.25	0.22 ***		13.01 ***	-0.18	0.242
		10	-0.07	0.31 ***		13.97 ***	-0.4 ***	0.198
	Moderate	0.7	-0.28 *	0.2 ***		8.6 ***	-0.15	0.433
		2	-0.13	0.21 ***		12.79 ***	-0.2 ***	0.279
		5	-0.21	0.23 ***		13.85 ***	-0.21	0.216
		10	-0.11	0.33 ***		14.79 ***	-0.42	0.178
	High	0.7	-0.23	0.2 ***		8.08 **	-0.14	0.333
		2	-0.15	0.2 ***		11.65 ***	-0.13 *	0.179
		5	-0.21	0.22 ***		12.61 ***	-0.18	0.184
		10	-0.09	0.33 ***		14.26 ***	-0.43	0.168
Uniform Cost Billfish q half	Nil	0.7	-0.29 *	0.2 ***		9.59 ***	-0.14	0.453
		2	-0.18	0.2 ***		14.81 ***	-0.18	0.318
		5	-0.27	0.22 ***		12.73 ***	-0.17	0.242
		10	-0.12	0.31 ***		12.28 ***	-0.38	0.202
	Moderate	0.7	-0.28 *	0.2 ***		8.53 ***	-0.15	0.432
		2	-0.17	0.2 ***		14.41 ***	-0.19	0.304
		5	-0.22	0.22 ***		14.52 ***	-0.19	0.246
		10	-0.09	0.32 ***		14.4 ***	-0.41	0.199
	High	0.7	-0.23	0.2 ***		8.34 **	-0.14	0.334
		2	-0.11	0.21 ***		12.28 ***	-0.19	0.25
		5	-0.23	0.21 ***		13.47 ***	-0.17	0.224
		10	-0.26	0.29 ***		13.8 ***	-0.3 ***	0.158

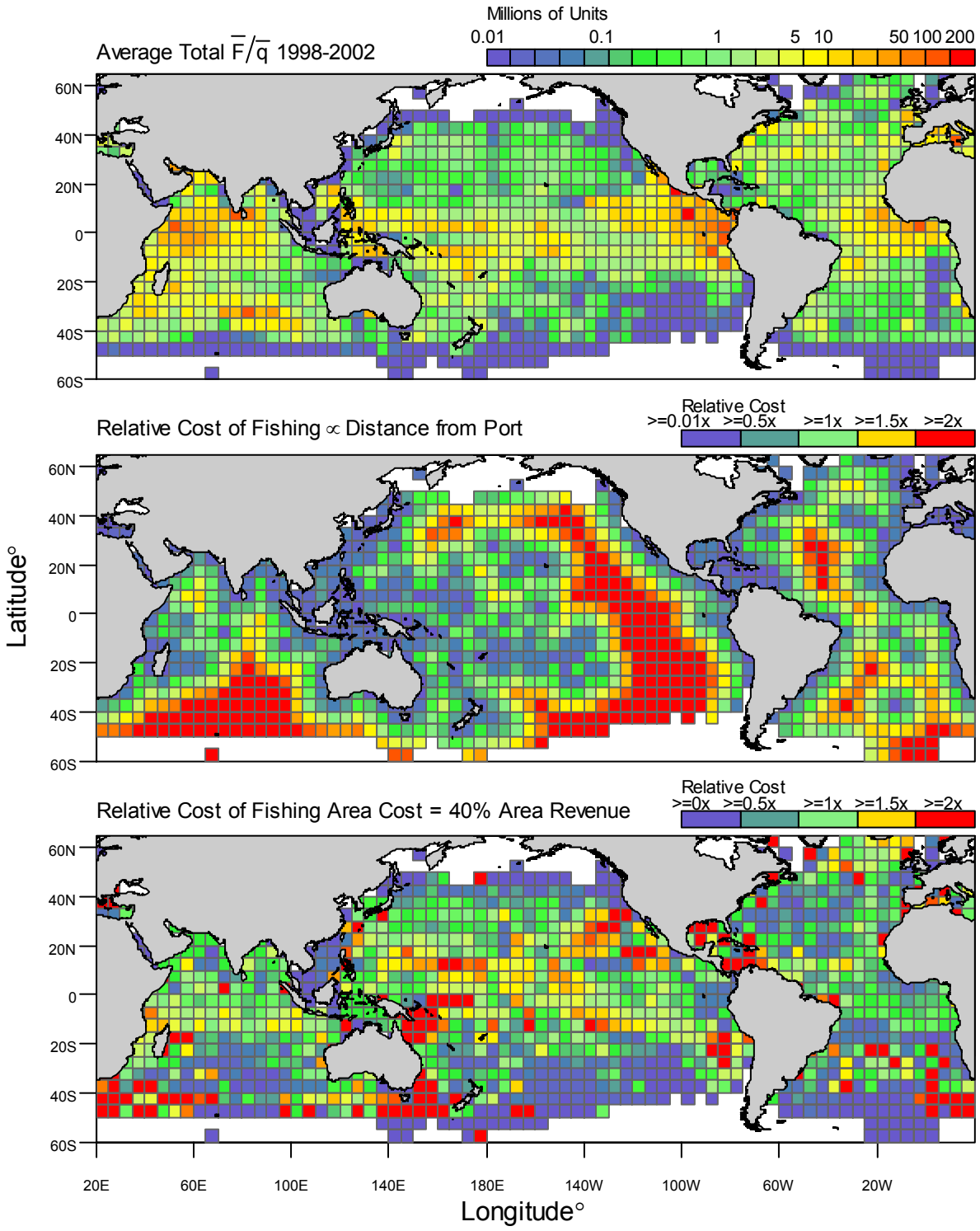

Figure 6.1 Average relative fishing mortality rate distribution from 1998-2002 (top panel). Estimated relative fishing cost by cell assuming cost is proportional to distance from port and total cost is 40% of total revenues (middle panel). Estimated relative fishing cost by cell assuming cost equals 40% of cell specific average revenue from 1998-2002 (bottom panel)

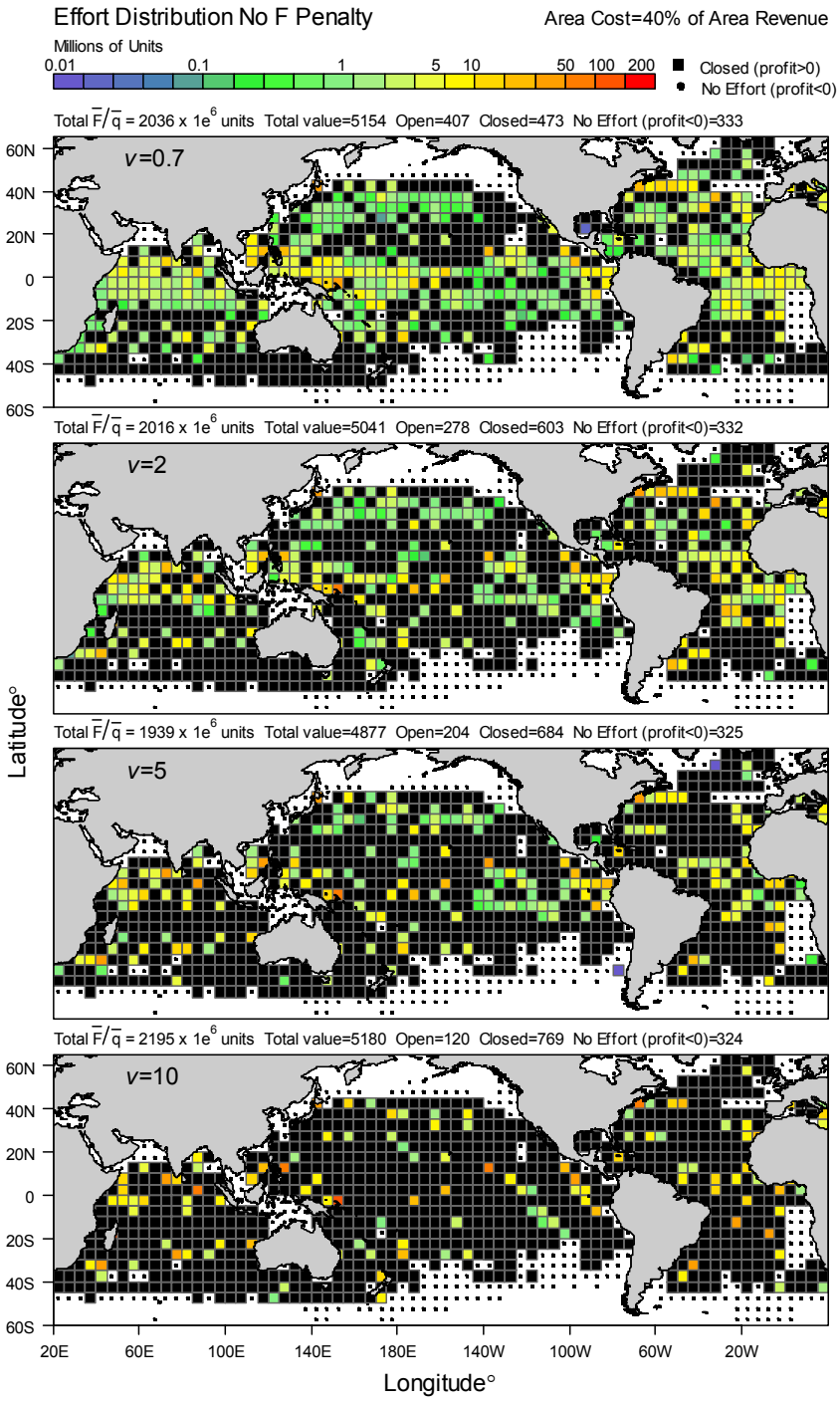

Figure 6.2 Distribution of mean relative fishing mortality for profit optimization scenarios, for various initial movement rates (v) assuming area cost is 40% of area revenue and no penalty is applied if stock specific target fishing mortality rates are exceeded. Black squares are closed areas and black dots are areas assumed not to attract effort, as no profit would be generated.

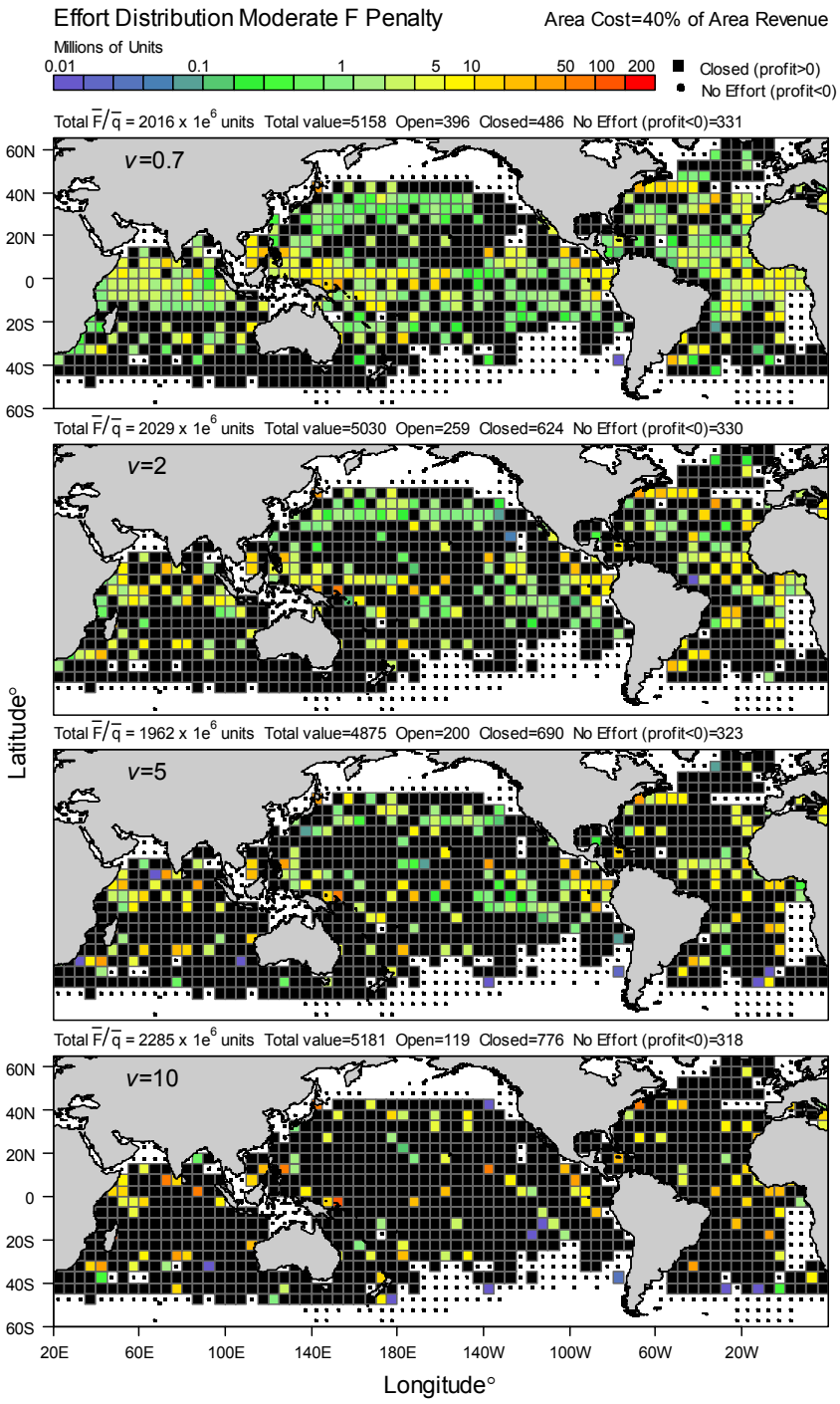

Figure 6.3 Distribution of mean relative fishing mortality for profit optimization scenarios for various initial movement rates (v) assuming area cost is 40% of area revenue and a moderate penalty is applied if stock specific target fishing mortality rates are exceeded. Black squares are closed areas and black dots are areas assumed not to attract effort, as no profit would be generated.

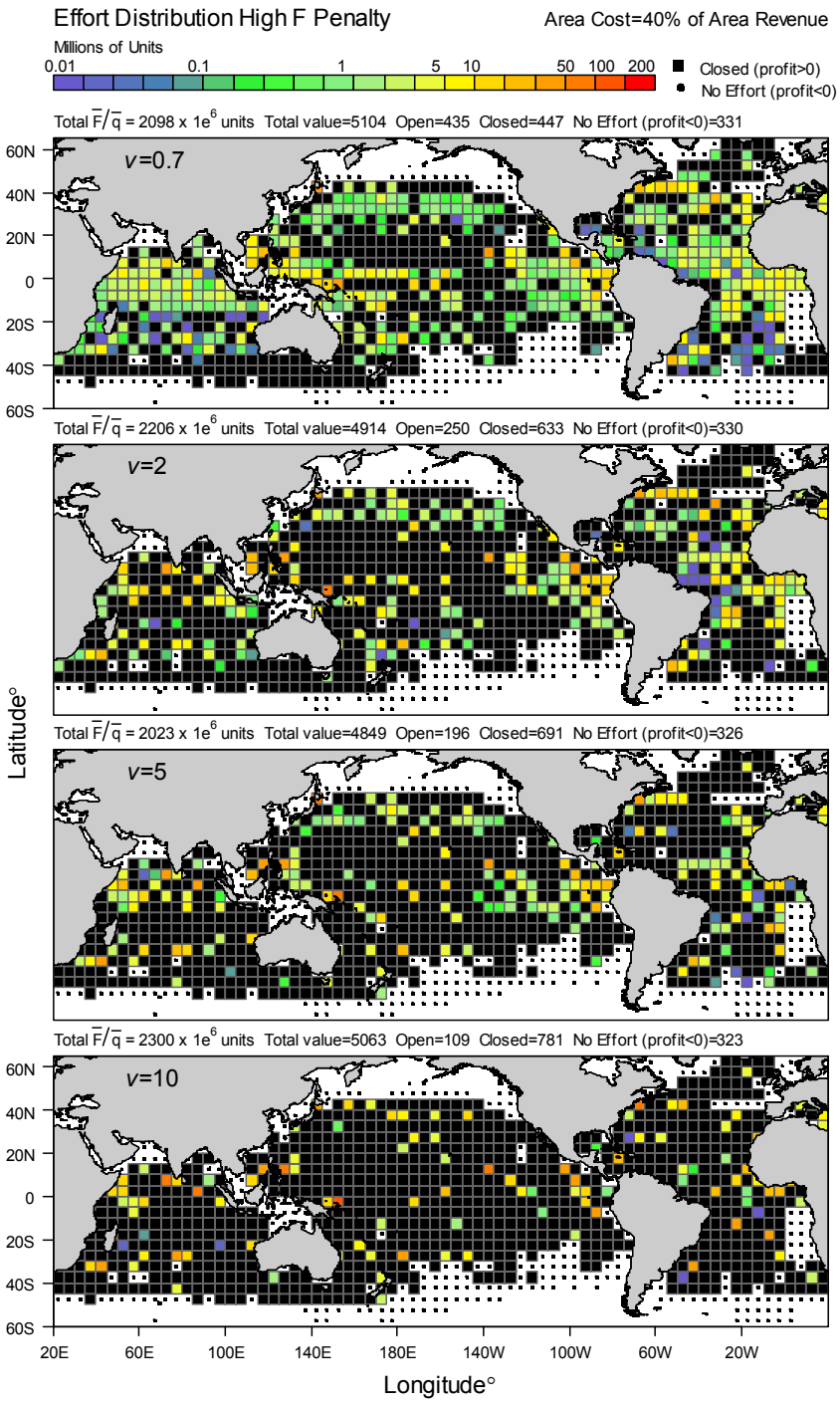

Figure 6.4 Distribution of mean relative fishing mortality for profit optimization scenarios for various initial movement rates (v) assuming area cost is 40% of areas revenue and a severe penalty is applied if stock specific target fishing mortality rates are exceeded. Black squares are closed areas and black dots are areas assumed not to attract effort, as no profit would be generated.

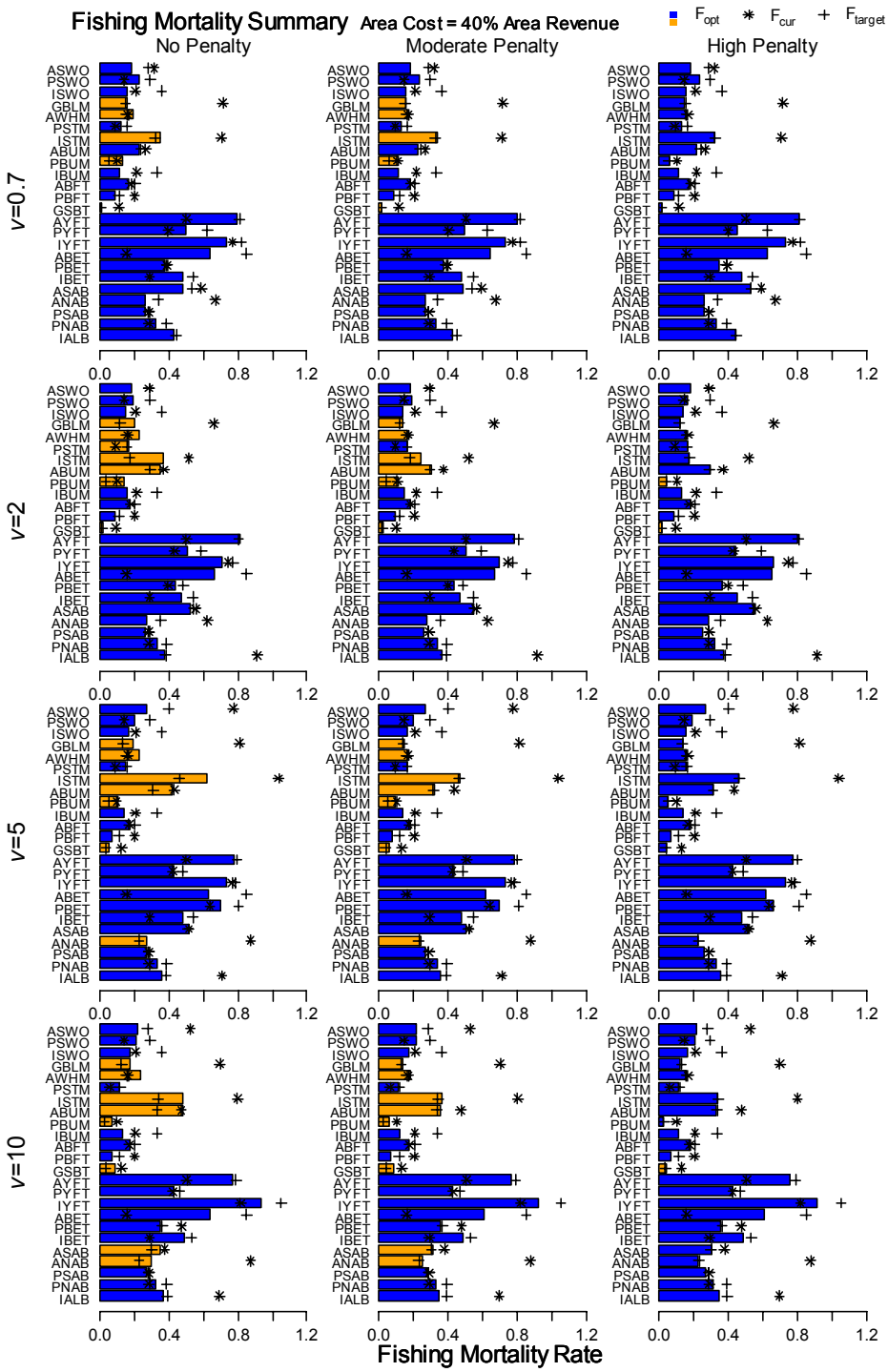

Figure 6.5 Fishing mortality summaries for each stock, for profit optimization scenarios for various initial movement rates and penalties for exceeding target fishing mortalities assuming area cost is 40% of area revenue. Blue or orange bars are estimated fishing mortality rates. Black stars indicate current fishing mortality rates. Black crosses indicate target mortality rates. Orange bars indicate target fishing mortality is exceeded.

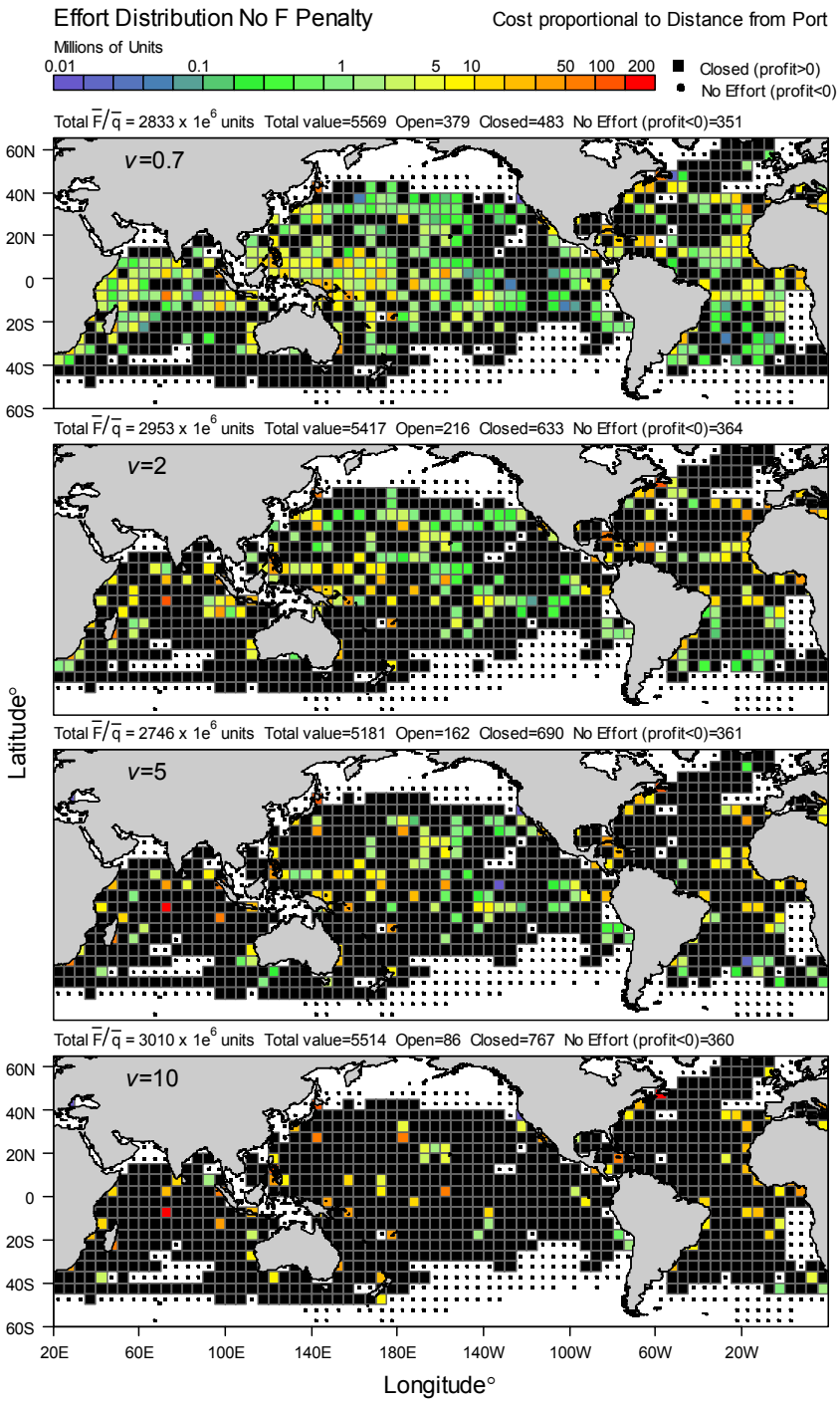

Figure 6.6 Distribution of mean relative fishing mortality for profit optimization scenarios for various initial movement rates (v) assuming area cost is a function of distance to port, total cost is 40% of total revenue and no penalty is applied if stock specific target fishing mortality rates are exceeded. Black squares are closed areas and black dots are areas assumed not to attract effort, as no profit would be generated.

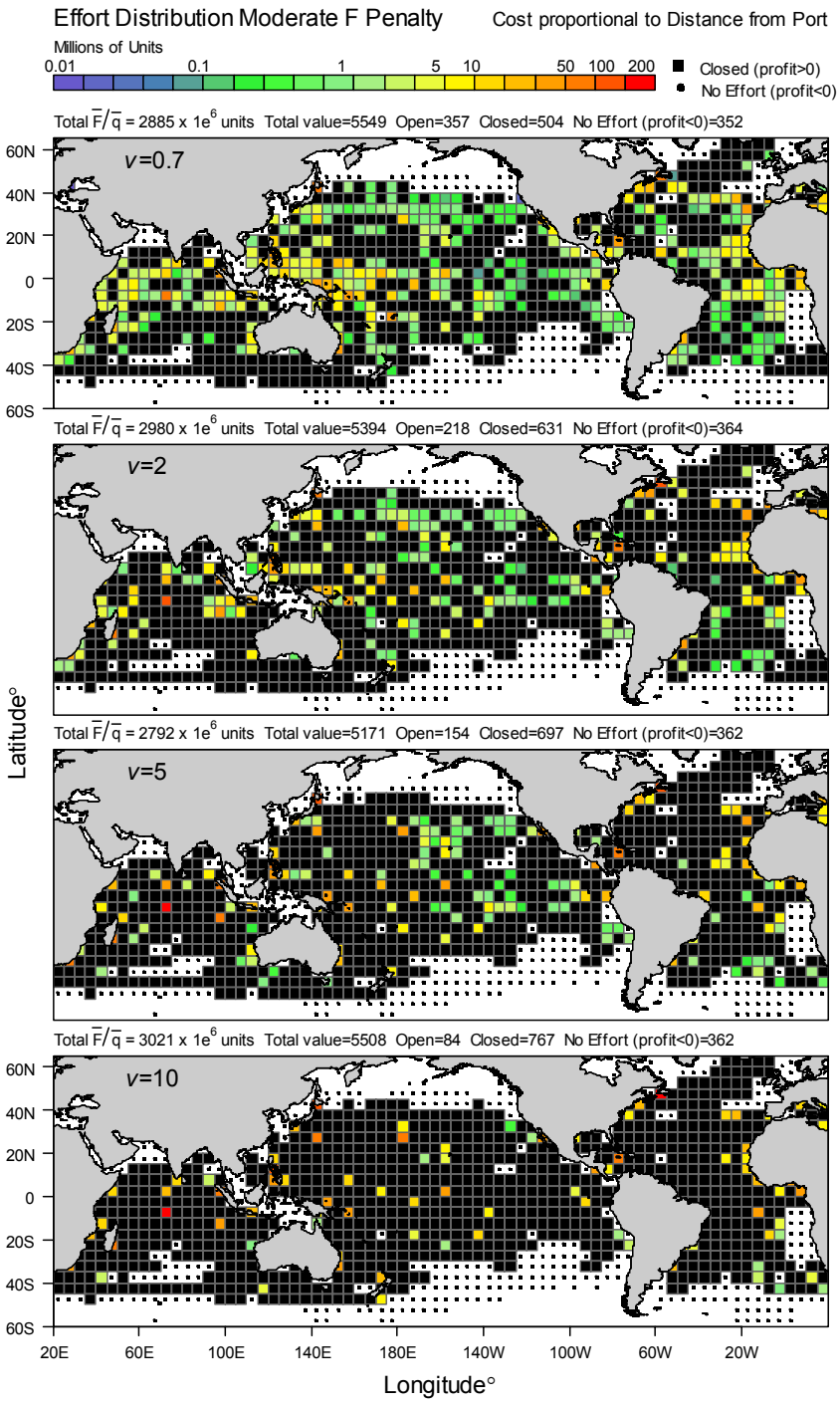

Figure 6.7 Distribution of mean relative fishing mortality for profit optimization scenarios for various initial movement rates (v) assuming area cost is a function of distance to port, total cost is 40% of total revenue and a moderate penalty is applied if stock specific target fishing mortality rates are exceeded. Black squares are closed areas and black dots are areas assumed not to attract effort, as no profit would be generated.

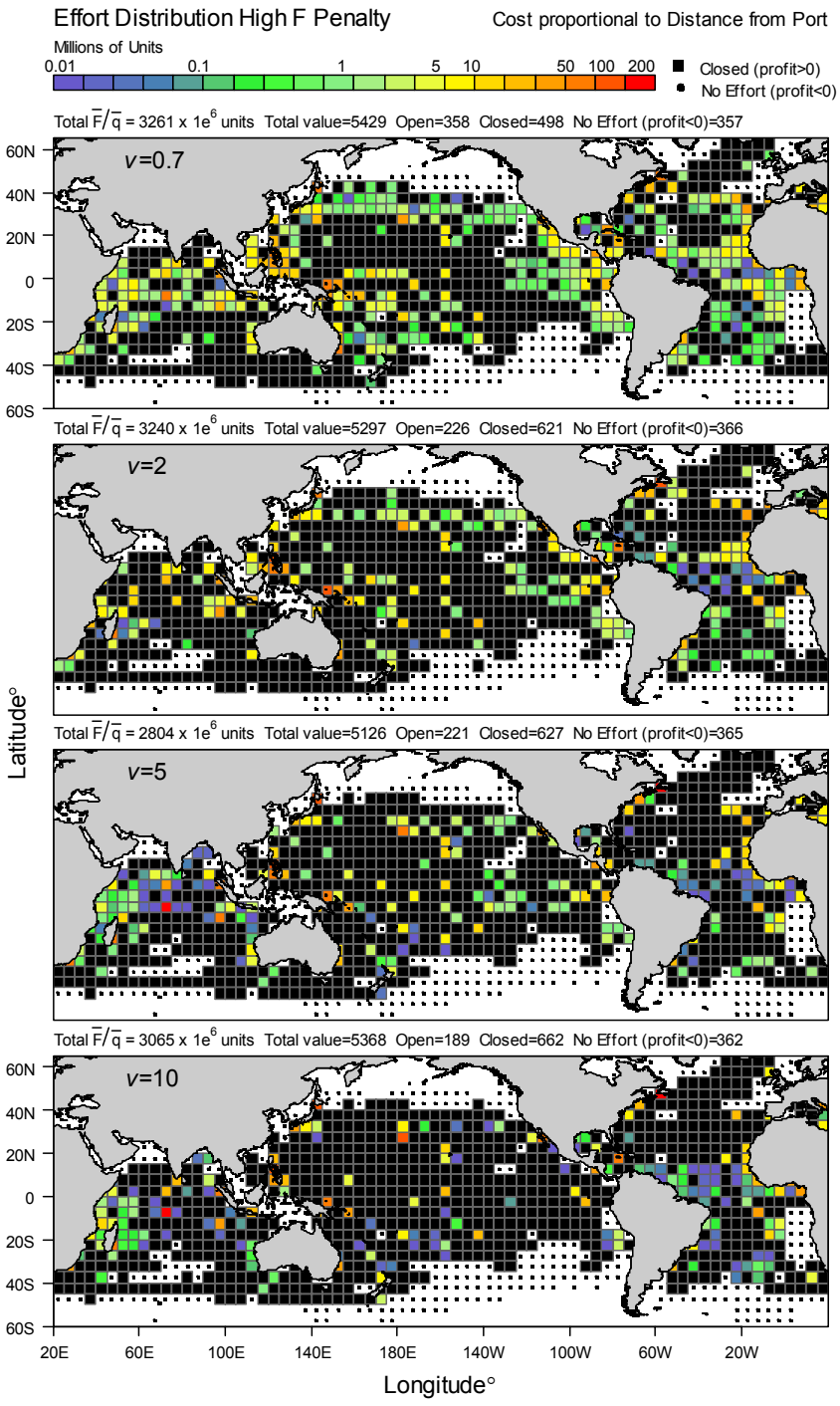

Figure 6.8 Distribution of mean relative fishing mortality for profit optimization scenarios for various initial movement rates (v) assuming area cost is a function of distance to port, total cost is 40% of total revenue and a severe penalty is applied if stock specific target fishing mortality rates are exceeded. Black squares are closed areas and black dots are areas assumed not to attract effort, as no profit would be generated.

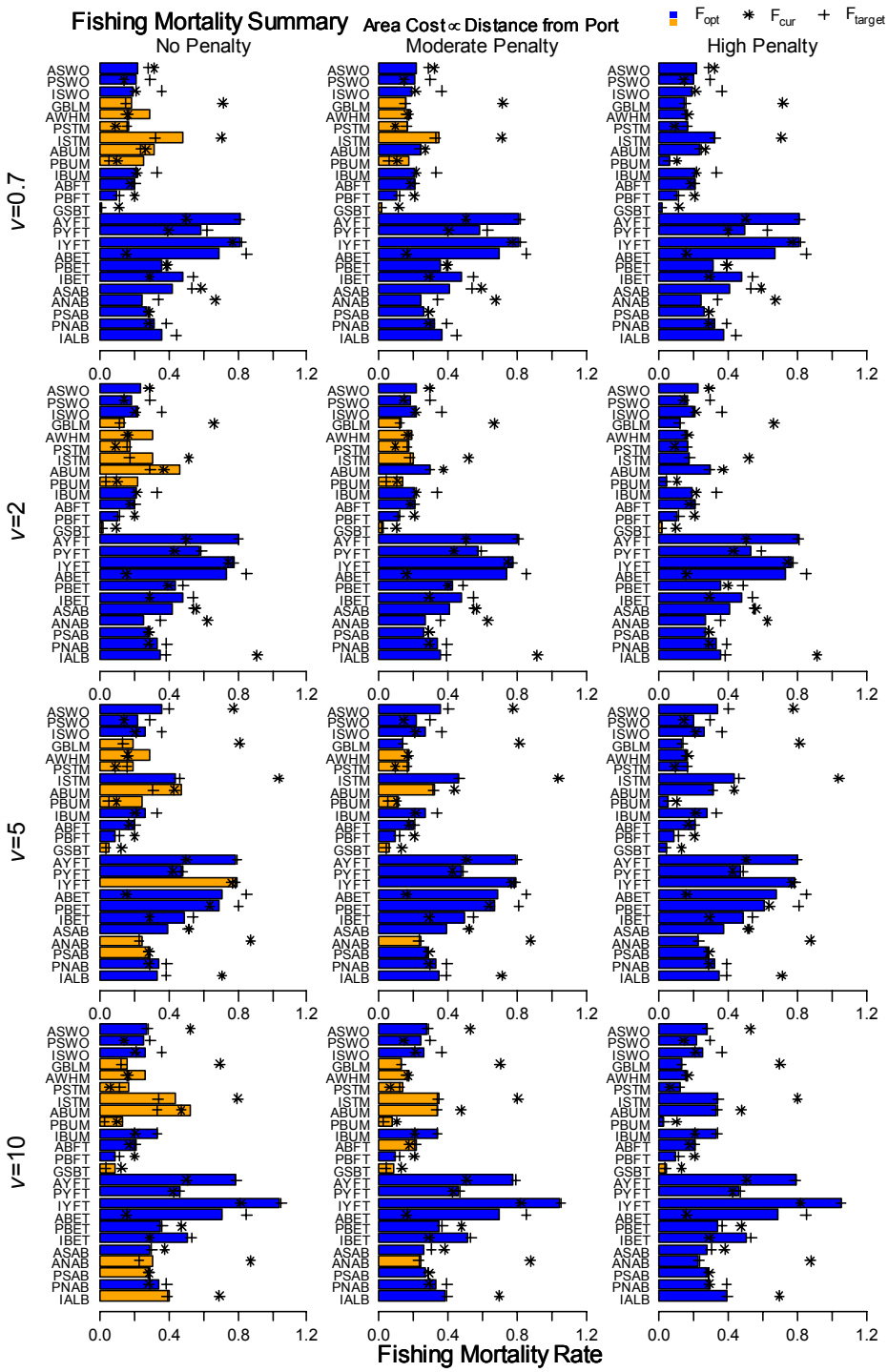

Figure 6.9 Fishing mortality summaries for each stock for profit optimization scenarios for various initial movement rates and penalties for exceeding target fishing mortalities assuming area cost is a function of distance to port, total cost is 40% of total revenue. Blue and orange are estimated fishing mortality rates. Black stars indicate current fishing mortality rates. Black crosses indicate target mortality rates. Orange bars indicate target fishing mortality is exceeded.

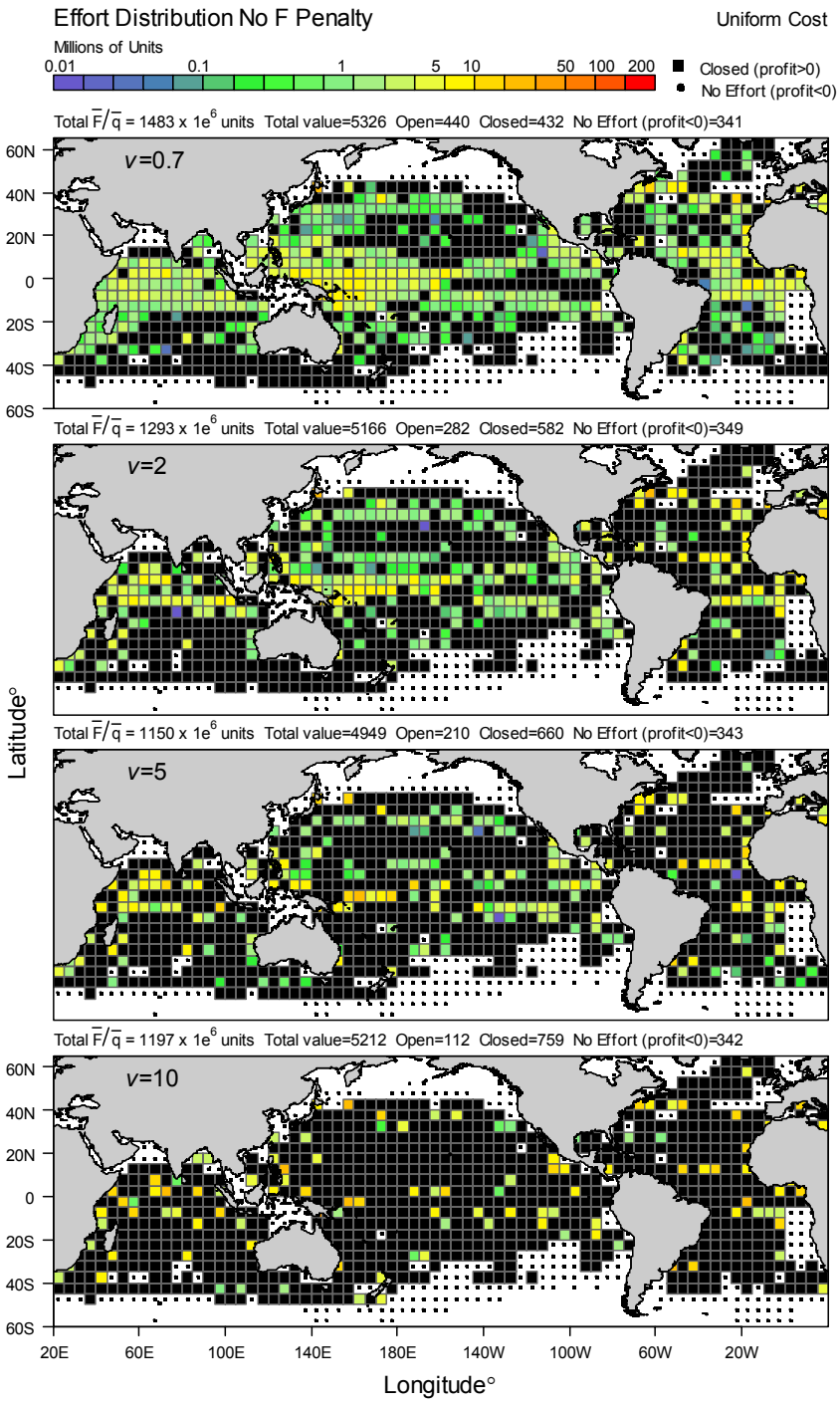

Figure 6.10 Distribution of mean relative fishing mortality for profit optimization scenarios for various initial movement rates (v) assuming area cost is uniform, total cost is 40% of total revenue and no penalty is applied if stock specific target fishing mortality rates are exceeded. Black squares are closed areas and black dots are areas assumed not to attract effort, as no profit would be generated.

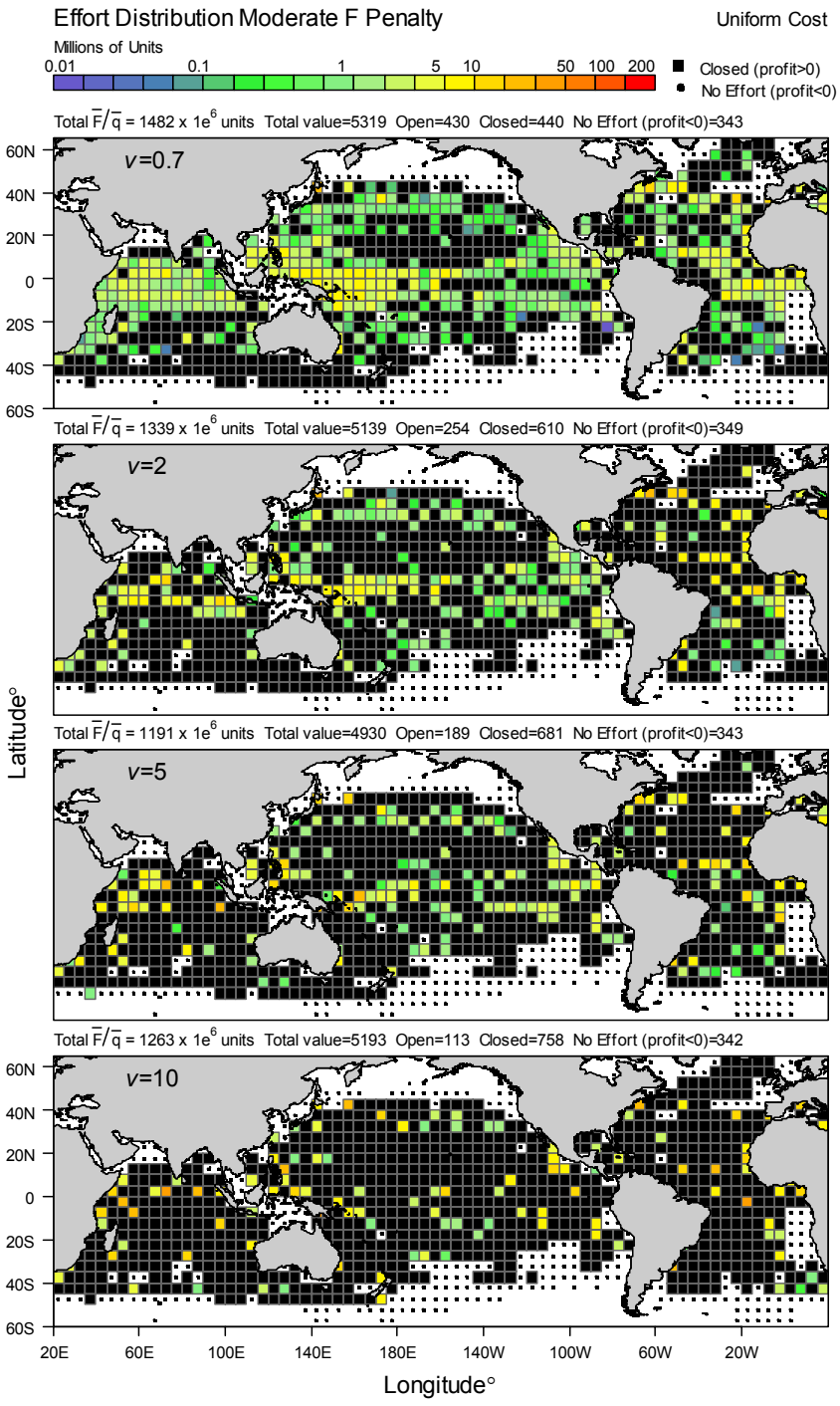

Figure 6.11 Distribution of mean relative fishing mortality for profit optimization scenarios for various initial movement rates (v) assuming area cost is uniform, total cost is 40% of total revenue and a moderate penalty is applied if stock specific target fishing mortality rates are exceeded. Black squares are closed areas and black dots are areas assumed not to attract effort, as no profit would be generated.

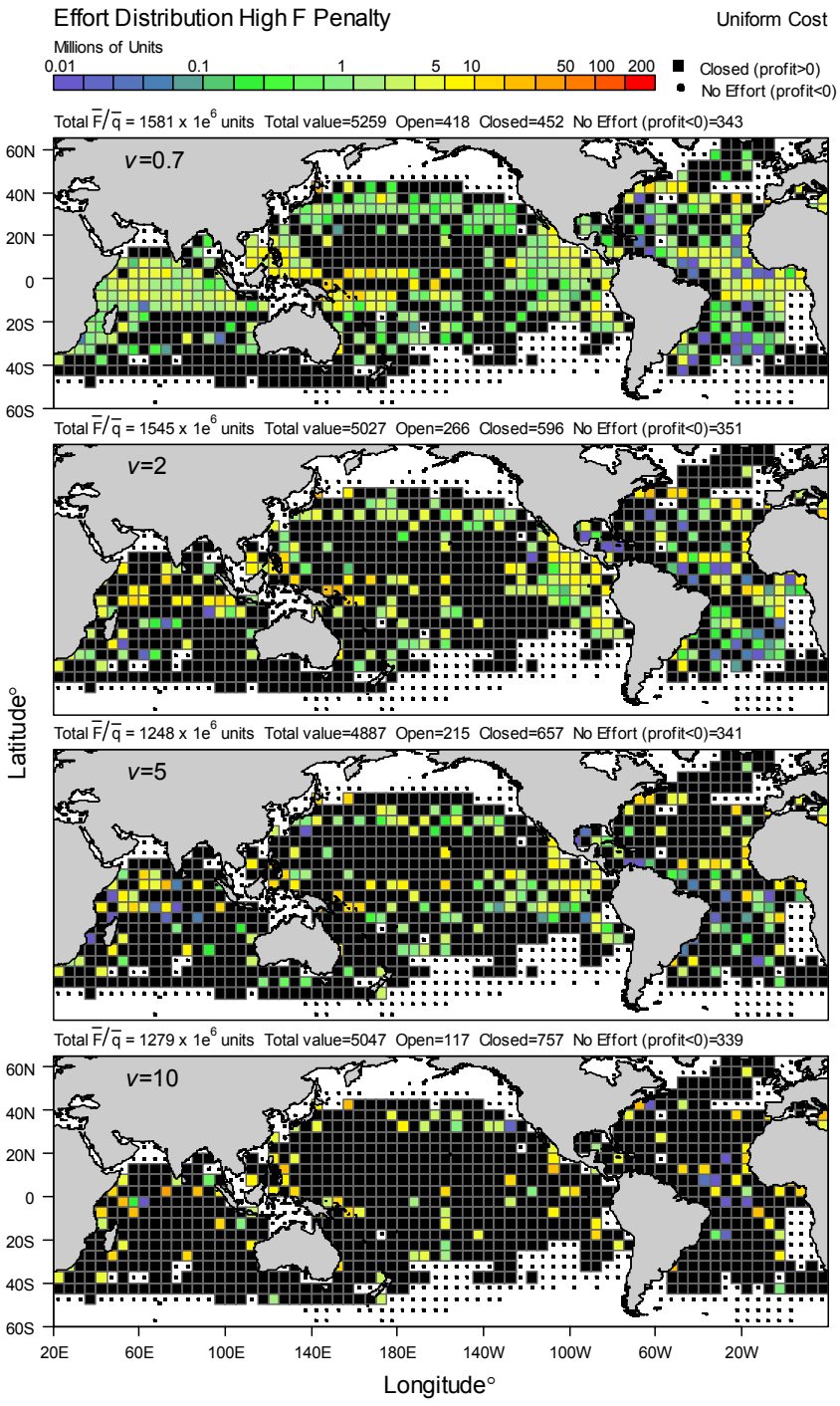

Figure 6.12 Distribution of mean relative fishing mortality for profit optimization scenarios for various initial movement rates (v) assuming area cost is uniform, total cost is 40% of total revenue and a severe penalty is applied if stock specific target fishing mortality rates are exceeded. Black squares are closed areas and black dots are areas assumed not to attract effort, as no profit would be generated.

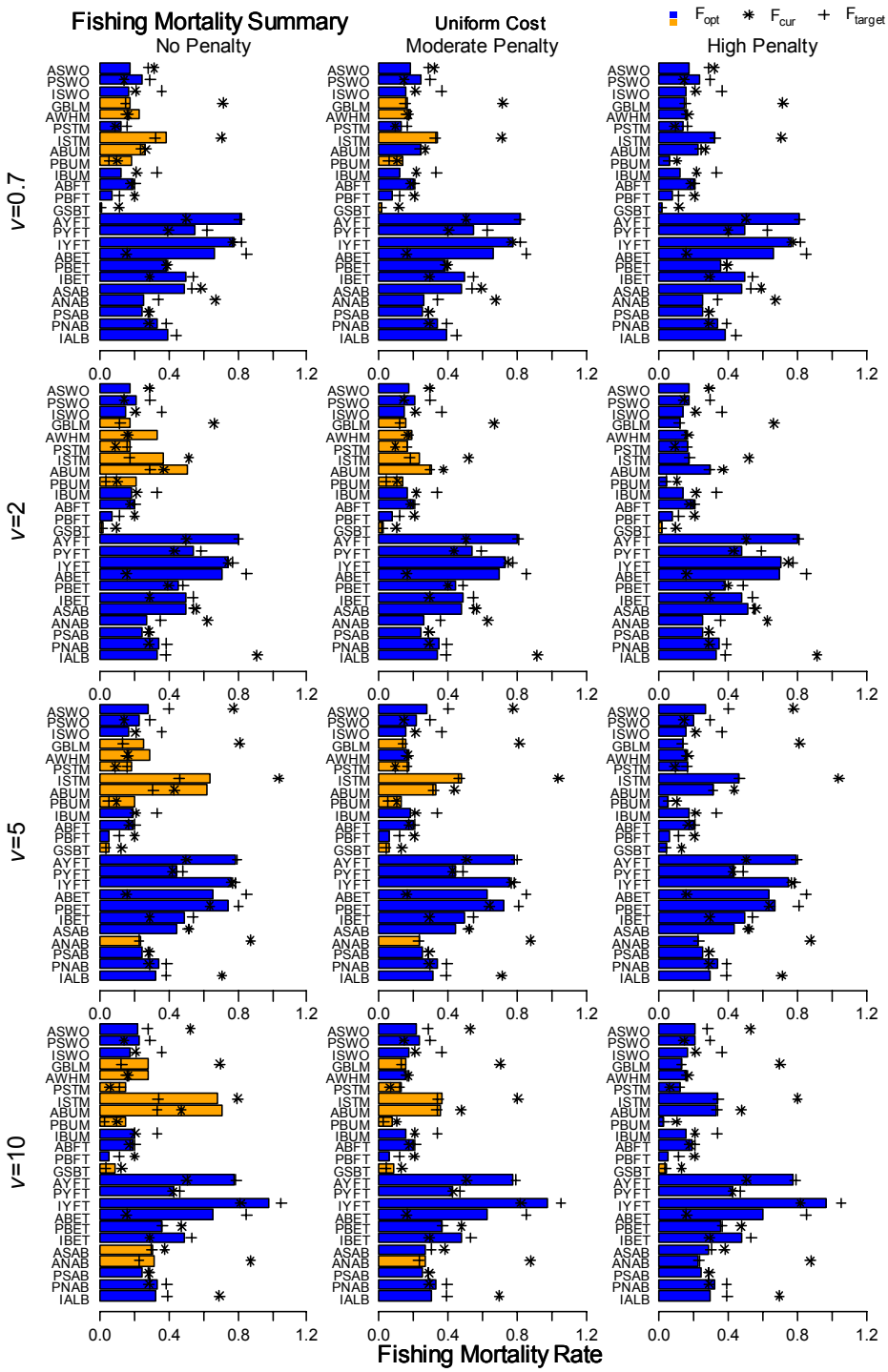

Figure 6.13 Fishing mortality summaries for each stock for profit optimization scenarios for various initial movement rates and penalties for exceeding target fishing mortalities assuming area cost is uniform, total cost is 40% of total revenue. Blue and orange are estimated fishing mortality rates. Black stars indicate current fishing mortality rates. Black crosses indicate target mortality rates. Orange bars indicate target fishing mortality is exceeded.

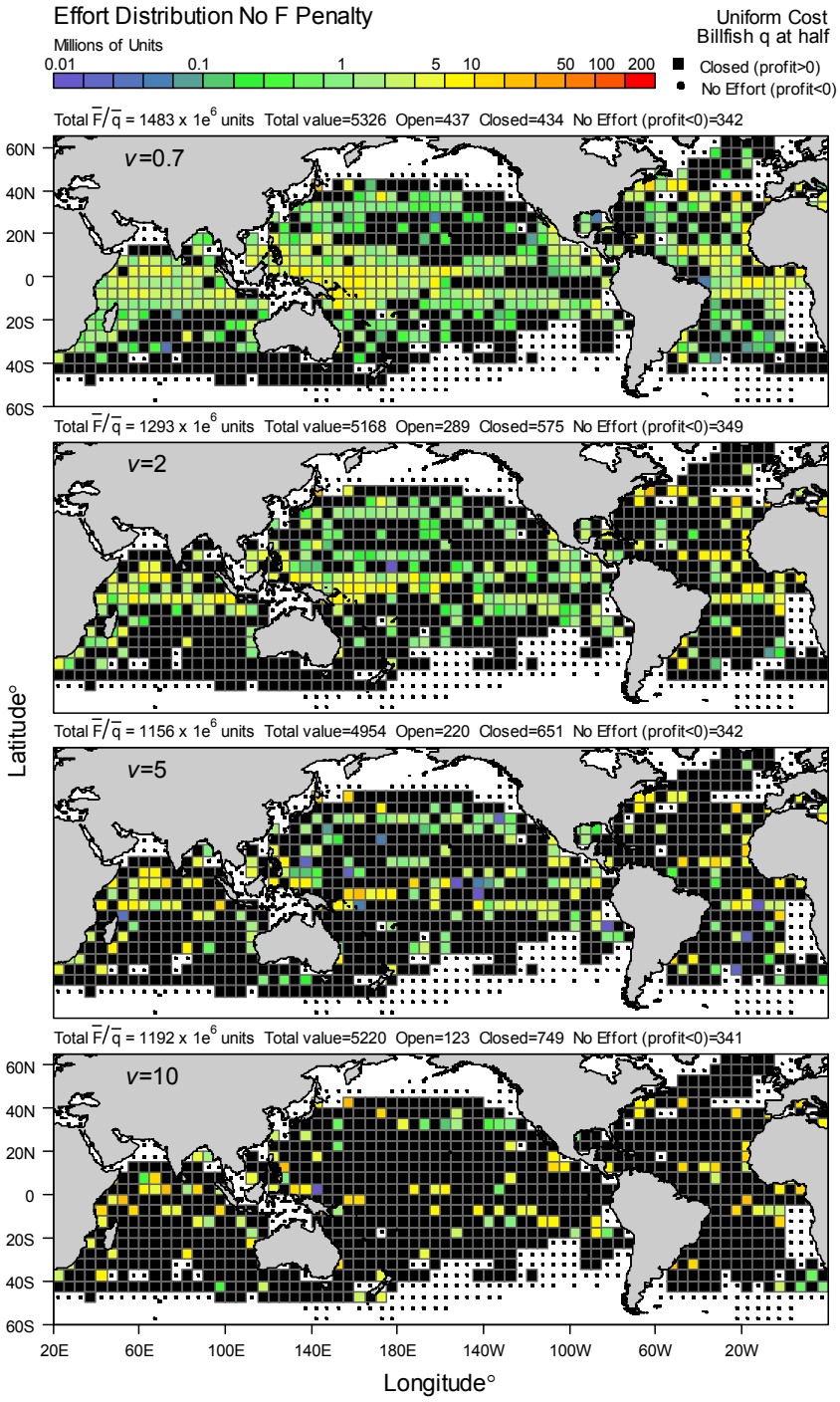

Figure 6.14 Distribution of mean relative fishing mortality for profit optimization scenarios for various initial movement rates (v) assuming area cost is uniform, total cost is 40% of total revenue, billfish q is halved and no penalty is applied if stock specific target fishing mortality rates are exceeded. Black squares are closed areas and black dots are areas assumed not to attract effort, as no profit would be generated.

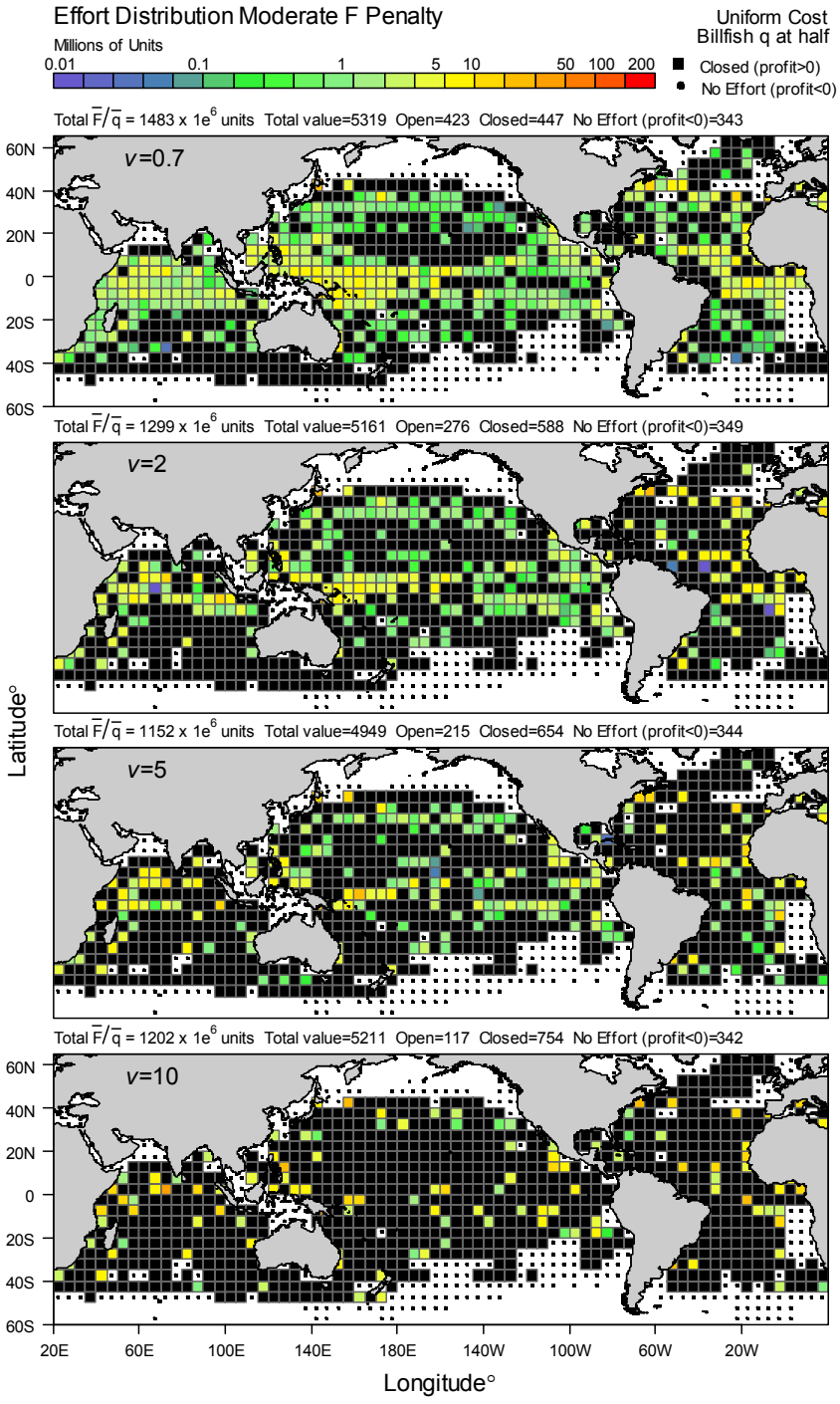

Figure 6.15 Distribution of mean relative fishing mortality for profit optimization scenarios for various initial movement rates (v) assuming area cost is uniform, total cost is 40% of total revenue, billfish q is halved and a moderate penalty is applied if stock specific target fishing mortality rates are exceeded. Black squares are closed areas and black dots are areas assumed not to attract effort, as no profit would be generated.

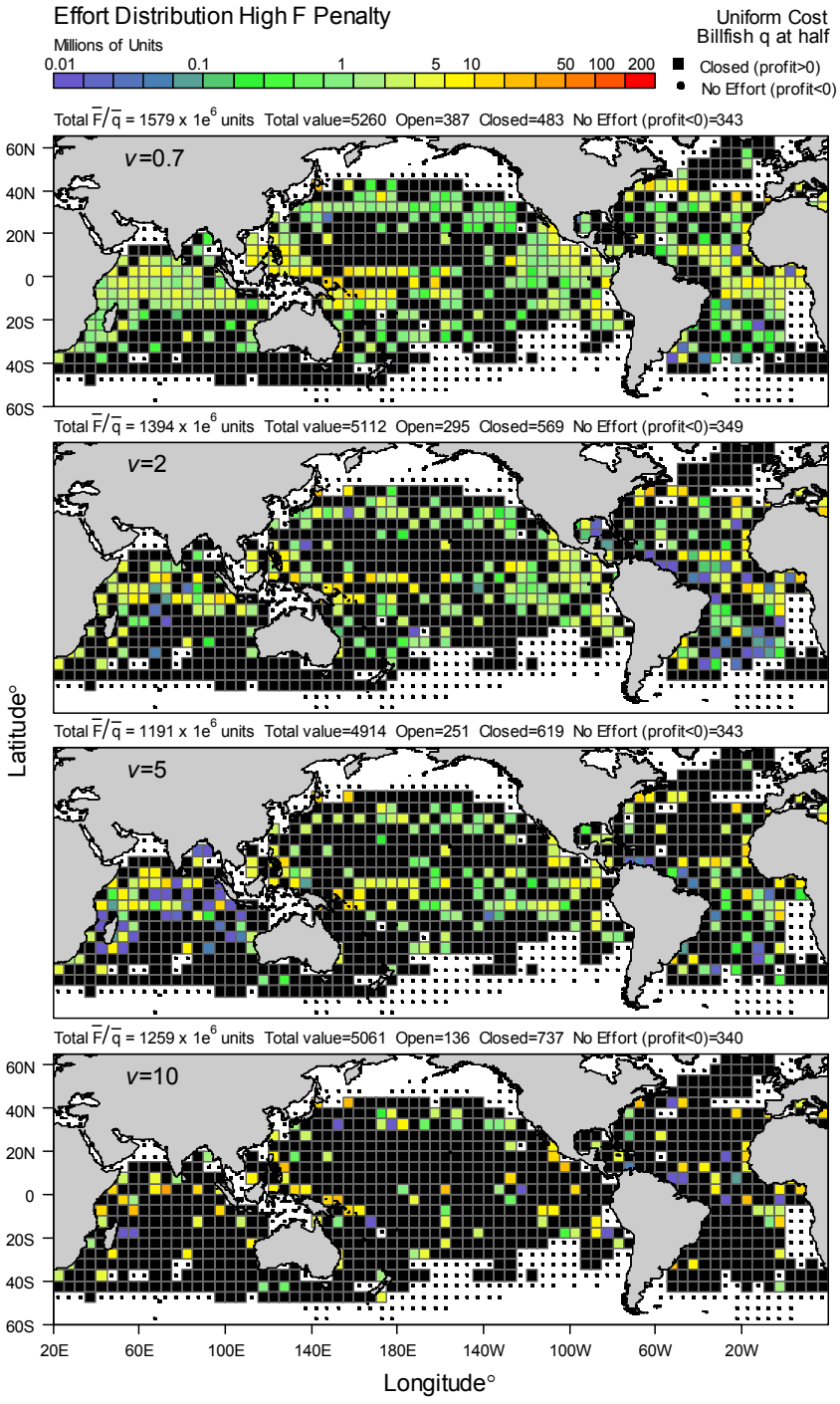

Figure 6.16 Distribution of mean relative fishing mortality for profit optimization scenarios for various initial movement rates (v) assuming area cost is uniform, total cost is 40% of total revenue, billfish q is halved and a severe penalty is applied if stock specific target fishing mortality rates are exceeded. Black squares are closed areas and black dots are areas assumed not to attract effort, as no profit would be generated.

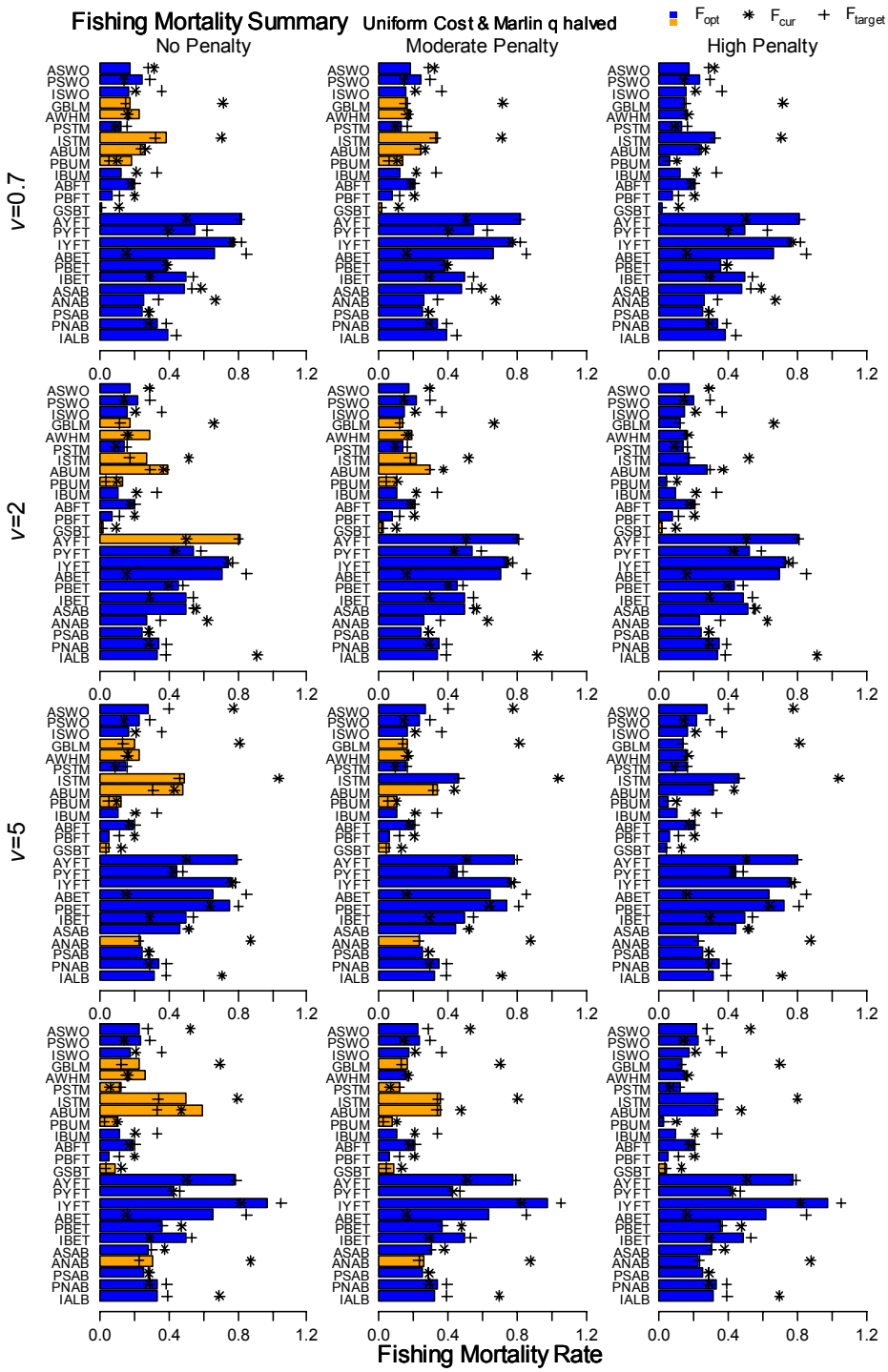

Figure 6.17 Fishing mortality summaries for each stock for profit optimization scenarios for various initial movement rates and penalties for exceeding target fishing mortalities assuming area cost is uniform, total cost is 40% of total revenue and billfish q is halved. Blue and orange bars are estimated fishing mortality rates. Black stars indicate current fishing mortality rates. Black crosses indicate target mortality rates. Orange bars indicate target fishing mortality is exceeded.

Chapter 7 Summary

William Cochran begins his text on sampling theory with a reminder, “Our knowledge, our attitudes, and our actions, are based to a very large extent on samples”. Much of the data available to fisheries scientists are the direct result of commercial fisheries, and have not been collected using unbiased sampling methods. Even basic statistics such as total catch and effort are estimated from sampling. Reliance on samples is even greater when more detailed information is desired, (e.g., aspects of catch composition or spatial location), requiring further refinements to port sampling or sampling of logbook information. Before making suppositions about the status of stocks as assessment scientists, we must be wary of the data in hand. Do available data reflect the true impact of a fishery in terms of numbers removed, effort, spatial distribution, aspects of stock composition, etc.? What is the relationship between data derived from the fishery and the state of the populations from which the catch statistics were taken?

There are a number of examples in tuna and billfish fisheries where catches have been underestimated. There is mounting evidence that illegal, unreported, and unregulated fishing (IUU) is not a trivial component of catch taken and substantial uncertainly has been introduced into assessments, (e.g., southern bluefin tuna or Atlantic bluefin tuna). Until recently, the magnitude of catches by Indonesia and the Philippines in the western-central Pacific Ocean was substantially underestimated. There is no simple solution to addressing these sampling problems. Substantial effort has gone into providing the best available data for tuna and billfish but as in Chapter 2 with the development of the global spatial database, assumptions must be made. Species descriptions that appear in Chapter 2 also rely heavily on observations made from fisheries. Spatial distributions, apparent growth pattern, seasonal movements, or vertical distributions presented are potentially biased. As a broader spectrum of sampling tools has become available, (e.g., sonar or satellite tags) our understanding of species biology is being refined and, in some cases, changing our perceived relationship between fisheries and harvested species.

Understanding the relationship between the state of a stock and observations of that state made by fisheries one of the challenges in fisheries assessments. The stock assessment literature is full

of warnings about biases introduced into assessments and potential errors in management that arise when assumed relationships between observations and state are erroneous. One of the most common biases introduced into assessments stems from assuming that changes in nominal *cpue* are proportional to changes in stock abundance. Provided fishing activity is essentially random with respect to species analyzed and no major developments occur that alter gear efficiency this assumption is likely valid. However, historical developments in the Japanese longline fishery preclude such a relationship from being true, and the distribution and nature of sampling effort relative to species distributions must be considered when inferring changes in stock levels. In Chapter 3, relative abundance trends derived using differing methods produced noticeable differences in population trends. Underlying each method was an explicit assumption about how Japanese longline fisheries sampled in space and time. Abundance trends derived using nominal *cpue*, averaging only over fished areas or assuming representative sampling of a static spatial distribution produce abundance trends that suggested greater levels of depletion or higher variability. These methods did not account for changes in the spatial and temporal distribution of Japanese fishing effort throughout the period examined and therefore do not correct for the biased sampling of all stocks. Methods that are considered more appropriate when deriving estimators from ratios involved averaging over all spatial strata. Provided fishery sampling within strata can be assumed effectively random, averaging required the imputation of values in time-areas strata not sampled.

Abundance trends derived using methods that attempted to correct for Japanese longline fishery sampling biases suggest less severe impacts of historic fishery removals on tuna and billfish stock when compared to other estimators. Species aggregated nominal *cpue* suggest tuna and billfish were depleted to <20% of 1950 levels. More appropriate estimators indicate only some stocks appear to have been reduced to levels <30% of 1950 levels (a number of marlin and bluefin stocks). Although the methods used to correct for change in gear efficiency are questionable, having only corrected for potential impact of gear depth, there is little question that accounting for changes in the spatial distribution of Japanese longline effort results in a noticeably different pattern of decline in most stocks as a result of industrialized fishing.

Although it is possible to generalize about stock status given apparent depletion levels using rules of thumb, potential reference points and status are usually determined by assessing underlying production relationships and fishery selectivity. In Chapter 4, a number of simple assessment methods were utilized to estimate underlying stock recruitment relationships and determine stock status relative to standard biological reference points. The methods presented modeled the component of stocks estimated to be vulnerable to longline gear and utilized relative abundance trends and reported catches. For a number of stocks, relative abundance trends were determined to be uninformative and informative prior distributions were assumed for current fishing mortality rates and in some instances for F_{msy}. Results from Chapter 4 were therefore conditional on assumed prior distributions for natural mortality rates, current fishing mortality rates, and F_{msy}. Recruitment reconstructions proved a valuable tool for determining when productivity estimates would not be possible. Over a range of estimates of current fishing mortality rates, resulting stock recruitment relationships for some stocks could be explained by a wide range of productivity estimates, from recruitment linearly related to stock size to apparently independent of stock size. For these stocks, even with prior information for current fishing mortality, estimation of stock productivity failed.

Stock reduction analyses and models forced with relative fishing mortality rates indicated a number of stocks were over-fished and subjected to over-fishing as of 2002. Atlantic Ocean stocks estimated to fall under this classification included northern and southern albacore tuna, yellowfin tuna, blue marlin, and white marlin. In the Indian Ocean albacore tuna, southern bluefin tuna, striped marlin, and black marlin also fell into this category with the fishing mortality ratio estimated for black marlin being the highest of all stocks. Pacific bigeye tuna, bluefin tuna, and blue marlin could also be classified in this category. Pacific Ocean yellowfin and southern albacore tuna were estimated to have been subjected to over-fishing but were not over-fished. The remaining stocks could be categorized as under exploited.

Relative abundance trends with sufficient contrast to estimate productivity parameters robustly were developed for only 7 of 24 stocks assessed. Over half of the assessments required informative priors on stock productivity. While it is common to have uninformative relative abundance trends requiring additional information to constrain assessments, the need for such

constraints raises a number of concerns. The most common data sources about fishing mortality rates are stock composition data, and mortality rates inferred from such data are sensitive to structural assumptions. Assumptions about selectivity pattern, recruitment strength, constant natural mortality, and cumulative impacts of size selective removals all strongly influence estimated fishing mortality rates; indeed, high risk of serious violations of these assumptions is one of the primary reasons composition data were not used in this study.

Unreasonable estimates of productivity were initially made for some stocks. When productivity estimates were constrained to values that were more reasonable given prior assessments of productivity, predicted abundance declines were underestimated relative to declines in relative abundance, (i.e., hyperdepletion). Although such deviations can be attributed to process or observation anomalies, the temporal pattern in the anomalies suggests some fundamental factor was missed when standardizing effort. Anomalies did not vary randomly but tended to shift from large positive values early in the history of the fishery to negative. It is likely that reduction in gear efficiency have been underestimated for some marlin, yellowfin, and albacore stocks because of changes in species targeting. In contrast, efficiency gains for bigeye tuna and bluefin have likely been underestimated. Without operational level information, it is not possible to determine what factors may have led to these biases.

The multi-species spatial model developed in Chapter 5 allowed movement and localized depletion affects to be incorporated into the assessment of stock productivity and status. This created a framework to assess the suitability of spatial imputation methods used to derive relative abundance trends. Parameter values estimated for the spatial model tended to be similar to those estimated using spatially aggregated models. No clear effect of increasing movement rates could be seen in parameter estimates. There was a tendency for current stock status to be estimated closer to optimal levels, i.e., fewer stocks experiencing over-fishing as of 2002. Southern bluefin tuna and black marlin were exceptions, with exploitation rates estimated to be much higher that those estimated in spatially aggregated models. Initial population distributions, advection-diffusion fields, and apparent recruitment distributions depended on initial movements rates. Higher initial movement rates resulted in the concentration of recruitment into fewer areas. Fishing mortality rates in the early part of the period were estimated sufficiently low that, even

with the inclusion of movement between areas, impact of local depletions were insufficient to cause population reductions in surrounding areas. This result implies that imputing catch rates in areas prior to fishing, using an average of the catch rate observed in the first few years of fishing is unlikely to distort relative abundance trends. However, fishing mortality rate increases over the period examined were estimated to be sufficiently high to cause reductions in surrounding areas later. Imputing catch rates over long periods later in the time series was likely problematic because as local depletion effect due to harvesting activities in surrounding areas were likely underestimated. Bluefin tuna abundance indices were affected the most by this effect, because imputation over long periods within high abundance areas was necessary.

In Chapter 6, the spatial model was used to explore a number of scenarios for spatial redistribution of fishing effort. This analysis sought the equilibrium effort distribution that would optimize total global profit from fisheries catching tuna and billfish under various assumed spatial costs, movement rates, and penalties for exceeding species-specific target exploitation rates. Assuming stock status had been estimated accurately, optimization in the absence of fishing mortality constraints indicates profit would be increased with a large reduction (>60%) in fishing effort. Furthermore, effort should be shifted into those areas determined to produce the highest value, with optimum fishing effort equaling 0 (closure) for a large proportion of areas (>60%). Closed areas tended to form a complex mosaic. For a number of areas, effort was excluded because they were determined to be unprofitable. The net result of the optimized effort reduction and redistribution was to reduce fishing mortality rates on the most valuable stock to levels below F_{msy}. The severity of effort reductions depended on the assumed costs and movement rates. The number of closed areas increased with movement rate. When movement rates were assumed low, increasing the penalty for exceeding target exploitation rates resulted in a greater portion of areas being closed and effort being shifted out of areas where valuable and vulnerable species overlapped. At the highest movement rates, severe fishing mortality penalties resulted in a higher portion of areas being opened relative to no penalty simulations, with effort increasing slightly and diffusing into areas of reduced species overlap but lower profitability. Reducing billfish catchability produced a noticeable reduction in the number of areas closed. If profit optimization is a management goal of RFMOs, gaming scenarios indicate that some

efficiency could be gained by closing large areas, provided overall effort is reduced and shifted into high value areas.

In his book "Wonderful life", Stephen J. Gould (1989) poses the question, "How should scientists operate when they must try to explain the results of history, those inordinately complex events that can occur but once in detailed glory?" Gould suggests the complexity of historic events precludes the use of experimental methods to determine causation, and that scientists must focus on developing a narrative. Stock assessment models are narratives aimed at describing historical information in order to provide a framework to evaluate status and explore future possibilities. The set of viable hypotheses is narrowed by matching model predictions against a variety of observations. The resulting credible range of narratives depends a great deal on our ability to understand how the details of history have influenced available observations. Catch and effort data of the Japanese longline fleet span the history of industrialized exploitation of tuna and billfish stocks, and provide a tantalizing data set from which to assess the impacts of fishing. However, even when reasonable and hopefully appropriate methods are used to account for changes in the fleet over time, it is questionable if sufficient detail is available to correct for all the changes that occurred over the period. Some of the assessment results presented in this thesis suggest critical historic details have not been accounted for, such that abundance trends derived from Japanese longline catch and effort still paint a biased picture of how some stocks responded to the impacts of industrialized fishing. If information on such critical details is unavailable, we can choose to ignore such periods at the expense of losing contrast and restrict the use of relative abundance time series to periods for which effort standardization is possible. For many tuna and billfish assessments, relative abundance trends are estimated from Japanese longline catch and effort data only for years after the period of rapid expansion, and this forces the assessments to rely heavily on composition information. Assumption about the mechanisms that gave rise to patterns in the available composition information can alter the assessment of stock productivity and it is prudent to question if such mechanisms are well understood. There is a possibility of establishing research programs that would aid in standardizing effort such as paired comparisons of different gear/technology configurations. For example, in Chapter 3 standardization of effort for changes in gear depth for each species was based on observations from a restricted area. Confidence in this component of effort standardization would be improved significantly if

observations were available from a broader suite of areas. Ultimately, our ability to reduce structural and numerical uncertainty may be limited when only fisheries dependent data are available. If the international community that utilizes tuna and billfish resources is motivated to improve assessments, there is the potential to develop innovative research programs such as the expansion of tagging programs to a larger scale to reduce the reliance of assessment on historical trend and composition data.

References

Allen, R., and Punsly, R. 1984. Catch rates as indices of abundance in yellowfin tuna, *Thunnus albacares*, in the eastern Pacific ocean. Bull. IATTC **18**(4).

Allison, G.W., Lubchenco, J., and Carr, M.H. 1998. Marine reserves are necessary but not sufficient for marine conservation. Ecol. Appl. **8**(1): S79-S92.

Alvarado Bremer, J.R., Mejuto, J., Gomez-Marquez, J., Boan, F., Carpintero, P., Rodriguez, J.M., Creig, T.W., and Ely, B. 1999. Hierarchical analysis of swordfish mitochondrial DNA substructure within the Atlantic Ocean. Collective Volume of Scientific Papers ICCAT **49**(1): 457-466.

Alves, A., de Barros, P., and Pinho, M.R. 2002. Age and growth studies of bigeye tuna *Thunnus obesus* from Madeira using vertebrae. Fisheries Research **54**(3): 389-393.

Amorim, A.F., Arfelli, C.A., Antero-Silva, J.N., Fagundes, L., Costa, F.E.S., and Assumpçao, R. 1998. Blue marlin (*Makaira nigricans*) and white marlin (*Tetrapturus albidus*) caught off Brazilian coast. Collective Volume of Scientific Papers ICCAT **47**: 163-184.

Arena, P., Potosci, A., and Cefali, A. 1980. Risultati preliminari di studi sull'etá, l'accrescimento a la prima maturitá sessuale dell' alalunga *Thunnus alalunga* (Bonn. 1788) del Tirreno. Mem. Biol. Mar. Oceanogr. **10**(3): 71-81.

Armas, R.G., Sosa-Nishizaki, O., Rodriguez, R.F., and Perez, V.A.L. 1999. Confirmation of the spawning area of the striped marlin, *Tetrapturus audax*, in the so-called core area of the eastern tropical Pacific off Mexico. Fish. Oceanogr. **8**(3): 238-242.

Arocha, F. 1997. The reproductive dynamics of swordfish *Xiphias gladius L.* and management implications in the northwestern Atlantic, Univ. Miami, Miami, FL.

Arocha, F., and Lee, D.W. 1995. The spawning of swordfish from the Northwest Atlantic. Collective Volume of Scientific Papers ICCAT **44**(3): 179-186.

Arocha, F., Lee, D.W., Marcano, L.A., and Marcano, J.S. 2001. Update information on the spawning of yellowfin tuna, *Thunnus albacares*, in the western central Atlantic. Collective Volume of Scientific Papers ICCAT **52**(1): 167-176.

Arocha, F., and Marcano, L. 2006. Life history characteristics of *Makaira nigricans*, *Tetrapturus albidus*, and *Istiophorus albicans* from the eastern Caribbean Sea and adjacent waters. In J. Nielsen, J. Dodson, K. Friedland, T. Hamon, N. Hughes, J. Musick and E. Verspoor, Eds. Proceedings of the Fourth World Fisheries Congress: Reconciling Fisheries with Conservation. Amer. Fish. Soc. Symp. 49, Bethesda, Maryland.: 587-597.

Arocha, F., Moreno, C., Beerkircher, L., Lee, D.W., and Marcano, L. 2003. Update on growth estimates for swordfish, *Xiphias gladius*, in the northwestern Atlantic. Collective Volume of Scientific Papers ICCAT **55**(4): 1416-1429.

Arrizabalaga, H., and Pereira, J.G. 2005. Bigeye pop-up tagging results in Azorian waters. Collective Volume of Scientific Papers ICCAT **57**(2): 137-150.

Arrizabalaga, H., Rodas, V., Ortiz de Zárate, V., Costas, E., and González-Garcés, A. 2002. Study on the migrations and stock structure of albacore (*Thunnua alalunga*) from the Atlantic Ocean and the Mediterranean Sea based on conventional tag release-recapture experiences. Collective Volume of Scientific Papers ICCAT **54**(2): 1479-1494.

Baglin, R.E. 1979. Sex composition, length-weight relationship, and reproduction of the white marlin, *Tetrapturus albidus*, in the western North-Atlantic Ocean. Fish. Bull. **76**(4): 919-926.

Baglin, R.E. 1982. Reproductive Biology of Western Atlantic Bluefin Tuna. Fish. Bull. **80**(1): 121-134.

Barbieri, M.A., Canales, C., Correa, V., Donoso, M., Casanga, A.G., Leiva, B., Montiel, A., and Yáñez, E. 1998. Development and present state of the swordfish, *Xiphias gladius*, fishery in Chile. U.S. Nat. Mar. Fish. Serv., NOAA Tech. Rep. NMFS **142**: 77-88.

Bard, F.X. 1981. Le thon germon (*Thunnus alalunga*) de l'Océan Atlantique, University of Paris.

Bard, F.X. 1983. Croissance de l'albacore (*Thunnus albacares*) Atlantique, d'apres les donnes des marquages. Collective Volume of Scientific Papers ICCAT **20**(1): 104-116.

Bard, F.X. 2001. Extensions of geographical and vertical habitat of albacore (*Thunnus alalunga*) in the North Atlantic. Possible consequences on the true rate of exploitation of this stock. Collective Volume of Scientific Papers ICCAT **52**(4): 1477-1456.

Bayliff, W.H. 1979. Migrations of yellowfin tuna in the eastern Pacific Ocean as determined from tagging experiments initiated during 1968–1974. Bull. IATTC **17**: 447-506.

Bayliff, W.H. 1994. A review of the biology and fisheries for northern bluefin tuna, *Thunnus thynnus* in the Pacific Ocean. In: Shomura RS, Majkowski J, Langi S, editors. Interactions of Pacific tuna fisheries. Proceedings of the First FAO Expert Consultation on Interactions of Pacific Tuna Fisheries; 1991 Dec 3-11; Noumea, New Caledonia **Volume 2**: 244-295.

Bayliff, W.H. 2000. Status of bluefin tuna in the Pacific Ocean. Stock Assessment Report IATTC: 211-254.

Bayliff, W.H., Ishizuka, Y., and Deriso, R. 1991. Growth, movements, and mortality of northern bluefin, *Thunnus thynnus*, in the Pacific Ocean, as determined from tagging experiments. Bull. IATTC **20**(1): 1-94.

Beacham, T.D., Brattey, J., Miller, K.M., Le, K.D., and Withler, R.E. 2002. Multiple stock structure of Atlantic cod (*Gadus morhua*) off Newfoundland and Labrador determined from genetic variation. ICES J. Mar. Sci. **59**(4): 650-665.

Bell, R.R. 1963. Synopsis of biological data on California bluefin tuna *Thunnus saliens* Jordan and Evermann 1926. FAO Fish. Rep. **6**(2): 380-421.

Benyon, P.R. 1968. A review of numerical methods for digital simulation. Simulation **11**: 219-238.

Bertignac, M., Lehodey, P., and Hampton, J. 1998. A spatial population dynamics simulation model of tropical tunas using a habitat index based on environmental parameters. Fish. Oceanogr. **7**(3-4): 326-334.

Beverly, S., Chapman, L., and Sokimi, W. 2003. Horizontal longline fishing-methods and techniques: a manual for fishermen. Secretariat of the Pacific Community. Noumea, New Caledonia

Beverly, S., Curran, D., Musyl, M., and Molony, B. 2009. Effects of eliminating shallow hooks from tuna longline sets on target and non-target species in the Hawaii-based pelagic tuna fishery. Fisheries Research **96**(2-3): 281-288.

Beverton, R.J.H., and Holt, S.J. 1957. On the Dynamics of Exploited Fish Populations. U.K. Ministry of Agrigulture, Fisheries and Food, Fisheries Investigations Series 2 **19**: 533.

Bigelow, K., Musyl, M.K., Poisson, F., and Kleiber, P. 2006. Pelagic longline gear depth and shoaling. Fisheries Research **77**(2): 173-183.

Bigelow, K.A., Hampton, J., and Miyabe, N. 2002. Application of a habitat-based model to estimate effective longline fishing effort and relative abundance of Pacific bigeye tuna (Thunnus obesus). Fish. Oceanogr. **11**(3): 143-155.

Bigelow, K.A., and Maunder, M.N. 2007. Does habitat or depth influence catch rates of pelagic species? Can. J. Fish. Aquat. Sci. **64**(11): 1581-1594.

Biro, P.A., and Post, J.R. 2008. Rapid depletion of genotypes with fast growth and bold personality traits from harvested fish populations. Proceedings of the National Academy of Sciences of the United States of America **105**(8): 2919-2922.

Blank, J.M., Morrissette, J.M., Landeira-Fernandez, A.M., Blackwell, S.B., Williams, T.D., and Block, B.A. 2004. In situ cardiac performance of Pacific bluefin tuna hearts in response to acute temperature change. J. Exp. Biol. **207**(5): 881-890.

Block, B.A. 1986. Structure of the brain and eye heater tissue in marlins, sailfish, spearfish. J. Morphol. **190**: 169-189.

Block, B.A., Booth, D.T., and Carey, F.G. 1992. Depth and Temperature of the Blue Marlin, Makaira-Nigricans, Observed by Acoustic Telemetry. Mar. Biol. **114**(2): 175-183.

Block, B.A., Dewar, H., Blackwell, S.B., Williams, T.D., Prince, E.D., Farwell, C.J., Boustany, A., Teo, S.L.H., Seitz, A., Walli, A., and Fudge, D. 2001. Migratory movements, depth preferences, and thermal biology of Atlantic bluefin tuna. Science **293**(5533): 1310-1314.

Block, B.A., Keen, J.E., Castillo, B., Dewar, H., Freund, E.V., Marcinek, D.J., Brill, R.W., and Farwell, C. 1997. Environmental preferences of yellowfin tuna (*Thunnus albacares*) at the northern extent of its range. Mar. Biol. **130**(1): 119-132.

Block, B.A., Teo, S.L.H., Walli, A., Boustany, A., Stokesbury, M.J.W., Farwell, C.J., Weng, K.C., Dewar, H., and Williams, T.D. 2005. Electronic tagging and population structure of Atlantic bluefin tuna. Nature **434**(7037): 1121-1127.

Boggs, C.H. 1989. Vital rate statistics for billfish stock assessment. *In* Planning the Future of Billfishes: Research and Management in the 90s and Beyond. Proceedings of the Second International Billfish Symposium, Kailua-Kona, Hawaii, August 1-5, 1988, Part 1: Fishery and Stock Synopses, Data Needs and Management. *Edited by* R.H. Stroud. National Coalition for Marine Conservation, Inc. pp. 225-233.

Bremer, J.R.A., Mejuto, J., Gomez-Marquez, J., Boan, F., Carpintero, P., Rodriguez, J.M., Vinas, J., Greig, T.W., and Ely, B. 2005. Hierarchical analyses of genetic variation of samples from breeding and feeding grounds confirm the genetic partitioning of northwest Atlantic and South Atlantic populations of swordfish (Xiphias gladius L.). J. Exp. Mar. Biol. Ecol. **327**(2): 167-182.

Brill, R., Bigelow, K., Musyl, M.K., Fritsches, K.A., and Warrant, E.J. 2005. Bigeye tuna (*Thunnus obesus*) behaviour and physiology and their relevance to stock assessments and fishery biology. Collective Volume of Scientific Papers ICCAT **57**(2): 142-161.

Brill, R., Lutcavage, M., Metzger, G., Bushnell, P., Arendt, M., Lucy, J., Watson, C., and Foley, D. 2002. Horizontal and vertical movements of juvenile bluefin tuna (*Thunnus thynnus*), in relation to oceanographic conditions of the western North Atlantic, determined with ultrasonic telemetry. Fish. Bull. **100**(2): 155-167.

Brill, R.W. 1994. A review of temperature and oxygen tolerance studies of tunas pertinent to fisheries oceanography, movement models and stock assessments. Fish. Oceanogr. **3**(3): 204-216.

Brill, R.W., Block, B.A., Boggs, C.H., Bigelow, K.A., Freund, E.V., and Marcinek, D.J. 1999. Horizontal movements and depth distribution of large adult yellowfin tuna (*Thunnus albacares*) near the Hawaiian Islands, recorded using ultrasonic telemetry: implications for the physiological ecology of pelagic fishes. Mar. Biol. **133**(3): 395-408.

Brill, R.W., Holts, D.B., Chang, R.K.C., Sullivan, S., Dewar, H., and Carey, F.G. 1993. Vertical and Horizontal Movements of Striped Marlin (*Tetrapturus audax*) near the Hawaiian-Islands, Determined by Ultrasonic Telemetry, with Simultaneous Measurement of Oceanic Currents. Mar. Biol. **117**(4): 567-574.

Brill, R.W., Lowe, T.E., and Cousins, K.L. 1998. How water temperature really limits the vertical movements of tunas and billfishes - It's the heart stupid. Abstract from the American Fisheries Society, International Congress on Biology of Fish, July 26-20, 1998, Towson University, Baltimore, MD.

Bromhead, D., Pepperell, J.G., Wise, B., and Findlay, J. 2004. Striped marlin: biology and fisheries. Bureau of Rural Sciences. Canberra.

Bromley, D.W. 2009. Abdicating responsibility: the deceits of fisheries policy. . Fisheries **34**(6): 280-290.

Bushnell, P.G., and Brill, R.W. 1992. Oxygen-Transport and Cardiovascular-Responses in Skipjack Tuna (*Katsuwonus pelamis*) and Yellowfin Tuna (*Thunnus albacares*) Exposed to Acute-Hypoxia. Journal of Comparative Physiology B-Biochemical Systemic and Environmental Physiology **162**(2): 131-143.

Caddy, J.F., Dickson, C.A., and Butler, M.J.A. 1976. Age and growth of giant bluefin tuna (*Thunnus thynnus thynnus*) in Canadian waters in 1975. Fisheries Research Board of Canada, Ottawa, Manuscript Report Series **1395**: 1-16.

Calkins, T.P. 1980. Synopsis of biological data on the bigeye tuna (*Thunnus obesus*) (Lowe 1839), in the Pacific ocean. Spec. Rep. IATTC **2**: 213-260.

Campbell, R.A. 2004. CPUE standardisation and the construction of indices of stock abundance in a spatially varying fishery using general linear models. Fisheries Research **70**(2-3): 209-227.

Campbell, R.A., and Tuck, G.N. 1998. Preliminary analysis of billfish catch rates in the Indian Ocean. In 7th expert consultation on Indian Ocean tunas. Victoria, Seychelles, 9-14 November, 1998. IOTC proceedings no. 1: 192-210.

Carey, F.G. 1982. A brain heater in the swordfish. Science **216**: 1327-1328.

Carey, F.G., and Robison, B.H. 1981. Daily Patterns in the Activities of Swordfish, Xiphias-Gladius, Observed by Acoustic Telemetry. Fish. Bull. **79**(2): 277-292.

Caton, A.E. 1994. Review of aspects of southern blufin tuna biology, population and fisheries. In: Shomura RS, Majkowski J, Langi S, editors. Interactions of Pacific tuna fisheries. Proceedings of the First FAO Expert Consultation on Interactions of Pacific Tuna Fisheries; 1991 Dec 3-11; Noumea, New Caledonia **Volume 2**: 296-343.

Caveriviere. 1975. Longeur predorsale, longeur a la fourche et poids des albacores (*Thunnus albacares*) de lÁtlantique. Document SCRS/75/73, unpublished.

CCSBT. 2005. Report of the Tenth Meeting of the Scientific Committee, 9 September 2004, Narita,Japan. CCSBT Sci. Com. Rep.

CCSBT. 2006a. Commission for the Conservation of Southern Bluefin Tuna Report of the Eleventh Meeting of the Scientific Committee 12-15 September 2006 Tokyo, Japan. Report CCSBT: 73.

CCSBT. 2006b. Report of the seventh meeting of the stock assessment group. CCSBT Stock. Assess. Rep. **CCSBTSAG7**: 93.

CCSBT Database. 2004. Commision for the Conservation of Souther Bluefin Tuna public domain database. Task II Catch, Effort, and Size. **updated June 2004**(accessed January 2005): http://www.ccsbt.org.

Chen, I.C., Lee, P.F., and Tzeng, W.N. 2005. Distribution of albacore (*Thunnus alalunga*) in the Indian Ocean and its relation to environmental factors. Fish. Oceanogr. **14**(1): 71-80.

Chen, S., and Watanabe, S. 1988. Age dependence of natural mortality coefficient in fish population dynamics. Nippon Suisan Gakkaishi **55**(2): 205-208.

Christensen, V. *In press*. MEY=MSY. Fish and Fisheries.

Christensen, V., and Walters, C.J. 2004. Trade-offs in ecosystem-scale optimization of fisheries management policies. Bull. Mar. Sci. **74**(3): 549-562.

Clark, C. 1976. Mathematical Bioeconomics: the optimal management of renewable resources. Wiley, New York.

Clark, C.W., and Mangel, M. 1979. Aggregation and Fishery Dynamics - Theoretical-Study of Schooling and the Purse Seine Tuna Fisheries. Fish. Bull. **77**(2): 317-337.

Clark, I. 1979. Practical geostatistics. Elsevier, London.

Coimbra, M.R.M. 1995. Proposed movements of the albacore tuna, *Thunnus alalunga*, in the South Atlantic Ocean, Tokyo University of Fisheries, Tokyo, Japan.

Cole, J.S. 1980. Synopsis of biological data on yellowfin tunas, *Thunnus albacares* (Bonnaterre, 1788), in the Pacific Ocean. Spec. Rep. IATTC **2**: 75-150.

Collette, B.B., and Nauen, C.E. 1983. FAO species 1983, catalogue. Vol. 2. Scombrids of the world. An annotated and illustrated catalogue of tunas, mackerels, bonitos and related species known to date. FAO Fish. Synop. **125**(2): 137.

Conand, F., and Richards, W.J. 1982. Distribution of tuna larvae between Madagascar and the equator, Indian Ocean. Biological Oceanography **1**(4): 321-336.

Corriero, A., Desantis, S., Deflorio, M., Acone, F., Bridges, C.R., De Serna, J.M., Megalofonou, P., and De Metrio, G. 2003. Histological investigation on the ovarian cycle of the bluefin tuna in the western and central Mediterranean. J. Fish Biol. **63**(1): 108-119.

Corriero, A., Karakulak, S., Santamaria, N., Deflorio, M., Spedicato, D., Addis, P., Desantis, S., Cirillo, F., Fenech-Farrugia, A., Vassallo-Agius, R., de la Serna, J.M., Oray, Y., Cau, A., Megalofonou, P., and De Metrio, G. 2005. Size and age at sexual maturity of female bluefin tuna (Thunnus thynnus L. 1758) from the Mediterranean Sea. J. Appl. Ichthyol. **21**(6): 483-486.

Cort, J.L. 1991. Age and growth of the bluefin tuna (*Thunnus thynnus*) in the Northeast Atlantic. Collective Volume of Scientific Papers ICCAT **35**(2): 213-230.

Costello, C., and Polasky, S. 2008. Optimal harvesting of stochastic spatial resources. J. Environ. Econ. Manage. **56**(1): 1-18.

Dagorn, L., Holland, K.N., Hallier, J.P., Taquet, M., Moreno, G., Sancho, G., Itano, D.G., Aumeeruddy, R., Girard, C., Million, J., and Fonteneau, A. 2006. Deep diving behavior observed in yellowfin tuna (Thunnus albacares). Aquat. Living Resour. **19**(1): 85-88.

Dagorn, L., Menczer, F., Bach, P., and Olson, R.J. 2000. Co-evolution of movement behaviours by tropical pelagic predatory fishes in response to prey environment: a simulation model. Ecol. Model. **134**(2-3): 325-341.

Davis, T.L.O., Farley, J.H., and Gunn, J.S. 2001. Size and age at 50% maturity in SBT. An integrated view from published information and new data from the spawning ground. CCSBT Sci. Com. Rep. **01/16**.

Davis, T.L.O., and Stanley, C.A. 2002. Vertical and horizontal movements of southern bluefin tuna (*Thunnus maccoyii*) in the Great Australian Bight observed with ultrasonic telemetry. Fish. Bull. **100**(3): 448-465.

DeMartini, E.E., Uchiyama, J.H., and Williams, H.A. 2000. Sexual maturity, sex ratio, and size composition of swordfish, *Xiphias gladius*, caught by the Hawaii-based pelagic longline fishery. Fish. Bull. **98**(3): 489-506.

Deriso, R., and Parma, A. 1987. On the odds of catching fish with angling gear. Trans. Am. Fish. Soc. **116**: 224-256.

Deriso, R.B., Punsly, R.G., and Bayliff, W.H. 1991. A Markov Movement Model of Yellowfin Tuna in the Eastern-Pacific-Ocean and Some Analyses for International Management. Fisheries Research **11**(3-4): 375-395.

Diaz-Jaimes, P., and Uribe-Alcocer, M. 2006. Spatial differentiation in the eastern Pacific yellowfin tuna revealed by microsatellite variation. Fish. Sci. **72**(3): 590-596.

Dizon, A.E. 1977. Effect of Dissolved-Oxygen Concentration and Salinity on Swimming Speed of 2 Species of Tunas. Fish. Bull. **75**(3): 649-653.

Domeier, M.L. 2006. An analysis of pacific striped marlin (*Tetrapturus audax*) horizontal movement patterns using pop-up satellite archival tags. Bull. Mar. Sci. **79**(3): 811-825.

Domeier, M.L., Dewar, H., and Nasby-Lucas, N. 2003. Mortality rate of striped marlin (*Tetrapturus audax*) caught with recreational tackle. Marine and Freshwater Research **54**(4): 435-445.

Dowling, N., and Campbell, R.A. 2002. Exploratory analyses of Japanese longline catch and effort data and calculation of annual abundance indices within the eastern Indian Ocean. Working Paper for TAC Setting Workshop for the SWT&BF - June 2002: 57.

Draganik, B., and Pelczarski, W. 1984. Growth and age of bigeye and yellowfin tuna in the central Atlantic as per data gathered by R/V "Wieczno". Collective Volume of Scientific Papers ICCAT **20**: 96-103.

Ehrhardt, N.M. 1992. Age and growth of swordfish, *Xiphias gladius*, in the northwestern Atlantic. Bull. Mar. Sci. **50**(2): 292-301.

Ehrhardt, N.M., Robbins, R.J., and Arocha, F. 1996. Age validation and growth of swordfish, *Xiphias gladius*, in the northwest Atlantic. Collective Volume of Scientific Papers ICCAT **45**(2): 358-367.

Eldridge, M.B., and Wares, P.G. 1974. Some biological observations of billfishes taken in the Eastern Pacific Ocean, 1967-1970. In: Shomura, R.S. and Williams, F., (Eds.) Proceedings of the International Billfish Symposium, Kailua-Kona, Hawaii, 9-12 August 1972. Part 2. Review and Contributed Papers. 89-101.

Farley, J.H., Clear, N.P., Leroy, B., Davis, T.L.O., and McPherson, G. 2006. Age, growth and preliminary estimates of maturity of bigeye tuna, Thunnus obesus, in the Australian region. Marine and Freshwater Research **57**(7): 713-724.

Farley, J.H., and Davis, T.L.O. 1998. Reproductive dynamics of southern bluefin tuna, Thunnus maccoyii. Fish. Bull. **96**(2): 223-236.

Farley, J.H., Davis, T.L.O., Gunn, J.S., Clear, N.P., and Preece, A.L. 2007. Demographic patterns of southern bluefin tuna, *Thunnus maccoyii*, as inferred from direct age data. Fisheries Research **83**(2-3): 151-161.

Fink, B.D., and Bayliff, W.H. 1970. Migrations of yellowfin and skipjack tuna in the eastern Pacific Ocean as determined by tagging experiments, 1952–1964. Bull. IATTC **15**: 1-227.

Fonteneau, A. 2005. An overview of yellowfin (*Thunnus albacares*) tuna stocks, fisheries and stock status worldwide. IOTC Working Paper **IOTC-2005-WPTT-21**: 1-38.

Fonteneau, A., Ariz, J., Delgado de Molina, A., and Pianet, R. 2005. A comparison of bigeye (*Thunnus obesus*) stocks and fisheries in the Atlantic, Indian and Pacific oceans. Collective Volume of Scientific Papers ICCAT **57**(2): 41-66.

Forrest, R.E., Martell, S.J.D., Melnychuk, M.C., and Walters, C.J. 2008. An age-structured model with leading management parameters, incorporating age-specific selectivity and maturity. Can. J. Fish. Aquat. Sci. **65**(2): 286-296.

Fournier, D.A. 2001. An introduction to AD model builder version 6.0.2. Otter Research. Sidney, British Columbia.

Fournier, D.A., Hampton, J., and Sibert, J.R. 1998. MULTIFAN-CL: a length-based, age-structured model for fisheries stock assessment, with application to South Pacific albacore, *Thunnus alalunga*. Can. J. Fish. Aquat. Sci. **55**(9): 2105-2116.

Francis, R.C. 1977. TUNPOP: a simulation of the dynamics and structure of the yellowfin tuna stock and surface fishery of the eastern Pacific Ocean. Bull. IATTC **17**(4): 233-279.

Fromentin, J.M., and Powers, J.E. 2005. Atlantic bluefin tuna: population dynamics, ecology, fisheries and management. Fish and Fisheries. **6**(4): 281-306.

Game, E.T., Grantham, H.S., Hobday, A.J., Pressey, R.L., Lombard, A.T., Beckley, L.E., Gjerde, K., Bustamante, R., Possingham, H.P., and Richardson, A.J. 2009. Pelagic protected areas: the missing dimension in ocean conservation. Trends Ecol. Evol. **24**(7): 360-369.

Gavaris, S., and Ianelli, J.N. 2002. Statistical issues in fisheries' stock assessments. Scandinavian Journal of Statistics **29**(2): 245-267.

Gelman, A., Carlin, J.B., Stern, H.S., and Rubin, D.B. 1995. Bayesian data analysis. Chapman and Hall, London, U.K.

Gillis, D.M., and Peterman, R.M. 1998. Implications of interference among fishing vessels and the ideal free distribution to the interpretation of CPUE. Can. J. Fish. Aquat. Sci. **55**(1): 37-46.

Goodyear, C.P. 1980. Compensation in fish populations. *In* Biological monitoring of fish. *Edited by* C. Hocutt and C.J. Stauffer. Lexington Books, D. C. Heath Co., Lexington, Mass.

Goodyear, C.P. 2003. Spatio-temporal distribution of longline catch per unit effort, sea surface temperature and Atlantic marlin. Marine and Freshwater Research **54**(4): 409-417.

Goodyear, C.P., Luo, J., Prince, E.D., and Serafy, J.E. 2006. Temperature-depth habitat utilization of blue marlin monitored with PSAT tags in the context of simulation modeling of pelagic longline CPUE. Collective Volume of Scientific Papers ICCAT **59**(1): 224-237.

Goodyear, C.P., and Prager, M.H. 2001. Fitting surplus-production models with missing catch data using ASPIC: evaluation with simulated data on Atlantic blue marlin. Collective Volume of Scientific Papers ICCAT **53**(1): 146-163.

Gordon, H.S. 1954. Economic theory of a common property resource: The fishery. Journal of Political Economy **62**: 124–142.

Gould, S.J. 1989. Wonderful life: the Burgess Shale and the nature of history. W. W. Norton & Co. Inc., New York, NY.

Graham, J.B., Lowell, W.R., Lai, N.C., and Laurs, R.M. 1989. O_2 Tension, Swimming-Velocity, and Thermal Effects on the Metabolic-Rate of the Pacific Albacore *Thunnus alalunga*. Experimental Biology **48**(2): 89-94.

Grant, B. 1969. Proposed migrations of albacore, *Thunnus alalunga*, in the Atlantic Ocean. Trans. Am. Fish. Soc. **98**(4): 589-598.

Grantham, H.S., Petersen, H.P., and Possingham, H.P. 2008. Reducing bycatch in the South African pelagic longline fishery: the utility of different approaches to fisheries closures. Endangered Species Research **5**: 291-299.

Graves, J.E., and Mcdowell, J.R. 1994. Genetic-Analysis of Striped Marlin (*Tetrapturus audax*) Population-Structure in the Pacific-Ocean. Can. J. Fish. Aquat. Sci. **51**(8): 1762-1768.

Graves, J.E., and McDowell, J.R. 2003. Stock structure of the world's istiophorid billfishes: a genetic perspective. Marine and Freshwater Research **54**(4): 287-298.

Greig, T.W., Alvarado-Bremer, J.R., and Ely, B. 1999. Nuclear markers provide additional evidence for population subdivision among Atlantic swordfish. Collective Volume of Scientific Papers ICCAT **49**(1).

Gulland, J. 1956. On the fishing effort in English demersal trawl fisheries. U.K. Ministry of Agrigulture, Fisheries and Food, Fisheries Investigations Series 2 **20**(5): 41.

Gulland, J. 1974. Catch per unit effort as a measure of abundance. Collective Volume of Scientific Papers ICCAT **3**: 1-11.

Gunn, J.S., and Block, B.A. 2001. Acoustic, archival and pop-up satellite tagging of tunas. In Tunas: Physiology, Ecology and Evolution (ed. B. A. Block and E. D. Stevens): 167-224. San Diego, CA: Academic Press.

Gunn, J.S., Patterson, T.A., and Pepperell, J.G. 2003. Short-term movement and behaviour of black marlin Makaira indica in the Coral Sea as determined through a pop-up satellite archival tagging experiment. Marine and Freshwater Research **54**(4): 515-525.

Haddon, M. 2001. Modelling and Quantitative methods in Fisheries. Chapman and Hall.

Hallier, J.-P. 2005. Movement of tropical tunas from the tuna associated baitboat fishery of Dakar and from BETYP and historical tagging operations in the Atlantic Ocean. Collective Volume of Scientific Papers ICCAT **57**(1): 76-99.

Hallier, J.-P., Stequert, B., Maury, O., and Bard, F.-X. 2005. Growth of bigeye tuna (*Thunnus obesus*) in the Eastern Atlantic Ocean from taggin-recapture data and otolith readings. Collective Volume of Scientific Papers ICCAT **57**(1): 181-194.

Hampton, J. 1991. Estimation of Southern Bluefin Tuna *Thunnus maccoyii* Natural Mortality and Movement Rates from Tagging Experiments. Fish. Bull. **89**(4): 591-610.

Hampton, J., Bigelow, K.A., and Labelle, M. 1998. A summary of current information on the biology, fisheries and stock assessment of bigeye tuna (Thunnus obesus) in the Pacific Ocean, with recommendations for data requirements and future research. SPC Tech. Rep. **36**: 1-46.

Hampton, J., and Fournier, D.A. 2001. A spatially disaggregated, length-based, age-structured population model of yellowfin tuna (*Thunnus albacares*) in the western and central Pacific Ocean. Marine and Freshwater Research **52**(7): 937-963.

Hampton, J., and Gunn, J. 1998. Exploitation and movements of yellowfin tuna (*Thunnus albacares*) and bigeye tuna (*T. obesus*) tagged in the north-western Coral Sea. Marine and Freshwater Research **49**(6): 475-489.

Hampton, J., Kleiber, P., Langley, A., Takeuchi, Y., and Ichinokawa, M. 2005a. Stock assessment of bigeye tuna in the western and central Pacific Ocean. WCPFCSC Working Paper **SC1**(SA WP-2): 77.

Hampton, J., Langley, A., and Kleiber, P. 2006a. Stock assessment of bigeye tuna in the western and central Pacific Ocean, including analysis of management optins. WCPFCSC Working Paper **SC2**(SA WP-2): 103.

Hampton, J., Langley, A., and Kleiber, P. 2006b. Stock assessment of yellowfin tuna in the western and central Pacific Ocean, including an analysis of management options. WCPFCSC Working Paper **SC2**(SA WP-1): 103.

Hampton, J., Sibert, J.R., Kleiber, P., Maunder, M.N., and Harley, S.J. 2005b. Decline of Pacific tuna populations exaggerated? Nature **434**(7037): E1-E2.

Hampton, J., and Williams, P. 2005. A description of tag-recapture data for bigeye tunna (*Thunnus obesus*) in the Western and Central Pacific Ocean. Collective Volume of Scientific Papers ICCAT **57**(2): 85-93.

Hanamoto, E. 1978. Fishery oceanography of striped marlin - III. Relation between fishing ground of striped marlin and submarine topography in the Southern Coral Sea. Bull. Jap. Soc. Sci. Fish. **44**: 19-26.

Hanamoto, E. 1987. Effects of oceanographic environment on bigeye tuna distribution. Bull. Jap. Soc. Fish. Oceanogr. **51**(3): 203-216.

Hannesson, R. 1998. Marine reserved: what would they acomplish? Mar. Resour. Econ. **13**: 159-170.

Harada, T. 1980. Maguro-rui yosei kenkyu no shinten to tenbo (Progress and future prospects in tuna culturing studies translation by Otsu, Tamio, U.S. Nat. Mar. Fish. Serv., Honolulu). Far Seas Fish. Res. Lab., Japan Tuna Research Conf., Proc.: 50-58.

Harley, S.J., Myers, R.A., and Dunn, A. 2001. Is catch-per-unit-effort proportional to abundance? Can. J. Fish. Aquat. Sci. **58**(9): 1760-1772.

Hayasi, S. 1974. Effort and cpue as mesure of abundance. Collected Volume of Scientific Papers ICCAT **3**: 32-50.

Hilborn, R. 1979. Comparison of Fisheries Control-Systems That Utilize Catch and Effort Data. Journal of the Fisheries Research Board of Canada **36**(12): 1477-1489.

Hilborn, R. 1990. Determination of Fish Movement Patterns from Tag Recoveries Using Maximum-Likelihood Estimators. Can. J. Fish. Aquat. Sci. **47**(3): 635-643.

Hilborn, R., and Mangel, M. 1997. The Ecological Detective. Princeton University Press, Princeton, New Jersey.

Hilborn, R., Pikitch, E.K., and Francis, R.C. 1993. Current Trends in Including Risk and Uncertainty in Stock Assessment and Harvest Decisions. Can. J. Fish. Aquat. Sci. **50**(4): 874-880.

Hilborn, R., Punt, A.E., and Orensanz, J. 2004. Beyond band-aids in fisheries management: Fixing world fisheries. Bull. Mar. Sci. **74**(3): 493-507.

Hilborn, R., and Walters, C. 1992. Quantitative fisheries stock assessment: choice, dynamics, and uncertainty. Chapman and Hall Inc., New York.

Hill, K.T., Cailliet, C.M., and Radtke, R.L. 1989. A comparative analysis of growth zones in four calcified structures of Pacific blue marlin, *Makaira nigricans*. Fish. Bull. **87**: 829-843.

Hinton, M.G. 2001. Status of blue marlin in the eastern Pacific Ocean. Stock Assessment Report IATTC **SAR1**: 284-319.

Hinton, M.G., and Bayliff, W.H. 2002. Status of stripped marlin in the Eastern Pacific Ocean in 2001 and outlook for 2002. Stock Assessment Report IATTC: 328-364.

Hinton, M.G., Bayliff, W.H., and Suter, J.M. 2004. Assessment of swordfish in the Eastern Pacific Ocean. Stock Assessment Report IATTC **4**: 291-326.

Hinton, M.G., Taylor, R.G., and Murphy, M.D. 1997. Use of gonad indices to estimate the status of reproductive activity of female swordfish, *Xiphias gladius*: A validated classification method. Fish. Bull. **95**(1): 80-84.

Hisada, K. 1973. Inverstigation on tuna hand-line fishing ground as some biological observations on yellowfin and bigeye tunas caught in the northwestern Coral Sea. Bull. Far Seas Fish. Res. Lab. **8**: 35-69.

Holdsworth, J., Saul, P., and Browne, G. 2003. Factors affecting striped marlin catch rate in the New Zealand recreational fishery. Marine and Freshwater Research **54**(4): 473-481.

Holland, K., Brill, R., and Chang, R.K.C. 1990a. Horizontal and Vertical Movements of Pacific Blue Marlin Captured and Released Using Sportfishing Gear. Fish. Bull. **88**(2): 397-402.

Holland, K.N., Brill, R.W., and Chang, R.K.C. 1990b. Horizontal and Vertical Movements of Yellowfin and Bigeye Tuna Associated with Fish Aggregating Devices. Fish. Bull. **88**(3): 493-507.

Honma, M. 1974. Estimation of overall effective fishing intensity of tuna longline fishery. Bull. Far Seas Fish. Res. Lab. **10**: 63-85.

Horodysky, A.Z., Kerstetter, D.W., and Graves, J.E. 2004. Habitat preference and diving behavior of white marlin (*Tetrapturus albidus*) released from the recreational rod-and-reel and commercial pelagic longline fishereis in the western north Atlantic Ocean: implications for habitat-based stock assessment models. Collective Volume of Scientific Papers ICCAT **56**(1): 160-168.

Horodysky, A.Z., Kerstetter, D.W., and Graves, J.E. 2005. Habitat utilization and vertical movements of white marlin (*Tetrapturus albidus*) released from commercial and recreational gear in the western North Atlantic Ocean: inferences from short-duration pop-up archival satellite tags (PSATs). ICCAT **SCRS/2005/034**.

Hoyle, S.D., Langley, A., and Hampton, J. 2008. Stock assessment of albacore tuna in the South Pacific Ocean. Western and Central Pacific Fisheries Commission Scientific Committee fourth regular session 11-22 August 2008 Port Moresby, Papua New Guinea **WCPFC-SC4-2008**(SA-WP-8): 126.

Hoyle, S.D., and Maunder, M.N. 2007. Status of yellowfin tuna in the Eastern Pacific Ocean in 2005 and outlook for 2006. Stock Assessment Report IATTC **SAR7-YFT-ENG**: 3-116.

Hsu, C.C. 1991. Parameters estimation of generalized von Bertalanffy growth equation. Acta Oceanogr. Taiwan. **26**: 66-77.

Hsu, C.C., and Chen, K.-S. 2006. Reconstructind von Bertalanffy growth equation of Pacific bluefin tuna (Thunnus orientalis) with additional spawner scales samples from the southwestern North Pacific Ocean. ISC Meeting Report **ISC/06/PBF-WG/05**: 1-10.

Huang, C.S., Wu, C.L., Kao, C.L., and Su, W.C. 1990. Age and growth of the Indian Ocean albacore, *Thunnus alalunga*, by scales. FAO/IPTP/TWS/90/53.

Hyde, J.R., Humphreys, R., Musyl, M., Lynn, E., and Vetter, R. 2006. A central north pacific spawning ground for striped marlin, Tetrapturus audax. Bull. Mar. Sci. **79**(3): 683-690.

IATTC. 2008. Tunas and billfishes in the Eastern Pacific Ocean 2007. Inter-American Tropical Tuna Commision Fishery Status Report **6**: 145.

IATTC Database. 2006. Inter-Americam Tropical Tuna Commision public domain data.

ICCAT. 1984. Meeting of the working group of juvenile tropical tunas. Collective Volume of Scientific Papers ICCAT **21**(1): 1-289.

ICCAT. 1987. Report of the swordfish assessment workshop. Collective Volume of Scientific Papers ICCAT **26**(2): 339-395.

ICCAT. 1991. Report of the yellowfin year program. Collective Volume of Scientific Papers ICCAT **36**: 1-36.

ICCAT. 1997. Report of the 1996 ICCAT SCRS Bluefin Tuna Stock Assessment Session. Collective Volume of Scientific Papers ICCAT **46**(1): 1-186.

ICCAT. 2003a. Report of the 2002 Atlantic Bluefin Stock Assessment Session. Collective Volume of Scientific Papers ICCAT **55**(3): 710-937.

ICCAT. 2003b. Report of the 2002 Atlantic Swordfish Stock Assessment Session. Collective Volume of Scientific Papers ICCAT **55**(4): 1289-1415.

ICCAT. 2003c. Report of the 2002 ICCAT White Marlin Stock Assessment Meeting. Collective Volume of Scientific Papers ICCAT **55**(2): 350-452.

ICCAT. 2004a. 2003 ICCAT Atlantic Yellowfin Stock Assessment Session. Collective Volume of Scientific Papers ICCAT **56**(2): 443-527.

ICCAT. 2004b. 2003 ICCAT Mediterranean swordfish stock assessment session. Collective Volume of Scientific Papers ICCAT **56**(3): 789-837.

ICCAT. 2005. Report of the 2004 ICCAT Bigeye Tuna Stock Assessment Session Collective Volume of Scientific Papers ICCAT **58**(1): 1-110.

ICCAT. 2006a. Report of the 2006 Atlantic Bluefin Tuna Stock Assessment Session. **SRCS/2006/013**: 137.

ICCAT. 2006b. Report of the 2006 ICCAT Atlantic Swordfish Stock Assessment. **SCI-040/2006**: 66.

ICCAT. 2006c. Report of the 2006 ICCAT Billfish Stock Assessment. **SCI-012/2006**: 75.

ICCAT. 2007a. Report of the 2007 ICCAT Albacore Stock Assessment Session. ICCAT Report: 84.

ICCAT. 2007b. Report of the 2007 ICCAT Bigeye Tuna Stock Assessment Session. ICCAT Report: 1000.

ICCAT. 2009. Report for biennial period, 2008-2009 Part 1(2008) Vol.2. International Commision for the Conservation of Atlantic Tuna Standing Committee on Research and Science Report **REP_EN_08-09_I_2**: 275.

ICCAT Database. 2006. International Commission for the Conservation of Atlantic Tunas public domain database. Task II Catch, Effort, and Size: http://www.iccat.int/en/ (accessed December 2006).

IOTC. 2004a. Report of the First Session of the IOTC Working Party on Temperate Tunas. IOTC Working Paper **IOTC-2004-WPTMT-R[EN]**: 1-18.

IOTC. 2004b. Report of the Seventh Session of the Scientific Committee Victoria, Seychelles, 8-12 November 2004. IOTC Scientific Committee Report **IOTC-2004-SC-R[EN]**: 1-91.

IOTC. 2005. Biological data on tuna and tuna-like species gathered at the IOTC Secretariat: Status report. IOTC Working Paper **IOTC-2005-WPTT-05**: 23.

IOTC. 2007. Report of the Tenth Session of the Scientific Committee Victoria, Seychelles, 5-9 November 2007. IOTC Scientific Committee Report **IOTC-2007-SC-R[EN]**: 133.

IOTC. 2008. Report of the Eleventh Session of the Scientific Committee. Victoria, Seychelles, 1-5 December 2008. IOTC Scientific Committee Report **IOTC-2008-SC-R[E]**: 166.

IOTC Database. 2006. Indian Ocean Tuna Commision public domain database. Task II Catch, Effort and Size: http://www.iotc.org (accessed December 2006).

ISC. 2005. Report of the nineteenth North Pacific albacore workshop, Fisheries and Oceans Canada, Pacific Biological Station, Nanaimo, B.C., Nanaimo, B.C., Canada.

ISC. 2006. Report of the sixth meeting of the International Scientific Committee for Tuna and Tuna-like Species in the North Pacific Ocean plenary session, March 23-27, 2006 La Jolla, California U.S.A. Annnex 5 Report of the Marlin Working Group meeting (November 15-21, 2005, Honolulu, HI, U.S.A.). ISC Meeting Report **MARWG**: 1-23.

ISC. 2007. Report of the seventh meeting of the Iternational Scientific Committee for tuna and tuna-like species in the North Pacific Ocean. Busan, Korea

Plenary Session, July 25-30, 2007 54.

ISC. 2008a. Report of the albacore working group workshop. International Scientific Committee for Tuna and Tuna-like Species in the North Pacific Ocean February 28 – March 6, 2008 La Jolla, California USA: 43.

ISC. 2008b. Report of the billfish working group workshop. International Scientific Committee for Tuna and Tuna-like Species in the North Pacific Ocean 11-19 June 2008 Tokyo University of Agriculture Abashiri, Hokkaido, Japan: 28.

ISC. 2008c. Report of the Pacific bluefin tuna working grpoup workshop. International Scientific Committee for Tuna and Tuna-like Species in the North Pacific Ocean May 28-June 4, 2008 Shimizu, Japan continued July 17-18, 2008 Takamatsu, Japan: 67.

Itoh, T. 2006. Sizes of adult bluefin tuna Thunnus orientalis in different areas of the western Pacific Ocean. Fish. Sci. **72**(1): 53-62.

Itoh, T., Tsuji, S., and Nitta, A. 2003a. Migration patterns of young Pacific bluefin tuna (*Thunnus orientalis*) determined with archival tags. Fish. Bull. **101**(3): 514-534.

Itoh, T., Tsuji, S., and Nitta, A. 2003b. Swimming depth, ambient water temperature preference, and feeding frequency of young Pacific bluefin tuna (*Thunnus orientalis*) determined with archival tags. Fish. Bull. **101**(3): 535-544.

Jones, J.B. 1991. Movements of Albacore Tuna (*Thunnus alalunga*) in the South-Pacific - Evidence from Parasites. Mar. Biol. **111**(1): 1-9.

Karakulak, S., Oray, I., Corriero, A., Aprea, A., Spedicato, D., Zubani, D., Santamaria, N., and De Metrio, G. 2004. First information on the reproductive biology of the bluefin tuna (*Thunnus thynnus*) in the eastern Mediterranean. . Collective Volume of Scientific Papers ICCAT **56**(4): 1158-1162.

Kikawa, S. 1962. Studies on the spawning activity of Pacific tunas, *Parathunnus mebachi* and *Neothunnus macropterus*, by the gonad index examination. Rep. Nankai Reg. Fish. Res. Lab **1**(43-56).

Kikawa, S. 1966. The distribution of maturing bigeye and yellowfin and an evaluation of their spawning potential in different areas in the longline grounds in the Pacific. Rep. Nankai Reg. Fish. Res. Lab. **23**: 131-208.

Kimura, D.K., Balsiger, J.W., and Ito, D.H. 1984. Generalized Stock Reduction Analysis. Can. J. Fish. Aquat. Sci. **41**(9): 1325-1333.

Kimura, D.K., and Tagart, J.V. 1982. Stock Reduction Analysis, Another Solution to the Catch Equations. Can. J. Fish. Aquat. Sci. **39**(11): 1467-1472.

Kimura, S., Nakai, M., and Sugimoto, T. 1997. Migration of albacore, *Thunnus alalunga*, in the North Pacific Ocean in relation to large oceanic phenomena. Fish. Oceanogr. **6**(2): 51-57.

Kitagawa, T., Kimura, S., Nakata, H., and Yamada, H. 2006. Thermal adaptation of Pacific bluefin tuna *Thunnus orientalis* to temperate waters. Fish. Sci. **72**(1): 149-156.

Kitagawa, T., Kimura, S., Nakata, H., and Yamada, H. 2007. Why do young Pacific bluefin tuna repeatedly dive to depths through the thermocline? Fish. Sci. **73**(1): 98-106.

Kitagawa, T., Nakata, H., Kimura, S., Itoh, T., Tsuji, S., and Nitta, A. 2000. Effect of ambient temperature on the vertical distribution and movement of Pacific bluefin tuna *Thunnus thynnus orientalis*. Marine Ecology-Progress Series **206**: 251-260.

Kitagawa, T., Nakata, H., Kimura, S., Sugimoto, T., and Yamada, H. 2002. Differences in vertical distribution and movement of Pacific bluefin tuna (*Thunnus thynnus orientalis*)

among areas: the East China Sea, the Sea of Japan and the western North Pacific. Marine and Freshwater Research **53**(2): 245-252.

Kleiber, P., and Hampton, J. 1994. Modeling Effects of Fads and Islands on Movement of Skipjack Tuna (*Katsuwonus pelamis*) - Estimating Parameters from Tagging Data. Can. J. Fish. Aquat. Sci. **51**(12): 2642-2653.

Kleiber, P., Hampton, J., Hinton, M.G., and Uozumi, Y. 2002. Update on Blue Marlin Stock Assessment. 15th Meeting of the Standing Committee on Tuna and Billfish Working Paper Honolulu, Hawaii, 22-27 July 2002 **BBRG-10**: 1-29.

Kleiber, P., and Maunder, M. 2008. Inherent bias in using aggregate CPUE to characterize abundance of fish species assemblages. Fisheries Research **93**: 140-145.

Kolody, D., Campbell, R.A., and Davies, N. 2006. A Multifan-CL stock assessment for South-west Pacific Swordfish 1952-2004. Western and Central Pacific Fisheries Commission Scientific committee second regular session 7-18 August 2006 Manila, Philippines **WCPFC-SC2** (ME-WP-3): 68.

Kopf, R.K., Davie, P.S., and Holdsworth, J.C. 2005. Size trends and population characteristics of striped marlin, *Tetrapturus audax* caught in the New Zealand recreational fishery. N. Z. J. Mar. Freshwat. Res. **39**(5): 1145-1156.

Korsmeyer, K.E., Dewar, H., Lai, N.C., and Graham, J.B. 1996. Tuna aerobic swimming performance: Physiological and environmental limits based on oxygen supply and demand. Comparative Biochemistry and Physiology B-Biochemistry & Molecular Biology **113**(1): 45-56.

Koto, T. 1969. Studies on the albacore - XIV. Distribution and movement of the albacore in the Indian and the Atlantic Oceans based on the catch statistics of japanese tuna longline fishery. Bull. Far Seas Fish. Res. Lab. **1**: 115-129.

Kume, S., and Joseph, J. 1966. Size composition, growth and sexual maturity of bigeye tuna, *Thunnus obesus (Lowe)*, from the Japanese long-line fishery in the eastrn Pacific Ocean. Bull. IATTC **11**(2): 47-99.

Labelle, M., and Hampton, J. 2003. Stock assessment of albacore tuna in the South Pacific Ocean. SCTB **SCTB16 ALB-1**: 31.

Labelle, M., Hampton, J., Bailey, K., Murray, T., Fournier, D.A., and Sibert, J.R. 1993. Determination of Age and Growth of South-Pacific Albacore (*Thunnus alalunga*) Using 3 Methodologies. Fish. Bull. **91**(4): 649-663.

Langley, A. 2006. The South Pacific albacore fishery: a summary of the status of the stock and fishery management issues of relevance to Pacific Island countries and territories. SPC Tech. Rep. **37**.

Langley, A., and Hampton, J. 2005. Stock assessment of albacore tuna in the south Pacific Ocean. Working Paper SA-WP3. 1st meeting of the Scientific Committee of the Western and Central Pacific Fisheries Commission. Noumea, New Caledonia 8-19 August,2005.

Langley, A., Hampton, J., Kleiber, P., and Hoyle, S.D. 2008. Stock assessment of bigeye tuna in the Western and Central Pacific Ocean, including analysis of management options. Western and Central Pacific Fisheries Commission Scientific Committee Fourth regular session 11-28 August 2006 Port Moresby, Papua New Guinea **WCPFC-SC4-2008**(SA-WP-1 Rev.1): 137.

Lauck, T., Clark, C.W., Mangel, M., and Munro, G.R. 1998. Implementing the precautionary principle in fisheries management through marine reserves. Ecol. Appl. **8**(1): S72-S78.

Laurs, R.M., and Dotson, R.C. 1992. Albacore. *In* California's Living Marine Resources and Their Utilization. *Edited by* W.S. Leet, C.M. Dewees and C.W. Haugen. Sea Grant Extension Program, Department of Wildlife and Fisheries Biology, University of California, Davis, CA. pp. 136-138.

Lee, L.K., and Yeh, S.Y. 1993. Studies on the age and growth of south Atlantic albacore (*Thunnus alalunga*) specimens collected from Taiwanese longliners. Collective Volume of Scientific Papers ICCAT **40**(2): 354-360.

Lee, P.-F., Chen, I.-C., and Tzeng, W.-N. 2005. Spatial and temporal distribution patterns of bigeye tuna (*Thunnus obesus*) in the Indian Ocean. Zool. Stud. **44**(2): 260-270.

Lee, Y.C., Hsu, C.C., Chang, S.K., and Liu, H.C. 1990. Yield per recruit analysis of the Indian Ocean albacore stock. IPTP Rep. **TWS/90/56**: 14.

Lee, Y.C., and Kuo, C.L. 1988. Age characters of albacore, *Thunnus alalunga*, in the Indian Ocean. IPTP Rep. **TWS/88/61**: 99-108.

Lee, Y.C., and Liu, H.C. 1992. Age determination, by vertebra reading, in Indian albacore, *Thunnus alalunga* (Bonnaterre). J. Fish. Soc. Taiwan **19**(2): 89-102.

Lehodey, P., Alheit, J., Barange, M., Baumgartner, T., Beaugrand, G., Drinkwater, K., Fromentin, J.M., Hare, S.R., Ottersen, G., Perry, R.I., Roy, C., Van der Lingen, C.D., and Werner, F. 2006. Climate variability, fish, and fisheries. J. Clim. **19**(20): 5009-5030.

Lehodey, P., Bertignac, M., Hampton, J., Lewis, A., and Picaut, J. 1997. El Nino Southern Oscillation and tuna in the western Pacific. Nature **389**(6652): 715-718.

Lehodey, P., Chai, F., and Hampton, J. 2003. Modelling climate-related variability of tuna populations from a coupled ocean-biogeochemical-populations dynamics model. Fish. Oceanogr. **12**(4-5): 483-494.

Lehodey, P., Hampton, J., and Leroy, B. 1999. Preliminary results on age and growth of bigeye tuna (*Thunnus obesus*) from the western and central Pacific Ocean as indicated by daily growth increments and tagging data. SCTB **SCTB12 BET-2**: 18.

Lehodey, P., and Leroy, B. 1999. Age and growth of yellowfin tuna (*Thunnus albacares*) from the western and central Pacific Ocean as indicated by daily growth increments and tagging data. SCTB **SCTB12 YFT-2**: 21.

Lehodey, P., Senina, I., and Murtugudde, R. 2008. A spatial ecosystem and populations dynamics model (SEAPODYM) - Modeling of tuna and tuna-like populations. Prog. Oceanogr. **78**(4): 304-318.

Lessa, R., and Duarte-Neto, P. 2004. Age and growth of yellowfin tuna (*Thunnus albacares*) in the western equatorial Atlantic, using dorsal fin spines. Fisheries Research **69**(2): 157-170.

Lu, H.-J., Lee, K.-T., and Liao, C.H. 1998. On the relationship between El nino/Southern ocillation and south Pacific albacore. Fisheries Research **39**(1): 1-7.

Lutcavage, M.E., Brill, R.W., Skomal, G.B., Chase, B.C., Goldstein, J.L., and Tutein, J. 2000. Tracking adult North Atlantic bluefin tuna (*Thunnus thynnus*) in the northwestern Atlantic using ultrasonic telemetry. Mar. Biol. **137**(2): 347-358.

Magnusson, A., and Hilborn, R. 2007. What makes fisheries data informative? Fish and Fisheries. **8**(4): 337-358.

Mangel, M., and Stamps, J. 2001. Trade-offs between growth and mortality and the maintenance of individual variation in growth. Evol. Ecol. Res. **3**(5): 583-593.

Marcinek, D.J., Blackwell, S.B., Dewar, H., Freund, E.V., Farwell, C., Dau, D., Seitz, A.C., and Block, B.A. 2001. Depth and muscle temperature of Pacific bluefin tuna examined with acoustic and pop-up satellite archival tags. Mar. Biol. **138**(4): 869-885.

Martell, S.J.D., Pine, W.E., and Walters, C.J. 2008. Parameterizing age-structured models from a fisheries management perspective. Can. J. Fish. Aquat. Sci. **65**(8): 1586-1600.

Martell, S.J.D., and Walters, C.J. 2002. Implementing harvest rate objectives by directly monitoring exploitation rates and estimating changes in catchability. Bull. Mar. Sci. **70**(2): 695-713.

Martins, C., Pinheiro, P., Travassos, P., and Hazin, F. 2007. Prelimary results on the reproductive biology of blue marlin, *Makaira nigricans* (Lacépède, 1803) in the tropical western Atlantic Ocean. Collective Volume of Scientific Papers ICCAT **60**(5): 1636-1642.

Mather, F.J., Jones, A.C., and Beardsley, G.L. 1972. Migration and distribution of white marlin and blue marlin in the Atlantic Ocean. Fish. Bull. **70**: 283-298.

Mather, F.J., Mason, J.M., and Jones, A.C. 1995. Historical document: life history and fisheries of Atlantic bluefin tuna. NOAA Techical Memorandum NMFS SEFSC **370**: 165.

Matsuda, Y., and Ouchi, K. 1984. Legal, political and economic constraints on Japanese strategies for distant-water tuna and skipjack fisheries in southeast asian seas and the Western Central Pacific. Mem. Kagoshima Univ. Res. Center S. Pac. **5**(3): 151-232.

Matsumoto, T., Saito, H., and Miyabe, N. 2005. Swimming behaviour of adult bigeye tuna using pop-up tags in the central Atlantic Ocean. Collective Volume of Scientific Papers ICCAT **57**(2): 151-170.

Maunder, M.N., Hinton, M.G., Bigelow, K.A., and Langley, A.D. 2006a. Developing indices of abundance using habitat data in a statistical framework. Bull. Mar. Sci. **79**(3): 545-559.

Maunder, M.N., and Hoyle, S.D. 2006a. Status of bigeye tuna in the Eastern Pacific Ocean in 2004 and outlook for 2005. Stock Assessment Report IATTC **SAR6-BET-ENG**: 103-206.

Maunder, M.N., and Hoyle, S.D. 2006b. Status of yellowfin tuna in the Eastern Pacific Ocean in 2004 and outlook for 2005. Stock Assessment Report IATTC: 3-102.

Maunder, M.N., and Hoyle, S.D. 2007. Status of bigeye tuna in the Eastern Pacific Ocean in 2005 and outlook for 2006. Stock Assessment Report IATTC **SAR7-BET-ENG**: 116-248.

Maunder, M.N., and Punt, A.E. 2004. Standardizing catch and effort data: a review of recent approaches. Fisheries Research **70**: 141-159.

Maunder, M.N., Sibert, J.R., Fonteneau, A., Hampton, J., Kleiber, P., and Harley, S.J. 2006b. Interpreting catch per unit effort data to assess the status of individual stocks and communities. ICES J. Mar. Sci. **63**(8): 1373-1385.

Mcallister, M.K., Pikitch, E.K., Punt, A.E., and Hilborn, R. 1994. A Bayesian-Approach to Stock Assessment and Harvest Decisions Using the Sampling Importance Resampling Algorithm. Can. J. Fish. Aquat. Sci. **51**(12): 2673-2687.

McDowell, J.R., and Graves, J.E. 2008. Population structure of striped marlin (*Kajikia audax*) in the Pacific Ocean based on analysis of microsatellite and mitochondrial DNA. Can. J. Fish. Aquat. Sci. **65**(7): 1307-1320.

Medina, A., Abascal, F.J., Megina, C., and Garcia, A. 2002. Stereological assessment of the reproductive status of female Atlantic northern bluefin tuna during migration to Mediterranean spawning grounds through the Strait of Gibraltar. J. Fish Biol. **60**(1): 203-217.

Meester, G. 2000. A mathematical programing and simulation-bases approach to determining critical factors in the design of effective marine reserves plans for coral reef fishes. Ph.D. dissertation. University of Miami.

Megalofonou, P. 1990. Size distribution, length-weight relationships, age and sex of albacore (*Thunnus alalunga*) in the Aegean Sea. Collective Volume of Scientific Papers ICCAT **32**: 154-162.

Megalofonou, P. 2000. Age and growth of Mediterranean albacore. J. Fish Biol. **57**(3): 700-715.

Mejuto, J., Iglesias, S., Rey, J.C., Alot, E., and Garcia, B. 1988. Relaciones talla-peso del pez espada (*Xiphias gladius*, L.) en las areas BIL-94 y BIL-95, por estratos espacio temporales. Collective Volume of Scientific Papers ICCAT **27**: 214-221.

Melo-Barrera, F.N., Felix-Uraga, R., and Quinonez-Velazquez, C. 2003. Growth and length-weight relationship of the striped marlin, *Tetrapturus audax* (Pisces : Istiophoridae), in Cabo San lucas, Baja California Sur, Mexico. Cienc. Mar. **29**(6): 305-315.

Merrett, N.R. 1971. Aspects of the biology of billfish (Istiophoridae) from the equatorial western Indian Ocean. J. Zool. **163**: 351-395.

Mimura, K. 1963. Synopsis of biological data on yellowfin tuna *Neothunnus macropterus* Temminck and Schlegel 1842 (Indian Ocean). in Rosa, H. (ed.). Proceedings of the world scientific meeting on the biology of tuna and related species. FAO Fish. Rep. **6**(2): 319-349.

Mimura, K., and Warashina, I. 1962. Studies on indomaguro (*Thunnus maccoyii*?) . Description of the development of the fishery, geographical differences and seasonal changes of distribution and relation which is seen among idomaguro, southern bluefin, and goshumaguro. Nankai Reg. Fish. Res. Lab. Rep. **16**: 135-154.

Miyabe, N. 1994. A review of the biology and fisheries for bigeye tuna, *Thunnus obesus*, in the Pacific Ocean. In: Shomura RS, Majkowski J, Langi S, editors. Interactions of Pacific tuna fisheries. Proceedings of the First FAO Expert Consultation on Interactions of Pacific Tuna Fisheries; 1991 Dec 3-11; Noumea, New Caledonia **Volume 2**: 207-243.

Miyake, M.P. 2004. A brief history of tuna fisheries of the world. In Bayliff, W. H., J. I. de Leiva Moreno, and J. Majkowski (eds). Second meeting of the Technical Advisory Committee of the FAO project Management of tuna fishing capacity: conservation and socio-economics. 15-18 March 2004. Madrid, Spain. FAO Fisheries Proceedings **2**: 23-50.

Miyake, M.P., Miyabe, N., and Nakano, H. 2004. Historical trends of tuna catches in the world. FAO Fish. Tech. Pap. **467**: 74.

Morita, H. 1998. Marine fisheries policies under the occupation (Senryoka no kaiyo gyogyo seisaku). *In* 50 Years of Japan Fisheries Agency (Suisancho 50 nenshi). *Edited by* I. Konuma. Japan Fisheries Agency, Tokyo. pp. 87-96 [in Japanese].

Mullon, C., Freon, P., and Cury, P. 2005. The dynamics of collapse in world fisheries. Fish and Fisheries. **6**(2): 111-120.

Murphy, T.C., and Sakagawa, G.T. 1977. A review and evaluation of estimates of natural mortality rates of tunas. Collective Volume of Scientific Papers ICCAT **6**(1): 117-123.

Myers, R.A., Bowen, K.G., and Barrowman, N.J. 1999. Maximum reproductive rate of fish at low population sizes. Can. J. Fish. Aquat. Sci. **56**(12): 2404-2419.

Myers, R.A., and Worm, B. 2003. Rapid worldwide depletion of predatory fish communities. Nature **423**(6937): 280-283.

Nakamura, E.L., and Uchiyama, J.H. 1966. Length-weight relations of Pacific tunas. Proceedings of the Governor's Conference on Pacific Fishery Resources, Hawaii, pp. 197-201.

Nakamura, H. 1969. Tuna distribution and migration. Fishing News, London.

Nakamura, I. 1985. Billfishes of the World: An Annotated and Illustrated Catalogue of Marlins, Sailfishes, Spearfishes and Swordfishes Known to Date, Food and Agriculture Organization of the United Nations, Rome, Italy.

National Research Council. 1995. Understanding Marine Biodiversity: a research agenda for the nation. National Academy Press, Washington, D. C. .

National Research Council. 1999. Sustaining Marine Fisheries. National Academy Press, Washington, D. C.

Nelder, J.A., and Wedderburn, R.W.M. 1972. Generalized Linear Models. Journal of the Royal Statistical Society Series A (General) **135**(3): 370-384.

Nikaido, H., Miyabe, N., and Ueyanagi, S. 1991. Spawning time and frequency of bigeye tuna, *Thunnus obesus*. Bull. Far Seas Fish. Res. Lab. **28**: 47-73.

Nishida, T., and Shono, H. 2007. Stock assessment of yellowfin tuna (*Thunnus albacares*) in the Indian Ocean by the age structured production model(ASPM) analyses. Working Paper IOTC **IOTC-2007-WPTT-12**.

Nishikawa, Y., Honma, M., Ueyanagi, S., and Kikawa, S. 1985. Average distribution of larvae of oceanic species of scombroid fishes, 1956-1981. Bull. Far Seas Fish. Res. Lab. **12**(S. Series): 1-99.

Nishikawa, Y., Kikawa, S., Honma, M., and Ueyanagi, S. 1978. Distribution atlas of larval tunas, billfishes and related species - Results of larval surveys by R/V Shunyo Maru, and Shoyo Maru, 1956-1975. Far Seas Fisheries Research Laboratory Shimuzu: 1-100.

Nishikawa, Y., and Ueyanagi, S. 1974. The distribution of the larvae of swordfish, Xiphias gladius, in the Indian and pacific Oceans. In Shomura, S., Williams, F. (eds.) Proceedings of the International Billfish Symposium; 9-12 August 1972 Kailua-Kona, HI. Part 2, Review and contributed papers. NOAA Technical Report NMFS **SSRF-675**: 261-264.

Okamoto, H. 2004. Search for the Japanese tuna fishing data before and just after World War II. Bull. Fish. Res. Agen. **13**: 15-34.

Oliveira, I.M., Hazin, F.H.V., Travassos, P., Pinheiro, P.B., and Hazin, H.G. 2007. Preliminary results on the reproductive biology of the white marlin, *Tetrapturus albidus* (Poey 1960) in the western equatorial Atlantic Ocean. Collective Volume of Scientific Papers ICCAT **60**(5): 1738-1745.

Olson, R.J. 1980. Synopsis of biological data on the southern bluefin tuna, *Thunnus maccoyii* (Castelnau, 1872). Spec. Rep. IATTC **2**: 155-211.

Ortega-Garcia, S., Klett-Traulsen, A., and Ponce-Diaz, G. 2003. Analysis of sportfishing catch rates of striped marlin (*Tetrapturus audax*) at Cabo San Lucas, Baja California Sur, Mexico, and their relation to sea surface temperature. Marine and Freshwater Research **54**(4): 483-488.

Ortiz, M., Prince, E.D., Serafy, J.E., Holts, D.B., Davy, K.B., Pepperell, J.G., Lowry, M.B., and Holdsworth, J.C. 2003. Global overview of the major constituent-based billfish tagging programs and their results since 1954. Marine and Freshwater Research **54**(4): 489-507.

Paloheimo, J.E., and Dickie, L.M. 1964. Abundance and fishing success. Journal du Conseil International pour l'Exploration de la Mer **155**: 152-163.

Parks, W., Bard, F.-X., Cayré, P., and Kume, S. 1982. Length-weight relations for bigeye tuna captured in the eastern Atlantic Ocean. Collective Volume of Scientific Papers ICCAT **17**(1): 214-225.

Parrack, M., and Phares, P. 1979. Aspects of the growth of Atlantic bluefin tuna determined from mark recapture data. Collective Volume of Scientific Papers ICCAT **8**(2): 356-366.

Pauly, D. 1980. On the interrelationships between natural mortality, growth parameters, and mean environmental temperature in 175 fish stocks. J Cons. **39**(2): 175-192.

Pauly, D., Christensen, V., Dalsgaard, J., Froese, R., and Torres, F. 1998. Fishing down marine food webs. Science **279**(5352): 860-863.

Penney, A. 1994. Morphometric relationships, annual catch-at-size for South African-caught South Atlantic albacore (*Thunnus alalunga*). Collective Volume of Scientific Papers ICCAT **XLII**(1): 371-382.

Pepperell, J.G. 2000a. Brief synopsis of the biology of the black marlin (*Makaira indica*), with reference to the Indian ocean. IOTC proceedings no. 3 **WPB00-09**: 214-220.

Pepperell, J.G. 2000b. Brief synopsis of the biology of the blue marlin (*Makaira nigricans*), with reference to the Indian ocean. IOTC proceedings no. 3 **WPB00-10**: 221-227.

Pillai, P.P., and Ueyanagi, S. 1978. Distribution and biology of the striped marlin *Tetrapturus audax* (Philippi) taken by the longline fishery in the Indian Ocean. Bull. Far Seas Fish. Res. Lab. **16**: 9-32.

Poisson, F., Marjolet, C., and Fauvel, C. 2001. Sexual maturity, spawning season and estimation of batch fecundity of swordfish (*Xiphias Gladius*) caught by the reunion-based pelagic longline fishery (SWOI). IOTC Proceedings no. 4: 120 -125.

Polacheck, T. 2006. Tuna longline catch rates in the Indian Ocean: Did industrial fishing result in a 90% rapid decline in the abundance of large predatory species? Mar. Policy **30**(5): 470-482.

Polacheck, T., Eveson, J.P., and Laslett, G.M. 2004. Increase in growth rates of southern bluefin tuna (*Thunnus maccoyii*) over four decades: 1960 to 2000. Can. J. Fish. Aquat. Sci. **61**(2): 307-322.

Polacheck, T., Eveson, J.P., Laslett, G.M., Pollock, K.H., and Hearn, W.S. 2006. Integrating catch-at-age and multiyear tagging data: a combined Brownie and Petersen estimation approach in a fishery context. Can. J. Fish. Aquat. Sci. **63**(3): 534-548.

Polacheck, T., Hilborn, R., and Punt, A.E. 1993. Fitting Surplus Production Models - Comparing Methods and Measuring Uncertainty. Can. J. Fish. Aquat. Sci. **50**(12): 2597-2607.

Porch, C.E. 1995. Trajectory-Based Approaches to Estimating Velocity and Diffusion from Tagging Data. Fish. Bull. **93**(4): 694-709.

Prager, M.H., Prince, E.D., and Lee, D.W. 1995. Empirical Length and Weight Conversion Equations for Blue Marlin, White Marlin, and Sailfish from the North-Atlantic Ocean. Bull. Mar. Sci. **56**(1): 201-210.

Praulai, C. 1998. Tuna Fisheries in then Eastern Indian Ocean, 1993-1998. Proceedings of the 7th Expert Consultation on Indian Ocean Tunas, Victoria, Seychelles, 9-14 November, 1998 **IOTC-1998-EC7-08**: 39-46.

Prince, E.D., Cowen, R.K., Orbesen, E.S., Luthy, S.A., Llopiz, J.K., Richardson, D.E., and Serafy, J.E. 2005. Movements and spawning of white marlin (*Tetrapturus albidus*) and blue marlin (*Makaira nigricans*) off Punta Cana, Dominican Republic. Fish. Bull. **103**(4): 659-669.

Prince, E.D., and Goodyear, C.P. 2006. Hypoxia-based habitat compression of tropical pelagic fishes. Fish. Oceanogr. **15**(6): 451-464.

Prince, E.D., Lee, D.W., Zweifel, J.R., and Brothers, E.B. 1991. Estimating age and growth of young Atlantic blue marlin, *Makaira nigricans*, from otolith microstructure. Fish. Bull. **89**: 441-459.

Proctor, C.H., Thresher, R.E., Gunn, J.S., Mills, D.J., Harrowfield, I.R., and Sie, S.H. 1995. Stock Structure of the Southern Bluefin Tuna *Thunnus maccoyii* - an Investigation Based on Probe Microanalysis of Otolith Composition. Mar. Biol. **122**(4): 511-526.

Punt, A.E., and Hilborn, R. 1997. Fisheries stock assessment and decision analysis: The Bayesian approach. Rev. Fish Biol. Fish. **7**(1): 35-63.

Quinn II, T.J., and Deriso, R. 1999. Quantitative fish dynamics. Oxford University Press, New York, New York.

R Development Core Team. 2008. R: A language and environment for statistical computing (v 2.8.0). R Foundation for Statistical Computing, Vienna, Austria. URL http://www.R-project.org.

Ramón, D., and Bailey, K. 1996. Spawning seasonality of albacore, *Thunnus alalunga*, in the South Pacific Ocean. Fish. Bull. **94**(4): 725-733.

Ravier, C., and Fromentin, J.M. 2001. Long-term fluctuations in the eastern Atlantic and Mediterranean bluefin tuna population. ICES J. Mar. Sci. **58**(6): 1299-1317.

Ravier, C., and Fromentin, J.M. 2002. Eastern Atlantic bluefin tuna: what we learnt from historical time-series of trap catches. Collective Volume of Scientific Papers ICCAT **54**: 507-516.

Reeb, C.A., Arcangeli, L., and Block, B.A. 2000. Structure and migration corridors in Pacific populations of the Swordfish *Xiphius gladius*, as inferred through analyses of mitochondrial DNA. Mar. Biol. **136**(6): 1123-1131.

Richards, W.J. 1976. Spawning of bluefin tuna (*Thunnus thynnus*) in the Atlantic Ocean and adjacent seas. Collective Volume of Scientific Papers ICCAT **5**(2): 267-278.

Ricker, W.E. 1975. Computation and interpretation of biological statistics of fish populatons. Fisheries Research Board of Canada **Bulletin No. 191**.

Roberts, C.M., Mason, L., and Hawkins, J.P. 2006. Roadmap to Recovery: A global network of marine reserves.

Roberts, P.E. 1980. Surface distribution of albacore tuna, *Thunnus alalunga* Bonnaterre, in relation to the Subtropical Convergence Zone east of New Zealand. N. Z. J. Mar. Freshwat. Res. **14**: 373-380.

Rodgveller, C.J., Lunsford, C.R., and Fujioka, J.T. 2008. Evidence of hook competition in longline surveys. Fish. Bull. **106**(4): 364-374.

Rose, G.A., and Kulka, D.W. 1999. Hyperaggregation of fish and fisheries: How catch-per-unit-effort increased as the northern cod (*Gadus morhua*) declined. Canadian Journal of Fisheries & Aquatic Sciences **56**(suppl. 1): 118-127.

Rose, G.A., and Leggett, W.C. 1991. Effects of Biomass Range Interactions on Catchability of Migratory Demersal Fish by Mobile Fisheries - an Example of Atlantic Cod (*Gadus morhua*). Can. J. Fish. Aquat. Sci. **48**(5): 843-848.

Ruzzante, D.E., Wroblewski, J.S., Taggart, C.T., Smedbol, R.K., Cook, D., and Goddard, S.V. 2000. Bay-scale population structure in coastal Atlantic cod in Labrador and Newfoundland, Canada. J. Fish Biol. **56**(2): 431-447.

Saito, H., and Yokawa, K. 2006. Use of pop-up tags to estimate vertical distribution of Atlantic blue marlin (*Makaira nigricans*) released from the commercial and research longline cruise during 2002 and 2003. Collective Volume of Scientific Papers ICCAT **59**(1): 252-264

Saito, S. 1973. Studies on fishing of albacore, *Thunnus alalunga* (Bonnaterre) by experimental deep-sea tuna longline. Mem. Fac. Fish. Hokkaido Univ. **21**: 107-184.

Sakagawa, G.T., and Bell, R.R. 1980. Swordfish, *Xiphias gladius*. In Shomura, R. S. (editor). 1980. Summary report of the billfish stock assessment workshop Pacific resources. U.S. Nat. Mar. Fish. Serv., NOAA-TM-NMFS-SWFC-5. 40-50.

Sanchirico, J.N., and Wilen, J.E. 1999. Bioeconomics of spatial exploitation in a patchy environment. J. Environ. Econ. Manage. **37**(2): 129-150.

Santiago, J. 1993. A new length-weight relationship for the North Atlantic albacore. Collective Volume of Scientific Papers ICCAT **XL**(2): 316-319.

Schaefer, K.M., and Fuller, D.W. 2002. Movements, behavior, and habitat selection of bigeye tuna (*Thunnus obesus*) in the eastern equatorial Pacific, ascertained through archival tags. Fish. Bull. **100**: 765-788.

Schaefer, K.M., and Fuller, D.W. 2005. Conventional and archival tagging of bigeye tuna (*Thunnus obesus*) in the eastern equitorial Pacific Ocean. Collective Volume of Scientific Papers ICCAT **57**(2): 67-84.

Schaefer, K.M., Fuller, D.W., and Block, B.A. 2007. Movements, behavior, and habitat utilization of yellowfin tuna (*Thunnus albacares*) in the northeastern Pacific Ocean, ascertained through archival tag data. Mar. Biol. **152**(3): 1432-1793.

Schaefer, K.M., Fuller, D.W., and Miyabe, N. 2005. Reproductive biology of bigeye tuna (*Thunnus obesus*) in the eastern and central Pacific Ocean. Bull. IATTC **23**(1): 1-33.

Schaefer, M.B. 1954. Some aspects of the dynamics of populations important to the management of commercial marine fisheries. Bull. IATTC **1**: 27–56.

Schaefer, M.B. 1955. Morphometric comparison of yellowfin tuna from southeast Polynesia, Central America, and Hawaii. Bull. IATTC **1**: 89-139.

Schaefer, M.B. 1957. A study of the dynamics of the fishery for yellowfin tuna in the Eastern Tropical Pacific Ocean. Bull. IATTC **2**: 245-285.

Schaefer, M.B. 1967. Fishery dynamics and present status of the yellowfin tuna population of the eastern Pacific Ocean. Bull. IATTC **12**(3): 87-139.

Schnute, J.T. 1987. Data, uncertainty, model ambiguity, and model identification. Nat. Resour. Model. **2**: 159-212.

Schnute, J.T., and Kronlund, A.R. 1996. A management oriented approach to stock recruitment analysis. Can. J. Fish. Aquat. Sci. **53**(6): 1281-1293.

Schnute, J.T., and Kronlund, A.R. 2002. Estimating salmon stock-recruitment relationships from catch and escapement data. Can. J. Fish. Aquat. Sci. **59**(3): 433-449.

Schnute, J.T., and Richards, L.J. 1998. Analytical models for fishery reference points. Can. J. Fish. Aquat. Sci. **55**(2): 515-528.

Serafy, J.E., Cowen, R.K., Paris, C.B., Capo, T.R., and Luthy, S.A. 2003. Evidence of blue marlin, *Makaira nigricans*, spawning in the vicinity of Exuma Sound, Bahamas. Marine and Freshwater Research **54**(4): 299-306.

Serafy, J.E., Kerstetter, D.W., and Rice, P.H. 2009. Can circle hook use benefit billfishes? Fish and Fisheries. **10**(2): 132-142.

Serventy, D.L. 1956. The southern bluefin tuna, *Thunnus thynnus maccoyii* (Castelnau), in Australian waters. Aust. J. Mar. Freshw. Res. **7**(1): 1-43.

Sharp, G.D. 1978. Behavioural and physiological properties of tunas and their effects on vulnerability to fishing gear. *In* The Physiological Ecology of Tunas. *Edited by* G.D. Sharp and A.E. Dizon. Academic Press, New York. pp. 397-449.

Shimada, B.M., and Schaefer, M.B. 1956. A study of changes in fishing effort, abundance, and yield for yellowfin and skipjack tuna in the Eastern Tropical Pacific Ocean. Bull. IATTC **1**(7): 350-469.

Shingu, C., Warashina, Y., and Matsuzaki, N. 1974. Distribution of bluefin tuna exploited by longline fishery in the western Pacific Ocean. Bull. Far Seas Fish. Res. Lab. **10**: 109-140.

Sibert, J., and Hampton, J. 2003. Mobility of tropical tunas and the implications for fisheries management. Mar. Policy **27**(1): 87-95.

Sibert, J., Hampton, J., Kleiber, P., and Maunder, M. 2006. Biomass, size, and trophic status of top predators in the Pacific Ocean. Science **314**(5806): 1773-1776.

Sibert, J.R., and Fournier, D.A. 1994. Evaluation of diffusion-advection equations for the estimation of movement patterns from tag recapture data. *In* Interactions of Pacific tuna fisheries. Proceedings of the First FAO Expert Consultation on Interaction of Pacific Tuna Fisheries, 31 December 1991, Noumea, New Caledonia. FAO Fish. Tech. Pap. No. 336/1. *Edited by* R.S. Shomura, J. Majkowski and S. Langi. pp. 108-121.

Sibert, J.R., Hampton, J., Fournier, D.A., and Bills, P.J. 1999. An advection-diffusion-reaction model for the estimation of fish movement parameters from tagging data, with application to skipjack tuna (*Katsuwonus pelamis*). Can. J. Fish. Aquat. Sci. **56**(6): 925-938.

Sibert, J.R., Musyl, M.K., and Brill, R.W. 2003. Horizontal movements of bigeye tuna (*Thunnus obesus*) near Hawaii determined by Kalman filter analysis of archival tagging data. Fish. Oceanogr. **12**(3): 141-151.

Sigler, M.F. 2000. Abundance estimation and capture of sablefish (*Anoplopoma fimbria*) by longline gear. Can. J. Fish. Aquat. Sci. **57**(6): 1270-1283.

Skillman, R.A., and Yong, M.Y.Y. 1976. Vonbertalanffy Growth-Curves for Striped Marlin, *Tetrapturus audax*, and Blue Marlin, *Makaira nigricans*, in Central North Pacific Ocean. Fish. Bull. **74**(3): 553-566.

SPC-OFP. 2006a. Estimates of annual catches in the WCPFC statistical area. Statistical Information paper, Western and Central Pacific Scientific Committee second regular session 7-18 August 2006 Manila, Philippines **WCPFC-SC2-2006/ST IP-1**: 26.

SPC-OFP. 2006b. Estimates of annual catches in the WCPFC statistical area. Western and Central Pacific Fisheries Commission Scientific committee second regular session 7-18 August 2006 Manila, Philippines **WCPFC-SC2-2006/ST IP-1**: 26.

SPC-OFP Database. 2006. Secretariat of the Pacific Community Oceanic Fisheries Programme public domain catch effort database. **updated October 2006** (accessed December 2006): http://www.spc.int/oceanfish.

Speare, P. 2003. Age and growth of black marlin, *Makaira indica*, in east coast Australian waters. Marine and Freshwater Research **54**(4): 307-314.

Squire, J.L., and Muhlia-Melo, A.F. 1993. A review of striped marlin (*Tetrapturus audax*), swordfish (*Xiphias gladius*), and sailfish (*Istiophorus platypterus*) fisheries and resource management by Mexico and the United States in the northeast Pacific Ocean. NMFS SWFSC Administrative Report **LJ-93-06**: 44.

Squire, J.L.J. 1974. Migration patterns of Istiophoridae in the Pacific Ocean as determined by cooperative tagging programs. In: Shomura, R.S. and Williams, F., (Eds.) Proceedings of the International Billfish Symposium Kailua-Kona, Hawaii, 9-12 August 1972. Part 2. Review and Contributed Papers. 226-235.

Squire, J.L.J., and Suzuki, Z. 1990. Migration trends of striped marlin (*Tetrapturus audax*) in the Pacific Ocean. In: Stroud, R.H., (Ed.) Planning the future of billfishes. Research and management in the 90's and beyond. Proceedings of the second international billfish symposium, Kailua-Kona, Hawaii, 1-5 August 1988. Part 2. Contributed papers.: 67-80.

Stamps, J.A. 2007. Growth-mortality tradeoffs and 'personality traits' in animals. Ecol. Lett. **10**(5): 355-363.

Stocker, M.E. 2005. Report of the Nineteenth North Pacific Albacore Workshop.Nineteenth North Pacific Albacore Workshop, Nanaimo, B.C., Canada, November 25-December 2, 2004. Fisheries and Oceans Canada, Pacific Biological Station, Nanaimo, B.C.: 127.

Sumaila, R.U., and Charles, A.T. 2002. Economic models of marine protected areas: an introduction. Nat. Resour. Model. **15**(3): 261-272.

Sun, C.L., Huang, C.L., and Yeh, S.Z. 2001. Age and growth of the bigeye tuna, *Thunnus obesus*, in the western Pacific Ocean. Fish. Bull. **99**(3): 502-509.

Sun, C.L., Wang, S.P., and Yeh, S.Z. 2002. Age and growth of the swordfish (*Xiphias gladius L.*) in the waters around Taiwan determined from anal-fin rays. Fish. Bull. **100**(4): 822-835.

Susca, V., Corriero, A., Bridges, C.R., and De Metrio, G. 2001. Study of the sexual maturity of female bluefin tuna: purification and partial characterization of vitellogenin and its use in an enzyme-linked immunosorbent assay. J. Fish Biol. **58**(3): 815-831.

Suzuki, Z. 1994. A review of the biology and fisheries for Yellowfin tuna (*Thunnus albacares*) in the western and central Pacific Ocean. In: Shomura RS, Majkowski J, Langi S, editors. Interactions of Pacific tuna fisheries. Proceedings of the First FAO Expert Consultation on Interactions of Pacific Tuna Fisheries; 1991 Dec 3-11; Noumea, New Caledonia **Volume 2**: 108-137.

Suzuki, Z., Tomlinson, P.K., and Honma, M. 1978. Population structure of Pacific Yellowfin tuna. Bull. IATTC **17**: 273–441.

Suzuki, Z., Warashina, Y., and Kishida, M. 1977. The comparison of catches by regular and deep tuna longline gears in the Western and Central Equitorial Pacific. Bull. Far Seas Fish. Res. Lab. **15**: 51-89.

Swain, D.P., and Sinclair, A.F. 1994. Fish Distribution and Catchability - What Is the Appropriate Measure of Distribution. Can. J. Fish. Aquat. Sci. **51**(5): 1046-1054.

Swain, D.P., and Wade, E.J. 2003. Spatial distribution of catch and effort in a fishery for snow crab (*Chionoecetes opilio*): tests of predictions of the ideal free distribution. Can. J. Fish. Aquat. Sci. **60**(8): 897-909.

Takahashi, M., Okamura, H., Yokawa, K., and Okazaki, M. 2003. Swimming behaviour and migration of a swordfish recorded by an archival tag. Marine and Freshwater Research **54**(4): 527-534.

Takeuchi, Y. 2007a. Estimation of quarterly catch of Japanese tuna purse seine operating in the north western Pacific and Sea of Japan catching medium to large bluefin tuna. ISC Working Paper **ISC/07/PBF-1/10**.

Takeuchi, Y. 2007b. Recalculation of length frequency data from Japanese tuna Purse Scene operating north western Pacific and Sea of Japan for use of Stock Synthesis II application. ISC Working Paper **ISC/07/PBF-1/08**.

Takeuchi, Y., and Takahashi, M. 2006. Estimates of natural mortality of age 0 Pacific bluefin tuna from conventional tagging data. ISC Meeting Report **ISC/06/PBF-WG/07**: 1-6.

Teo, S.L.H., Boustany, A., Dewar, H., Stokesbury, M.J.W., Weng, K.C., Beemer, S., Seitz, A.C., Farwell, C.J., Prince, E.D., and Block, B.A. 2007. Annual migrations, diving behavior, and thermal biology of Atlantic bluefin tuna, *Thunnus thynnus*, on their Gulf of Mexico breeding grounds. Mar. Biol. **151**(1): 1-18.

Thorogood, J. 1987. Age and growth-rate determination of southern bluefin tuna, *Thunnus maccoyii*, using otolith banding. J. Fish Biol. **30**(1): 7-14.

Tserpes, G., and Tsimenides, N. 1995. Determination of Age and Growth of Swordfish, *Xiphias gladius* L, 1758, in the Eastern Mediterranean Using Anal-Fin Spines. Fish. Bull. **93**(3): 594-602.

Tsuji, S. 2007. Overview of existing data collection and monitoring mechanisms for tuna stock and fisheries management. Report of the Joint Meeting of Tuna RFMOs January 22-26, 2007 Kobe, Japan(TunaRFMOs2007/5): 30-36.

Turner, S.C., and Restrepo, V.R. 1994. A review of the growth rate of West Atlantic bluefin tuna, *Thunnus thynnus*, estimated from marked and recaptured fish. Collective Volume of Scientific Papers ICCAT **42**(1): 170-172.

Tyler, J.A., and Rose, K.A. 1994. Individual Variability and Spatial Heterogeneity in Fish Population-Models. Rev. Fish Biol. Fish. **4**(1): 91-123.

Uda, M. 1957. A consideration on the log years trend of the fisheries fluctuation in relation to sea consditions. Bull. Jap. Soc. Sci. Fish. **23**(7-8): 368-372.

Ueyanagi, S. 1969. Observations on the distribution of tuna larva in the Indo-Pacific Ocean with emphasis on the deliniation of spawning areas of albacore, *Thunnus alalunga*. Bull. Far Seas Fish. Res. Lab. **2**: 117-219.

Ueyanagi, S., and Wares, P.G. 1975. Synopsis of biological data on striped marlin, *Tetrapturus audax* (Philippi, 1887). In: Shomura, R.S. and Williams, F., (Eds.) Proceedings of the international billfish symposium, Kailua-Kona, Hawaii, 9-12 August 1972, Part 3. Species synopses. 132-159.

Uozumi, Y. 2003. Historical perspective of global billfish stock assessment. Marine and Freshwater Research **54**(4): 555-565.

Vanpouille, K., Poisson, F., Taquet, M., Ogor, A., and Troadec, H. 2001. Atelier de travail sur les poissons a rostre Commision Thoniere de l'Ocean Indien etude de la croissance de l'espadon (*Xiphias gladius*). IOTC Proceedings no. 4 **WPB01-06**: 126-143.

Walters, C. 2003. Folly and fantasy in the analysis of spatial catch rate data. Can. J. Fish. Aquat. Sci. **60**(12): 1433-1436.

Walters, C., and Ludwig, D. 1994. Calculation of Bayes Posterior Probability-Distributions for Key Population Parameters. Can. J. Fish. Aquat. Sci. **51**(3): 713-722.

Walters, C., Pauly, D., and Christensen, V. 1999. Ecospace: prediction of mesoscale spatial patterns in trophic relationships of exploited ecosystems, with emphasis on the impacts of marine protected areas. Ecosystems **2**(6): 539-554.

Walters, C.J., and Bonfil, R. 1999. Multispecies spatial assessment models for the British Columbia groundfish trawl fishery. Can. J. Fish. Aquat. Sci. **56**(4): 601-628.

Walters, C.J., Christensen, V., Martell, S.J., and Kitchell, J.F. 2005. Possible ecosystem impacts of applying MSY policies from single-species assessment. ICES J. Mar. Sci. **62**(3): 558-568.

Walters, C.J., and Hilborn, R. 2005. Exploratory assessment of historical recruitment patterns using relative abundance and catch data. Can. J. Fish. Aquat. Sci. **62**(9): 1985-1990.

Walters, C.J., and Martell, S.J.D. 2004. Fisheries ecology and management. Princeton University Press, Princeton, NJ.

Walters, C.J., Martell, S.J.D., and Korman, J. 2006. A stochastic approach to stock reduction analysis. Can. J. Fish. Aquat. Sci. **63**(1): 212-223.

Wang, C.-H. 1988. Seasonal changes of the distribution of South Pacific albacore based on Taiwan's tuna longline fisheries, 1971-1985. Nat.Taiwan Univ.Sci.Rep.Acta Oceanogr.Taiwanica **20**: 13-40.

Wang, S.P., Sun, C.L., and Yeh, S.Z. 2003. Sex ratios and sexual maturity of swordfish (*Xiphias gladius* L.) in the waters of Taiwan. Zool. Stud. **42**(4): 529-539.

Wang, S.P., Sun, C.L., Yeh, S.Z., Chiang, W.C., Su, N.J., Chang, Y.J., and Liu, C.H. 2006. Length distributions, weight-length relationships, and sex ratios at lengths for the billfishes in taiwan waters. Bull. Mar. Sci. **79**(3): 865-869.

Ward, P., and Hindmarsh, S. 2007. An overview of historical changes in the fishing gear and practices of pelagic longliners, with particular reference to Japan's Pacific fleet. Rev. Fish Biol. Fish. **17**(4): 501-516.

Ward, P., and Myers, R.A. 2005a. Inferring the depth distribution of catchability for pelagic fishes and correcting for variations in the depth of longline fishing gear. Can. J. Fish. Aquat. Sci. **62**(5): 1130-1142.

Ward, P., and Myers, R.A. 2005b. Shifts in open-ocean fish communities coinciding with the commencement of commercial fishing. Ecology **86**(4): 835-847.

WCPFC. 2008. The Commission for the Conservation and Management of Highly Migratory Fish Stocks in the Western and Central Pacific Ocean. Scientific Committee Fourth Regular Session, 11-22 August 2008, Port Moresby, Papua New Guinea Summary Report. 266.

Whitelaw, W. 2003. Recreational billfish catches and gamefishing facilities of Pacific Island nations in the Western and Central Pacific Ocean. Marine and Freshwater Research **54**(4): 463-471.

Wild, A. 1986. Growth of yellowfin tuna, *Thunnus albacares*, in the eastern Pacific Ocean based on otolith increments. Bull. IATTC **18**: 421-482.

Wild, A. 1994. A review of the biology and fisheries for Yellowfin tuna (*Thunnus albacares*) in the eastern Pacific Ocean. In: Shomura RS, Majkowski J, Langi S, editors. Interactions of Pacific tuna fisheries. Proceedings of the First FAO Expert Consultation on Interactions of Pacific Tuna Fisheries; 1991 Dec 3-11; Noumea, New Caledonia **Volume 2**: 52-107.

Wilson, C.A., and Dean, J.M. 1983. The potential use of sagittae for estimating age of Atlantic swordfish, *Xiphias gladius*. In Prince, E.D. and Pulos, L.M. (eds) Proceedings of the International Workshop on Age Determination of Oceanic Pelagic Fishes: Tunas, Billfishes and Sharks. NOAA Tech. Rep. NMFS **8**: 151-156.

Wilson, S.G., Lutcavage, M.E., Brill, R.W., Genovese, M.P., Cooper, A.B., and Everly, A.W. 2005. Movements of bluefin tuna (*Thunnus thynnus*) in the northwestern Atlantic Ocean recorded by pop-up satellite archival tags. Mar. Biol. **146**(2): 409-423.

Worm, B., Barbier, E.B., Beaumont, N., Duffy, J.E., Folke, C., Halpern, B.S., Jackson, J.B.C., Lotze, H.K., Micheli, F., Palumbi, S.R., Sala, E., Selkoe, K.A., Stachowicz, J.J., and Watson, R. 2006. Impacts of biodiversity loss on ocean ecosystem services. Science **314**(5800): 787-790.

Worm, B., Hilborn, R., Baum, J.K., Branch, T.A., Collie, J.S., Costello, C., Fogarty, M.J., Fulton, E.A., Hutchings, J.A., Jennings, S., Jensen, O.P., Lotze, H.K., Mace, P.M., McClanahan, T.R., Minto, C., Palumbi, S.R., Parma, A.M., Ricard, D., Rosenberg, A.A., Watson, R., and Zeller, D. 2009. Rebuilding Global Fisheries. Science **325**(5940): 578-585.

Worm, B., Lotze, H.K., and Myers, R.A. 2003. Predator diversity hotspots in the blue ocean. Proceedings of the National Academy of Sciences of the United States of America **100**(17): 9884-9888.

Worm, B., Sandow, M., Oschlies, A., Lotze, H.K., and Myers, R.A. 2005. Global patterns of predator diversity in the open oceans. Science **309**(5739): 1365-1369.

Yabuta, Y., Yukinawa, M., and Warshuna, Y. 1960. Growth and age of yellowfin tuna II. Age determination (scale method). Rep. Nankai Reg. Fish. Res. Lab. **12**: 63-74.

Yamanaka, H. 1963. Synopsis of biological data on kuromaguro *Thunnus orientalis* (Temminck and Schlegel) 1842 (Pacific Ocean). in Rosa, H. (ed.). Proceedings of the world scientific meeting on the biology of tuna and related species. FAO Fish. Rep. **6**(2): 180-217.

Yesaki, M. 1983. Observations on the biology of yellowfin (*Thunnus albacares*) and skipjack (*Katsuwonus pelamis*) tunas in Philippine waters. IPTP Rep. **IPTP/83/WP/7**: 66.

Yukinawa, M. 1970. Age and growth of southern bluefin tuna *Thunnus maccoyii* (Castelnau) by use of scales. Bull. Far Seas Fish. Res. Lab. **3**: 229-257.

Yukinawa, M., and Yabuta, Y. 1967. Age and growth of the bluefin tuna, *Thunnus thynnus* (Linnaeus), in the North Pacific Ocean. Rep. Nankai Reg. Fish. Res. Lab. **25**: 1-28.

Appendix for Chapter 2

Table 8.1 Proportion (p) of nominal catch reported spatially by longline fleets in the Atlantic Ocean. Fleet ID. was assigned to facilitate plotting and corresponds to the ICCAT fleet ID in the ICCAT task II database.

Fleet ID	ICCAT ID	ICCAT Fleet	p	Fleet ID	ICCAT ID	ICCAT Fleet	p
1	1	Algerie	0.00	54	71	EC.Italy (Ligurian sea)	0.00
2	2	Argentina	0.60	55	72	EC.Italy (Sardenha)	0.00
3	3	Brazil (Barbados)	0.00	56	73	EC.Italy (Tyrrhenian sea)	0.00
4	4	Brazil (Bolivia)	0.00	57	76	Japan	0.95
5	5	Brazil (Bolivia - Natal)	1.00	58	77	Korea, Republic of	0.33
6	6	Brazil	0.40	59	78	Libya	0.23
7	8	Brazil (based in Itajai)	0.77	60	79	EC.Malta	0.16
8	9	Brazil (based in Cabedelo)	1.00	61	80	Maroc	0.00
9	10	Brazil (based in Natal)	0.08	62	81	Norway	0.50
10	11	Brazil (based in Rio Grande)	0.75	63	82	EC.Poland	0.00
11	12	Brazil (based in Santos)	0.01	64	83	EC.Portugal	0.75
12	14	Brazil (Belize)	0.73	65	84	EC.Portugal (Mainland based)	0.14
13	15	Brazil (Canada)	0.03	66	85	EC.Portugal (Azores based)	5.11
14	16	Brazil (Canada - Natal)	0.22	67	86	EC.Portugal (Madeira based)	19.40
15	17	Brazil (España)	0.75	68	88	South Africa (Korea)	4.98
16	18	Brazil (España - Cabedelo)	0.39	69	89	South Africa (Namibia)	1.81
17	19	Brazil (España - NATAL)	0.01	70	91	South Africa (Seychelles)	0.00
18	20	Brazil (Eq. Guinea)	0.99	71	92	South Africa (St. Vincent)	2.33
19	21	Brazil (Guyan)	0.53	72	93	South Africa	0.11
20	22	Brazil (Guyan - Natal)	0.00	73	94	EC.España	0.60
21	23	Brazil (Honduras)	0.44	74	97	EC.España (Coruña based)	1.00
22	25	Brazil (Honduras - Cabedelo)	0.11	75	103	Tunisie	0.11
23	26	Brazil (Honduras - Natal)	0.03	76	106	U.S.A.	0.42
24	27	Brazil (Honduras - Santos)	0.23	77	113	Panama	0.00
25	28	Brazil (Iceland)	1.03	78	114	Venezuela	0.28
26	29	Brazil (Iceland - Natal)	0.12	79	115	Venezuela (foreign based)	1.05
27	30	Brazil (Japan)	0.92	80	116	Grenada	0.44
28	31	Brazil (Korea)	0.34	81	117	Mexico	1.61
29	33	Brazil (Panama)	0.43	82	119	U.S.S.R.	0.32
30	35	Brazil (Panama - Cabedelo)	0.39	83	123	Sierra Leone	0.41
31	36	Brazil (Panama - Natal)	0.24	84	124	Trinidad and Tobago	0.00
32	37	Brazil (Portugal)	0.93	85	125	Trinidad & Tobago (Trinidad)	1.00
33	38	Brazil (Portugal-Cabedelo)	1.00	86	127	Uruguay	0.39
34	39	Brazil (Taipei)	0.84	87	130	EC.Cyprus	0.49
35	40	Brazil (USA)	0.70	88	141	Sta. Helena	1.00
36	41	Brazil (USA - Natal)	0.29	89	143	Barbados	0.00
37	42	Brazil (Uruguay)	0.86	90	145	Cape Verde	1.00
38	43	Brazil (Uruguay - Itajai)	1.34	91	146	EC.Ireland	0.00
39	44	Brazil (Uruguay - Cabedelo)	0.34	92	157	Guinea Ecuatorial	0.00
40	45	Brazil (St. Vincent)	0.59	93	159	UK.Bermuda	0.00
41	47	Brazil (Vanuatu)	0.15	94	164	Croatia	0.00
42	49	Canada	0.29	95	168	St. Vincent and Grenadines	0.21
43	50	Canada (Japan)	0.00	96	169	EC.United Kingdom	0.00
44	51	Chinese Taipei	0.75	97	170	Namibia	0.01
45	52	Cuba	0.50	98	174	China, People's Republic of	0.79
46	54	EC.France	0.00	99	186	Iceland	4.36
47	61	EC.Greece	0.11	100	188	Faroe Islands	0.13
48	62	EC.Italy	0.11	101	189	Philippines	0.71
49	64	EC.Italy (Strait of Sicily)	1.00	102	190	Philippines (based in Manila)	1.00
50	65	EC.Italy (Adriatic sea)	0.00	103	191	Cambodia	0.00
51	67	EC.Italy (South Adriatic sea)	0.00	104	193	FR-Saint Pierre et Miquelon	0.00
52	69	EC.Italy (North Ionian sea)	0.12	105	196	Seychelles	0.00
53	70	EC.Italy (South Ionian sea)	0.00				

Table 8.2 Proportion (p) of nominal catch reported spatially by longline fleets in the Indian Ocean. Fleet ID. was assigned to facilitate plotting and corresponds to the IOTC fleet ID in the IOTC task II database.

Fleet ID	IOTC ID	IOTC Fleet	p	Fleet ID	IOTC ID	IOTC Fleet	p
1	AUS	Australia	0.47	15	OMN	Oman	1.00
2	CHN	China	0.71	16	PAK	Pakistan	0.00
3	TWN	Taiwan,China	0.87	17	PHL	Philippines	0.63
4	FRA	France	0.00	18	PRT	Portugal	0.00
5	FRA-REU	France-Reunion	0.80	19	SYC	Seychelles	0.33
6	GIN	Guinea	1.00	20	ZAF	South Africa	0.94
7	IND	India	1.16	21	SUN	Soviet Union	0.00
8	IDN	Indonesia	0.00	22	ESP	Spain	0.80
9	IRN	Iran, Islamic Republic	0.00	24	THA	Thailand	0.00
10	JPN	Japan	0.98	26	NEI-OTH	NEI-Other	0.00
11	KOR	Korea, Republic of	0.57	28	NEI-DFRZ	NEI-Deep-freezing	0.00
12	MYS	Malaysia	0.00	29	NEI-ICE	NEI-Fresh Tuna	0.00
13	MDV	Maldives	0.00	30	KEN	Kenya	0.00
14	MUS	Mauritius	0.15	32	URY	Uruguay	0.00

Table 8.3 Estimated total landings (number in thousands) of longline vulnerable individuals caught by all gears combined, for the stocks as defined in this study.

Year	GBLM	IALB	IBET	IYFT	GSBT	IBUM	ISTM	ISWO
1950	0.00	0.22	0.00	56.13	0.00	0.00	0.00	0.00
1951	0.00	0.22	0.00	68.03	0.00	0.00	0.00	0.00
1952	22.81	3.46	5.24	139.66	6.08	5.76	2.37	0.09
1953	47.08	56.93	30.15	206.45	49.33	19.79	6.59	0.73
1954	70.00	145.38	124.98	516.53	30.77	45.94	21.41	3.59
1955	50.50	169.51	171.49	1029.40	25.78	50.96	20.49	5.49
1956	80.62	283.32	281.67	1285.14	120.56	74.96	47.93	12.04
1957	96.89	264.52	221.61	797.83	417.60	57.80	52.02	10.38
1958	90.45	349.22	208.48	637.77	226.15	64.48	51.42	14.67
1959	77.38	585.98	191.42	707.98	1003.46	67.98	66.65	13.66
1960	85.69	629.29	304.93	1039.21	1189.44	59.83	59.65	17.59
1961	90.85	836.41	298.69	988.07	1210.73	52.65	72.18	21.31
1962	95.32	1081.94	425.99	1421.18	632.73	50.63	52.54	26.68
1963	80.45	805.33	293.75	830.23	968.34	33.82	46.35	23.87
1964	77.01	1089.44	363.22	787.69	722.15	51.26	53.92	27.73
1965	82.05	715.85	413.49	960.61	722.52	55.47	91.59	29.27
1966	79.52	878.75	513.23	1416.57	684.15	53.50	113.17	32.27
1967	69.14	1537.83	581.13	1188.18	933.62	60.13	121.20	43.95
1968	79.59	1154.70	879.47	3080.08	832.35	51.53	86.01	41.88
1969	79.51	1412.69	790.21	1998.71	845.91	46.85	104.68	47.64
1970	79.14	790.21	700.60	1240.98	705.01	51.65	89.49	52.78
1971	67.00	783.00	559.17	1640.88	698.19	42.77	50.42	43.70
1972	54.36	755.17	482.50	1309.17	803.55	43.37	44.88	41.46
1973	46.53	1575.60	427.76	948.80	651.52	26.21	30.11	30.00
1974	53.07	1840.03	700.46	1042.33	673.27	30.50	68.11	38.66
1975	50.34	654.43	950.74	1118.23	539.40	37.86	53.12	44.91
1976	29.36	1065.38	767.48	1088.12	687.55	31.41	69.50	36.68
1977	28.70	848.53	947.48	1935.73	555.31	26.10	94.91	34.98
1978	36.93	1266.67	1215.48	1538.95	533.20	47.48	162.95	47.62
1979	44.97	1284.51	877.37	1405.66	540.77	37.87	91.97	49.38
1980	39.69	956.24	898.05	1306.29	617.14	36.23	118.09	47.54
1981	46.78	1002.59	869.29	1208.46	550.00	39.15	141.18	52.02
1982	47.16	1731.74	1105.87	1530.16	405.41	51.77	78.57	68.30
1983	56.37	1386.60	1194.52	1621.39	488.82	63.82	93.01	81.92
1984	47.07	1263.05	1050.00	2517.57	408.75	62.68	90.70	76.46
1985	42.32	728.22	1197.42	2937.34	352.86	62.82	113.85	103.41
1986	42.06	1641.83	1286.74	3519.80	274.59	86.66	167.21	128.12
1987	55.87	1633.48	1436.48	3836.14	258.38	97.66	130.37	142.86
1988	64.26	1669.33	1590.09	5087.46	206.60	76.94	99.00	217.57
1989	43.34	1283.96	1514.81	4922.90	239.66	65.75	80.47	173.51
1990	42.80	1406.44	1651.42	5840.58	197.67	59.94	43.94	178.39
1991	50.75	1595.20	1928.51	5593.79	241.98	64.73	84.14	179.95
1992	55.65	2026.40	1825.14	7363.75	265.32	86.62	65.40	281.05
1993	52.35	2177.16	2302.69	10220.92	309.08	102.54	132.01	418.57
1994	57.14	1807.92	2398.11	7815.01	238.87	103.72	122.47	450.06
1995	47.14	1589.16	2400.34	7834.71	218.11	86.92	106.17	510.63
1996	40.18	2104.54	2659.84	7876.91	224.36	103.76	106.11	529.59
1997	55.64	2098.12	2934.82	7699.62	217.25	134.56	80.45	538.28
1998	63.01	2743.71	3057.79	7132.72	265.40	137.34	84.50	606.70
1999	61.00	2541.59	3407.57	8363.96	269.24	159.88	82.91	565.10
2000	58.63	2721.98	2976.49	7718.00	228.78	126.60	60.87	557.14
2001	47.32	2733.84	2614.14	7293.77	258.85	85.96	49.51	485.80
2002	54.01	2136.79	3010.80	7638.49	231.54	102.03	51.86	587.88

continued on next page

Year	PNAB	PSAB	PBET	PYFT	PBFT	PBUM	PSTM	PSWO
1950	1896.97	267.53	13.73	97.55	32.59	23.28	0.10	65.94
1951	1757.85	132.71	51.74	138.86	32.59	35.98	0.24	66.38
1952	3984.30	217.35	751.77	662.80	56.60	172.75	115.42	243.04
1953	3368.11	199.92	701.55	904.02	45.97	191.96	96.94	253.65
1954	2675.32	743.12	511.57	834.82	47.24	124.48	200.50	283.23
1955	2342.47	687.40	798.60	789.67	82.74	171.42	149.85	295.61
1956	2980.23	644.91	923.78	928.40	111.87	151.58	172.75	320.17
1957	3633.79	779.77	1298.35	1714.36	87.31	242.04	162.94	315.03
1958	2436.17	1365.00	1638.59	1794.92	44.49	237.28	219.56	414.18
1959	2319.46	1354.39	1506.67	2495.58	76.38	209.93	213.79	383.43
1960	2699.13	1619.91	1697.23	4527.30	96.20	195.37	191.22	445.16
1961	2312.96	1693.52	2153.98	4922.26	93.07	294.40	245.31	442.60
1962	2141.97	2486.15	1971.38	4160.97	91.66	319.95	316.22	268.30
1963	2842.62	2226.44	2575.40	4110.87	86.10	323.44	369.54	258.50
1964	2550.45	1658.51	1812.62	4525.19	59.07	233.58	541.27	205.00
1965	2731.58	1595.39	1431.06	4244.57	66.38	183.08	458.71	252.67
1966	2883.34	2524.21	1607.45	4736.63	51.14	173.38	374.47	284.24
1967	3570.37	2461.79	1672.90	3665.08	34.01	160.69	431.17	269.88
1968	2987.33	1829.07	1473.17	4652.89	45.44	144.77	523.52	300.78
1969	2934.30	1715.00	1916.60	5588.92	17.63	167.64	362.60	361.33
1970	2617.99	2099.40	1437.96	6223.71	15.07	205.02	474.49	298.23
1971	3165.64	2287.71	1428.78	4991.25	20.36	130.38	427.49	205.57
1972	3687.54	2424.08	1859.27	7420.17	21.83	156.20	288.93	197.71
1973	3474.89	2799.30	1842.55	8016.84	13.25	163.09	291.13	226.37
1974	3709.38	2423.21	1660.40	7580.36	20.30	154.32	290.19	226.61
1975	2833.45	1268.62	1817.69	7264.07	23.62	116.15	285.14	269.16
1976	4010.08	1596.19	2579.99	8684.48	12.26	141.68	260.31	327.98
1977	2135.24	2274.85	2939.40	7565.03	27.63	148.59	185.11	298.60
1978	3295.65	2464.92	2776.48	8017.98	57.71	157.99	210.36	333.56
1979	2379.03	1690.56	2694.74	8283.11	72.37	159.29	244.45	269.91
1980	2459.87	2049.80	2822.71	8015.51	54.15	171.72	263.25	289.80
1981	2592.25	2452.95	2382.95	8305.63	72.92	189.63	299.02	345.18
1982	2381.00	2007.83	2316.28	6788.03	55.55	174.23	284.76	306.30
1983	1853.00	1893.33	2366.53	7111.37	42.55	157.16	210.94	307.40
1984	2687.56	1515.83	2329.94	8362.85	13.15	201.30	189.47	313.01
1985	2010.17	1864.96	2904.17	10034.34	12.07	176.66	194.50	369.26
1986	1449.90	2324.33	3226.04	10467.00	21.41	206.42	288.92	377.39
1987	1473.00	1762.31	3352.94	11979.55	24.61	212.15	334.00	415.02
1988	1308.81	2352.12	2604.66	11142.67	10.99	217.62	327.11	390.87
1989	1249.87	1791.36	2616.38	12424.23	17.43	176.06	225.50	334.84
1990	1417.89	1434.95	3349.43	12814.09	9.87	176.51	160.89	341.49
1991	1128.90	1685.68	3300.65	12334.24	19.75	218.54	179.28	307.00
1992	1631.01	2504.15	3109.12	13910.41	22.67	181.90	173.59	354.77
1993	1642.59	2199.31	2655.36	13407.98	29.84	192.41	206.05	334.37
1994	2275.83	2611.12	3598.69	12963.08	34.03	254.59	207.31	300.02
1995	2300.99	1995.19	3160.73	12536.66	24.01	243.23	203.34	258.80
1996	2490.58	1949.17	3241.29	11322.04	24.63	171.55	176.78	272.93
1997	2772.84	2339.82	3734.84	14244.17	28.74	183.36	196.72	330.67
1998	2457.94	2819.13	3479.26	15060.44	15.08	207.57	157.82	380.20
1999	3371.96	2237.47	3358.71	13690.45	51.06	199.02	136.49	332.65
2000	2346.86	2356.58	4288.33	14271.96	36.56	190.19	102.35	403.54
2001	2337.91	3279.35	3905.68	17326.33	15.06	221.79	105.04	393.04
2002	2803.87	3831.18	3666.69	17365.56	18.81	206.49	99.00	310.82

continued on next page

Year	ANAB	ASAB	ABET	AYFT	ABFT	ABUM	AWHM	ASWO
1950	650.99	0.00	9.80	15.60	95.97	0.00	0.00	32.96
1951	561.05	0.00	20.03	17.65	112.04	0.00	0.00	26.00
1952	532.27	0.00	24.48	36.23	146.27	0.00	0.00	31.90
1953	557.89	0.00	35.79	46.79	146.64	0.00	0.00	32.94
1954	774.87	0.00	35.56	44.29	137.61	0.00	0.00	40.52
1955	567.15	0.00	58.31	54.63	154.29	0.00	0.00	42.73
1956	761.48	1.06	33.78	53.71	104.31	0.50	0.01	60.17
1957	884.62	31.47	108.90	337.11	131.00	8.70	0.83	76.13
1958	1142.08	89.42	61.36	869.74	129.64	9.97	1.36	94.42
1959	1142.89	400.91	120.68	1286.84	100.44	22.61	6.78	107.23
1960	1171.95	503.78	146.00	1359.70	100.46	27.96	13.38	75.96
1961	1048.00	486.89	262.93	1073.82	116.16	44.80	40.65	107.87
1962	1465.21	891.23	418.71	1105.20	177.71	112.97	117.94	135.55
1963	1614.39	631.41	376.02	1134.76	156.02	97.83	88.72	257.64
1964	1932.45	1169.91	385.16	1209.23	155.88	86.72	171.24	290.92
1965	1628.16	732.49	668.13	1190.06	144.70	47.34	136.87	259.15
1966	1279.63	752.01	309.92	834.24	102.40	25.94	106.90	259.98
1967	1467.95	740.98	388.77	994.85	107.01	19.01	68.46	262.77
1968	1365.53	871.50	405.51	1364.87	67.79	24.85	81.28	305.63
1969	1199.49	1652.17	594.10	1574.97	71.80	32.95	77.03	370.82
1970	1474.47	1828.29	750.65	1422.37	64.91	28.87	82.09	386.39
1971	1560.77	1742.37	1194.21	1455.87	73.56	37.38	83.55	361.04
1972	1653.73	2168.99	838.12	1762.43	63.25	21.13	84.31	254.83
1973	1990.39	1249.61	955.65	1675.52	64.17	30.50	80.49	258.62
1974	1761.86	1082.60	1083.79	1740.12	125.57	28.18	69.91	248.86
1975	1750.69	809.23	1131.68	2047.92	127.97	36.97	75.82	264.12
1976	2592.75	1004.83	781.28	2020.36	138.19	22.26	62.24	275.34
1977	2352.03	1076.60	905.30	2165.68	127.75	17.25	38.27	241.47
1978	1921.36	1203.87	849.37	2158.03	91.99	14.79	27.46	391.58
1979	1954.12	1085.28	747.98	1975.62	85.85	12.86	32.75	456.16
1980	1559.51	1132.59	1096.53	2065.39	95.53	16.24	42.43	515.83
1981	1370.05	1128.53	1139.83	2467.39	105.33	19.81	50.49	411.36
1982	1876.36	1304.12	1292.74	2537.06	110.91	25.14	37.15	602.43
1983	2037.03	712.79	1001.68	2519.81	115.50	20.39	74.46	594.90
1984	1624.28	742.04	1169.38	1729.62	118.81	29.07	45.29	702.82
1985	1970.00	1223.95	1396.40	2374.72	121.05	32.66	63.42	984.69
1986	2381.10	1531.75	1114.80	2298.06	99.26	23.25	68.52	888.63
1987	1782.25	1756.99	992.57	2215.52	99.81	20.22	55.76	893.62
1988	1383.90	1170.73	1136.61	2124.67	130.31	29.34	51.33	1255.15
1989	1058.58	1232.75	1341.93	2484.15	103.39	44.51	73.25	1164.83
1990	1134.02	1551.54	1441.77	2857.84	121.75	44.22	56.38	942.88
1991	984.36	1293.96	1627.28	2608.04	133.78	40.51	56.19	900.69
1992	892.84	1916.82	1532.31	2401.78	157.17	25.14	41.16	988.52
1993	1408.32	1550.81	1700.15	2304.41	169.22	31.43	63.06	1128.78
1994	1424.11	1500.41	1862.70	2512.55	257.89	39.87	58.42	1155.04
1995	1380.16	969.98	1605.51	2195.22	262.26	29.44	53.33	1300.62
1996	1029.81	1430.20	1605.62	2140.33	261.67	46.44	59.59	1217.85
1997	1018.72	1182.51	1482.42	1924.77	267.41	46.09	46.25	1347.77
1998	1088.12	1155.78	1426.13	2016.83	197.32	42.81	43.22	1331.26
1999	1477.78	1052.48	1585.36	1984.80	192.23	41.89	43.02	1416.23
2000	1534.11	1297.35	1566.34	1945.10	198.35	37.15	25.62	1474.33
2001	1541.68	1748.73	1380.47	2313.00	201.66	33.26	27.90	1397.83
2002	1091.97	1461.87	1226.40	2024.52	208.25	22.86	31.97	1199.58

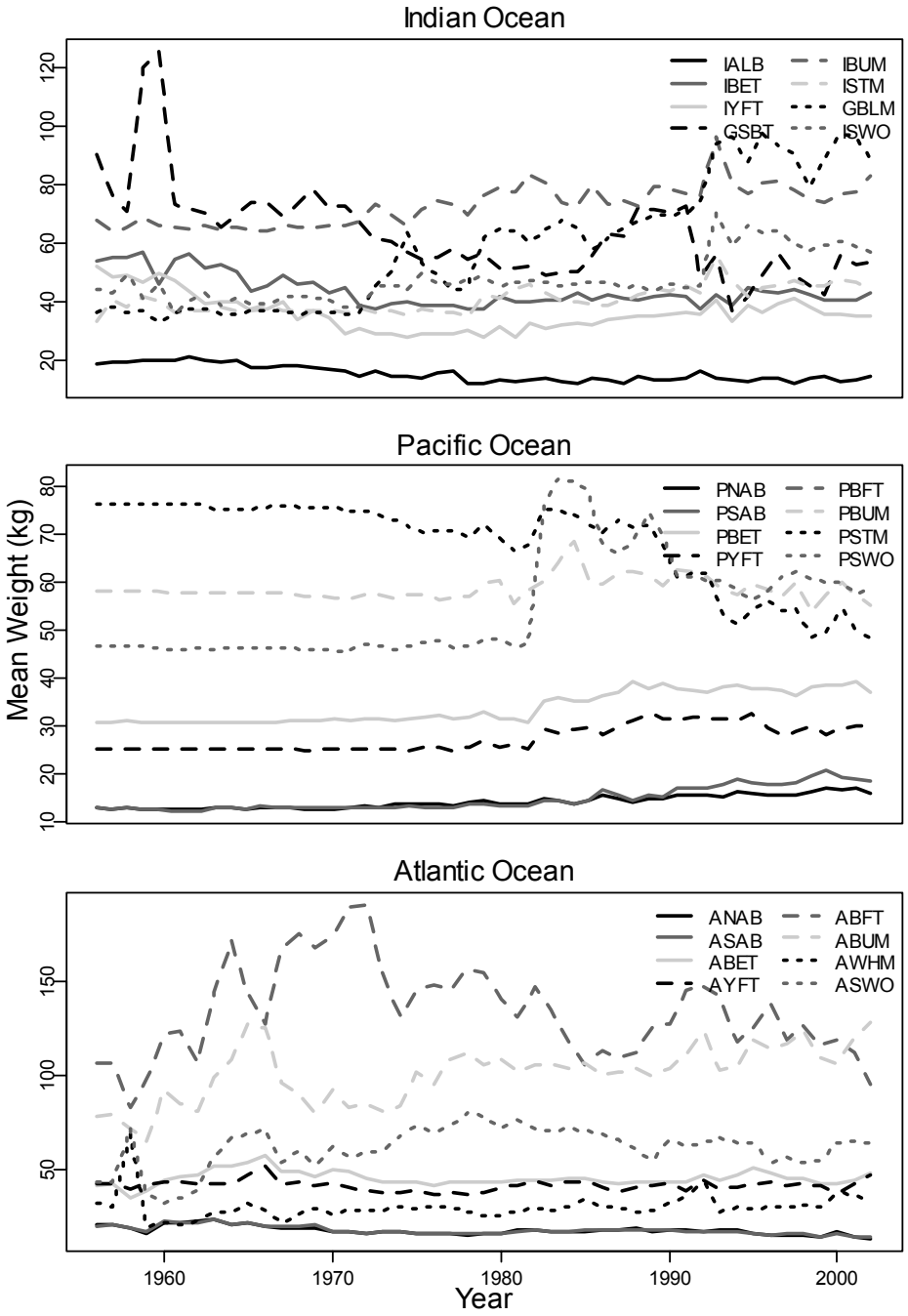

Figure 8.1Estimated mean weight (kg) of species caught by longline in each ocean. Indian and Pacific oceans weights were calculated from monthly spatial 5°x5° Japanese biomass and numbers caught. Atlantic Ocean weights were calculated from monthly spatial 5°x5° Japanese biomass and numbers caught as well as Task II size frequency data.

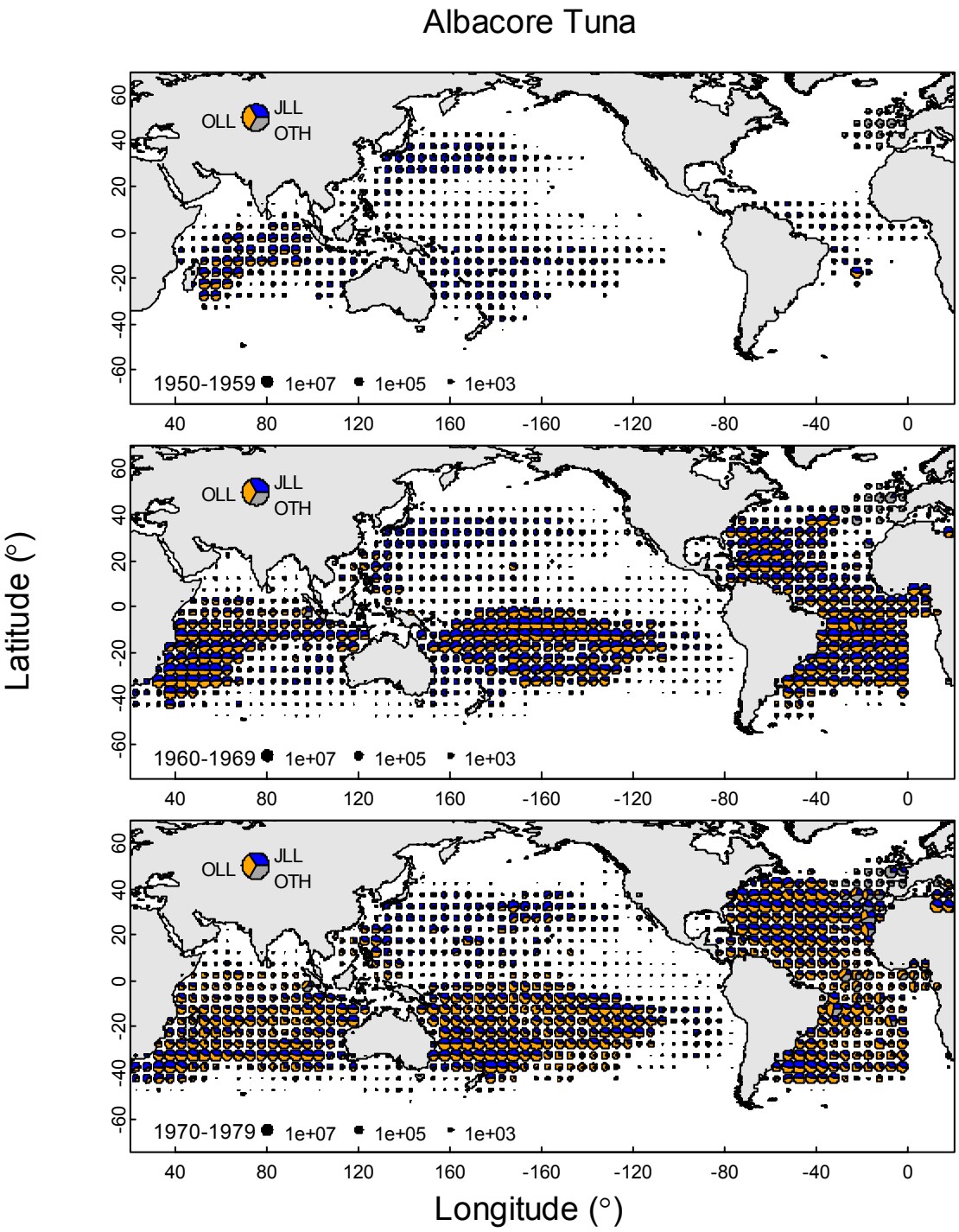

Figure 8.2 Estimated mean spatial (5°x5°) catch (in numbers of individuals) for albacore tuna of longline vulnerable size from 1950-1979 by decade. Size of circle reflects the magnitude of catch. Blue, orange, and white divisions represent catch from Japanese longline, all other nations' longlines, and all nations all other gear combined respectively. Due to insufficient public domain spatial data for other gear types, catch of North Pacific albacore is underestimated.

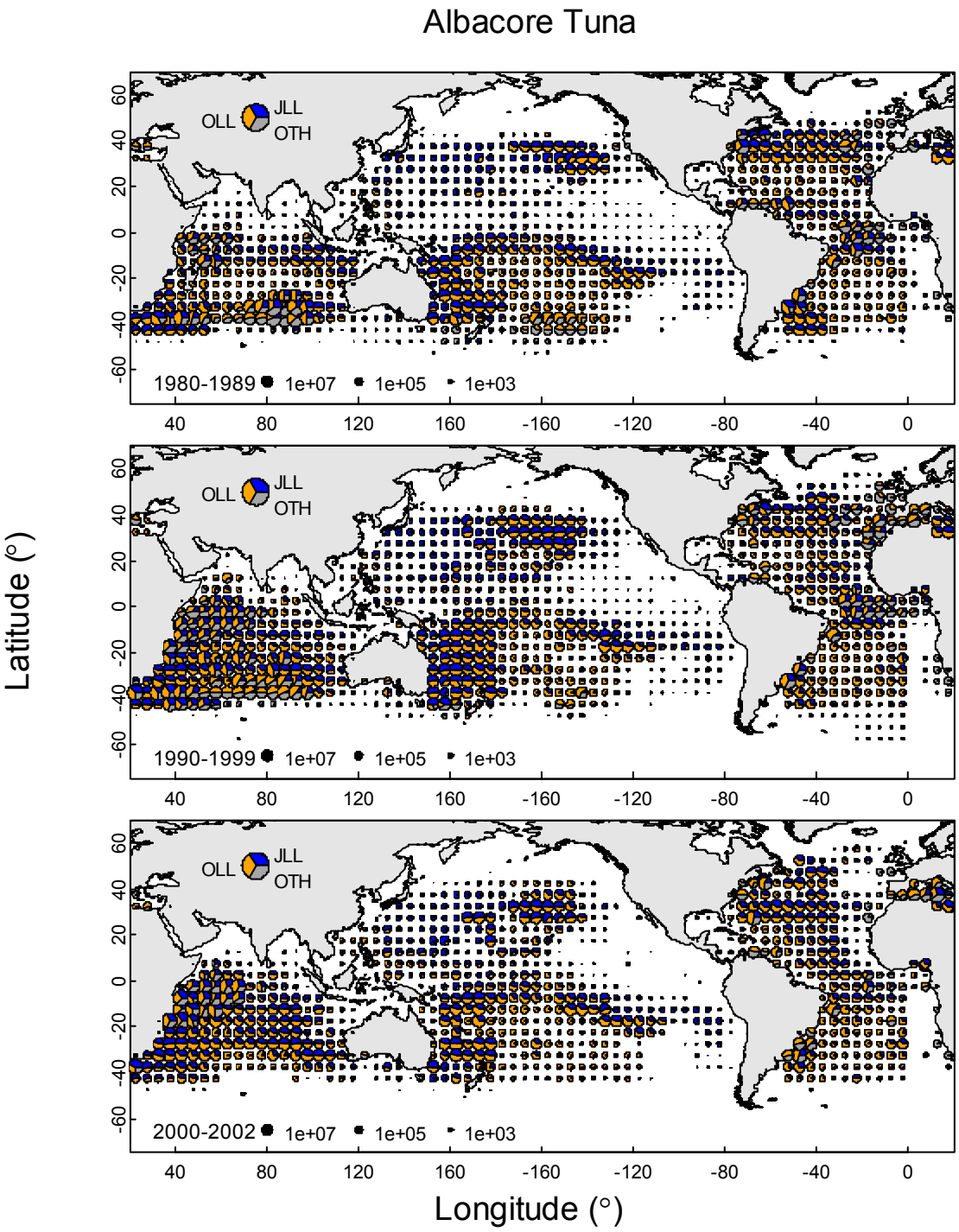

Figure 8.3 Estimated mean spatial (5°x5°) catch (in numbers of individuals) for albacore tuna of longline vulnerable size from 1980-2002 by decade. Size of circle reflects the magnitude of catch. Blue, orange, and white divisions represent catch from Japanese longline, all other nations' longlines, and all nations all other gear combined respectively. Due to insufficient public domain spatial data for other gear types, catch of North Pacific albacore is underestimated.

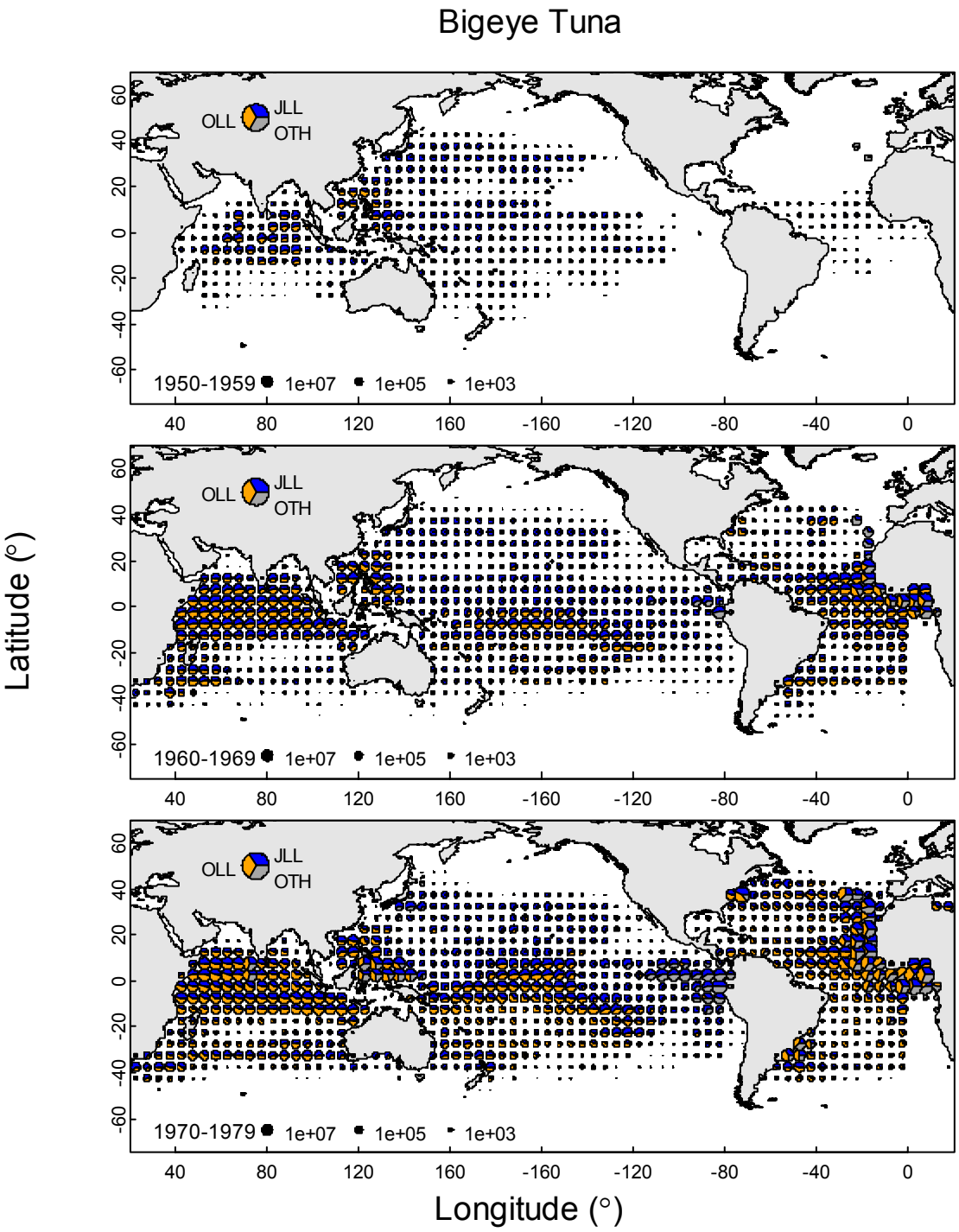

Figure 8.4 Estimated mean spatial (5°x5°) catch (in numbers of individuals) for bigeye tuna of longline vulnerable size from 1950-1979 by decade. Size of circle reflects the magnitude of catch. Blue, orange, and white divisions represent catch from Japanese longline, all other nations' longlines, and all nations all other gear combined respectively.

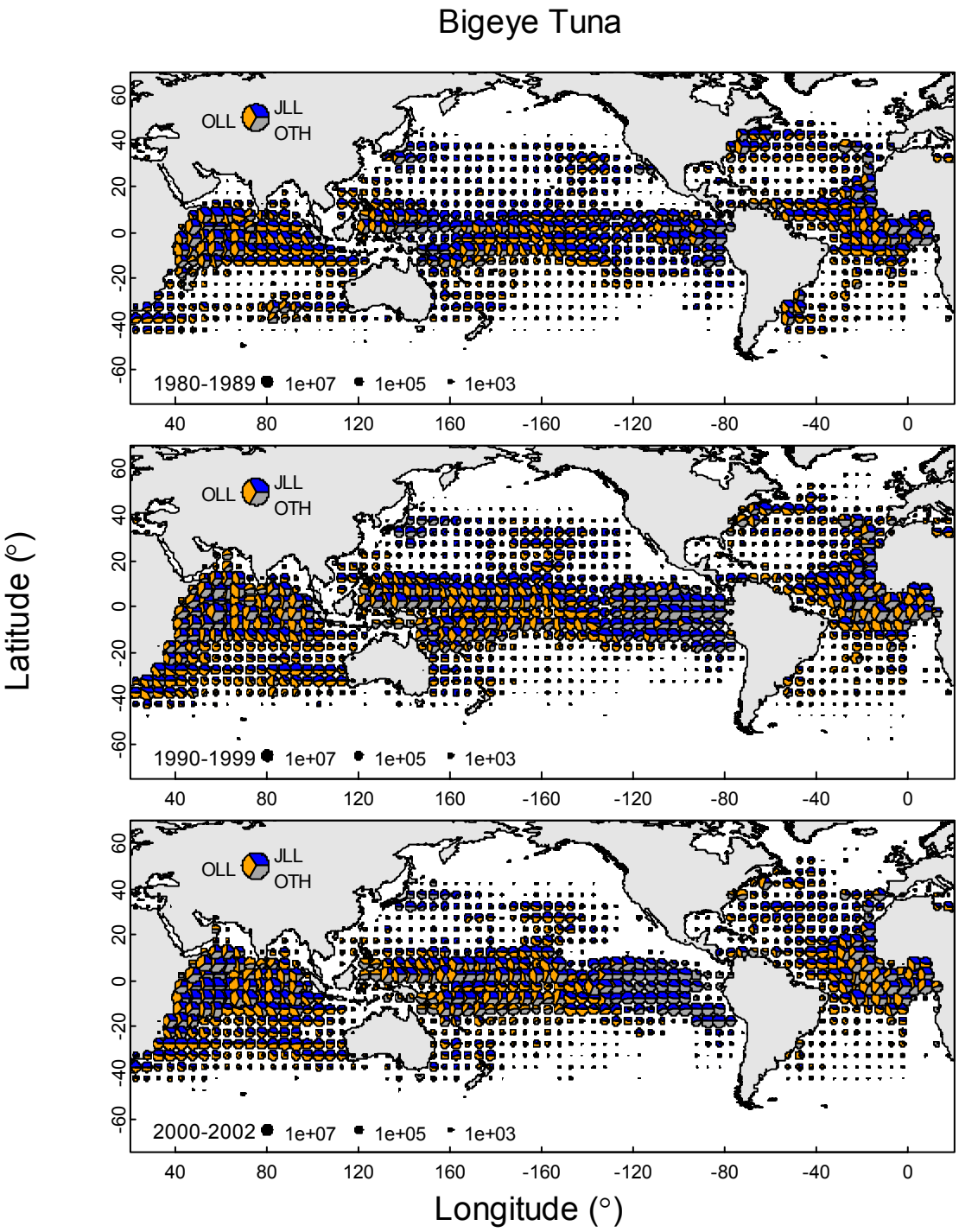

Figure 8.5 Estimated mean spatial (5°x5°) catch (in numbers of individuals) for bigeye tuna of longline vulnerable size from 1980-2002 by decade. Size of circle reflects the magnitude of catch. Blue, orange, and white divisions represent catch from Japanese longline, all other nations' longlines, and all nations all other gear combined respectively.

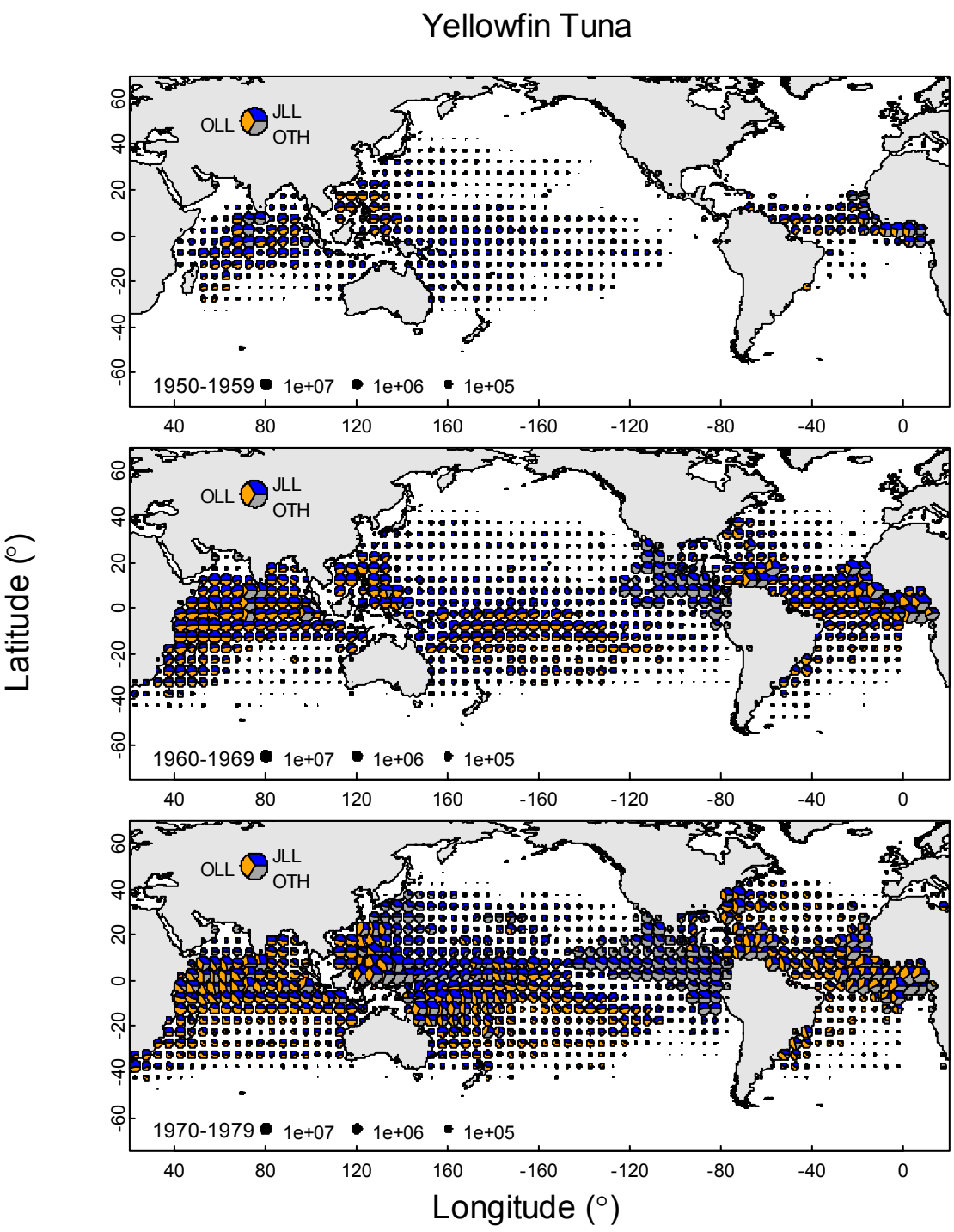

Figure 8.6 Estimated mean spatial (5°x5°) catch (in numbers of individuals) for yellowfin tuna of longline vulnerable size from 1950-1979 by decade. Size of circle reflects the magnitude of catch. Blue, orange, and white divisions represent catch from Japanese longline, all other nations' longlines, and all nations all other gear combined respectively.

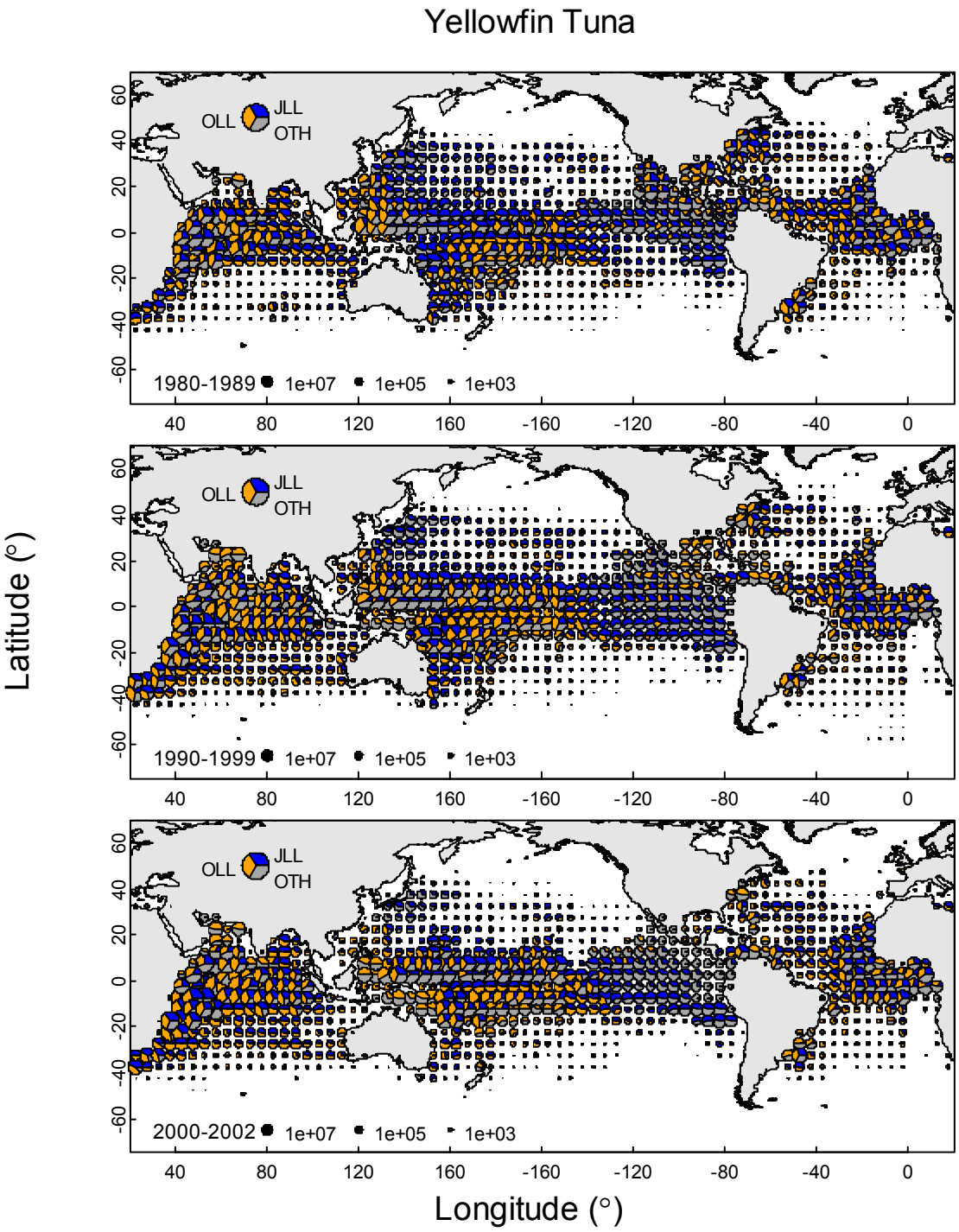

Figure 8.7 Estimated mean spatial (5°x5°) catch (in numbers of individuals) for yellowfin tuna of longline vulnerable size from 1980-2002 by decade. Size of circle reflects the magnitude of catch. Blue, orange, and white divisions represent catch from Japanese longline, all other nations' longlines, and all nations all other gear combined respectively.

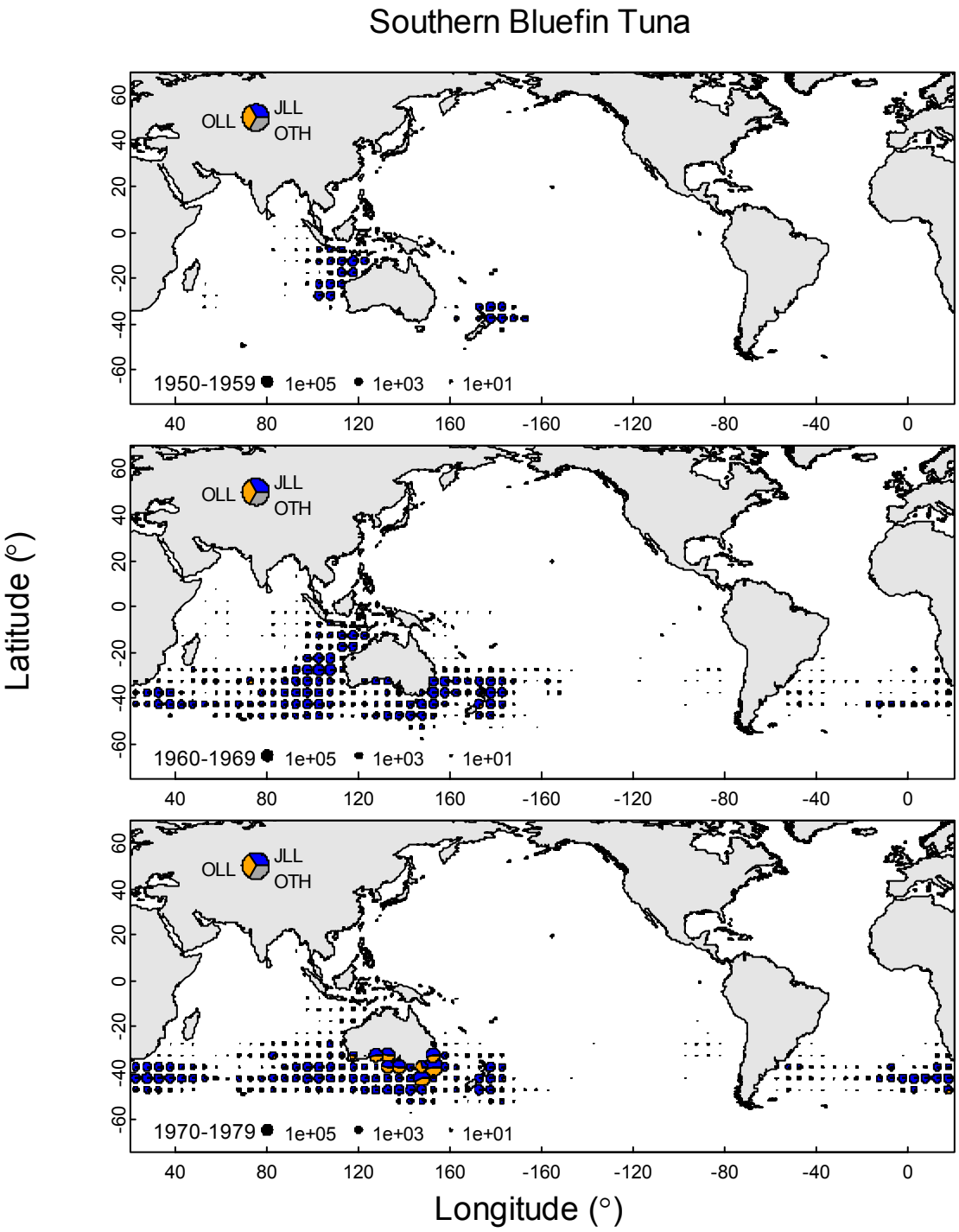

Figure 8.8 Estimated mean spatial (5°x5°) catch (in numbers of individuals) for southern bluefin tuna of longline vulnerable size from 1950-1979 by decade. Size of circle reflects the magnitude of catch. Blue, orange, and white divisions represent catch from Japanese longline, all other nations' longlines, and all nations all other gear combined respectively.

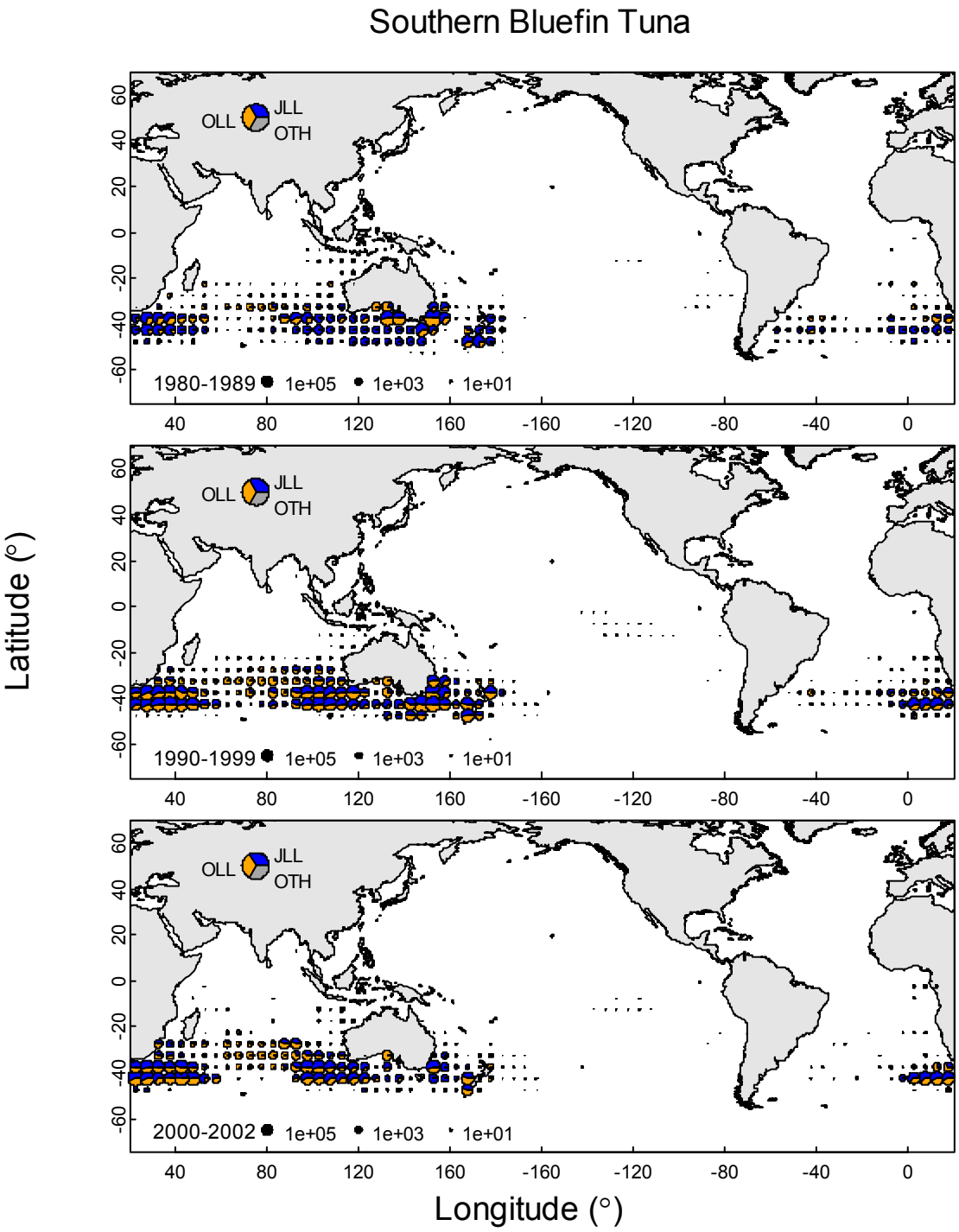

Figure 8.9 Estimated mean spatial (5°x5°) catch (in numbers of individuals) for southern bluefin tuna of longline vulnerable size from 1980-2002 by decade. Size of circle reflects the magnitude of catch. Blue, orange, and white divisions represent catch from Japanese longline, all other nations' longlines, and all nations all other gear combined respectively.

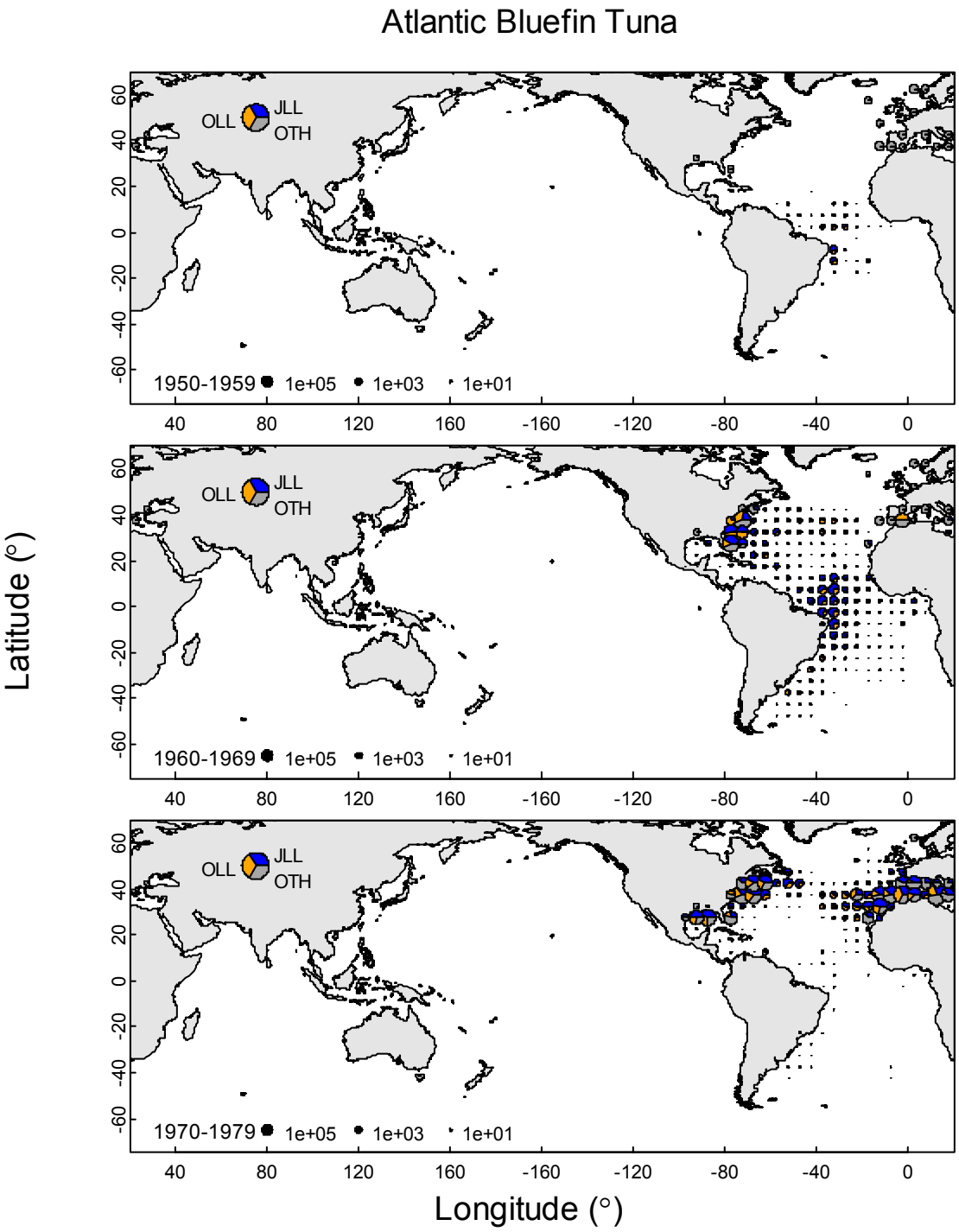

Figure 8.10 Estimated mean spatial (5°x5°) catch (in numbers of individuals) for Atlantic bluefin tuna of longline vulnerable size from 1950-1979 by decade. Size of circle reflects the magnitude of catch. Blue, orange, and white divisions represent catch from Japanese longline, all other nations' longlines, and all nations all other gear combined respectively.

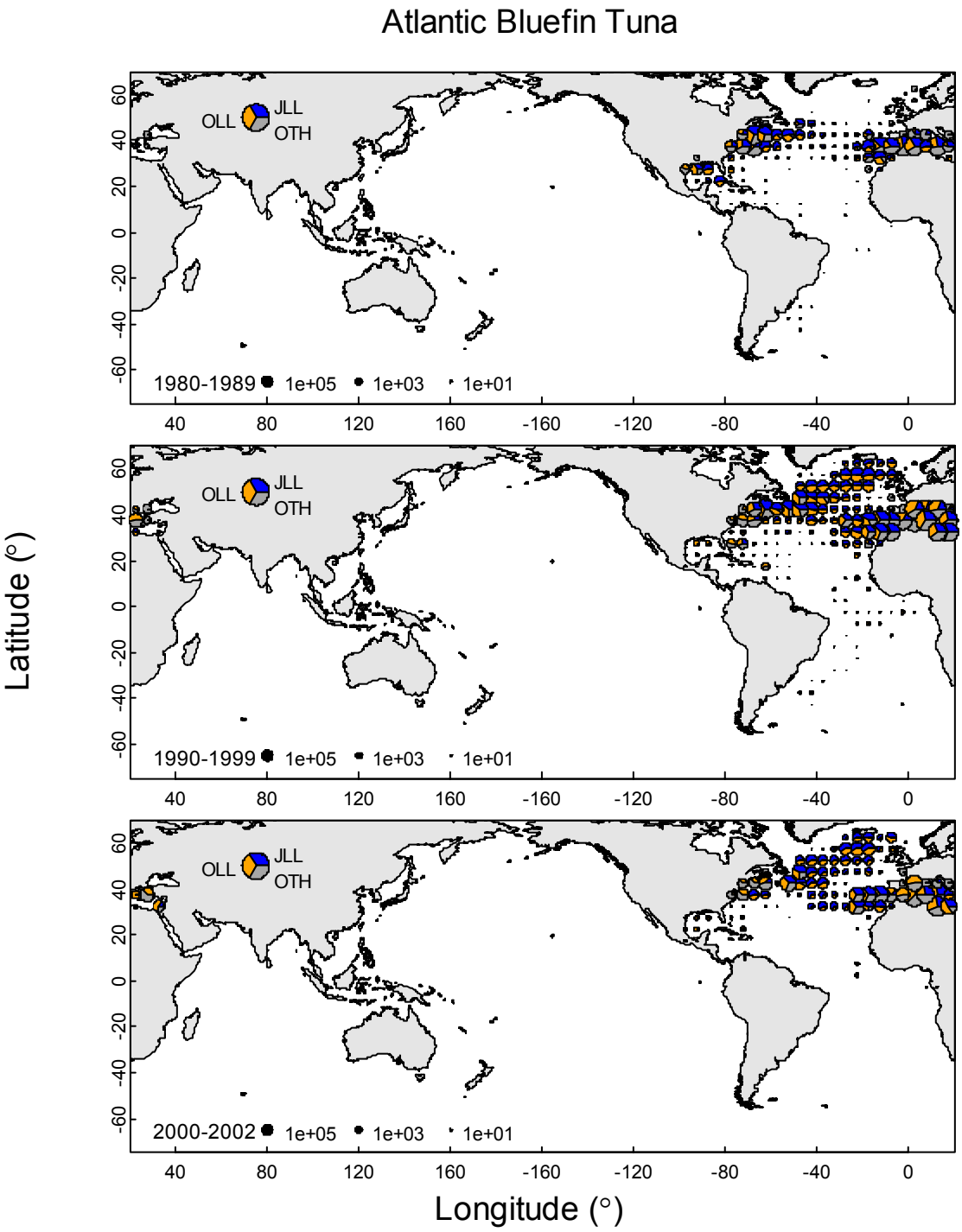

Figure 8.11 Estimated mean spatial (5°x5°) catch (in numbers of individuals) for Atlantic bluefin tuna of longline vulnerable size from 1980-2002 by decade. Size of circle reflects the magnitude of catch. Blue, orange, and white divisions represent catch from Japanese longline, all other nations' longlines, and all nations all other gear combined respectively.

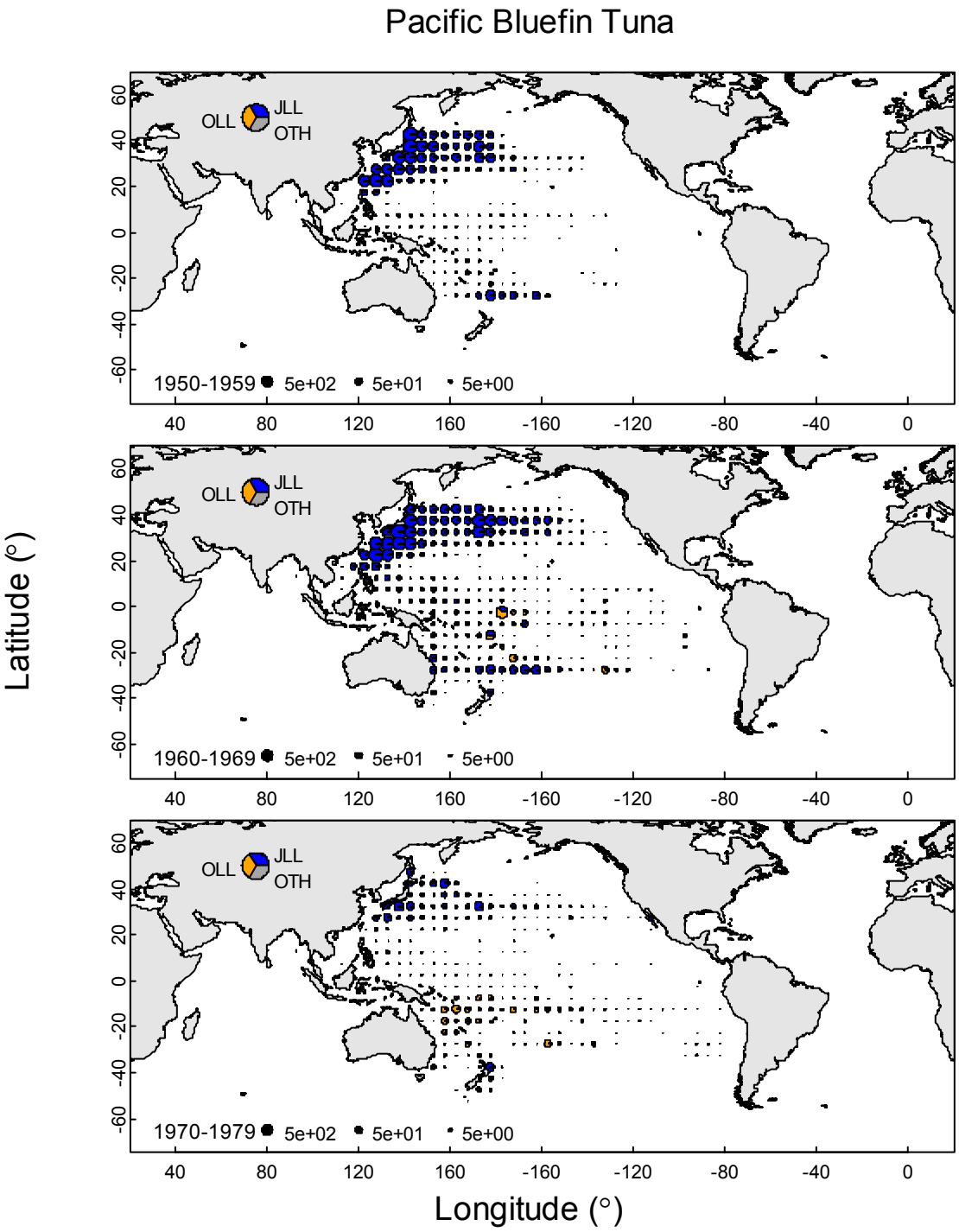

Figure 8.12 Estimated mean spatial (5°x5°) catch (in numbers of individuals) for North Pacific bluefin tuna of longline vulnerable size from 1950-1979 by decade. Size of circle reflects the magnitude of catch. Blue, orange, and white divisions represent catch from Japanese longline, all other nations' longlines, and all nations all other gear combined respectively. Due to insufficient public domain spatial data for other gear types, catch of North Pacific bluefin tuna is underestimated.

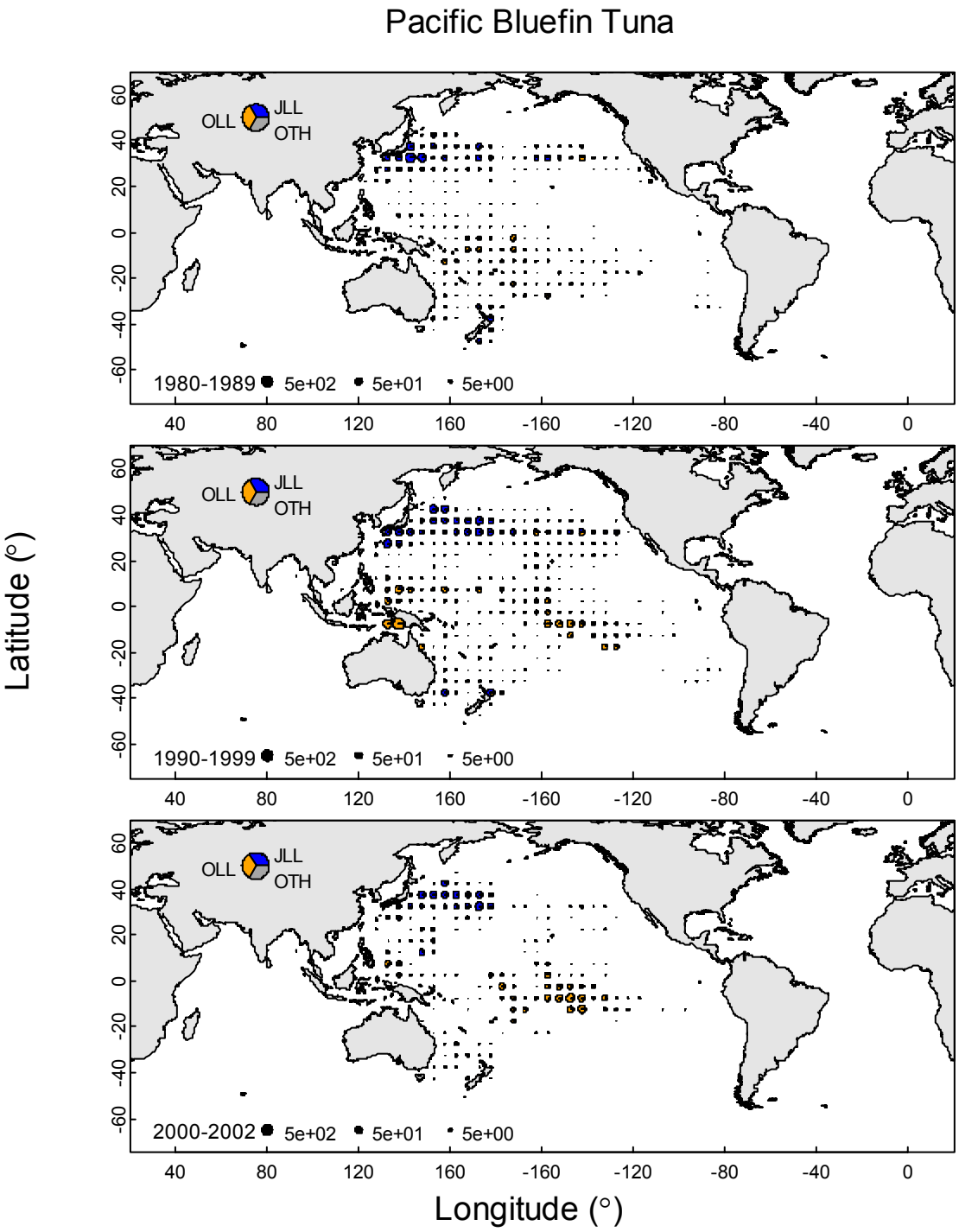

Figure 8.13 Estimated mean spatial (5°x5°) catch (in numbers of individuals) for North Pacific bluefin tuna of longline vulnerable size from 1980-2002 by decade. Size of circle reflects the magnitude of catch. Blue, orange, and white divisions represent catch from Japanese longline, all other nations' longlines, and all nations all other gear combined respectively. Due to insufficient public domain spatial data for other gear types, catch of North Pacific bluefin tuna is underestimated.

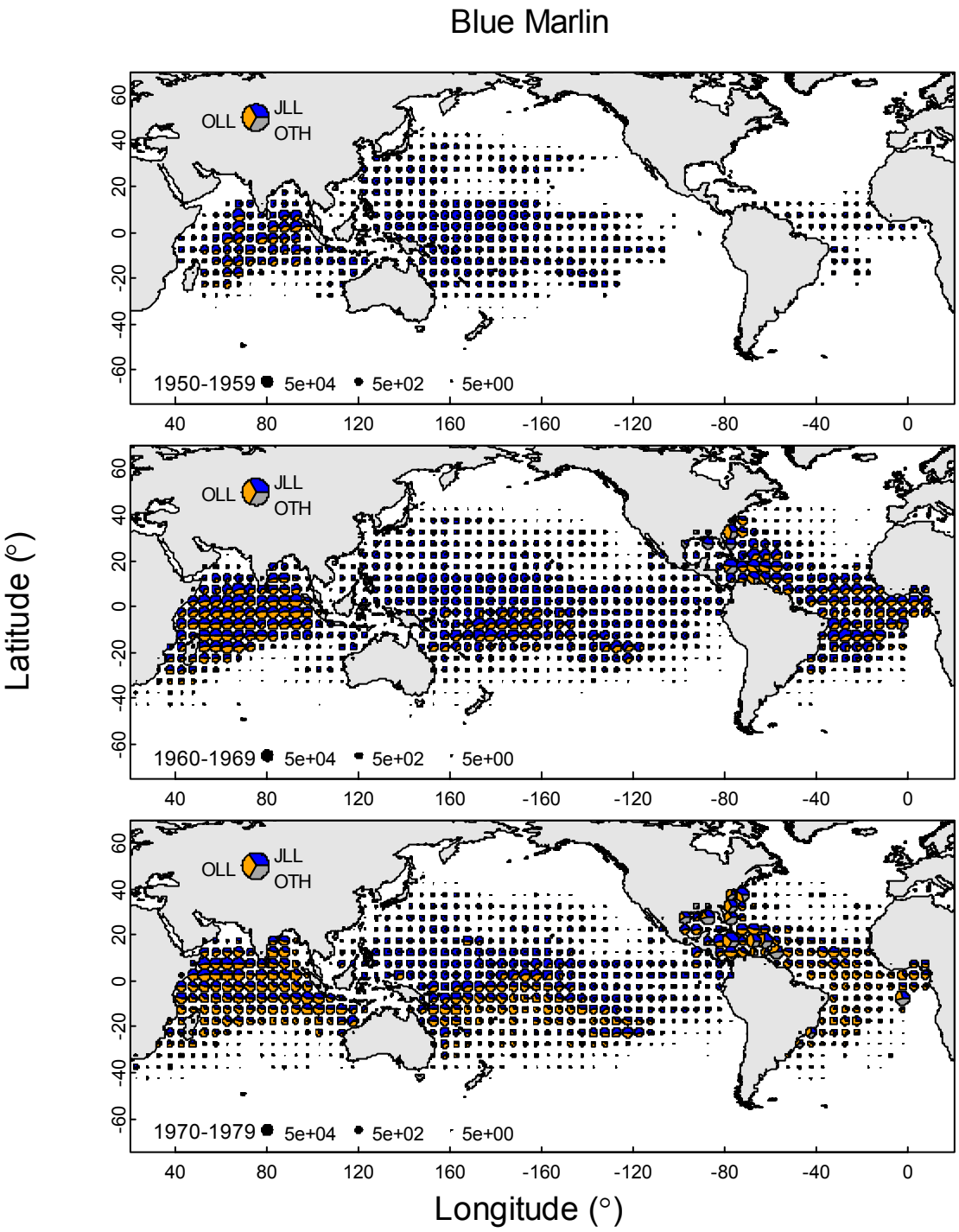

Figure 8.14 Estimated mean spatial (5°x5°) catch (in numbers of individuals) for blue marlin of longline vulnerable size from 1950-1979 by decade. Size of circle reflects the magnitude of catch. Blue, orange, and white divisions represent catch from Japanese longline, all other nations' longlines, and all nations all other gear combined respectively.

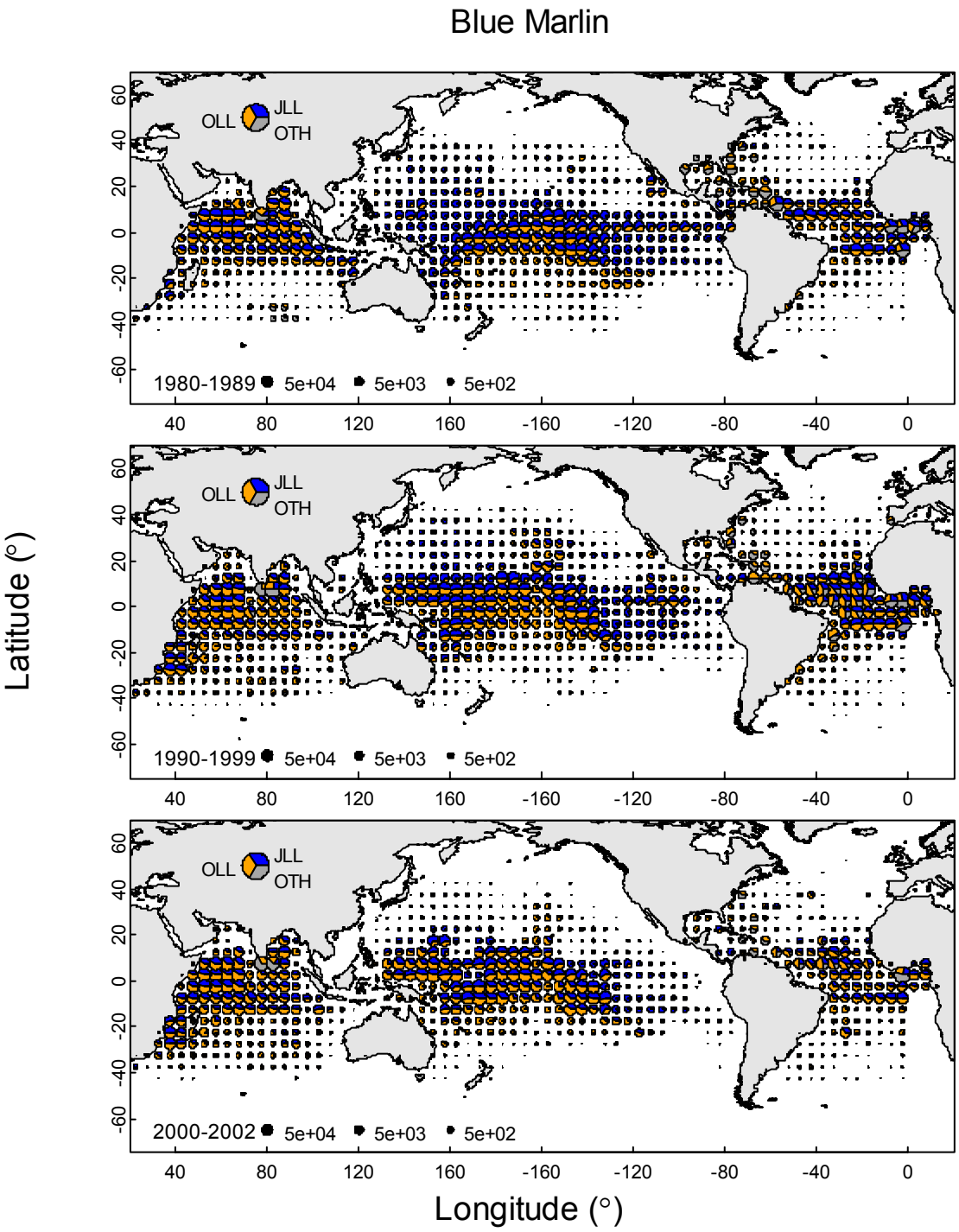

Figure 8.15 Estimated mean spatial (5°x5°) catch (in numbers of individuals) for blue marlin of longline vulnerable size from 1980-2002 by decade. Size of circle reflects the magnitude of catch. Blue, orange, and white divisions represent catch from Japanese longline, all other nations' longlines, and all nations all other gear combined respectively.

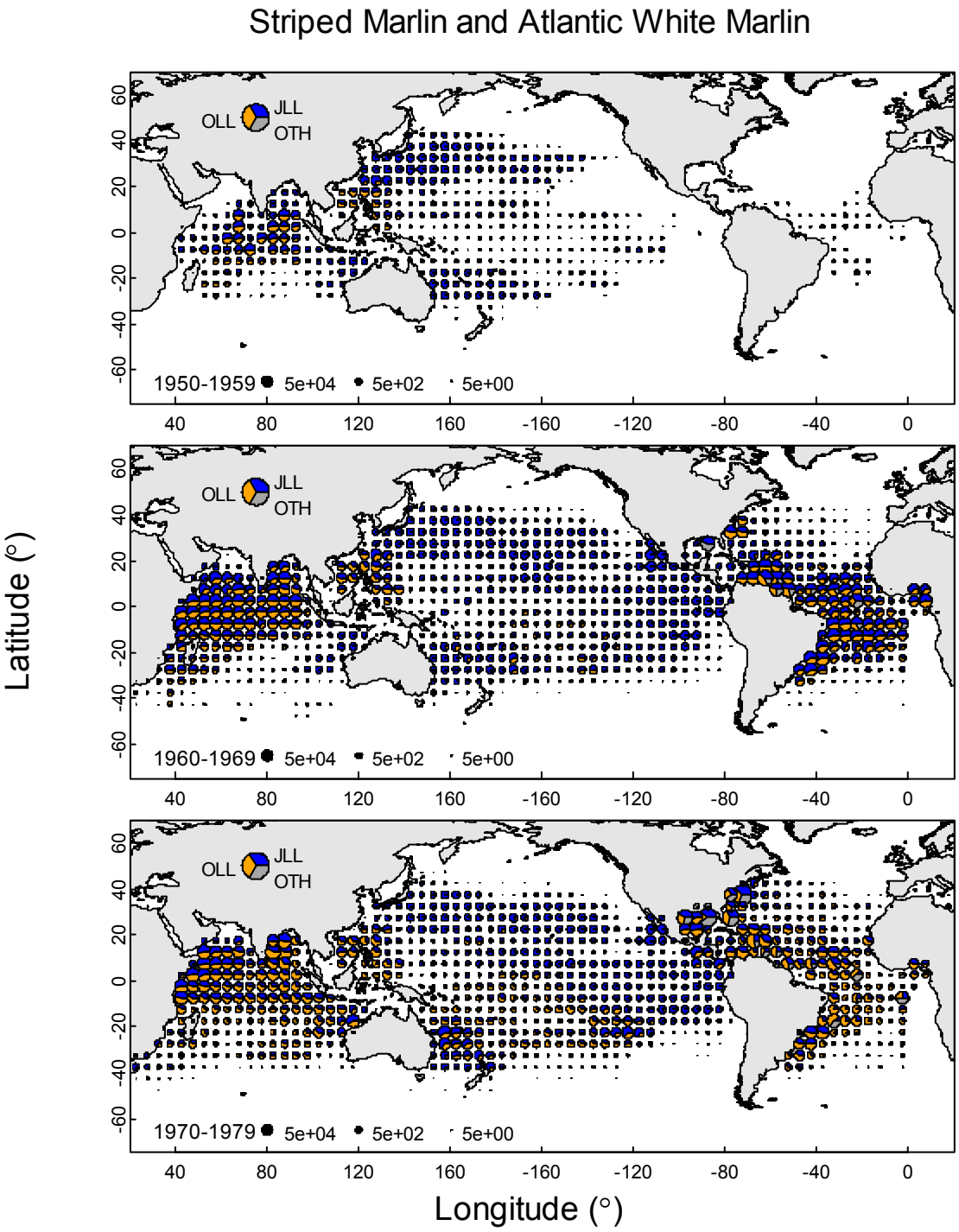

Figure 8.16 Estimated mean spatial (5°x5°) catch (in numbers of individuals) for Indo-Pacific striped marlin and Atlantic white marlin of longline vulnerable size from 1950-1979 by decade. Size of circle reflects the magnitude of catch. Blue, orange, and white divisions represent catch from Japanese longline, all other nations' longlines, and all nations all other gear combined respectively.

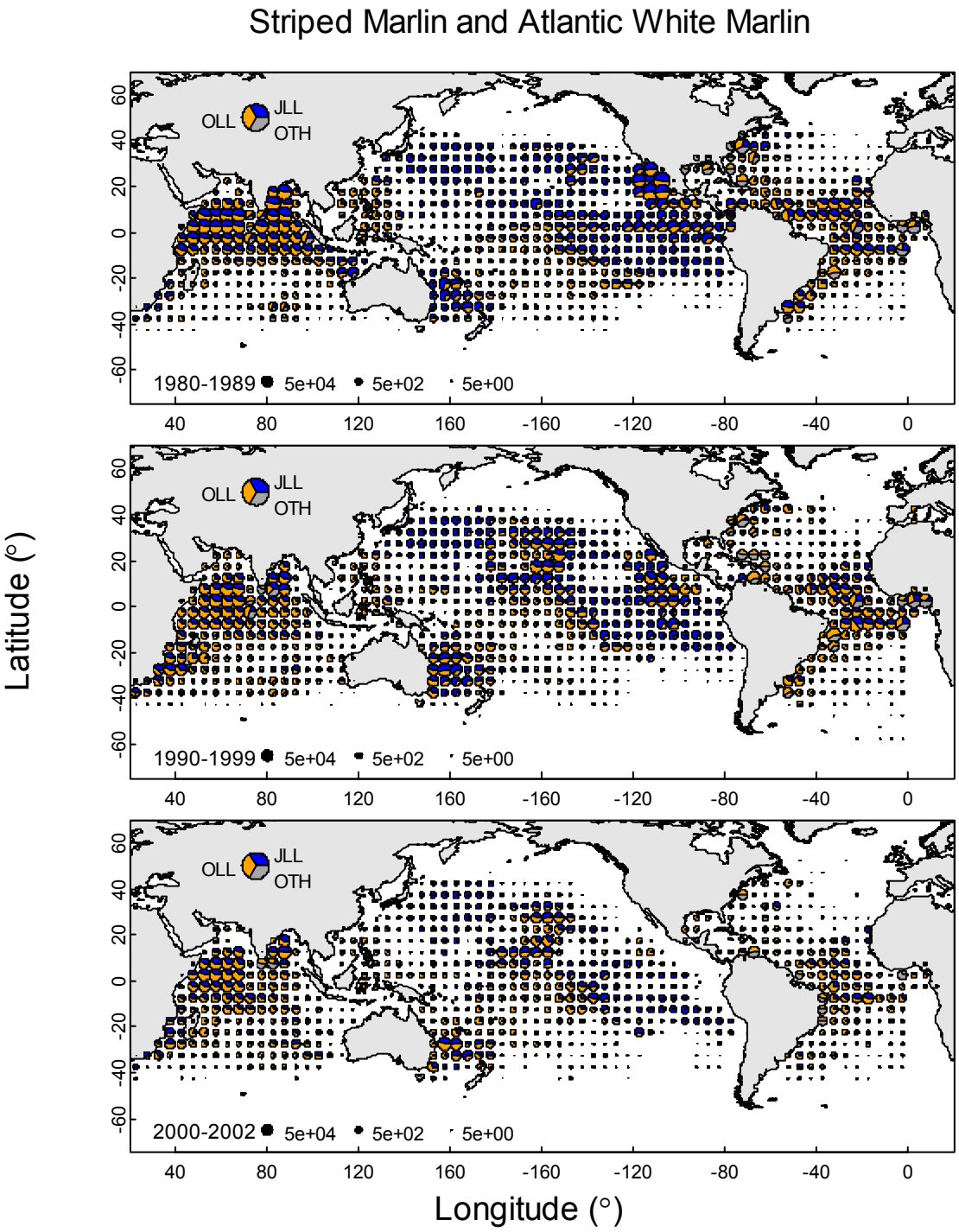

Figure 8.17 Estimated mean spatial (5°x5°) catch (in numbers of individuals) for Indo-Pacific striped marlin and Atlantic white marlin of longline vulnerable size from 1980-2002 by decade. Size of circle reflects the magnitude of catch. Blue, orange, and white divisions represent catch from Japanese longline, all other nations' longlines, and all nations all other gear combined respectively.

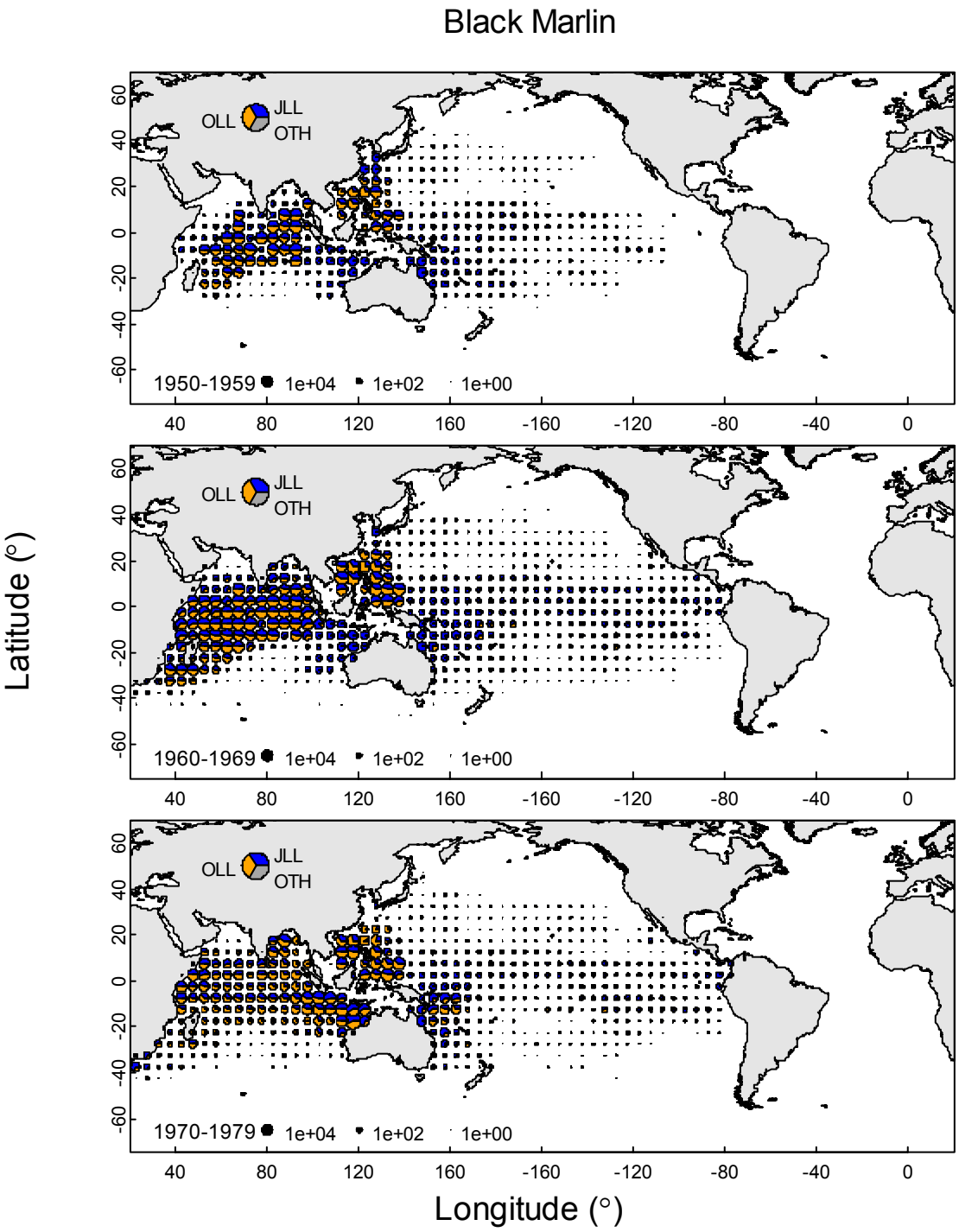

Figure 8.18 Estimated mean spatial (5°x5°) catch (in numbers of individuals) for Indo-Pacific black marlin of longline vulnerable size from 1950-1979 by decade. Size of circle reflects the magnitude of catch. Blue, orange, and white divisions represent catch from Japanese longline, all other nations' longlines, and all nations all other gear combined respectively.

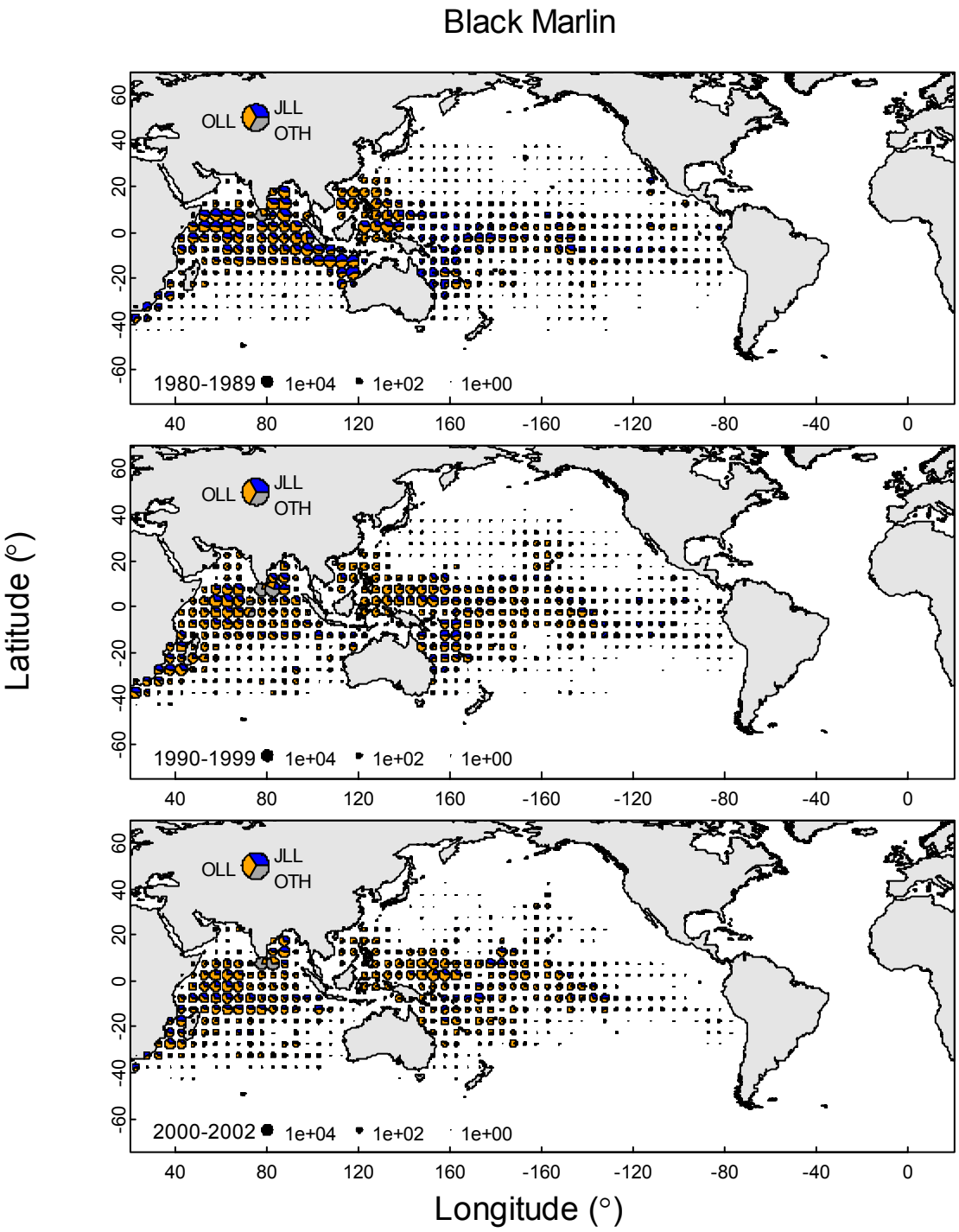

Figure 8.19 Estimated mean spatial (5°x5°) catch (in numbers of individuals) for Indo-Pacific black marlin of longline vulnerable size from 1980-2002 by decade. Size of circle reflects the magnitude of catch. Blue, orange, and white divisions represent catch from Japanese longline, all other nations' longlines, and all nations all other gear combined respectively.

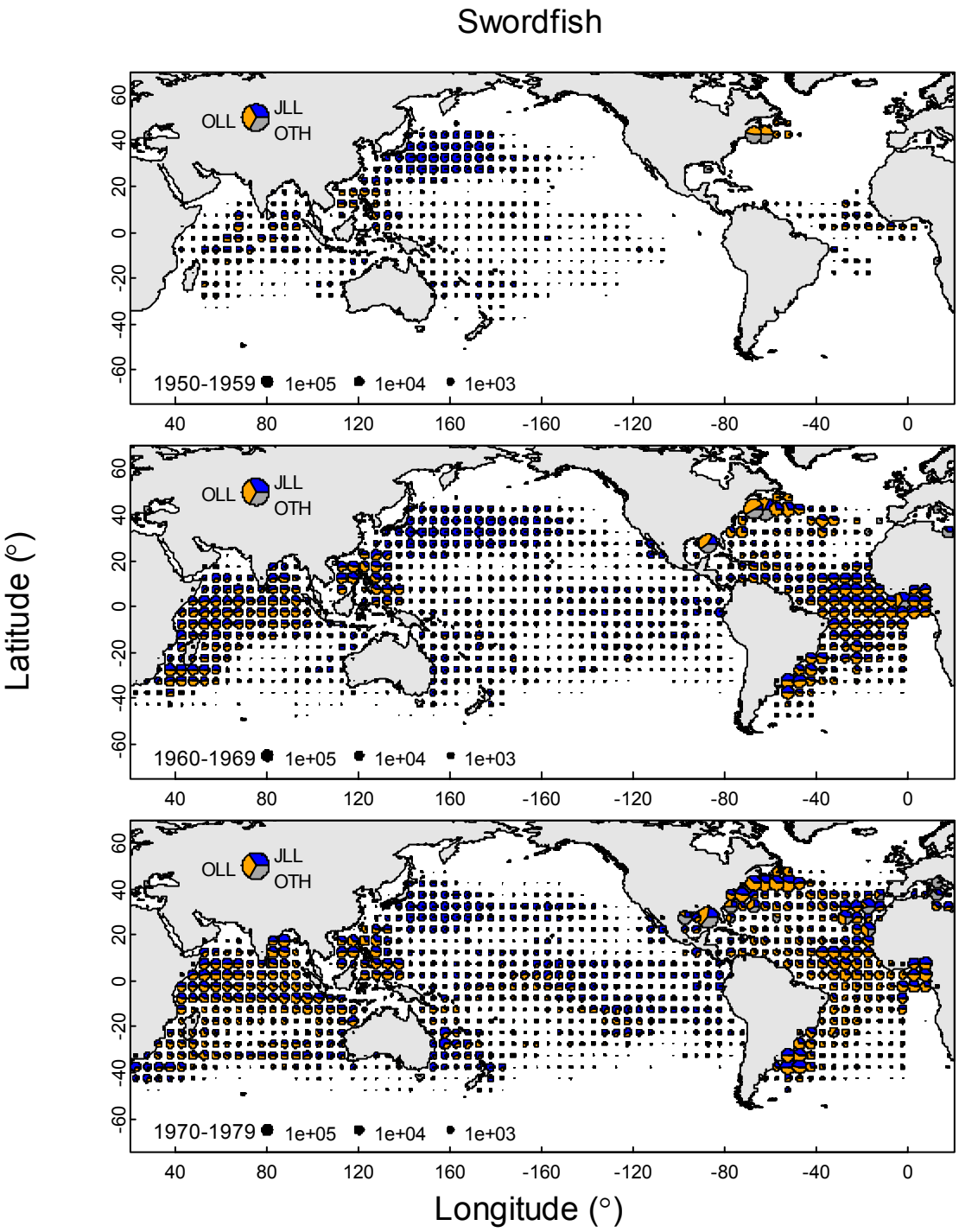

Figure 8.20 Estimated mean spatial (5°x5°) catch (in numbers of individuals) for swordfish of longline vulnerable size from 1950-1979 by decade. Size of circle reflects the magnitude of catch. Blue, orange, and white divisions represent catch from Japanese longline, all other nations' longlines, and all nations all other gear combined respectively.

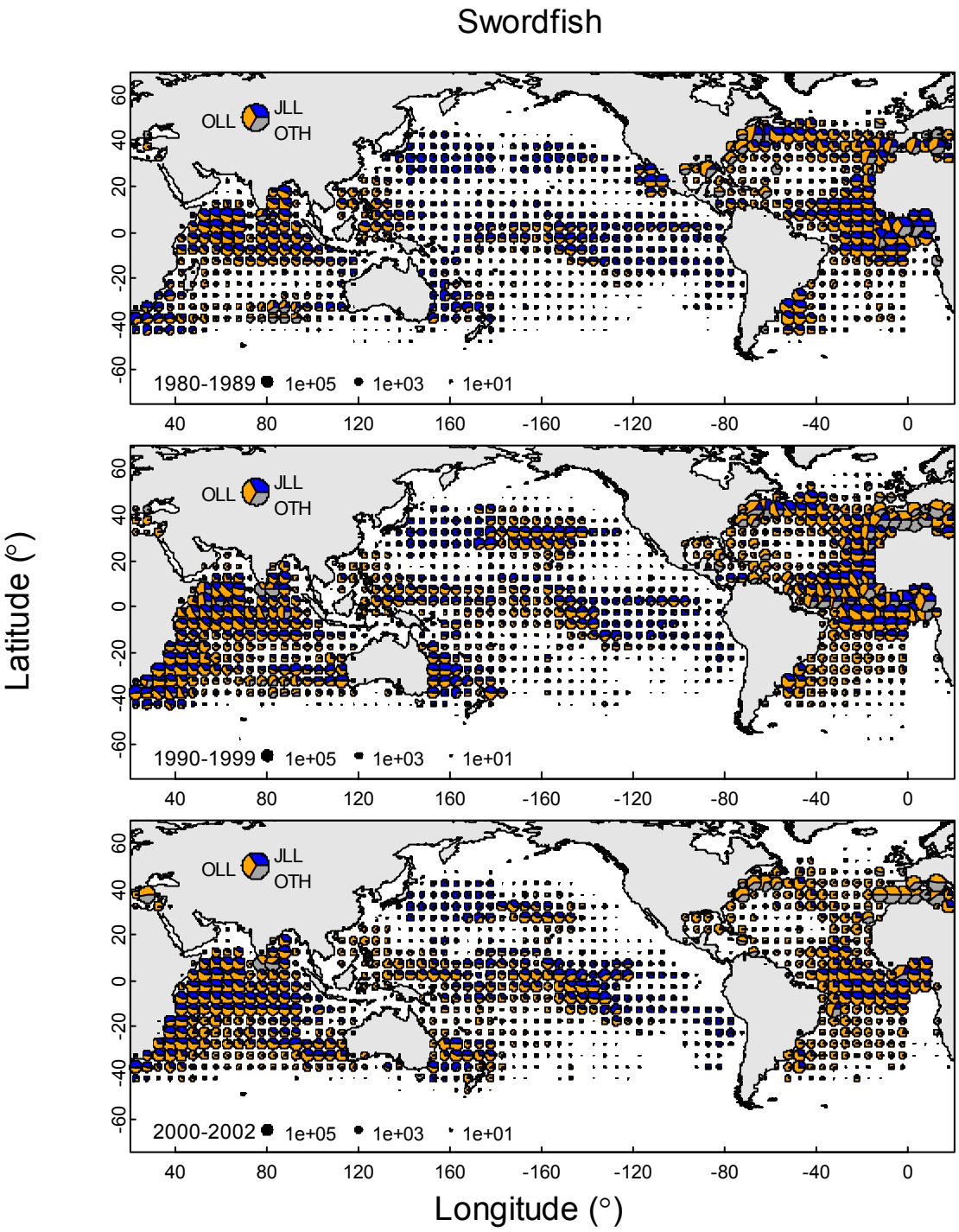

Figure 8.21 Estimated mean spatial (5°x5°) catch (in numbers of individuals) for swordfish of longline vulnerable size from 1980-2002 by decade. Size of circle reflects the magnitude of catch. Blue, orange, and white divisions represent catch from Japanese longline, all other nations' longlines, and all nations all other gear combined respectively.

Appendix for Chapter 3

Table 9.1 Yearly average *cpue* values calculated using the SF31 spatial filling method.

	IALB	PNAB	PSAB	ANAB	ASAB	IBET	PBET	ABET
1950		0.000358	0.002354				0.002474	
1951		0.000358	0.002355				0.002476	
1952	0.001801	0.000396	0.002337			0.000701	0.002528	
1953	0.0018	0.000391	0.002359			0.000696	0.002515	
1954	0.0018	0.000313	0.002429			0.000694	0.00244	
1955	0.001836	0.000252	0.00232			0.000721	0.002453	
1956	0.001769	0.000237	0.002285	0.001135	0.001744	0.000701	0.002476	0.000641
1957	0.001743	0.000258	0.002275	0.001135	0.001745	0.000675	0.002531	0.000642
1958	0.001783	0.000296	0.00234	0.001139	0.001747	0.000669	0.002554	0.000633
1959	0.00175	0.000241	0.002376	0.001134	0.001799	0.000637	0.002415	0.000643
1960	0.001622	0.000294	0.002581	0.001138	0.001798	0.000664	0.002481	0.000647
1961	0.001595	0.000239	0.002633	0.001118	0.001666	0.000627	0.002408	0.000695
1962	0.001443	0.000241	0.002448	0.001139	0.001523	0.00063	0.002142	0.0007
1963	0.00134	0.000238	0.001991	0.001159	0.001524	0.000651	0.001924	0.000701
1964	0.001372	0.000242	0.001926	0.001131	0.001532	0.000609	0.001596	0.000662
1965	0.001258	0.000217	0.002017	0.000991	0.00135	0.000544	0.001457	0.000686
1966	0.001262	0.000369	0.002028	0.001013	0.001205	0.000551	0.001537	0.000641
1967	0.00118	0.000375	0.00176	0.001044	0.001182	0.000564	0.001529	0.000643
1968	0.001083	0.000376	0.00156	0.000995	0.001238	0.000583	0.001433	0.000682
1969	0.000937	0.000345	0.001509	0.000955	0.00114	0.000551	0.00154	0.000646
1970	0.000725	0.000328	0.001417	0.001018	0.001037	0.000588	0.001203	0.000609
1971	0.000633	0.000266	0.001274	0.000746	0.000985	0.000497	0.001172	0.00056
1972	0.000643	0.000335	0.001214	0.000646	0.000916	0.000499	0.001252	0.000535
1973	0.000606	0.000363	0.001157	0.000647	0.000918	0.000513	0.001252	0.000593
1974	0.00057	0.000378	0.001046	0.000596	0.000922	0.000483	0.001184	0.000593
1975	0.000495	0.00031	0.001031	0.000557	0.000895	0.0004	0.001192	0.000542
1976	0.000539	0.000313	0.001012	0.000536	0.000895	0.000419	0.001237	0.000529
1977	0.000511	0.000367	0.00105	0.000534	0.000898	0.000533	0.001385	0.000593
1978	0.000468	0.000306	0.00104	0.000483	0.000857	0.000596	0.001227	0.000566
1979	0.000456	0.000326	0.00102	0.000457	0.00085	0.000538	0.001193	0.000649
1980	0.000455	0.000322	0.000986	0.000456	0.000761	0.000536	0.001099	0.000651
1981	0.000474	0.000336	0.001014	0.000441	0.000723	0.000562	0.001009	0.000565
1982	0.000473	0.000357	0.001037	0.00042	0.000696	0.000596	0.001078	0.00058
1983	0.000455	0.000341	0.00104	0.000421	0.000686	0.000564	0.001119	0.000582
1984	0.000441	0.000325	0.001007	0.000401	0.000654	0.000525	0.00104	0.000636
1985	0.000449	0.000311	0.000995	0.000377	0.000649	0.000517	0.00125	0.00065
1986	0.000482	0.00028	0.000978	0.000347	0.000623	0.00056	0.001219	0.000655
1987	0.000502	0.000288	0.000983	0.000293	0.000584	0.000582	0.001118	0.00073
1988	0.000475	0.000259	0.000991	0.000272	0.000565	0.000562	0.000955	0.000699
1989	0.000434	0.000236	0.000948	0.000248	0.000548	0.000533	0.001022	0.000632
1990	0.000395	0.000278	0.000974	0.000252	0.000551	0.00051	0.001108	0.000581
1991	0.000313	0.000284	0.000954	0.000244	0.000493	0.000494	0.001013	0.000614
1992	0.000283	0.00032	0.00097	0.000244	0.000433	0.000454	0.000969	0.000586
1993	0.000293	0.000355	0.001018	0.000241	0.000425	0.000471	0.000923	0.000586
1994	0.00027	0.000479	0.000999	0.000248	0.000405	0.000481	0.000915	0.000538
1995	0.000254	0.000512	0.000981	0.000248	0.000373	0.000446	0.000849	0.000556
1996	0.000236	0.000551	0.000954	0.000242	0.000369	0.000436	0.000839	0.000498
1997	0.000238	0.000575	0.001011	0.000219	0.000372	0.0004	0.000895	0.000483
1998	0.000242	0.000548	0.001034	0.000206	0.000377	0.000398	0.000923	0.000481
1999	0.000247	0.000528	0.001005	0.000172	0.000372	0.000378	0.000814	0.000499
2000	0.000231	0.000516	0.001016	0.000154	0.000377	0.000359	0.000824	0.000492
2001	0.000238	0.000485	0.001003	0.000133	0.00036	0.000345	0.0008	0.000459
2002	0.000224	0.000422	0.000976	0.000115	0.000356	0.000306	0.000773	0.000421

continued on next page

	IYFT	PYFT	AYFT	GSBT	PBFT	ABFT	IBUM	PBUM
1950		0.002563		0.001067	1.11E-05			0.000587
1951		0.002576		0.001067	1.11E-05			0.000581
1952	0.002501	0.00262		0.001066	1.19E-05		0.000197	0.000601
1953	0.002499	0.002633		0.00107	1.21E-05		0.0002	0.000601
1954	0.002529	0.002469		0.001077	8.91E-06		0.000203	0.000562
1955	0.002769	0.002406		0.001057	9.49E-06		0.000201	0.000556
1956	0.002419	0.002493	0.002407	0.001045	1.19E-05	6.99E-05	0.000172	0.000544
1957	0.002016	0.002544	0.002359	0.001091	1.01E-05	7.03E-05	0.000162	0.000506
1958	0.001801	0.00237	0.002476	0.001094	6.84E-06	6.92E-05	0.000164	0.000465
1959	0.001849	0.002296	0.002385	0.001128	1.25E-05	7.32E-05	0.000153	0.000438
1960	0.001809	0.002488	0.002122	0.001086	9.62E-06	7.77E-05	0.000129	0.000396
1961	0.001631	0.002148	0.001618	0.001059	1.57E-05	7.28E-05	0.000118	0.000375
1962	0.001533	0.001917	0.00138	0.001071	1.28E-05	8.77E-05	9.77E-05	0.00034
1963	0.001278	0.00178	0.001262	0.000956	7.64E-06	9.86E-05	8.51E-05	0.000291
1964	0.001069	0.001741	0.001085	0.000843	6.86E-06	7.95E-05	8.82E-05	0.000248
1965	0.000991	0.001782	0.000825	0.000757	6.14E-06	6.57E-05	7.2E-05	0.000198
1966	0.001113	0.001807	0.00078	0.000695	4.3E-06	6.2E-05	6.62E-05	0.000187
1967	0.000782	0.001427	0.000954	0.000619	3.11E-06	5.72E-05	5.37E-05	0.000176
1968	0.001222	0.001576	0.000897	0.000556	2.89E-06	5.25E-05	5.12E-05	0.000161
1969	0.00092	0.001591	0.000836	0.000521	3.06E-06	5.1E-05	4.57E-05	0.000171
1970	0.000736	0.001574	0.00075	0.000466	2.8E-06	4.78E-05	4.09E-05	0.000192
1971	0.000838	0.001404	0.000714	0.000428	2.45E-06	4.36E-05	4.02E-05	0.000155
1972	0.000811	0.001413	0.000705	0.000416	2.24E-06	4.29E-05	4.3E-05	0.000151
1973	0.000733	0.001315	0.00065	0.000367	2.25E-06	4.62E-05	4.35E-05	0.000153
1974	0.000565	0.001195	0.000685	0.000354	1.99E-06	6.39E-05	4.2E-05	0.000133
1975	0.000592	0.001239	0.000576	0.000332	2.74E-06	4.78E-05	3.64E-05	0.000112
1976	0.000621	0.001273	0.000576	0.000368	3.36E-06	5.54E-05	3.82E-05	0.00012
1977	0.000682	0.001411	0.000592	0.000376	3.69E-06	5.51E-05	4.54E-05	0.000121
1978	0.000616	0.001564	0.00058	0.000338	3.86E-06	5.55E-05	4.71E-05	0.000126
1979	0.000565	0.001361	0.000575	0.00032	3.33E-06	5E-05	4.25E-05	0.000123
1980	0.000525	0.001384	0.000562	0.000315	2.93E-06	5.49E-05	4.3E-05	0.000128
1981	0.000524	0.001131	0.000544	0.000295	3.45E-06	5.08E-05	4.01E-05	0.000122
1982	0.000568	0.001137	0.000517	0.000284	3.68E-06	4.96E-05	3.93E-05	0.000128
1983	0.000599	0.001306	0.000515	0.000274	2.35E-06	4.27E-05	4.24E-05	0.000139
1984	0.000587	0.001116	0.000535	0.000267	2.55E-06	4.62E-05	4.36E-05	0.000146
1985	0.000562	0.001185	0.00053	0.000257	1.69E-06	4.97E-05	4E-05	0.00013
1986	0.000622	0.001321	0.000514	0.000228	1.6E-06	4.56E-05	3.61E-05	0.000141
1987	0.000634	0.001282	0.000514	0.00022	1.62E-06	4.96E-05	3.6E-05	0.00014
1988	0.000641	0.001262	0.000549	0.000217	1.72E-06	4.47E-05	3.28E-05	0.000143
1989	0.000576	0.00119	0.000504	0.000216	1.66E-06	4.32E-05	3.04E-05	0.000135
1990	0.000565	0.001188	0.000482	0.000218	1.76E-06	4.08E-05	2.76E-05	0.000125
1991	0.000531	0.001142	0.000465	0.000218	1.73E-06	3.75E-05	2.57E-05	0.000132
1992	0.000512	0.00115	0.000457	0.00022	2.43E-06	3.78E-05	2.43E-05	0.000136
1993	0.000544	0.001158	0.000438	0.000236	3.01E-06	4.5E-05	2.61E-05	0.000144
1994	0.000506	0.001154	0.000455	0.00024	2.51E-06	4.52E-05	2.93E-05	0.000149
1995	0.000498	0.001207	0.000475	0.000236	2.23E-06	5.19E-05	2.7E-05	0.000157
1996	0.00056	0.00126	0.000466	0.00021	2.69E-06	4.68E-05	2.5E-05	0.000132
1997	0.000501	0.001238	0.000456	0.000207	2.74E-06	4.48E-05	2.47E-05	0.000141
1998	0.000466	0.00109	0.000473	0.000206	3E-06	4.44E-05	2.58E-05	0.000148
1999	0.000477	0.001006	0.000437	0.000201	3.02E-06	4.52E-05	2.79E-05	0.000134
2000	0.000498	0.00116	0.000431	0.000209	2.72E-06	4.82E-05	2.56E-05	0.000127
2001	0.000506	0.001051	0.000431	0.000209	1.9E-06	5.23E-05	2.15E-05	0.000128
2002	0.000476	0.000887	0.000415	0.000208	2.12E-06	5.06E-05	1.68E-05	0.000123

continued on next page

	ABUM	ISTM	PSTM	AWHM	GBLM	ISWO	PSWO	ASWO
1950			0.000469		0.000162		0.000138	
1951			0.000469		0.000162		0.000138	
1952		0.000164	0.000476		0.000164	3.91E-05	0.000138	
1953		0.000165	0.000468		0.000162	3.91E-05	0.000136	
1954		0.000164	0.000474		0.000161	3.85E-05	0.000136	
1955		0.000161	0.000462		0.000165	3.9E-05	0.000151	
1956	0.000165	0.000163	0.000466	0.000166	0.000151	3.96E-05	0.000146	6.6E-05
1957	0.000167	0.000158	0.000453	0.000168	0.000143	3.84E-05	0.00015	6.61E-05
1958	0.000164	0.000154	0.000451	0.000166	0.000136	4.28E-05	0.000154	6.59E-05
1959	0.000156	0.000164	0.000457	0.000164	0.000128	3.79E-05	0.000156	6.46E-05
1960	0.000147	0.000136	0.000445	0.000164	0.000125	3.89E-05	0.000147	6.32E-05
1961	0.000163	0.000133	0.000457	0.000183	0.000116	3.63E-05	0.000158	6.7E-05
1962	0.000157	0.000128	0.000483	0.000208	0.000108	3.79E-05	0.00016	7.03E-05
1963	0.000134	0.000121	0.000453	0.000207	9.59E-05	3.9E-05	0.000169	7.51E-05
1964	0.000108	0.00012	0.000461	0.000202	8.7E-05	3.56E-05	0.000149	7.46E-05
1965	8.8E-05	0.000139	0.000464	0.000192	8.27E-05	3.63E-05	0.000143	7.43E-05
1966	7.89E-05	0.000128	0.000427	0.000211	8.72E-05	3.78E-05	0.000148	7.47E-05
1967	7.18E-05	0.000112	0.000468	0.000203	8.54E-05	4.02E-05	0.000132	7.27E-05
1968	7.3E-05	0.00011	0.000455	0.000192	7.69E-05	3.87E-05	0.000144	8E-05
1969	7.38E-05	9.36E-05	0.000397	0.000187	8.46E-05	3.99E-05	0.000154	8.09E-05
1970	6.68E-05	8.77E-05	0.000439	0.000184	7.47E-05	4.55E-05	0.000166	8.56E-05
1971	6.39E-05	7.77E-05	0.000453	0.000154	6.87E-05	4.39E-05	0.000147	7.32E-05
1972	6.19E-05	7.23E-05	0.000355	0.00015	6.45E-05	4.7E-05	0.000152	7.46E-05
1973	6.12E-05	7.16E-05	0.000288	0.000149	6.1E-05	4.55E-05	0.000158	7.53E-05
1974	5.9E-05	8.88E-05	0.000275	0.000151	4.98E-05	4.35E-05	0.000143	7.48E-05
1975	5.88E-05	7.77E-05	0.000287	0.000143	5.09E-05	4.29E-05	0.000152	7.46E-05
1976	5.52E-05	8.61E-05	0.000257	0.000136	5.16E-05	4.23E-05	0.000152	7.36E-05
1977	5.17E-05	0.00012	0.000227	0.000131	4.85E-05	4.72E-05	0.000156	7.77E-05
1978	5.12E-05	0.000128	0.000222	0.00013	5.23E-05	5.37E-05	0.000148	7.38E-05
1979	5.15E-05	0.00012	0.000307	0.000127	4.78E-05	5.36E-05	0.000139	7.3E-05
1980	5.19E-05	0.000122	0.000298	0.000127	4.82E-05	4.94E-05	0.00014	7.59E-05
1981	5.18E-05	0.000103	0.00028	0.00012	4.65E-05	5.17E-05	0.00014	7.77E-05
1982	5.47E-05	8.4E-05	0.000296	0.000113	4.16E-05	5.35E-05	0.000128	8.3E-05
1983	5.43E-05	7.37E-05	0.00025	0.000109	4.36E-05	5.14E-05	0.000129	8.17E-05
1984	5.65E-05	7.95E-05	0.000242	0.000106	4.41E-05	5.36E-05	0.000123	8.3E-05
1985	5.64E-05	7.81E-05	0.000269	0.000108	4.45E-05	6.06E-05	0.000133	9.42E-05
1986	5.31E-05	8.16E-05	0.000275	0.000112	4.29E-05	5.62E-05	0.000139	8.65E-05
1987	5.35E-05	7.46E-05	0.000301	0.000111	4.18E-05	5.93E-05	0.000146	8.85E-05
1988	5.39E-05	6.71E-05	0.000297	0.000112	4.01E-05	6.06E-05	0.000143	9.15E-05
1989	5.29E-05	6.32E-05	0.000278	0.000106	3.75E-05	5.67E-05	0.000141	8.86E-05
1990	4.92E-05	5.7E-05	0.000263	0.000107	3.38E-05	5.85E-05	0.000142	9.7E-05
1991	4.56E-05	5.84E-05	0.000267	0.000104	3.46E-05	5.69E-05	0.000133	8.45E-05
1992	4.58E-05	5.55E-05	0.000256	9.8E-05	3.4E-05	5.87E-05	0.000135	7.82E-05
1993	4.93E-05	5.34E-05	0.000275	9.52E-05	3.3E-05	5.99E-05	0.000136	8.3E-05
1994	5.08E-05	4.98E-05	0.000273	9.47E-05	3.31E-05	5.72E-05	0.000134	7.8E-05
1995	4.67E-05	4.7E-05	0.000277	9.18E-05	3.02E-05	5.13E-05	0.000129	7.46E-05
1996	4.95E-05	4.49E-05	0.000282	9.12E-05	2.86E-05	5.16E-05	0.000134	7.07E-05
1997	4.88E-05	4.21E-05	0.000306	8.81E-05	2.82E-05	5.25E-05	0.000135	6.46E-05
1998	4.8E-05	3.94E-05	0.000304	8.64E-05	2.91E-05	5.21E-05	0.000132	6.56E-05
1999	4.88E-05	4.01E-05	0.000281	8.53E-05	2.77E-05	4.57E-05	0.000128	6.38E-05
2000	4.73E-05	3.73E-05	0.000269	7.91E-05	2.68E-05	4.33E-05	0.000133	5.35E-05
2001	4.37E-05	3.72E-05	0.000261	7.34E-05	2.5E-05	4.05E-05	0.000145	4.67E-05
2002	4.13E-05	3.24E-05	0.000248	7.2E-05	2.55E-05	3.84E-05	0.00015	4.53E-05

Appendix for Chapter 4

Table 10.1 F_{msy} and MSY estimates from recruitment reconstructions assuming Beverton-holt (BH) and Ricker (R) recruitment relationships for 3 current fishing mortality estimates (Fcur or F) and a known natural mortality rate M. Values are presented as mode (95% credible interval) and (-) indicates a point estimate.* indicates where estimates have exceeded maximum or minimum values.

Stock	Method	M	Fcur	Fmsy	MSY
IALB	BH F=0.25M*	0.27(-)	0.07(-)	0(0-0.02)	0.01(0-0.36)
	BH F=M*	0.27(-)	0.27(-)	0.05(0-0.11)	0.44(0-1.19)
	BH F=3M	0.27(-)	0.81(-)	0.34(0.21-0.71)	1.44(1.06-2.01)
	R F=0.25M*	0.27(-)	0.07(-)	0(0-0.01)	0.01(0-0.21)
	R F=M*	0.27(-)	0.27(-)	0.02(0-0.05)	0.15(0-0.7)
	R F=3M	0.27(-)	0.81(-)	0.16(0.11-0.22)	1.18(0.84-1.6)
IBET	BH F=0.25M*	0.4(-)	0.1(-)	0.01(0-0.14)	0.39(0-86.62)
	BH F=M*	0.4(-)	0.4(-)	1.4(0.54-2.32)	3.5(2.28-4.11)
	BH F=3M*	0.4(-)	1.2(-)	1.66(1.21-2.36)	1.74(1.53-1.98)
	R F=0.25M*	0.4(-)	0.1(-)	0.01(0-0.09)	0.31(0-115.88)
	R F=M	0.4(-)	0.4(-)	0.41(0.3-0.56)	2.33(1.78-2.98)
	R F=3M*	0.4(-)	1.2(-)	1.94(1.35-2.37)	3.01(2.3-3.48)
IYFT	BH F=0.25M*	0.7(-)	0.18(-)	0.06(0-0.11)	1.46(0.01-3.7)
	BH F=M	0.7(-)	0.7(-)	0.31(0.19-0.48)	3.35(2.14-4.68)
	BH F=3M*	0.7(-)	2.1(-)	1.99(0.83-4.03)	4.39(3.06-5.53)
	R F=0.25M*	0.7(-)	0.18(-)	0.03(0-0.08)	0.68(0-2.73)
	R F=M	0.7(-)	0.7(-)	0.2(0.12-0.27)	2.75(1.63-4.05)
	R F=3M	0.7(-)	2.1(-)	0.58(0.42-0.8)	3.3(2.41-4.4)
GSBT	BH F=0.25M*	0.1(-)	0.02(-)	0.15(0.01-0.56)	0.48(0.03-0.93)
	BH F=M	0.1(-)	0.1(-)	0.05(0.03-0.08)	0.17(0.12-0.23)
	BH F=3M	0.1(-)	0.3(-)	0.1(0.08-0.12)	0.47(0.38-0.62)
	R F=0.25M*	0.1(-)	0.02(-)	0.01(0-0.04)	0.04(0-0.23)
	R F=M	0.1(-)	0.1(-)	0.04(0.03-0.06)	0.17(0.12-0.23)
	R F=3M	0.1(-)	0.3(-)	0.12(0.1-0.14)	0.46(0.39-0.59)
IBUM	BH F=0.25M*	0.25(-)	0.06(-)	0.02(0.01-0.08)	0.02(0-0.09)
	BH F=M	0.25(-)	0.25(-)	0.15(0.08-0.28)	0.06(0.03-0.09)
	BH F=3M*	0.25(-)	0.75(-)	0.7(0.35-1.44)	0.08(0.06-0.1)
	R F=0.25M*	0.25(-)	0.06(-)	0.01(0-0.02)	0(0-0.03)
	R F=M	0.25(-)	0.25(-)	0.05(0.02-0.08)	0.02(0.01-0.05)
	R F=3M	0.25(-)	0.75(-)	0.17(0.13-0.23)	0.05(0.04-0.07)
ISTM	BH F=0.25M*	0.5(-)	0.12(-)	0.01(0-0.11)	0.03(0-9.34)
	BH F=M	0.5(-)	0.5(-)	0.39(0.29-0.57)	0.08(0.06-0.09)
	BH F=3M*	0.5(-)	1.5(-)	1.64(0.95-2.89)	0.08(0.07-0.1)
	R F=0.25M*	0.5(-)	0.12(-)	0.01(0-0.09)	0.03(0-9.62)
	R F=M	0.5(-)	0.5(-)	0.35(0.27-0.44)	0.08(0.07-0.09)
	R F=3M	0.5(-)	1.5(-)	1.16(0.93-1.43)	0.09(0.08-0.1)
GBLM	BH F=0.25M*	0.15(-)	0.04(-)	0.01(0-0.02)	0(0-0.01)
	BH F=M	0.15(-)	0.15(-)	0.05(0.03-0.07)	0.02(0.01-0.03)
	BH F=3M	0.15(-)	0.45(-)	0.15(0.12-0.19)	0.04(0.04-0.05)
	R F=0.25M*	0.15(-)	0.04(-)	0(0-0.01)	0(0-0)
	R F=M	0.15(-)	0.15(-)	0.03(0.02-0.05)	0.02(0.01-0.03)
	R F=3M	0.15(-)	0.45(-)	0.13(0.11-0.15)	0.05(0.04-0.05)
ISWO	BH F=0.25M*	0.21(-)	0.05(-)	0.01(0-0.07)	0.59(0.05-45.94)
	BH F=M	0.21(-)	0.21(-)	0.02(0.02-0.03)	4.45(0.22-54.17)
	BH F=3M	0.21(-)	0.63(-)	0.06(0.04-0.07)	4.95(0.22-53.77)
	R F=0.25M*	0.21(-)	0.05(-)	0.01(0-0.05)	0.64(0.05-44.52)
	R F=M	0.21(-)	0.21(-)	0.02(0.02-0.03)	4.21(0.22-52.56)
	R F=3M	0.21(-)	0.63(-)	0.06(0.04-0.08)	4.99(0.23-51.73)

continued next

Stock	Method	M	Fcur	Fmsy	MSY
PNAB	BH F=0.25M*	0.27(-)	0.07(-)	0.86(0.13-1.57)	6.05(3.11-7.48)
	BH F=M*	0.27(-)	0.27(-)	1.03(0.43-1.57)	3.01(2.5-3.4)
	BH F=3M*	0.27(-)	0.81(-)	1.26(0.69-1.6)	2.54(2.31-2.93)
	R F=0.25M	0.27(-)	0.07(-)	0.3(0.14-0.52)	4.36(2.94-6.42)
	R F=M	0.27(-)	0.27(-)	0.59(0.38-0.9)	2.83(2.46-3.41)
	R F=3M*	0.27(-)	0.81(-)	1.22(0.78-1.58)	2.57(2.33-3.09)
PSAB	BH F=0.25M	0.27(-)	0.07(-)	0.07(0.03-0.14)	1.98(0.63-3.6)
	BH F=M	0.27(-)	0.27(-)	0.23(0.16-0.34)	2.04(1.67-2.53)
	BH F=3M	0.27(-)	0.81(-)	0.84(0.53-1.51)	2.18(1.93-2.51)
	R F=0.25M	0.27(-)	0.07(-)	0.05(0.01-0.08)	1.45(0.25-2.71)
	R F=M	0.27(-)	0.27(-)	0.16(0.13-0.2)	1.86(1.54-2.2)
	R F=3M	0.27(-)	0.81(-)	0.44(0.39-0.51)	2.04(1.89-2.23)
PBET	BH F=0.25M*	0.4(-)	0.1(-)	0.05(0-0.1)	1.28(0.02-2.87)
	BH F=M	0.4(-)	0.4(-)	0.29(0.21-0.43)	2.63(2.12-3.31)
	BH F=3M*	0.4(-)	1.2(-)	1.96(1.56-2.37)	3.27(3.04-3.48)
	R F=0.25M*	0.4(-)	0.1(-)	0.04(0-0.07)	0.96(0.01-2.32)
	R F=M	0.4(-)	0.4(-)	0.2(0.15-0.24)	2.27(1.86-2.73)
	R F=3M	0.4(-)	1.2(-)	0.62(0.53-0.72)	2.62(2.36-2.92)
PYFT	BH F=0.25M	0.7(-)	0.18(-)	0.14(0.08-0.22)	9.34(5.16-14.18)
	BH F=M	0.7(-)	0.7(-)	0.92(0.61-1.57)	13.17(10.56-16.92)
	BH F=3M*	0.7(-)	2.1(-)	3.7(3.28-4.17)	11.51(10.85-12.22)
	R F=0.25M	0.7(-)	0.18(-)	0.11(0.06-0.16)	7.83(4.23-11.42)
	R F=M	0.7(-)	0.7(-)	0.45(0.37-0.53)	9.84(8.5-11.34)
	R F=3M	0.7(-)	2.1(-)	1.55(1.3-1.81)	10.73(9.59-12)
PBFT	BH F=0.25M*	0.28(-)	0.07(-)	0.19(0.03-1.28)	0.04(0-0.11)
	BH F=M	0.28(-)	0.28(-)	0.21(0.11-0.5)	0.03(0.02-0.04)
	BH F=3M	0.28(-)	0.83(-)	0.38(0.25-0.63)	0.04(0.03-0.08)
	R F=0.25M*	0.28(-)	0.07(-)	0.05(0.01-0.13)	0.01(0-0.05)
	R F=M	0.28(-)	0.28(-)	0.16(0.09-0.25)	0.03(0.02-0.05)
	R F=3M	0.28(-)	0.83(-)	0.4(0.27-0.56)	0.05(0.03-0.17)
PBUM	BH F=0.25M	0.25(-)	0.06(-)	0.13(0.06-0.27)	0.23(0.11-0.4)
	BH F=M	0.25(-)	0.25(-)	0.26(0.18-0.42)	0.17(0.14-0.22)
	BH F=3M	0.25(-)	0.75(-)	0.56(0.42-0.9)	0.18(0.16-0.2)
	R F=0.25M	0.25(-)	0.06(-)	0.05(0.02-0.08)	0.1(0.02-0.19)
	R F=M	0.25(-)	0.25(-)	0.14(0.11-0.17)	0.15(0.12-0.19)
	R F=3M	0.25(-)	0.75(-)	0.37(0.32-0.43)	0.19(0.17-0.22)
PSTM	BH F=0.25M	0.5(-)	0.12(-)	0.16(0.08-0.27)	0.24(0.19-16.55)
	BH F=M	0.5(-)	0.5(-)	0.47(0.32-0.84)	0.33(0.23-25.74)
	BH F=3M	0.5(-)	1.5(-)	1.04(0.73-2.09)	0.39(0.24-26.81)
	R F=0.25M	0.5(-)	0.12(-)	0.15(0.09-0.25)	0.25(0.19-30.26)
	R F=M	0.5(-)	0.5(-)	0.52(0.36-0.8)	0.35(0.24-30.46)
	R F=3M	0.5(-)	1.5(-)	1.43(1.03-2.27)	0.39(0.24-36.21)
PSWO	BH F=0.25M*	0.21(-)	0.05(-)	0.53(0.06-1.22)	1.02(0.34-1.35)
	BH F=M*	0.21(-)	0.21(-)	0.88(0.33-1.23)	0.48(0.35-0.53)
	BH F=3M*	0.21(-)	0.63(-)	0.81(0.46-1.24)	0.33(0.3-0.35)
	R F=0.25M	0.21(-)	0.05(-)	0.26(0.03-0.58)	0.89(0.37-1.62)
	R F=M*	0.21(-)	0.21(-)	0.67(0.31-1.16)	0.57(0.37-0.83)
	R F=3M*	0.21(-)	0.63(-)	1.08(0.94-1.25)	0.39(0.36-0.42)

continued next

Stock	Method	M	Fcur	Fmsy	MSY
ANAB	BH F=0.25M*	0.27(-)	0.07(-)	0(0-0.01)	0(0-0.06)
	BH F=M*	0.27(-)	0.27(-)	0(0-0.02)	0.02(0-6.56)
	BH F=3M	0.27(-)	0.81(-)	0.16(0.13-0.2)	1.09(0.95-1.24)
	R F=0.25M*	0.27(-)	0.07(-)	0(0-0)	0.01(0-0.04)
	R F=M*	0.27(-)	0.27(-)	0(0-0.02)	0.02(0-11.91)
	R F=3M	0.27(-)	0.81(-)	0.16(0.13-0.19)	1.15(1-1.33)
ASAB	BH F=0.25M*	0.27(-)	0.07(-)	0(0-0.01)	0.01(0-0.1)
	BH F=M	0.27(-)	0.27(-)	0.09(0.06-0.12)	0.67(0.49-0.88)
	BH F=3M	0.27(-)	0.81(-)	0.48(0.37-0.68)	1.15(1.03-1.32)
	R F=0.25M*	0.27(-)	0.07(-)	0(0-0.01)	0.01(0-0.05)
	R F=M	0.27(-)	0.27(-)	0.07(0.05-0.09)	0.61(0.43-0.79)
	R F=3M	0.27(-)	0.81(-)	0.31(0.27-0.36)	1.12(1-1.24)
ABET	BH F=0.25M*	0.4(-)	0.1(-)	0.24(0.01-1.64)	2.1(0.63-51.55)
	BH F=M*	0.4(-)	0.4(-)	1.24(0.37-2.32)	1.68(1.01-2.03)
	BH F=3M*	0.4(-)	1.2(-)	1.37(0.4-2.31)	0.97(0.73-1.16)
	R F=0.25M*	0.4(-)	0.1(-)	0.16(0.01-0.31)	1.64(0.58-34.97)
	R F=M	0.4(-)	0.4(-)	0.95(0.46-1.76)	2.02(1.23-3.15)
	R F=3M*	0.4(-)	1.2(-)	2.03(1.7-2.38)	1.46(1.27-1.65)
AYFT	BH F=0.25M	0.7(-)	0.18(-)	0.09(0.04-0.15)	1.02(0.29-1.83)
	BH F=M	0.7(-)	0.7(-)	0.47(0.37-0.62)	1.86(1.57-2.2)
	BH F=3M*	0.7(-)	2.1(-)	2.88(1.89-4.1)	2.19(1.95-2.38)
	R F=0.25M	0.7(-)	0.18(-)	0.07(0.02-0.11)	0.81(0.11-1.62)
	R F=M	0.7(-)	0.7(-)	0.35(0.28-0.41)	1.86(1.5-2.26)
	R F=3M	0.7(-)	2.1(-)	1.08(0.94-1.23)	2.13(1.9-2.38)
ABFT	BH F=0.25M*	0.15(-)	0.04(-)	0.28(0-0.86)	0.42(0.01-0.71)
	BH F=M*	0.15(-)	0.15(-)	0.53(0.19-0.87)	0.21(0.14-0.26)
	BH F=3M*	0.15(-)	0.45(-)	0.7(0.53-0.89)	0.14(0.13-0.16)
	R F=0.25M*	0.15(-)	0.04(-)	0.13(0-0.36)	0.34(0-1.12)
	R F=M	0.15(-)	0.15(-)	0.29(0.16-0.47)	0.21(0.14-0.31)
	R F=3M*	0.15(-)	0.45(-)	0.66(0.44-0.88)	0.18(0.14-0.21)
ABUM	BH F=0.25M	0.25(-)	0.06(-)	0.07(0.02-0.13)	0.02(0.01-0.04)
	BH F=M	0.25(-)	0.25(-)	0.18(0.13-0.26)	0.03(0.02-0.03)
	BH F=3M	0.25(-)	0.75(-)	0.53(0.32-1.25)	0.03(0.02-0.03)
	R F=0.25M	0.25(-)	0.06(-)	0.04(0.01-0.07)	0.01(0-0.03)
	R F=M	0.25(-)	0.25(-)	0.14(0.1-0.17)	0.02(0.02-0.03)
	R F=3M	0.25(-)	0.75(-)	0.38(0.3-0.48)	0.03(0.03-0.04)
AWHM	BH F=0.25M*	0.32(-)	0.08(-)	0.02(0.01-0.04)	0.49(0.03-14.47)
	BH F=M	0.32(-)	0.32(-)	0.13(0.1-0.29)	0.17(0.04-13.48)
	BH F=3M*	0.32(-)	0.96(-)	0.51(0.26-1.73)	0.05(0.04-6.56)
	R F=0.25M*	0.32(-)	0.08(-)	0.02(0.02-0.04)	0.52(0.03-14.36)
	R F=M	0.32(-)	0.32(-)	0.14(0.11-0.27)	0.23(0.04-13.77)
	R F=3M	0.32(-)	0.96(-)	0.43(0.3-1.05)	0.1(0.04-12.71)
ASWO	BH F=0.25M*	0.21(-)	0.05(-)	0.01(0-0.96)	1.85(0.01-92.94)
	BH F=M	0.21(-)	0.21(-)	0.03(0.02-0.06)	4.57(0.46-120.9)
	BH F=3M	0.21(-)	0.63(-)	0.07(0.06-0.09)	12.47(0.74-125.56)
	R F=0.25M*	0.21(-)	0.05(-)	0(0-0.19)	1.21(0.02-103.56)
	R F=M	0.21(-)	0.21(-)	0.03(0.02-0.05)	5.31(0.46-127.07)
	R F=3M	0.21(-)	0.63(-)	0.08(0.06-0.1)	12.15(0.76-127.86)

Table 10.2 Biological reference points Fratio, the ratio of current fishing mortality to the fishing mortality that produces MSY, and Nratio, the ratio of current stock size to the stock size that produced MSY when fished at Fmsy. Estimates are from recruitment reconstructions assuming Beverton-holt (BH) and Ricker (R) recruitment relationships for 3 current fishing mortality estimates (Fcur or F) and a known natural mortality rate M. Values are presented as, mode (95% credible interval) and (-) indicates a point estimate.

Stock	Method	Fratio	Nratio
IALB	BH F=0.25M	24.95(3.51-70.32)	10.6(2.06-31.95)
	BH F=M	5.95(2.52-89.66)	0.99(0.73-5.34)
	BH F=3M	2.38(1.14-3.89)	0.74(0.58-1.12)
	R F=0.25M	33.48(5.67-71.47)	10.31(2.06-23.78)
	R F=M	14.84(5.12-177.05)	1.18(0.65-9.11)
	R F=3M	4.98(3.66-7.05)	0.43(0.37-0.49)
IBET	BH F=0.25M	8.92(0.71-102.87)	1.59(0-10.14)
	BH F=M	0.29(0.17-0.75)	2.87(1.69-4.11)
	BH F=3M	0.72(0.51-0.99)	2.27(1.79-3.02)
	R F=0.25M	13.78(1.07-100.43)	1.56(0-9.48)
	R F=M	0.97(0.72-1.36)	1.27(1.18-1.36)
	R F=3M	0.62(0.51-0.89)	1.54(1.39-1.64)
IYFT	BH F=0.25M	3.1(1.55-62.41)	1.68(1.24-14.65)
	BH F=M	2.26(1.45-3.71)	1.01(0.8-1.23)
	BH F=3M	1.05(0.52-2.52)	1.63(0.94-2.76)
	R F=0.25M	5.68(2.31-114.4)	1.98(1.18-25.58)
	R F=M	3.55(2.56-5.63)	0.77(0.63-0.93)
	R F=3M	3.61(2.63-5.01)	0.64(0.52-0.74)
GSBT	BH F=0.25M	0.17(0.04-1.71)	3.23(2.34-6.51)
	BH F=M	1.92(1.27-3.03)	0.74(0.6-0.89)
	BH F=3M	3.04(2.53-3.62)	0.17(0.11-0.24)
	R F=0.25M	1.94(0.69-12.5)	2.75(1.51-13.44)
	R F=M	2.38(1.77-3.39)	0.59(0.51-0.68)
	R F=3M	2.57(2.18-3.07)	0.2(0.14-0.26)
IBUM	BH F=0.25M	2.51(0.78-10.91)	2.61(1.51-8.21)
	BH F=M	1.72(0.88-3.15)	1.12(0.94-1.37)
	BH F=3M	1.07(0.52-2.16)	1.27(0.82-2.13)
	R F=0.25M	7.25(2.51-14.83)	3.69(1.52-7.17)
	R F=M	5(3.19-11.35)	0.85(0.66-1.36)
	R F=3M	4.31(3.29-5.84)	0.45(0.39-0.51)
ISTM	BH F=0.25M	9.31(1.16-122.43)	0.64(0-1.6)
	BH F=M	1.27(0.87-1.74)	0.57(0.45-0.71)
	BH F=3M	0.91(0.52-1.58)	0.72(0.45-1.12)
	R F=0.25M	10.48(1.35-119.49)	0.61(0-1.57)
	R F=M	1.43(1.13-1.83)	0.49(0.42-0.55)
	R F=3M	1.29(1.05-1.6)	0.48(0.42-0.54)
GBLM	BH F=0.25M	4.71(1.81-8.71)	3.89(2.05-6.41)
	BH F=M	3.07(2.13-4.61)	0.79(0.69-0.9)
	BH F=3M	3.04(2.38-3.73)	0.41(0.33-0.5)
	R F=0.25M	8.78(4.88-10.7)	4.64(2.86-5.62)
	R F=M	4.36(3.22-6.53)	0.67(0.58-0.78)
	R F=3M	3.45(2.95-4.08)	0.33(0.28-0.38)
ISWO	BH F=0.25M	6.74(0.77-42.69)	0.1(0-1.8)
	BH F=M	8.84(6.66-11.94)	0.01(0-0.35)
	BH F=3M	11.4(8.88-15.41)	0.01(0-0.25)
	R F=0.25M	6.83(1-41.61)	0.1(0-1.67)
	R F=M	8.61(6.61-11.42)	0.01(0-0.32)
	R F=3M	10.64(8.29-14.62)	0.01(0-0.26)

continued next page

Stock	Method	Fratio	Nratio
PNAB	BH F=0.25M	0.08(0.04-0.5)	5.27(1.72-8.18)
	BH F=M	0.26(0.17-0.63)	3.15(1.48-4.47)
	BH F=3M	0.64(0.51-1.18)	1.56(0.74-2.01)
	R F=0.25M	0.23(0.13-0.47)	2.54(1.74-3.04)
	R F=M	0.46(0.3-0.7)	1.94(1.31-2.46)
	R F=3M	0.66(0.51-1.03)	1.48(0.78-1.88)
PSAB	BH F=0.25M	0.93(0.49-2.48)	1.76(1.49-2.15)
	BH F=M	1.19(0.79-1.68)	1.3(1.09-1.61)
	BH F=3M	0.97(0.54-1.52)	1.49(1.07-2.36)
	R F=0.25M	1.39(0.83-6.15)	1.58(1.33-2.5)
	R F=M	1.7(1.38-2.13)	1(0.9-1.1)
	R F=3M	1.82(1.58-2.1)	0.85(0.77-0.92)
PBET	BH F=0.25M	2.03(1.01-33.47)	1.52(1.24-6.31)
	BH F=M	1.37(0.92-1.94)	1.1(0.93-1.31)
	BH F=3M	0.61(0.51-0.77)	1.98(1.66-2.32)
	R F=0.25M	2.78(1.38-44.16)	1.51(1.17-8.25)
	R F=M	2.05(1.65-2.61)	0.85(0.77-0.92)
	R F=3M	1.95(1.66-2.28)	0.78(0.71-0.84)
PYFT	BH F=0.25M	1.23(0.8-2.2)	1.43(1.27-1.57)
	BH F=M	0.76(0.45-1.14)	1.62(1.33-2.17)
	BH F=3M	0.57(0.5-0.64)	2.5(2.25-2.8)
	R F=0.25M	1.59(1.11-2.76)	1.32(1.17-1.49)
	R F=M	1.56(1.31-1.87)	1.07(0.99-1.13)
	R F=3M	1.36(1.16-1.61)	1.12(1.04-1.2)
PBFT	BH F=0.25M	0.36(0.05-2.19)	1.91(1.23-4.43)
	BH F=M	1.29(0.55-2.5)	0.69(0.35-1.2)
	BH F=3M	2.21(1.31-3.32)	0.27(0.09-0.53)
	R F=0.25M	1.28(0.54-5.74)	1.35(0.86-3.35)
	R F=M	1.69(1.1-3.1)	0.49(0.25-0.63)
	R F=3M	2.05(1.49-3.09)	0.25(0.05-0.38)
PBUM	BH F=0.25M	0.48(0.23-0.97)	1.92(1.65-2.29)
	BH F=M	0.96(0.59-1.38)	1.24(1.01-1.63)
	BH F=3M	1.34(0.84-1.8)	0.87(0.68-1.28)
	R F=0.25M	1.36(0.83-3.54)	1.59(1.25-2.71)
	R F=M	1.78(1.44-2.25)	0.78(0.69-0.87)
	R F=3M	2.03(1.76-2.33)	0.53(0.47-0.59)
PSTM	BH F=0.25M	0.77(0.46-1.47)	0.58(0-0.97)
	BH F=M	1.05(0.6-1.57)	0.3(0-0.71)
	BH F=3M	1.44(0.72-2.06)	0.18(0-0.6)
	R F=0.25M	0.81(0.5-1.44)	0.54(0-0.89)
	R F=M	0.96(0.63-1.38)	0.31(0-0.66)
	R F=3M	1.05(0.66-1.46)	0.25(0-0.61)
PSWO	BH F=0.25M	0.1(0.04-0.86)	3.66(1.3-6.37)
	BH F=M	0.24(0.17-0.63)	3.22(1.64-4.16)
	BH F=3M	0.77(0.51-1.38)	1.48(0.85-2.12)
	R F=0.25M	0.2(0.09-1.64)	2.1(0.66-2.52)
	R F=M	0.32(0.18-0.67)	2.05(1.48-2.45)
	R F=3M	0.58(0.5-0.67)	1.65(1.52-1.79)

continued next page

Stock	Method	Fratio	Nratio
ANAB	BH F=0.25M	37.26(9.73-72.24)	8.03(2.31-18.79)
	BH F=M	81.71(13.21-275.15)	1.07(0-4.52)
	BH F=3M	4.98(4.04-6.15)	0.26(0.21-0.3)
	R F=0.25M	37.28(14.31-72.59)	6.62(2.32-14.89)
	R F=M	90.06(15.53-276.37)	1.07(0-4.34)
	R F=3M	5.2(4.32-6.3)	0.23(0.2-0.26)
ASAB	BH F=0.25M	23.89(6.17-67.58)	7.68(2.52-21.33)
	BH F=M	3.09(2.28-4.34)	0.73(0.65-0.81)
	BH F=3M	1.69(1.19-2.18)	0.78(0.65-0.99)
	R F=0.25M	31.5(9.62-72.01)	8.49(2.95-19.75)
	R F=M	3.87(3-5.3)	0.64(0.57-0.7)
	R F=3M	2.62(2.27-3.04)	0.51(0.48-0.55)
ABET	BH F=0.25M	0.42(0.06-7.67)	1.71(0-4.21)
	BH F=M	0.32(0.17-1.09)	2.61(1.29-4.03)
	BH F=3M	0.87(0.52-2.97)	1.65(0.55-2.52)
	R F=0.25M	0.62(0.32-6.95)	1.43(0.01-1.6)
	R F=M	0.42(0.23-0.86)	1.65(1.31-1.95)
	R F=3M	0.59(0.5-0.71)	1.61(1.46-1.74)
AYFT	BH F=0.25M	1.86(1.16-4.45)	1.1(0.86-1.57)
	BH F=M	1.48(1.13-1.92)	0.77(0.65-0.91)
	BH F=3M	0.73(0.51-1.11)	1.32(0.95-1.75)
	R F=0.25M	2.55(1.54-9.29)	1.03(0.78-2.19)
	R F=M	2.03(1.69-2.52)	0.56(0.49-0.62)
	R F=3M	1.95(1.71-2.24)	0.51(0.46-0.55)
ABFT	BH F=0.25M	0.14(0.04-13.83)	3.79(1.04-7.59)
	BH F=M	0.28(0.17-0.77)	3.44(1.87-5.04)
	BH F=3M	0.64(0.51-0.84)	2.21(1.71-2.76)
	R F=0.25M	0.3(0.1-24.39)	2.21(0.02-4.14)
	R F=M	0.52(0.32-0.93)	1.83(1.52-2.1)
	R F=3M	0.69(0.51-1.02)	1.66(1.38-1.87)
ABUM	BH F=0.25M	0.95(0.48-2.55)	1.57(1.29-2.08)
	BH F=M	1.39(0.95-1.97)	0.88(0.7-1.1)
	BH F=3M	1.42(0.6-2.34)	0.76(0.48-1.51)
	R F=0.25M	1.61(0.91-4.57)	1.42(1.13-2.42)
	R F=M	1.83(1.47-2.38)	0.68(0.58-0.78)
	R F=3M	1.96(1.56-2.51)	0.52(0.41-0.62)
AWHM	BH F=0.25M	3.35(1.88-5.34)	0.02(0-0.48)
	BH F=M	2.46(1.1-3.18)	0.07(0-0.56)
	BH F=3M	1.88(0.55-3.69)	0.31(0-1.08)
	R F=0.25M	3.34(1.95-5.33)	0.02(0-0.45)
	R F=M	2.28(1.19-2.93)	0.05(0-0.52)
	R F=3M	2.23(0.92-3.19)	0.13(0-0.64)
ASWO	BH F=0.25M	7.88(0.05-53.01)	1.16(0-4.81)
	BH F=M	8.37(3.36-11.47)	0.03(0-0.81)
	BH F=3M	9.12(6.88-11.01)	0.01(0-0.26)
	R F=0.25M	13.21(0.27-53.84)	0.48(0-2.68)
	R F=M	8.26(4.12-11.19)	0.03(0-0.69)
	R F=3M	8.38(6.34-10.45)	0.01(0-0.27)

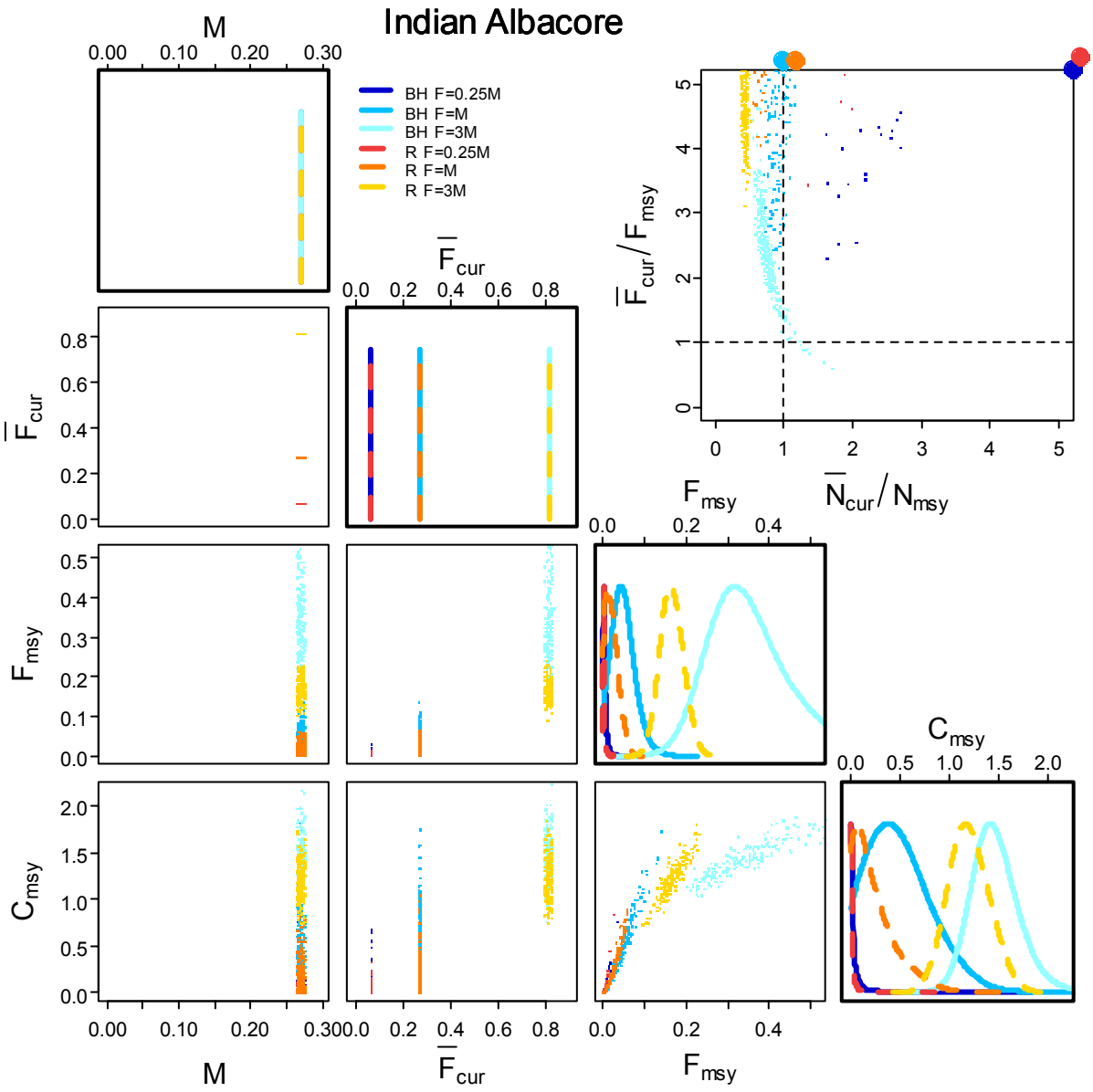

Figure 10.1 Indian Ocean albacore tuna leading parameter joint distributions (lower triangular), marginal posterior distributions (diagonal) and biological reference points (upper triangular) for F_{msy} and MSY (C_{msy}) estimated from recruitment reconstructions assuming Beverton-Holt (BH) and Ricker (R) recruitment relationships for three current fishing mortality estimates (F_{cur} or F) and a known natural mortality rate M. Biological reference points are the ratio of current fishing mortality to the fishing mortality which produces MSY, and the ratio of current stock size to the stock size that produces MSY when fished at F_{msy}. Filled circles outside the upper triangular plot indicate ratios greater than 5. If both ratios are greater than 5 the filled circles lay in the top right corner.

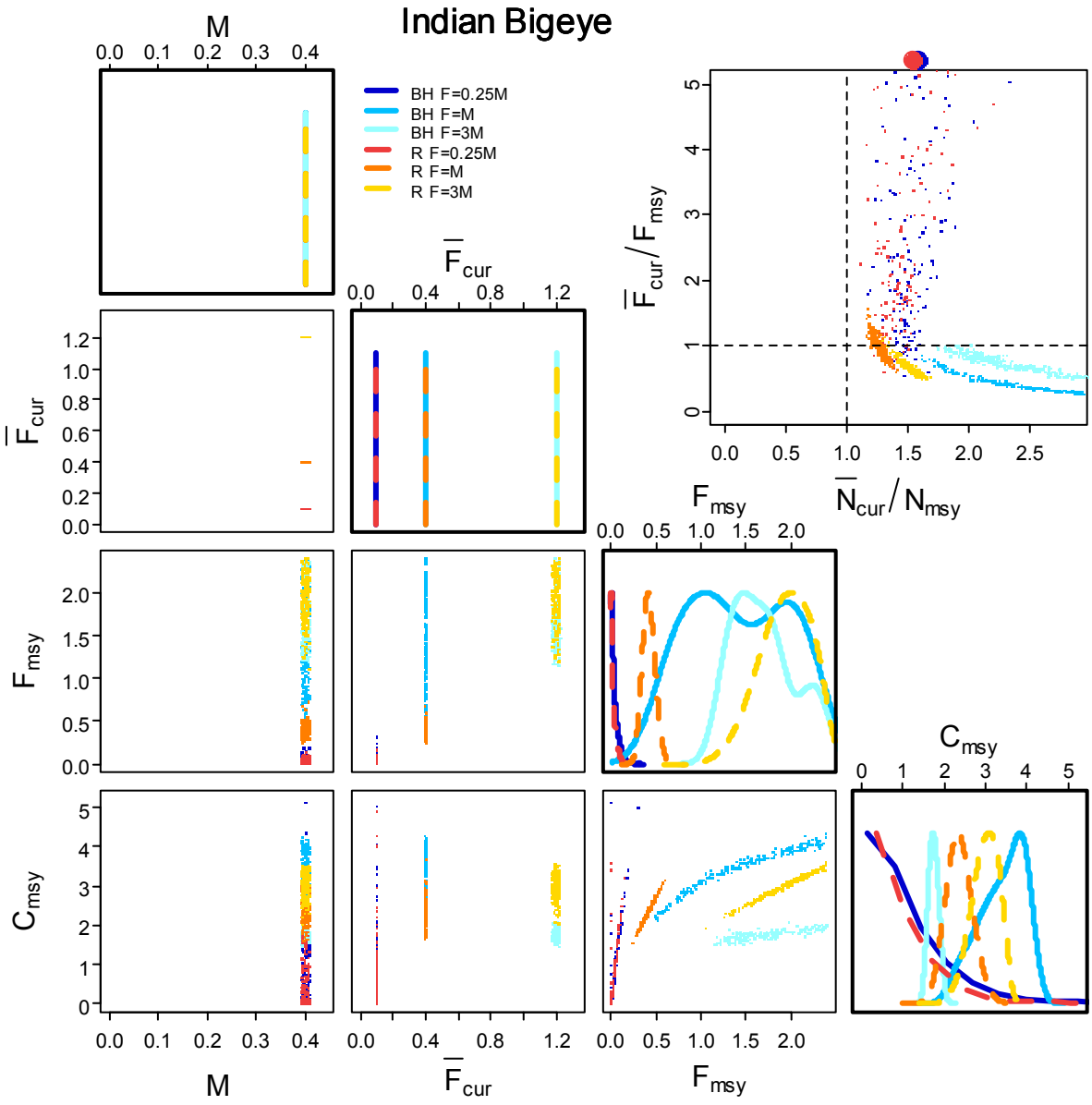

Figure 10.2 Indian Ocean bigeye tuna leading parameter joint distributions (lower triangular), marginal posterior distributions (diagonal) and biological reference points (upper triangular) for F_{msy} and MSY (C_{msy}) estimated from recruitment reconstructions assuming Beverton-Holt (BH) and Ricker (R) recruitment relationships for three current fishing mortality estimates (F_{cur} or F) and a known natural mortality rate M. Biological reference points are the ratio of current fishing mortality to the fishing mortality which produces MSY, and the ratio of current stock size to the stock size that produces MSY when fished at F_{msy}. Filled circles outside the upper triangular plot indicate ratios greater than 5. If both ratios are greater than 5 the filled circles lay in the top right corner.

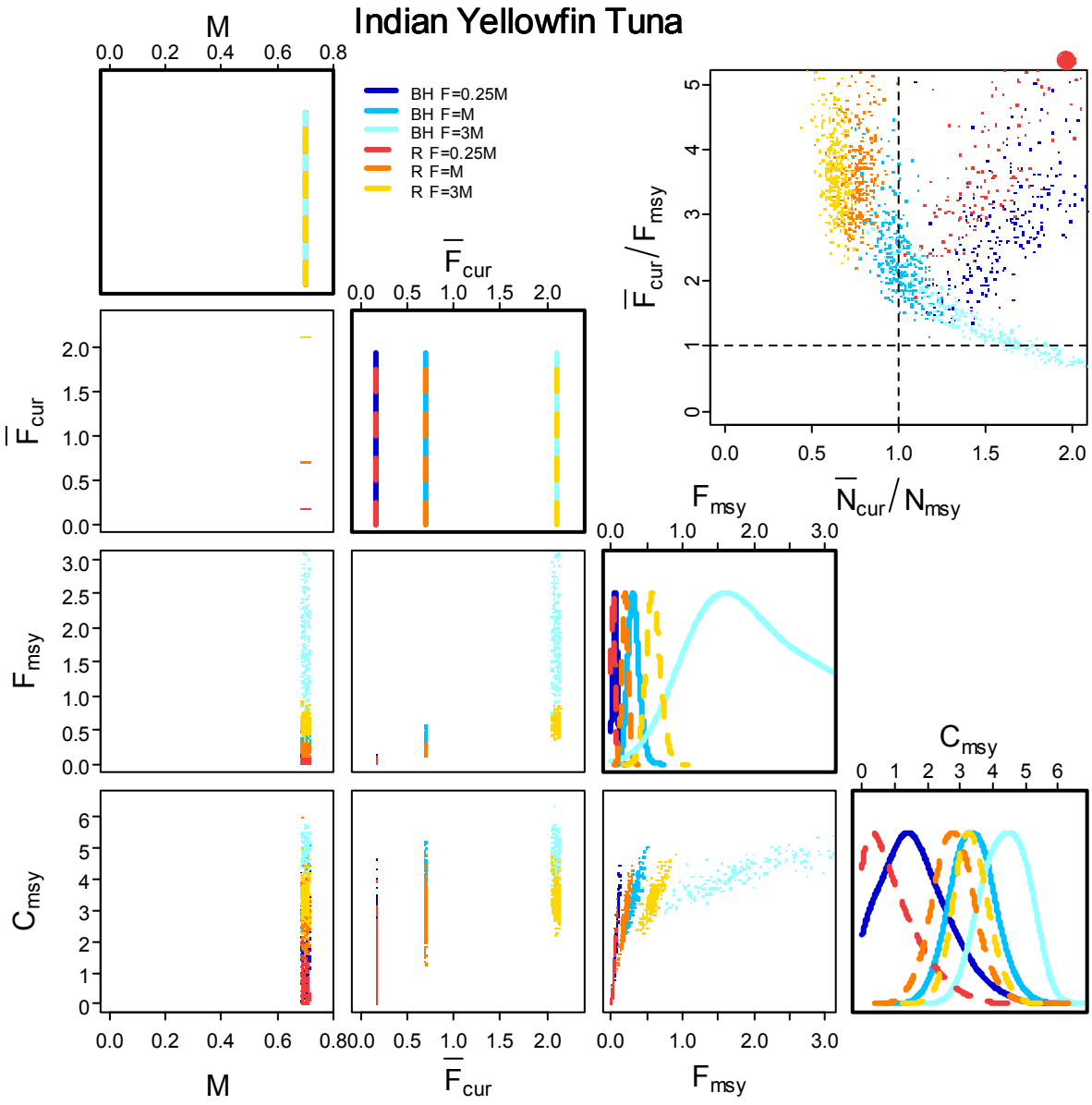

Figure 10.3 Indian Ocean yellowfin tuna leading parameter joint distributions (lower triangular), marginal posterior distributions (diagonal) and biological reference points (upper triangular) for F_{msy} and MSY (C_{msy}) estimated from recruitment reconstructions assuming Beverton-Holt (BH) and Ricker (R) recruitment relationships for three current fishing mortality estimates (F_{cur} or F) and a known natural mortality rate M. Biological reference points are the ratio of current fishing mortality to the fishing mortality which produces MSY, and the ratio of current stock size to the stock size that produces MSY when fished at F_{msy}. Filled circles outside the upper triangular plot indicate ratios greater than 5. If both ratios are greater than 5 the filled circles lay in the top right corner.

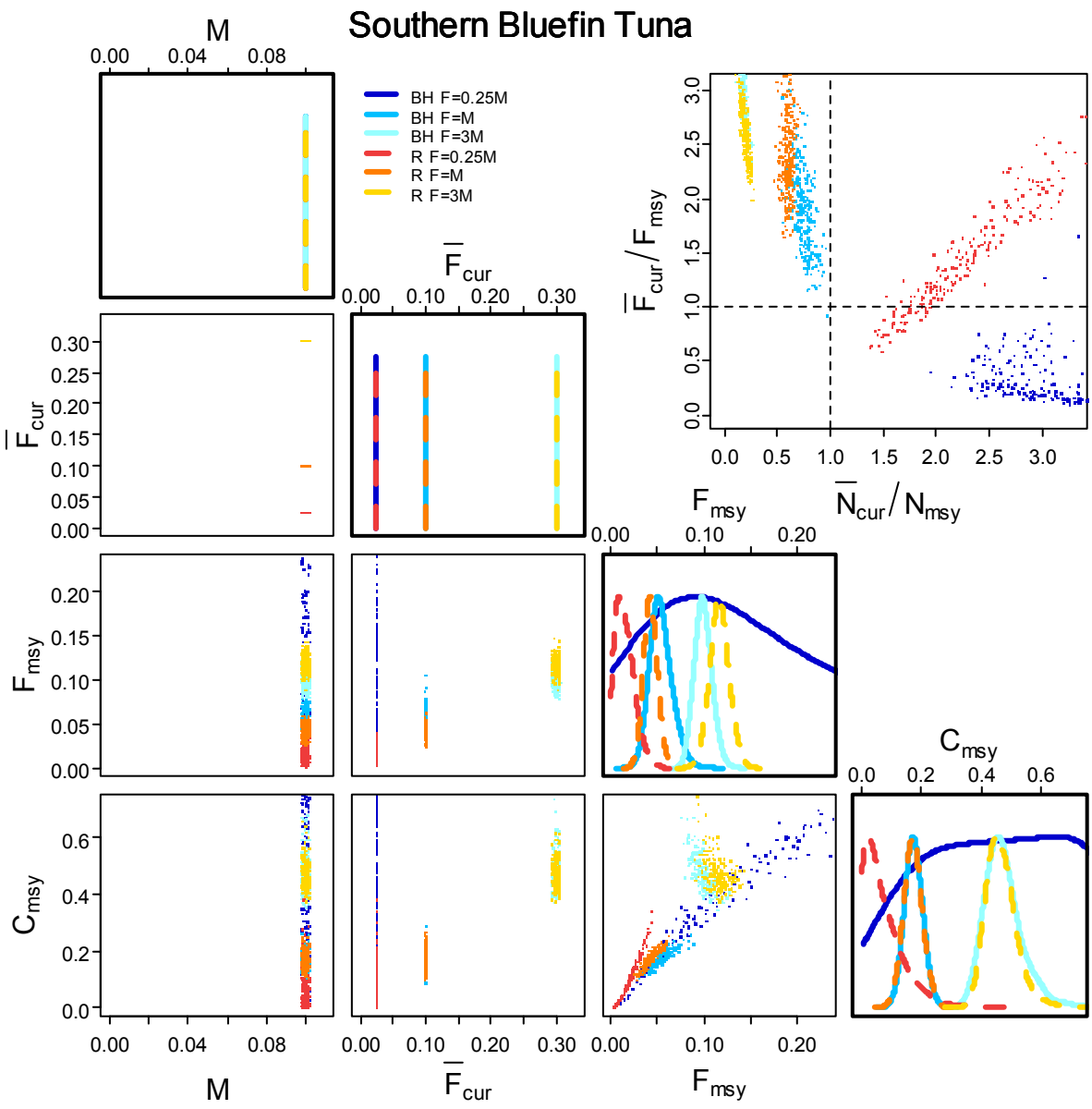

Figure 10.4 Southern bluefin tuna leading parameter joint distributions (lower triangular), marginal posterior distributions (diagonal) and biological reference points (upper triangular) for F_{msy} and MSY (C_{msy}) estimated from recruitment reconstructions assuming Beverton-Holt (BH) and Ricker (R) recruitment relationships for three current fishing mortality estimates (F_{cur} or F) and a known natural mortality rate M. Biological reference points are the ratio of current fishing mortality to the fishing mortality which produces MSY, and the ratio of current stock size to the stock size that produces MSY when fished at F_{msy}. Filled circles outside the upper triangular plot indicate ratios greater than 5. If both ratios are greater than 5 the filled circles lay in the top right corner.

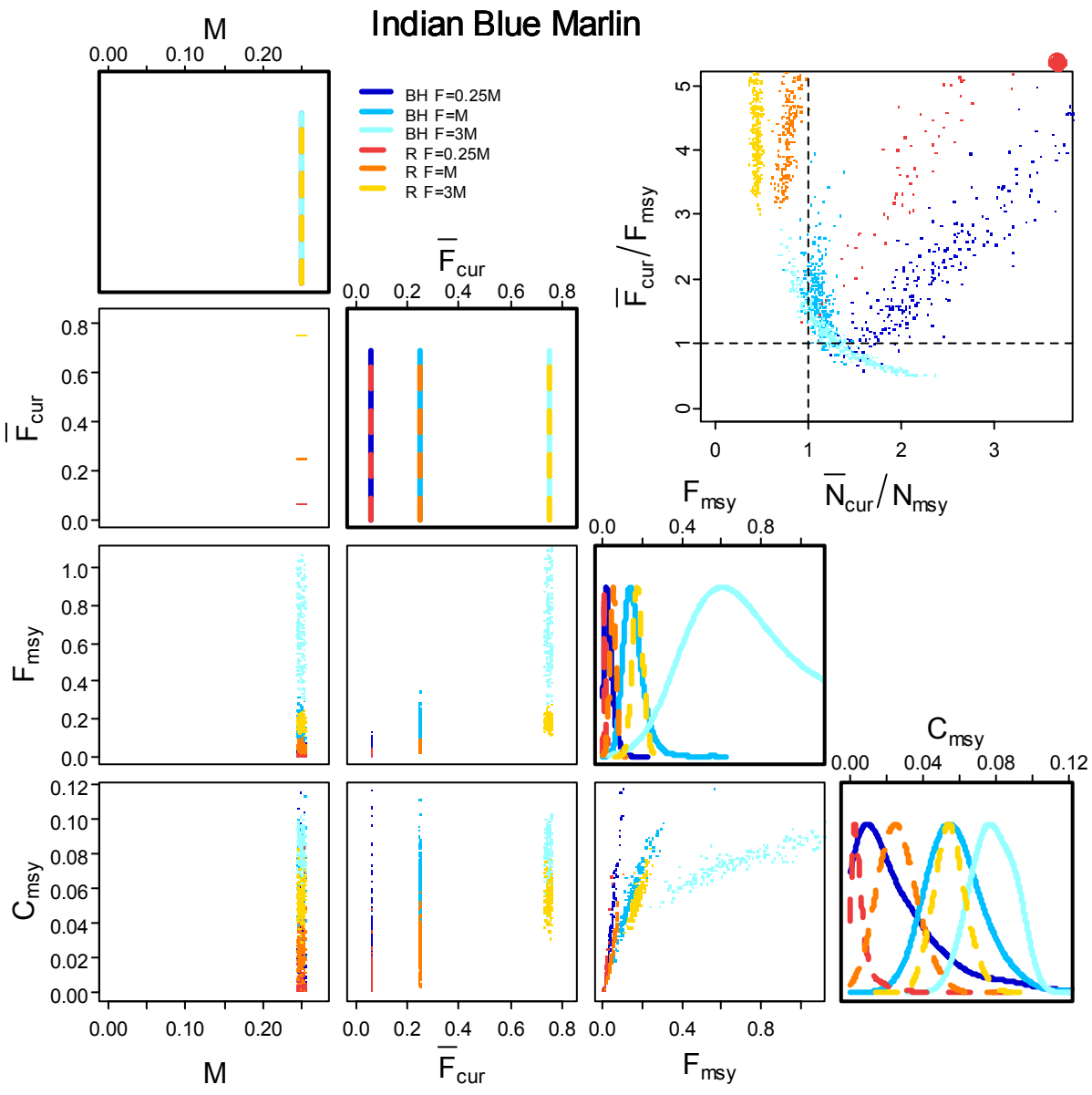

Figure 10.5 Indian Ocean blue marlin leading parameter joint distributions (lower triangular), marginal posterior distributions (diagonal) and biological reference points (upper triangular) for F_{msy} and MSY (C_{msy}) estimated from recruitment reconstructions assuming Beverton-Holt (BH) and Ricker (R) recruitment relationships for three current fishing mortality estimates (F_{cur} or F) and a known natural mortality rate M. Biological reference points are the ratio of current fishing mortality to the fishing mortality which produces MSY, and the ratio of current stock size to the stock size that produces MSY when fished at F_{msy}. Filled circles outside the upper triangular plot indicate ratios greater than 5. If both ratios are greater than 5 the filled circles lay in the top right corner.

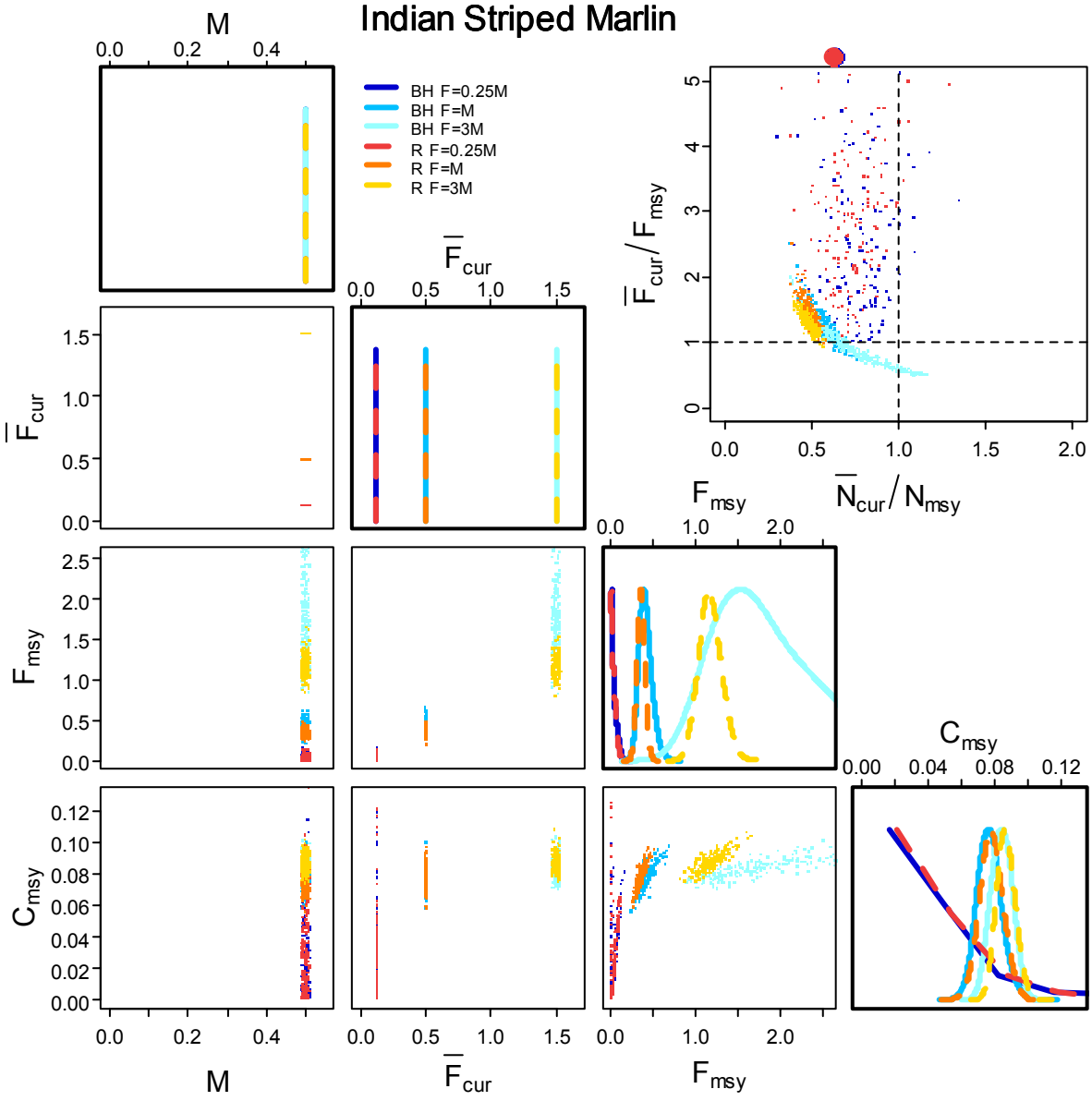

Figure 10.6 Indian Ocean striped marlin leading parameter joint distributions (lower triangular), marginal posterior distributions (diagonal) and biological reference points (upper triangular) for F_{msy} and MSY (C_{msy}) estimated from recruitment reconstructions assuming Beverton-Holt (BH) and Ricker (R) recruitment relationships for three current fishing mortality estimates (F_{cur} or F) and a known natural mortality rate M. Biological reference points are the ratio of current fishing mortality to the fishing mortality which produces MSY, and the ratio of current stock size to the stock size that produces MSY when fished at F_{msy}. Filled circles outside the upper triangular plot indicate ratios greater than 5. If both ratios are greater than 5 the filled circles lay in the top right corner.

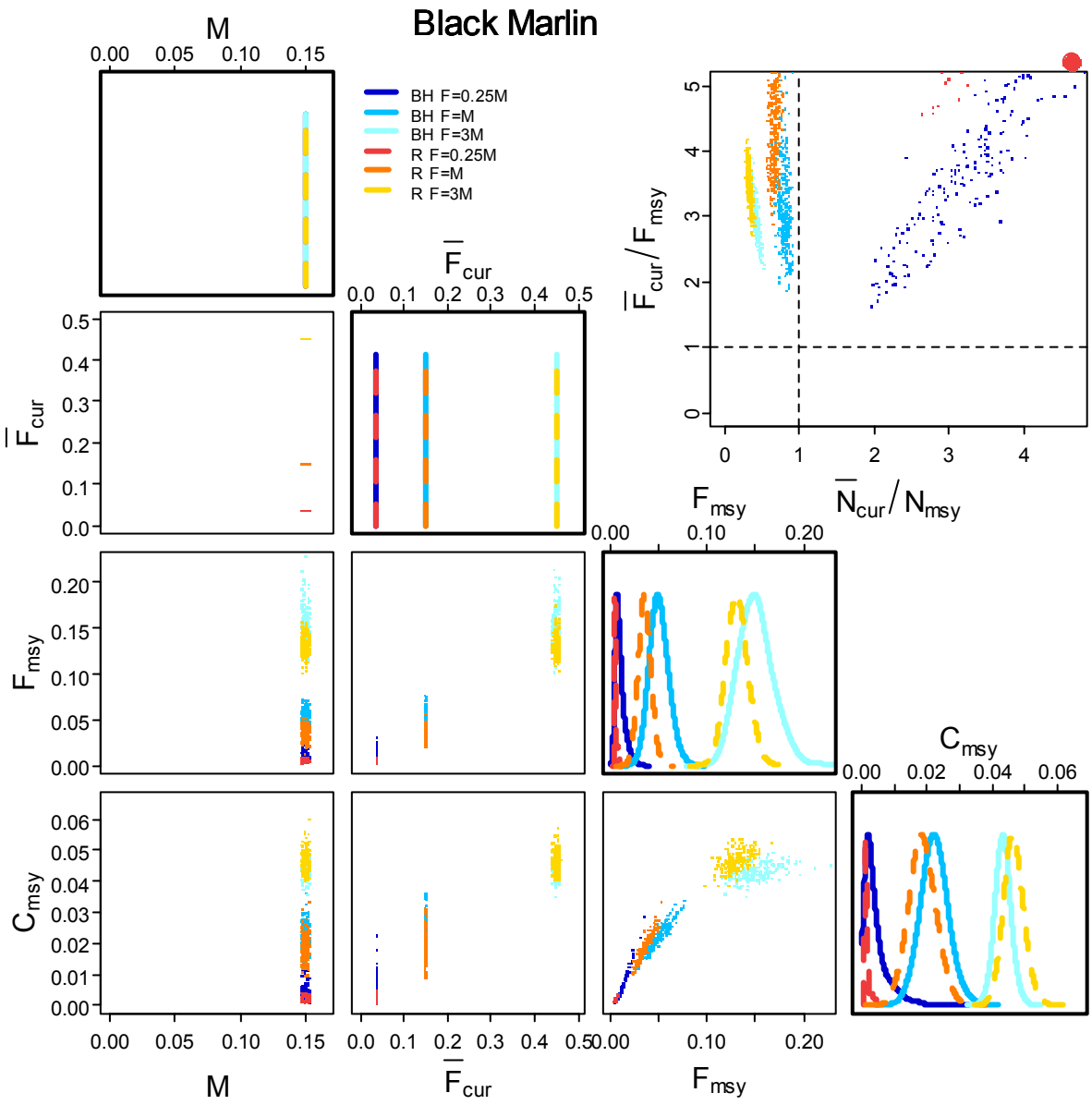

Figure 10.7 Indo-Pacific black marlin leading parameter joint distributions (lower triangular), marginal posterior distributions (diagonal) and biological reference points (upper triangular) for F_{msy} and MSY (C_{msy}) estimated from recruitment reconstructions assuming Beverton-Holt (BH) and Ricker (R) recruitment relationships for three current fishing mortality estimates (F_{cur} or F) and a known natural mortality rate M. Biological reference points are the ratio of current fishing mortality to the fishing mortality which produces MSY, and the ratio of current stock size to the stock size that produces MSY when fished at F_{msy}. Filled circles outside the upper triangular plot indicate ratios greater than 5. If both ratios are greater than 5 the filled circles lay in the top right corner.

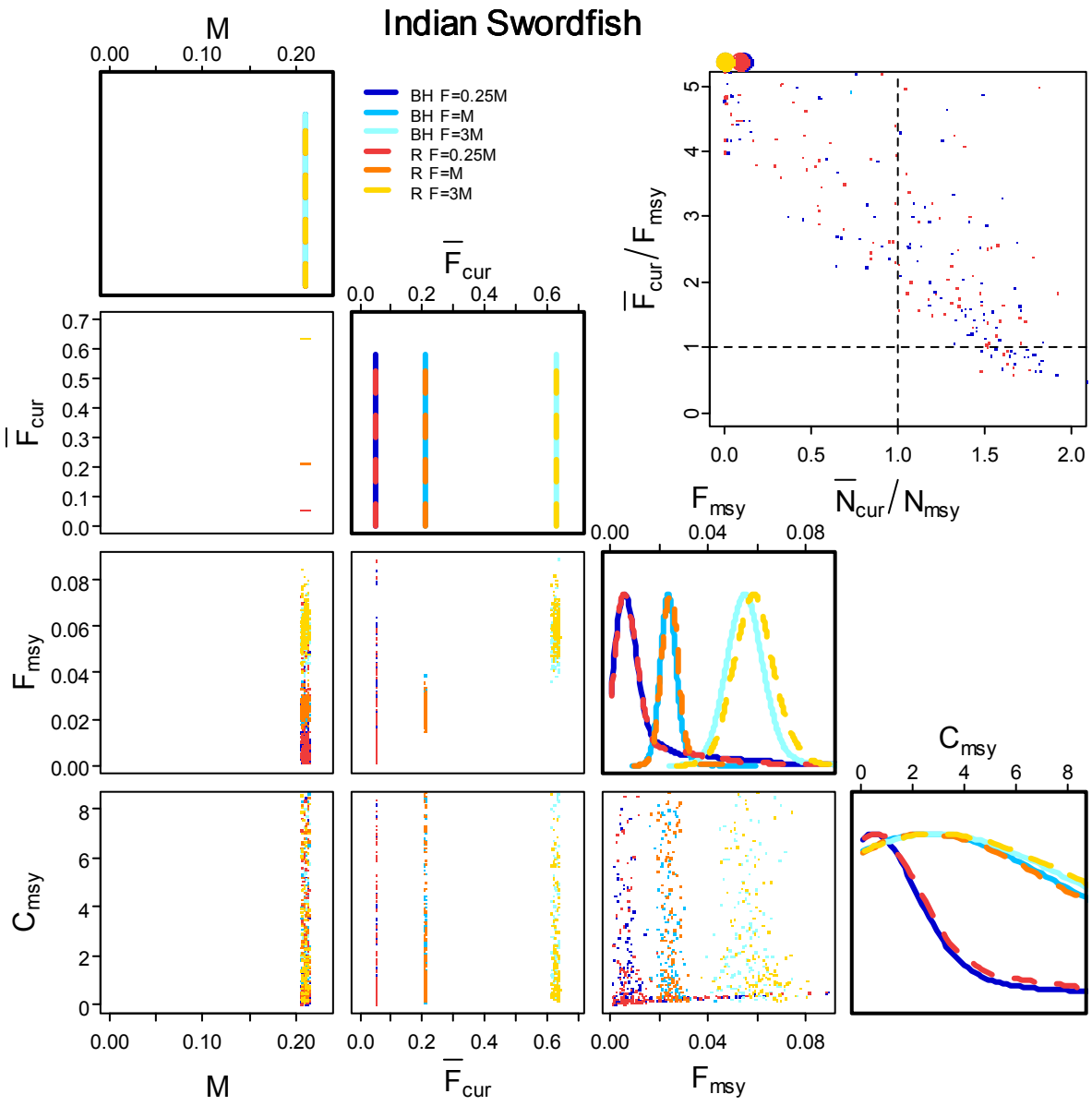

Figure 10.8 Indian Ocean swordfish leading parameter joint distributions (lower triangular), marginal posterior distributions (diagonal) and biological reference points (upper triangular) for F_{msy} and MSY (C_{msy}) estimated from recruitment reconstructions assuming Beverton-Holt (BH) and Ricker (R) recruitment relationships for three current fishing mortality estimates (F_{cur} or F) and a known natural mortality rate M. Biological reference points are the ratio of current fishing mortality to the fishing mortality which produces MSY, and the ratio of current stock size to the stock size that produces MSY when fished at F_{msy}. Filled circles outside the upper triangular plot indicate ratios greater than 5. If both ratios are greater than 5 the filled circles lay in the top right corner.

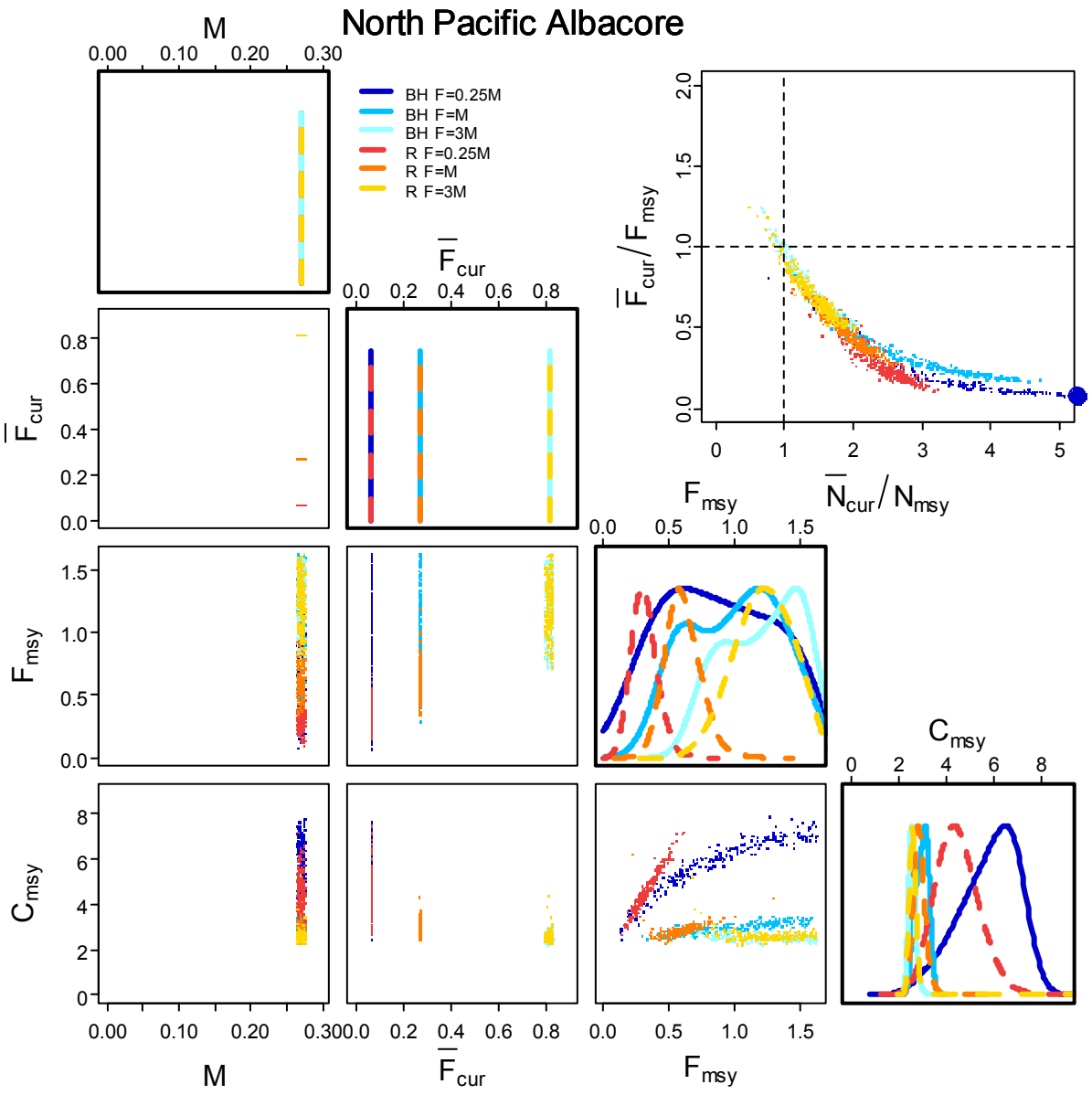

Figure 10.9 Pacific Ocean northern albacore tuna leading parameter joint distributions (lower triangular), marginal posterior distributions (diagonal) and biological reference points (upper triangular) for F_{msy} and MSY (C_{msy}) estimated from recruitment reconstructions assuming Beverton-Holt (BH) and Ricker (R) recruitment relationships for three current fishing mortality estimates (F_{cur} or F) and a known natural mortality rate M. Biological reference points are the ratio of current fishing mortality to the fishing mortality which produces MSY, and the ratio of current stock size to the stock size that produces MSY when fished at F_{msy}. Filled circles outside the upper triangular plot indicate ratios greater than 5. If both ratios are greater than 5 the filled circles lay in the top right corner.

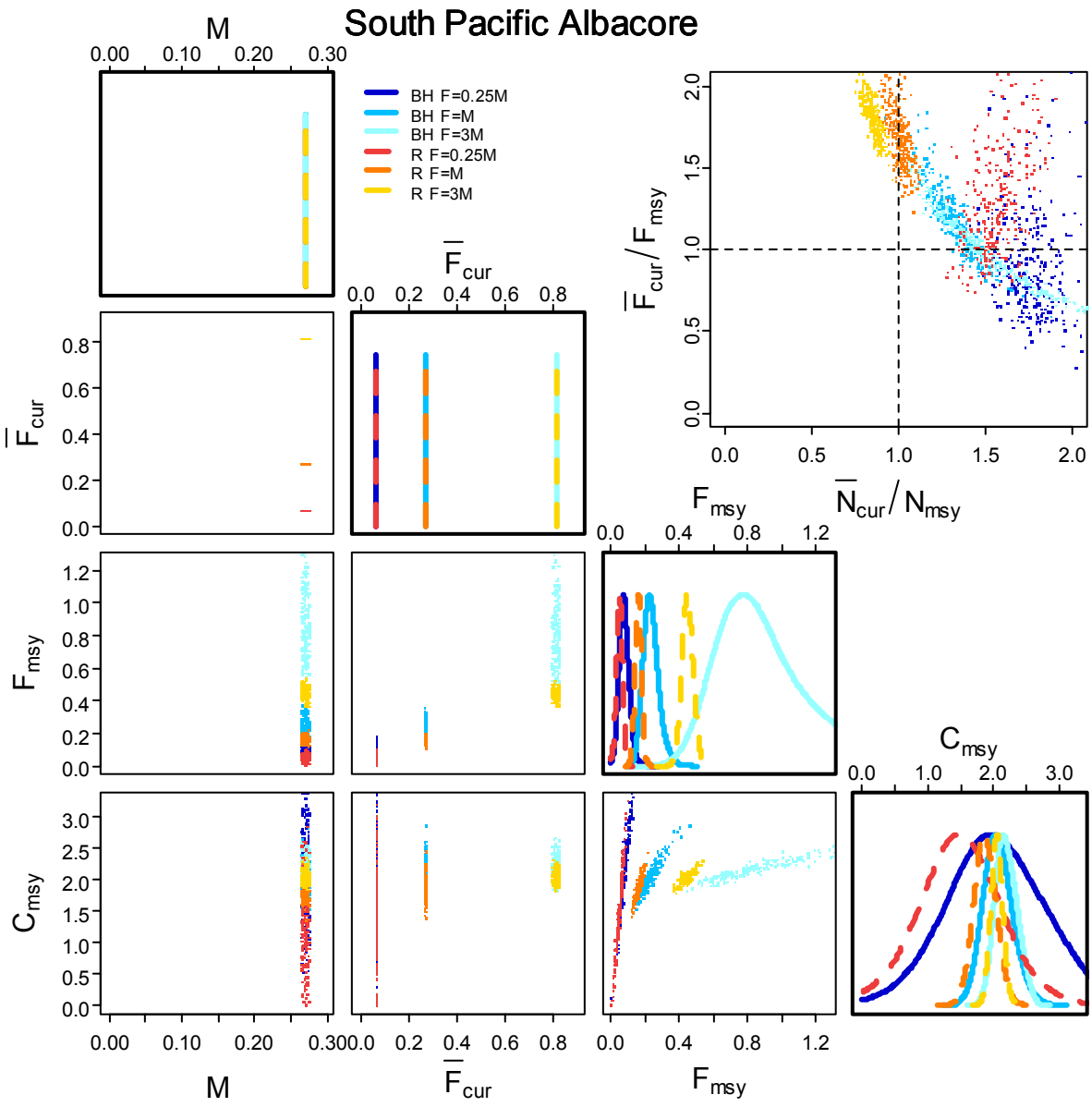

Figure 10.10 Pacific Ocean southern albacore tuna leading parameter joint distributions (lower triangular), marginal posterior distributions (diagonal) and biological reference points (upper triangular) for F_{msy} and MSY (C_{msy}) estimated from recruitment reconstructions assuming Beverton-Holt (BH) and Ricker (R) recruitment relationships for three current fishing mortality estimates (F_{cur} or F) and a known natural mortality rate M. Biological reference points are the ratio of current fishing mortality to the fishing mortality which produces MSY, and the ratio of current stock size to the stock size that produces MSY when fished at F_{msy}. Filled circles outside the upper triangular plot indicate ratios greater than 5. If both ratios are greater than 5 the filled circles lay in the top right corner.

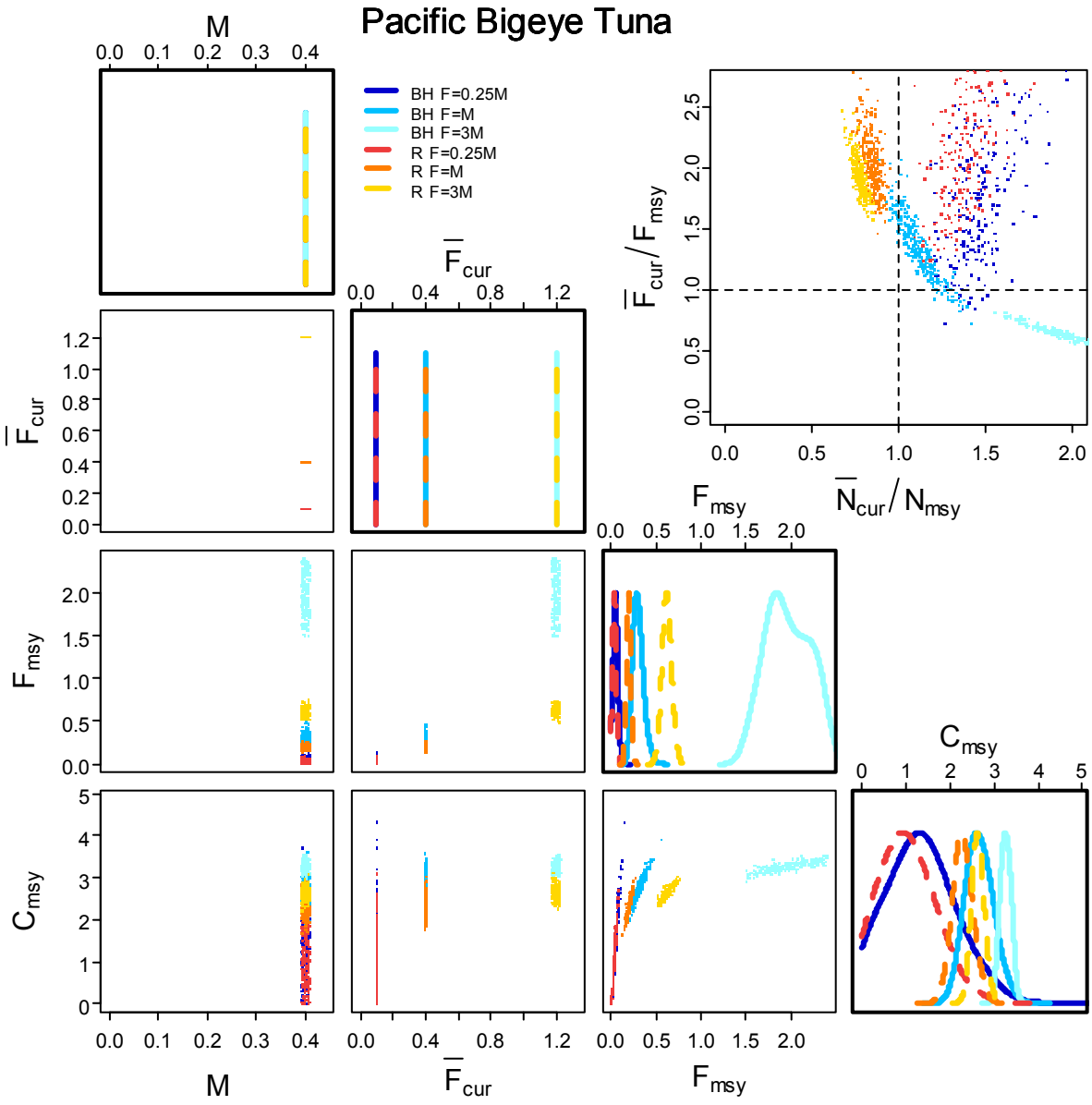

Figure 10.11 Pacific Ocean bigeye tuna leading parameter joint distributions (lower triangular), marginal posterior distributions (diagonal) and biological reference points (upper triangular) for F_{msy} and MSY (C_{msy}) estimated from recruitment reconstructions assuming Beverton-Holt (BH) and Ricker (R) recruitment relationships for three current fishing mortality estimates (F_{cur} or F) and a known natural mortality rate M. Biological reference points are the ratio of current fishing mortality to the fishing mortality which produces MSY, and the ratio of current stock size to the stock size that produces MSY when fished at F_{msy}. Filled circles outside the upper triangular plot indicate ratios greater than 5. If both ratios are greater than 5 the filled circles lay in the top right corner.

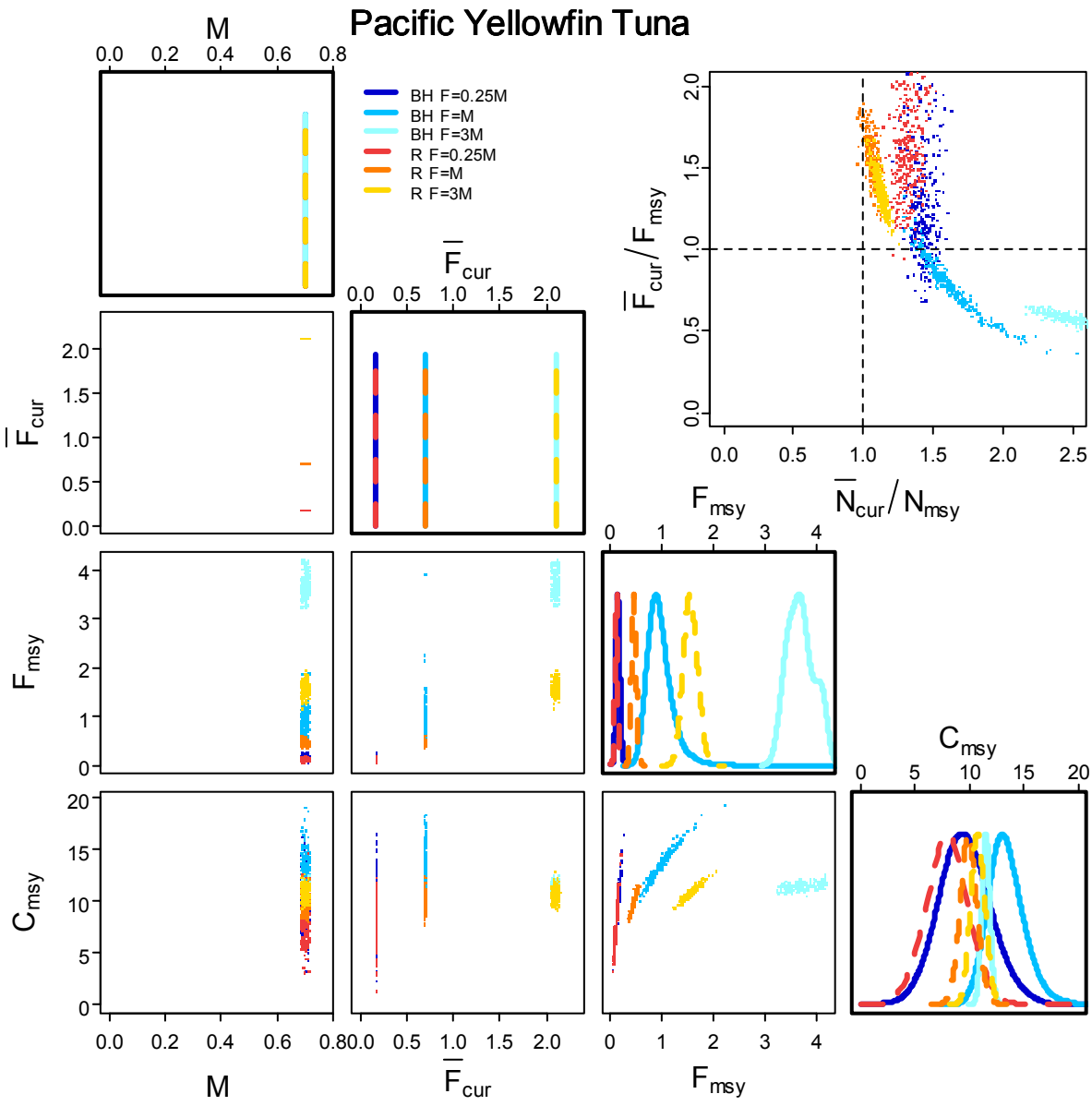

Figure 10.12 Pacific Ocean yellowfin tuna leading parameter joint distributions (lower triangular), marginal posterior distributions (diagonal) and biological reference points (upper triangular) for F_{msy} and MSY (C_{msy}) estimated from recruitment reconstructions assuming Beverton-Holt (BH) and Ricker (R) recruitment relationships for three current fishing mortality estimates (F_{cur} or F) and a known natural mortality rate M. Biological reference points are the ratio of current fishing mortality to the fishing mortality which produces MSY, and the ratio of current stock size to the stock size that produces MSY when fished at F_{msy}. Filled circles outside the upper triangular plot indicate ratios greater than 5. If both ratios are greater than 5 the filled circles lay in the top right corner.

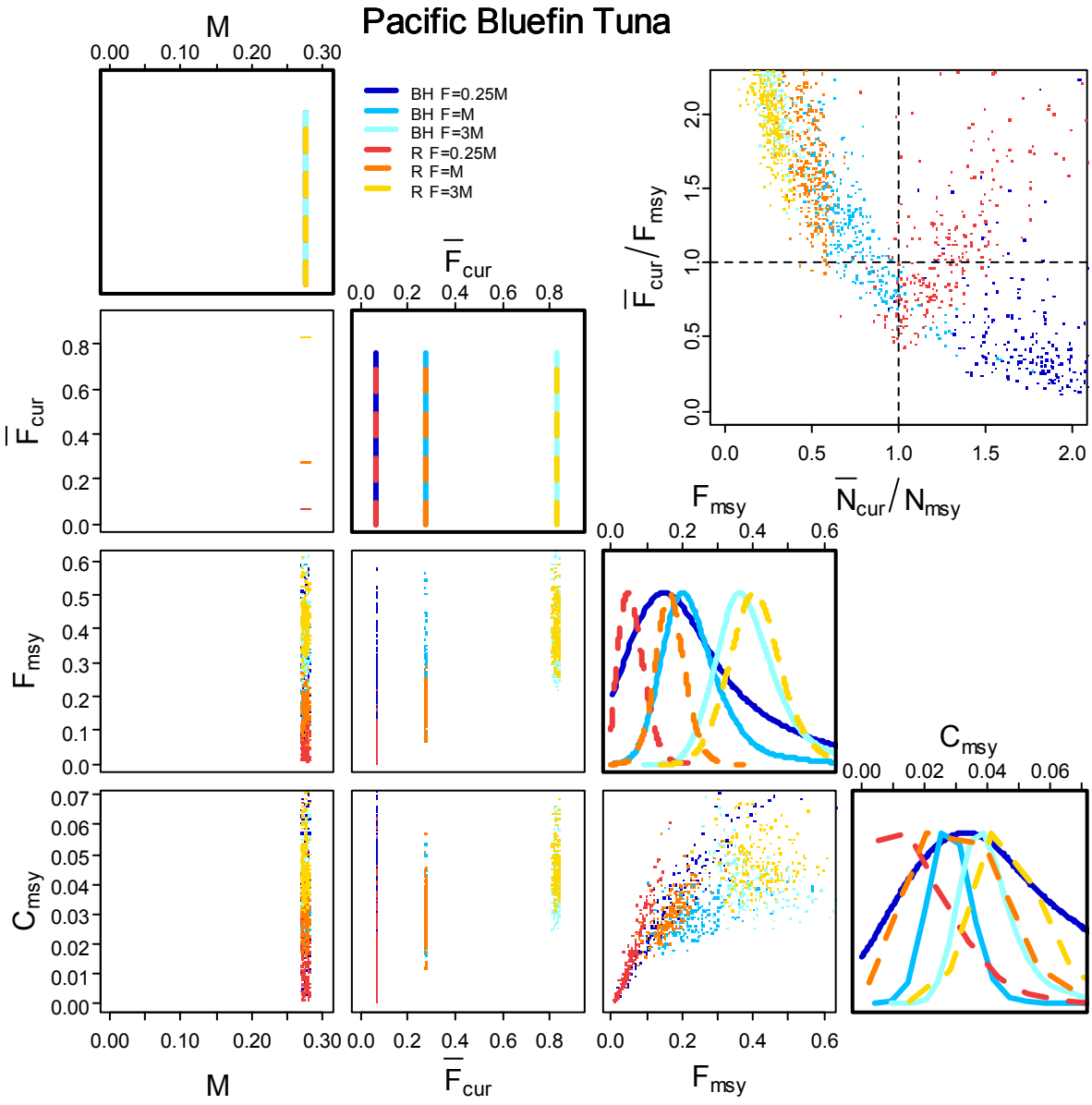

Figure 10.13 Pacific Ocean bluefin tuna leading parameter joint distributions (lower triangular), marginal posterior distributions (diagonal) and biological reference points (upper triangular) for F_{msy} and MSY (C_{msy}) estimated from recruitment reconstructions assuming Beverton-Holt (BH) and Ricker (R) recruitment relationships for three current fishing mortality estimates (F_{cur} or F) and a known natural mortality rate M. Biological reference points are the ratio of current fishing mortality to the fishing mortality which produces MSY, and the ratio of current stock size to the stock size that produces MSY when fished at F_{msy}. Filled circles outside the upper triangular plot indicate ratios greater than 5. If both ratios are greater than 5 the filled circles lay in the top right corner.

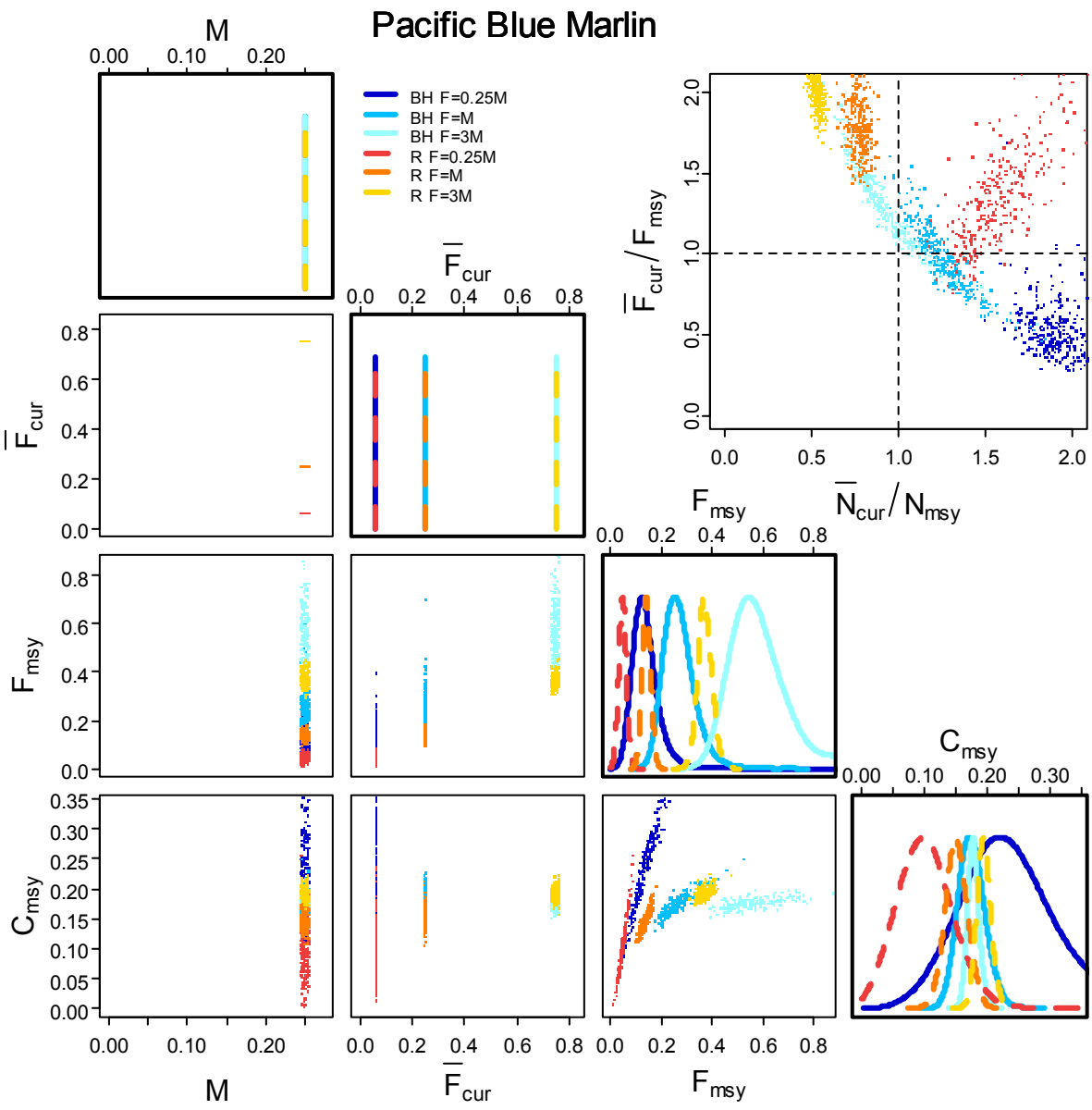

Figure 10.14 Pacific Ocean blue marlin leading parameter joint distributions (lower triangular), marginal posterior distributions (diagonal) and biological reference points (upper triangular) for F_{msy} and MSY (C_{msy}) estimated from recruitment reconstructions assuming Beverton-Holt (BH) and Ricker (R) recruitment relationships for three current fishing mortality estimates (F_{cur} or F) and a known natural mortality rate M. Biological reference points are the ratio of current fishing mortality to the fishing mortality which produces MSY, and the ratio of current stock size to the stock size that produces MSY when fished at F_{msy}. Filled circles outside the upper triangular plot indicate ratios greater than 5. If both ratios are greater than 5 the filled circles lay in the top right corner.

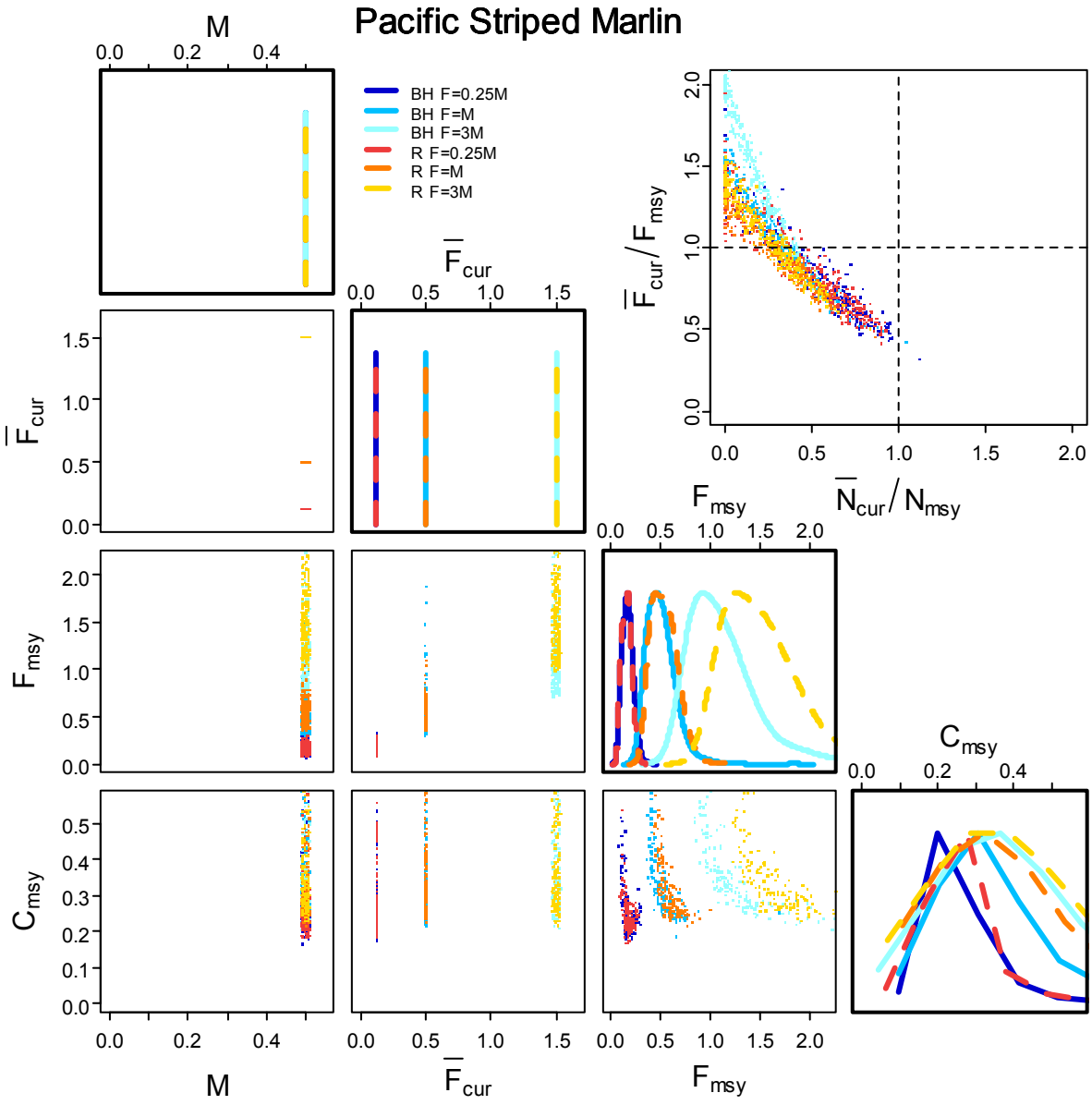

Figure 10.15 Pacific Ocean striped marlin leading parameter joint distributions (lower triangular), marginal posterior distributions (diagonal) and biological reference points (upper triangular) for F_{msy} and MSY (C_{msy}) estimated from recruitment reconstructions assuming Beverton-Holt (BH) and Ricker (R) recruitment relationships for three current fishing mortality estimates (F_{cur} or F) and a known natural mortality rate M. Biological reference points are the ratio of current fishing mortality to the fishing mortality which produces MSY, and the ratio of current stock size to the stock size that produces MSY when fished at F_{msy}. Filled circles outside the upper triangular plot indicate ratios greater than 5. If both ratios are greater than 5 the filled circles lay in the top right corner.

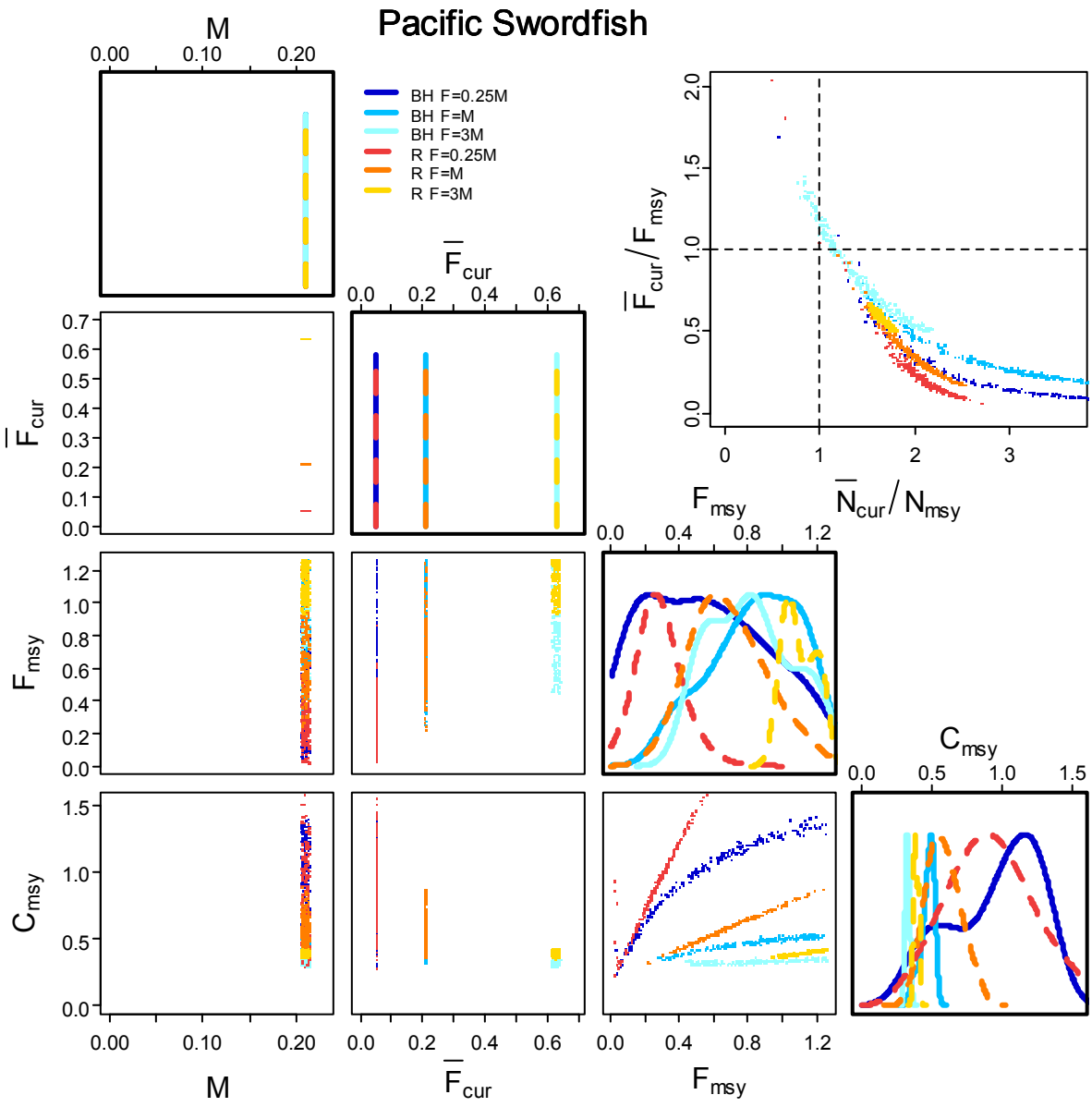

Figure 10.16 Pacific Ocean swordfish leading parameter joint distributions (lower triangular), marginal posterior distributions (diagonal) and biological reference points (upper triangular) for F_{msy} and MSY (C_{msy}) estimated from recruitment reconstructions assuming Beverton-Holt (BH) and Ricker (R) recruitment relationships for three current fishing mortality estimates (F_{cur} or F) and a known natural mortality rate M. Biological reference points are the ratio of current fishing mortality to the fishing mortality which produces MSY, and the ratio of current stock size to the stock size that produces MSY when fished at F_{msy}. Filled circles outside the upper triangular plot indicate ratios greater than 5. If both ratios are greater than 5 the filled circles lay in the top right corner.

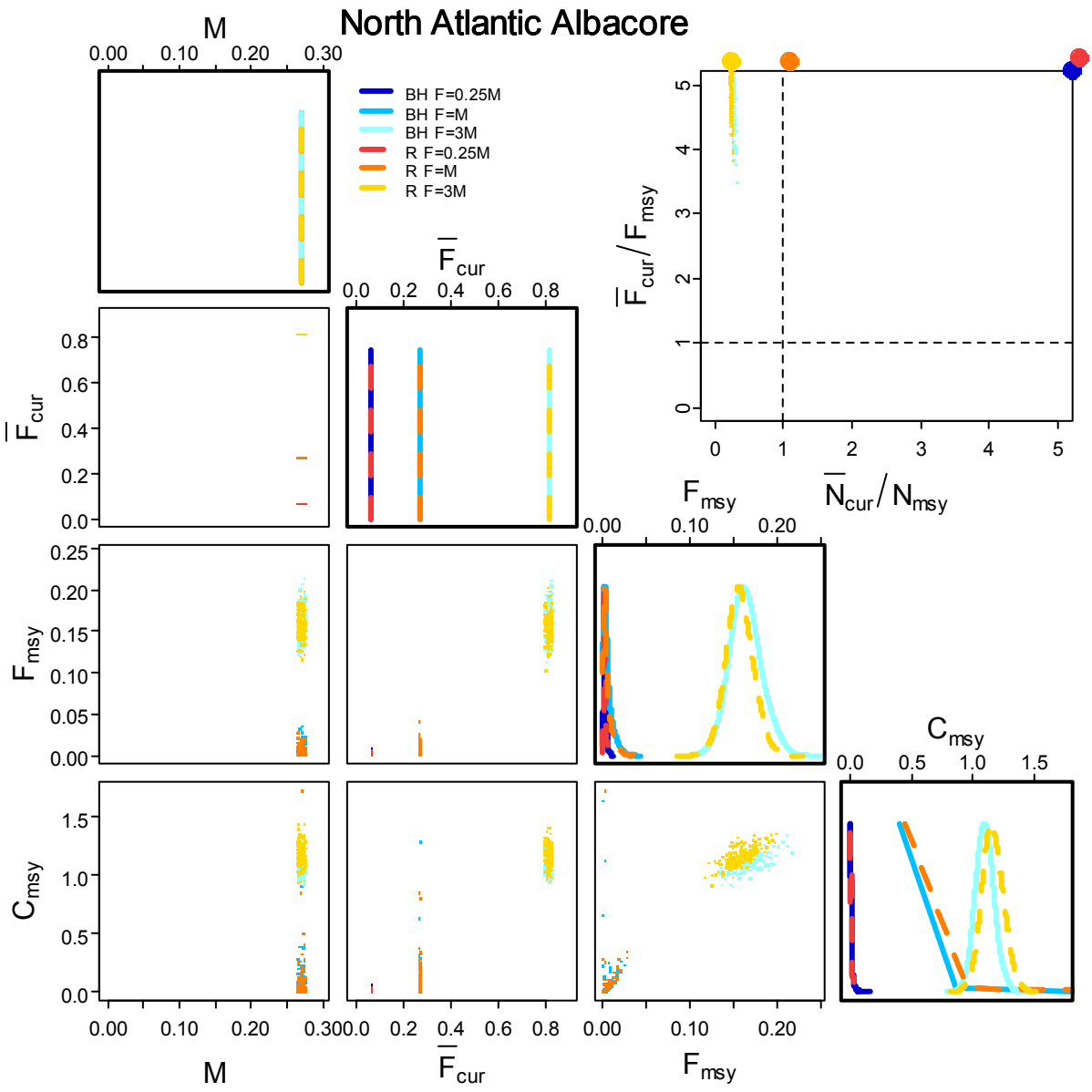

Figure 10.17 Atlantic Ocean northern albacore tuna leading parameter joint distributions (lower triangular), marginal posterior distributions (diagonal) and biological reference points (upper triangular) for F_{msy} and MSY (C_{msy}) estimated from recruitment reconstructions assuming Beverton-Holt (BH) and Ricker (R) recruitment relationships for three current fishing mortality estimates (F_{cur} or F) and a known natural mortality rate M. Biological reference points are the ratio of current fishing mortality to the fishing mortality which produces MSY, and the ratio of current stock size to the stock size that produces MSY when fished at F_{msy}. Filled circles outside the upper triangular plot indicate ratios greater than 5. If both ratios are greater than 5 the filled circles lay in the top right corner.

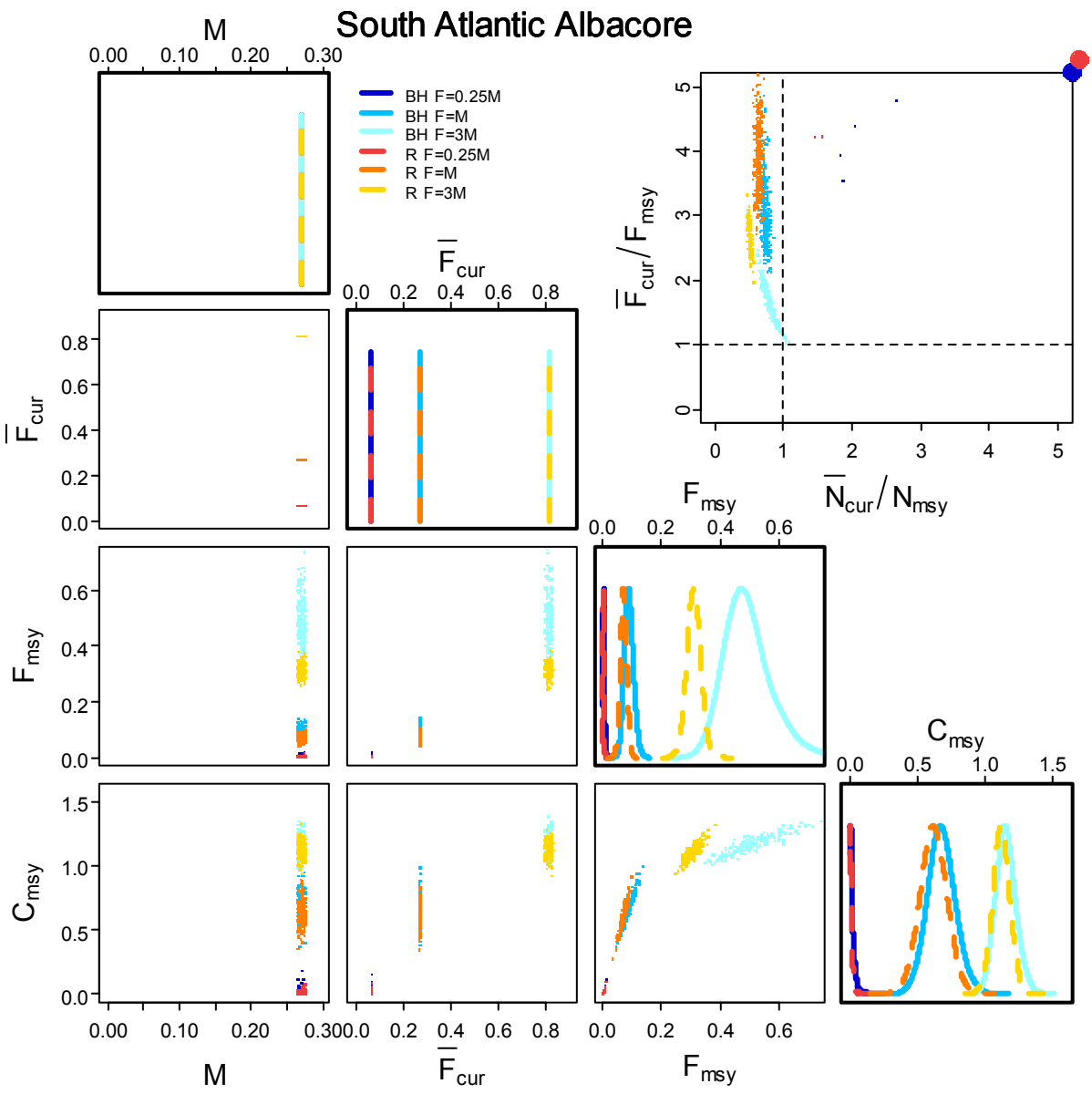

Figure 10.18 Atlantic Ocean southern albacore tuna leading parameter joint distributions (lower triangular), marginal posterior distributions (diagonal) and biological reference points (upper triangular) for F_{msy} and MSY (C_{msy}) estimated from recruitment reconstructions assuming Beverton-Holt (BH) and Ricker (R) recruitment relationships for three current fishing mortality estimates (F_{cur} or F) and a known natural mortality rate M. Biological reference points are the ratio of current fishing mortality to the fishing mortality which produces MSY, and the ratio of current stock size to the stock size that produces MSY when fished at F_{msy}. Filled circles outside the upper triangular plot indicate ratios greater than 5. If both ratios are greater than 5 the filled circles lay in the top right corner.

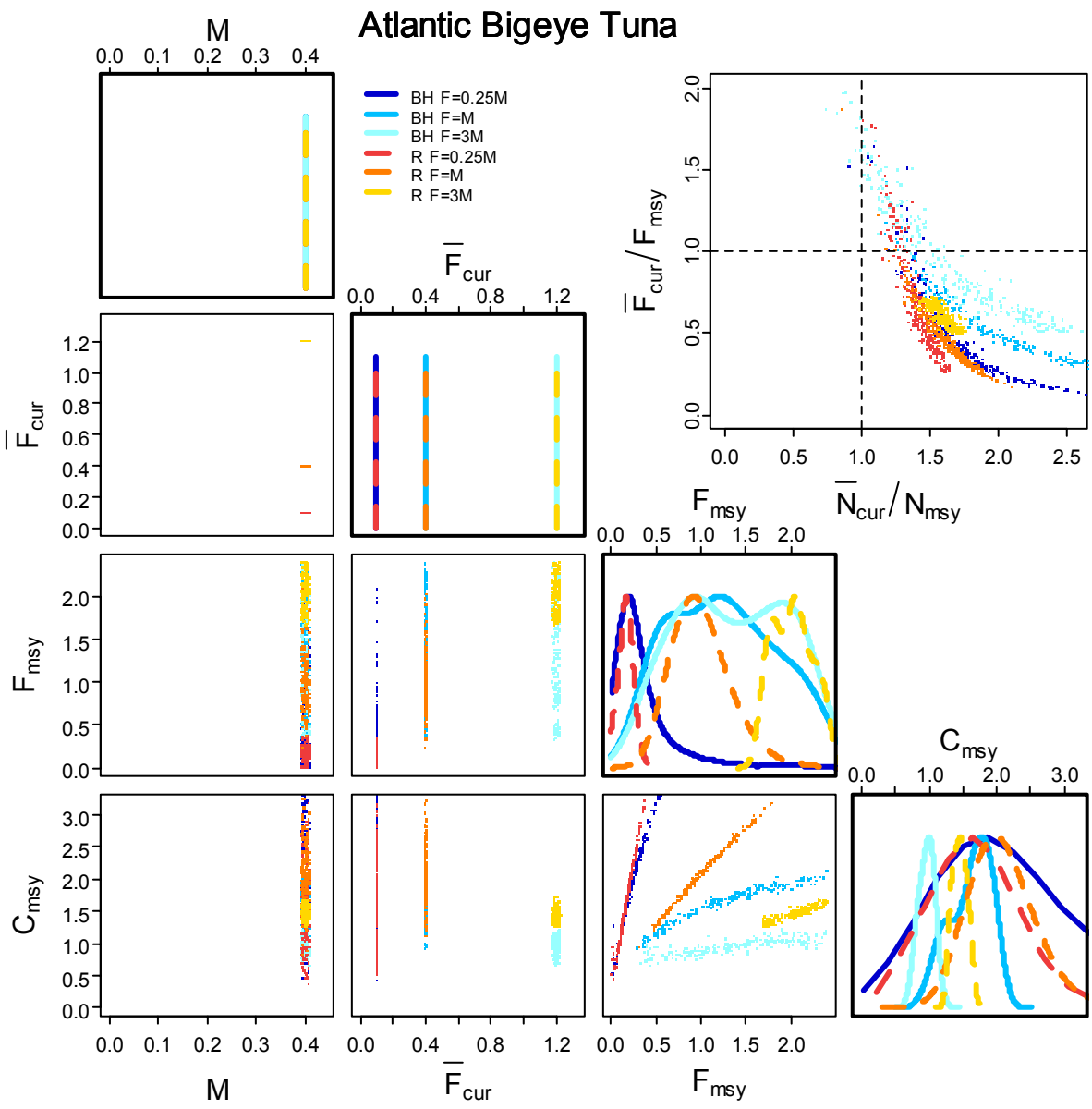

Figure 10.19 Atlantic Ocean bigeye tuna leading parameter joint distributions (lower triangular), marginal posterior distributions (diagonal) and biological reference points (upper triangular) for F_{msy} and MSY (C_{msy}) estimated from recruitment reconstructions assuming Beverton-Holt (BH) and Ricker (R) recruitment relationships for three current fishing mortality estimates (F_{cur} or F) and a known natural mortality rate M. Biological reference points are the ratio of current fishing mortality to the fishing mortality which produces MSY, and the ratio of current stock size to the stock size that produces MSY when fished at F_{msy}. Filled circles outside the upper triangular plot indicate ratios greater than 5. If both ratios are greater than 5 the filled circles lay in the top right corner.

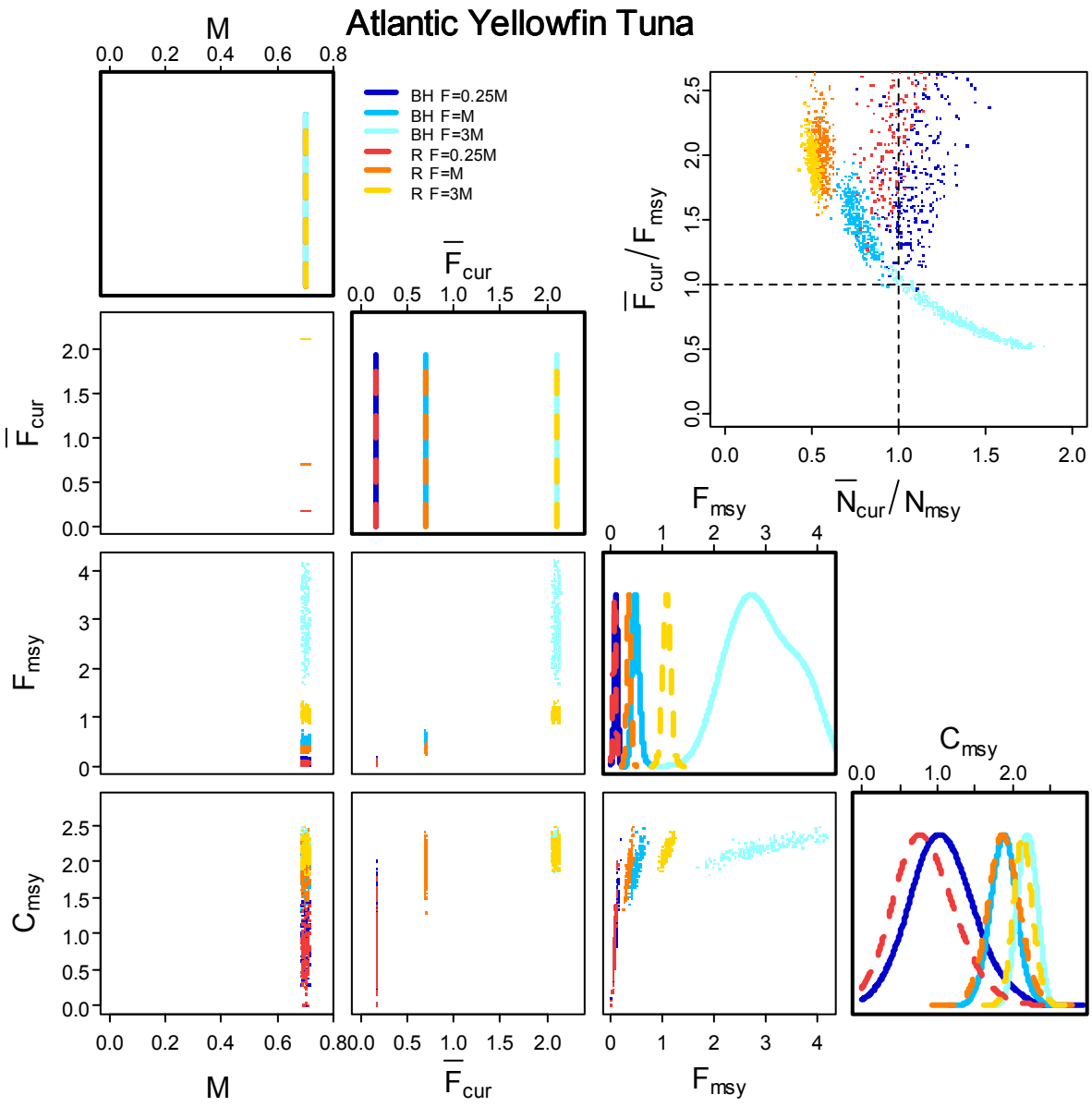

Figure 10.20 Atlantic Ocean yellowfin tuna leading parameter joint distributions (lower triangular), marginal posterior distributions (diagonal) and biological reference points (upper triangular) for F_{msy} and MSY (C_{msy}) estimated from recruitment reconstructions assuming Beverton-Holt (BH) and Ricker (R) recruitment relationships for three current fishing mortality estimates (F_{cur} or F) and a known natural mortality rate M. Biological reference points are the ratio of current fishing mortality to the fishing mortality which produces MSY, and the ratio of current stock size to the stock size that produces MSY when fished at F_{msy}. Filled circles outside the upper triangular plot indicate ratios greater than 5. If both ratios are greater than 5 the filled circles lay in the top right corner.

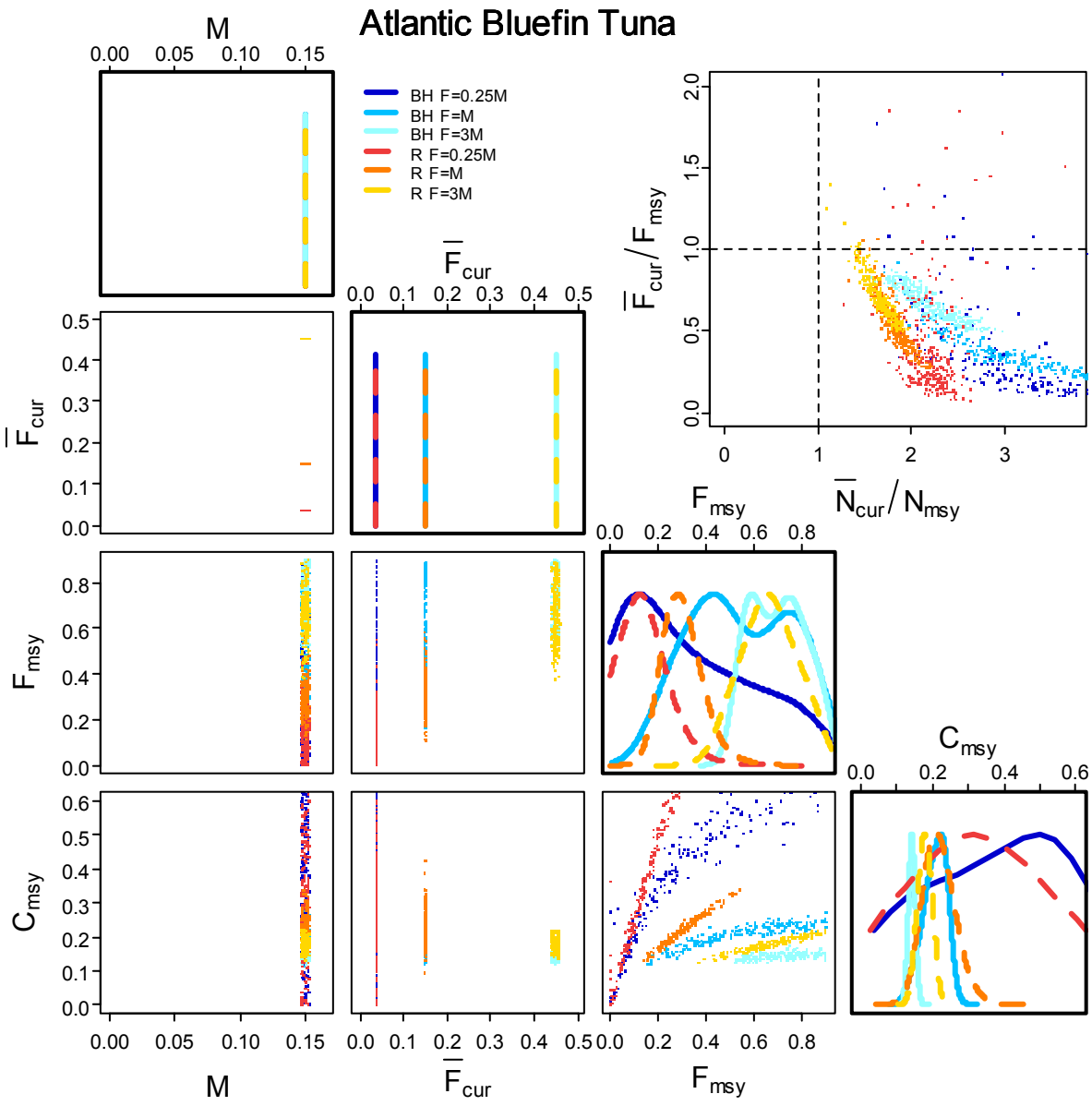

Figure 10.21 Atlantic Ocean bluefin tuna leading parameter joint distributions (lower triangular), marginal posterior distributions (diagonal) and biological reference points (upper triangular) for F_{msy} and MSY (C_{msy}) estimated from recruitment reconstructions assuming Beverton-Holt (BH) and Ricker (R) recruitment relationships for three current fishing mortality estimates (F_{cur} or F) and a known natural mortality rate M. Biological reference points are the ratio of current fishing mortality to the fishing mortality which produces MSY, and the ratio of current stock size to the stock size that produces MSY when fished at F_{msy}. Filled circles outside the upper triangular plot indicate ratios greater than 5. If both ratios are greater than 5 the filled circles lay in the top right corner.

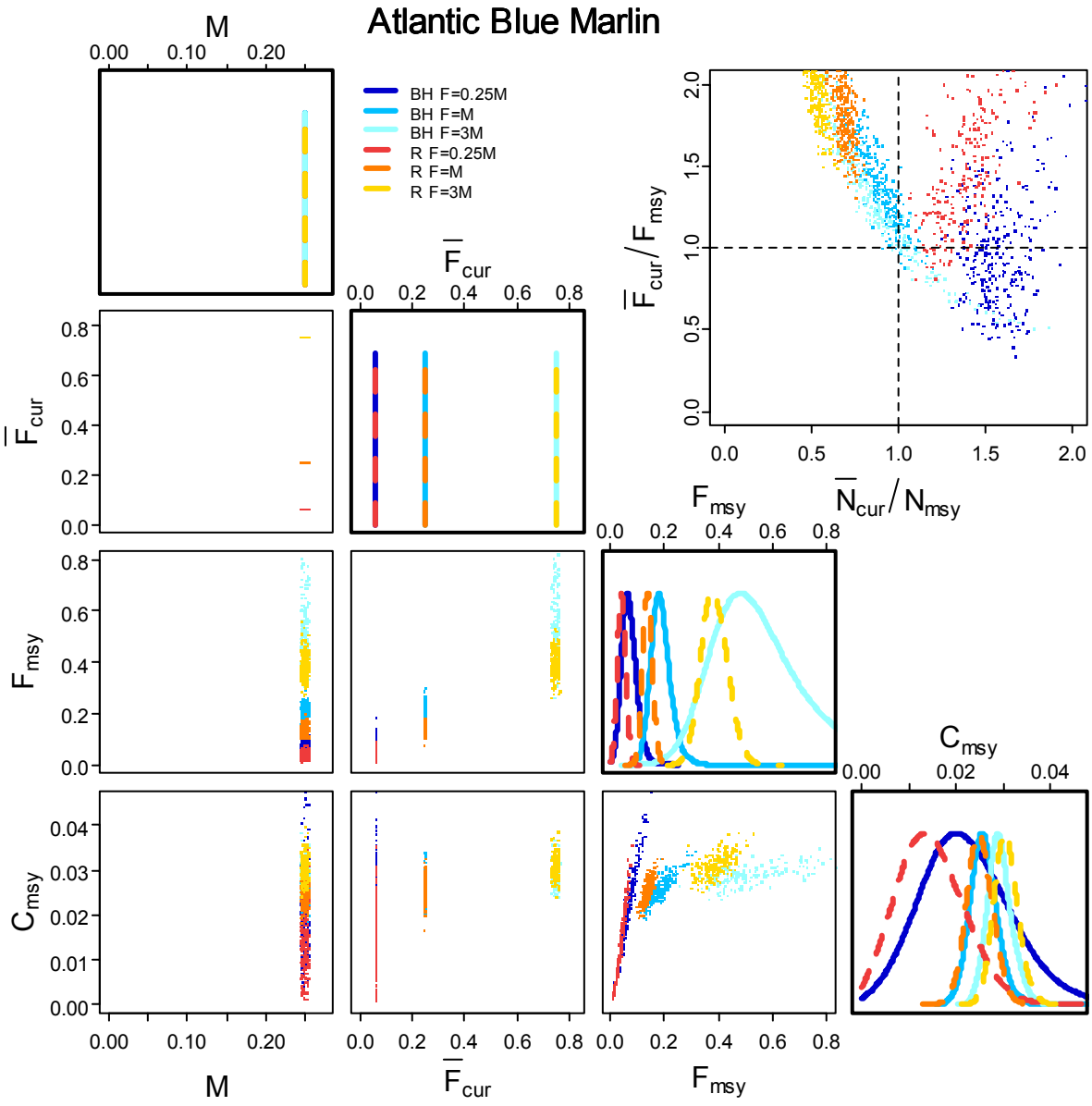

Figure 10.22 Atlantic Ocean blue marlin leading parameter joint distributions (lower triangular), marginal posterior distributions (diagonal) and biological reference points (upper triangular) for F_{msy} and MSY (C_{msy}) estimated from recruitment reconstructions assuming Beverton-Holt (BH) and Ricker (R) recruitment relationships for three current fishing mortality estimates (F_{cur} or F) and a known natural mortality rate M. Biological reference points are the ratio of current fishing mortality to the fishing mortality which produces MSY, and the ratio of current stock size to the stock size that produces MSY when fished at F_{msy}. Filled circles outside the upper triangular plot indicate ratios greater than 5. If both ratios are greater than 5 the filled circles lay in the top right corner.

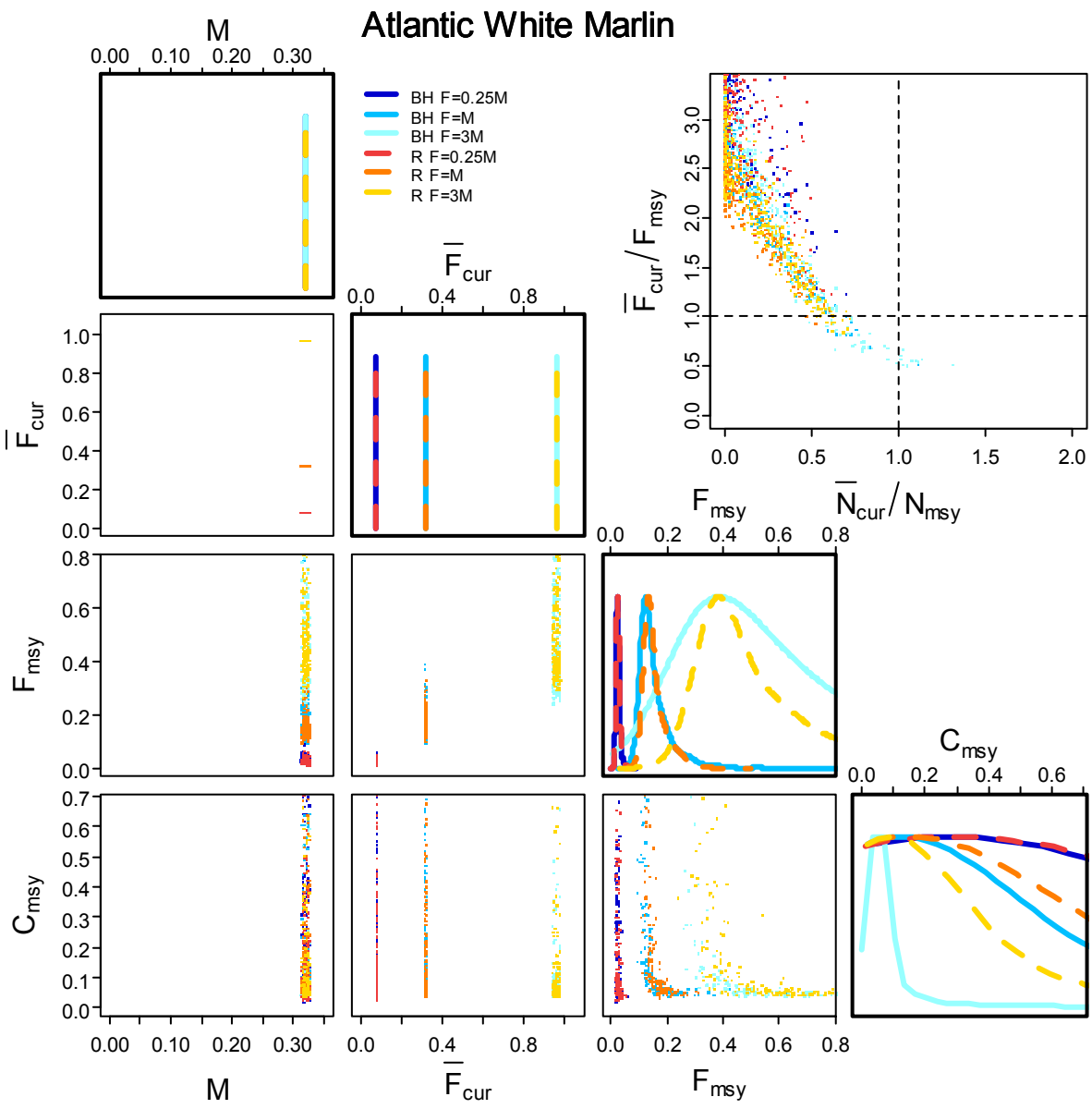

Figure 10.23 Atlantic Ocean white marlin leading parameter joint distributions (lower triangular), marginal posterior distributions (diagonal) and biological reference points (upper triangular) for F_{msy} and MSY (C_{msy}) estimated from recruitment reconstructions assuming Beverton-Holt (BH) and Ricker (R) recruitment relationships for three current fishing mortality estimates (F_{cur} or F) and a known natural mortality rate M. Biological reference points are the ratio of current fishing mortality to the fishing mortality which produces MSY, and the ratio of current stock size to the stock size that produces MSY when fished at F_{msy}. Filled circles outside the upper triangular plot indicate ratios greater than 5. If both ratios are greater than 5 the filled circles lay in the top right corner.

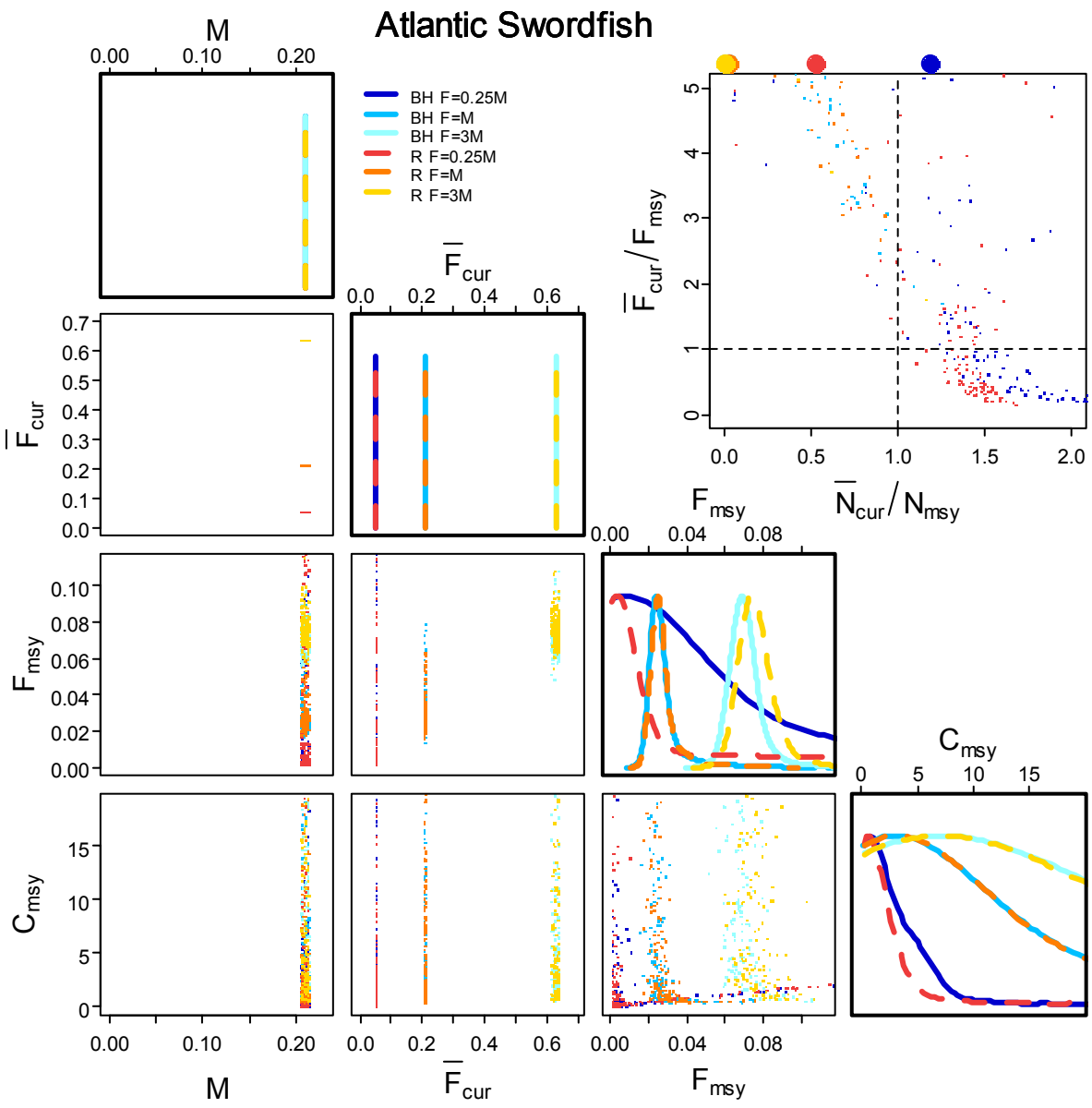

Figure 10.24 Atlantic Ocean swordfish leading parameter joint distributions (lower triangular), marginal posterior distributions (diagonal) and biological reference points (upper triangular) for F_{msy} and MSY (C_{msy}) estimated from recruitment reconstructions assuming Beverton-Holt (BH) and Ricker (R) recruitment relationships for three current fishing mortality estimates (F_{cur} or F) and a known natural mortality rate M. Biological reference points are the ratio of current fishing mortality to the fishing mortality which produces MSY, and the ratio of current stock size to the stock size that produces MSY when fished at F_{msy}. Filled circles outside the upper triangular plot indicate ratios greater than 5. If both ratios are greater than 5 the filled circles lay in the top right corner.

Table 10.3 Parameter estimates from stock reduction analysis (SRA) with process error assumed low or high and from the E* forced method. Parameters are presented as prior mode (95% interval) posterior 50% quantile as an approximation to posterior mode (95% interval). A single set of numbers indicates no prior was used.

Stock	Method	M	Fcur	Fmsy	MSY	N1950/N0
IALB	**SRA Low**	0.27(0.24-0.3) 0.26(0.24-0.29)	0.58(0.37-0.91) 1.14(0.57-1.2)	0.3726(0.33-0.59) 0.3(0.25-0.45)	1.48(1.39-1.89)	1(0.91-1.1) 1.1(0.95-1.15)
	SRA High	0.27(0.24-0.3) 0.27(0.24-0.29)	0.58(0.37-0.91) 1.56(0.64-1.38)	0.3726(0.33-0.59) 0.28(0.22-0.39)	1.66(1.69-2.8)	1(0.91-1.1) 1.15(0.98-1.19)
	F/q Forced	0.27(0.24-0.3) 0.26(0.23-0.29)	0.58(0.37-0.91) 1.19(0.94-1.46)	0.3726(0.33-0.59) 0.41(0.3-0.54)	1.42(1.26-1.62)	1(0.91-1.1) 1.05(0.95-1.16)
IBET	**SRA Low**	0.4(0.34-0.47) 0.39(0.34-0.46)	0.3(0.24-0.38) 0.3(0.25-0.36)	0.552(0.43-1.02) 0.47(0.33-0.77)	2.94(2.42-3.73)	1(0.91-1.1) 1.1(0.96-1.15)
	SRA High	0.4(0.34-0.47) 0.47(0.34-0.45)	0.3(0.24-0.38) 0.36(0.25-0.38)	0.552(0.43-1.02) 0.47(0.33-0.78)	2.81(2.37-4)	1(0.91-1.1) 1.07(0.94-1.13)
	F/q Forced	0.4(0.34-0.47) 0.4(0.35-0.46)	0.3(0.24-0.38) 0.29(0.24-0.34)	0.552(0.43-1.02) 0.53(0.35-0.8)	2.96(2.39-3.72)	1(0.91-1.1) 1.05(0.95-1.15)
IYFT	**SRA Low**	0.7(0.53-0.92) 0.79(0.51-0.89)	0.6(0.38-0.96) 0.67(0.41-0.95)	0.966(0.55-2.46) 0.26(0.25-1.4)	4.37(4.41-10.85)	1(0.91-1.1) 1.11(0.94-1.15)
	SRA High	0.7(0.53-0.92) 1.23(0.54-0.89)	0.6(0.38-0.96) 0.56(0.32-0.73)	0.966(0.55-2.46) 0.14(0.11-0.3)	5.31(4.9-10.76)	1(0.91-1.1) 1.06(0.95-1.15)
	F/q Forced	0.7(0.53-0.92) 0.64(0.49-0.85)	0.6(0.38-0.96) 0.74(0.48-1.05)	0.966(0.55-2.46) 0.78(0.39-1.62)	6.15(4.39-9.35)	1(0.91-1.1) 1.03(0.93-1.14)
GSBT	**SRA Low**	0.1(0.096-0.104) 0.1(0.1-0.1)	0.12(0.1-0.13)	0.05(0.04-0.06)	0.26(0.23-0.28)	1(0.91-1.1) 1(0.91-1.11)
	SRA High	0.1(0.096-0.104) 0.1(0.1-0.1)	0.12(0.09-0.14)	0.06(0.04-0.08)	0.27(0.21-0.31)	1(0.91-1.1) 0.96(0.9-1.09)
	F/q Forced	0.1(0.096-0.104) 0.1(0.1-0.1)	0.12(0.1-0.13)	0.05(0.04-0.06)	0.26(0.23-0.28)	1(0.91-1.1) 0.99(0.9-1.1)
IBUM	**SRA Low**	0.25(0.23-0.28) 0.24(0.22-0.27)	0.2(0.17-0.23) 0.22(0.18-0.24)	0.345(0.31-0.54) 0.3(0.24-0.43)	0.11(0.09-0.14)	1(0.91-1.1) 1.07(0.94-1.14)
	SRA High	0.25(0.23-0.28) 0.26(0.22-0.27)	0.2(0.17-0.23) 0.22(0.17-0.24)	0.345(0.31-0.54) 0.3(0.24-0.42)	0.14(0.12-0.21)	1(0.91-1.1) 1.03(0.92-1.12)
	F/q Forced	0.25(0.23-0.28) 0.24(0.22-0.27)	0.2(0.17-0.23) 0.21(0.18-0.25)	0.345(0.31-0.54) 0.32(0.24-0.43)	0.15(0.12-0.2)	1(0.91-1.1) 1.03(0.94-1.13)
ISTM	**SRA Low**	0.5(0.41-0.61) 0.49(0.41-0.59)	0.23(0.11-0.32)	0.1(0-0.18)	0.05(0-0.07)	1(0.91-1.1) 1.02(0.92-1.11)
	SRA High	0.5(0.41-0.61) 0.57(0.38-0.54)	0.64(0.1-0.39)	0.37(0.04-0.26)	0.08(0.04-0.08)	1(0.91-1.1) 0.99(0.92-1.11)
	F/q Forced	0.5(0.41-0.61) 0.49(0.41-0.6)	0.33(0.13-0.5)	0.16(0-0.3)	0.06(0-0.07)	1(0.91-1.1) 1(0.91-1.11)
GBLM	**SRA Low**	0.15(0.14-0.16) 0.15(0.14-0.16)	0.45(0.33-0.63)	0.09(0.05-0.12)	0.03(0.03-0.04)	1(0.9-1.1) 1.13(0.96-1.18)
	SRA High	0.15(0.14-0.16) 0.15(0.14-0.16)	0.44(0.26-0.47)	0.11(0.05-0.13)	0.04(0.03-0.04)	1(0.9-1.1) 1.02(0.94-1.15)
	F/q Forced	0.15(0.14-0.16) 0.15(0.14-0.16)	0.37(0.29-0.47)	0.11(0.07-0.15)	0.04(0.03-0.04)	1(0.9-1.1) 1.05(0.95-1.15)
ISWO	**SRA Low**	0.21(0.19-0.23) 0.22(0.2-0.23)	0.3(0.24-0.38) 0.18(0.18-0.3)	0.2898(0.28-0.44) 0.28(0.23-0.36)	0.47(0.35-0.5)	1(0.91-1.1) 0.89(0.86-1.05)
	SRA High	0.21(0.19-0.23) 0.23(0.2-0.23)	0.3(0.24-0.38) 0.18(0.18-0.27)	0.2898(0.28-0.44) 0.26(0.22-0.35)	0.36(0.25-0.4)	1(0.91-1.1) 0.85(0.84-1.02)
	F/q Forced	0.21(0.19-0.23) 0.22(0.2-0.23)	0.3(0.24-0.38) 0.21(0.16-0.26)	0.2898(0.28-0.44) 0.3(0.24-0.37)	0.29(0.23-0.37)	1(0.91-1.1) 0.95(0.86-1.06)

continued next page

Stock	Method	M	Fcur	Fmsy	MSY	N1950/N0
PNAB	**SRA Low**	0.27(0.24-0.3) 0.28(0.25-0.31)	0.4(0.29-0.55) 0.23(0.2-0.34)	0.3726(0.33-0.6) 0.32(0.27-0.48)	2.77(2.6-3.05)	1(0.21-4.81) 0.31(0.21-0.46)
	SRA High	0.27(0.24-0.3) 0.28(0.24-0.3)	0.4(0.29-0.55) 0.38(0.21-0.36)	0.3726(0.33-0.6) 0.44(0.3-0.5)	2.64(2.41-3.09)	1(0.21-4.81) 0.27(0.24-0.44)
	F/q Forced	0.27(0.24-0.3) 0.27(0.25-0.3)	0.4(0.29-0.55) 0.29(0.22-0.37)	0.3726(0.33-0.6) 0.39(0.3-0.53)	2.66(2.49-3.04)	1(0.21-4.81) 0.27(0.18-0.41)
PSAB	**SRA Low**	0.27(0.24-0.3) 0.25(0.23-0.29)	0.21(0.18-0.25) 0.26(0.2-0.27)	0.14(0.07-0.18)	1.78(1.22-2.04)	1(0.91-1.1) 1.15(0.99-1.19)
	SRA High	0.27(0.24-0.3) 0.27(0.23-0.29)	0.21(0.18-0.25) 0.27(0.21-0.3)	0.17(0.07-0.18)	1.95(1.22-2.04)	1(0.91-1.1) 1.07(0.99-1.19)
	F/q Forced	0.27(0.24-0.3) 0.25(0.23-0.28)	0.21(0.18-0.25) 0.25(0.21-0.29)	0.2(0.14-0.27)	1.86(1.62-2.13)	1(0.91-1.1) 1.05(0.96-1.15)
PBET	**SRA Low**	0.4(0.34-0.47) 0.38(0.32-0.45)	0.45(0.31-0.64) 0.52(0.35-0.68)	0.23(0.11-0.42)	2.41(1.68-3.01)	1(0.91-1.1) 1.18(1-1.2)
	SRA High	0.4(0.34-0.47) 0.43(0.33-0.44)	0.45(0.31-0.64) 0.74(0.34-0.67)	0.33(0.11-0.37)	2.6(1.77-3.07)	1(0.91-1.1) 1.09(0.97-1.16)
	F/q Forced	0.4(0.34-0.47) 0.36(0.31-0.43)	0.45(0.31-0.64) 0.65(0.47-0.84)	0.77(0.35-2.23)	3.12(2.55-4.05)	1(0.91-1.1) 1.03(0.94-1.14)
PYFT	**SRA Low**	0.7(0.53-0.92) 0.69(0.51-0.88)	0.35(0.27-0.46) 0.37(0.28-0.47)	0.21(0.09-0.37)	9.61(5.73-12.85)	1(0.91-1.1) 1.24(1.01-1.23)
	SRA High	0.7(0.53-0.92) 1(0.48-0.81)	0.35(0.27-0.46) 0.38(0.25-0.43)	0.13(0.06-0.23)	7.09(4.49-11.5)	1(0.91-1.1) 1.1(0.95-1.17)
	F/q Forced	0.7(0.53-0.92) 0.58(0.42-0.76)	0.35(0.27-0.46) 0.42(0.31-0.6)	0.43(0.24-2.59)	11.68(9.22-19.65)	1(0.91-1.1) 1.09(0.98-1.19)
PBFT	**SRA Low**	0.276(0.25-0.31) 0.27(0.24-0.3)	0.08(0-0.16)	0.05(0.01-0.09)	0.01(0-5.15)	1(0.2-4.76) 4.38(2.17-16.93)
	SRA High	0.276(0.25-0.31) 0.28(0.25-0.31)	0.79(0.02-0.25)	0.31(0.03-0.2)	0.04(0.02-0.04)	1(0.2-4.76) 0.62(0.96-5.3)
	F/q Forced	0.276(0.25-0.31) 0.27(0.25-0.31)	0.2(0.03-0.41)	0.11(0.02-0.21)	0.02(0.01-0.03)	1(0.2-4.76) 1.91(0.84-9.08)
PBUM	**SRA Low**	0.25(0.23-0.28) 0.25(0.23-0.27)	0.1(0.09-0.11) 0.1(0.09-0.11)	0.03(0-0.06)	0.07(0-0.13)	1(0.9-1.1) 1.05(0.92-1.12)
	SRA High	0.25(0.23-0.28) 0.27(0.23-0.28)	0.1(0.09-0.11) 0.1(0.09-0.11)	0.03(0.01-0.07)	0.14(0.04-0.24)	1(0.9-1.1) 1.04(0.92-1.13)
	F/q Forced	0.25(0.23-0.28) 0.24(0.22-0.27)	0.1(0.09-0.11) 0.1(0.09-0.11)	0.03(0-0.06)	0.07(0-0.13)	1(0.9-1.1) 1.03(0.92-1.14)
PSTM	**SRA Low**	0.5(0.41-0.61) 0.49(0.4-0.61)	0.04(0.02-0.05)	0.07(0-0.1)	0.17(0.01-0.21)	1(0.91-1.1) 0.97(0.9-1.1)
	SRA High	0.5(0.41-0.61) 0.66(0.4-0.58)	0.06(0.01-0.05)	0.14(0.01-0.15)	0.21(0.05-0.36)	1(0.91-1.1) 0.98(0.91-1.1)
	F/q Forced	0.5(0.41-0.61) 0.49(0.41-0.6)	0.04(0.02-0.06)	0.07(0.02-0.11)	0.17(0.07-0.21)	1(0.91-1.1) 0.99(0.9-1.1)
PSWO	**SRA Low**	0.21(0.19-0.23) 0.21(0.19-0.23)	0.15(0.13-0.17) 0.14(0.13-0.16)	0.2898(0.28-0.43) 0.29(0.23-0.36)	0.44(0.38-0.48)	1(0.21-4.74) 0.58(0.5-0.64)
	SRA High	0.21(0.19-0.23) 0.22(0.19-0.23)	0.15(0.13-0.17) 0.14(0.13-0.16)	0.2898(0.28-0.43) 0.29(0.23-0.36)	0.42(0.37-0.47)	1(0.21-4.74) 0.54(0.47-0.6)
	F/q Forced	0.21(0.19-0.23) 0.21(0.2-0.23)	0.15(0.13-0.17) 0.14(0.13-0.16)	0.2898(0.28-0.43) 0.29(0.23-0.37)	0.4(0.36-0.45)	1(0.21-4.74) 0.51(0.44-0.58)

continued next page

Stock	Method	M	Fcur	Fmsy	MSY	N1950/N0
ANAB	**SRA Low**	0.27(0.24-0.3) 0.24(0.23-0.29)	0.4(0.29-0.55) 0.93(0.59-0.98)	0.3726(0.33-0.6) 0.14(0.13-0.22)	1.02(0.99-1.23)	1(0.21-4.75) 1.05(0.91-1.44)
	SRA High	0.27(0.24-0.3) 0.27(0.23-0.29)	0.4(0.29-0.55) 1.06(0.5-0.9)	0.3726(0.33-0.6) 0.16(0.15-0.27)	1.12(1.12-1.78)	1(0.21-4.75) 0.98(0.99-1.53)
	F/q Forced	0.27(0.24-0.3) 0.26(0.24-0.29)	0.4(0.29-0.55) 0.89(0.75-1.04)	0.3726(0.33-0.6) 0.21(0.17-0.26)	1.18(1.09-1.26)	1(0.21-4.75) 0.76(0.62-0.95)
ASAB	**SRA Low**	0.27(0.24-0.3) 0.24(0.23-0.29)	0.94(0.69-1.67)	0.23(0.15-0.33)	0.97(0.84-1.07)	1(0.91-1.1) 1.09(0.95-1.15)
	SRA High	0.27(0.24-0.3) 0.27(0.23-0.29)	1.03(0.44-1.01)	0.3(0.12-0.33)	1.07(0.81-1.15)	1(0.91-1.1) 1.03(0.94-1.14)
	F/q Forced	0.27(0.24-0.3) 0.26(0.23-0.29)	0.59(0.48-0.73)	0.33(0.23-0.48)	1.06(0.96-1.17)	1(0.91-1.1) 1.02(0.92-1.13)
ABET	**SRA Low**	0.4(0.34-0.47) 0.47(0.39-0.51)	0.175(0.15-0.2) 0.15(0.14-0.18)	0.552(0.43-1.01) 0.65(0.43-0.93)	2.73(2.12-3.17)	1(0.91-1.1) 0.91(0.86-1.01)
	SRA High	0.4(0.34-0.47) 0.52(0.37-0.48)	0.175(0.15-0.2) 0.17(0.14-0.19)	0.552(0.43-1.01) 0.55(0.38-0.86)	2.43(1.86-3.03)	1(0.91-1.1) 0.91(0.86-0.98)
	F/q Forced	0.4(0.34-0.47) 0.44(0.38-0.51)	0.175(0.15-0.2) 0.16(0.14-0.17)	0.552(0.43-1.01) 0.67(0.46-0.99)	2.68(2.15-3.3)	1(0.91-1.1) 0.93(0.85-1.01)
AYFT	**SRA Low**	0.7(0.53-0.93) 0.38(0.39-0.72)	0.51(0.34-0.76) 1.05(0.52-1.06)	0.966(0.54-2.47) 1.35(0.35-1.47)	2.37(1.85-2.59)	1(0.91-1.1) 1.1(0.96-1.16)
	SRA High	0.7(0.53-0.93) 0.89(0.48-0.77)	0.51(0.34-0.76) 0.79(0.38-0.8)	0.966(0.54-2.47) 0.27(0.16-0.35)	2.11(1.91-3.06)	1(0.91-1.1) 1.12(0.97-1.17)
	F/q Forced	0.7(0.53-0.93) 0.44(0.35-0.57)	0.51(0.34-0.76) 1.28(0.92-1.59)	0.966(0.54-2.47) 1.6(0.88-2.81)	2.14(1.98-2.37)	1(0.91-1.1) 1.04(0.94-1.14)
ABFT	**SRA Low**	0.15(0.14-0.16) 0.15(0.14-0.16)	0.18(0.16-0.21) 0.16(0.15-0.19)	0.207(0.21-0.29) 0.2(0.17-0.24)	0.17(0.15-0.19)	1(0.21-4.54) 1.12(0.89-1.36)
	SRA High	0.15(0.14-0.16) 0.15(0.14-0.16)	0.18(0.16-0.21) 0.18(0.15-0.2)	0.207(0.21-0.29) 0.21(0.18-0.25)	0.16(0.13-0.18)	1(0.21-4.54) 0.77(0.64-0.99)
	F/q Forced	0.15(0.14-0.16) 0.15(0.14-0.16)	0.18(0.16-0.21) 0.17(0.14-0.19)	0.207(0.21-0.29) 0.21(0.18-0.25)	0.14(0.13-0.16)	1(0.21-4.54) 0.9(0.7-1.15)
ABUM	**SRA Low**	0.25(0.23-0.28) 0.24(0.22-0.27)	0.28(0.16-0.41)	0.12(0.05-0.17)	0.02(0.02-0.03)	1(0.91-1.1) 1.07(0.94-1.14)
	SRA High	0.25(0.23-0.28) 0.25(0.22-0.27)	0.3(0.16-0.32)	0.17(0.08-0.21)	0.03(0.02-0.03)	1(0.91-1.1) 1.04(0.93-1.13)
	F/q Forced	0.25(0.23-0.28) 0.24(0.22-0.27)	0.32(0.21-0.44)	0.19(0.11-0.32)	0.02(0.02-0.03)	1(0.91-1.1) 1.03(0.92-1.13)
AWHM	**SRA Low**	0.32(0.28-0.36) 0.38(0.3-0.39)	0.2(0.17-0.23) 0.13(0.14-0.2)	0.09(0.07-0.16)	0.04(0.03-0.05)	1(0.91-1.1) 0.9(0.87-1.06)
	SRA High	0.32(0.28-0.36) 0.4(0.3-0.38)	0.2(0.17-0.23) 0.15(0.14-0.19)	0.15(0.1-0.37)	0.04(0.03-0.07)	1(0.91-1.1) 0.93(0.88-1.07)
	F/q Forced	0.32(0.28-0.36) 0.34(0.3-0.39)	0.2(0.17-0.23) 0.17(0.14-0.2)	0.16(0.11-0.24)	0.04(0.04-0.05)	1(0.91-1.1) 0.96(0.87-1.06)
ASWO	**SRA Low**	0.21(0.19-0.23) 0.22(0.2-0.23)	0.4(0.29-0.55) 0.14(0.16-0.3)	0.2898(0.28-0.44) 0.28(0.23-0.37)	1.44(1.01-1.44)	1(0.91-1.1) 0.82(0.83-1.01)
	SRA High	0.21(0.19-0.23) 0.23(0.2-0.23)	0.4(0.29-0.55) 0.19(0.17-0.28)	0.2898(0.28-0.44) 0.28(0.23-0.36)	1.19(0.84-1.32)	1(0.91-1.1) 0.79(0.79-0.94)
	F/q Forced	0.21(0.19-0.23) 0.22(0.2-0.23)	0.4(0.29-0.55) 0.18(0.14-0.23)	0.2898(0.28-0.44) 0.3(0.24-0.38)	1.14(0.88-1.42)	1(0.91-1.1) 0.91(0.82-1)

Table 10.4 Biological reference point estimates from stock reduction analysis (SRA) with process error assumed low or high and from F/q forced method. Parameters are presented as posterior 50% quantile (95% interval). Fratio is the ratio of current fishing mortality rate to Fmsy. Nratio is the ratio of current stock size to the stock size that would produce MSY if fished at Fmsy

Stock	Method	Fratio	Nratio
IALB	**SRA Low**	0.77(0.24-0.29)	0.83(0.57-1.2)
	SRA High	0.55(2.01-4.92)	0.58(0.47-0.75)
	F/q Forced	0.4(2.24-3.7)	0.41(0.32-0.54)
IBET	**SRA Low**	1.76(0.24-0.29)	0.83(0.57-1.2)
	SRA High	1.61(0.39-0.94)	1.76(1.47-2.2)
	F/q Forced	1.83(0.36-0.78)	1.84(1.55-2.28)
IYFT	**SRA Low**	0.91(0.24-0.29)	0.83(0.57-1.2)
	SRA High	0.45(1.59-4.36)	0.5(0.4-0.66)
	F/q Forced	1.13(0.44-1.67)	1.16(0.75-1.93)
GSBT	**SRA Low**	0.46(0.24-0.29)	0.83(0.57-1.2)
	SRA High	0.47(1.59-2.67)	0.48(0.41-0.55)
	F/q Forced	0.45(1.96-2.45)	0.45(0.4-0.5)
IBUM	**SRA Low**	1.5(0.24-0.29)	0.83(0.57-1.2)
	SRA High	1.12(0.45-0.86)	1.17(0.88-1.54)
	F/q Forced	1.68(0.48-0.91)	1.68(1.41-1.99)
ISTM	**SRA Low**	0.53(0.24-0.29)	0.83(0.57-1.2)
	SRA High	0.56(1.24-3.73)	0.51(0.4-0.65)
	F/q Forced	0.55(1.58-66.02)	0.54(0.45-0.66)
GBLM	**SRA Low**	0.37(0.24-0.29)	0.83(0.57-1.2)
	SRA High	0.42(3.32-5.47)	0.41(0.36-0.47)
	F/q Forced	0.35(2.98-4.04)	0.35(0.3-0.4)
ISWO	**SRA Low**	1.96(0.24-0.29)	0.83(0.57-1.2)
	SRA High	2.35(0.58-1.07)	2.42(2.09-2.82)
	F/q Forced	1.77(0.51-0.95)	1.77(1.51-2.07)
PNAB	**SRA Low**	1.37(0.24-0.29)	0.83(0.57-1.2)
	SRA High	1.35(0.51-0.98)	1.54(1.07-2)
	F/q Forced	1.31(0.52-1)	1.32(0.94-1.74)
PSAB	**SRA Low**	1.13(0.24-0.29)	0.83(0.57-1.2)
	SRA High	1.18(1.44-3.62)	1.02(0.82-1.24)
	F/q Forced	1.06(1-1.6)	1.06(0.92-1.25)
PBET	**SRA Low**	0.93(0.24-0.29)	0.83(0.57-1.2)
	SRA High	0.97(1.58-3.66)	0.88(0.72-1.09)
	F/q Forced	1.26(0.33-1.38)	1.39(0.89-2.64)
PYFT	**SRA Low**	1.18(0.24-0.29)	0.83(0.57-1.2)
	SRA High	0.95(1.56-5.07)	0.95(0.81-1.14)
	F/q Forced	1.28(0.21-1.41)	1.35(1.06-3.66)
PBFT	**SRA Low**	1.15(0.24-0.29)	0.83(0.57-1.2)
	SRA High	0.36(0.57-1.52)	0.93(0.47-2.01)
	F/q Forced	0.55(0.69-3.07)	0.7(0.29-2.3)
PBUM	**SRA Low**	0.81(0.24-0.29)	0.83(0.57-1.2)
	SRA High	0.53(1.52-12.62)	0.51(0.39-0.66)
	F/q Forced	0.72(1.6-75.57)	0.66(0.47-0.98)
PSTM	**SRA Low**	1.13(0.24-0.29)	0.83(0.57-1.2)
	SRA High	1.2(0.21-2.04)	1.18(1.02-1.39)
	F/q Forced	1.13(0.48-1.58)	1.13(0.98-1.29)
PSWO	**SRA Low**	1.92(0.24-0.29)	0.83(0.57-1.2)
	SRA High	1.94(0.39-0.63)	1.94(1.67-2.24)
	F/q Forced	1.78(0.38-0.62)	1.78(1.53-2.07)

Continued on next page

Stock	Method	Fratio	Nratio
ANAB	**SRA Low**	4.5(3.08-6.18)	0.4(0.33-0.51)
	SRA High	3.38(2.15-5.08)	0.41(0.33-0.51)
	F/q Forced	4.17(3.79-4.57)	0.25(0.21-0.28)
ASAB	**SRA Low**	4.36(3.42-5.89)	0.6(0.53-0.7)
	SRA High	3.39(2.58-4.39)	0.63(0.54-0.75)
	F/q Forced	1.81(1.45-2.17)	0.64(0.56-0.78)
ABET	**SRA Low**	0.25(0.17-0.37)	2.34(1.94-2.9)
	SRA High	0.29(0.19-0.43)	2.17(1.82-2.67)
	F/q Forced	0.23(0.16-0.33)	2.45(2.06-3.05)
AYFT	**SRA Low**	1.07(0.56-1.9)	1.27(0.82-2.14)
	SRA High	2.27(1.63-3.18)	0.51(0.41-0.62)
	F/q Forced	0.8(0.49-1.14)	1.23(0.87-1.92)
ABFT	**SRA Low**	0.82(0.67-1)	1.58(1.41-1.76)
	SRA High	0.82(0.67-1.01)	1.72(1.44-2.04)
	F/q Forced	0.79(0.64-0.98)	1.32(1.14-1.52)
ABUM	**SRA Low**	2.4(1.71-3.52)	0.69(0.56-0.85)
	SRA High	1.79(1.22-2.67)	0.78(0.63-0.96)
	F/q Forced	1.65(1.19-2.14)	0.71(0.57-0.91)
AWHM	**SRA Low**	1.49(1.05-2.44)	0.54(0.44-0.67)
	SRA High	0.91(0.49-1.57)	0.8(0.64-1.07)
	F/q Forced	1.04(0.75-1.32)	0.87(0.68-1.15)
ASWO	**SRA Low**	0.74(0.52-1.08)	1.7(1.42-2)
	SRA High	0.75(0.54-1.05)	1.9(1.66-2.18)
	F/q Forced	0.59(0.43-0.81)	1.87(1.57-2.18)

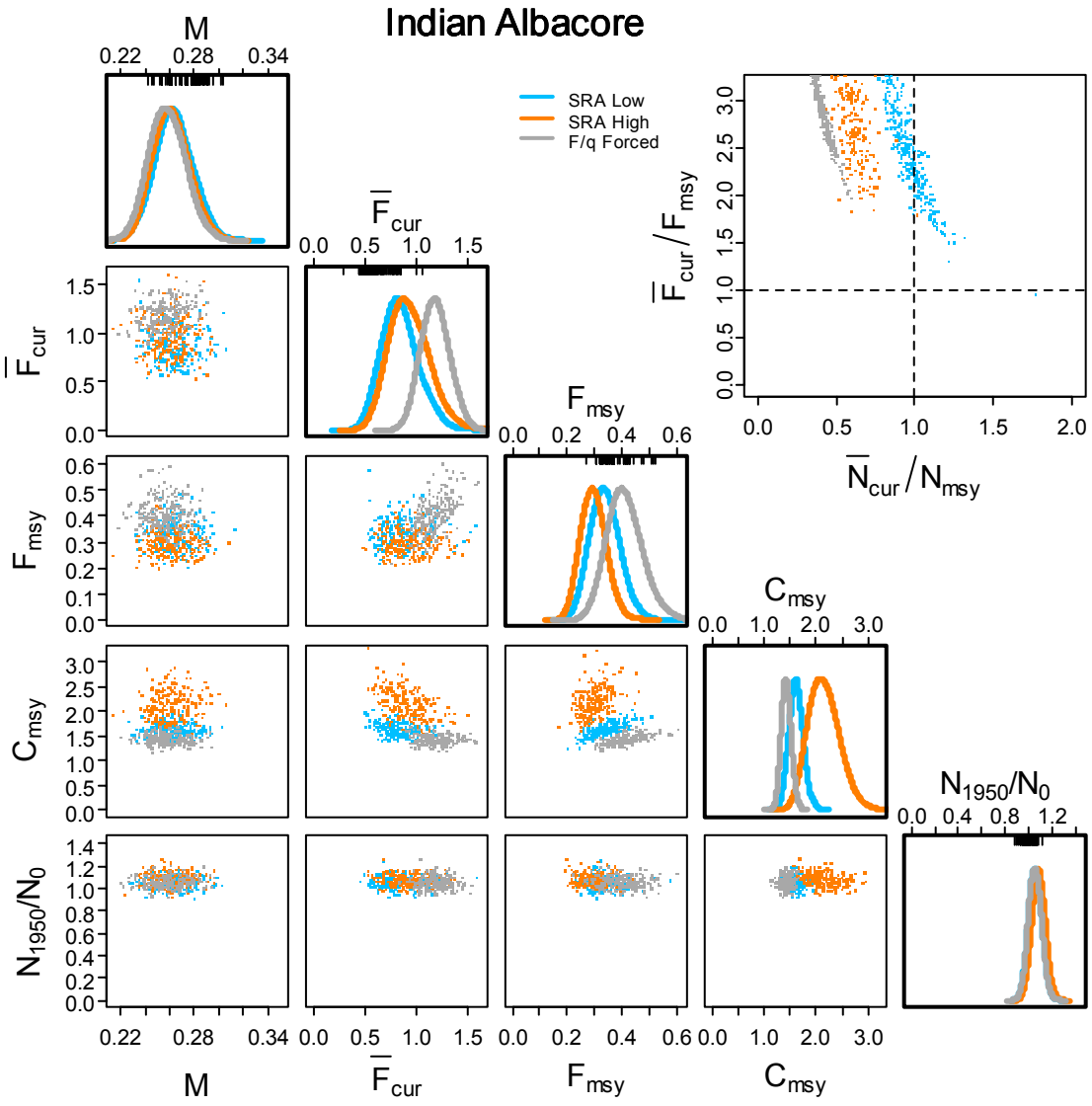

Figure 10.25 Indian Ocean albacore tuna leading parameter joint distribution (lower triangular), marginal posterior distributions (diagonal) and biological reference points (upper triangular) for natural mortality (M), current fishing mortality (F_{cur}), fishing mortality that produced MSY (F_{msy}), MSY (C_{msy}) and the ratio of population in 1950 to that expected in the absence of fishing. Biological reference points in the top right corner are the ratio of current fishing mortality to the fishing mortality that produces MSY, and the ratio of current stock size to the stock size that produces MSY. Filled circles outside the upper triangular plot indicate ratios greater than 5. Blue lines and points are from SRA where variance in recruitment anomalies was assumed low. Orange lines and points are from SRA where variance in recruitment anomalies was assumed high. Light grey lines and points are from the relative fishing mortality rate forced numbers dynamic model. Rug plots on the top of distributions on the diagonal demark prior distributions.

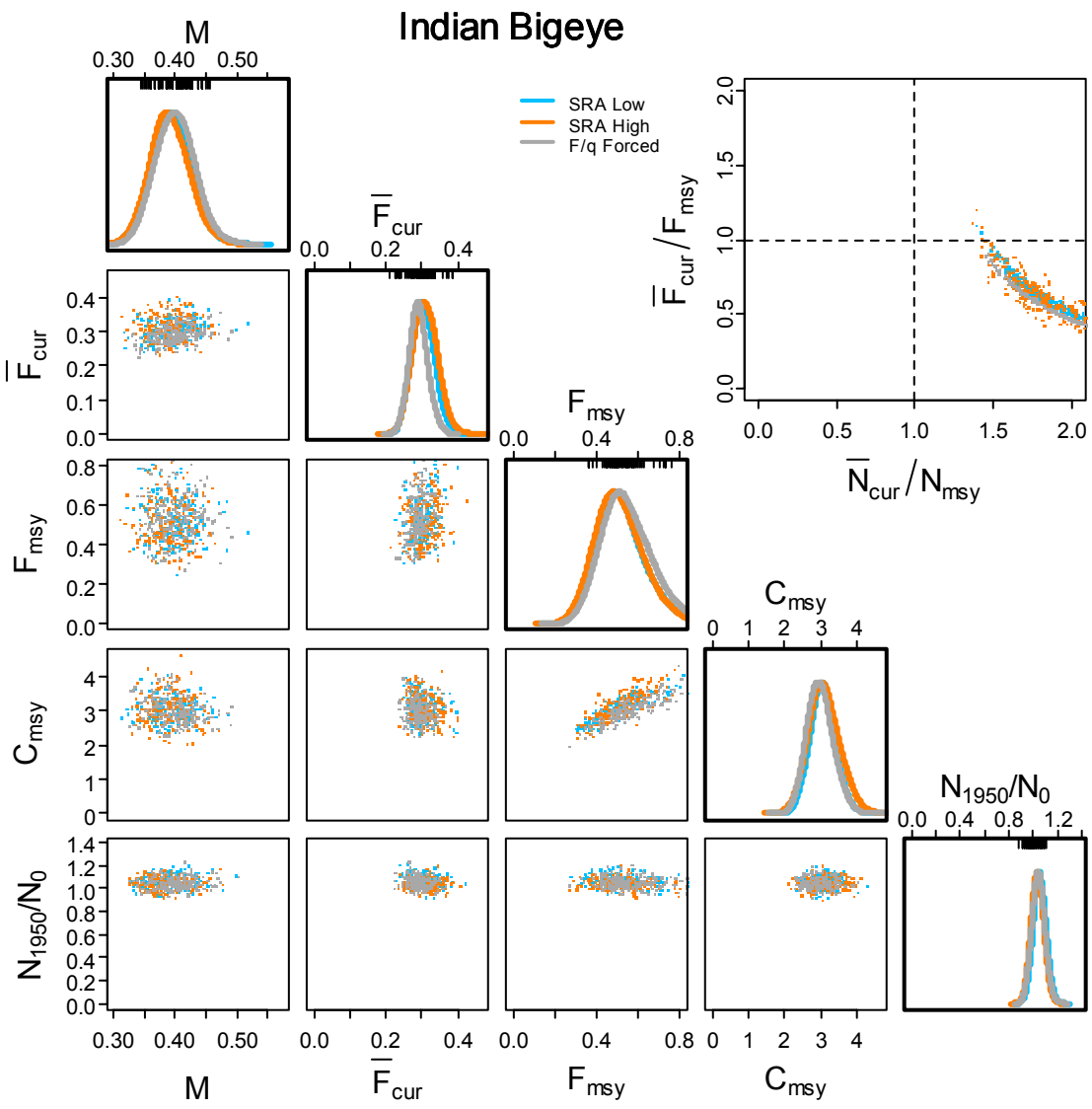

Figure 10.26 Indian Ocean bigeye tuna leading parameter joint distribution (lower triangular), marginal posterior distributions (diagonal) and biological reference points (upper triangular) for natural mortality (M), current fishing mortality (F_{cur}), fishing mortality that produced MSY (F_{msy}), MSY (C_{msy}) and the ratio of population in 1950 to that expected in the absence of fishing. Biological reference points in the top right corner are the ratio of current fishing mortality to the fishing mortality that produces MSY, and the ratio of current stock size to the stock size that produces MSY. Filled circles outside the upper triangular plot indicate ratios greater than 5. Blue lines and points are from SRA where variance in recruitment anomalies was assumed low. Orange lines and points are from SRA where variance in recruitment anomalies was assumed high. Light grey lines and points are from the relative fishing mortality rate forced numbers dynamic model. Rug plots on the top of distributions on the diagonal demark prior distributions.

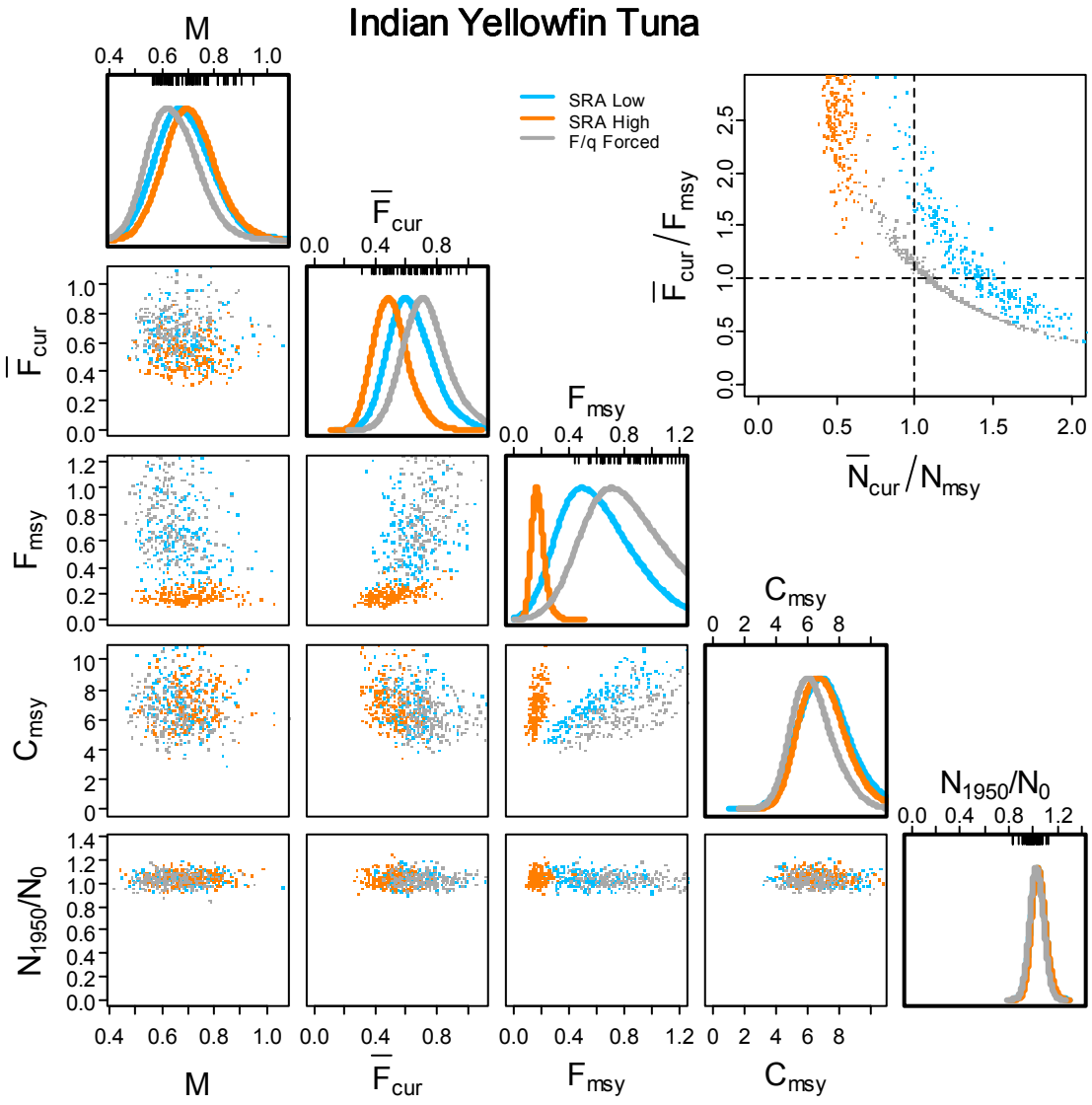

Figure 10.27 Indian Ocean yellowfin tuna leading parameter joint distribution (lower triangular), marginal posterior distributions (diagonal) and biological reference points (upper triangular) for natural mortality (M), current fishing mortality (F_{cur}), fishing mortality that produced MSY (F_{msy}), MSY (C_{msy}) and the ratio of population in 1950 to that expected in the absence of fishing. Biological reference points in the top right corner are the ratio of current fishing mortality to the fishing mortality that produces MSY, and the ratio of current stock size to the stock size that produces MSY. Filled circles outside the upper triangular plot indicate ratios greater than 5. Blue lines and points are from SRA where variance in recruitment anomalies was assumed low. Orange lines and points are from SRA where variance in recruitment anomalies was assumed high. Light grey lines and points are from the relative fishing mortality rate forced numbers dynamic model. Rug plots on the top of distributions on the diagonal demark prior distributions.

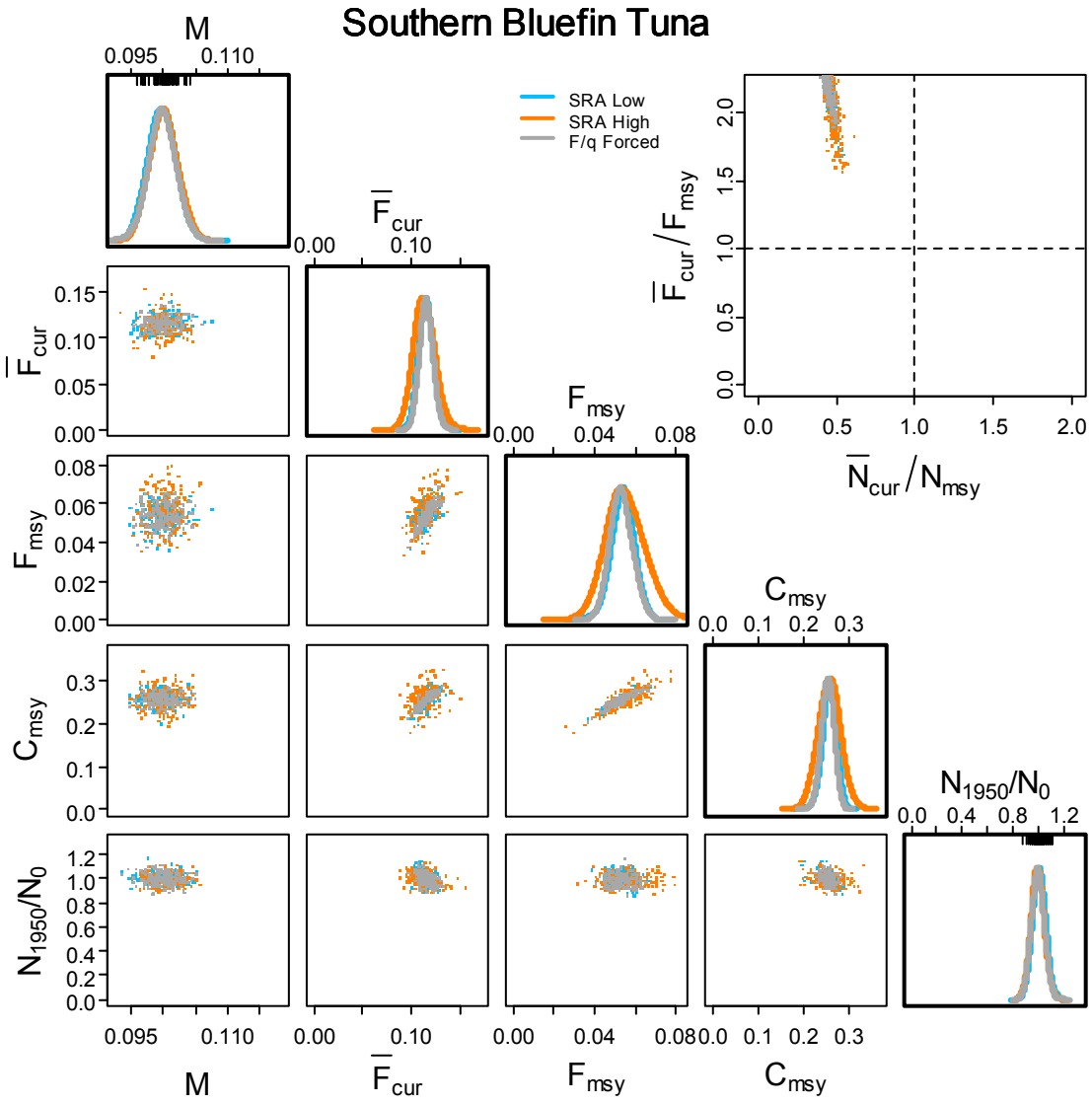

Figure 10.28 Southern bluefin tuna leading parameter joint distribution (lower triangular), marginal posterior distributions (diagonal) and biological reference points (upper triangular) for natural mortality (M), current fishing mortality (F_{cur}), fishing mortality that produced MSY (F_{msy}), MSY (C_{msy}) and the ratio of population in 1950 to that expected in the absence of fishing. Biological reference points in the top right corner are the ratio of current fishing mortality to the fishing mortality that produces MSY, and the ratio of current stock size to the stock size that produces MSY. Filled circles outside the upper triangular plot indicate ratios greater than 5. Blue lines and points are from SRA where variance in recruitment anomalies was assumed low. Orange lines and points are from SRA where variance in recruitment anomalies was assumed high. Light grey lines and points are from the relative fishing mortality rate forced numbers dynamic model. Rug plots on the top of distributions on the diagonal demark prior distributions.

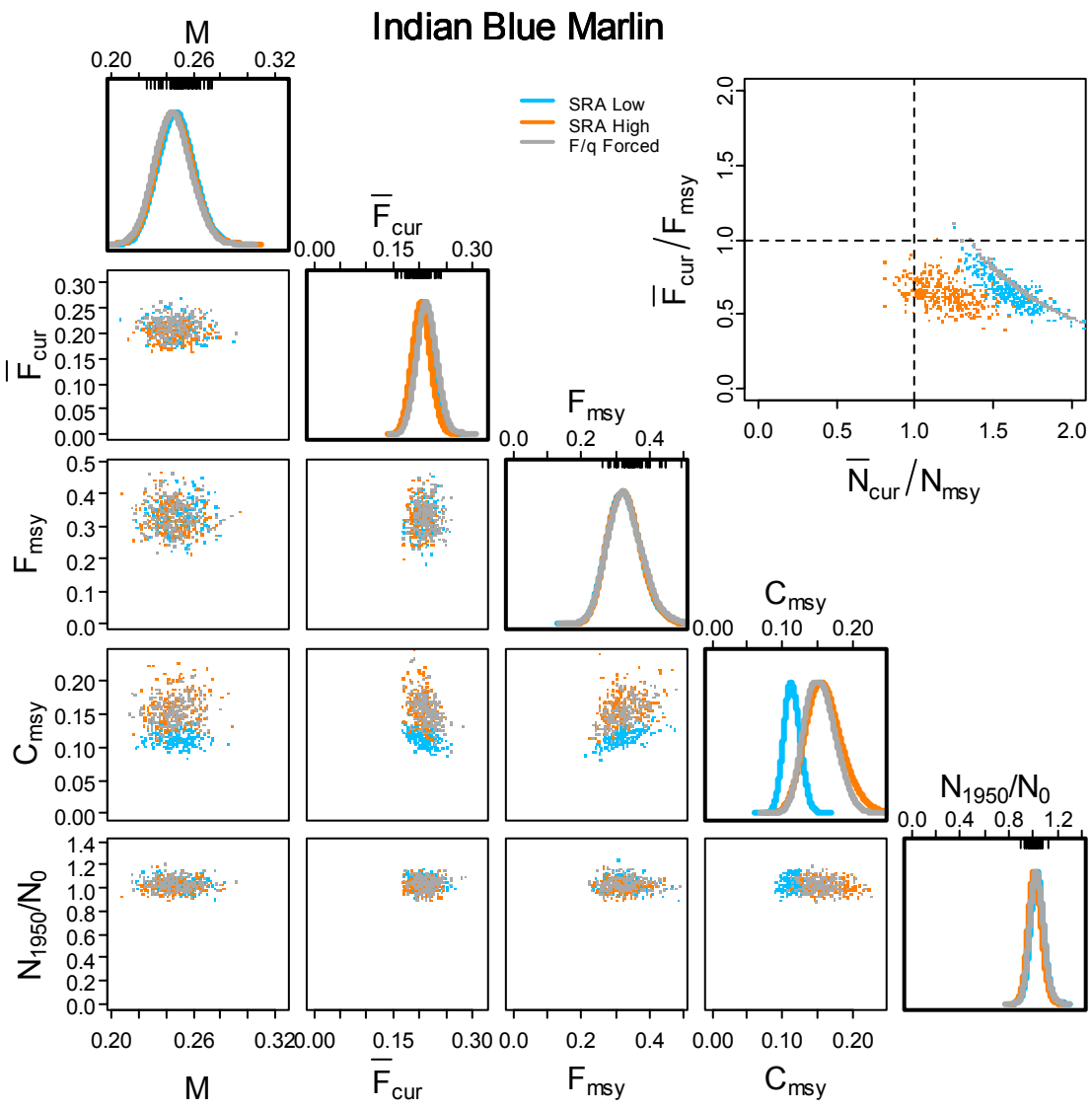

Figure 10.29 Indian Ocean blue marlin leading parameter joint distribution (lower triangular), marginal posterior distributions (diagonal) and biological reference points (upper triangular) for natural mortality (M), current fishing mortality (F_{cur}), fishing mortality that produced MSY (F_{msy}), MSY (C_{msy}) and the ratio of population in 1950 to that expected in the absence of fishing. Biological reference points in the top right corner are the ratio of current fishing mortality to the fishing mortality that produces MSY, and the ratio of current stock size to the stock size that produces MSY. Filled circles outside the upper triangular plot indicate ratios greater than 5. Blue lines and points are from SRA where variance in recruitment anomalies was assumed low. Orange lines and points are from SRA where variance in recruitment anomalies was assumed high. Light grey lines and points are from the relative fishing mortality rate forced numbers dynamic model. Rug plots on the top of distributions on the diagonal demark prior distributions.

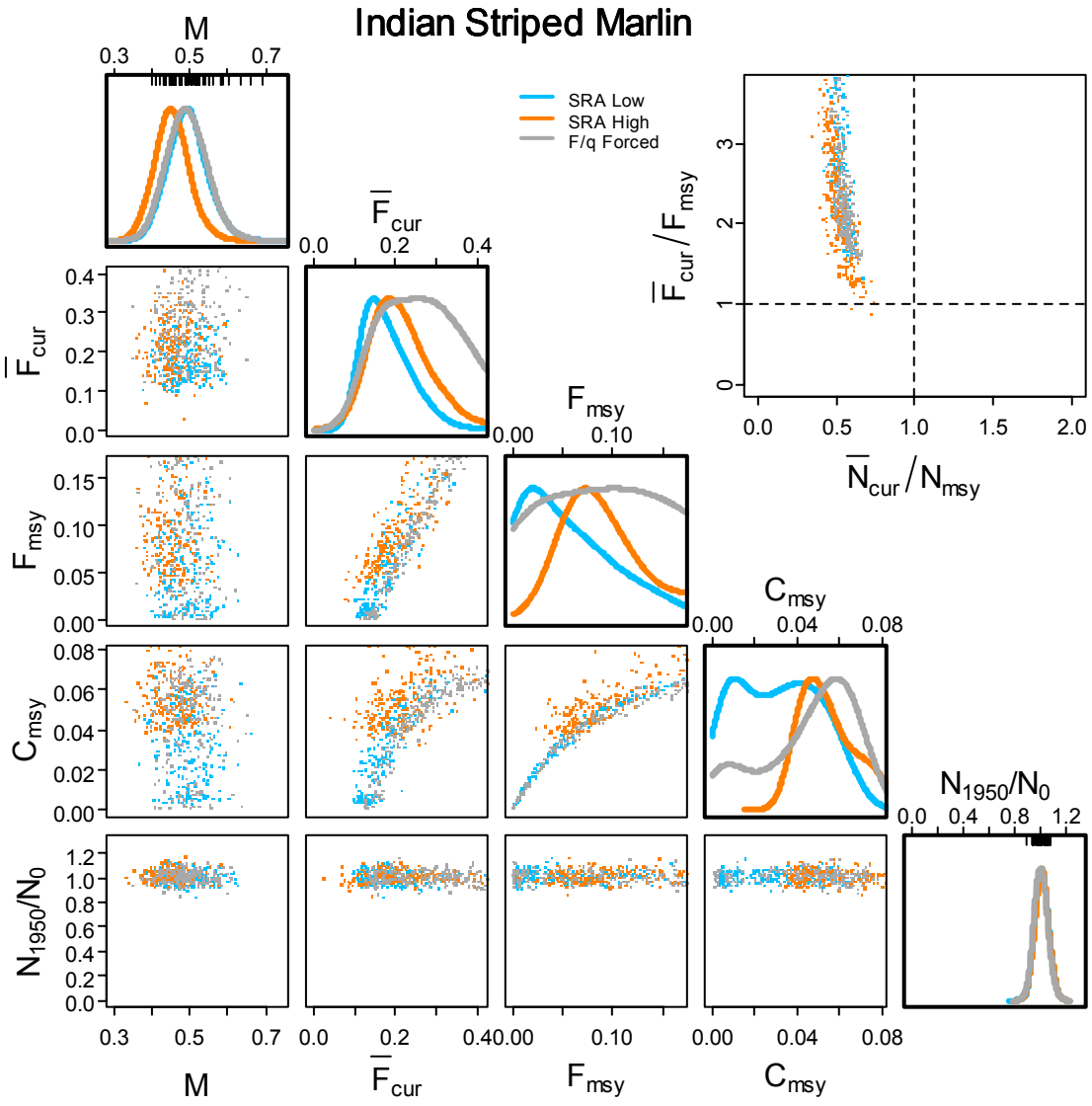

Figure 10.30 Indian Ocean striped marlin leading parameter joint distribution (lower triangular), marginal posterior distributions (diagonal) and biological reference points (upper triangular) for natural mortality (M), current fishing mortality (F_{cur}), fishing mortality that produced MSY (F_{msy}), MSY (C_{msy}) and the ratio of population in 1950 to that expected in the absence of fishing. Biological reference points in the top right corner are the ratio of current fishing mortality to the fishing mortality that produces MSY, and the ratio of current stock size to the stock size that produces MSY. Filled circles outside the upper triangular plot indicate ratios greater than 5. Blue lines and points are from SRA where variance in recruitment anomalies was assumed low. Orange lines and points are from SRA where variance in recruitment anomalies was assumed high. Light grey lines and points are from the relative fishing mortality rate forced numbers dynamic model. Rug plots on the top of distributions on the diagonal demark prior distributions.

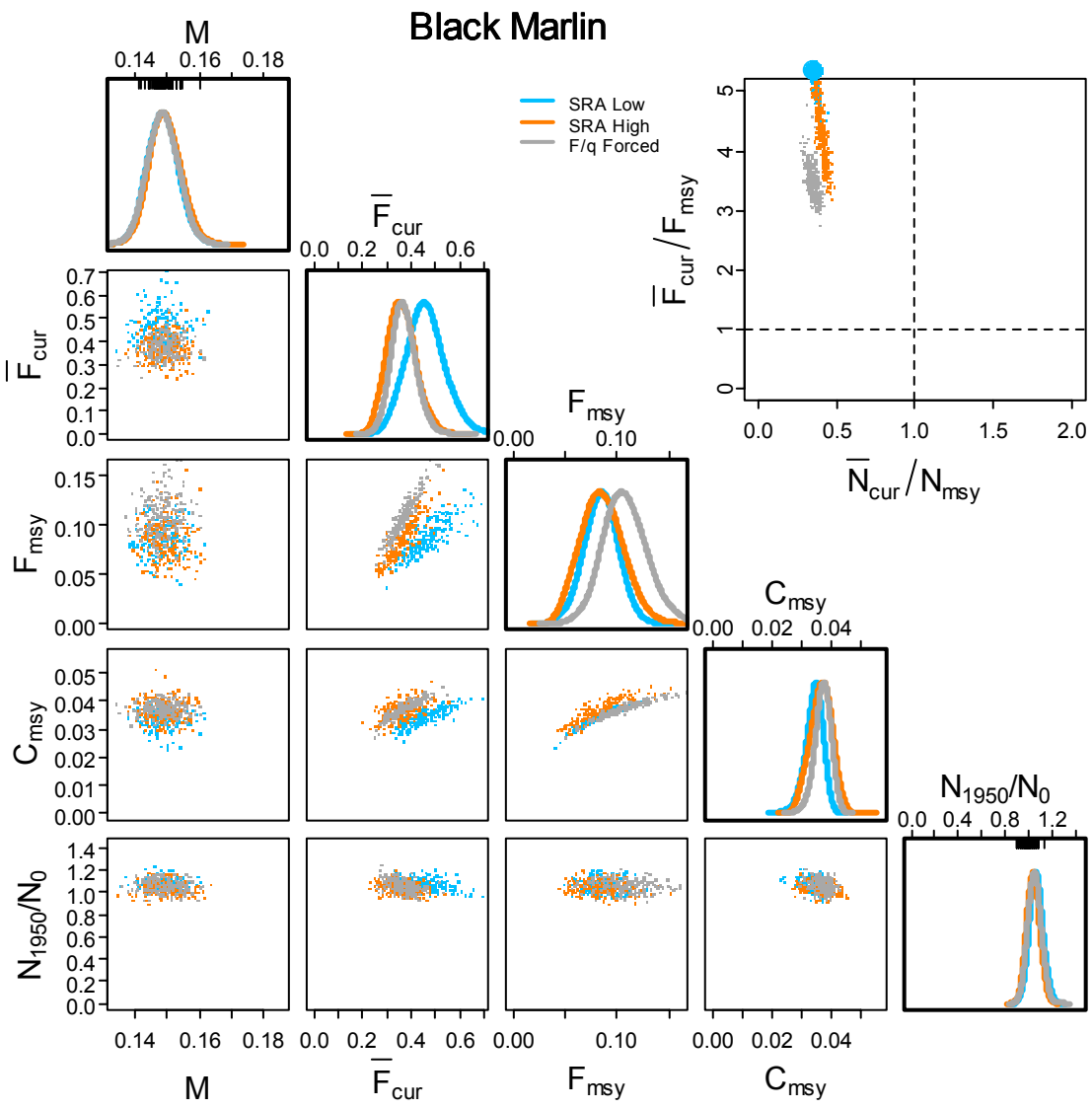

Figure 10.31 Indo-Pacific black marlin leading parameter joint distribution (lower triangular), marginal posterior distributions (diagonal) and biological reference points (upper triangular) for natural mortality (M), current fishing mortality (F_{cur}), fishing mortality that produced MSY (F_{msy}), MSY (C_{msy}) and the ratio of population in 1950 to that expected in the absence of fishing. Biological reference points in the top right corner are the ratio of current fishing mortality to the fishing mortality that produces MSY, and the ratio of current stock size to the stock size that produces MSY. Filled circles outside the upper triangular plot indicate ratios greater than 5. Blue lines and points are from SRA where variance in recruitment anomalies was assumed low. Orange lines and points are from SRA where variance in recruitment anomalies was assumed high. Light grey lines and points are from the relative fishing mortality rate forced numbers dynamic model. Rug plots on the top of distributions on the diagonal demark prior distributions.

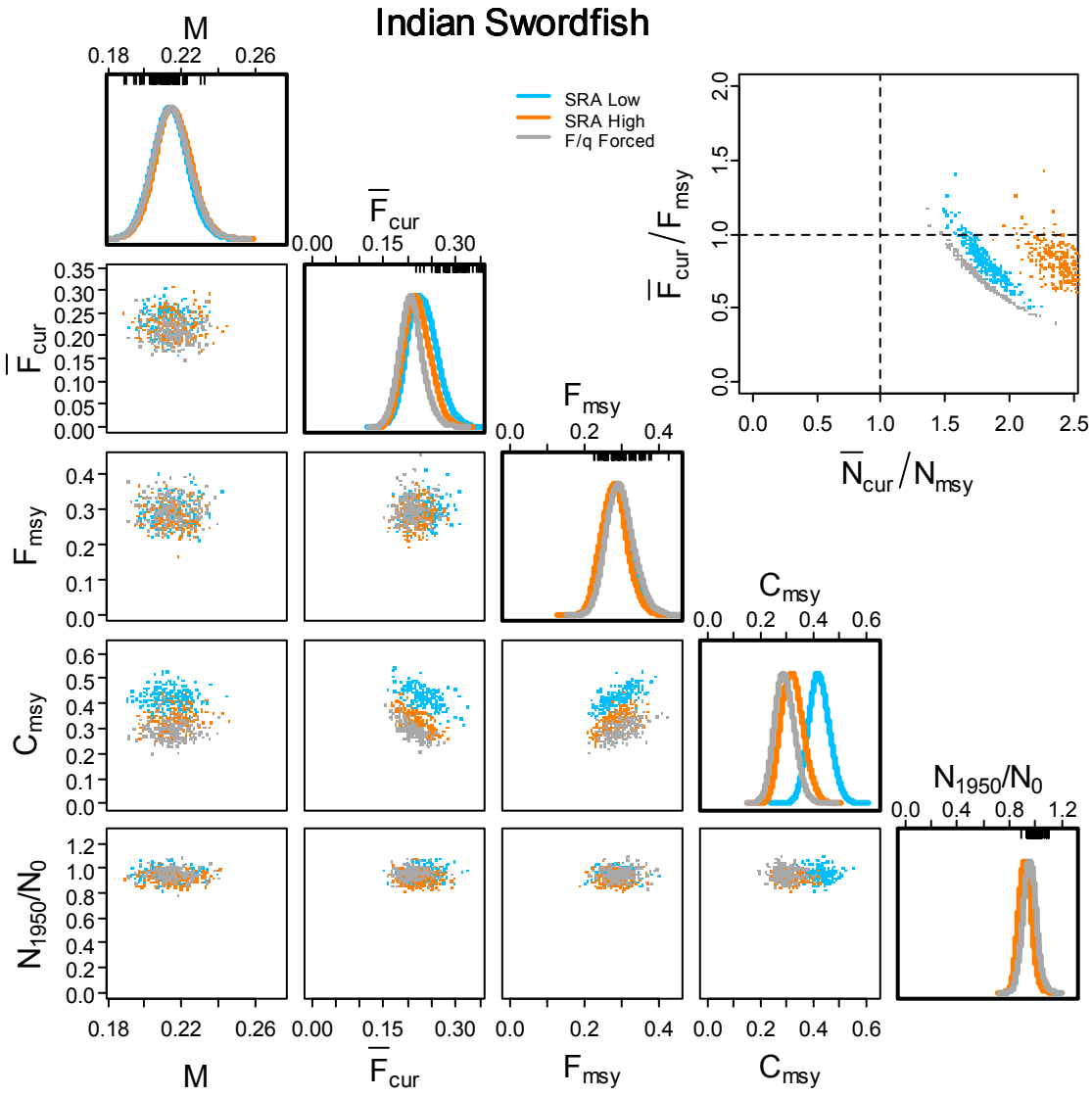

Figure 10.32 Indian Ocean swordfish leading parameter joint distribution (lower triangular), marginal posterior distributions (diagonal) and biological reference points (upper triangular) for natural mortality (M), current fishing mortality (F_{cur}), fishing mortality that produced MSY (F_{msy}), MSY (C_{msy}) and the ratio of population in 1950 to that expected in the absence of fishing. Biological reference points in the top right corner are the ratio of current fishing mortality to the fishing mortality that produces MSY, and the ratio of current stock size to the stock size that produces MSY. Filled circles outside the upper triangular plot indicate ratios greater than 5. Blue lines and points are from SRA where variance in recruitment anomalies was assumed low. Orange lines and points are from SRA where variance in recruitment anomalies was assumed high. Light grey lines and points are from the relative fishing mortality rate forced numbers dynamic model. Rug plots on the top of distributions on the diagonal demark prior distributions.

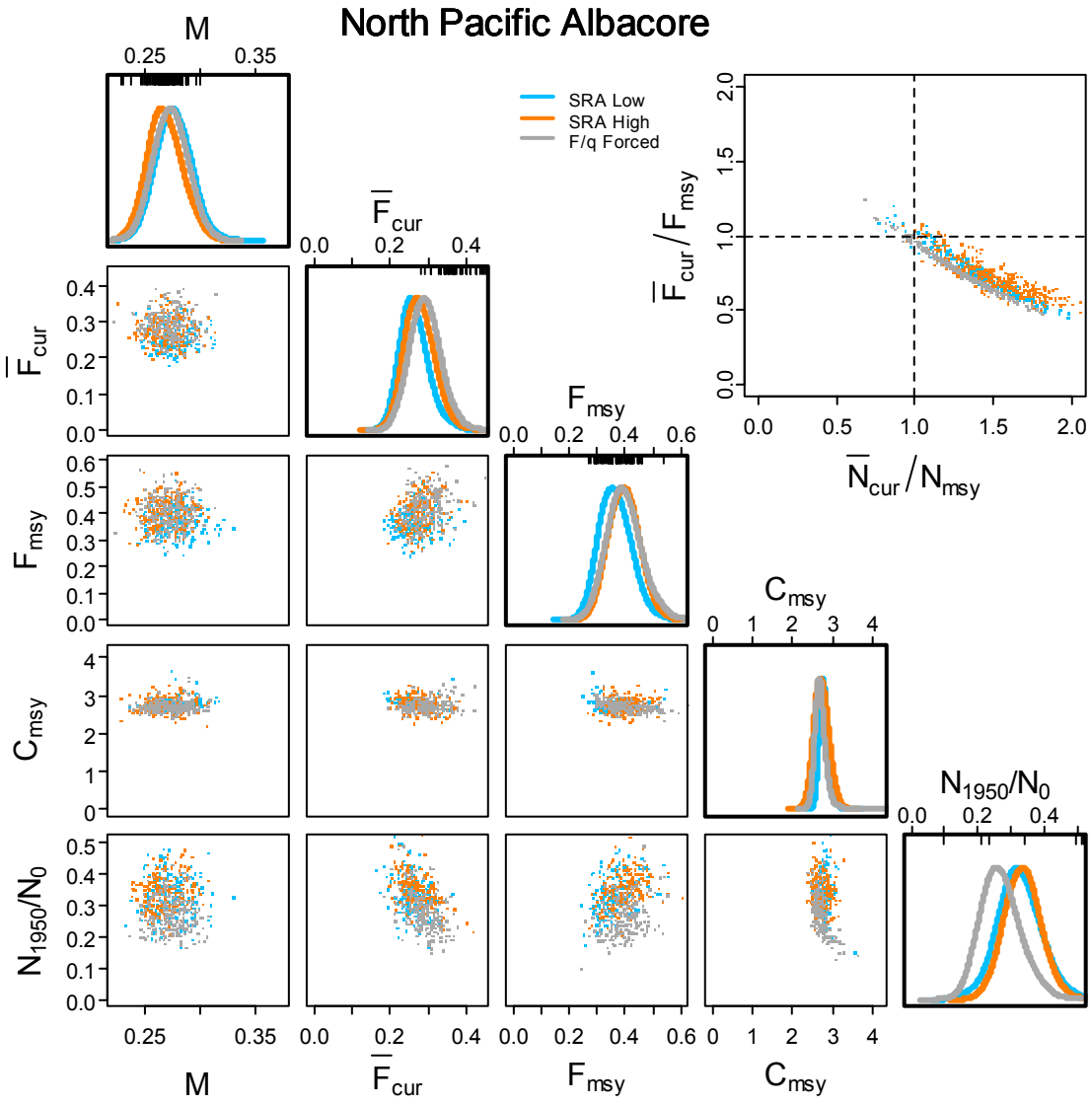

Figure 10.33 Pacific Ocean northern albacore tuna leading parameter joint distribution (lower triangular), marginal posterior distributions (diagonal) and biological reference points (upper triangular) for natural mortality (M), current fishing mortality (F_{cur}), fishing mortality that produced MSY (F_{msy}), MSY (C_{msy}) and the ratio of population in 1950 to that expected in the absence of fishing. Biological reference points in the top right corner are the ratio of current fishing mortality to the fishing mortality that produces MSY, and the ratio of current stock size to the stock size that produces MSY. Filled circles outside the upper triangular plot indicate ratios greater than 5. Blue lines and points are from SRA where variance in recruitment anomalies was assumed low. Orange lines and points are from SRA where variance in recruitment anomalies was assumed high. Light grey lines and points are from the relative fishing mortality rate forced numbers dynamic model. Rug plots on the top of distributions on the diagonal demark prior distributions.

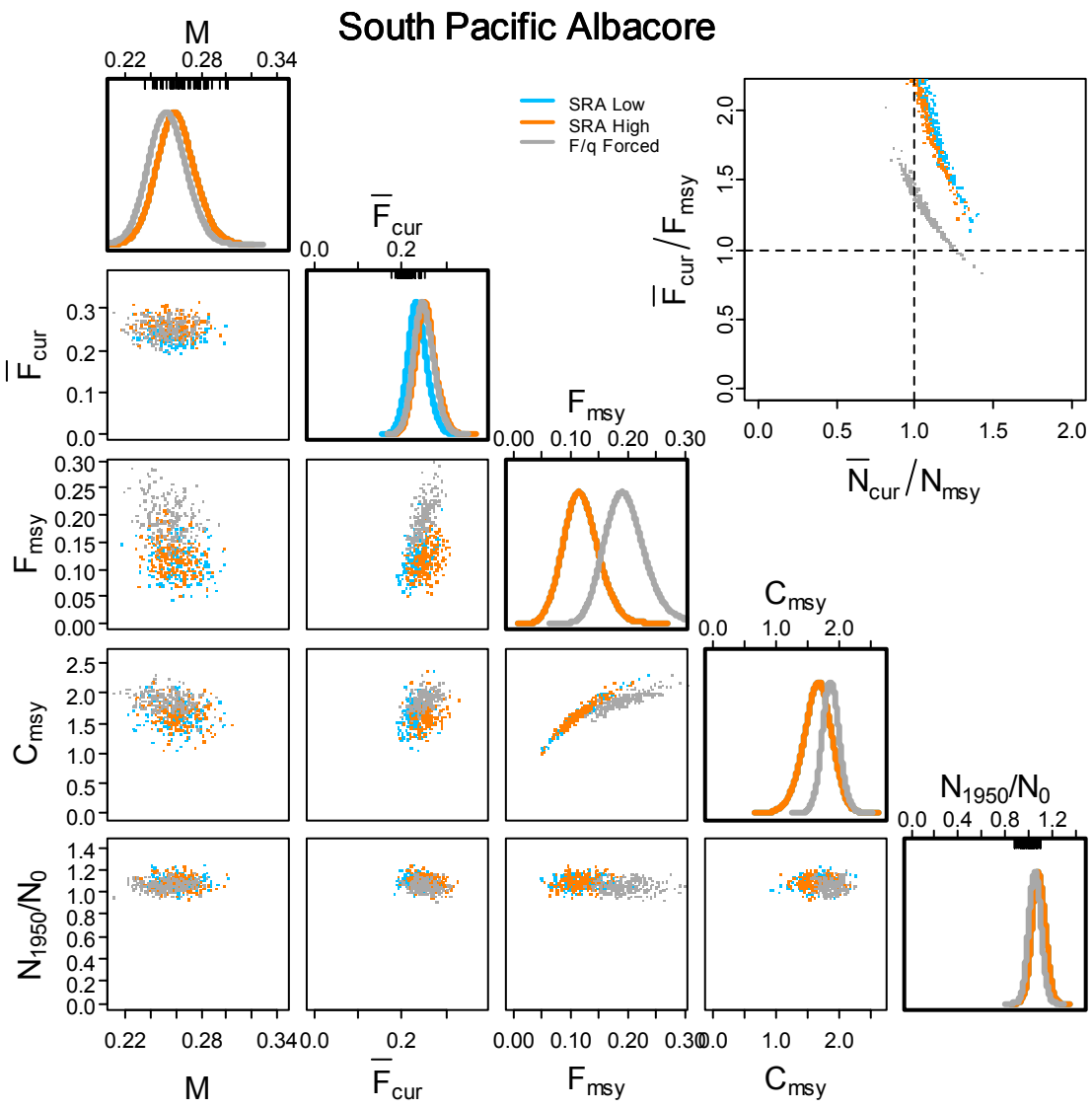

Figure 10.34 Pacific Ocean southern albacore tuna leading parameter joint distribution (lower triangular), marginal posterior distributions (diagonal) and biological reference points (upper triangular) for natural mortality (M), current fishing mortality (F_{cur}), fishing mortality that produced MSY (F_{msy}), MSY (C_{msy}) and the ratio of population in 1950 to that expected in the absence of fishing. Biological reference points in the top right corner are the ratio of current fishing mortality to the fishing mortality that produces MSY, and the ratio of current stock size to the stock size that produces MSY. Filled circles outside the upper triangular plot indicate ratios greater than 5. Blue lines and points are from SRA where variance in recruitment anomalies was assumed low. Orange lines and points are from SRA where variance in recruitment anomalies was assumed high. Light grey lines and points are from the relative fishing mortality rate forced numbers dynamic model. Rug plots on the top of distributions on the diagonal demark prior distributions.

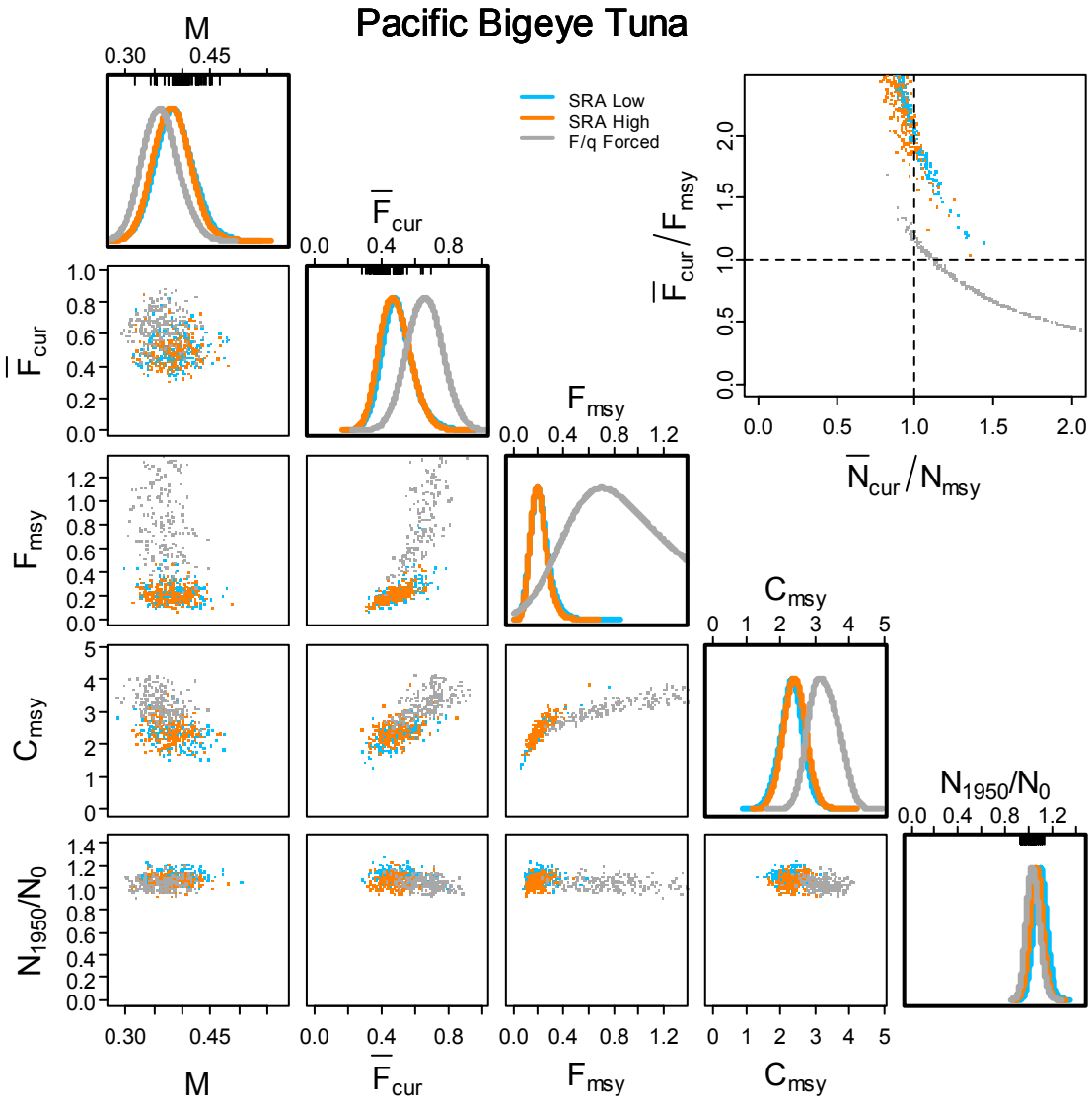

Figure 10.35 Pacific Ocean bigeye tuna leading parameter joint distribution (lower triangular), marginal posterior distributions (diagonal) and biological reference points (upper triangular) for natural mortality (M), current fishing mortality (F_{cur}), fishing mortality that produced MSY (F_{msy}), MSY (C_{msy}) and the ratio of population in 1950 to that expected in the absence of fishing. Biological reference points in the top right corner are the ratio of current fishing mortality to the fishing mortality that produces MSY, and the ratio of current stock size to the stock size that produces MSY. Filled circles outside the upper triangular plot indicate ratios greater than 5. Blue lines and points are from SRA where variance in recruitment anomalies was assumed low. Orange lines and points are from SRA where variance in recruitment anomalies was assumed high. Light grey lines and points are from the relative fishing mortality rate forced numbers dynamic model. Rug plots on the top of distributions on the diagonal demark prior distributions.

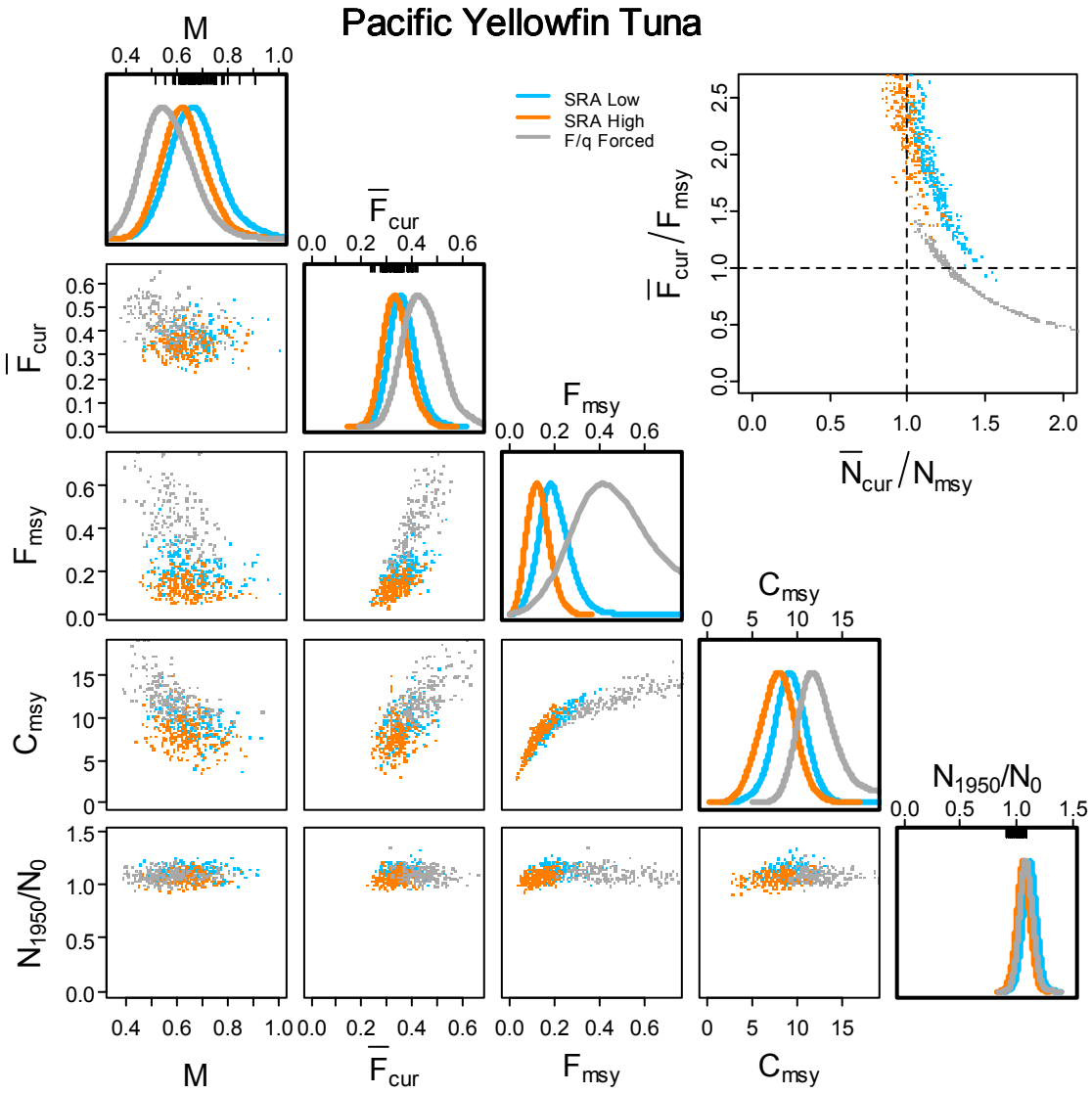

Figure 10.36 Pacific Ocean yellowfin tuna leading parameter joint distribution (lower triangular), marginal posterior distributions (diagonal) and biological reference points (upper triangular) for natural mortality (M), current fishing mortality (F_{cur}), fishing mortality that produced MSY (F_{msy}), MSY (C_{msy}) and the ratio of population in 1950 to that expected in the absence of fishing. Biological reference points in the top right corner are the ratio of current fishing mortality to the fishing mortality that produces MSY, and the ratio of current stock size to the stock size that produces MSY. Filled circles outside the upper triangular plot indicate ratios greater than 5. Blue lines and points are from SRA where variance in recruitment anomalies was assumed low. Orange lines and points are from SRA where variance in recruitment anomalies was assumed high. Light grey lines and points are from the relative fishing mortality rate forced numbers dynamic model. Rug plots on the top of distributions on the diagonal demark prior distributions.

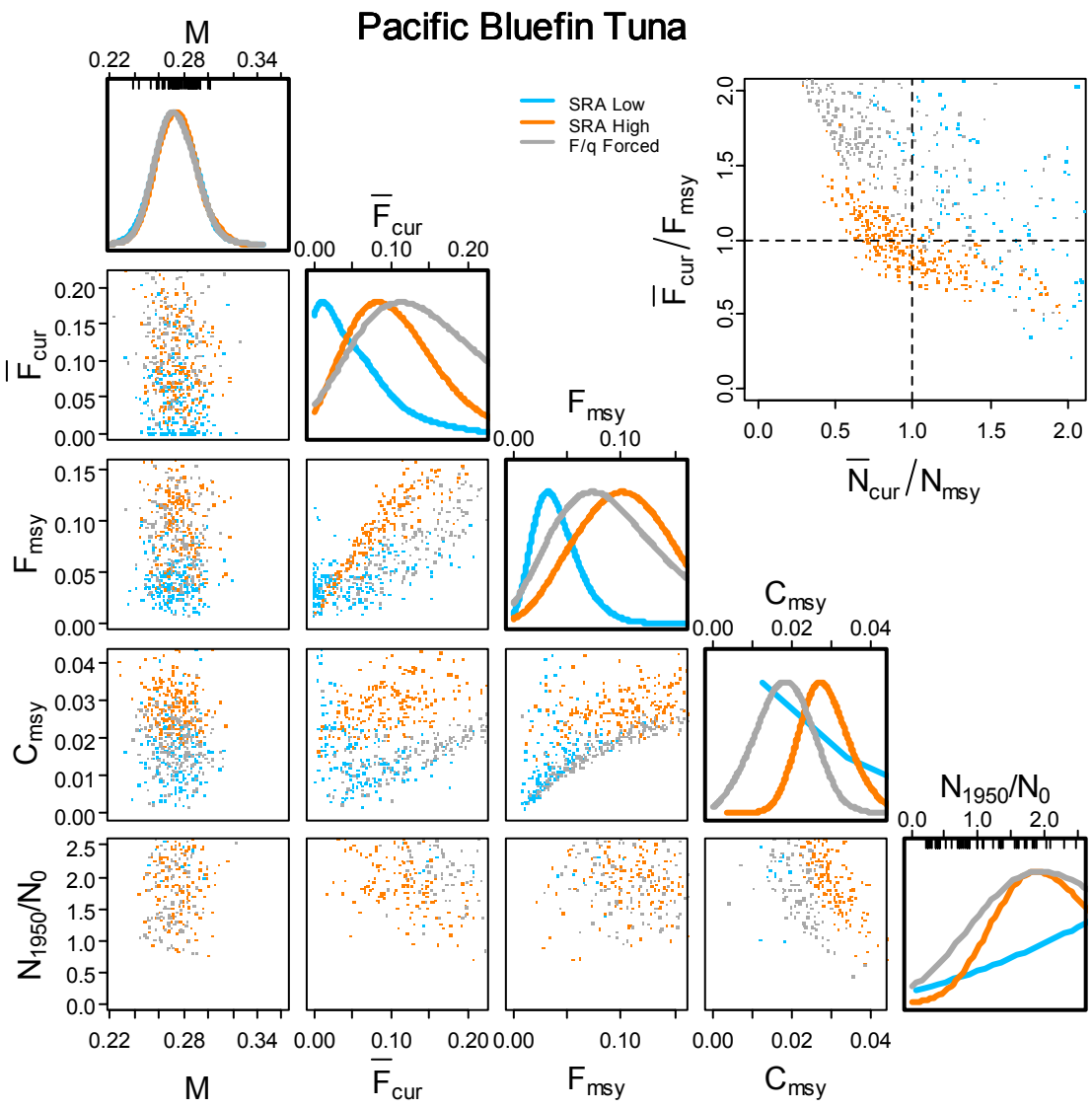

Figure 10.37 Pacific Ocean bluefin tuna leading parameter joint distribution (lower triangular), marginal posterior distributions (diagonal) and biological reference points (upper triangular) for natural mortality (M), current fishing mortality (F_{cur}), fishing mortality that produced MSY (F_{msy}), MSY (C_{msy}) and the ratio of population in 1950 to that expected in the absence of fishing. Biological reference points in the top right corner are the ratio of current fishing mortality to the fishing mortality that produces MSY, and the ratio of current stock size to the stock size that produces MSY. Filled circles outside the upper triangular plot indicate ratios greater than 5. Blue lines and points are from SRA where variance in recruitment anomalies was assumed low. Orange lines and points are from SRA where variance in recruitment anomalies was assumed high. Light grey lines and points are from the relative fishing mortality rate forced numbers dynamic model. Rug plots on the top of distributions on the diagonal demark prior distributions.

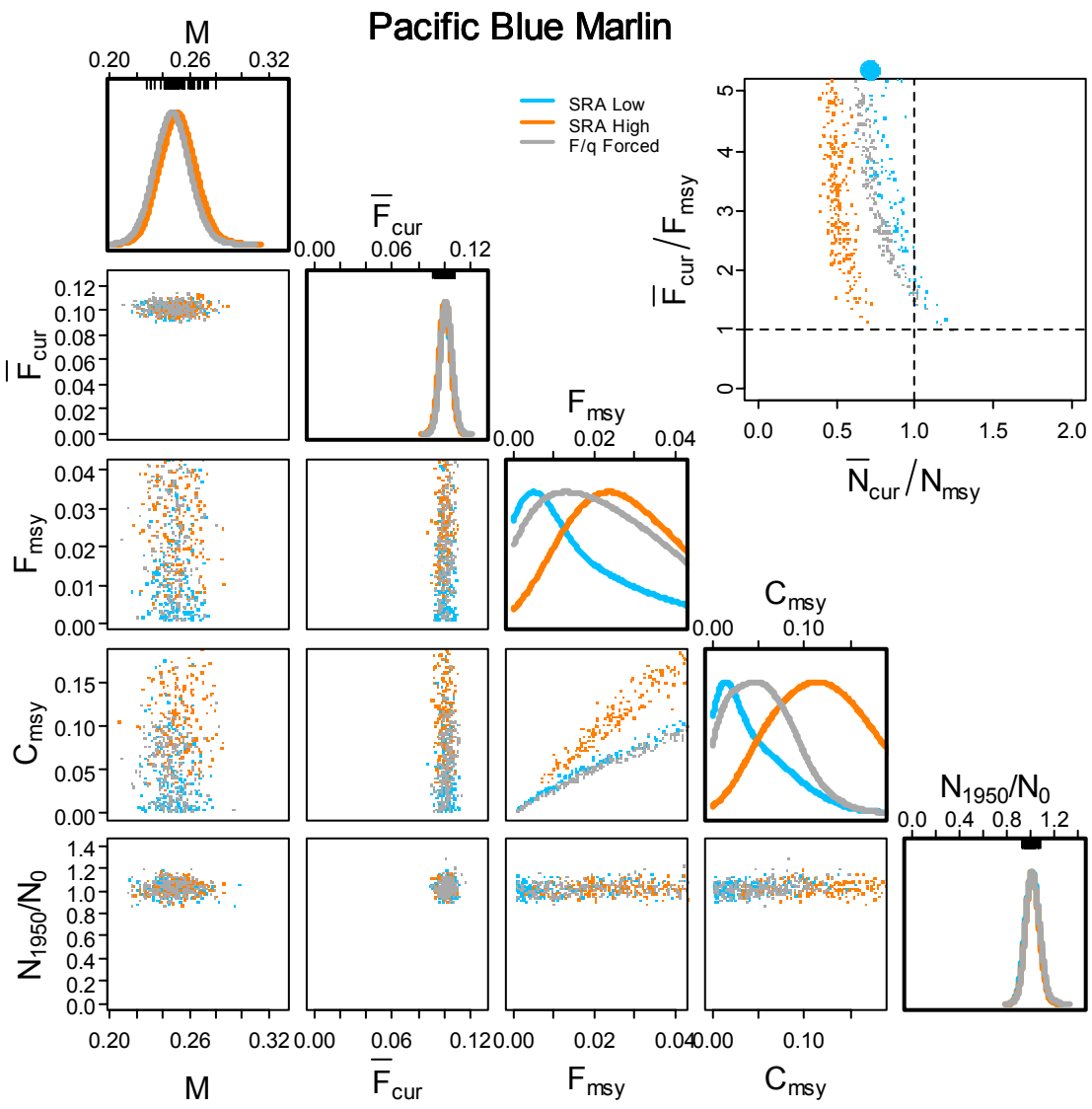

Figure 10.38 Pacific Ocean blue marlin leading parameter joint distribution (lower triangular), marginal posterior distributions (diagonal) and biological reference points (upper triangular) for natural mortality (M), current fishing mortality (F_{cur}), fishing mortality that produced MSY (F_{msy}), MSY (C_{msy}) and the ratio of population in 1950 to that expected in the absence of fishing. Biological reference points in the top right corner are the ratio of current fishing mortality to the fishing mortality that produces MSY, and the ratio of current stock size to the stock size that produces MSY. Filled circles outside the upper triangular plot indicate ratios greater than 5. Blue lines and points are from SRA where variance in recruitment anomalies was assumed low. Orange lines and points are from SRA where variance in recruitment anomalies was assumed high. Light grey lines and points are from the relative fishing mortality rate forced numbers dynamic model. Rug plots on the top of distributions on the diagonal demark prior distributions.

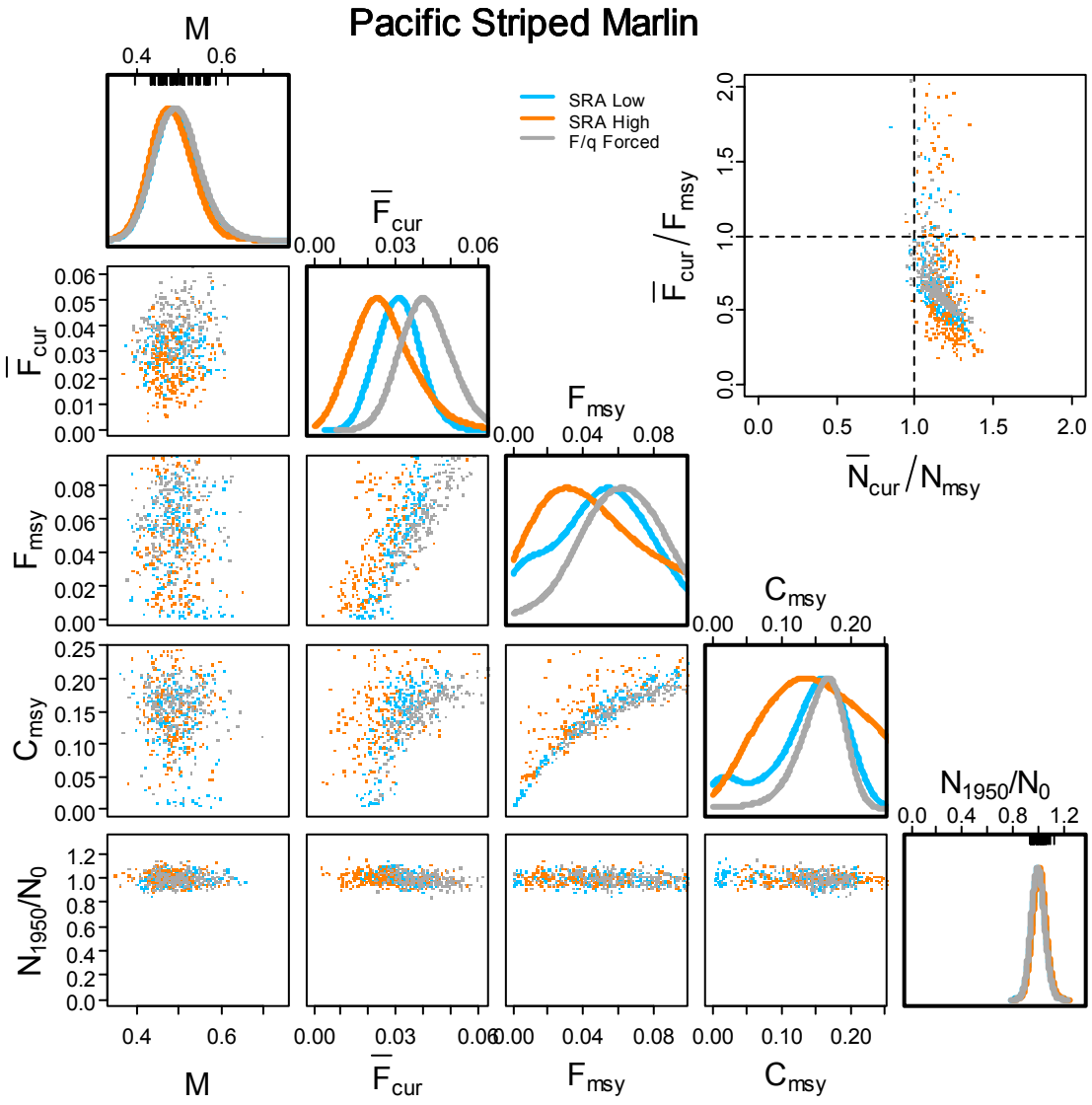

Figure 10.39 Pacific Ocean striped marlin leading parameter joint distribution (lower triangular), marginal posterior distributions (diagonal) and biological reference points (upper triangular) for natural mortality (M), current fishing mortality (F_{cur}), fishing mortality that produced MSY (F_{msy}), MSY (C_{msy}) and the ratio of population in 1950 to that expected in the absence of fishing. Biological reference points in the top right corner are the ratio of current fishing mortality to the fishing mortality that produces MSY, and the ratio of current stock size to the stock size that produces MSY. Filled circles outside the upper triangular plot indicate ratios greater than 5. Blue lines and points are from SRA where variance in recruitment anomalies was assumed low. Orange lines and points are from SRA where variance in recruitment anomalies was assumed high. Light grey lines and points are from the relative fishing mortality rate forced numbers dynamic model. Rug plots on the top of distributions on the diagonal demark prior distributions.

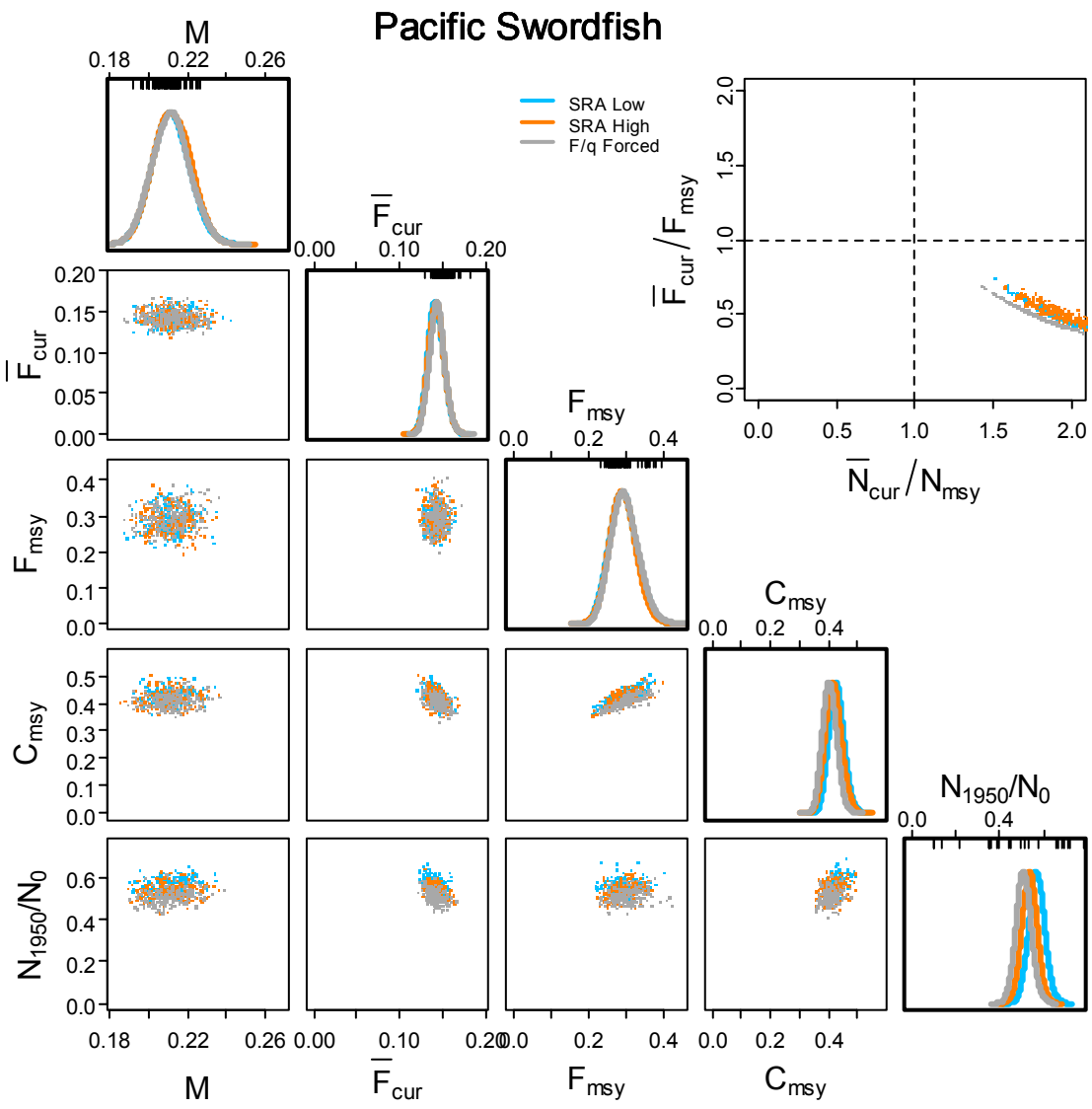

Figure 10.40 Pacific Ocean swordfish leading parameter joint distribution (lower triangular), marginal posterior distributions (diagonal) and biological reference points (upper triangular) for natural mortality (M), current fishing mortality (F_{cur}), fishing mortality that produced MSY (F_{msy}), MSY (C_{msy}) and the ratio of population in 1950 to that expected in the absence of fishing. Biological reference points in the top right corner are the ratio of current fishing mortality to the fishing mortality that produces MSY, and the ratio of current stock size to the stock size that produces MSY. Filled circles outside the upper triangular plot indicate ratios greater than 5. Blue lines and points are from SRA where variance in recruitment anomalies was assumed low. Orange lines and points are from SRA where variance in recruitment anomalies was assumed high. Light grey lines and points are from the relative fishing mortality rate forced numbers dynamic model. Rug plots on the top of distributions on the diagonal demark prior distributions.

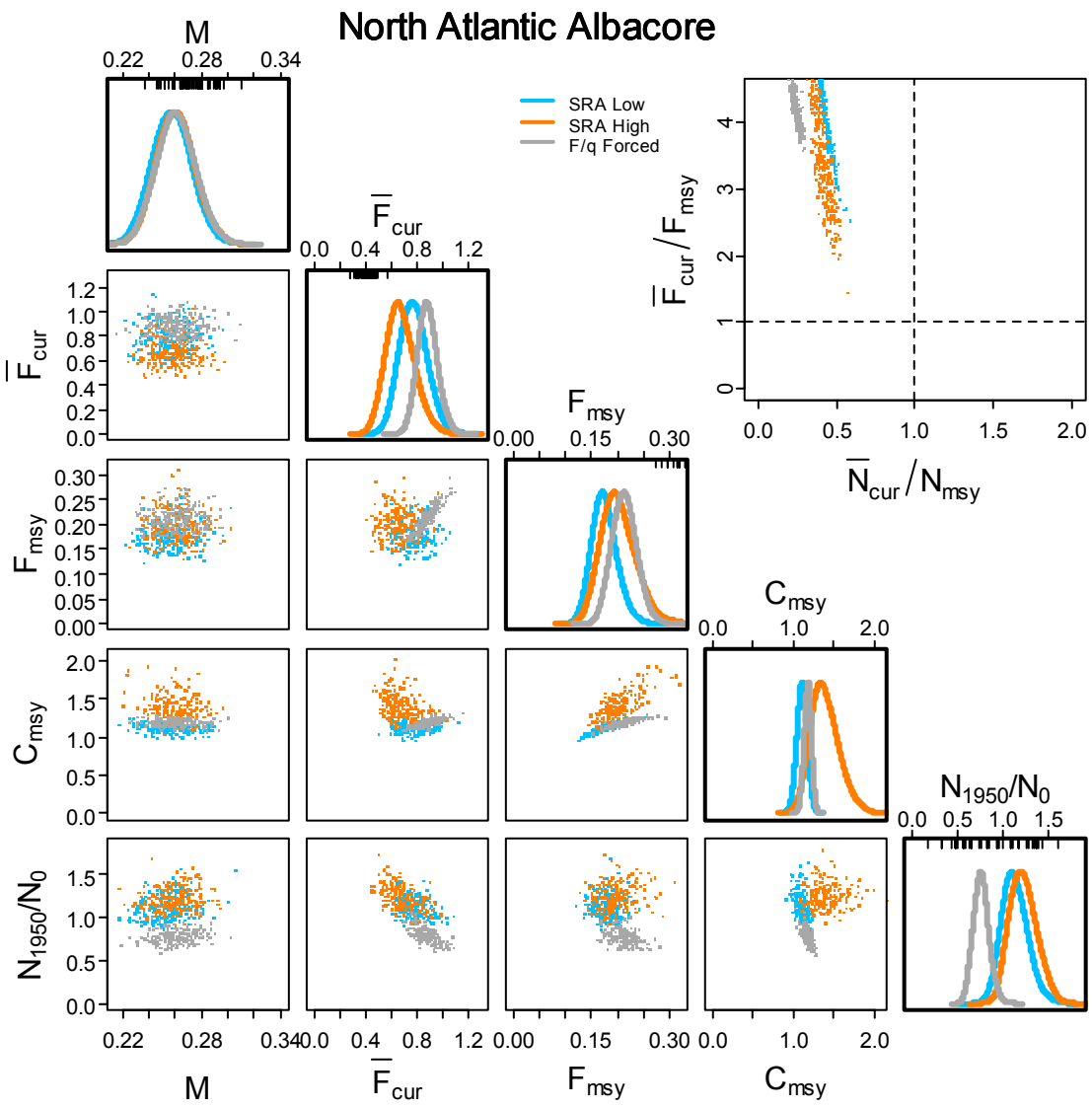

Figure 10.41 Atlantic Ocean northern albacore tuna leading parameter joint distribution (lower triangular), marginal posterior distributions (diagonal) and biological reference points (upper triangular) for natural mortality (M), current fishing mortality (F_{cur}), fishing mortality that produced MSY (F_{msy}), MSY (C_{msy}) and the ratio of population in 1950 to that expected in the absence of fishing. Biological reference points in the top right corner are the ratio of current fishing mortality to the fishing mortality that produces MSY, and the ratio of current stock size to the stock size that produces MSY. Filled circles outside the upper triangular plot indicate ratios greater than 5. Blue lines and points are from SRA where variance in recruitment anomalies was assumed low. Orange lines and points are from SRA where variance in recruitment anomalies was assumed high. Light grey lines and points are from the relative fishing mortality rate forced numbers dynamic model. Rug plots on the top of distributions on the diagonal demark prior distributions.

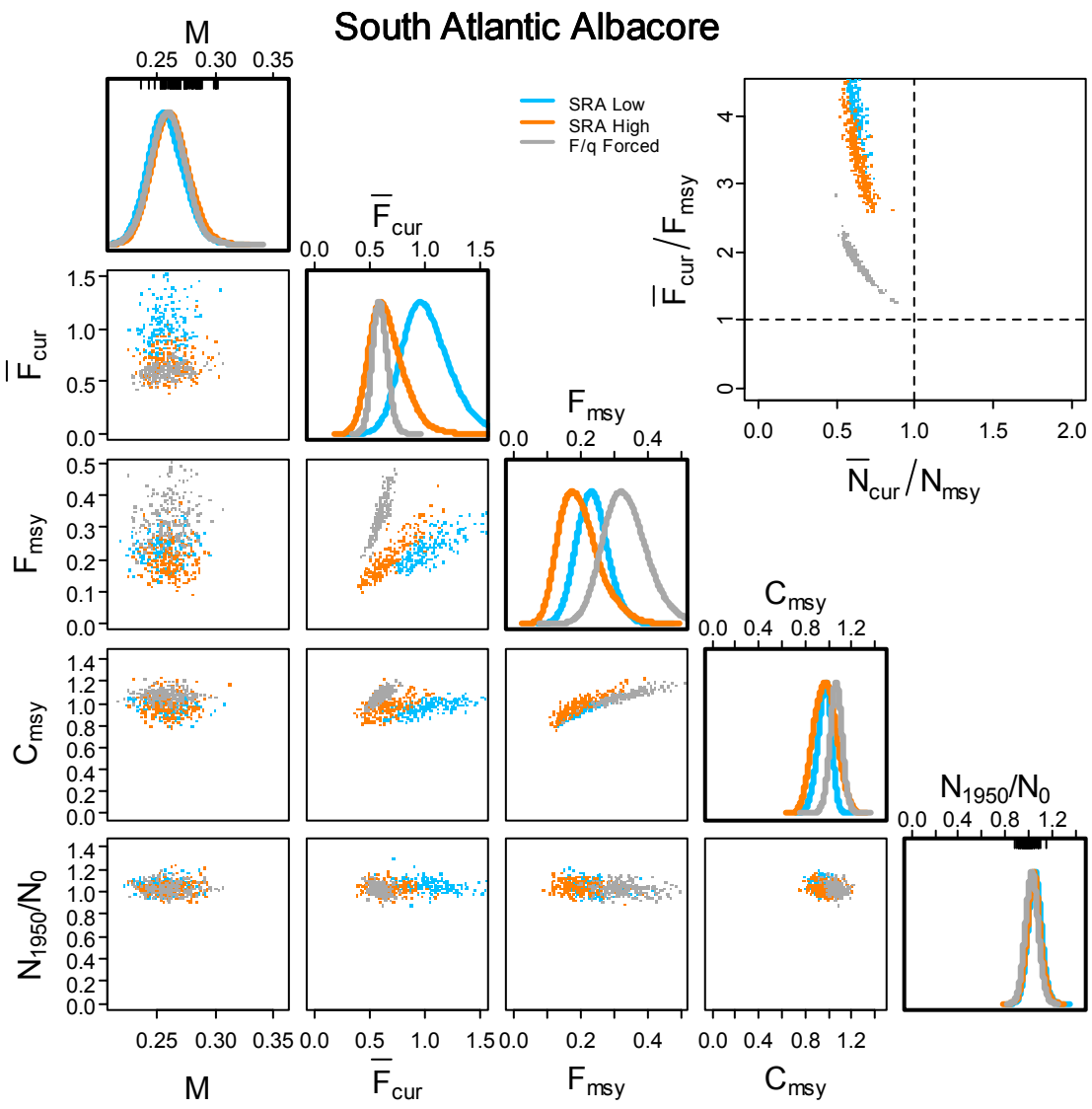

Figure 10.42 Atlantic Ocean southern albacore tuna leading parameter joint distribution (lower triangular), marginal posterior distributions (diagonal) and biological reference points (upper triangular) for natural mortality (M), current fishing mortality (F_{cur}), fishing mortality that produced MSY (F_{msy}), MSY (C_{msy}) and the ratio of population in 1950 to that expected in the absence of fishing. Biological reference points in the top right corner are the ratio of current fishing mortality to the fishing mortality that produces MSY, and the ratio of current stock size to the stock size that produces MSY. Filled circles outside the upper triangular plot indicate ratios greater than 5. Blue lines and points are from SRA where variance in recruitment anomalies was assumed low. Orange lines and points are from SRA where variance in recruitment anomalies was assumed high. Light grey lines and points are from the relative fishing mortality rate forced numbers dynamic model. Rug plots on the top of distributions on the diagonal demark prior distributions.

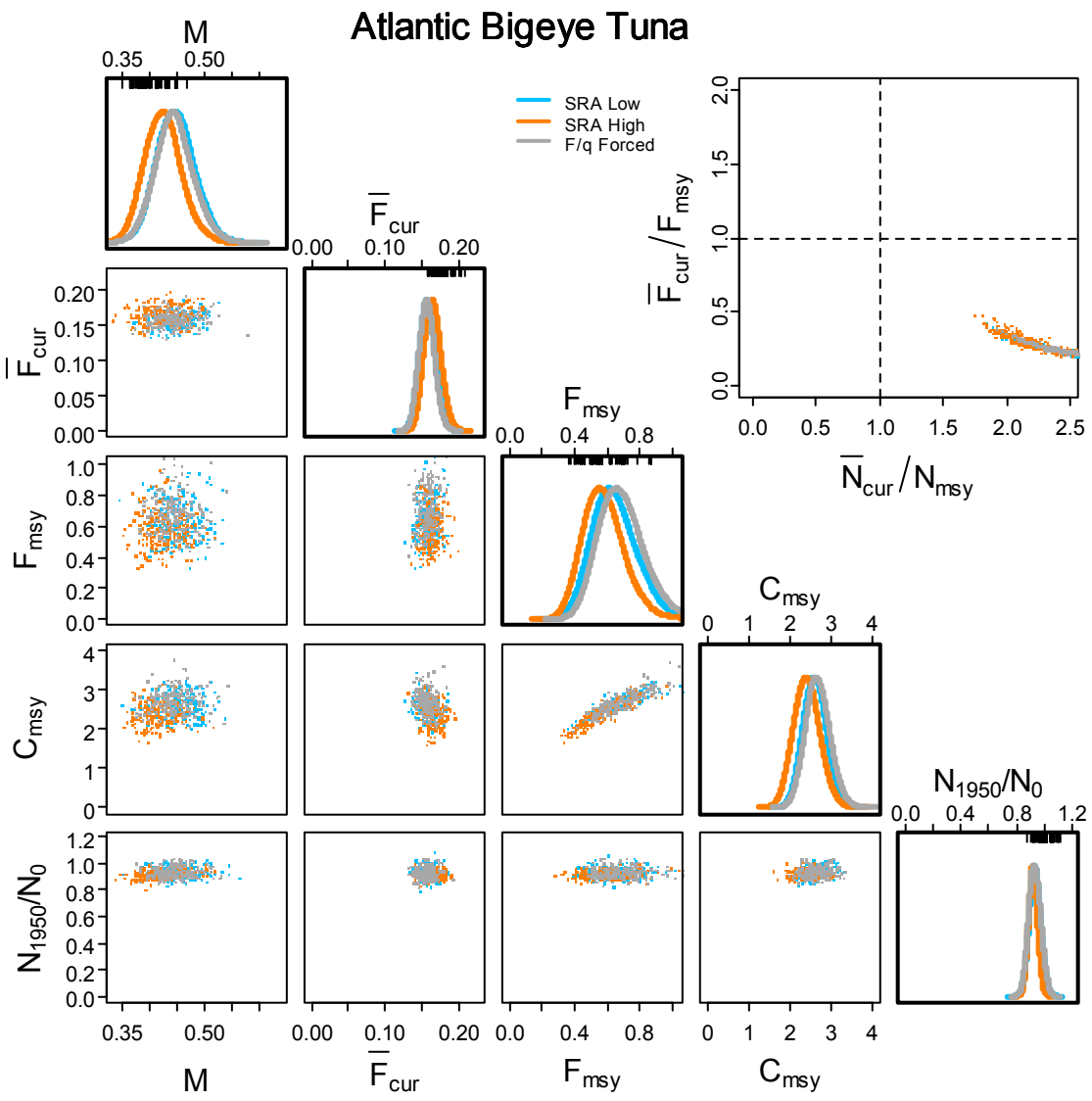

Figure 10.43 Atlantic Ocean bigeye tuna leading parameter joint distribution (lower triangular), marginal posterior distributions (diagonal) and biological reference points (upper triangular) for natural mortality (M), current fishing mortality (F_{cur}), fishing mortality that produced MSY (F_{msy}), MSY (C_{msy}) and the ratio of population in 1950 to that expected in the absence of fishing. Biological reference points in the top right corner are the ratio of current fishing mortality to the fishing mortality that produces MSY, and the ratio of current stock size to the stock size that produces MSY. Filled circles outside the upper triangular plot indicate ratios greater than 5. Blue lines and points are from SRA where variance in recruitment anomalies was assumed low. Orange lines and points are from SRA where variance in recruitment anomalies was assumed high. Light grey lines and points are from the relative fishing mortality rate forced numbers dynamic model. Rug plots on the top of distributions on the diagonal demark prior distributions.

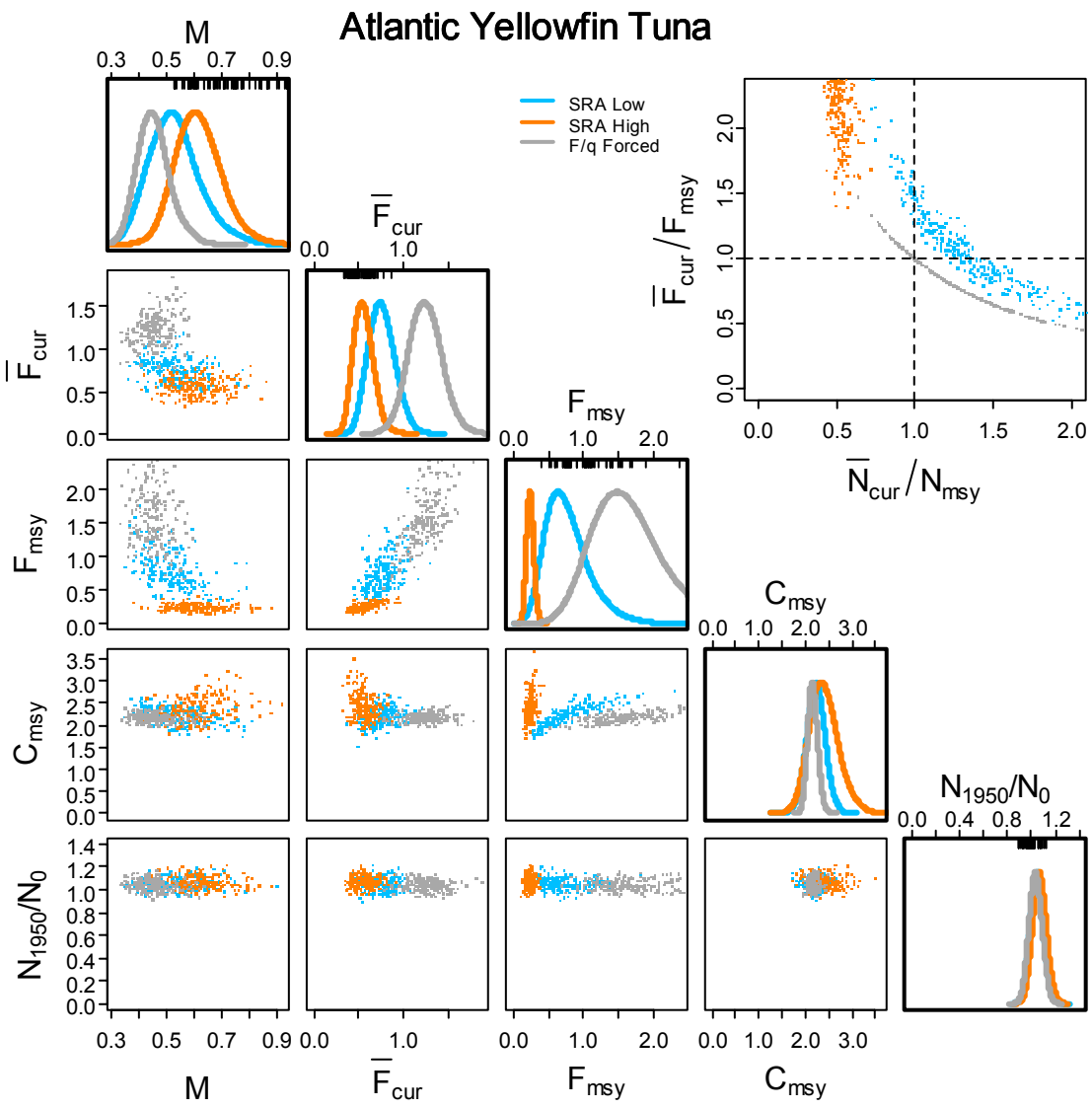

Figure 10.44 Atlantic Ocean yellowfin tuna leading parameter joint distribution (lower triangular), marginal posterior distributions (diagonal) and biological reference points (upper triangular) for natural mortality (M), current fishing mortality (F_{cur}), fishing mortality that produced MSY (F_{msy}), MSY (C_{msy}) and the ratio of population in 1950 to that expected in the absence of fishing. Biological reference points in the top right corner are the ratio of current fishing mortality to the fishing mortality that produces MSY, and the ratio of current stock size to the stock size that produces MSY. Filled circles outside the upper triangular plot indicate ratios greater than 5. Blue lines and points are from SRA where variance in recruitment anomalies was assumed low. Orange lines and points are from SRA where variance in recruitment anomalies was assumed high. Light grey lines and points are from the relative fishing mortality rate forced numbers dynamic model. Rug plots on the top of distributions on the diagonal demark prior distributions.

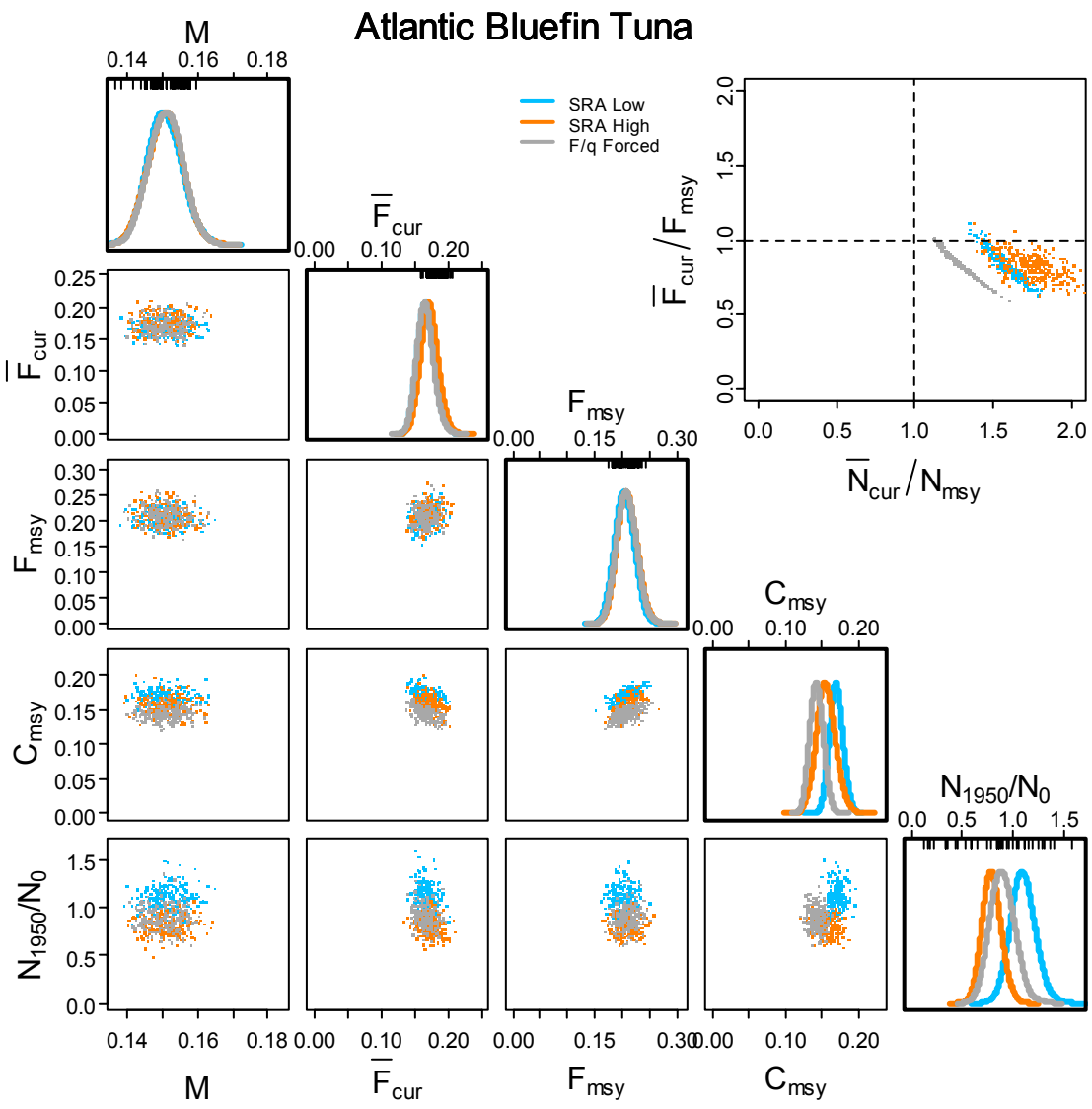

Figure 10.45 Atlantic Ocean bluefin tuna leading parameter joint distribution (lower triangular), marginal posterior distributions (diagonal) and biological reference points (upper triangular) for natural mortality (M), current fishing mortality (F_{cur}), fishing mortality that produced MSY (F_{msy}), MSY (C_{msy}) and the ratio of population in 1950 to that expected in the absence of fishing. Biological reference points in the top right corner are the ratio of current fishing mortality to the fishing mortality that produces MSY, and the ratio of current stock size to the stock size that produces MSY. Filled circles outside the upper triangular plot indicate ratios greater than 5. Blue lines and points are from SRA where variance in recruitment anomalies was assumed low. Orange lines and points are from SRA where variance in recruitment anomalies was assumed high. Light grey lines and points are from the relative fishing mortality rate forced numbers dynamic model. Rug plots on the top of distributions on the diagonal demark prior distributions.

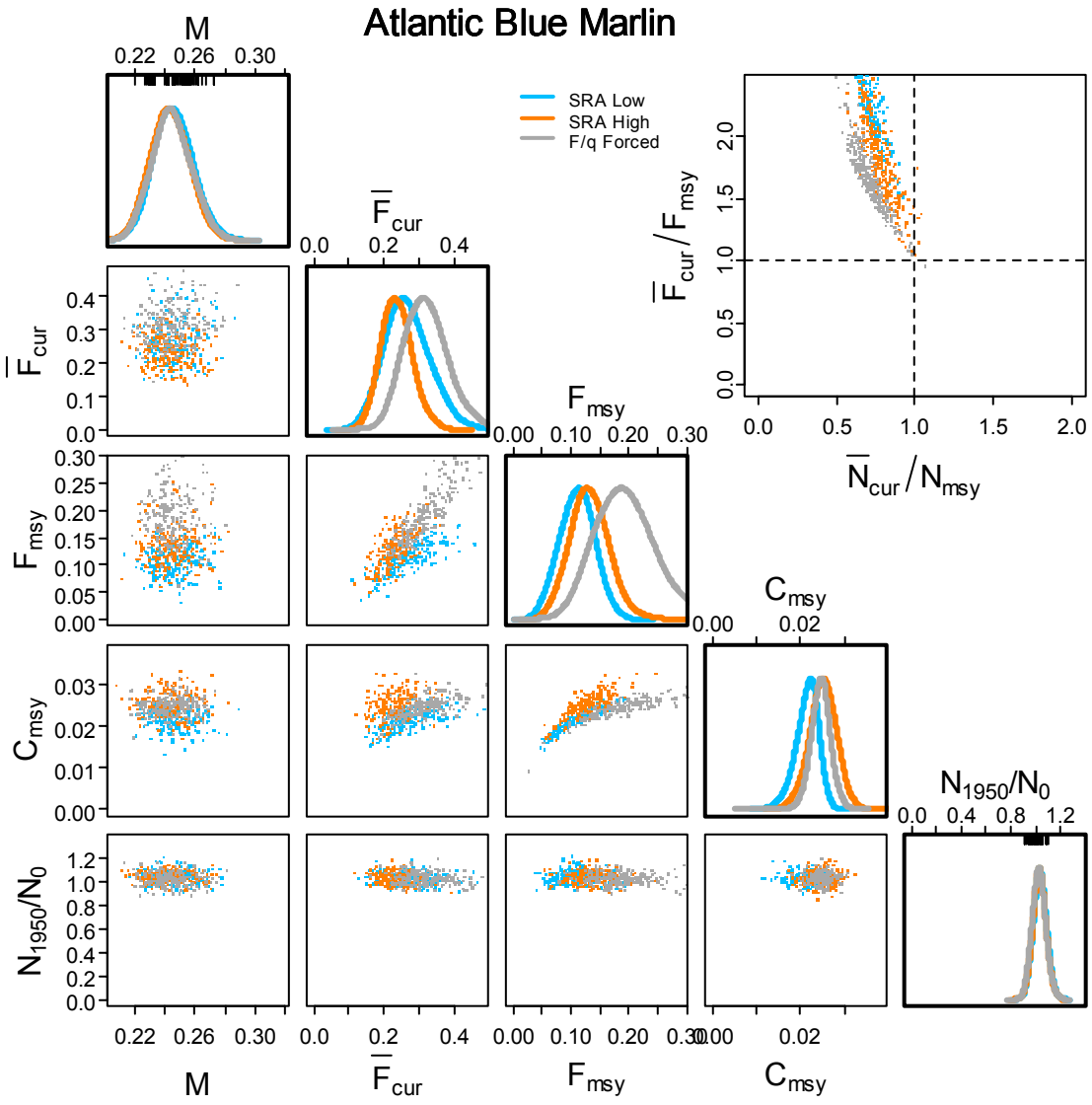

Figure 10.46 Atlantic Ocean blue marlin leading parameter joint distribution (lower triangular), marginal posterior distributions (diagonal) and biological reference points (upper triangular) for natural mortality (M), current fishing mortality (F_{cur}), fishing mortality that produced MSY (F_{msy}), MSY (C_{msy}) and the ratio of population in 1950 to that expected in the absence of fishing. Biological reference points in the top right corner are the ratio of current fishing mortality to the fishing mortality that produces MSY, and the ratio of current stock size to the stock size that produces MSY. Filled circles outside the upper triangular plot indicate ratios greater than 5. Blue lines and points are from SRA where variance in recruitment anomalies was assumed low. Orange lines and points are from SRA where variance in recruitment anomalies was assumed high. Light grey lines and points are from the relative fishing mortality rate forced numbers dynamic model. Rug plots on the top of distributions on the diagonal demark prior distributions.

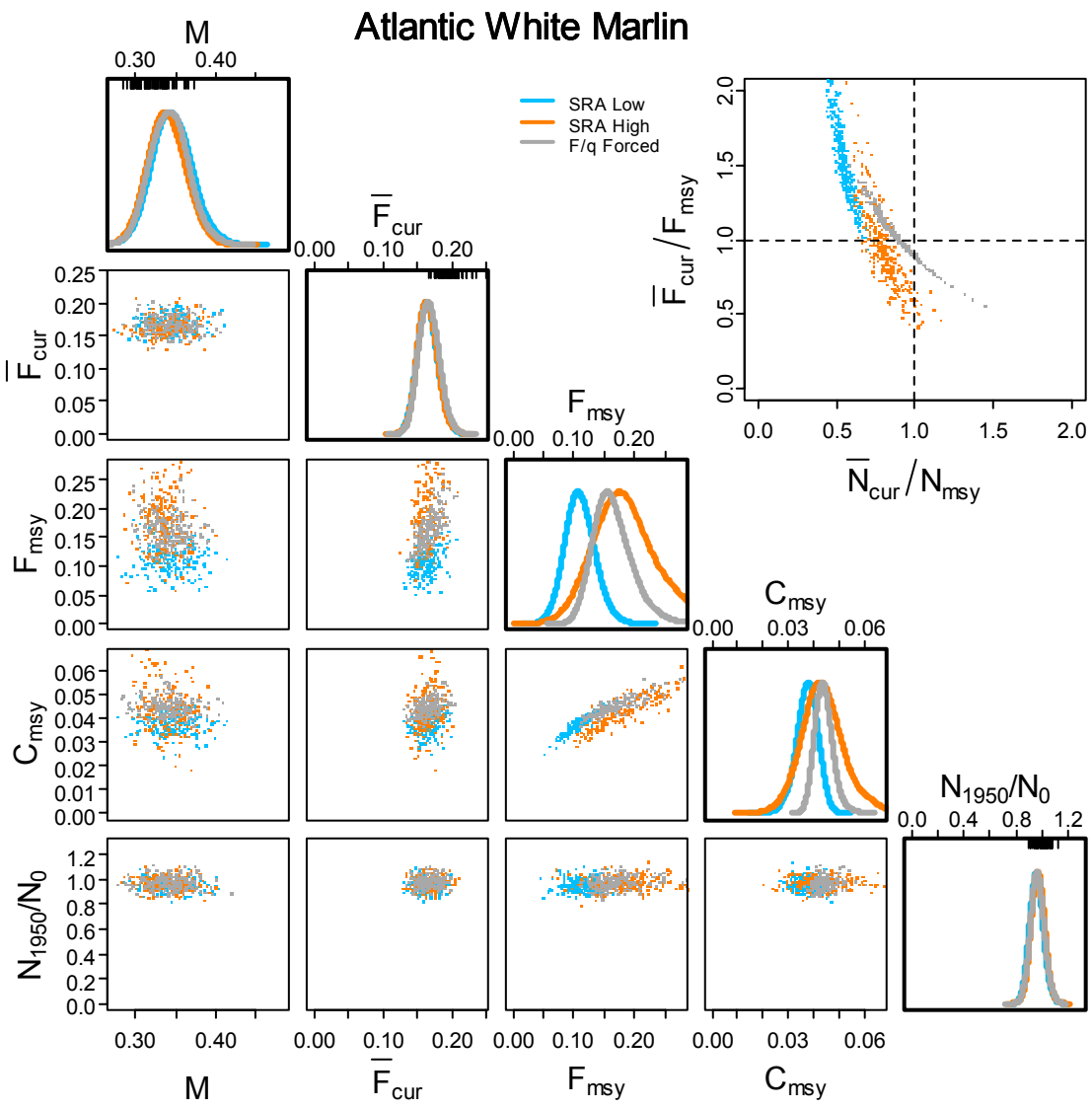

Figure 10.47 Atlantic Ocean white marlin leading parameter joint distribution (lower triangular), marginal posterior distributions (diagonal) and biological reference points (upper triangular) for natural mortality (M), current fishing mortality (F_{cur}), fishing mortality that produced MSY (F_{msy}), MSY (C_{msy}) and the ratio of population in 1950 to that expected in the absence of fishing. Biological reference points in the top right corner are the ratio of current fishing mortality to the fishing mortality that produces MSY, and the ratio of current stock size to the stock size that produces MSY. Filled circles outside the upper triangular plot indicate ratios greater than 5. Blue lines and points are from SRA where variance in recruitment anomalies was assumed low. Orange lines and points are from SRA where variance in recruitment anomalies was assumed high. Light grey lines and points are from the relative fishing mortality rate forced numbers dynamic model. Rug plots on the top of distributions on the diagonal demark prior distributions.

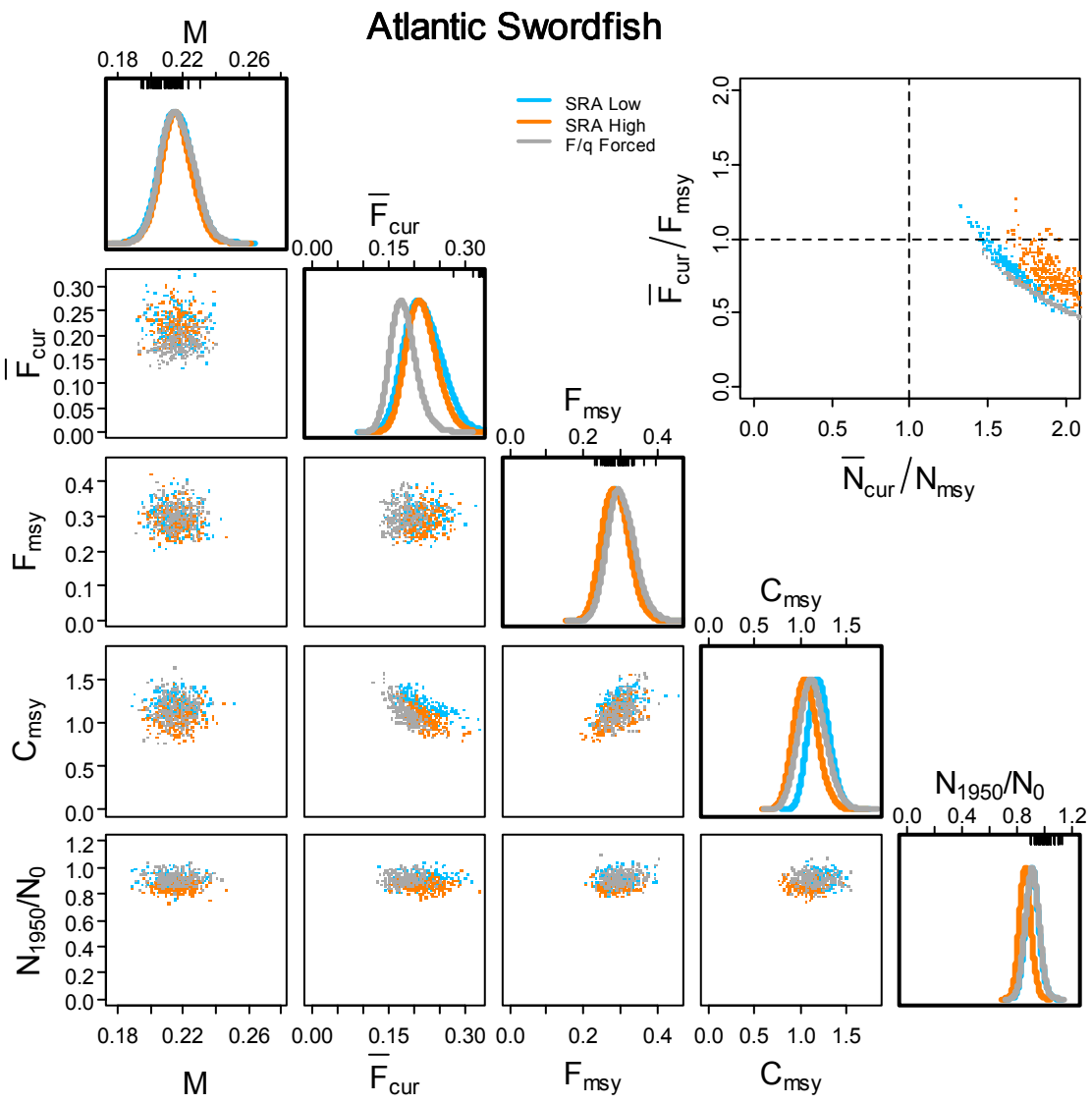

Figure 10.48 Atlantic Ocean swordfish leading parameter joint distribution (lower triangular), marginal posterior distributions (diagonal) and biological reference points (upper triangular) for natural mortality (M), current fishing mortality (F_{cur}), fishing mortality that produced MSY (F_{msy}), MSY (C_{msy}) and the ratio of population in 1950 to that expected in the absence of fishing. Biological reference points in the top right corner are the ratio of current fishing mortality to the fishing mortality that produces MSY, and the ratio of current stock size to the stock size that produces MSY. Filled circles outside the upper triangular plot indicate ratios greater than 5. Blue lines and points are from SRA where variance in recruitment anomalies was assumed low. Orange lines and points are from SRA where variance in recruitment anomalies was assumed high. Light grey lines and points are from the relative fishing mortality rate forced numbers dynamic model. Rug plots on the top of distributions on the diagonal demark prior distributions.

Appendix for Chapter 5

Table 11.1 Leading parameter MLE values and 95% credible interval for various initial movement rates, from fitting the spatial model to catch data. See Table 4.1 for prior distributions.

Stock	Movement	M	Fcur	Fmsy	MSY	N1950/N0
IALB	**v=0.7**	0.27(0.24-0.3)	1.31(0.74-2.3)	0.44(0.31-0.62)	1.48(1.21-1.79)	1.09(0.99-1.21)
	v=2	0.27(0.24-0.29)	0.91(0.7-1.16)	0.38(0.29-0.51)	1.4(1.18-1.66)	0.98(0.89-1.08)
	v=5	0.27(0.24-0.3)	0.71(0.55-0.91)	0.39(0.29-0.51)	1.46(1.21-1.77)	0.98(0.89-1.09)
	v=10	0.26(0.24-0.29)	0.7(0.54-0.88)	0.39(0.3-0.52)	1.44(1.19-1.73)	0.98(0.89-1.08)
IBET	**v=0.7**	0.4(0.34-0.47)	0.29(0.23-0.36)	0.53(0.33-0.89)	2.95(2.1-4.17)	1(0.9-1.1)
	v=2	0.4(0.34-0.46)	0.29(0.23-0.36)	0.53(0.33-0.87)	2.97(2.16-4.07)	1(0.91-1.11)
	v=5	0.4(0.34-0.47)	0.29(0.23-0.37)	0.53(0.33-0.9)	2.97(2.08-4.31)	1(0.91-1.11)
	v=10	0.4(0.34-0.47)	0.29(0.23-0.37)	0.53(0.32-0.87)	2.96(2.02-4.25)	1(0.9-1.1)
IYFT	**v=0.7**	0.64(0.49-0.86)	0.77(0.51-1.14)	0.81(0.4-1.72)	5.62(3.66-8.67)	1.03(0.93-1.14)
	v=2	0.65(0.46-0.95)	0.74(0.49-1.09)	0.77(0.37-1.62)	5.57(3.6-8.55)	1.01(0.91-1.12)
	v=5	0.67(0.5-0.88)	0.76(0.51-1.17)	0.78(0.38-1.58)	5.45(3.6-8.37)	1(0.91-1.11)
	v=10	0.7(0.53-0.93)	0.82(0.54-1.24)	1.04(0.47-2.34)	6.26(3.94-10.21)	1(0.9-1.1)
GSBT	**v=0.7**	0.1(0.1-0.1)	0.11(0.07-0.18)	0.01(0-0.08)	0.1(0.02-0.45)	1(0.91-1.11)
	v=2	0.1(0.1-0.1)	0.1(0.06-0.14)	0.02(0-0.05)	0.11(0.04-0.29)	1.04(0.94-1.14)
	v=5	0.1(0.1-0.1)	0.13(0-8.17)	0.04(0-97.71)	0.18(0.01-5.58)	0.97(0.73-1.31)
	v=10	0.1(0.1-0.1)	0.13(0.07-0.24)	0.04(0.01-0.18)	0.19(0.07-0.48)	0.97(0.87-1.09)
IBUM	**v=0.7**	0.25(0.23-0.27)	0.21(0.18-0.25)	0.33(0.25-0.43)	0.17(0.13-0.22)	1.03(0.93-1.13)
	v=2	0.25(0.22-0.27)	0.21(0.18-0.25)	0.33(0.25-0.44)	0.18(0.14-0.23)	1.02(0.93-1.13)
	v=5	0.24(0.22-0.27)	0.21(0.18-0.25)	0.33(0.26-0.43)	0.18(0.14-0.24)	1.03(0.94-1.13)
	v=10	0.25(0.22-0.27)	0.21(0.17-0.24)	0.33(0.26-0.43)	0.19(0.14-0.25)	1.02(0.93-1.13)
ISTM	**v=0.7**	0.51(0.42-0.62)	0.71(0.43-1.19)	0.32(0.15-0.75)	0.07(0.06-0.09)	0.99(0.9-1.09)
	v=2	0.49(0.41-0.6)	0.52(0.27-1.01)	0.18(0.07-0.47)	0.06(0.04-0.09)	1(0.9-1.1)
	v=5	0.5(0.41-0.6)	1.04(0.68-1.58)	0.46(0.24-0.89)	0.07(0.06-0.09)	0.99(0.9-1.1)
	v=10	0.54(0.44-0.65)	0.8(0.54-1.18)	0.34(0.17-0.65)	0.07(0.06-0.09)	0.99(0.89-1.09)
GBLM	**v=0.7**	0.15(0.14-0.16)	0.72(0.5-1)	0.15(0.1-0.22)	0.04(0.04-0.05)	1.01(0.91-1.11)
	v=2	0.15(0.14-0.16)	0.66(0.47-0.96)	0.12(0.08-0.19)	0.04(0.03-0.04)	1.01(0.92-1.11)
	v=5	0.15(0.14-0.16)	0.8(0.59-1.11)	0.13(0.09-0.19)	0.04(0.04-0.04)	1.01(0.92-1.12)
	v=10	0.15(0.14-0.16)	0.7(0.44-1.11)	0.13(0.07-0.23)	0.04(0.03-0.05)	1.01(0.92-1.12)
ISWO	**v=0.7**	0.21(0.19-0.23)	0.21(0.16-0.26)	0.36(0.28-0.45)	0.33(0.25-0.42)	1(0.91-1.1)
	v=2	0.21(0.19-0.23)	0.21(0.17-0.26)	0.36(0.29-0.46)	0.33(0.26-0.42)	1(0.91-1.1)
	v=5	0.21(0.19-0.23)	0.21(0.17-0.26)	0.36(0.29-0.46)	0.33(0.26-0.42)	1(0.91-1.1)
	v=10	0.21(0.19-0.23)	0.21(0.17-0.26)	0.36(0.28-0.45)	0.33(0.25-0.42)	1(0.91-1.1)
PNAB		**Insufficient spatial data**				
PSAB	**v=0.7**	0.27(0.24-0.3)	0.29(0.24-0.34)	0.29(0.13-0.61)	1.99(1.36-2.89)	1(0.91-1.1)
	v=2	0.27(0.24-0.3)	0.29(0.24-0.34)	0.27(0.07-1.32)	1.95(0.98-4.24)	1(0.91-1.1)
	v=5	0.27(0.24-0.3)	0.29(0.24-0.34)	0.28(0.03-2.33)	1.98(0.72-5.43)	1(0.91-1.1)
	v=10	0.27(0.24-0.3)	0.29(0.24-0.34)	0.28(0.03-2.55)	1.94(0.72-5.48)	1(0.91-1.1)
PBET	**v=0.7**	0.4(0.34-0.47)	0.39(0.28-0.54)	0.39(0.17-0.84)	2.88(2.12-3.92)	1(0.91-1.09)
	v=2	0.4(0.35-0.47)	0.4(0.31-0.51)	0.49(0.26-0.89)	3.06(2.41-3.96)	1.01(0.92-1.1)
	v=5	0.4(0.34-0.46)	0.64(0.5-0.81)	0.81(0.45-1.43)	3.07(2.5-3.72)	0.98(0.9-1.09)
	v=10	0.4(0.34-0.47)	0.48(0.35-0.65)	0.37(0.2-0.64)	2.54(2.05-3.11)	1.03(0.93-1.13)
PYFT	**v=0.7**	0.64(0.5-0.83)	0.4(0.31-0.51)	0.63(0.25-1.62)	15.38(10.25-23.91)	0.99(0.9-1.09)
	v=2	0.66(0.51-0.86)	0.43(0.33-0.57)	0.58(0.26-1.32)	12.67(9.19-17.96)	1.03(0.94-1.13)
	v=5	0.69(0.55-0.89)	0.42(0.33-0.54)	0.48(0.25-0.92)	11.05(8.2-14.93)	1.01(0.92-1.12)
	v=10	0.67(0.53-0.87)	0.42(0.33-0.55)	0.46(0.24-0.88)	10.71(7.95-14.12)	1.01(0.91-1.12)
PBFT		**Insufficient spatial data**				

Continued next page

Stock	Movement	M	Fcur	Fmsy	MSY	N1950/N0
PBUM	**v=0.7**	0.24(0.22-0.27)	0.1(0.1-0.11)	0.05(0.03-0.1)	0.08(0.06-0.12)	1.04(0.94-1.15)
	v=2	0.25(0.22-0.27)	0.1(0.09-0.11)	0.04(0.02-0.08)	0.06(0.04-0.12)	1.03(0.93-1.15)
	v=5	0.24(0.22-0.27)	0.1(0.09-0.11)	0.05(0.02-0.12)	0.07(0.04-0.14)	0.98(0.9-1.09)
	v=10	0.25(0.23-0.28)	0.1(0.09-0.11)	0.03(0.01-0.09)	0.05(0.02-0.14)	1.02(0.92-1.12)
PSTM	**v=0.7**	0.5(0.41-0.6)	0.09(0.06-0.13)	0.16(0.11-0.24)	0.17(0.15-0.2)	1(0.91-1.11)
	v=2	0.5(0.41-0.61)	0.09(0.03-0.31)	0.16(0.05-0.5)	0.17(0.13-0.23)	1(0.91-1.1)
	v=5	0.5(0.41-0.61)	0.09(0.03-0.3)	0.16(0.05-0.49)	0.17(0.13-0.22)	1(0.91-1.1)
	v=10	0.5(0.41-0.62)	0.06(0-2.67)	0.11(0-39.46)	0.13(0.02-1.06)	1(0.85-1.18)
PSWO		**Insufficient spatial data**				
ANAB	**v=0.7**	0.25(0.23-0.28)	0.67(0.48-0.93)	0.34(0.25-0.45)	2.45(1.89-3.28)	2.82(1.17-7.11)
	v=2	0.26(0.23-0.29)	0.62(0.47-0.85)	0.35(0.26-0.48)	2.46(1.85-3.34)	1.55(0.66-3.81)
	v=5	0.27(0.24-0.3)	0.87(0.61-1.23)	0.23(0.17-0.3)	1.23(0.77-1.94)	1.02(0.31-3.16)
	v=10	0.27(0.24-0.3)	0.87(0.61-1.24)	0.23(0.17-0.3)	1.23(0.83-1.82)	1.02(0.25-3.94)
ASAB	**v=0.7**	0.27(0.24-0.3)	0.59(0.36-0.99)	0.54(0.16-1.78)	1.32(0.96-1.79)	1(0.92-1.1)
	v=2	0.28(0.25-0.31)	0.56(0.41-0.73)	0.55(0.25-1.16)	1.24(0.98-1.56)	0.99(0.89-1.09)
	v=5	0.28(0.25-0.31)	0.51(0.3-0.88)	0.52(0.11-2.33)	1.27(0.85-1.9)	1.02(0.92-1.13)
	v=10	0.28(0.25-0.31)	0.38(0.17-0.79)	0.3(0.09-0.99)	1.07(0.82-1.42)	1.05(0.95-1.16)
ABET	**v=0.7**	0.4(0.34-0.47)	0.16(0.14-0.18)	0.85(0.46-1.5)	3.12(2.23-4.24)	1(0.91-1.1)
	v=2	0.4(0.34-0.47)	0.16(0.14-0.18)	0.85(0.48-1.52)	3.16(2.28-4.24)	1(0.91-1.1)
	v=5	0.4(0.33-0.48)	0.16(0.14-0.18)	0.84(0.46-1.5)	3.14(2.32-4.25)	1(0.9-1.1)
	v=10	0.4(0.33-0.48)	0.16(0.14-0.18)	0.85(0.48-1.56)	3.14(2.32-4.27)	1(0.9-1.11)
AYFT	**v=0.7**	0.68(0.52-0.91)	0.5(0.34-0.74)	0.8(0.37-1.64)	2.52(0.97-6.74)	1(0.91-1.1)
	v=2	0.68(0.53-0.91)	0.5(0.34-0.75)	0.82(0.37-1.71)	2.55(1-6.51)	1(0.91-1.1)
	v=5	0.68(0.51-0.89)	0.5(0.34-0.75)	0.79(0.38-1.7)	2.62(1.01-6.83)	1(0.91-1.1)
	v=10	0.68(0.52-0.9)	0.51(0.34-0.75)	0.78(0.37-1.66)	2.94(1.14-7.37)	1(0.91-1.1)
ABFT	**v=0.7**	0.15(0.14-0.16)	0.18(0.16-0.21)	0.21(0.17-0.24)	0.17(0.15-0.2)	0.57(0.35-0.96)
	v=2	0.15(0.14-0.16)	0.18(0.15-0.21)	0.2(0.18-0.24)	0.17(0.15-0.2)	0.47(0.29-0.79)
	v=5	0.15(0.14-0.16)	0.17(0.15-0.2)	0.21(0.17-0.24)	0.19(0.16-0.22)	0.4(0.24-0.65)
	v=10	0.15(0.14-0.16)	0.17(0.15-0.2)	0.21(0.17-0.24)	0.19(0.16-0.22)	0.47(0.28-0.79)
ABUM	**v=0.7**	0.25(0.23-0.27)	0.21(0.18-0.25)	0.33(0.25-0.43)	0.17(0.13-0.22)	1.03(0.93-1.13)
	v=2	0.25(0.22-0.27)	0.21(0.18-0.25)	0.33(0.25-0.44)	0.18(0.14-0.23)	1.02(0.93-1.13)
	v=5	0.24(0.22-0.27)	0.21(0.18-0.25)	0.33(0.26-0.43)	0.18(0.14-0.24)	1.03(0.94-1.13)
	v=10	0.25(0.22-0.27)	0.21(0.17-0.24)	0.33(0.26-0.43)	0.19(0.14-0.25)	1.02(0.93-1.13)
AWHM	**v=0.7**	0.25(0.23-0.27)	0.26(0.11-0.63)	0.24(0.08-0.74)	0.03(0.02-0.04)	1(0.91-1.1)
	v=2	0.25(0.22-0.27)	0.37(0.19-0.74)	0.29(0.12-0.74)	0.03(0.02-0.04)	1(0.91-1.11)
	v=5	0.25(0.22-0.27)	0.43(0.16-1.24)	0.31(0.09-1)	0.03(0.02-0.03)	1.01(0.91-1.11)
	v=10	0.25(0.23-0.28)	0.48(0.28-0.83)	0.33(0.17-0.68)	0.03(0.02-0.03)	1.01(0.91-1.11)
ASWO	**v=0.7**	0.32(0.28-0.36)	0.17(0.14-0.19)	0.16(0.06-0.37)	0.05(0.03-0.06)	1(0.9-1.1)
	v=2	0.32(0.28-0.36)	0.17(0.14-0.2)	0.16(0.07-0.33)	0.05(0.03-0.06)	1(0.9-1.1)
	v=5	0.32(0.28-0.36)	0.17(0.14-0.2)	0.16(0.08-0.3)	0.05(0.03-0.06)	1(0.91-1.11)
	v=10	0.32(0.28-0.36)	0.17(0.14-0.2)	0.16(0.08-0.29)	0.05(0.03-0.06)	1(0.9-1.1)

Table 11.2 Biological reference points estimated by fitting the spatial model to catch data, given various base mixing rates *v*.

Stock	Movement	Fcur/Fmsy	Ncur/Nmsy
IALB	**v=0.7**	3.02(1.93-4.59)	0.61(0.39-0.95)
	v=2	2.36(1.71-3.33)	0.7(0.5-0.98)
	v=5	1.83(1.32-2.54)	0.78(0.54-1.09)
	v=10	1.77(1.31-2.43)	0.66(0.45-0.99)
IBET	**v=0.7**	0.53(0.31-0.91)	1.62(1.22-2.15)
	v=2	0.54(0.33-0.91)	1.68(1.28-2.2)
	v=5	0.54(0.3-0.96)	1.47(1.04-2.03)
	v=10	0.55(0.32-0.96)	1.48(1.07-2.02)
IYFT	**v=0.7**	0.93(0.46-1.96)	1.28(0.76-2.08)
	v=2	0.97(0.48-1.9)	1.1(0.65-1.88)
	v=5	0.97(0.48-1.91)	1.02(0.57-1.86)
	v=10	0.77(0.35-1.74)	1.27(0.66-2.42)
GSBT	**v=0.7**	9.27(2.02-44.21)	0.33(0.24-0.47)
	v=2	6.05(2.21-17.07)	0.47(0.28-0.79)
	v=5	3.6(0.08-123.4)	0.46(0.06-3.18)
	v=10	3.62(1.23-11.23)	0.38(0.22-0.65)
IBUM	**v=0.7**	0.64(0.47-0.88)	2.11(1.81-2.46)
	v=2	0.65(0.47-0.87)	2.02(1.73-2.37)
	v=5	0.63(0.46-0.87)	2.03(1.72-2.4)
	v=10	0.61(0.45-0.84)	1.97(1.66-2.34)
ISTM	**v=0.7**	2.18(1.41-3.32)	0.88(0.56-1.42)
	v=2	2.96(1.86-4.58)	0.64(0.41-1.04)
	v=5	2.26(1.53-3.35)	0.87(0.5-1.57)
	v=10	2.36(1.56-3.66)	0.64(0.29-1.38)
GBLM	**v=0.7**	4.75(3.86-5.86)	0.95(0.75-1.19)
	v=2	5.64(4.56-6.86)	0.6(0.45-0.81)
	v=5	5.99(5.05-7.09)	0.49(0.33-0.72)
	v=10	5.5(4.5-6.76)	0.39(0.2-0.75)
ISWO	**v=0.7**	0.58(0.42-0.8)	2.1(1.8-2.45)
	v=2	0.58(0.42-0.8)	2(1.69-2.34)
	v=5	0.58(0.42-0.81)	1.97(1.66-2.35)
	v=10	0.58(0.42-0.8)	2.03(1.68-2.43)
PNAB		**Insufficient spatial data**	
PSAB	**v=0.7**	0.99(0.47-2.08)	1.18(0.69-2)
	v=2	0.98(0.23-3.93)	1.11(0.38-3.34)
	v=5	1.08(0.13-8.72)	0.95(0.17-5.52)
	v=10	1.04(0.11-8.14)	0.94(0.14-7.25)
PBET	**v=0.7**	1.02(0.62-1.75)	1.18(0.82-1.67)
	v=2	0.82(0.52-1.31)	1.34(0.98-1.83)
	v=5	0.79(0.49-1.25)	1.34(0.93-1.93)
	v=10	1.3(0.92-1.86)	0.86(0.65-1.12)
PYFT	**v=0.7**	0.63(0.31-1.4)	1.68(1.06-2.55)
	v=2	0.71(0.39-1.38)	1.4(0.91-2.05)
	v=5	0.89(0.55-1.48)	1.12(0.79-1.56)
	v=10	0.91(0.55-1.55)	1.09(0.75-1.54)
PBFT		**Insufficient spatial data**	

continued on next page

Stock	Movement	Fcur/Fmsy	Ncur/Nmsy
PBUM	**v=0.7**	1.86(1.08-3.19)	0.61(0.43-0.86)
	v=2	2.69(1.34-5.22)	0.53(0.37-0.77)
	v=5	1.96(0.88-4.48)	0.64(0.38-1.02)
	v=10	3.86(1.17-13.53)	0.48(0.29-0.76)
PSTM	**v=0.7**	0.57(0.46-0.71)	0.88(0.7-1.13)
	v=2	0.57(0.43-0.74)	0.8(0.58-1.1)
	v=5	0.57(0.42-0.78)	0.81(0.5-1.29)
	v=10	0.52(0.07-4.89)	0.8(0.49-1.31)
PSWO		**Insufficient spatial data**	
ANAB	**v=0.7**	1.99(1.31-3.12)	1.89(1.58-2.26)
	v=2	1.78(1.18-2.69)	2(1.62-2.43)
	v=5	3.86(2.42-6.03)	1.17(0.68-2)
	v=10	3.79(2.41-6.11)	0.94(0.4-2.24)
ASAB	**v=0.7**	1.09(0.46-2.54)	1.51(0.75-3.07)
	v=2	1.03(0.55-1.94)	1.3(0.74-2.25)
	v=5	1.02(0.35-2.96)	1.27(0.51-3.19)
	v=10	1.25(0.7-2.25)	0.86(0.53-1.36)
ABET	**v=0.7**	0.19(0.1-0.34)	2.48(1.73-3.56)
	v=2	0.19(0.1-0.34)	2.38(1.65-3.43)
	v=5	0.19(0.11-0.36)	2.53(1.72-3.52)
	v=10	0.19(0.1-0.35)	2.52(1.73-3.55)
AYFT	**v=0.7**	0.62(0.26-1.48)	1.14(0.54-2.41)
	v=2	0.63(0.26-1.45)	0.93(0.4-2.24)
	v=5	0.62(0.27-1.52)	0.89(0.26-2.82)
	v=10	0.64(0.27-1.49)	0.97(0.38-2.63)
ABFT	**v=0.7**	0.88(0.71-1.11)	1.66(1.48-1.86)
	v=2	0.86(0.7-1.07)	1.63(1.45-1.83)
	v=5	0.83(0.66-1.02)	1.68(1.48-1.91)
	v=10	0.84(0.68-1.04)	1.7(1.52-1.91)
ABUM	**v=0.7**	1.11(0.64-1.9)	1.24(0.84-1.84)
	v=2	1.26(0.8-2.03)	1.08(0.73-1.58)
	v=5	1.39(0.96-2.02)	0.86(0.53-1.34)
	v=10	1.43(0.98-2.08)	0.73(0.46-1.17)
AWHM	**v=0.7**	1.07(0.45-2.54)	0.83(0.31-2.24)
	v=2	1.06(0.51-2.13)	0.74(0.31-1.87)
	v=5	1.05(0.54-2.07)	0.65(0.22-1.96)
	v=10	1.07(0.56-2.01)	0.51(0.12-2.22)
ASWO	**v=0.7**	1.12(0.82-1.5)	2.2(1.94-2.51)
	v=2	0.99(0.69-1.42)	2.39(2.07-2.76)
	v=5	1.94(1.07-3.62)	2.04(1.5-2.76)
	v=10	1.87(1.32-2.63)	1.85(1.56-2.2)

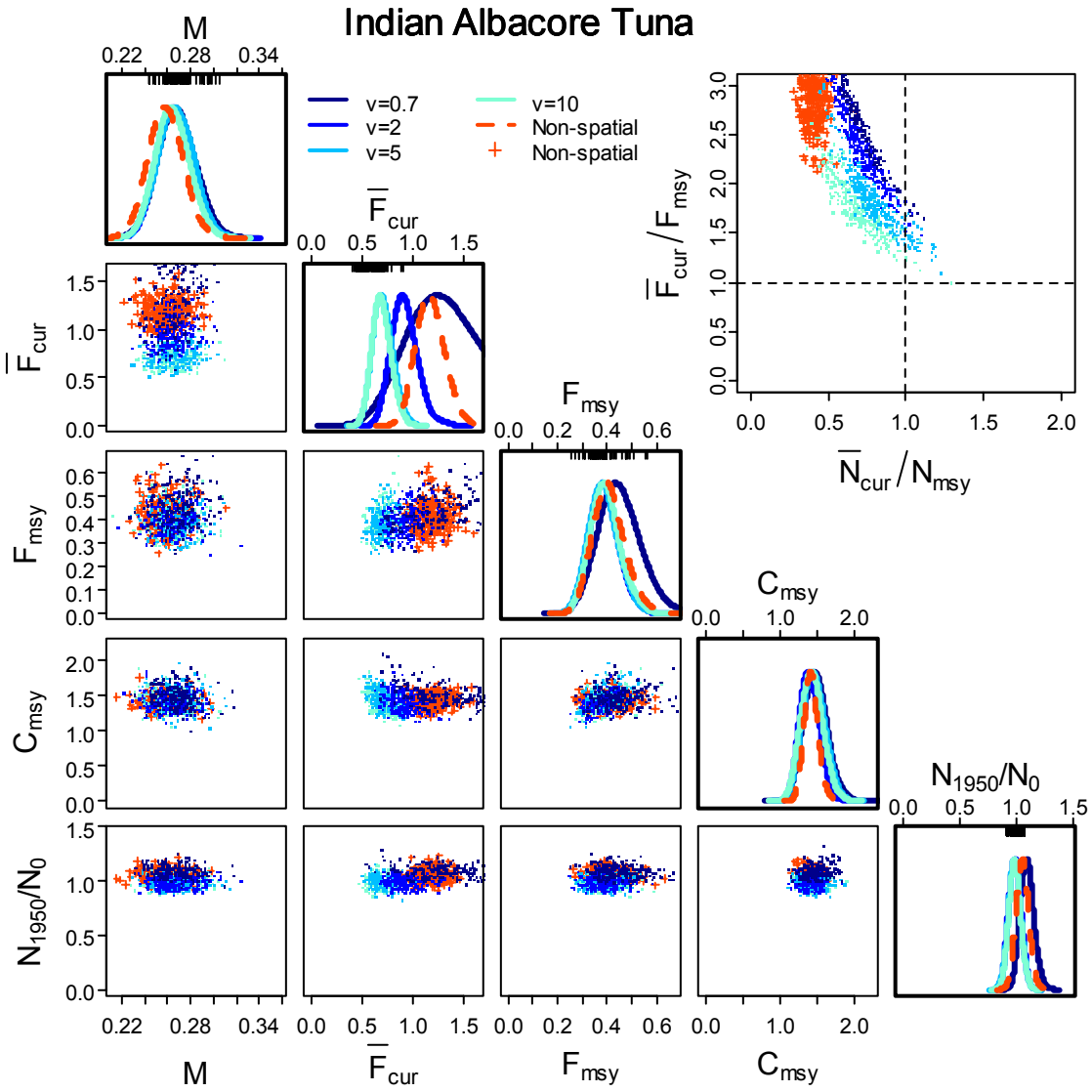

Figure 11.1 Indian Ocean albacore tuna leading parameter joint distribution (lower triangular), marginal posterior distributions (diagonal) and biological reference points (upper triangular) for natural mortality (M), current fishing mortality (F_{cur}), fishing mortality that produced MSY (F_{msy}), MSY (C_{msy}) and the ratio of population in 1950 to that expected in the absence of fishing from fitting the spatial model to catch data. Biological reference points in the top right corner are the ratio of current fishing mortality to the fishing mortality that produces MSY, and the ratio of current stock size to the stock size that produces MSY. Filled circles outside the upper triangular plot indicate ratios greater than 5. Blue lines and points are from spatial model runs under different intial movement rates. Dark orange lines are from the relative fishing mortality rate forced numbers dynamic model. Rug plots on the top of distributions on the diagonal demark prior distributions.

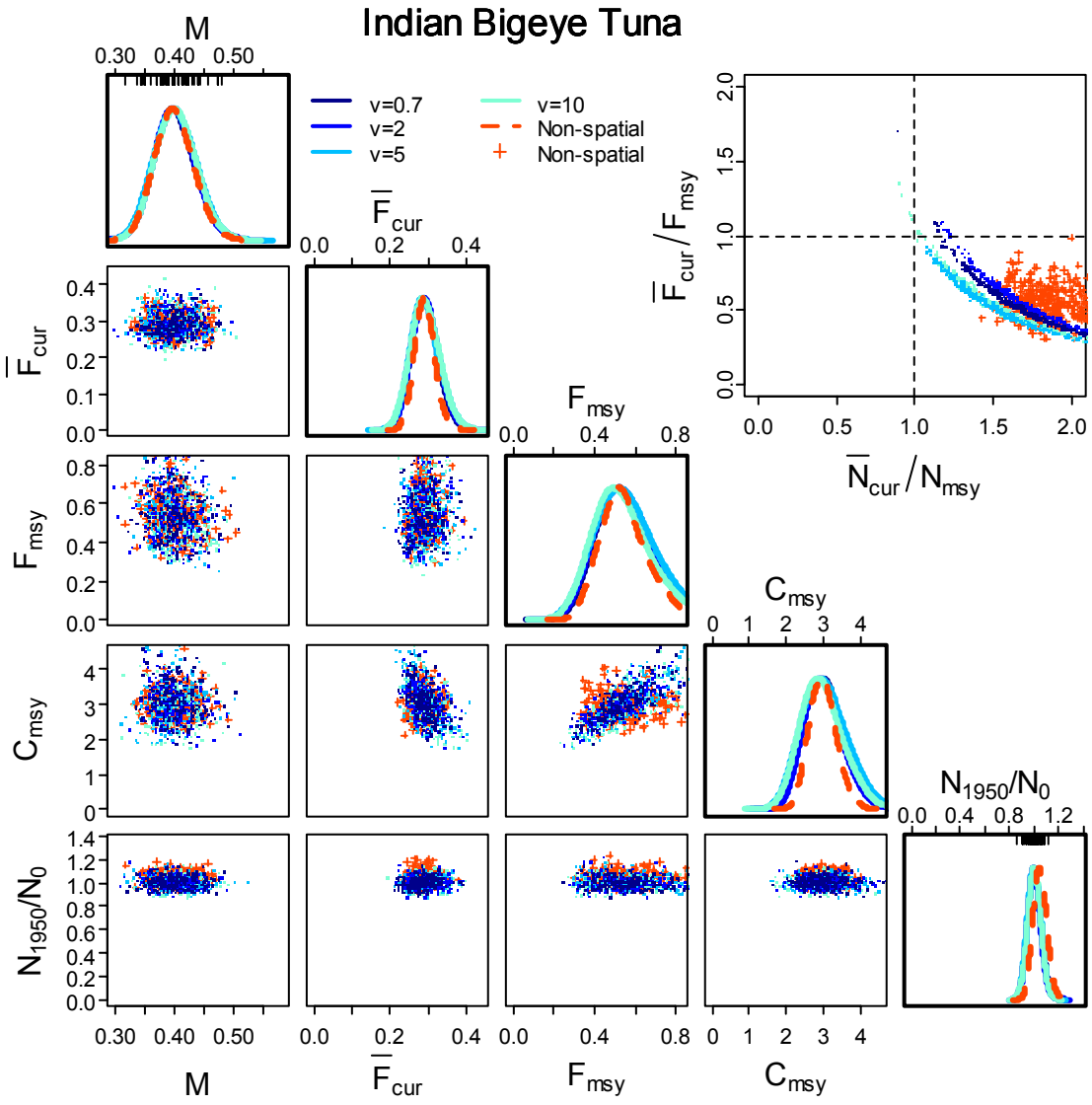

Figure 11.2 Indian Ocean bigeye tuna leading parameter joint distribution (lower triangular), marginal posterior distributions (diagonal) and biological reference points (upper triangular) for natural mortality (M), current fishing mortality (F_{cur}), fishing mortality that produced MSY (F_{msy}), MSY (C_{msy}) and the ratio of population in 1950 to that expected in the absence of fishing from fitting the spatial model to catch data. Biological reference points in the top right corner are the ratio of current fishing mortality to the fishing mortality that produces MSY, and the ratio of current stock size to the stock size that produces MSY. Filled circles outside the upper triangular plot indicate ratios greater than 5. Blue lines and points are from spatial model runs under different intial movement rates. Dark orange lines are from the relative fishing mortality rate forced numbers dynamic model. Rug plots on the top of distributions on the diagonal demark prior distributions.

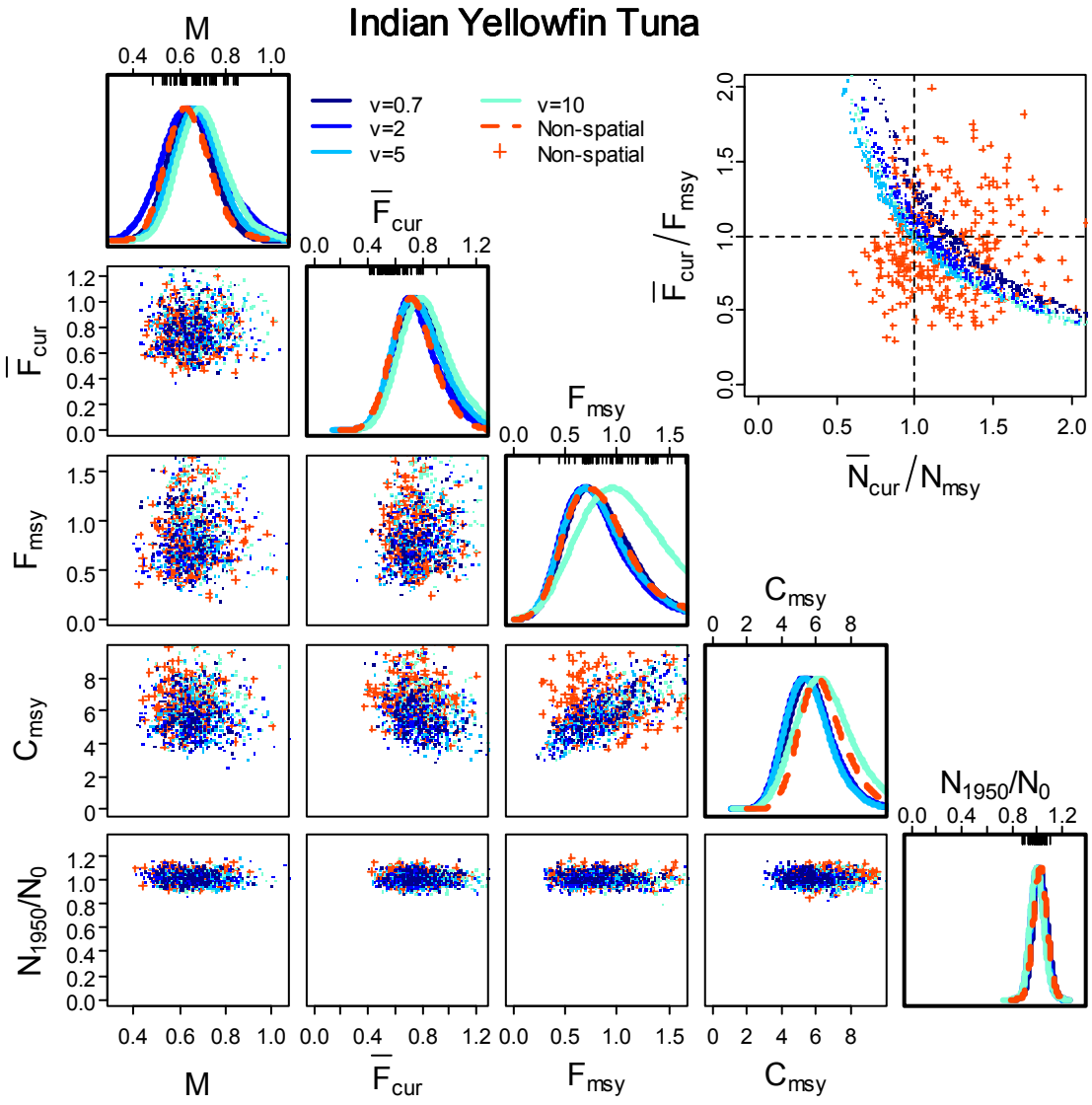

Figure 11.3 Indian Ocean yellowfin tuna leading parameter joint distribution (lower triangular), marginal posterior distributions (diagonal) and biological reference points (upper triangular) for natural mortality (M), current fishing mortality (F_{cur}), fishing mortality that produced MSY (F_{msy}), MSY (C_{msy}) and the ratio of population in 1950 to that expected in the absence of fishing from fitting the spatial model to catch data. Biological reference points in the top right corner are the ratio of current fishing mortality to the fishing mortality that produces MSY, and the ratio of current stock size to the stock size that produces MSY. Filled circles outside the upper triangular plot indicate ratios greater than 5. Blue lines and points are from spatial model runs under different intial movement rates. Dark orange lines are from the relative fishing mortality rate forced numbers dynamic model. Rug plots on the top of distributions on the diagonal demark prior distributions.

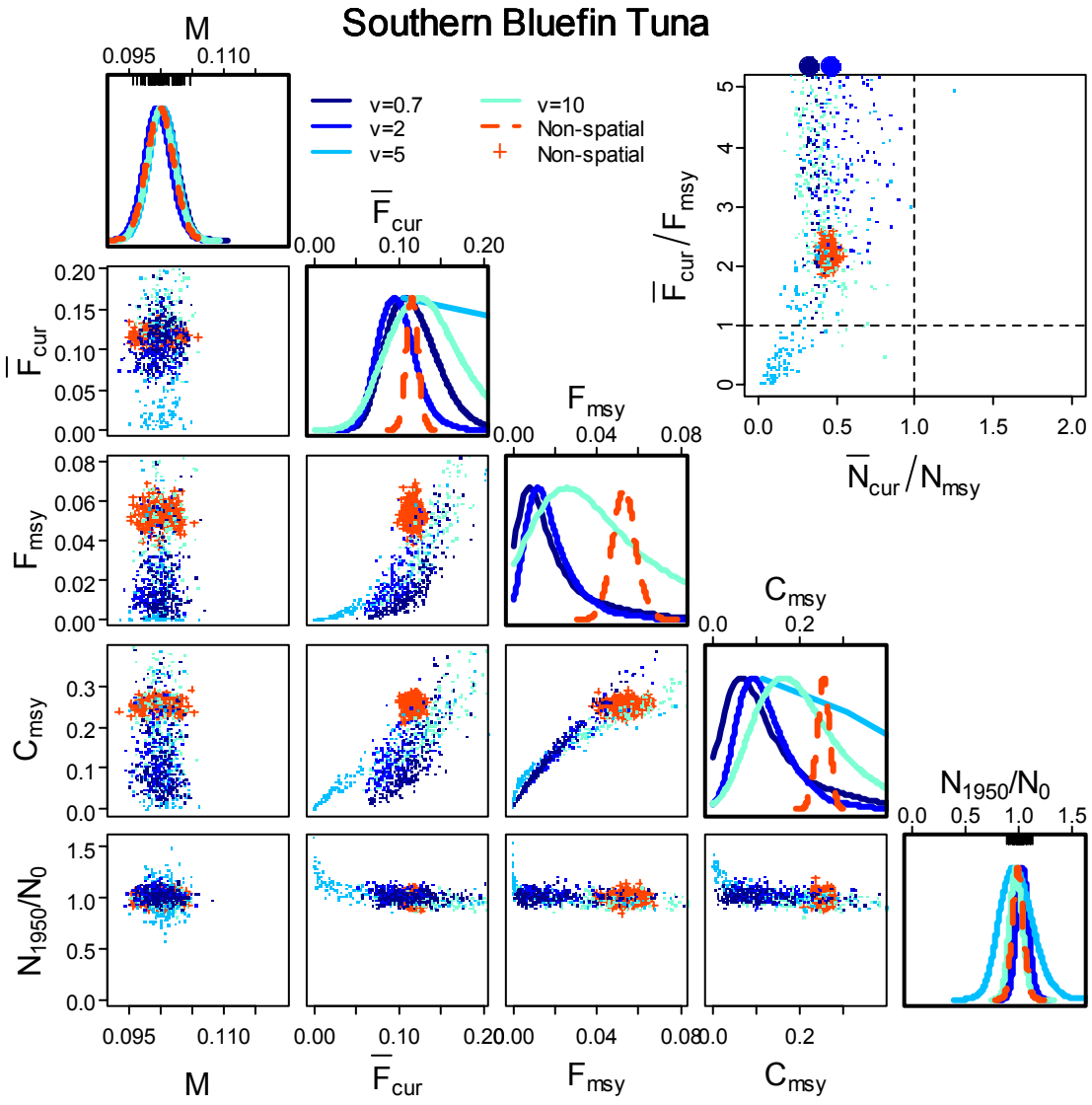

Figure 11.4 Southern bluefin tuna leading parameter joint distribution (lower triangular), marginal posterior distributions (diagonal) and biological reference points (upper triangular) for natural mortality (M), current fishing mortality (F_{cur}), fishing mortality that produced MSY (F_{msy}), MSY (C_{msy}) and the ratio of population in 1950 to that expected in the absence of fishing from fitting the spatial model to catch data. Biological reference points in the top right corner are the ratio of current fishing mortality to the fishing mortality that produces MSY, and the ratio of current stock size to the stock size that produces MSY. Filled circles outside the upper triangular plot indicate ratios greater than 5. Blue lines and points are from spatial model runs under different intial movement rates. Dark orange lines are from the relative fishing mortality rate forced numbers dynamic model. Rug plots on the top of distributions on the diagonal demark prior distributions.

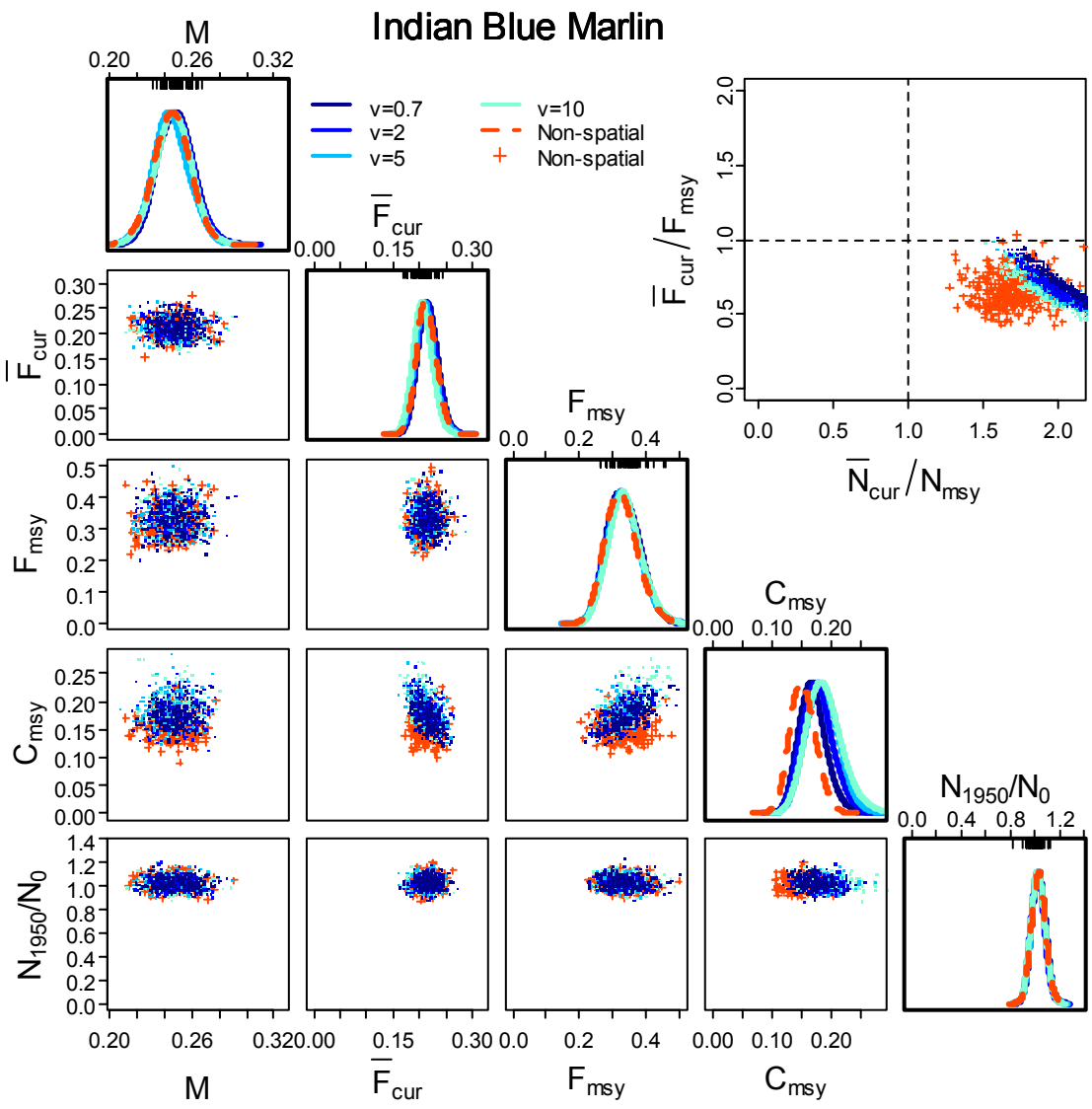

Figure 11.5 Indian Ocean blue marlin leading parameter joint distribution (lower triangular), marginal posterior distributions (diagonal) and biological reference points (upper triangular) for natural mortality (M), current fishing mortality (F_{cur}), fishing mortality that produced MSY (F_{msy}), MSY (C_{msy}) and the ratio of population in 1950 to that expected in the absence of fishing from fitting the spatial model to catch data. Biological reference points in the top right corner are the ratio of current fishing mortality to the fishing mortality that produces MSY, and the ratio of current stock size to the stock size that produces MSY. Filled circles outside the upper triangular plot indicate ratios greater than 5. Blue lines and points are from spatial model runs under different intial movement rates. Dark orange lines are from the relative fishing mortality rate forced numbers dynamic model. Rug plots on the top of distributions on the diagonal demark prior distributions.

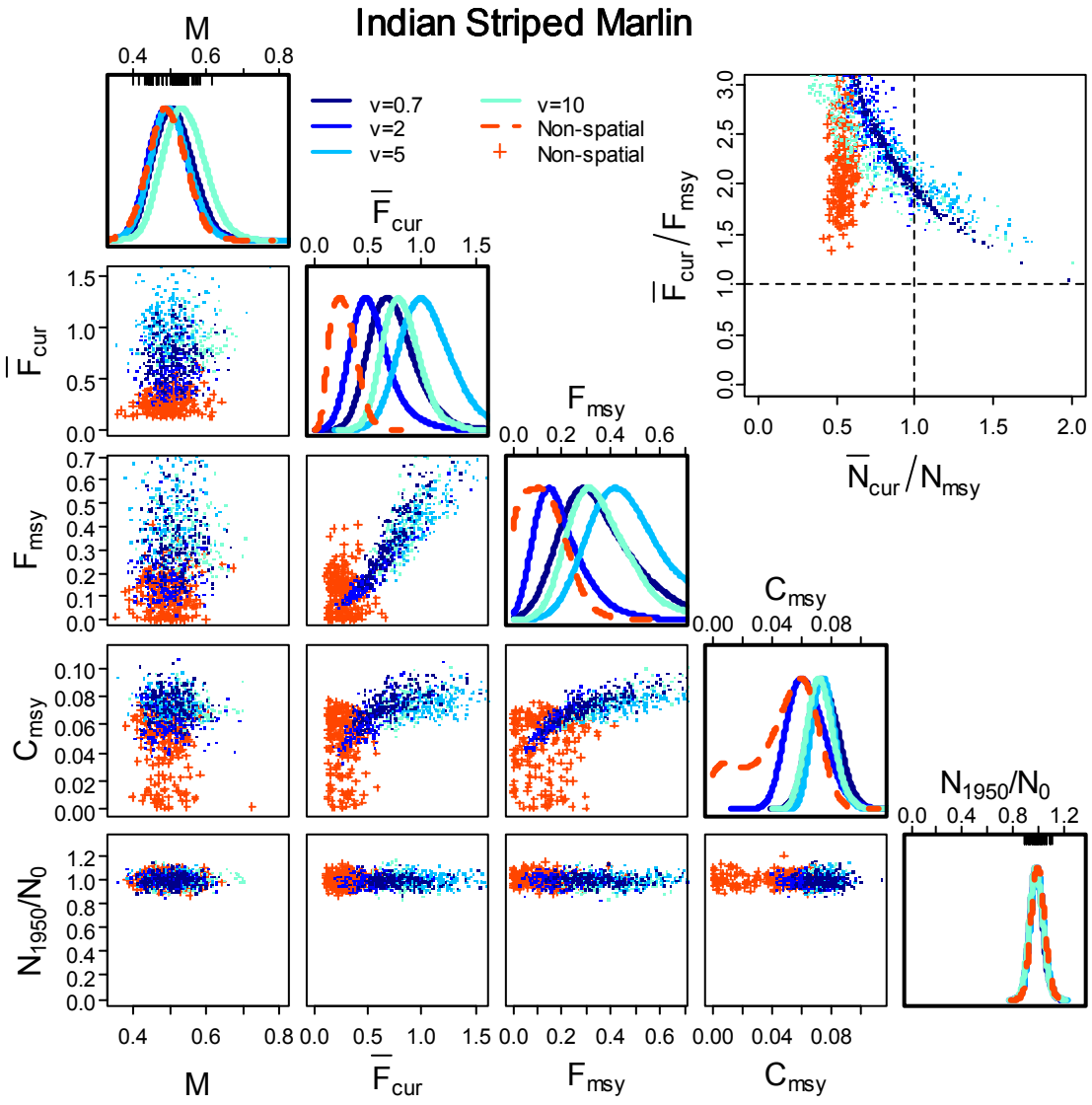

Figure 11.6 Indian Ocean striped marlin leading parameter joint distribution (lower triangular), marginal posterior distributions (diagonal) and biological reference points (upper triangular) for natural mortality (M), current fishing mortality (F_{cur}), fishing mortality that produced MSY (F_{msy}), MSY (C_{msy}) and the ratio of population in 1950 to that expected in the absence of fishing from fitting the spatial model to catch data. Biological reference points in the top right corner are the ratio of current fishing mortality to the fishing mortality that produces MSY, and the ratio of current stock size to the stock size that produces MSY. Filled circles outside the upper triangular plot indicate ratios greater than 5. Blue lines and points are from spatial model runs under different intial movement rates. Dark orange lines are from the relative fishing mortality rate forced numbers dynamic model. Rug plots on the top of distributions on the diagonal demark prior distributions.

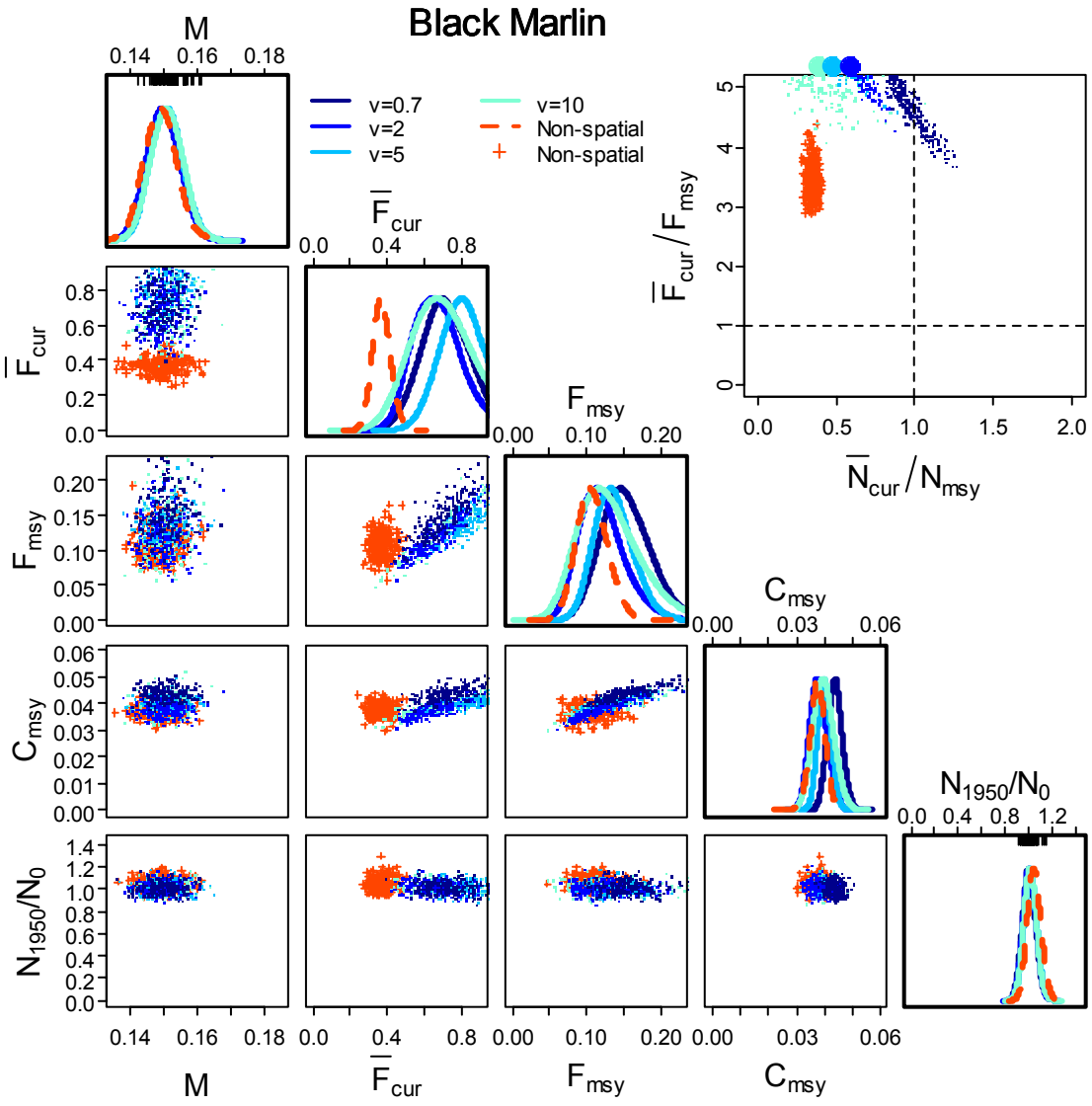

Figure 11.7 Indo-Pacific black marlin leading parameter joint distribution (lower triangular), marginal posterior distributions (diagonal) and biological reference points (upper triangular) for natural mortality (M), current fishing mortality (F_{cur}), fishing mortality that produced MSY (F_{msy}), MSY (C_{msy}) and the ratio of population in 1950 to that expected in the absence of fishing from fitting the spatial model to catch data. Biological reference points in the top right corner are the ratio of current fishing mortality to the fishing mortality that produces MSY, and the ratio of current stock size to the stock size that produces MSY. Filled circles outside the upper triangular plot indicate ratios greater than 5. Blue lines and points are from spatial model runs under different intial movement rates. Dark orange lines are from the relative fishing mortality rate forced numbers dynamic model. Rug plots on the top of distributions on the diagonal demark prior distributions.

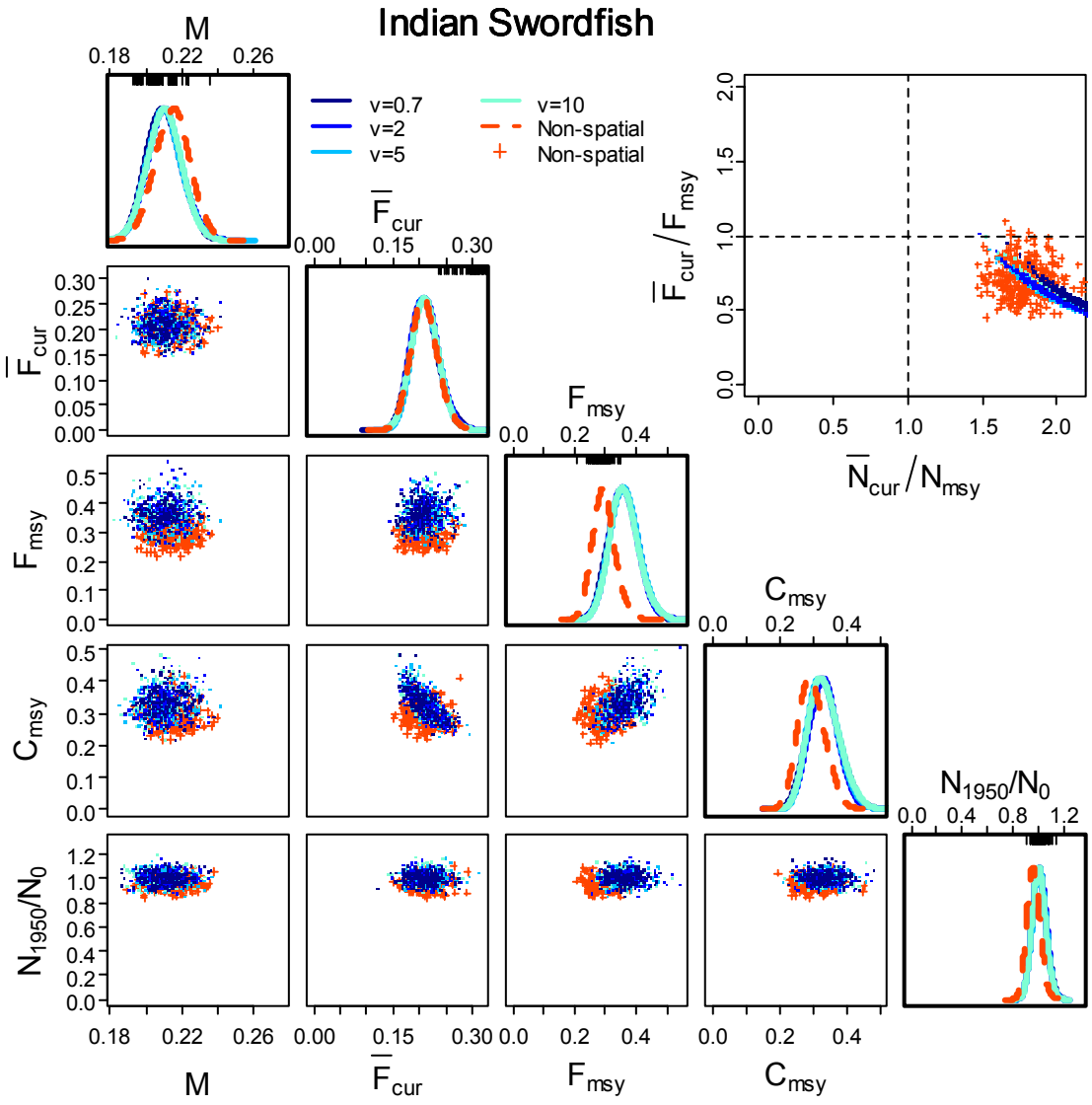

Figure 11.8 Indian Ocean swordfish leading parameter joint distribution (lower triangular), marginal posterior distributions (diagonal) and biological reference points (upper triangular) for natural mortality (M), current fishing mortality (F_{cur}), fishing mortality that produced MSY (F_{msy}), MSY (C_{msy}) and the ratio of population in 1950 to that expected in the absence of fishing from fitting the spatial model to catch data. Biological reference points in the top right corner are the ratio of current fishing mortality to the fishing mortality that produces MSY, and the ratio of current stock size to the stock size that produces MSY. Filled circles outside the upper triangular plot indicate ratios greater than 5. Blue lines and points are from spatial model runs under different intial movement rates. Dark orange lines are from the relative fishing mortality rate forced numbers dynamic model. Rug plots on the top of distributions on the diagonal demark prior distributions.

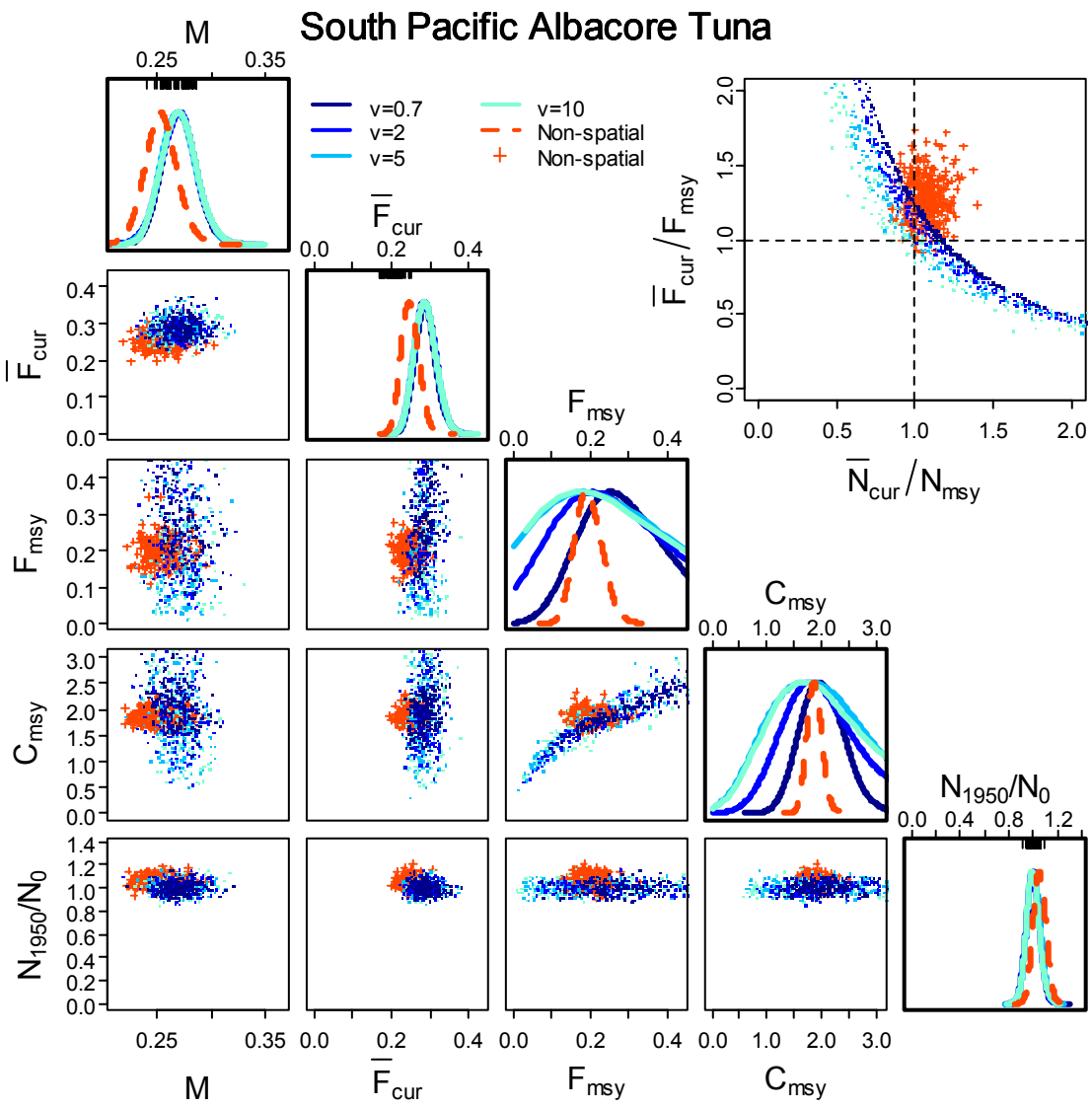

Figure 11.9 Pacific Ocean southern albacore tuna leading parameter joint distribution (lower triangular), marginal posterior distributions (diagonal) and biological reference points (upper triangular) for natural mortality (M), current fishing mortality (F_{cur}), fishing mortality that produced MSY (F_{msy}), MSY (C_{msy}) and the ratio of population in 1950 to that expected in the absence of fishing from fitting the spatial model to catch data. Biological reference points in the top right corner are the ratio of current fishing mortality to the fishing mortality that produces MSY, and the ratio of current stock size to the stock size that produces MSY. Filled circles outside the upper triangular plot indicate ratios greater than 5. Blue lines and points are from spatial model runs under different intial movement rates. Dark orange lines are from the relative fishing mortality rate forced numbers dynamic model. Rug plots on the top of distributions on the diagonal demark prior distributions.

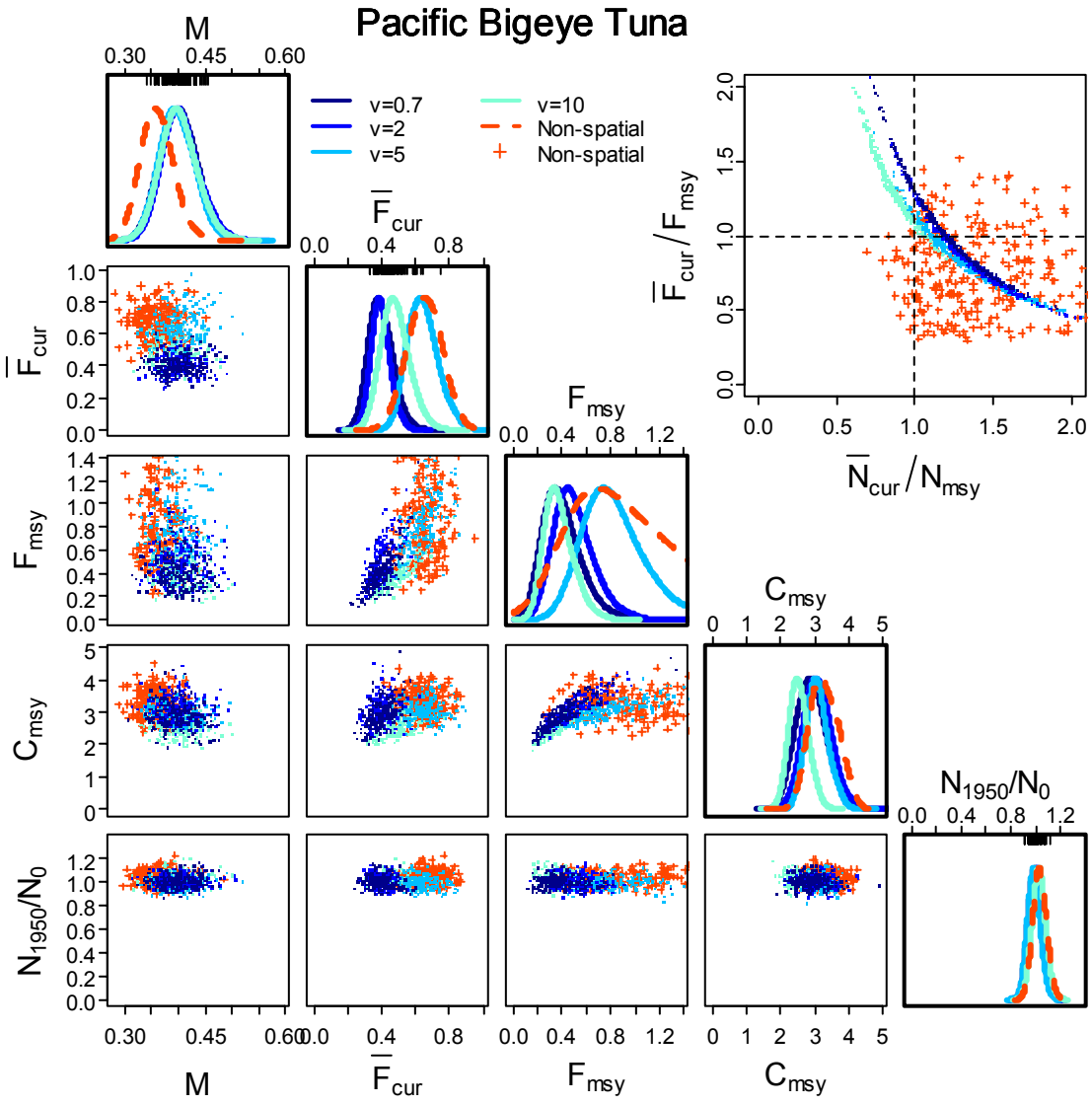

Figure 11.10 Pacific Ocean bigeye tuna leading parameter joint distribution (lower triangular), marginal posterior distributions (diagonal) and biological reference points (upper triangular) for natural mortality (M), current fishing mortality (F_{cur}), fishing mortality that produced MSY (F_{msy}), MSY (C_{msy}) and the ratio of population in 1950 to that expected in the absence of fishing from fitting the spatial model to catch data. Biological reference points in the top right corner are the ratio of current fishing mortality to the fishing mortality that produces MSY, and the ratio of current stock size to the stock size that produces MSY. Filled circles outside the upper triangular plot indicate ratios greater than 5. Blue lines and points are from spatial model runs under different intial movement rates. Dark orange lines are from the relative fishing mortality rate forced numbers dynamic model. Rug plots on the top of distributions on the diagonal demark prior distributions.

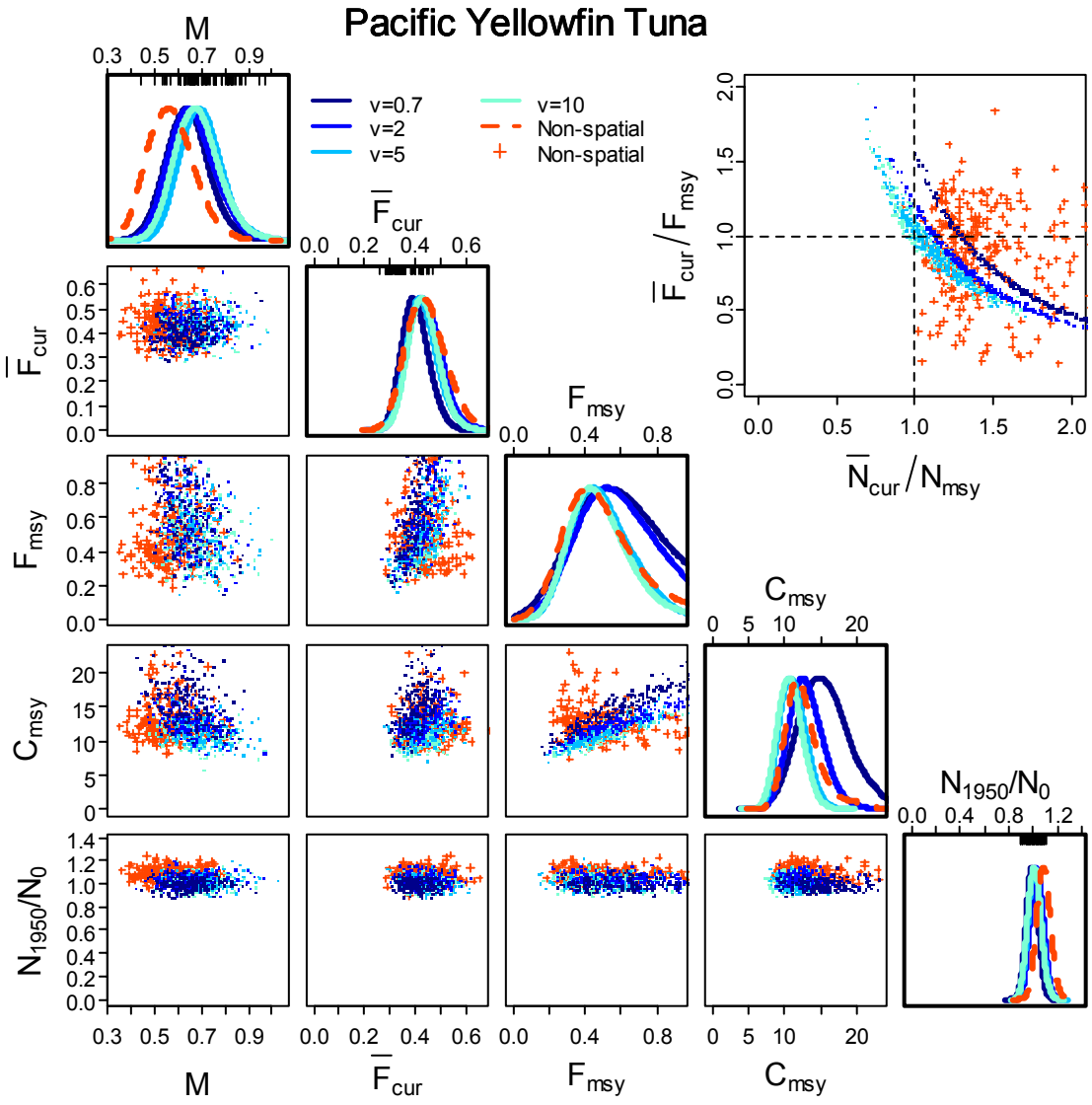

Figure 11.11 Pacific Ocean yellowfin tuna leading parameter joint distribution (lower triangular), marginal posterior distributions (diagonal) and biological reference points (upper triangular) for natural mortality (M), current fishing mortality (F_{cur}), fishing mortality that produced MSY (F_{msy}), MSY (C_{msy}) and the ratio of population in 1950 to that expected in the absence of fishing from fitting the spatial model to catch data. Biological reference points in the top right corner are the ratio of current fishing mortality to the fishing mortality that produces MSY, and the ratio of current stock size to the stock size that produces MSY. Filled circles outside the upper triangular plot indicate ratios greater than 5. Blue lines and points are from spatial model runs under different intial movement rates. Dark orange lines are from the relative fishing mortality rate forced numbers dynamic model. Rug plots on the top of distributions on the diagonal demark prior distributions.

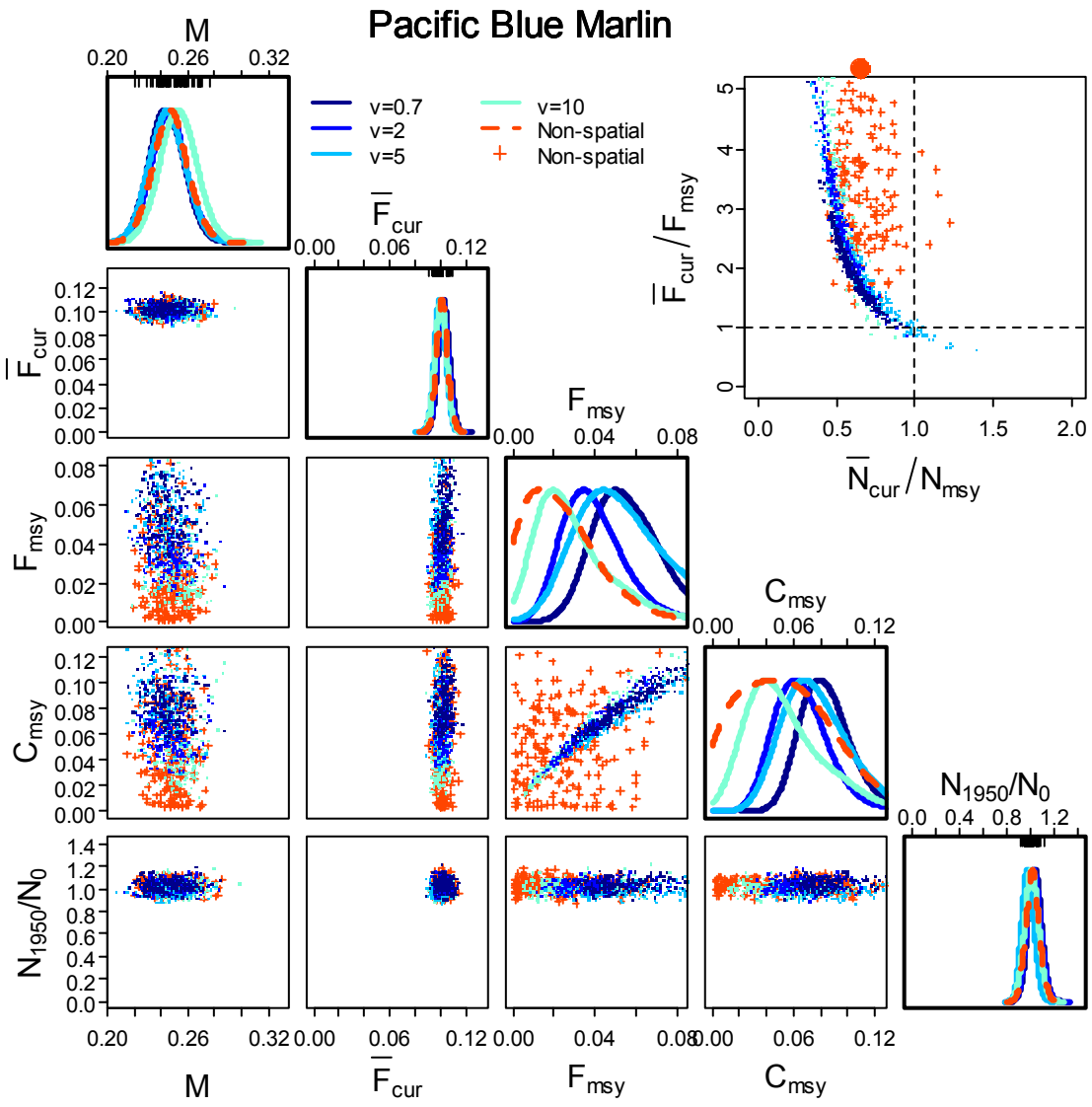

Figure 11.12 Pacific Ocean blue marlin leading parameter joint distribution (lower triangular), marginal posterior distributions (diagonal) and biological reference points (upper triangular) for natural mortality (M), current fishing mortality (F_{cur}), fishing mortality that produced MSY (F_{msy}), MSY (C_{msy}) and the ratio of population in 1950 to that expected in the absence of fishing from fitting the spatial model to catch data. Biological reference points in the top right corner are the ratio of current fishing mortality to the fishing mortality that produces MSY, and the ratio of current stock size to the stock size that produces MSY. Filled circles outside the upper triangular plot indicate ratios greater than 5. Blue lines and points are from spatial model runs under different intial movement rates. Dark orange lines are from the relative fishing mortality rate forced numbers dynamic model. Rug plots on the top of distributions on the diagonal demark prior distributions.

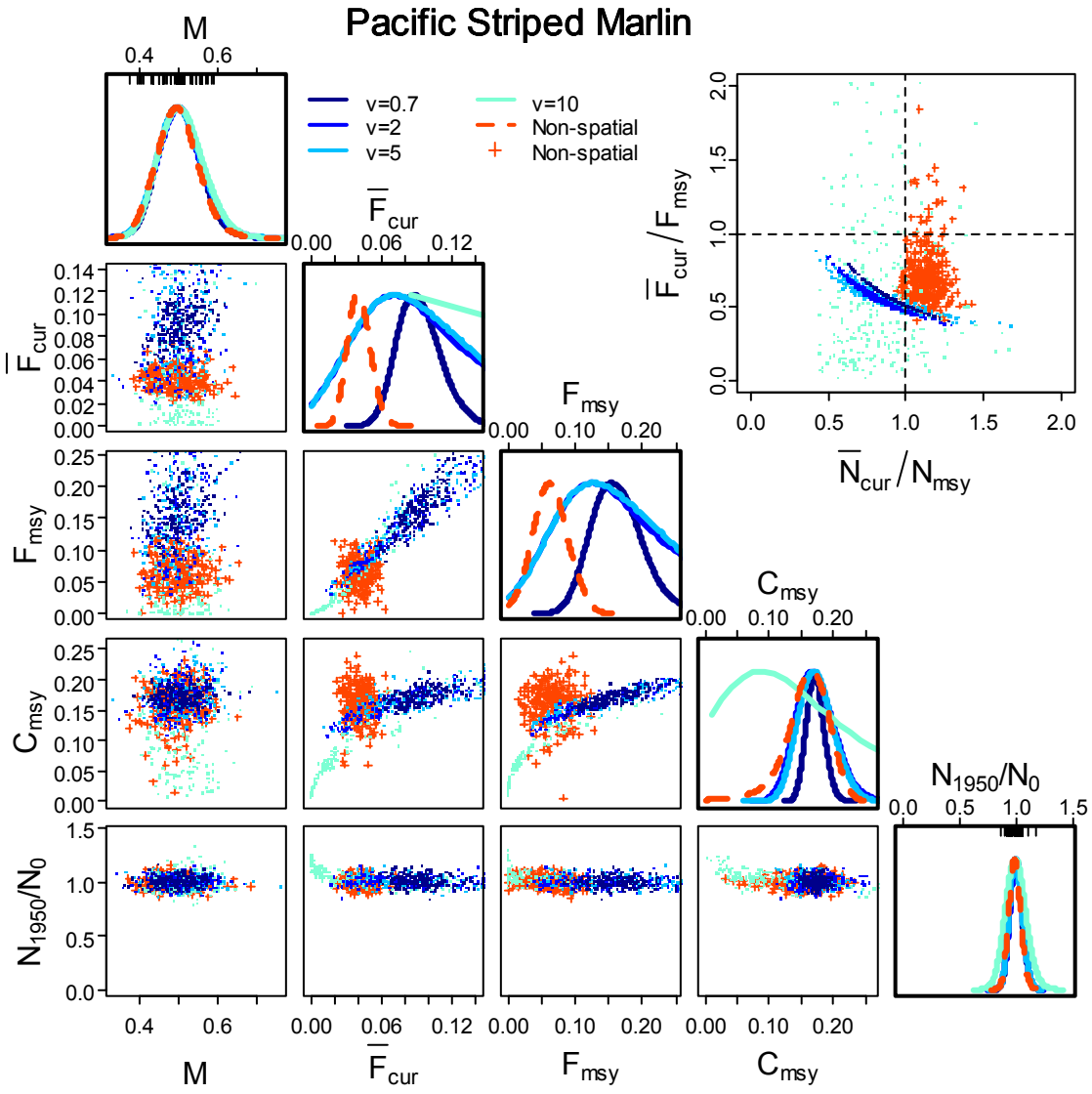

Figure 11.13 Pacific Ocean striped marlin leading parameter joint distribution (lower triangular), marginal posterior distributions (diagonal) and biological reference points (upper triangular) for natural mortality (M), current fishing mortality (F_{cur}), fishing mortality that produced MSY (F_{msy}), MSY (C_{msy}) and the ratio of population in 1950 to that expected in the absence of fishing from fitting the spatial model to catch data. Biological reference points in the top right corner are the ratio of current fishing mortality to the fishing mortality that produces MSY, and the ratio of current stock size to the stock size that produces MSY. Filled circles outside the upper triangular plot indicate ratios greater than 5. Blue lines and points are from spatial model runs under different intial movement rates. Dark orange lines are from the relative fishing mortality rate forced numbers dynamic model. Rug plots on the top of distributions on the diagonal demark prior distributions.

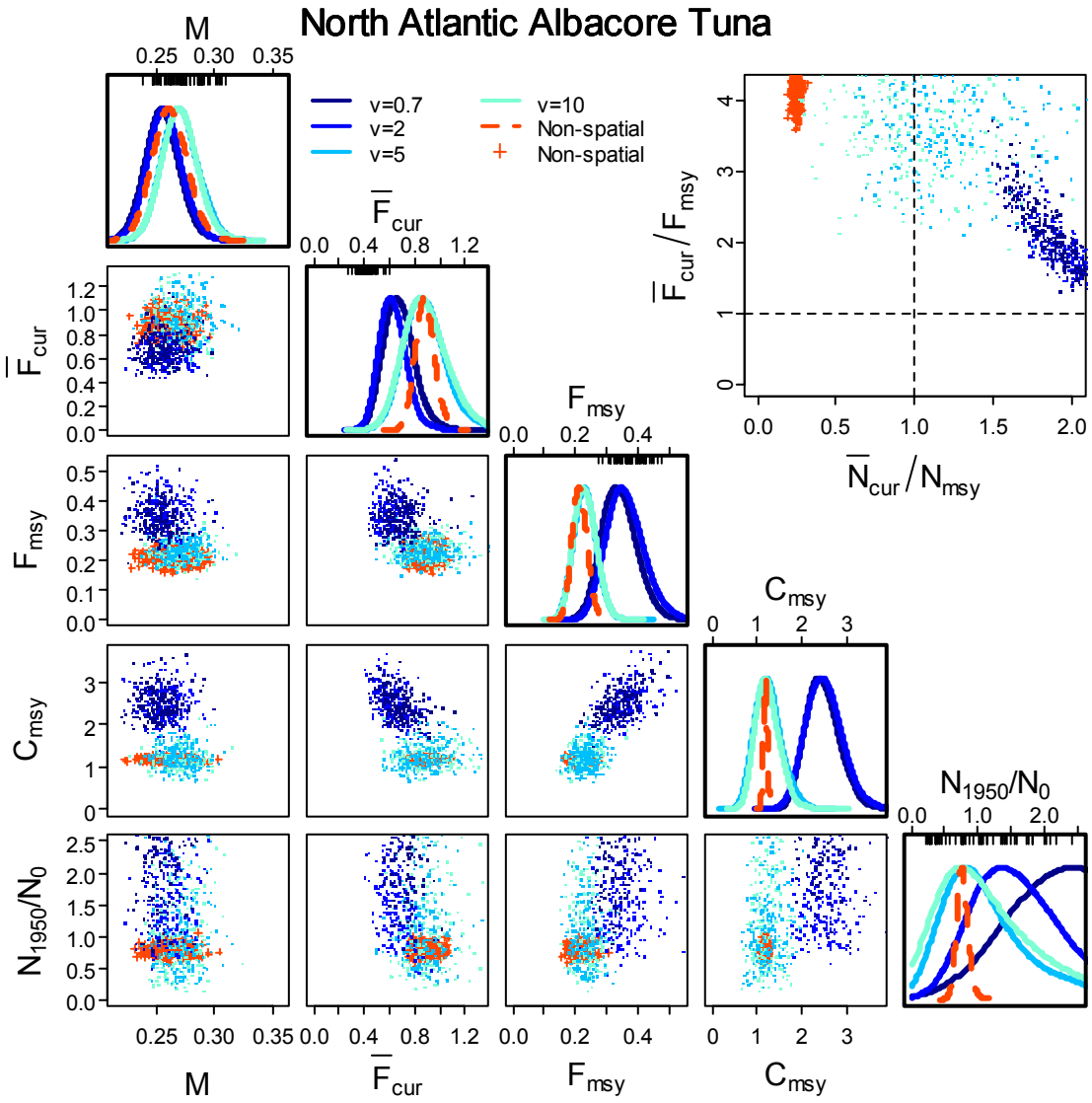

Figure 11.14 Atlantic Ocean northern albacore tuna leading parameter joint distribution (lower triangular), marginal posterior distributions (diagonal) and biological reference points (upper triangular) for natural mortality (M), current fishing mortality (F_{cur}), fishing mortality that produced MSY (F_{msy}), MSY (C_{msy}) and the ratio of population in 1950 to that expected in the absence of fishing from fitting the spatial model to catch data. Biological reference points in the top right corner are the ratio of current fishing mortality to the fishing mortality that produces MSY, and the ratio of current stock size to the stock size that produces MSY. Filled circles outside the upper triangular plot indicate ratios greater than 5. Blue lines and points are from spatial model runs under different intial movement rates. Dark orange lines are from the relative fishing mortality rate forced numbers dynamic model. Rug plots on the top of distributions on the diagonal demark prior distributions.

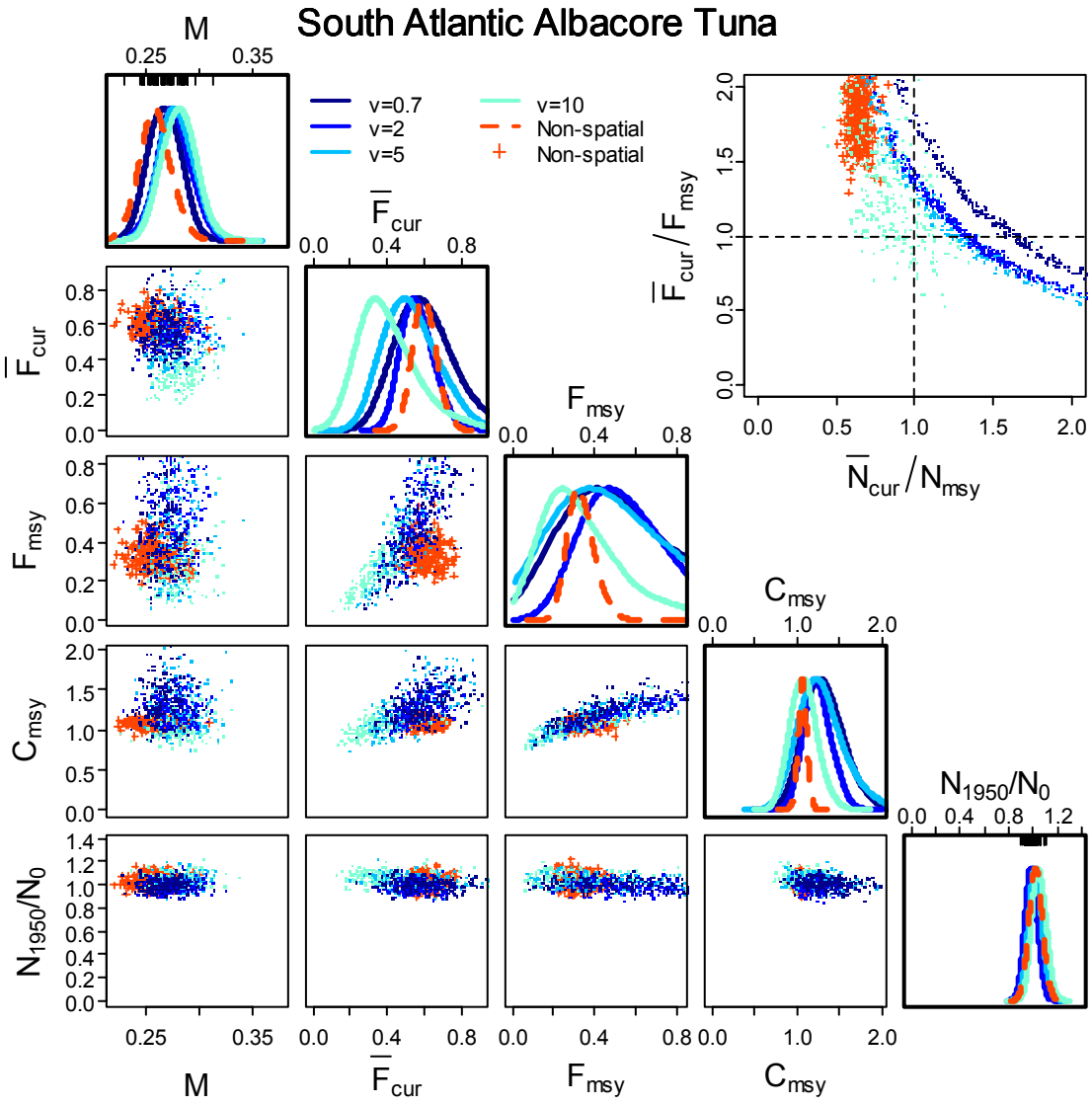

Figure 11.15 Atlantic Ocean southern albacore tuna leading parameter joint distribution (lower triangular), marginal posterior distributions (diagonal) and biological reference points (upper triangular) for natural mortality (M), current fishing mortality (F_{cur}), fishing mortality that produced MSY (F_{msy}), MSY (C_{msy}) and the ratio of population in 1950 to that expected in the absence of fishing from fitting the spatial model to catch data. Biological reference points in the top right corner are the ratio of current fishing mortality to the fishing mortality that produces MSY, and the ratio of current stock size to the stock size that produces MSY. Filled circles outside the upper triangular plot indicate ratios greater than 5. Blue lines and points are from spatial model runs under different intial movement rates. Dark orange lines are from the relative fishing mortality rate forced numbers dynamic model. Rug plots on the top of distributions on the diagonal demark prior distributions.

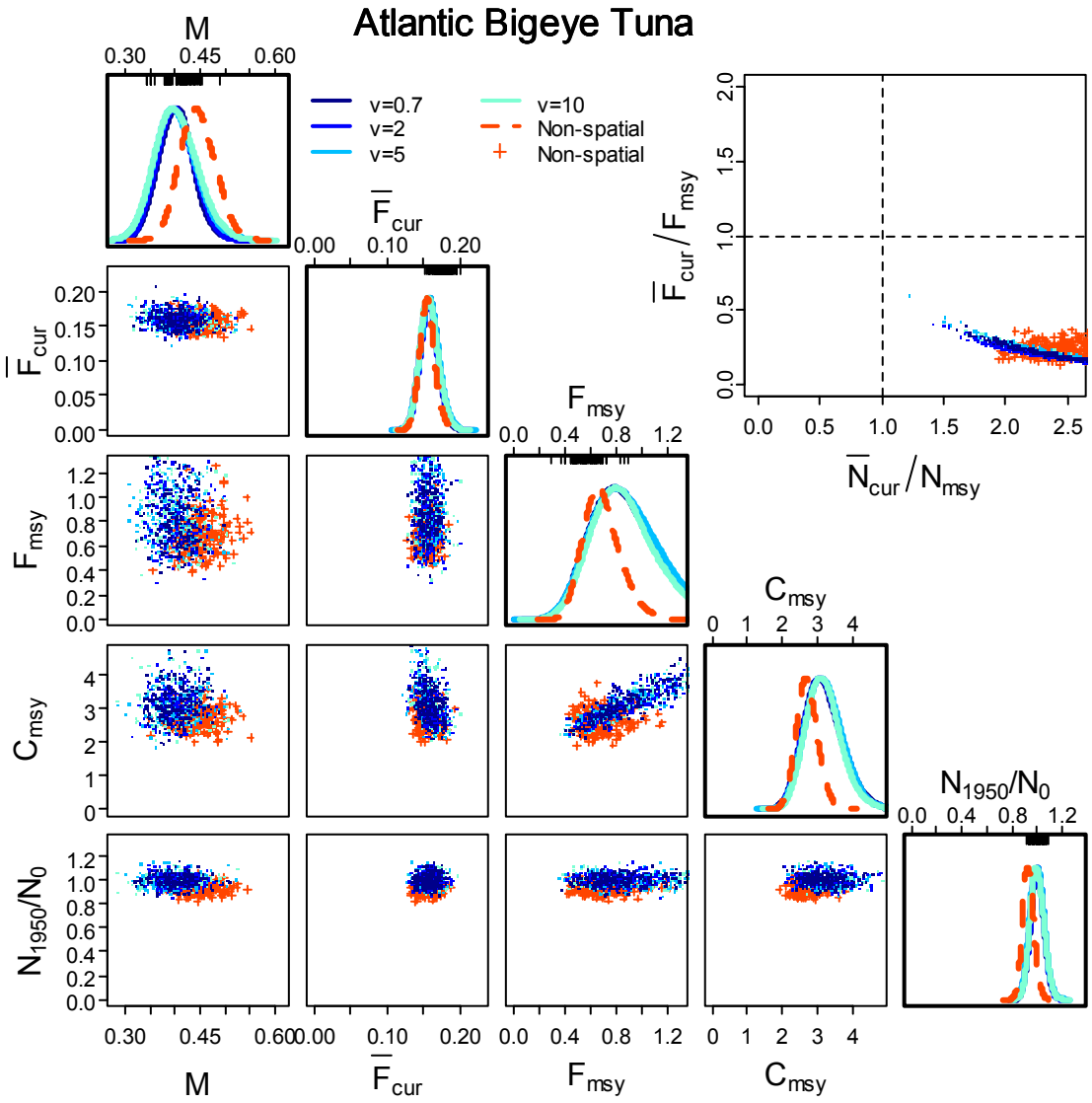

Figure 11.16 Atlantic Ocean bigeye tuna leading parameter joint distribution (lower triangular), marginal posterior distributions (diagonal) and biological reference points (upper triangular) for natural mortality (M), current fishing mortality (F_{cur}), fishing mortality that produced MSY (F_{msy}), MSY (C_{msy}) and the ratio of population in 1950 to that expected in the absence of fishing from fitting the spatial model to catch data. Biological reference points in the top right corner are the ratio of current fishing mortality to the fishing mortality that produces MSY, and the ratio of current stock size to the stock size that produces MSY. Filled circles outside the upper triangular plot indicate ratios greater than 5. Blue lines and points are from spatial model runs under different intial movement rates. Dark orange lines are from the relative fishing mortality rate forced numbers dynamic model. Rug plots on the top of distributions on the diagonal demark prior distributions.

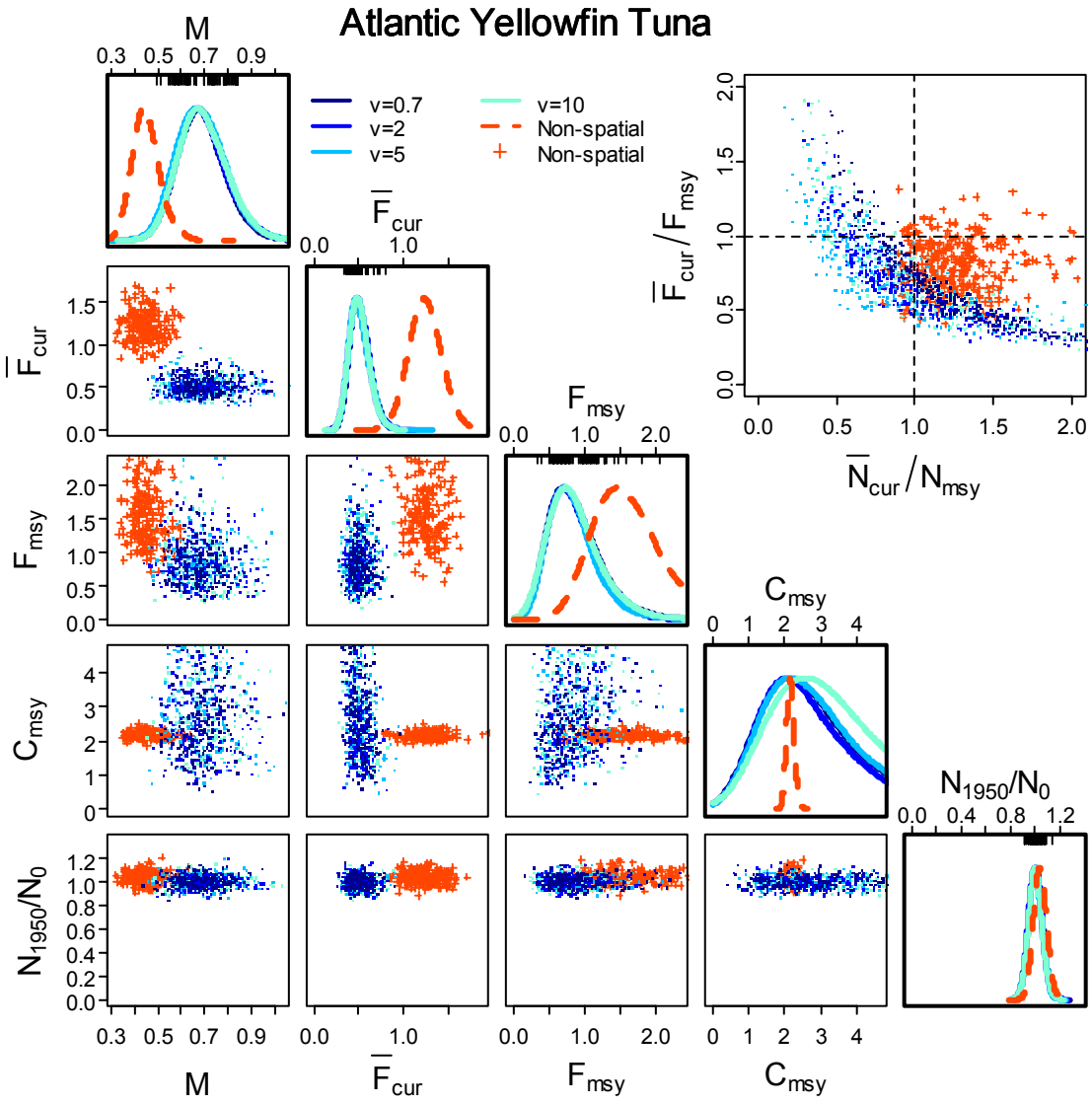

Figure 11.17 Atlantic Ocean yellowfin tuna leading parameter joint distribution (lower triangular), marginal posterior distributions (diagonal) and biological reference points (upper triangular) for natural mortality (M), current fishing mortality (F_{cur}), fishing mortality that produced MSY (F_{msy}), MSY (C_{msy}) and the ratio of population in 1950 to that expected in the absence of fishing from fitting the spatial model to catch data. Biological reference points in the top right corner are the ratio of current fishing mortality to the fishing mortality that produces MSY, and the ratio of current stock size to the stock size that produces MSY. Filled circles outside the upper triangular plot indicate ratios greater than 5. Blue lines and points are from spatial model runs under different intial movement rates. Dark orange lines are from the relative fishing mortality rate forced numbers dynamic model. Rug plots on the top of distributions on the diagonal demark prior distributions.

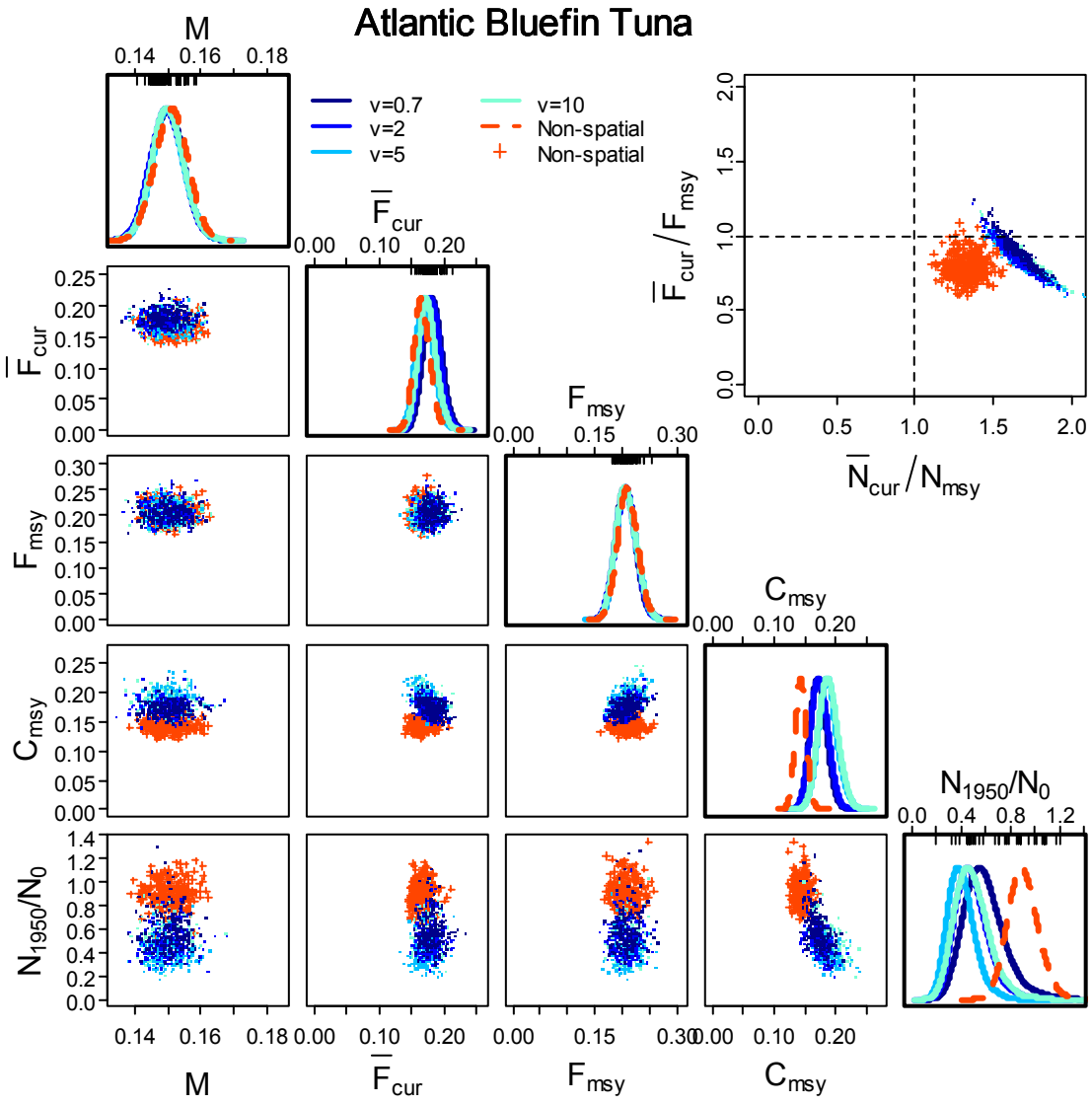

Figure 11.18 Atlantic Ocean bluefin tuna leading parameter joint distribution (lower triangular), marginal posterior distributions (diagonal) and biological reference points (upper triangular) for natural mortality (M), current fishing mortality (F_{cur}), fishing mortality that produced MSY (F_{msy}), MSY (C_{msy}) and the ratio of population in 1950 to that expected in the absence of fishing from fitting the spatial model to catch data. Biological reference points in the top right corner are the ratio of current fishing mortality to the fishing mortality that produces MSY, and the ratio of current stock size to the stock size that produces MSY. Filled circles outside the upper triangular plot indicate ratios greater than 5. Blue lines and points are from spatial model runs under different intial movement rates. Dark orange lines are from the relative fishing mortality rate forced numbers dynamic model. Rug plots on the top of distributions on the diagonal demark prior distributions.

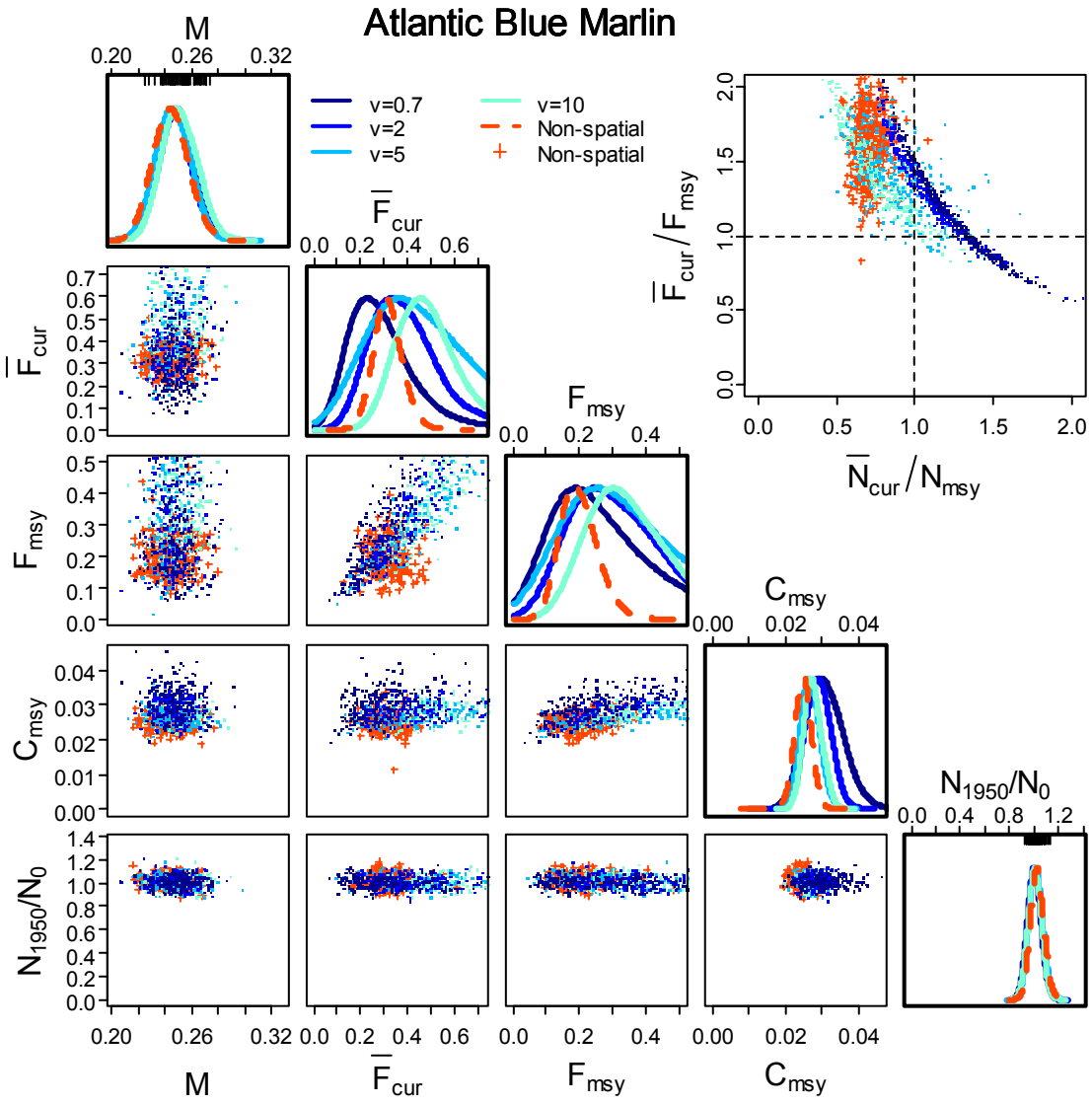

Figure 11.19 Atlantic Ocean blue marlin leading parameter joint distribution (lower triangular), marginal posterior distributions (diagonal) and biological reference points (upper triangular) for natural mortality (M), current fishing mortality (F_{cur}), fishing mortality that produced MSY (F_{msy}), MSY (C_{msy}) and the ratio of population in 1950 to that expected in the absence of fishing from fitting the spatial model to catch data. Biological reference points in the top right corner are the ratio of current fishing mortality to the fishing mortality that produces MSY, and the ratio of current stock size to the stock size that produces MSY. Filled circles outside the upper triangular plot indicate ratios greater than 5. Blue lines and points are from spatial model runs under different intial movement rates. Dark orange lines are from the relative fishing mortality rate forced numbers dynamic model. Rug plots on the top of distributions on the diagonal demark prior distributions.

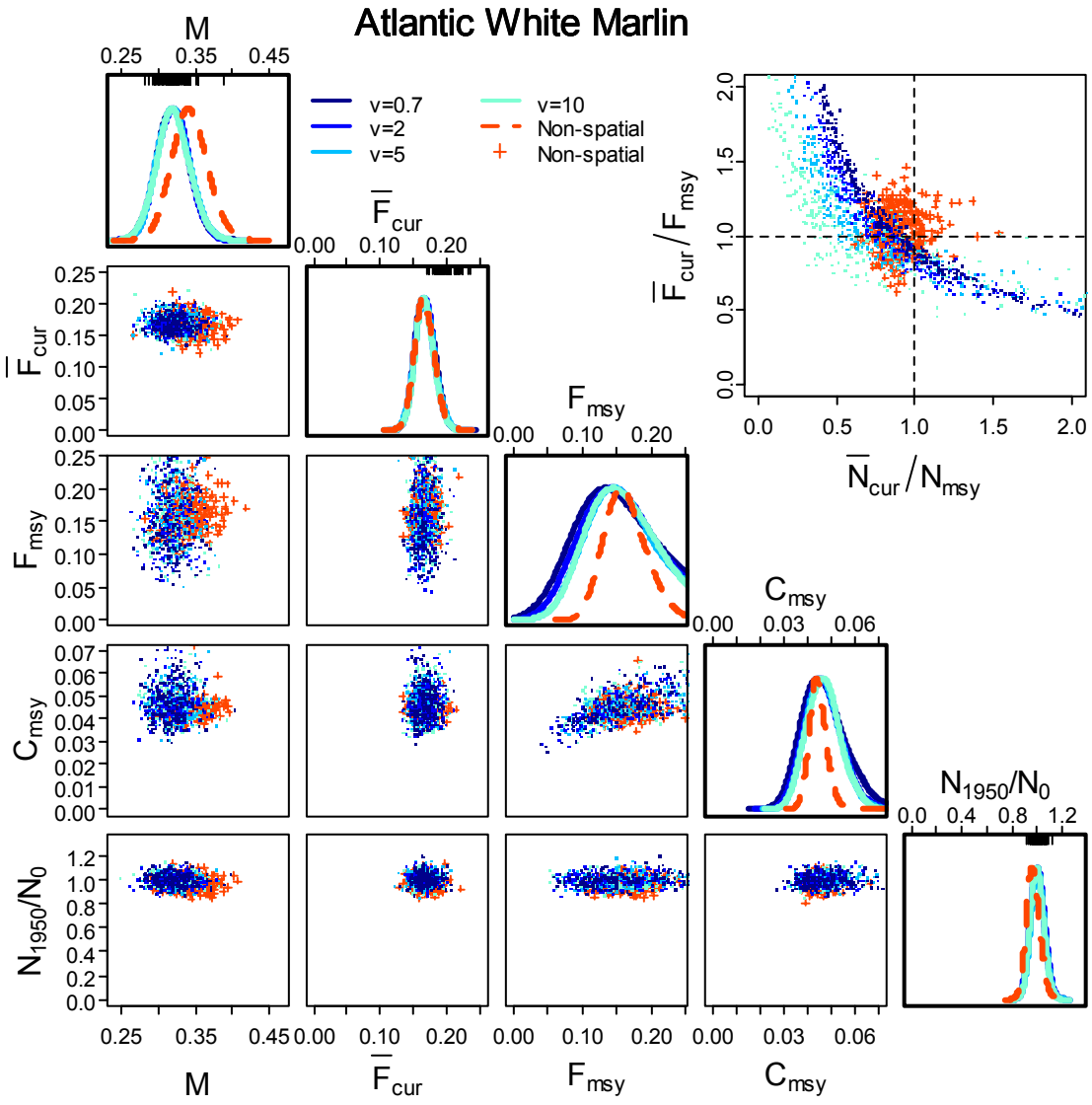

Figure 11.20 Atlantic Ocean white marlin leading parameter joint distribution (lower triangular), marginal posterior distributions (diagonal) and biological reference points (upper triangular) for natural mortality (M), current fishing mortality (F_{cur}), fishing mortality that produced MSY (F_{msy}), MSY (C_{msy}) and the ratio of population in 1950 to that expected in the absence of fishing from fitting the spatial model to catch data. Biological reference points in the top right corner are the ratio of current fishing mortality to the fishing mortality that produces MSY, and the ratio of current stock size to the stock size that produces MSY. Filled circles outside the upper triangular plot indicate ratios greater than 5. Blue lines and points are from spatial model runs under different intial movement rates. Dark orange lines are from the relative fishing mortality rate forced numbers dynamic model. Rug plots on the top of distributions on the diagonal demark prior distributions.

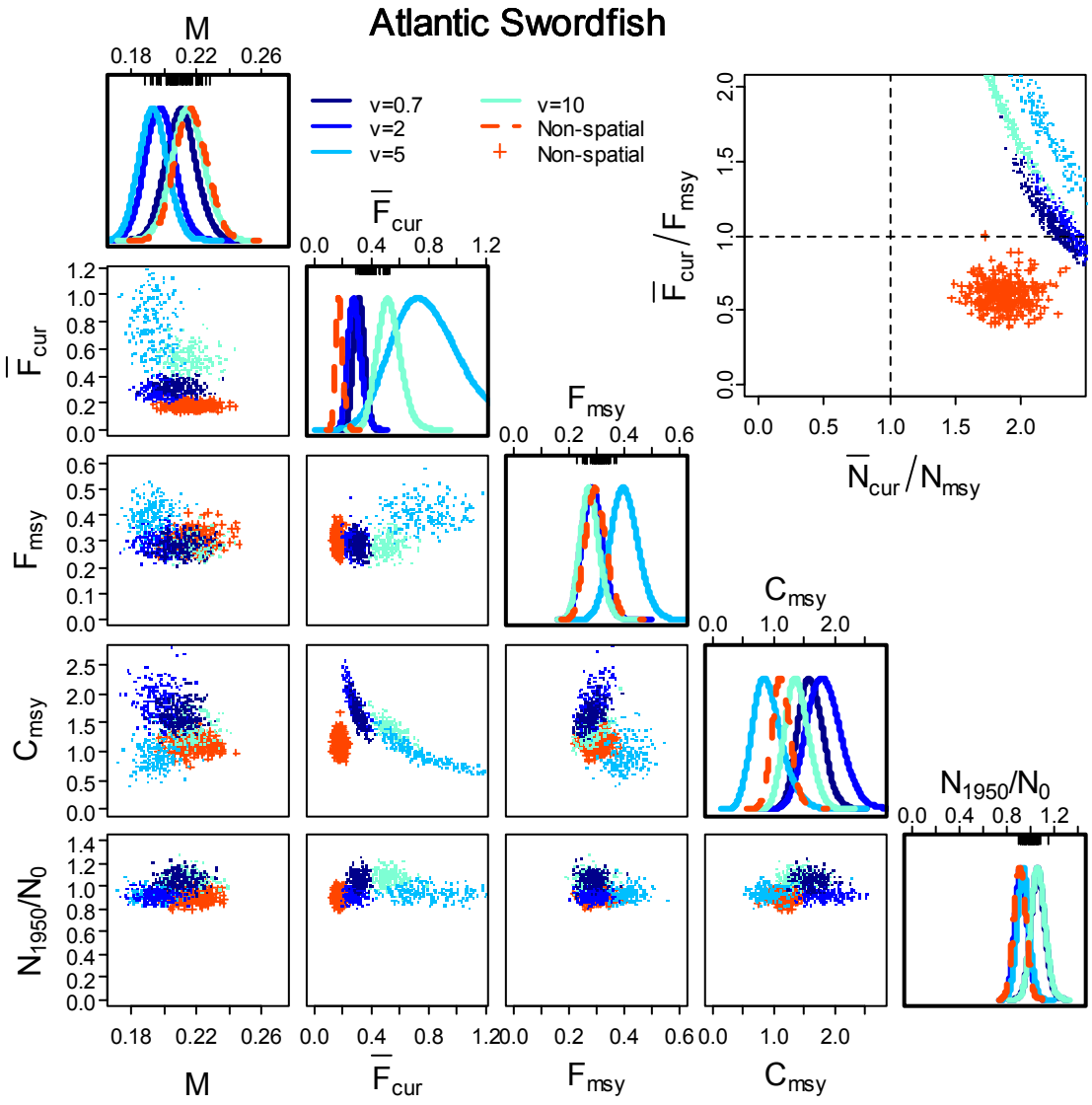

Figure 11.21 Atlantic Ocean swordfish leading parameter joint distribution (lower triangular), marginal posterior distributions (diagonal) and biological reference points (upper triangular) for natural mortality (M), current fishing mortality (F_{cur}), fishing mortality that produced MSY (F_{msy}), MSY (C_{msy}) and the ratio of population in 1950 to that expected in the absence of fishing from fitting the spatial model to catch data. Biological reference points in the top right corner are the ratio of current fishing mortality to the fishing mortality that produces MSY, and the ratio of current stock size to the stock size that produces MSY. Filled circles outside the upper triangular plot indicate ratios greater than 5. Blue lines and points are from spatial model runs under different intial movement rates. Dark orange lines are from the relative fishing mortality rate forced numbers dynamic model. Rug plots on the top of distributions on the diagonal demark prior distributions.

Appendix for Chapter 6

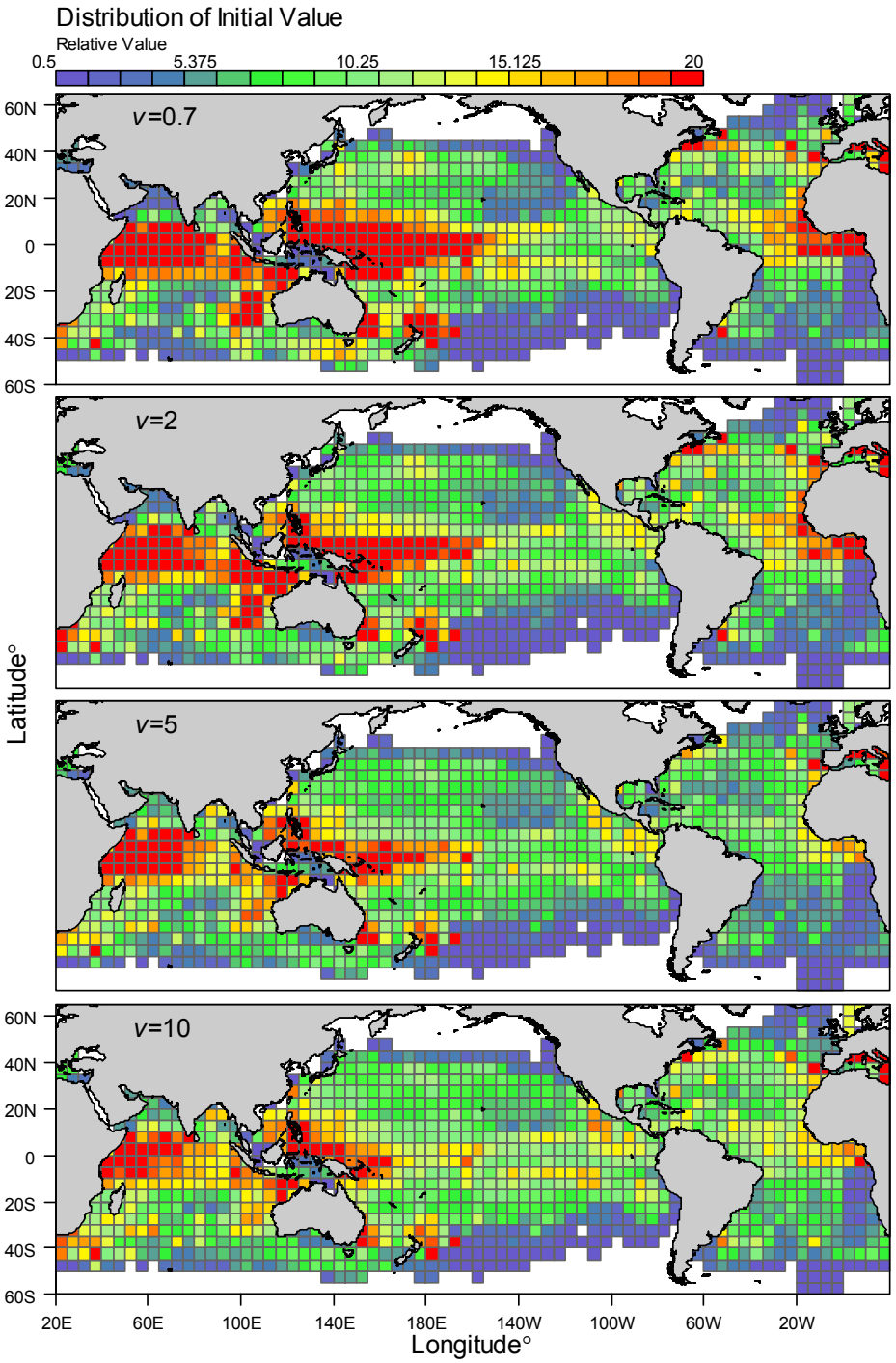

Figure 12.1 Estimated total initial value (initial population size x weight x price) for various initial movement rate scenarios summed over all stocks.

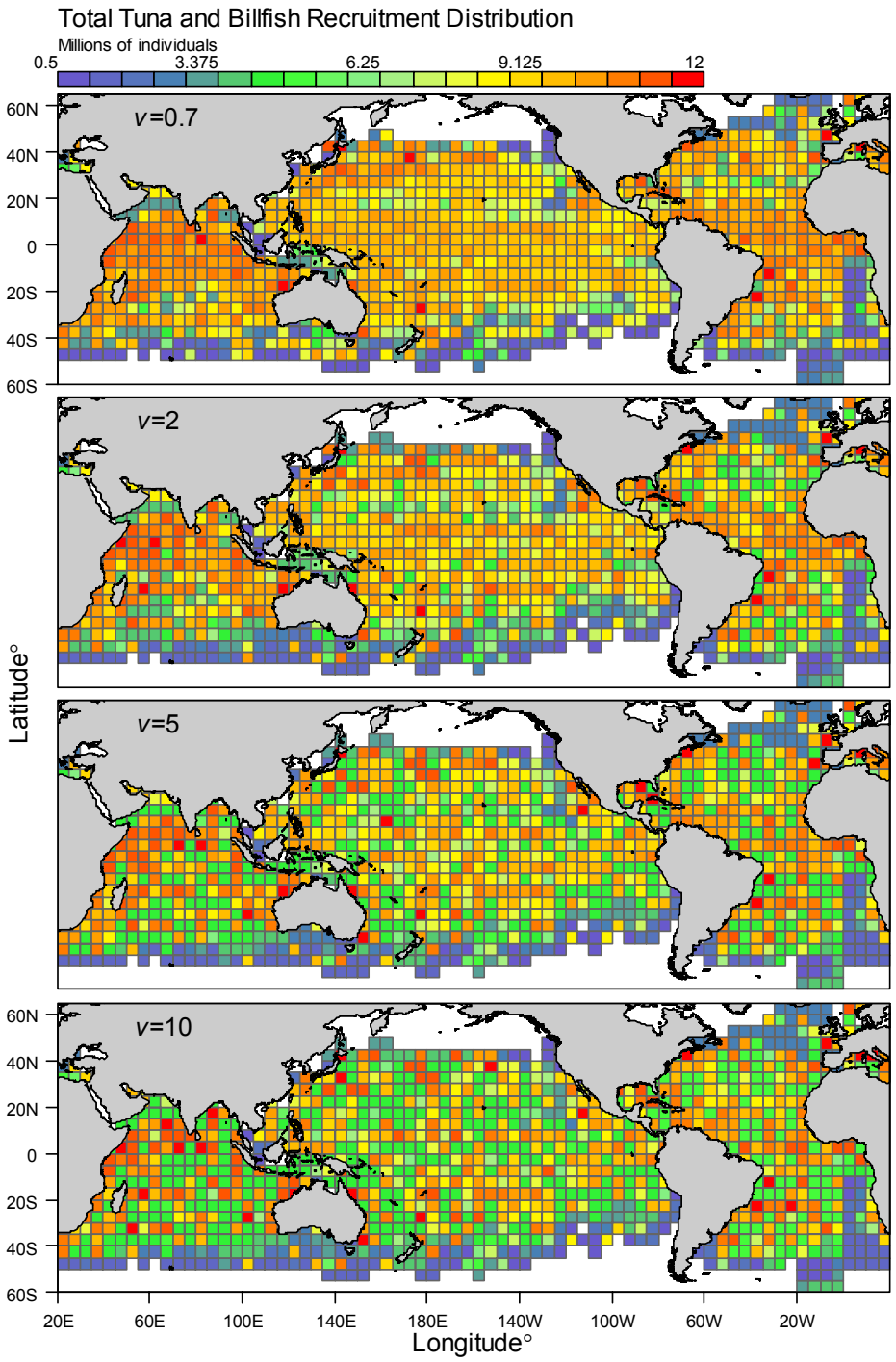

Figure 12.2 Estimated total initial recruitment for all species combined, under various initial movement rate scenarios.

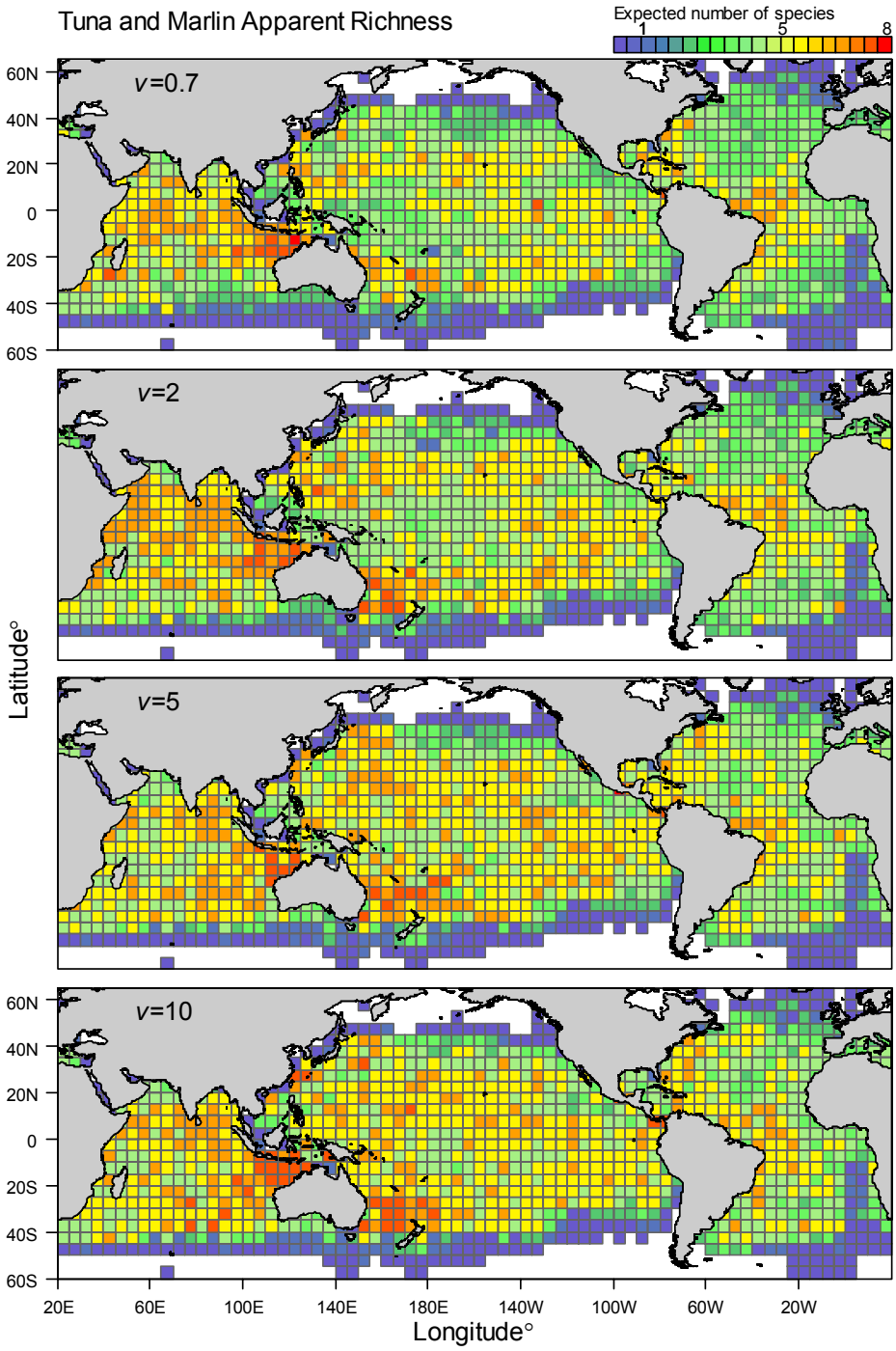

Figure 12.3 Estimated tuna and marlin species richness. Richness was calculated as the expected number of species arising in a random sample of 100 individuals from each cell. Sampling probability depended on estimated initial population size.